Central and Eastern United States Seismic Source Characterization for Nuclear Facilities

Volume 3: Chapters 8 to 11

U.S. Nuclear Regulatory Commission
Office of Nuclear Regulatory Research
Washington DC 20555
NUREG-2115

U.S. Department of Energy
1000 Independence Avenue SW
Washington, DC 20585
Report # DOE/NE-0140

Electric Power Research Institute
3420 Hillview Avenue
Palo Alto, CA 94304
Report # 1021097

AVAILABILITY OF REFERENCE MATERIALS IN NRC PUBLICATIONS

NRC Reference Material

As of November 1999, you may electronically access NUREG-series publications and other NRC records at NRC's Public Electronic Reading Room at http://www.nrc.gov/reading-rm.html. Publicly released records include, to name a few, NUREG-series publications; *Federal Register* notices; applicant, licensee, and vendor documents and correspondence; NRC correspondence and internal memoranda; bulletins and information notices; inspection and investigative reports; licensee event reports; and Commission papers and their attachments.

NRC publications in the NUREG series, NRC regulations, and *Title 10, Energy*, in the Code of *Federal Regulations* may also be purchased from one of these two sources.

1. The Superintendent of Documents
   U.S. Government Printing Office
   Mail Stop SSOP
   Washington, DC 20402–0001
   Internet: bookstore.gpo.gov
   Telephone: 202-512-1800
   Fax: 202-512-2250
2. The National Technical Information Service
   Springfield, VA 22161–0002
   www.ntis.gov
   1–800–553–6847 or, locally, 703–605–6000

A single copy of each NRC draft report for comment is available free, to the extent of supply, upon written request as follows:

Address: U.S. Nuclear Regulatory Commission
Office of Administration
Publications Branch
Washington, DC 20555-0001
E-mail: DISTRIBUTION.SERVICES@NRC.GOV
Facsimile: 301–415–2289

Some publications in the NUREG series that are posted at NRC's Web site address http://www.nrc.gov/reading-rm/doc-collections/nuregs are updated periodically and may differ from the last printed version. Although references to material found on a Web site bear the date the material was accessed, the material available on the date cited may subsequently be removed from the site.

Non-NRC Reference Material

Documents available from public and special technical libraries include all open literature items, such as books, journal articles, and transactions, *Federal Register* notices, Federal and State legislation, and congressional reports. Such documents as theses, dissertations, foreign reports and translations, and non-NRC conference proceedings may be purchased from their sponsoring organization.

Copies of industry codes and standards used in a substantive manner in the NRC regulatory process are maintained at—

The NRC Technical Library
Two White Flint North
11545 Rockville Pike
Rockville, MD 20852–2738

These standards are available in the library for reference use by the public. Codes and standards are usually copyrighted and may be purchased from the originating organization or, if they are American National Standards, from—

American National Standards Institute
11 West 42nd Street
New York, NY 10036–8002
www.ansi.org
212–642–4900

Legally binding regulatory requirements are stated only in laws; NRC regulations; licenses, including technical specifications; or orders, not in NUREG-series publications. The views expressed in contractor-prepared publications in this series are not necessarily those of the NRC.

The NUREG series comprises (1) technical and administrative reports and books prepared by the staff (NUREG–XXXX) or agency contractors (NUREG/CR–XXXX), (2) proceedings of conferences (NUREG/CP–XXXX), (3) reports resulting from international agreements (NUREG/IA–XXXX), (4) brochures (NUREG/BR–XXXX), and (5) compilations of legal decisions and orders of the Commission and Atomic and Safety Licensing Boards and of Directors' decisions under Section 2.206 of NRC's regulations (NUREG–0750).

Central and Eastern United States Seismic Source Characterization for Nuclear Facilities

Cosponsors

U.S. Department of Energy
1000 Independence Avenue SW
Washington, DC 20585

R. H. Lagdon, Jr.
Chief of Nuclear Safety
Office of the Under Secretary for Nuclear Security, S-5

M.E. Shields
Project Manager
Office of Nuclear Energy, NE-72

Electric Power Research Institute
3420 Hillview Avenue
Palo Alto, CA 94304

J. F. Hamel
Program Manager
Advanced Nuclear Technology

U.S. Nuclear Regulatory Commission
Office of Nuclear Regulatory Research
Washington DC 20555

R.G. Roche-Rivera
NRC Project Manager

*This document was **not** developed under a 10CFR50 Appendix B program.*

SPONSORS' ACKNOWLEDGMENTS

The project sponsors would like to acknowledge the following individuals for directing the project:

Coppersmith Consulting, Inc.
2121 N. California Blvd., #290
Walnut Creek, CA 94596

Technical Integration (TI) Lead
K.J. Coppersmith

Savannah River Nuclear Solutions, LLC
Savannah River Site
Building 730-4B, Room 313
Aiken, SC 29808

CEUS SSC Project Manager
L.A. Salomone

This document describes research sponsored by the Electric Power Research Institute (EPRI), U.S. Department of Energy (U.S. DOE) under Award Number DE-FG07-08ID14908, and the U.S. Nuclear Regulatory Commission (U.S. NRC) under Award Number NCR-04-09-144.

This publication is a corporate document that should be cited in the literature in the following manner:

Technical Report: Central and Eastern United States Seismic Source Characterization for Nuclear Facilities. EPRI, Palo Alto, CA, U.S. DOE, and U.S. NRC: 2012.

AUTHORS

This document was prepared by the following investigators:

Technical Integration Lead	Kevin J. Coppersmith
Project Manager	Lawrence A. Salomone
Technical Integration Team	Chris W. Fuller Laura L. Glaser Kathryn L. Hanson Ross D. Hartleb William R. Lettis Scott C. Lindvall Stephen M. McDuffie Robin K. McGuire Gerry L. Stirewalt Gabriel R. Toro Robert R. Youngs
Database Manager	David L. Slayter
Technical Support	Serkan B. Bozkurt Randolph J. Cumbest Valentina Montaldo Falero Roseanne C. Perman Allison M. Shumway Frank H. Syms Martitia (Tish) P. Tuttle, Paleoliquefaction Data Resource

ABSTRACT

This report describes a new seismic source characterization (SSC) model for the Central and Eastern United States (CEUS). It will replace the *Seismic Hazard Methodology for the Central and Eastern United States*, EPRI Report NP-4726 (July 1986) and the *Seismic Hazard Characterization of 69 Nuclear Plant Sites East of the Rocky Mountains,* Lawrence Livermore National Laboratory Model, (Bernreuter et al., 1989). The objective of the CEUS SSC Project is to develop a new seismic source model for the CEUS using a Senior Seismic Hazard Analysis Committee (SSHAC) Level 3 assessment process. The goal of the SSHAC process is to represent the center, body, and range of technically defensible interpretations of the available data, models, and methods. Input to a probabilistic seismic hazard analysis (PSHA) consists of both seismic source characterization and ground motion characterization. These two components are used to calculate probabilistic hazard results (or seismic hazard curves) at a particular site. This report provides a new seismic source model.

Results and Findings

The product of this report is a regional CEUS SSC model. This model includes consideration of an updated database, full assessment and incorporation of uncertainties, and the range of diverse technical interpretations from the larger technical community. The SSC model will be widely applicable to the entire CEUS, so this project uses a ground motion model that includes generic variations to allow for a range of representative site conditions (deep soil, shallow soil, hard rock). Hazard and sensitivity calculations were conducted at seven test sites representative of different CEUS hazard environments.

Challenges and Objectives

The regional CEUS SSC model will be of value to readers who are involved in PSHA work, and who wish to use an updated SSC model. This model is based on a comprehensive and traceable process, in accordance with SSHAC guidelines in NUREG/CR-6372, *Recommendations for Probabilistic Seismic Hazard Analysis: Guidance on Uncertainty and Use of Experts*. The model will be used to assess the present-day composite distribution for seismic sources along with their characterization in the CEUS and uncertainty. In addition, this model is in a form suitable for use in PSHA evaluations for regulatory activities, such as Early Site Permit (ESPs) and Combined Operating License Applications (COLAs).

Applications, Values, and Use

Development of a regional CEUS seismic source model will provide value to those who (1) have submitted an ESP or COLA for Nuclear Regulatory Commission (NRC) review before 2011; (2) will submit an ESP or COLA for NRC review after 2011; (3) must respond to safety issues resulting from NRC Generic Issue 199 (GI-199) for existing plants and (4) will prepare PSHAs to meet design and periodic review requirements for current and future nuclear facilities. This work replaces a previous study performed approximately 25 years ago. Since that study was

completed, substantial work has been done to improve the understanding of seismic sources and their characterization in the CEUS. Thus, a new regional SSC model provides a consistent, stable basis for computing PSHA for a future time span. Use of a new SSC model reduces the risk of delays in new plant licensing due to more conservative interpretations in the existing and future literature.

Perspective

The purpose of this study, jointly sponsored by EPRI, the U.S. Department of Energy (DOE), and the NRC was to develop a new CEUS SSC model. The team assembled to accomplish this purpose was composed of distinguished subject matter experts from industry, government, and academia. The resulting model is unique, and because this project has solicited input from the present-day larger technical community, it is not likely that there will be a need for significant revision for a number of years. See also Sponsors' Perspective for more details.

Approach

The goal of this project was to implement the CEUS SSC work plan for developing a regional CEUS SSC model. The work plan, formulated by the project manager and a technical integration team, consists of a series of tasks designed to meet the project objectives. This report was reviewed by a participatory peer review panel (PPRP), sponsor reviewers, the NRC, the U.S. Geological Survey, and other stakeholders. Comments from the PPRP and other reviewers were considered when preparing the report. The SSC model was completed at the end of 2011.

Keywords

Probabilistic seismic hazard analysis (PSHA)
Seismic source characterization (SSC)
Seismic source characterization model
Central and Eastern United States (CEUS)

CONTENTS

LIST OF FIGURES

LIST OF TABLES

EXECUTIVE SUMMARY

The Central and Eastern United States Seismic Source Characterization for Nuclear Facilities (CEUS SSC) Project was conducted over the period from April 2008 to December 2011 to provide a regional seismic source model for use in probabilistic seismic hazard analyses (PSHAs) for nuclear facilities. The study replaces previous regional seismic source models conducted for this purpose, including the Electric Power Research Institute–Seismicity Owners Group (EPRI-SOG) model (EPRI, 1988, 1989) and the Lawrence Livermore National Laboratory model (Bernreuter et al., 1989). Unlike the previous studies, the CEUS SSC Project was sponsored by multiple stakeholders—namely, the EPRI Advanced Nuclear Technology Program, the Office of Nuclear Energy and the Office of the Chief of Nuclear Safety of the U.S. Department of Energy (DOE), and the Office of Nuclear Regulatory Research of the Nuclear Regulatory Commission (NRC). The study was conducted using Senior Seismic Hazard Analysis Committee (SSHAC) Study Level 3 methodology to provide high levels of confidence that the data, models, and methods of the larger technical community have been considered and the center, body, and range of technically defensible interpretations have been included.

The regional seismic source characterization (SSC) model defined by this study can be used for site-specific PSHAs, provided that appropriate site-specific assessments are conducted as required by current regulations and regulatory guidance for the nuclear facility of interest. This model has been designed to be compatible with current and anticipated ground-motion characterization (GMC) models. The current recommended ground-motion models for use at nuclear facilities are those developed by EPRI (2004, 2006a, 2006b). The ongoing Next Generation Attenuation–East (NGA-East) project being supported by the NRC, DOE, and EPRI will provide ground-motion models that are appropriate for use with the CEUS SSC model. The methodology for a SSHAC Level 3 project as applied to the CEUS SSC Project is explained in the SSHAC report (Budnitz et al., 1997), which was written to discuss the evolution of expert assessment methodologies conducted during the previous three decades for purposes of probabilistic risk analyses. The methodological guidance provided in the SSHAC report was intended to build on the lessons learned from those previous studies and, specifically, to arrive at processes that would make it possible to avoid the issues encountered by the previous studies (NRC, 2011).

The SSHAC assessment process, which differs only slightly for Level 3 and 4 studies, is a technical process accepted in the NRC's seismic regulatory guidance (Regulatory Guide 1.208) for ensuring that uncertainties in data and scientific knowledge have been properly represented in seismic design ground motions consistent with the requirements of the seismic regulation 10 CFR Part 100.23 ("Geologic and Seismic Siting Criteria"). Therefore, the goal of the SSHAC assessment process is the proper and complete representation of knowledge and uncertainties in the SSC and GMC inputs to the PSHA (or similar hazard analysis). As discussed extensively in the SSHAC report (Budnitz et al., 1997) and affirmed in NRC (2011), a SSHAC assessment process consists of two important sequential activities, *evaluation* and *integration.* For a Level 3 assessment, these activities are conducted by the Technical Integration (TI) Team under the leadership of the TI Lead. As described in NRC (2011),

> The fundamental goal of a SSHAC process is to carry out properly and document completely the activities of evaluation and integration, defined as:
>
>> *Evaluation:* The consideration of the complete set of data, models, and methods proposed by the larger technical community that are relevant to the hazard analysis.
>>
>> *Integration:* Representing the center, body, and range of technically defensible interpretations in light of the evaluation process (i.e., informed by the assessment of existing data, models, and methods).

Each of the assessment and model-building activities of the CEUS SSC Project is associated with the evaluation and integration steps in a SSHAC Level 3 process. Consistent with the requirements of a SSHAC process, the specific roles and responsibilities of all project participants were defined in the Project Plan, and adherence to those roles was the responsibility of the TI Lead and the Project Manager. The technical assessments are made by the TI Team, who carry the principal responsibility of evaluation and integration, under the technical leadership of the TI Lead. The Database Manager and other technical support individuals assist in the development of work products. Resource and proponent experts participate by presenting their data, models, and interpretations at workshops and through technical interchange with the TI Team throughout the project. The Participatory Peer Review Panel (PPRP) is responsible for a continuous review of both the SSHAC process being followed and the technical assessments being made. The project management structure is headed by the Project Manager, who serves as the liason with the sponsors and the PPRP and manages the activities of all participants. The SSHAC Level 3 assessment process and implementation is discussed in depth in Chapter 2 of this report.

Each of the methodology steps in the SSHAC guidelines (Budnitz, 1997) was addressed adequately during the CEUS SSC Project. Furthermore, the project developed a number of enhancements to the process steps for conducting a SSHAC Study Level 3 project. For example, the SSHAC guidelines call for process steps that include developing a preliminary assessment model, calculating hazard using that model in order to identify the key issues, and finalizing the model in light of the feedback provided from the hazard calculations and sensitivity analyses. Because of the regional nature of the project and the multitude of assessments required, four rounds of model-building and three rounds of feedback were conducted. These activities ensured that all significant issues and uncertainties were identified and that the appropriate effort was devoted to the issues of most significance to the hazard results. A comparison of the activities conducted during the CEUS SSC Project with those recommended in the SSHAC guidelines themselves (Section 2.6) led to the conclusion that the current standards of practice have been met for a SSHAC Study Level 3 process—both those that are documented in the SSHAC report and those that resulted from precedents set by projects conducted since the SSHAC report was issued.

The catalog of past earthquakes that have occurred in a region is an important source of information for the quantification of future seismic hazards. This is particularly true in stable continental regions (SCRs) such as the CEUS where the causative mechanisms and structures for the occurrence of damaging earthquakes are generally poorly understood, and the rates of crustal deformation are low such that surface and near-surface indications of stresses in the crust and the buildup and release of crustal strains are difficult to quantify. Because the earthquake catalog is used in the characterization of the occurrence of future earthquakes in the CEUS, developing an updated earthquake catalog for the study region was an important focus of the CEUS SSC Project. The specific goals for earthquake catalog development and methods used to attain those goals are given in Chapter 3.

The earthquake catalog development consists of four main steps: catalog compilation, assessment of a uniform size measure to apply to each earthquake, identification of dependent earthquakes (catalog declustering), and assessment of the completeness of the catalog as a function of location, time, and earthquake size. An important part of the catalog development process was review by seismologists with extensive knowledge and experience in catalog compilation. The result is an earthquake catalog covering the entire study region for the period from 1568 through the end of 2008. Earthquake size is defined in terms of the moment magnitude scale (Hanks and Kanamori, 1979), consistent with the magnitude scale used in modern ground-motion prediction equations (GMPEs) for CEUS earthquakes. A significant contribution of the CEUS SSC Project is the work conducted to develop an updated and consistent set of conversion relationships between various earthquake size measures (instrumental magnitudes and intensity) and moment magnitude.

The conceptual SSC framework described in Chapter 4 was developed early in the CEUS SSC Project in order to provide a consistent approach and philosophy to SSC by the TI Team. This framework provides the basic underpinnings of the SSC model developed for the project, and it led to the basic structure and elements of the master logic tree developed for the SSC model. In considering the purpose of the CEUS SSC Project, the TI Team identified three attributes that are needed for a conceptual SSC framework:

1. A systematic, documented approach to treating alternatives using logic trees, including alternative conceptual models for future spatial distributions of seismicity (e.g., stationarity); alternative methods for expressing the future temporal distribution of seismicity (e.g., renewal models, Poisson models); and alternative data sets for characterizing seismic sources (e.g., paleoseismic data, historical seismicity data).
2. A systematic approach to identifying applicable data for the source characterization, evaluating the usefulness of the data, and documenting the consideration given to the data by the TI Team.
3. A methodology for identifying seismic sources based on defensible criteria for defining a seismic source, incorporating the lessons learned in SSC over the past two decades, and identifying the range of approaches and models that can be shown to be significant to hazard.

Each of these needs was addressed by the methodology used in the project. For example, the need for a systematic approach to identifying and evaluating the data and information that underlie the source characterization assessments was met by the development of Data Summary and Data Evaluation tables. These tables were developed for each seismic source to document the information available at the time of the CEUS SSC assessments (the Data Summary tables) and the way those data were used in the characterization process (the Data Evaluation tables). Given the evolution of approaches to identifying seismic sources, it is appropriate to provide a set of criteria and the logic for their application in the CEUS SSC Project. In the project, unique seismic sources are defined to account for distinct differences in the following criteria:

- Earthquake recurrence rate
- Maximum earthquake magnitude (Mmax)
- Expected future earthquake characteristics (e.g., style of faulting, rupture orientation, depth distribution)
- Probability of activity of tectonic feature(s)

Rather than treat these criteria as operating simultaneously or without priority, the CEUS SSC methodology works through them sequentially. Further, because each criterion adds complexity to the seismic source model, it is applied only if its application would lead to hazard-significant changes in the model. In this way, the model becomes only as complex as required by the available data and information.

The CEUS SSC master logic tree is tied to the conceptual SSC framework that establishes the context for the entire seismic source model. The master logic tree depicts the alternative interpretations and conceptual models that represent the range of defensible interpretations, and the relative weights assessed for the alternatives. By laying out the alternatives initially, the subsequent detailed source evaluations were conducted within a framework that ensures consistency across the sources. Important elements of the master logic tree are as follows:

- Representation of the sources defined based on paleoseismic evidence for the occurrence of repeated large-magnitude earthquakes (RLMEs, defined as two or more earthquakes with $\mathbf{M} \geq 6.5$).
- Alternatives to the spatial distribution of earthquakes based on differences in maximum magnitudes (Mmax zones approach).
- Representation of uncertainty in spatial stationarity of observed seismicity based on smoothing of recurrence parameters.
- Representation of possible differences in future earthquake characteristics (e.g., style, seismogenic thickness, and orientation of ruptures), which lead to definition of seismotectonic zones in the logic tree (seismotectonic zones approach).

The methodologies used by the project to make the SSC assessments are discussed in Chapter 5. The heart of any SSC model for PSHA is a description of the future spatial and temporal distribution of earthquakes. Continued analysis of the historical seismicity record and network monitoring by regional and local seismic networks has led to acceptance within the community that the general spatial patterns of observed small- to moderate-magnitude earthquakes provide predictive information about the spatial distribution of future large-magnitude earthquakes. The analyses leading to this conclusion have focused on whether the observed patterns of earthquakes have varied through time; therefore, in effect, this is an assessment of uncertainty in whether small- to moderate-magnitude earthquakes have been relatively stationary through time. However, the available data on larger-magnitude earthquakes and their relationship to the spatial distribution of smaller earthquakes based on the observed record are quite limited. These data are not sufficient to allow confidence in the predictions generated by empirical spatial models. For this reason, geologic and geophysical data are needed to specify the locations of future earthquakes in addition to the observed patterns of seismicity.

Detailed studies in the vicinity of large historical and instrumental earthquakes, and liquefaction phenomena associated with them, coupled with field and laboratory studies of geotechnical properties, are leading to a stronger technical basis for (1) placing limits on the locations of paleoearthquakes interpreted by the distribution of liquefaction phenomena and (2) defining their magnitudes. In some cases, the paleoseismic evidence for RLMEs is compelling, and the TI Team has included the RLME source in the SSC model. The locations of RLME sources notwithstanding, the spatial distribution of distributed seismicity sources has advanced in PSHA largely because of the assumption of spatial stationarity, and the SSC and hazard community uses approaches to "smooth" observed seismicity to provide a map that expresses the future spatial pattern of recurrence rates. The CEUS SSC model is based largely on the assumption, typical in PSHA studies, that spatial stationarity of seismicity is expected to persist for a period of approximately 50 years.

Estimating Mmax in SCRs such as the CEUS is highly uncertain despite considerable interest and effort by the scientific community over the past few decades. Mmax is defined as the upper truncation point of the earthquake recurrence curve for individual seismic sources, and the typically broad distribution of Mmax for any given source reflects considerable epistemic uncertainty. Because the maximum magnitude for any given seismic source in the CEUS occurs rarely relative to the period of observation, the use of the historical seismicity record provides important but limited constraints on the magnitude of the maximum event. Because of the independent constraints on earthquake size, those limited constraints are used to estimate the magnitudes of RLME. For distributed seismicity source zones, two approaches are used to assess Mmax: the Bayesian approach and the Kijko approach. In the Bayesian procedure (Johnston et al., 1994), the prior distribution is based on the magnitudes of earthquakes that occurred worldwide within tectonically analogous regions. As part of the CEUS SSC Project, the TI Team pursued the refinement and application of the Bayesian Mmax approach becauses it provides a quantitative and repeatable process for assessing Mmax.

The TI Team also explored alternative approaches for the assessment of Mmax that provide quantitative and repeatable results, and the team identified the approach developed by Kijko (2004) as a viable alternative. While the Kijko approach requires fewer assumptions than the Bayesian approach in that it uses only the observed earthquake statistics for the source, this is offset by the need for a relatively larger data sample in order to get meaningful results. Both approaches have the positive attribute that they are repeatable given the same data and they can be readily updated given new information. The relative weighting of the two approaches for inclusion in the logic tree is source-specific, a function of the numbers of earthquakes that are present within the source upon which to base the Mmax assessment: sources with fewer earthquakes are assessed to have little or no weight for the Kijko approach, while those with larger numbers of events are assessed higher weight for the Kijko approach. In all cases, because of the stability of the Bayesian approach and the preference for "analogue" approaches within the larger technical community, the Bayesian approach is assessed higher weight than the Kijko approach for all sources.

A major effort was devoted to updating the global set of SCR earthquakes and to assessing statistically significant attributes of those earthquakes following the approach given in Johnston et al. (1994). In doing so, it was found that the only significant attribute defining the prior distribution is the presence or absence of Mesozoic-or-younger extension. The uncertainty in this assessment is reflected in the use of two alternative priors: one that takes into account the presence or absence of crustal domains having this attribute, and another that combines the entire CEUS region as a single SCR crustal domain with a single prior distribution. The use of the Bayesian—and Kijko—approach requires a definition of the largest observed magnitude within each source, and this assessment, along with the associated uncertainty, was incorporated into the Mmax distributions for each seismic source. Consideration of global analogues led to the assessment of an upper truncation to all Mmax distributions at 8¼ and a lower truncation at 5½. The broad distributions of Mmax for the various seismic source zones reflect the current epistemic uncertainty in the largest earthquake magnitude within each seismic source.

The CEUS SSC model is based to a large extent on an assessment that spatial stationarity of seismicity will persist for time periods of interest for PSHA (approximately the next 50 years). Stationarity in this sense does not mean that future locations and magnitudes of earthquakes will occur exactly where they have occurred in the historical and instrumental record. Rather, the degree of spatial stationarity varies as a function of the type of data available to define the seismic source. RLME sources are based largely on paleoseismic evidence for repeated large-magnitude ($M \geq 6.5$) earthquakes that occur in approximately the same location over periods of a few thousand years. On the other hand, patterns of seismicity away from the RLME sources within the Mmax and seismotectonic zones are defined from generally small- to moderate-magnitude earthquakes that have occurred during a relatively short (i.e., relative to the repeat times of large events) historical and instrumental record. Thus, the locations of future events are not as tightly constrained by the locations of past events as for RLME sources. The spatial smoothing operation is based on calculations of earthquake recurrence within one-quarter-degree or half-degree cells, with allowance for "communication" between the cells. Both *a*- and *b*-values are allowed to vary, but the degree of variation has been optimized such that *b*-values vary little across the study region.

The approach used to smooth recurrence parameters is a refinement of the penalized-likelihood approach used in EPRI-SOG (EPRI, 1988), but it is designed to include a number of elements that make the formulation more robust, realistic, and flexible. These elements include the reformulation in terms of magnitude bins, the introduction of magnitude-dependent weights, catalog incompleteness, the effect of Mmax, spatial variation of parameters within the source zone, and the prior distributions of *b*. A key assessment made by the TI Team was the weight assigned to various magnitude bins in the assessment of smoothing parameters (Cases A, B, and E). This assessment represents the uncertainty in the interpretation that smaller magnitudes define the future locations and variation in recurrence parameters. Appropriately, the penalized-likelihood approach results in higher spatial variation (less smoothing) when the low-magnitude bins are included with high weight, and much less variation (higher smoothing) in the case where the lower-magnitude bins are given low or zero weight. The variation resulting from the final set of weights reflects the TI Team's assessment of the epistemic uncertainty in the spatial variation of recurrence parameters throughout the SSC model.

The earthquake recurrence models for the RLME sources are somewhat simpler than those for distributed seismicity sources because the magnitude range for individual RLMEs is relatively narrow and their spatial distribution is limited geographically such that spatial variability is not a concern. This limits the problem to one of estimating the occurrence rate in time of a point process. The data that are used to assess the occurrence rates are derived primarily from paleoseismic studies and consist of two types: data that provide estimated ages of the paleoearthquakes such that the times between earthquakes can be estimated, and data that provide an estimate of the number of earthquakes that have occurred after the age of a particular stratigraphic horizon. These data are used to derive estimates of the RLME occurrence rates and their uncertainty.

The estimation of the RLME occurrence rates is dependent on the probability model assumed for the temporal occurrence of these earthquakes. The standard model applied for most RLME sources in this study is the Poisson model, in which the probability of occurrence of an RLME in a specified time period is completely characterized by a single parameter, λ, the rate of RLME occurrence. The Poisson process is "memoryless"—that is, the probability of occurrence in the next time interval is independent of when the most recent earthquake occurred, and the time between earthquakes is exponentially distributed with a standard deviation equal to the mean time between earthquakes. For two RLME sources (Reelfoot Rift–New Madrid fault system and the Charleston source), the data are sufficient to suggest that the occurrence of RLMEs is more periodic in nature (the standard deviation is less than the mean time between earthquakes). For these RLME sources a simple renewal model can also be used to assess the probability of earthquake occurrence. In making an estimate of the probability of occurrence in the future, this model takes into account the time that has elapsed since the most recent RLME occurrence.

The CEUS SSC model has been developed for use in future PSHAs. To make this future use possible, the SSC model must be combined with a GMC model. At present, the GMPEs in use for SCRs such as the CEUS include limited information regarding the characteristics of future earthquakes. In anticipation of the possible future development of GMPEs for the CEUS that will make it possible to incorporate similar types of information, a number of characteristics of future earthquakes in the CEUS are assessed. In addition to characteristics that might be important for ground motion assessments, there are also assessed characteristics that are potentially important to the modeling conducted for hazard analysis. Future earthquake characteristics assessed include the tectonic stress regime, sense of slip/style of faulting, strike and dip of ruptures, seismogenic crustal thickness, fault rupture area versus magnitude relationship, rupture length-to-width aspect ratio, and relationship of ruptures to source boundaries.

Chapters 6 and 7 include discussions of the seismic sources that are defined by the Mmax zones and the seismotectonic zones branches of the master logic tree. Because of convincing evidence for their existence, both approaches include RLME sources. The rarity of repeated earthquakes relative to the period of historical observation means that evidence for repeated events comes largely from the paleoseismic record. By identifying the RLMEs and including them in the SSC model, there is no implication that the set of RLMEs included is in fact the total set of RLMEs that might exist throughout the study region. This is because the presently available studies that locate and characterize the RLMEs have been concentrated in certain locations and are not systematic across the entire study region. Therefore, the evidence for the existence of the RLMEs is included in the model where it exists, but the remaining parts of the study region are also assessed to have significant earthquake potential, which is evidenced by the inclusion of moderate-to-large magnitudes in the Mmax distributions for every Mmax zone or seismotectonic zone.

In Chapter 6, each RLME source is described in detail by the following factors: (1) evidence for temporal clustering, (2) geometry and style of faulting, (3) RLME magnitude, and (4) RLME recurrence. The descriptions document how the data have been evaluated and assessed to arrive at the various elements of the final SSC model, including all expressions of uncertainty. The Data Summary and Data Evaluation tables (Appendices C and D) complement the discussions in the text, documenting all the data that were considered in the course of data evaluation and integration process for each particular seismic source.

Alternative models for the distributed seismicity zones that serve as background zones to the RLME sources are either Mmax zones or seismotectonic zones. The Mmax zones are described in Chapter 6 and are defined according to constraints on the prior distributions for the Bayesian approach to estimating Mmax. The seismotectonic zones are described in Chapter 7 and are identified based on potential differences in Mmax as well as future earthquake characteristics. Each seismotectonic zone in the CEUS SSC model is described according to the following attributes: (1) background information from various data sets; (2) bases for defining the seismotectonic zone; (3) basis for the source geometry; (4) basis for the zone Mmax (e.g., largest observed earthquake); and (5) future earthquake characteristics. Uncertainties in the seismotectonic zone characteristics are described and are represented in the logic trees developed for each source.

For purposes of demonstrating the CEUS SSC model, seismic hazard calculations were conducted at seven demonstration sites throughout the study region, as described in Chapter 8. The site locations were selected to span a range of seismic source types and levels of seismicity. The results from the seismic hazard calculations are intended for scientific use to demonstrate the model, and they should not be used for engineering design. Mean hazard results are given for a range of spectral frequencies (PGA, 10 Hz, and 1 Hz) and for a range of site conditions. All calculations were made using the EPRI (2004, 2006) ground-motion models such that results could be compared to understand the SSC effects alone. Sensitivity analyses were conducted to provide insight into the dominant seismic sources and the important characteristics of the dominant seismic source at each site. The calculated mean hazard results are compared with the results using the SSC model from the 2008 U.S. Geological Survey national seismic hazard maps and the SSC model from the Combined Operating License applications for new nuclear power reactors. The hazard results using the CEUS SSC model given in Chapter 8 are reasonable and readily understood relative to the results from other studies, and sensitivities of the calculated hazard results can be readily explained by different aspects of the new model. The TI Team concludes that the SSC model provides reasonable and explainable calculated seismic hazard results, and the most important aspects of the SSC model to the calculated hazard (e.g., recurrence rates of RLME sources, recurrence parameters for distributed seismicity sources, Mmax) and their uncertainties have all been appropriately addressed.

Presumably, the GMC model input to the PSHA calculations will be replaced in the future by the results of the ongoing NGA-East project. The calculated hazard at the demonstration sites in Chapter 8 comes from the regional CEUS SSC model and does not include any local refinements that might be necessary to account for local seismic sources. Depending on the regulatory guidance that is applicable for the facility of interest, additional site-specific studies may be required to provide local refinements to the model.

To assist future users of the CEUS SSC model, Chapter 9 presents a discussion on the use of the model for PSHA. The basic elements of the model necessary for hazard calculations are given in the Hazard Input Document (HID). This document provides all necessary parameter values and probability distributions for use in a modern PSHA computer code. The HID does not, however, provide any justification for the values, since that information is given in the text of this report.

Chapter 9 also describes several simplifications to seismic sources that can be made to increase efficiency in seismic hazard calculations. These simplifications are recommended on the basis of sensitivity studies of alternative hazard curves that represent a range of assumptions on a parameter’s value. Sensitivities are presented using the test sites in this study. For applications of the seismic sources from this study, similar sensitivity studies should be conducted for the particular site of interest to confirm these results and to identify additional simplifications that might be appropriate. For the seismic sources presented, only those parameters that can be simplified are discussed and presented graphically. The sensitivity studies consisted of determining the sensitivity of hazard to logic tree branches for each node of the logic tree describing that source. The purpose was to determine which nodes of the logic tree could be collapsed to a single branch in order to achieve more efficient hazard calculations without compromising the accuracy of overall hazard results.

Finally, this report provides a discussion of the level of precision that is associated with seismic hazard estimates in the CEUS. This discussion addresses how seismic hazard estimates might change if the analysis were repeated by independent experts having access to the same basic information (geology, tectonics, seismicity, ground-motion equations, site characterization). It also addresses how to determine whether the difference in hazard would be significant if this basic information were to change and that change resulted in a difference in the assessed seismic hazard. This analysis was performed knowing that future data and models will continue to be developed and that a mechanism for evaluating the significance of that information is needed. Based on the precision model evaluated, if an alternative assumption or parameter is used in a seismic hazard study, and it potentially changes the calculated hazard (annual frequency of exceedence) by less than 25 percent for ground motions with hazards in the range 10^{-4} to 10^{-6}, that potential change is within the level of precision at which one can calculate seismic hazard. It should be noted, however, that a certain level of precision does not relieve users from performing site-specific studies to identify potential capable seismic sources within the site region and vicinity as well as to identify newer models and data. Also, this level of precision does not relieve users from fixing any errors that are discovered in the CEUS SSC model as it is implemented for siting critical facilities. In addition, NRC has not defined a set value for requiring or not requiring siting applicants to revise or update PSHAs.

Included in the report are appendices that summarize key data sets and analyses: the earthquake catalog, the Data Summary and Data Evaluation tables, the paleoliquefaction database, the HID, and documentation important to the SSHAC process. These data and analyses will assist future users of the CEUS SSC model in the implementation of the model for purposes of PSHA. The entire report and database will be provided on a website after the Final Project Report is issued.

The TI Team, Project Manager, and Sponsors determined the approach for quality assurance on the CEUS SSC Project in 2008, taking into account the SSHAC assessment process and national standards. The approach was documented in the CEUS SSC Project Plan dated June 2008 and discussed in more detail in the CEUS SSC Report (Appendix L). Beyond the assurance of quality arising from the external scientific review process, it is the collective, informed judgment of the TI Team (via the process of evaluation and integration) and the concurrence of the PPRP (via the participatory peer review process), as well as adherence to the national standard referred to in Appendix L, that ultimately lead to the assurance of quality in the process followed and in the products that resulted from the SSHAC hazard assessment framework.

October 24, 2011

Cliff Munson
Senior Technical Advisor
Office of New Reactors
U.S. Nuclear Regulatory Commission
Washington, DC 20555

Robert Roche
Project Manager
Office of Nuclear Regulatory Research
U.S. Nuclear Regulatory Commission
Washington, DC 20555

Richard H. Lagdon, Jr.
Chief of Nuclear Safety
Office of the Under Secretary for Nuclear Security, S-5
U.S. Department of Energy
1000 Independence Avenue SW
Washington, DC 20585

Thomas P. Miller
Senior Technical Advisor
Office of Nuclear Energy, NE-72/GTN
U.S. Department of Energy
1000 Independence Avenue SW
Washington, DC 20585

Jeffrey F. Hamel
Advanced Nuclear Technology Program Manager
Electric Power Research Institute
3420 Hillview Avenue
Palo Alto, CA 94304

Gentlemen:

Reference: *Central and Eastern United States Seismic Source Characterization for Nuclear Facilities Project:* Participatory Peer Review Panel Final Report

Introduction

This letter constitutes the final report of the PPRP[1] ("the Panel") for the *Central and Eastern United States Seismic Source Characterization for Nuclear Facilities Project* (the "CEUS SSC Project" or "the Project"). The eight Panel members (Jon P. Ake, Walter J. Arabasz, William J. Hinze, Annie M. Kammerer, Jeffrey K. Kimball, Donald P. Moore, Mark D. Petersen, J. Carl Stepp) participated in the Project in a manner fully consistent with the SSHAC Guidance.[2] The Panel was actively engaged in all phases and activities of the Project's implementation, including final development of the Project Plan and planning of the evaluation and integration activities, which are the core of the SSHAC assessment process.

[1] Participatory Peer Review Panel

[2] Budnitz, R. J., G. Apostolakis, D. M. Boore, L. S. Cluff, K. L. Coppersmith, C. A. Cornell, and P. A. Morris, 1997. *Recommendations for Probabilistic Seismic Hazard Analysis: Guidance on Uncertainty and the Use of Experts* (known as the "Senior Seismic Hazard Analysis Committee Report," or the "SSHAC Guidance"). NUREG/CR-6372, U. S. Nuclear Regulatory Commission. TIC; 235076. Washington, DC.

The Panel's involvement, described more fully later in this letter, also included review of analyses performed by the Project to support the evaluation and integration processes, review of interim evaluation and integration products, and review of the interim draft project report and the final project report. Additionally, panel members participated in specific analyses as resource experts, and panel members were observers in or participated as resource experts in eight of the eleven Technical Integrator Team (TI Team) working meetings held to implement the integration phase of the assessment process. We want to express our appreciation for the opportunity to participate in the CEUS SSC Project in this way.

In the remainder of this letter we provide our observations and conclusions on key elements of the project implementation process, and we summarize our reviews of the draft and final project reports. As we explain in our comments, assurance that the center, body, and range of the technically-defensible interpretations ("CBR of the TDI")[3] have been properly represented in the CEUS SSC Model fundamentally comes from implementing the structure and rigor of the SSHAC Guidance itself. We are aware that the SSHAC Guidance is accepted by the Nuclear Regulatory Commission and the Department of Energy for developing seismic hazard models that provide reasonable assurance, consistent with the seismic safety decision-making practices of these agencies, of compliance with their seismic safety policies and regulatory requirements. For these reasons, we describe aspects of the SSHAC Guidance to provide context for our observations and conclusions.

Project Plan: Conformity to the SSHAC Assessment Process

The SSHAC Guidance recognizes that observed data, available methods, models, and interpretations all contain uncertainties. These uncertainties lead to alternative scientific analyses and interpretations. In other words, experts in the broad technical community do not hold a single interpretation. Accepting this scientific situation, the SSHAC assessment process is designed to engage the scientific community in an orderly assessment of relevant data, methods, models, and interpretations that constitute current scientific knowledge as the basis for development of a seismic hazard model that represents the CBR of the TDI.

The assessment process is carried out by means of two main activities: *evaluation* and *integration*.[4] In implementation, the evaluation activities are structured to inform the integration activities. The evaluations are carried out by means of workshops in which the TI Team engages proponents of alternative interpretations that represent the range of relevant current community knowledge. Resource experts in the various relevant data sets are also engaged. The workshops have the dual purposes of, first, evaluating the degree to which alternative interpretations are supported by observed data and, second, defining uncertainties in the degree to which the interpretations are defensible, given the observed data. Integration is carried out by individual evaluator experts or evaluator expert teams (Level 4 process) or by a Technical Integrator (TI) Team (Level 3 process) who, informed by the evaluation activities, characterize the range of

---

[3] See Section 2.1 in the CEUS SSC Final Report for discussion of concepts relating to the center, body, and range of the "technically-defensible interpretations" vs. the center, body, and range of the "informed technical community."

[4] For an excellent discussion of this two-stage process, see *Practical Implementation Guidelines for SSHAC Level 3 and 4 Hazard Studies*, USNRC NUREG-XXXX, Draft for Review, Office of Nuclear Regulatory Research, May 2011.

defensible alternative interpretations in an integrated hazard model and assess the scientific uncertainty distribution. Based on our review of the Project Plan and our subsequent discussions with the Project Team, we concurred that the Plan conformed with the SSHAC Guidance, incorporating lessons learned from fourteen years experience using the Guidance, and that the planned implementation was structured to properly carry out the SSHAC assessment process for development of the CEUS SSC Model.

SSHAC Level 3 Assessment Process

The SSHAC Guidance describes implementation processes for four levels of assessment depending on the scientific complexity of the assessment and the intended use of the assessed hazard model. For an assessment such as the regional SSC model for the Central and Eastern United States, which will be used at many sites for making safety and licensing decisions for nuclear facilities, the SSHAC Guidance recommends using an assessment Level 3 or Level 4.

There are process differences between a Level 3 and Level 4 implementation, but the objective is the same: to obtain from multiple proponent experts information that supports an informed assessment of the range of existent relevant interpretations and associated uncertainties that together represent current community knowledge and to perform an informed assessment of the CBR of the TDI. We understand that within the SSHAC assessment process "technically defensible" means that observed data are sufficient to support evaluation of the interpretation and the corresponding uncertainty.

In a Level 4 assessment process a TI Team facilitates the assessment, identifying and engaging proponent and resource experts, performing supporting analyses, and conducting knowledge evaluation workshops and assessment integration working meetings. Multiple experts or teams of experts perform as evaluators of the range of existent interpretations and as integrators of the hazard model. The individual evaluator experts or evaluator expert teams take ownership of their individual or team assessments. In a Level 3 assessment all of these activities are consolidated under a single TI Team consisting of a TI Lead, multiple evaluator experts representing the scope of required scientific expertise, and experienced data and hazard analysts.

As we noted earlier in this report, assurance that the CBR of the TDI is properly represented in a hazard model comes from rigorously implementing the SSHAC assessment process itself. We note that an important lesson learned from multiple implementations of the SSHAC Guidance over the past fourteen years is that the Level 3 and Level 4 assessment processes provide comparably high assurance that the relevant scientific knowledge and the community uncertainty distribution are properly assessed and represented in the hazard model. The Level 3 assessment is significantly more integrated and cohesive and is more efficient to implement. These considerations led us to endorse use of the Level 3 assessment for implementation of the CEUS SSC Project in our Workshop No. 1 review letter. During the course of the Project we observed that the higher level of cohesiveness inherent in the Level 3 assessment process leads to significantly improved communication, facilitating the experts' performance of their technical work.

Overall Project Organization

A complex project with multiple sponsors such as the CEUS SSC Project cannot be successful unless it is well organized and energetically managed so that the various participants understand the interconnectedness of their activities and perform their technical work as a cohesive group. In this regard the adopted project management structure allowed the Project Manager to provide integrated overall project leadership, manage the database development activities, and effectively maintain communication with the PPRP and project sponsors while allowing TI Team lead to concentrate on the structural and technical activities of the assessment as the Project unfolded. <u>We conclude that the project organization was effective overall and particularly so with regard to facilitating the TI Team's implementation of the assessment process.</u>

Implementing the SSHAC Level 3 Assessment Process

Irrespective of the level of implementation, evaluation and integration are the main activities of a SSHAC assessment. The evaluation activities aim to identify and evaluate all relevant available data, models, methods, and scientific interpretations as well as uncertainties associated with each of them. The integration activities, informed by the evaluations, aim to represent the CBR of the TDI in a fully integrated SSC model.

Evaluation

Consistent with the SSHAC Guidance the evaluation phase of the CEUS SSC project accomplished a comprehensive evaluation of the data, models, methods, and scientific interpretations existent in the larger technical community that are relevant to the SSC model. In significant part the process was carried out in three structured workshops, each focusing on accomplishing a specific step in the evaluation process.

The first workshop (WS-1) focused on evaluations of relevant geological, geophysical, and seismological datasets (including data quality and uncertainties) and on identification of hazard-significant data and hazard-significant SSC assessment issues. It became clear that a number of issues relating to the earthquake catalog, the paleoliquefaction data set, the potential-field geophysical data, updating procedures for assessing maximum earthquake magnitude, and development of procedures for assessing earthquake recurrence would require focused analyses. These analyses were appropriately carried out within the TI Team working interactively with appropriate resource experts recognized by the larger scientific and technical community.

WS-2 focused on evaluations of the range of alternative scientific interpretations, methods, and models within the larger scientific community and on corresponding uncertainties. WS-3 focused on evaluations of hazard feedback derived at seven representative test locations using a preliminary CEUS SSC model. Specifically, the workshop focused on the identification of the key issues of most significance to completing the SSC model assessment.

Experience has shown that evaluations to gain understanding of the quality of various data sets and uncertainties associated with them are essential for fully informing an SSC assessment. We observed that in WS-1 resource experts for the various data sets did a high-quality job of describing the data sets and giving their perspective about the data quality and associated uncertainties. <u>We conclude that the understanding of data quality and uncertainties gained in WS-1 together with continued interactions between the TI Team and data resource experts</u>

significantly informed the TI Team's evaluations. The TI Team's evaluations of the data quality and uncertainties are well documented in the innovative "Data Summary Tables" and "Data Evaluation Tables" included in the Project Report. Importantly, the TI Team continued to effectively engage data resource experts in productive analyses of potential-field geophysical data, the earthquake catalog, development of the paleoearthquake data set (including an integrated assessment of the paleoliquefaction data in order to extend the earthquake catalog), the development of methods for assessing maximum earthquakes, and the development of earthquake recurrence analyses. All of these focused analyses strongly informed the assessment process. Moreover, documentation of the analyses resulted in stand-alone products of the Project that will serve future users of the CEUS SSC Model.

The compilation and evaluation of potentially relevant methods, models, and alternative scientific interpretations representing the community knowledge and corresponding uncertainties must be considered the core process activity of any SSHAC assessment. This step was largely carried out in WS-2. Success in defining the community knowledge depends on fully engaging proponent experts representing the range of methods, models, and interpretations existent at the time. Full engagement means that the proponent experts completely and clearly describe their interpretations and the data that support them and provide their individual evaluations of corresponding uncertainties. We observed that the actions taken by the Project and TI Team to explain the workshop goals and to guide participants toward meeting those goals was very productive. We conclude that the workshop was highly successful in meeting the stated goals and that it fully met the expectation of the SSHAC Guidance with respect to evaluating the range of alternative scientific interpretations. The discussions during the workshop and between the TI Team and Panel following the workshop evolved the "SSC Framework" concept, which provided transparent criteria that framed the TI Team's systematic identification and assessment of seismic sources throughout the CEUS.

Feedback from hazard calculations and sensitivity analyses is an important step in a SSHAC assessment to understand the importance of elements of the model and inform the final assessments. For development of a regional SSC model to be used for site-specific probabilistic seismic hazard analyses (PSHAs) at many geographically distributed sites, feedback based on the preliminary model is particularly important. Following WS-2 a preliminary SSC model termed "the SSC sensitivity model," was developed and used for hazard sensitivity calculations that were evaluated in WS-3. While the SSC sensitivity model was clearly preliminary, the evaluation of sensitivity results that took place in WS-3 provided important feedback for completing analyses and for supporting the TI Team's development of the preliminary CEUS SSC model. The Panel was able to review the preliminary model and provide feedback in a subsequent project briefing meeting on March 24, 2010.

Together the three workshops provided the TI Team interactions with the appropriate range of resource and proponent experts. These experts were carefully identified to present, discuss, and debate the data, models, and methods that together form the basis for assuring that the CBR of the TDI have been properly represented in the hazard model. Experts representing academia, government, and private industry participated. The TI Team also reached out to a wide range of experts as they developed the database and performed the integration activities to develop the SSC model. The Panel participated throughout this process, and is satisfied that the TI Team fully engaged appropriate experts to accomplish the goals of a SSHAC Guidance.

Integration

Consistent with the SSHAC Guidance, integration is the process of assessing the CBR of the TDI and representing the assessment in the SSC model. Informed by the evaluation process, the integration process includes representation of the range of defensible methods, models, and interpretations of the larger technical community together with new models and methods developed by analyses during the evaluation and integration process.

For the CEUS SSC Project, development of the earthquake catalog, methods for assessing and representing maximum earthquake magnitudes, and methods for earthquake recurrence assessment continued during the integration process. The Panel reviewed all the analyses at various stages of development and provided comments and recommendations. The TI Team performed the integration process by means of eleven working meetings. Members of the Panel participated in most of these working meetings as observers or resource experts. The full Panel participated in the discussions during both feedback meetings and provided formal comments and recommendations following the meetings. <u>We observed that the integration process was thorough and that it acceptably complied with the SSHAC Guidance. Based on our participation and observations we conclude that the integrated CEUS SSC Model appropriately represents the center, body, and range of current methods, models and technically defensible interpretations.</u>

PPRP Engagement

Consistent with the SSHAC Guidance, the Panel was fully engaged in peer-review interactions with the TI Team and the Project Manager of the CEUS SSC Project throughout the entire project period—from development of the Project Plan in early to mid 2008 through production of the Final Project Report in mid to late 2011.[5] The Panel provided both written and oral peer-review comments on both technical and process aspects at many stages of the Project's evolution. Key PPRP activities, leading up to this final report, have included:

- Review of the Project Plan.
- Formulation of a PPRP implementation plan, specifically for the CEUS SSC Project, to ensure adherence to the general guidance provided by SSHAC and NUREG-1563 for the scope and goals of a PPRP review.
- Involvement in *each* of the three Project workshops, including advising in the planning stage; participating collectively as a review panel during the workshop (and individually as resource experts when requested by the TI Team), providing timely comments on technical and process issues; and submitting a written report of the Panel's observations and recommendations following each workshop.
- Development and implementation of a process, together with the TI Team, to document the resolution of recommendations made in PPRP formal communications.
- Participation as observers (and occasionally as resource experts when requested by the TI Team) in eight of the TI Team's 11 working meetings.
- Peer-review and written comments, including several informal reports, on the TI Team's intermediate work products, particularly early versions of the CEUS SSC Model.

---

[5] See CEUS SSC Final Report: Section 2.5, Table 2.2-1, and Appendix I

- Direct interaction with the TI Team and Project Manager in more than 20 teleconferences and four face-to-face briefings—in addition to the three workshops and eight working meetings of the TI Team noted above.
- Extensive, critical peer-review of the Project's 2010 Draft Report and 2011 Final Report.

The Panel, collectively and individually, fully understood the SSHAC Guidance for a structured participatory peer review and the requirements for a Level 3 assessment process; had full and frequent access to information and interacted extensively with the TI Team and Project Manager throughout the entire project; provided peer-review comments at numerous stages; and, as documented within the Final Project Report, was fully engaged to meet its peer-review obligations in an effective way.

Project Report

The SSHAC Guidance makes clear that adequate documentation of process and results is crucial for their understanding and use by others in the technical community, by later analysis teams, and by the project sponsors. The Panel understood what was needed to conform to the SSHAC requirements, and it was committed to ensuring that the documentation of technical details associated with the CEUS SSC Model in the Project Report was clear and complete. The Panel was equally committed to ensuring the transparency of process aspects of the project, both in implementation and in description in the Project Report.

The Panel provided lengthy compilations of review comments (see Appendix I of the Project Report) for both the 2010 Draft Report and the 2011 Final Report. These included hundreds of comments, categorized as general, specific, relating to clarity and completeness, or editorial. The massive amount of detail provided by the TI Team in the Project Report and the intensiveness of the Panel's review comments both reflect great diligence and a mutual understanding by the TI Team and the PPRP of the thoroughness and high quality of documentation expected in the Project Report.

The Project Manager and the TI Lead provided review criteria to the Panel for both the draft and final versions of the Project Report. The criteria for reviewing the Draft Report[6] covered the range of technical and process issues consistent with requirements of the SSHAC Guidance, including draft implementation guidance (see footnote #4). Key criteria, among others, include sufficiency of explanatory detail; adequate consideration of the full range of data, models, and methods—and the views of the larger technical community; adequate justification of the data evaluation process, logic-tree weights, and other technical decisions; proper treatment of uncertainties; and conformance to a SSHAC Level 3 assessment process. To be clear, the PPRP is charged with judging the adequacy of the documented *justification* for the CEUS SSC Model and its associated logic-tree weights. The TI Team "owns" the Model and logic-tree weights.

Criteria for reviewing the Final Report focused on reaching closure to comments made on the Draft Report and ensuring that no substantive issues remained unresolved. To that end, among its many review comments on the Final Report the Panel identified "mandatory" comments, which the TI Team was required to address in the final version of the Project Report.

[6] See PPRP report dated October 4, 2010, in Appendix I of CEUS SSC Final Report

The Panel made thorough, extensive efforts in its documented reviews of the 2010 Draft Report and the 2011 Final Report (as well as in many related interactions with the TI Team) to ensure a high-quality Project Report that fully meets SSHAC requirements for clear, complete, and transparent documentation of all aspects of the CEUS SSC Project. We are pleased to confirm that implementation of the CEUS SSC Project fully conformed with the SSHAC Guidance and that the resulting CEUS SSC Model properly meets the SSHAC goal of representing the center, body, and range of technically-defensible interpretations.

This concludes our PPRP Final Report for the CEUS SSC Project.

Jon P. Ake	Walter J. Arabasz	William J. Hinze
Annie M. Kammerer	Jeffrey K. Kimball	Donald P. Moore
Mark D. Petersen	J. Carl Stepp	

Copy:
Lawrence A. Salomone
Kevin J. Coppersmith
Brent Gutierrez

PROJECT ACKNOWLEDGMENTS

This study was sponsored by the Electric Power Research Institute (EPRI) Advanced Nuclear Technology Action Plan Committee, the U.S. Department of Energy (DOE) Office of Nuclear Energy and Office of the Chief of Nuclear Safety, and the U.S. Nuclear Regulatory Commission (NRC) Office of Nuclear Regulatory Research. Technical experts from the DOE, NRC, U.S. Geological Survey, Defense Nuclear Facility Safety Board, industry, and academia participated in the study as part of the Technical Integration (TI) Team or as members of the Participatory Peer Review Panel (PPRP). Any statements, opinions, findings, conclusions, or recommendations expressed in this material are those of the authors and do not necessarily reflect those of the participating or sponsoring agencies.

Jeffrey F. Hamel was the EPRI Advanced Nuclear Technology Program Manager. Lawrence A. Salomone of Savannah River Nuclear Solutions, LLC, served as the Project Manager for the study. Kevin J. Coppersmith of Coppersmith Consulting Inc., served as the lead for the TI Team. J. Carl Stepp of Earthquake Hazards Solutions, and Walter J. Arabasz, Research Professor Emeritus of Geology and Geophysics at the University of Utah, served as Co-chairmen for the PPRP. The entire Central and Eastern United States Seismic Source Characterization Project Team and their roles are discussed in Section 2 and are shown on the project oganization chart (Figure 2.3-1) of the report.

The authors of the report wish to acknowledge the contributions of the following people: the resource experts who participated in Workshop 1, the proponent experts who participated in Workshop 2, and the technical experts who provided valuable insights, perspective, and references throughout the study. The names of all these contributors are listed in Table 2.2-2.

In addition, the authors of the report appreciate the support of Geraldine Moore-Butler as administrative assistant and Nancy L. Sutherland as technical editor for the project. This report was assembled at AMEC.

SPONSORS' PERSPECTIVE

This report describes a new seismic source characterization model for the Central and Eastern United States (CEUS) for use in probabilistic seismic hazard analysis (PSHA) for nuclear facilities. PSHA has become a generally accepted procedure for supporting seismic design, seismic safety and decision making for both industry and government. Input to a PSHA consists of seismic source characterization (SSC) and ground motion characterization (GMC); these two components are necessary to calculate probabilistic hazard results (or seismic hazard curves) at a particular geographic location.

The 1986 Electric Power Research Institute and Seismicity Owners Group (EPRI-SOG) study included both an SSC and GMC component. Recent applications for new commercial reactors have followed U.S. Nuclear Regulatory Commission (NRC) regulatory guidance (RG 1.208) by using the EPRI-SOG source model as a starting point and updating it as appropriate on a site-specific basis. This CEUS SSC Project has developed a new SSC model for the CEUS to replace the SSC component of the EPRI-SOG study.

The CEUS SSC Project was conducted using a Senior Seismic Hazard Analysis Committee (SSHAC) Level 3 process, as described in the NRC publication, *Recommendations for Probabilistic Seismic Hazard Analysis: Guidance on Uncertainty and Use of Experts* (NUREG/CR-6372). The goal of the SSHAC process is to represent the center, body, and range of technically defensible interpretations of the available data, models, and methods. The CEUS SSC model is applicable to any site within the CEUS and can be used with the EPRI 2004/2006 GMC model to calculate seismic hazard at any site of interest. Long-term efforts to replace the EPRI 2004/2006 GMC model with the Next Generation Attenuation Relationships for Central and Eastern North America obtained from the NGA-East Project is scheduled for completion in 2014.

The updated CEUS SSC model provides industry and government with the following: a new model for the commercial nuclear industry to perform PSHAs for future reactor license applications; the NRC to support its review of early site permit (ESP) and construction and operating license (COL) applications; and the U.S. Department of Energy (DOE) to support modern PSHAs to meet design and periodic review requirements for its current and future nuclear facilities. Specific benefits of the model are as follows:

- **Consistency:** For many sites, seismic sources at distances up to 300 km (186 mi.) or more significantly contribute to hazard at some spectral frequencies. Consequently, seismic hazard models for many sites have significant geologic overlap. If done separately, there is a likelihood of conflicting assessments for the same regions. A regional source model allows for consistent input into a PSHA. An updated conceptual SSC framework that provides a consistent basis for identifying and characterizing seismic sources in the CEUS has been developed. The NRC will no longer need to review each time each applicant's regional SSC model when the accepted CEUS SSC model is used. This will avoid lengthy review of the regional SSC model in ESP and COL applications for sites within the CEUS that use the accepted regional CEUS SSC model to develop its site-specific SSC model.

- **Stability:** This CEUS SSC model was developed using the accepted state-of-practice SSHAC methodology that involved the following tasks:
  - Development of a comprehensive database and new tools for documenting the data consideration process.
  - Multiple workshops to identify applicable data, debate alternative hypotheses, and discuss feedback.
  - Multiple working meetings by the Technical Integration (TI) Team to develop the SSC model and fully incorporate uncertainties.
  - Technical advancements in a number of areas, such as developing a uniform earthquake catalog, developing an updated approach for assessing maximum magnitude, compiling data evaluation tables, incorporating paleoseismic data, and using spatial smoothing tools.
  - Participatory peer review, including four panel briefings, multiple interactions, and periodic formal feedback.
  - Proper documentation of all process and technical aspects of the project.

  Experience has shown that stability is best achieved through proper and thorough characterization of our knowledge and uncertainties, coupled with the involvement of the technical community, regulators, and oversight groups.

- **Greater Longevity:** An explicit goal of the SSHAC methodology is to represent the center, body, and range of the technically defensible interpretations of the available data, models, and methods. Using the SSHAC process provides reasonable assurance that this goal has been achieved. Representing the center, body, and range of interpretations at the time of the study means that as new information is acquired and various interpretations evolve as a result, the current thinking at any point is more likely to be addressed in the study. As new information becomes available, an existing SSC will require periodic reviews to evaluate the implications of the new findings. The need for updates to a particular study is now better understood as a result of findings of the CEUS SSC Project sensitivity studies to determine the significance of source characteristics.

- **Cost and Schedule Savings:** The CEUS SSC model can be used to perform a PSHA at any geographic location within the CEUS. It is applicable at any point within the CEUS, subject to site-specific refinements required by facility-specific regulations or regulatory guidance. Having stable, consistent input into a regional PSHA will reduce the time and cost required to complete a commercial nuclear site's ESP or COL licensing application, prepare a DOE site's PSHA, and develop design input for new commercial and DOE mission-critical nuclear facilities.

- **Advancement of Science:** The CEUS SSC Project provides new data, models, and methods. This information was shared at three workshops with international observers as a means to provide technology transfer for application in other regions. The CEUS SSC earthquake catalog, which merges and reconciles several catalogs and provides a uniform moment magnitude for all events, and the CEUS SSC paleoliquefaction database provide a new baseline for future research and updates. New approaches used in this project for spatial smoothing of recurrence parameters, assessment of maximum magnitude, and systematical documentation of all data considered and evaluated also benefit future research and PSHA updates.

The sponsors of the CEUS SSC Project are utilities and vendors on the EPRI Advanced Nuclear Technology Action Plan Committee, the DOE Office of Nuclear Energy, the DOE Office of the Chief of Nuclear Safety, and the NRC Office of Nuclear Regulatory Research. Technical experts from the DOE, NRC, U.S. Geological Survey (USGS), and Defense Nuclear Facility Safety Board (DNFSB) participated in the study as part of the TI Team or as members of the Participatory Peer Review Panel (PPRP).

The product of the CEUS SSC Project is a robust peer-reviewed regional CEUS SSC model for use in PSHAs. This model will be applicable to the entire CEUS, providing an important baseline for future research and updates. The CEUS SSC Project demonstrates that a SSHAC Level 3 approach can achieve the goals of considering the knowledge and uncertainties of the larger technical community within a robust and transparent framework. The value of the new CEUS SSC model has been enhanced by the participation of key stakeholders from industry, government, and academia who were part of the CEUS SSC Project Team.

Looking forward, the NRC will publish NUREG-2117 (2012), *Practical Implementation Guidelines for SSHAC Level 3 and 4 Hazard Studies* that provides SSHAC guidance on the need to update a regional model. The guidance covers updating both regional and site-specific assessments. It addresses the "refinement" process of starting with a regional model and refining it for site-specific applications.

ABBREVIATIONS

AD	anno domini (in the year of the Lord)
AFE	annual frequency of exceedance
AIC	Akaike information criterion
ALM	Alabama-Louisiana-Mississippi (zone of possible paleoseismic features)
AM	Atlantic Margin (seismotectonic zone)
AHEX	Atlantic Highly Extended Crust (seismotectonic zone)
ANSS	U.S. Advanced National Seismic System
ANT	Advanced Nuclear Technology
APC	Action Plan Comittee
BA	Blytheville arch
BC	before Christ
BCFZ	Big Creek fault zone
BFZ	Blytheville fault zone
BL	Bootheel lineament
BMA	Brunswick magnetic anomaly
BP	before present
BPT	Brownian passage time
BTP	Branch Technical Position
CAD	computer-aided design

CBR	center, body, and range
CCFZ	Crittenden County fault zone
CDZ	Commerce deformation zone
CENA	Central and Eastern North America
CERI	Center for Earthquake Research and Information
CEUS	Central and Eastern United States
CFZ	Commerce fault zone
CFR	Code of Federal Regulations
CGL	Commerce geophysical lineament
CGRGC	Cottonwood Grove–Rough Creek graben
CI	confidence interval
CNWRA	Center for Nuclear Waste Regulatory Analysis
COCORP	Consortium for Continental Reflection Profiling
COCRUST	Consortium for Crustal Reconnaissance Using Seismic Techniques
COL	combined construction and operating license
COLA	combined operating license application
COMP	composite prior, composite superdomain
CON	contemporary (with earthquake occurrence)
COV	coefficient of variation
CPT	cone penetration test
CVSZ	Central Virginia seismic zone
D&G	Dewey and Gordon (1984 catalog)
DEM	digital elevation model

DNFSB	Defense Nuclear Facilities Safety Board
DOE	U.S. Department of Energy
DWM	Division of Waste Management
ECC	Extended Continental Crust
ECC-AM	Extended Continental Crust–Atlantic Margin (seismotectonic zone)
ECC-GC	Extended Continental Crust–Gulf Coast (seismotectonic zone)
ECFS	East Coast fault system
ECFS-C	East Coast fault system—central segment
ECFS-N	East Coast fault system—northern segment
ECFS-S	East Coast fault system—southern segment
EC-SFS	East Coast–Stafford fault system
ECMA	East Coast magnetic anomaly
ECRB	East Continent rift basin
ECTM	Eastern Canada Telemetered Network
E[**M**]	expected moment magnitude listed in the CEUS SSC catalog for an earthquake
ENA	eastern North America
EP	Eau Plain shear zone
EPRI	Electric Power Research Institute
EPRI-SOG	Electric Power Research Institute–Seismicity Owners Group
ERM	Eastern rift margin
ERM-N	Eastern rift margin—north
ERM-RP	Eastern rift margin—river (fault) picks
ERM-S	Eastern rift margin—south

ERM-SCC	Eastern rift margin—south/Crittenden County
ERM-SRP	Eastern rift margin—south/river (fault) picks
ERRM	Eastern Reelfoot Rift Margin
ESP	early site permit
ESRI	Environmental Systems Research Institute
ETSZ	Eastern Tennessee seismic zone
EUS	Eastern United States
FAFC	Fluorspar Area fault complex
FGDC	Federal Geographic Data Committee
ft	foot or feet
FTP	file transfer protocol
ft/s	feet per second
ft/yr	feet per year
FWLA	Fugro William Lettis & Associates
FWR	Fort Wayne rift
Ga	billion years ago
GC	Gulf Coast
GCVSZ	Giles County, Virginia, seismic zone
GHEX	Gulf Coast Highly Extended Crust (seismotectonic zone)
GIS	geographic information system
GLTZ	Great Lakes tectonic zone
GMC	ground-motion characterization (model)
GMH	Great Meteor Hotspot (seismotectonic zone)

GMPE	ground-motion prediction equation
GMRS	ground-motion response spectra
GPR	ground-penetrating radar
GPS	global positioning system
GSC	Geological Survey of Canada
Gyr	gigayears (10^9 years)
HF	Humboldt fault
HID	hazard input document
I_0	maximum intensity
IAEA	International Atomic Energy Agency
IBEB	Illinois Basin Extended Basement (seismotectonic zone)
IPEEE	Individual Plant Examination for External Events
IRM	Iapetan rifted margin
ISC	International Seismological Centre
ITC	informed technical community
ka	thousand years ago
K-Ar	potassium-argon
km	kilometer(s)
km^2	square kilometer(s)
km/sec	kilometers per second
K-S	Kijko-Sellevoll
K-S-B	Kijko-Sellevoll-Bayes
kyr	thousand years

LDO	Lamont-Doherty Earth Observatory (catalog)
LHS	Latin hypercube sampling
LLNL	Lawrence Livermore National Laboratory
ln(FA)	logarithm of felt area (with felt area measured in km^2)
LS	least squares
LSA	La Salle anticlinal belt
LWLS	locally weighted least squares
m	meter(s)
M	magnitude
M, M_W	moment magnitudes
Ma	million years ago
MAR	Marianna (RLME source)
m_b	body-wave magnitude (short period)
m_{bLg}	body-wave magnitude determined from higher-mode (L_g) surface waves
M_C	coda magnitude
MCMC	Markov Chain Monte Carlo
M_D	duration magnitude
MESE	Mesozoic and younger extended crust
MESE-N	Mesozoic-and-younger extended crust or Mmax zone that is "narrow"
MESE-W	Mesozoic-and-younger extended crust or Mmax zone that is "wide"
mi.	mile(s)
$mi.^2$	square mile(s)
MIDC	midcontinent

MidC	Midcontinent-Craton (seismotectonic zone)
Mfa	felt-area magnitude
M_L	local magnitude
M_{max}, Mmax	maximum magnitude
MMI	modified Mercalli intensity
mm/yr	millimeters per year
M_N	Nuttli magnitude
M_o	Scalar seismic moment
MRS	Midcontinent rift system
m/s	meters per second
M_S	surface-wave magnitude
MSF	Meeman-Shelby fault
M_w	
Myr	million years
NAD83	North American Datum of 1983
NAP	Northern Appalachian (seismotectonic zone)
Nd	neodymium
NEDB	National Earthquake Database
NEI	Nuclear Energy Institute
NEIC	National Earthquake Information Center
NF	Niagara fault zone
NMESE	Non-Mesozoic and younger extended crust
NMESE-N	Mesozoic-and-younger extended crust or Mmax zone that is “narrow”

NMESE-W	Mesozoic-and-younger extended crust or Mmax zone that is “wide”
NMFS	New Madrid fault system
NMN	New Madrid North fault
NMS	New Madrid South fault
NMSZ	New Madrid seismic zone
NN	New Madrid north (fault segment as designated by Johnston and Schweig, 1996)
NOAA	National Oceanic and Atmospheric Administration
NPP	nuclear power plant(s)
NR	Nemaha Ridge
NRC	U.S. Nuclear Regulatory Commission
NRHF	Nemaha Ridge–Humboldt fault
NSHMP	National Seismic Hazard Mapping Project
NW	New Madrid west (fault segment as designated by Johnston and Schweig, 1996)
OKA	Oklahoma aulacogen (seismotectonic zone)
OKO	Oklahoma Geological Survey Leonard Geophysical Observatory (catalog)
OSL	optically stimulated luminescence
P_a	probability of activity (of being seismogenic)
PEZ	Paleozoic Extended Crust (seismotectonic zone)
PGA	peak ground acceleration
PM	Project Manager
PPRP	Participatory Peer Review Panel
PSHA	probabilistic seismic hazard analysis
PVHA	probabilistic volcanic hazard analysis

RCG	Rough Creek graben
RF	Reelfoot fault
RFT	Reelfoot thrust (fault)
RLME	repeated large-magnitude earthquake (source)
RR	Reelfoot rift zone
RS	Reelfoot South (fault segment)
SA	spectral acceleration
SCL	St. Charles lineament
SCML	south-central magnetic lineament
SCR	stable continental region
SCSN	South Carolina Seismic Network
SEUS	Southeastern United States (catalog)
SEUSSN	Southeastern United States Seismic Network
SGFZ	Ste. Genevieve fault zone
SHmax	maximum horizontal stress, compression, or principal stress
SLR	St. Lawrence rift (seismotectonic zone)
SLTZ	Spirit Lake tectonic zone
SLU	Saint Louis University (catalog)
SNM	Sanford et al. (2002 catalog)
SOG	Seismicity Owners Group
SPT	standard penetration test
SRA	Stover, Reagor, and Algermissen (1984 catalog)
SRTM	Shuttle Radar Topography Mission

SSC	seismic source characterization
SSE	safe shutdown earthquake
SSHAC	Senior Seismic Hazard Analysis Committee
Str&Tur	Street and Turcotte (1977 catalog)
SUSN	Southeastern United States Network
TC	technical community
TFI	technical facilitator/integrator
TI	technical integration
USGS	U.S. Geological Survey
USNSN	U.S. National Seismograph Network
UTC	Coordinated Universal Time
V_P/V_S	ratio of P-wave velocity to S-wave velocity
WES	Weston Observatory (catalog)
WIPP	Waste Isolation Pilot Project
WQSZ	Western Quebec seismic zone
WRFZ	White River fault zone
WUS	Western United States
WVFS	Wabash Valley fault system
WVSZ	Wabash Valley seismic zone
WWSSN	World-Wide Standardized Seismograph Network

8
CHAPTER 8
DEMONSTRATION HAZARD CALCULATIONS

8.1 Background on Demonstration Hazard Calculations

Demonstration hazard calculations were made at seven test sites to illustrate the effects that the seismic sources have on calculated seismic hazard, and to compare with hazards from previous CEUS seismic source models. All of these calculations were made for demonstration purposes only and should not be used for design or analysis decisions for any engineered facility.

Seven test sites were selected for demonstration calculations. These are listed in Table 8.1-1, along with the reason for choosing each site. A map of the seven sites is shown on Figure 8.1-1.

Seismic hazard was calculated for hard rock conditions using the ground motion equations from EPRI (2004, 2006). For these equations, hard rock is defined as rock with a shear wave velocity (V_S) of 2,800 m/s (9,200 ft/s). Most of the seismic hazard results presented in this section are for hard rock conditions (labeled "rock" in Section 8.2).

For calculating hazard on hard rock, the EPRI (2004) ground-motion equations were used with the EPRI (2006) aleatory standard deviations. These equations use distance to the surface projection of the rupture ("Joyner Boore distance") and closest distance to the rupture, when the earthquake rupture is defined. When (for seismic hazard calculations) the rupture geometry is unknown and the earthquake is represented as a point, the EPRI (2004) report includes correction terms for the distance measures and for the aleatory standard deviation, to modify these parameters for point-source conditions. These modifications were implemented within the seismic hazard calculations.

For cases where the causative fault geometry is known (or at least modeled), the distance measures from a site to the rupture are calculated explicitly. The three central faults of the New Madrid fault system are an example. For cases where fault locations are unknown but fault orientation is known (or at least modeled), the hazard calculation assumes a uniform spatial distribution of rupture within the defined geometry of the source, each rupture with the correct orientation. Relationships between earthquake magnitude and rupture length are given in the HID for each applicable source.

Seismic hazard results are also presented in this section for two soil conditions: shallow, stiff soil and deep, soft soil. These give a range of hazard results that might be expected at the seven test sites. For example, a deep soil site might be expected to affect long period ground motions from a large, distant earthquake, and the generic deep-soil model adopted here will represent that effect.

Two hypothetical soil profiles were used; V_S versus depth plots for these two profiles are shown on Figures 8.1-2 (for the shallow soil site) and 8.1-3 (for the deep soil site). Generic mean amplification factors for the two soil profiles are shown on Figures 8.1-4 and 8.1-5 for 10 Hz spectral acceleration (SA), 1 Hz SA, and peak ground acceleration (PGA). As expected, the shallow soil profile amplifies high frequencies, and the deep soil profile amplifies low frequencies. Uncertainties in amplification factor were included, with logarithmic standard deviations dependent on spectral frequency and amplitude. These standard deviations include the effect of uncertainties in V_S versus depth and in soil parameters, and range from 0.07 to 0.25.

Demonstration results are included in Section 8.2 for hard rock, shallow soil, and deep soil site conditions at the seven test sites. These hazard results are plotted for annual frequencies of exceedance from 10^{-3} to 10^{-6}. Note that seismic hazard calculations for critical facilities may require calculations over a different range—in particular, down to annual frequencies of exceedance of 10^{-7}.

8.2 Demonstration Hazard Calculations

This section presents demonstration hazard calculations for the seven test sites. Figures with hazard results in Sections 8.2.1 through 8.2.7 are presented first for hard rock site conditions (labeled “rock” below) in the order outlined below for each site. The results are then presented for rock, shallow soil, and deep soil. Finally, sensitivity plots are presented showing how sensitive the hazard is to some of the input assumptions.

Rock Hazard

Figures a–c: Mean rock hazard and 0.85, 0.5, and 0.15 fractile hazard curves for 10 Hz SA, 1 Hz SA, and PGA. Digital values for the rock hazard curves are provided in Tables 8.2.1-1 to 8.2.7-1; corresponding figures are indicated in the table titles.

Figures d–f: Total mean rock hazard and contribution by background and RLME source for 10 Hz SA, 1 Hz SA, and PGA.

Figures g–i: Contribution to mean rock hazard by individual background source for 10 Hz SA, 1 Hz SA, and PGA.

Hazard Comparisons

Figures j–l: Comparison of mean rock hazard from three source models for 10 Hz SA, 1 Hz SA, and PGA. This comparison shows total hazard for the current CEUS SSC source model and for two other source models, all using the EPRI (2004, 2006) ground-motion model. One source model is the USGS model developed for the National Seismic Hazard Mapping Project (Petersen et al., 2008). The other is the “COLA” model that has been used for nuclear power plant licensing applications since 2003. This is the EPRI-SOG (EPRI, 1988) model updated with more recent characterizations of several seismic sources. The updated New Madrid fault source (NMFS) is based on the Clinton and Bellefonte applications, and the updated Charleston seismic zone is based on the Vogtle application. Also, maximum magnitude (M_{max}) values for some seismic sources near the Gulf of Mexico coastline were updated to reflect recent seismicity. Calculations of hazard for all three models use the EPRI (2004, 2006) ground-motion equations, so the differences in hazard presented here between the three models is attributable to differences in the source models themselves.

Shallow Soil Hazard

Figures m–o: Total mean shallow-soil hazard and contribution by background and RLME source for 10 Hz SA, 1 Hz SA, and PGA.

Deep Soil Hazard

Figures p–r: Total mean deep-soil hazard and contribution by background and RLME source for 10 Hz SA, 1 Hz SA, and PGA.

All Site Conditions

Figures s–u: Total mean hazard for rock, shallow soil, and deep soil conditions for 10 Hz SA, 1 Hz SA, and PGA.

Hazard Sensitivity

Figures v and w: Mean rock hazard for Mmax background sources and for seismotectonic background sources for 10 Hz SA and 1 Hz SA. Note that the hazard from RLME sources is not included in these plots, and that each set of background sources is given a weight of unity for these plots only. The legends in these plots indicate the weights assigned in the logic tree for total hazard calculations.

Figures x and y: Mean rock hazard sensitivity to M_{max} for the dominant background source for 10 Hz SA and 1 Hz SA. These hazard curves include the weight assigned to the dominant background source, but assign a weight of unity to the individual M_{max} values (for these plots only). The legends in these plots indicate the total weight assigned in hazard calculations to each M_{max} value, including the probability of activity.

Figures z and aa: Mean rock hazard sensitivity to seismicity parameter smoothing Cases A, B, and E for background sources only for 10 Hz SA and 1 Hz SA. These hazard curves assign a weight of unity to each smoothing case (for these plots only). The legends in these plots indicate the weight assigned in hazard calculations to each smoothing case.

Figures bb, cc, and dd: Mean rock hazard sensitivity to the eight seismicity parameter realizations, for 10 Hz SA and smoothing Cases A, B, and E for background sources only. These hazard curves assign a weight of unity to each smoothing case (for these plots only). The legends in these plots indicate the weight assigned in hazard calculations to each realization.

Figures ee, ff, and gg: Sensitivity plots similar to the previous three, for 1 Hz SA.

Sensitivity to In-Cluster and Out-of-Cluster Assumption

The sensitivity of seismic hazard to the New Madrid fault in-cluster vs. out-of-cluster assumption is straightforward to determine. The mean in-cluster annual activity rate is 2.3×10^{-3} (over all in-cluster branches), the mean out-of-cluster annual activity rate is 5.0×10^{-4}, which is a factor of 4.6 difference. Thus hazard curves for these two cases would differ by about a factor of 4.6 (this is approximate because the in-cluster model assumes multiple earthquakes, but the out-of-cluster model assumes only a single earthquake).

8.2.1 Central Illinois Site

Hazard results are shown on Figures 8.2-1a through 8.2-1gg for the Central Illinois site. Figures 8.2-1a, 8.2-1b, and 8.2-1c show mean and fractile rock hazard curves for 10 Hz SA, 1 Hz SA, and PGA, respectively. Figure 8.2-1b shows that the mean rock hazard curve for 1 Hz SA lies close to the 0.85 fractile hazard curve at some amplitudes. This results from the contribution of the NMFS RLME source for 1 Hz SA, as discussed below.

Figures 8.2-1d and 8.2-1f show that for 10 Hz SA and PGA, background sources give the highest contributions to hazard. Among background sources, Figures 8.2-1g and 8.2-1i indicate that the highest contributions to 10 Hz SA and PGA hazard come from the MidC seismotectonic sources, the NMESE-N Mmax source, and the IBEB seismotectonic source. The MidC and NMESE-N sources are host sources, while the IBEB source is a major contributor to hazard because of its close proximity to the site and its weighted mean M_{max} value of **M** 7.4. For comparison, the MidC seismotectonic zones have a weighted mean M_{max} value of **M** 6.6, and the NMESE-N Mmax source has a weighted mean M_{max} value of **M** 7.1.

For 1 Hz SA, Figure 8.2-1e shows that the NMFS RLME source dominates total rock hazard for ground motions up to about 0.33 g, and background sources dominate total rock hazard at higher amplitudes. Also note that the ERM-S RLME source has a higher hazard than the ERM-N RLME source, even though the ERM-N RLME source is closer to the site. This is caused by the ERM-S RLME source having a weighted mean M_{max} of **M** 7.2 and the ERM-N RLME source having a weighted mean M_{max} of **M** 6.9. Figure 8.2-1h shows the contribution to 1 Hz SA by background source.

When the NMFS dominates the hazard and lies a great distance from a site (in this case about 320 km, or 200 mi., from the Central Illinois site), the mean hazard often corresponds to a high fractile hazard curve (the 0.85 fractile or higher). The reason is that for the EPRI (2004, 2006) ground-motion model at great distances, one or a few equations within the EPRI (2004, 2006) model give high ground motions and dominate the mean hazard. These few equations have low weight, but their large contribution to the mean hazard results in a mean hazard that corresponds to a high fractile hazard curve.

Figures 8.2-1j and 8.2-1l show that the CEUS SSC model results in higher rock hazard at the site than the COLA or USGS models for 10 Hz SA and PGA, respectively. This is caused by the IBEB source (mean M_{max} of **M** 7.4) dominating the high-frequency hazard for the CEUS SSC model at this site. The COLA and USGS mean values of M_{max} for the area encompassed by the IBEB source are lower. Additionally, the IBEB source concentrates historical seismicity within the source boundaries, whereas large regional sources (of the COLA and USGS source models) allow seismicity to be smoothed over a wider region.

Figure 8.2-1k shows that the three seismic source models result in similar hazards for 1 Hz SA. The NMFS dominates rock hazard at 1 Hz SA, as discussed above, and the New Madrid sources are similar in all three models, resulting in similar hazard for 1 Hz SA.

Figures 8.2-1m through 8.2-1r indicate similar contributions by seismic source for shallow and deep soil as were found for rock. These figures show that for PGA and 10 Hz SA, background sources dominate the total soil hazard at the site. For 1 Hz SA, the NMFS RLME source dominates total soil hazard up to about 0.35 g (for shallow soil) or about 0.8 g (for deep soil). At higher amplitudes, background sources dominate the 1 Hz SA soil hazard.

Figure 8.2-1t shows that for 1 Hz SA, rock and shallow soil have similar total hazard at the site, but amplification caused by deep soil greatly increases the total hazard at the site. For 10 Hz SA and PGA (Figures 8.2-1s and 8.2-1u), shallow soil amplifies ground motions slightly, and deep soil deamplifies ground motions at the site, except for low PGA amplitudes. At PGA amplitudes less than 0.35 g, deep soil shows amplifications of ground motion (see Figure 8.1-5).

Sensitivity results for background sources (Figures 8.2-1v through 8.2-1gg) show the following:

- There is little difference in hazard between Mmax and seismotectonic sources.
- The hazard is sensitive to M_{max} values for the IBEB seismotectonic source, which is expected.
- Smoothing Case E shows the highest hazard, followed by Cases B and A. This is consistent with seismicity rates in the IBEB seismotectonic source for these three smoothing cases.
- The hazard is sensitive to the eight realizations of seismicity parameters for the three smoothing cases, which is expected.

8.2.2 Chattanooga Site

Hazard results are shown on Figures 8.2-2a through 8.2-2gg for the Chattanooga site. Figures 8.2-2a, 8.2-2b, and 8.2-2c show mean and fractile rock hazard curves for 10 Hz SA, 1 Hz SA, and PGA, respectively.

Figures 8.2-2d and 8.2-2f show that for 10 Hz SA and PGA, background sources give the highest contributions to rock hazard. Among background sources, Figures 8.2-2g and 8.2-2i indicate that the highest contributions to 10 Hz SA and PGA hazard come from the PEZ-N seismotectonic source and the NMESE-N Mmax source. Both sources are host sources.

For 1 Hz SA, Figure 8.2-2e shows that the NMFS RLME source dominates total rock hazard for ground motions up to about 0.15 g, and background sources dominate total rock hazard at higher amplitudes. However, even at amplitudes below 0.15 g, background sources have an important contribution to total hazard. Figure 8.2-2h shows the contribution to 1 Hz SA by background source.

Figures 8.2-2j and 8.2-2l show that the CEUS SSC model and USGS model result in nearly identical hazards for lower amplitudes, but above about 0.6 and 0.3 g, the USGS model results in higher rock hazards for 10 Hz SA and PGA, respectively. This is related to the mean M_{max} value for the USGS model for the region encompassing eastern Tennessee, which is higher than the mean M_{max} values for this region in the CEUS SSC and COLA models. Figure 8.2-2k shows that the CEUS SSC model results in rock hazard at the site that lies between the hazard from the COLA and USGS models for 1 Hz SA. The difference in M_{max} values between the source models also plays a role in the comparison of 1 Hz hazard.

Figures 8.2-2m through 8.2-2r indicate similar contributions by seismic source for shallow and deep soil as were found for rock. These figures show that for 10 Hz SA and PGA, background sources give the highest contributions to hazard. For 1 Hz SA, the NMFS dominates total hazard for ground motions up to about 0.15 g for shallow soil and 0.35 g for deep soil, and background sources dominate total hazard at higher amplitudes.

Figure 8.2-2t shows that for 1 Hz SA, rock and shallow soil have similar total hazard at the site, but amplification caused by deep soil greatly increases the total hazard at the site. For 10 Hz SA (Figure 8.2-2s), shallow soil amplifies ground motions slightly, and deep soil deamplifies ground motions at the site. The same is true for PGA (Figure 8.2-2u), except for amplitudes less than 0.35 g where deep soil shows amplification of ground motion (see Figure 8.1-5).

Sensitivity results for background sources (Figures 8.2-2v through 8.2-2gg) show the following:

- There is little difference in hazard between Mmax and seismotectonic sources.
- There is little sensitivity in hazard M_{max} values for the PEZ-N seismotectonic source at 10 Hz SA, but at 1 Hz SA the sensitivity is more pronounced, which is expected.
- Smoothing Case A shows the highest hazard, followed by Cases B and E, and there is sensitivity to the three cases. This is consistent with seismicity rates in the PEZ-N seismotectonic source for these three smoothing cases.
- The hazard is sensitive to the eight realizations of seismicity parameters for the three smoothing cases, which is expected.

8.2.3 Houston Site

Hazard results are shown on Figures 8.2-3a through 8.2-3gg for the Houston site. Figures 8.2-3a, 8.2-3b, and 8.2-3c show mean and fractile rock hazard curves for 10 Hz SA, 1 Hz SA, and PGA, respectively. Figure 8.2-3b shows that the mean rock hazard lies above the 0.85 fractile between about 0.045 and 0.25 g. This results from the contribution of the NMFS RLME source at 1 Hz SA, which is discussed below.

Figures 8.2-3d and 8.2-3f show that for 10 Hz SA and PGA, background sources give the highest contributions to hazard except at low amplitudes. For 10 Hz SA amplitudes below about 0.03 g, and PGA amplitudes below about 0.015 g, the NMFS gives hazard that slightly exceeds that from background sources. Among background sources, Figures 8.2-3g and 8.2-3i indicate that the highest contributions to 10 Hz SA and PGA hazard come from the GHEX and ECC-GC seismotectonic sources and the MESE-N Mmax source. The GHEX and MESE-N are host sources, while ECC-GC is a major contributor to hazard because of its proximity to the site and its higher seismicity rate.

For 1 Hz SA, Figure 8.2-3e shows that the NMFS RLME source dominates total rock hazard for ground motions. When the NMFS dominates the hazard and lies a great distance from a site (in this case about 780 km, or 485 mi., from the Houston site), the mean hazard often corresponds to a high fractile hazard curve (the 0.85 fractile or higher). The reason is that for the EPRI (2004, 2006) ground-motion model at great distances, one or a few equations within the EPRI (2004, 2006) model give high ground motions and dominate the mean hazard. These few equations have low weight, but their large contribution to the mean hazard results in a mean hazard that corresponds to a high fractile hazard curve. Figure 8.2-3h shows the contribution to 1 Hz SA by background source.

Figures 8.2-3j and 8.2-3l show that hazard from the CEUS SSC model lies between hazards from the COLA and USGS models for 10 Hz SA and PGA, respectively. Figure 8.2-3k shows that for 1 Hz SA, all three models result in similar rock hazard, up to approximately 0.05 g. At higher amplitudes, the USGS model results in higher rock hazard. The NMFS dominates rock hazard at

1 Hz SA, as discussed above, and the New Madrid sources are similar in all three models. Higher 1 Hz SA hazard from the USGS model at amplitudes above 0.05 g probably relates to the USGS treatment of background sources in the vicinity of Houston.

Figures 8.2-3m through 8.2-3r indicate similar contributions by seismic source for shallow and deep soil as were found for rock. These figures show that for 10 Hz SA and PGA, background sources give the highest contributions to hazard except at low amplitudes (less than about 0.04 g for 10 Hz SA for shallow and deep soil, and less than about 0.03 g for PGA for shallow and deep soil). At these low amplitudes the NMFS is the dominant contributor to hazard. For 1 Hz SA, the NMFS dominates total hazard for ground motions at all amplitudes, which was the conclusion for rock hazard (Figure 8.2-3e).

Figure 8.2-3t shows that for 1 Hz SA, rock and shallow soil have similar total hazard at the site, but amplification caused by the deep soil greatly increases the total hazard at the site. For 10 Hz SA and PGA (Figures 8.2-3s and 8.2-3u), shallow soil amplifies ground motions slightly, while deep soil hazard exhibits deamplification above about 0.35 g (for PGA) and 0.09 g (for 10 Hz SA), and amplification below those amplitudes. This is consistent with the amplification factor for deep soil (Figure 8.1-5).

Sensitivity results for background sources (Figures 8.2-3v through 8.2-3gg) show the following:

- Hazard from the seismotectonic sources exceeds that of the Mmax sources because of the higher seismicity rate of seismotectonic source ECC-GC and its close proximity to the site.
- There is little sensitivity of hazard to M_{max} values for the GHEX seismotectonic source at 10 Hz SA, but at 1 Hz SA the sensitivity is slightly more pronounced, which is expected.
- Smoothing Cases A and E show the highest hazard, followed by Case B. This is consistent with seismicity rates in the GHEX source for these three smoothing cases.
- The hazard is sensitive to the eight realizations of seismicity parameters for the three smoothing cases, which is expected. The hazard is especially sensitive to the eight realizations for Case B, as seen for 10 Hz and 1 Hz SA, where two of the eight realizations indicate very low seismicity near the site.

8.2.4 Jackson Site

Hazard results are shown on Figures 8.2-4a through 8.2-4gg for the Jackson site. Figures 8.2-4a, 8.2-4b, and 8.2-4c show the mean and fractile rock hazard curves for 10 Hz SA, 1 Hz SA, and PGA, respectively. Figure 8.2-4b shows the mean rock hazard overlapping the 0.85 fractile hazard between about 0.2 and 0.32 g. This results from the contribution of the NMFS RLME source at 1 Hz SA, which is discussed below.

For 10 Hz SA and PGA, Figures 8.2-4d and 8.2-4f show that the NMFS is the highest contributor to hazard at amplitudes below 0.35 g (for 10 Hz SA) and 0.15 g (for PGA). Above these amplitudes, the highest contribution to total hazard comes from the background sources. Among background sources, Figures 8.2-4g and 8.2-4i indicate that the highest contributions to 10 Hz SA and PGA hazard come from the ECC-GC seismotectonic source, and at lower amplitudes, from the RR and RR-RCG seismotectonic sources. ECC-GC is the host source, while the RR and RR-RCG sources are a major contributor to low-amplitude hazard because of the use of midcontinent attenuation equations for these sources, whereas Gulf attenuation equations are used for all other background sources.

For 1 Hz SA, Figure 8.2-4e shows that the NMFS RLME source dominates total rock hazard for ground motions. When the NMFS dominates the hazard and lies a great distance from a site (in this case about 360 km, or 225 mi., from the Jackson site), the mean hazard often corresponds to a high fractile hazard curve (the 0.85 fractile or higher). The reason is that for the EPRI (2004, 2006) ground-motion model at great distances, one or a few equations within the EPRI (2004, 2006) model give high ground motions and dominate the mean hazard. These few equations have low weight, but their large contribution to the mean hazard results in a mean hazard that corresponds to a high fractile hazard curve. Figure 8.2-4h shows the contribution to 1 Hz SA by background source.

Figures 8.2-4j and 8.2-4l show that the CEUS SSC model results in 10 Hz SA and PGA hazard that lies between the hazards from the COLA and USGS models. Figure 8.2-4k indicates that for 1 Hz SA, all three models have similar rock hazard up to approximately 0.15 g. Above that amplitude the USGS model indicates somewhat higher rock hazard. The NMFS dominates rock hazard at 1 Hz SA, as discussed above, and the New Madrid sources are similar in all three models, resulting in similar hazard for 1 Hz SA.

Figures 8.2-4m through 8.2-4r indicate similar contributions by seismic source for shallow and deep soil to those found for rock. That is, for 10 Hz SA and PGA, background sources dominate the total soil hazard at higher ground-motion amplitudes, while at lower amplitudes the NMFS dominates. For 1 Hz SA, the NMFS RLME source dominates total hazard for both shallow and deep soil.

Figures 8.2-4s through 8.2-4u show that at 10 Hz SA, there is slight amplification of shallow soil and a deamplification of deep soil. At 1 Hz SA, rock and shallow soil have similar total hazard at the site, but amplification caused by the deep soil greatly increases the total hazard at the site. For PGA, shallow soil amplifies ground motions, resulting in a higher hazard curve. Deep soil deamplifies ground motions for PGA above 0.35 g, resulting in a lower hazard curve, and the opposite is true for PGA below about 0.35 g. This is consistent with the deep soil amplification factor (Figure 8.1-5).

Sensitivity results for background sources (Figures 8.2-4v through 8.2-4gg) show the following:

- Hazard from the seismotectonic sources exceeds hazard from the Mmax sources because seismicity rates in the seismotectonic sources (specifically, the ECC-GC source) are higher than for Mmax sources (specifically, the MESE-N).
- There is little sensitivity in hazard M_{max} values for the ECC-GC seismotectonic source at 10 Hz SA, but at 1 Hz SA the sensitivity is slightly more pronounced, which is expected.
- Smoothing Cases A, B, and E show very similar hazard for 10 Hz SA and 1 Hz SA.
- Seismic hazard is sensitive to the eight realizations of seismicity parameters for Case A, with one realization indicating very low hazard (very low rates of seismicity). There is less sensitivity to the eight realizations for Cases B and E.

8.2.5 Manchester Site

Hazard results are shown on Figures 8.2-5a through 8.2-5gg for the Manchester site. Figures 8.2-5a, 8.2-5b, and 8.2-5c show the mean and fractile rock hazard curves for 10 Hz SA, 1 Hz SA, and PGA, respectively.

Figures 8.2-5d through 8.2-5f show that for 10 Hz SA, 1 Hz SA, and PGA, the background sources are the highest contributor to hazard. The only RLME modeled for the Manchester hazard is the Charlevoix RLME, but its great distance (about 440 km, or 275 mi.) from the site means that it makes only a minor contribution to hazard at any frequency. Among background sources, Figures 8.2-5g and 8.2-5i indicate that the highest contribution to 10 Hz SA and PGA hazard comes from the NAP seismotectonic source, which is a host source. MESE-N and STUDY-R make the largest contributions of the Mmax sources. Figure 8.2-5h shows the contribution to 1 Hz SA by background source.

Figures 8.2-5j and 8.2-5l show that for 10 Hz SA and PGA, the CEUS SSC model results in hazard similar to that of the COLA model. The USGS model indicates similar hazard at low amplitudes, but above about 0.5 g for 10 Hz SA and 0.35 g for PGA, the USGS model results in higher hazard. Figure 8.2-5k shows that for 1 Hz SA, the CEUS SSC model results in somewhat higher hazard than the COLA model, but (at amplitudes exceeding about 0.03 g) the USGS model results in the highest hazard between the three.

Figures 8.2-5m through 8.2-5r indicate similar contributions from background sources for shallow and deep soil as were found for rock. These figures show that for 10 Hz SA, 1 Hz SA, and PGA, background sources dominate the total soil hazard at the site, and that the Charlevoix RLME is not a large contributor to hazard because of its great distance from the site.

Figure 8.2-5t shows that for 1 Hz SA, rock and shallow soil have similar total hazard at the site, but amplification caused by the deep soil greatly increases the total hazard at the site. For 10 Hz SA and PGA (Figures 8.2-5s and 8.2-5u), shallow soil amplifies ground motions slightly, and deep soil deamplifies ground motions at the site, except for low PGA amplitudes. At PGA amplitudes less than 0.35 g, deep soil shows amplifications of ground motion (see Figure 8.1-5).

Sensitivity results for background sources (Figures 8.2-5v through 8.2-5gg) show the following:

- Mmax and seismotectonic sources indicate very similar hazards.
- There is little sensitivity in hazard M_{max} values for the NAP seismotectonic source at 10 Hz SA, but at 1 Hz SA the sensitivity is slightly more pronounced, which is expected.
- Smoothing Case A shows the highest hazard, followed by Cases B and E. This is consistent with seismicity rates in the NAP seismotectonic source for these three smoothing cases.
- The hazard is sensitive to the eight realizations for the three smoothing cases, which is expected. The hazard is somewhat more sensitive to the eight realizations for Case B than for Cases A and E.

8.2.6 Savannah Site

Hazard results are shown on Figures 8.2-6a through 8.2-6gg for the Savannah site. Figures 8.2-6a, 8.2-6b, and 8.2-6c show mean and fractile rock hazard curves for 10 Hz SA, 1 Hz SA, and PGA, respectively.

Figures 8.2-6d and 8.2-6f show that for 10 Hz SA and PGA, the Charleston RLME is the highest contributor to rock hazard, but background sources contribute significantly at higher amplitudes. For PGA, at amplitudes higher than about 1.25 g, background sources indicate the highest contribution to hazard. Among background sources, Figures 8.2-6g through 8.2-6i indicate that the highest contribution comes from the ECC-AM seismotectonic source for 10 Hz SA, 1 Hz SA, and PGA. MESE-N makes the largest contribution of the Mmax sources. ECC-AM and MESE-N are both host sources.

For 1 Hz SA, Figure 8.2-6e shows that the Charleston RLME dominates total rock hazard for all amplitudes and that the background sources are less significant contributors than for 10 Hz SA or PGA.

Figures 8.2-6j through 8.2-6l show that the CEUS SSC model produces higher hazard at Savannah than the COLA and USGS models, except at higher amplitudes (above 1.8, 0.45, and 0.8 g for 10 Hz SA, 1 Hz SA, and PGA, respectively) where the USGS model shows higher hazard. This is primarily a result of differences in Charleston source geometries between the three models, which have an important effect at a very close site like Savannah. For a more distant site, hazard resulting from the three models is expected to be similar. In particular, sites located to the northwest would lie perpendicular to predominant rupture orientations in the Charleston RLME and would not be highly affected by assumptions on source geometries.

Figures 8.2-6m through 8.2-6r indicate similar contributions by seismic source for shallow and deep soil as were found for rock. These figures show that for 10 Hz SA and PGA, the Charleston RLME is the highest contributor to hazard, and background sources contribute significantly at higher amplitudes. For 1 Hz SA, the background sources are less significant contributors to hazard than at 10 Hz SA or PGA.

Figures 8.2-6s through 8.2-6u show that at 10 Hz SA, there is slight amplification of shallow soil and a deamplification of deep soil. At 1 Hz SA, rock and shallow soil have similar total hazard at the site, but amplification caused by the deep soil greatly increases the total hazard at the site. For PGA, shallow soil shows higher hazard than rock, while deep soil shows lower hazard than rock above about 0.35 g and higher hazard below that amplitude. This is consistent with the deep soil amplification factor for PGA (Figure 8.1-5).

Sensitivity results for background sources (Figures 8.2-6v through 8.2-6gg) show the following:

- There is little difference in hazard between Mmax and seismotectonic sources.
- There is little sensitivity in hazard M_{max} values for the ECC-AM seismotectonic source at 10 Hz SA, but at 1 Hz SA the sensitivity is slightly more pronounced, which is expected.
- Smoothing Case A shows the highest hazard, followed by Cases E and B. This is consistent with seismicity rates in the ECC-AM seismotectonic source for these three smoothing cases.
- The hazard is sensitive to the eight realizations of seismicity parameters for the three smoothing cases, which is expected.

8.2.7 Topeka Site

Hazard results are shown on Figures 8.2-7a through 8.2-7gg for the Topeka site. Figures 8.2-7a, 8.2-7b, and 8.2-7c show the mean and fractile rock hazard curves for 10 Hz SA, 1 Hz SA, and

PGA, respectively. Figure 8.2-7b shows the mean rock hazard being equivalent to the 0.85 fractile between about 0.1 and 0.15 g. This results from the contribution of the NMFS RLME source at 1 Hz SA, which is discussed below.

For 10 Hz SA and PGA, Figures 8.2-7d and 8.2-7f show that background sources give the highest contributions to hazard. Among background sources, Figures 8.2-7g and 8.2-7i indicate that the highest contributions come from the MidC-A seismotectonic source, the NMESE-N Mmax sources, and the STUDY-R Mmax source. All of these are host sources.

For 1 Hz SA, Figure 8.2-7e shows that the NMFS RLME source dominates total rock hazard for ground motions up to about 0.2 g, and background sources dominate total rock hazard at higher amplitudes. When the NMFS dominates the hazard and lies a great distance from a site (in this case about 580 km, or 360 mi., from the Topeka site), the mean hazard often corresponds to a high fractile hazard curve (the 0.85 fractile or higher). The reason is that for the EPRI (2004, 2006) ground-motion model at great distances, one or a few equations within the EPRI (2004, 2006) model give high ground motions and dominate the mean hazard. These few equations have low weight, but their large contribution to the mean hazard results in a mean hazard that corresponds to a high fractile hazard curve. Contribution by background source for 1 Hz SA is shown on Figure 8.2-7h.

Figures 8.2-7j and 8.2-7l show that the CEUS SSC model results in slightly higher rock hazard at the site than the COLA or USGS models for 10 Hz SA and PGA, respectively. Figure 8.2-7k shows that for 1 Hz SA, hazards resulting from the three models are very similar. The NMFS dominates rock hazard at 1 Hz SA, as discussed above, and the New Madrid sources are similar in all three models, resulting in similar hazard for 1 Hz SA.

Figures 8.2-7m through 8.2-7r indicate similar contributions by seismic source for shallow and deep soil as were found for rock. These figures show that for 10 Hz SA and PGA, background sources give the highest contributions to hazard. For 1 Hz SA, the NMFS dominates total hazard for ground motions up to about 0.25 g for shallow soil and 0.55 g for deep soil, and background sources dominate total hazard at higher amplitudes.

Figures 8.2-7s through 8.2-7u show that at 10 Hz SA, there is a slight amplification of shallow soil and a deamplification of deep soil. At 1 Hz SA, rock and shallow soil have similar total hazard at the site, but amplification caused by the deep soil greatly increases the total hazard at the site. For PGA, shallow soil is amplified, but deep soil shows lower hazard than rock above about 0.35 g, and higher hazard below this amplitude. This is consistent with the deep soil amplification factor for PGA (Figure 8.1-5).

Sensitivity results for background sources (Figures 8.2-7v through 8.2-7gg) show the following:

- Mmax sources indicate higher hazard than seismotectonic sources. The maximum magnitudes and local seismicity rates in Mmax sources are higher than the corresponding values in seismotectonic sources, which explains this difference.
- There is a moderate sensitivity in hazard M_{max} values for the MidC-A seismotectonic source at 10 Hz SA, but at 1 Hz SA the sensitivity is more pronounced, which is expected.
- Smoothing Case B shows the highest hazard, followed by Cases E and A. This is consistent with seismicity rates in the MidC-A seismotectonic source for these three smoothing cases.

- The hazard is sensitive to the eight realizations of seismicity parameters for the three smoothing cases, which is expected. The hazard is especially sensitivity to the eight realizations for Case A, as seen for 10 Hz and 1 Hz SA.

Table 8.1-1
Description of Seven Test Sites

Test Site Name	N. Latitude	W. Longitude	Reason for Selection
Central Illinois	40.000	–90.000	Hazard from New Madrid seismic zone and paleoearthquake zones in central Illinois
Chattanooga	35.064	–85.255	Hazard from Eastern Tennessee seismic zone
Houston	29.760	–95.363	Hazard in Gulf Coast region
Jackson	32.312	–90.178	Hazard from New Madrid seismic zone
Manchester	42.991	–71.463	Hazard in New England
Savannah	32.082	–81.097	Hazard from Charleston source
Topeka	39.047	–95.682	Hazard in central plains region

Table 8.2.1-1
Mean and Select Fractiles for Rock Hazard at Central Illinois: Digital Data for Figures 8.2-1a through 8.2-1c

Frequency	Spectral Accel. (g)	Mean	0.15	0.5	0.85
10 Hz	0.1	1.27E-3	4.37E-4	9.33E-4	2.00E-3
	0.15	5.98E-4	1.91E-4	4.07E-4	9.33E-4
	0.2	3.37E-4	1.06E-4	2.34E-4	5.01E-4
	0.3	1.45E-4	4.47E-5	1.02E-4	2.04E-4
	0.5	4.91E-5	1.59E-5	3.63E-5	7.76E-5
	0.7	2.44E-5	7.41E-6	1.82E-5	3.89E-5
	1	1.16E-5	3.47E-6	9.12E-6	1.95E-5
	1.5	4.79E-6	1.32E-6	3.47E-6	8.51E-6
	2	2.45E-6	6.17E-7	1.74E-6	4.27E-6
	3	8.61E-7	1.78E-7	5.75E-7	1.62E-6
	5	1.90E-7	2.75E-8	1.10E-7	3.55E-7
	7	6.14E-8	6.68E-9	3.16E-8	1.18E-7
	10	1.64E-8	1.23E-9	7.41E-9	3.06E-8
1 Hz	0.01	4.48E-3	1.86E-3	3.72E-3	7.16E-3
	0.015	2.90E-3	1.00E-3	2.46E-3	4.90E-3
	0.02	2.08E-3	6.17E-4	1.62E-3	3.72E-3
	0.03	1.21E-3	2.69E-4	8.13E-4	2.29E-3
	0.05	5.16E-4	7.76E-5	2.69E-4	9.33E-4
	0.07	2.62E-4	3.16E-5	1.10E-4	4.37E-4
	0.1	1.15E-4	1.12E-5	4.17E-5	1.66E-4
	0.15	4.00E-5	3.24E-6	1.29E-5	5.13E-5
	0.2	1.75E-5	1.32E-6	5.25E-6	2.09E-5
	0.3	5.02E-6	3.43E-7	1.51E-6	6.46E-6
	0.5	9.67E-7	5.13E-8	3.31E-7	1.51E-6
	0.7	3.29E-7	1.38E-8	1.14E-7	5.75E-7
	1	1.07E-7	3.24E-9	3.39E-8	2.04E-7

Frequency	Spectral Accel. (g)	Mean	0.15	0.5	0.85
PGA	0.1	3.27E-4	8.32E-5	2.04E-4	5.01E-4
	0.15	1.42E-4	3.89E-5	9.55E-5	2.04E-4
	0.2	7.90E-5	2.24E-5	5.50E-5	1.18E-4
	0.3	3.56E-5	1.05E-5	2.57E-5	5.89E-5
	0.5	1.34E-5	3.47E-6	9.77E-6	2.40E-5
	0.7	6.93E-6	1.51E-6	4.57E-6	1.29E-5
	1	3.23E-6	5.75E-7	2.00E-6	6.03E-6
	1.5	1.22E-6	1.55E-7	6.17E-7	2.29E-6
	2	5.55E-7	5.31E-8	2.51E-7	1.00E-6
	3	1.58E-7	9.77E-9	5.89E-8	2.69E-7
	5	2.40E-8	7.59E-10	6.46E-9	3.89E-8
	7	5.68E-9	1.10E-10	1.23E-9	8.51E-9
	10	1.03E-9	1.20E-11	1.72E-10	1.41E-9

Table 8.2.2-1
Mean and Select Fractiles for Rock Hazard at Chattanooga: Digital Data for Figures 8.2-2a through 8.2-2c)

Frequency	Spectral Accel. (g)	Mean	0.15	0.5	0.85
10 Hz	0.1	1.77E-3	6.61E-4	1.41E-3	2.82E-3
	0.15	9.63E-4	3.55E-4	7.08E-4	1.62E-3
	0.2	6.17E-4	2.19E-4	4.37E-4	1.07E-3
	0.3	3.25E-4	1.10E-4	2.19E-4	5.75E-4
	0.5	1.41E-4	4.62E-5	8.91E-5	2.69E-4
	0.7	7.85E-5	2.40E-5	5.13E-5	1.45E-4
	1	4.04E-5	1.20E-5	2.57E-5	7.76E-5
	1.5	1.75E-5	4.90E-6	1.12E-5	3.16E-5
	2	9.08E-6	2.29E-6	5.62E-6	1.70E-5
	3	3.23E-6	7.08E-7	1.86E-6	5.62E-6
	5	7.12E-7	1.26E-7	3.80E-7	1.32E-6
	7	2.29E-7	3.16E-8	1.18E-7	4.07E-7
	10	6.04E-8	6.46E-9	2.75E-8	1.10E-7
1 Hz	0.01	5.39E-3	2.29E-3	4.57E-3	8.51E-3
	0.015	3.40E-3	1.23E-3	2.82E-3	5.62E-3
	0.02	2.38E-3	7.08E-4	1.86E-3	4.27E-3
	0.03	1.34E-3	3.31E-4	9.33E-4	2.46E-3
	0.05	5.64E-4	1.02E-4	3.31E-4	1.00E-3
	0.07	2.90E-4	4.47E-5	1.45E-4	4.68E-4
	0.1	1.33E-4	1.82E-5	6.10E-5	2.04E-4
	0.15	5.06E-5	6.03E-6	2.16E-5	7.76E-5
	0.2	2.45E-5	2.82E-6	1.05E-5	3.89E-5
	0.3	8.50E-6	8.13E-7	3.72E-6	1.43E-5
	0.5	2.18E-6	1.45E-7	9.33E-7	3.98E-6
	0.7	8.76E-7	4.17E-8	3.55E-7	1.68E-6
	1	3.19E-7	1.01E-8	1.10E-7	6.17E-7

Frequency	Spectral Accel. (g)	Mean	0.15	0.5	0.85
PGA	0.1	6.36E-4	2.04E-4	4.37E-4	1.07E-3
	0.15	3.44E-4	1.10E-4	2.19E-4	6.17E-4
	0.2	2.21E-4	6.76E-5	1.45E-4	4.07E-4
	0.3	1.17E-4	3.39E-5	7.24E-5	2.19E-4
	0.5	4.88E-5	1.20E-5	3.06E-5	8.91E-5
	0.7	2.58E-5	5.62E-6	1.59E-5	4.79E-5
	1	1.22E-5	2.14E-6	6.92E-6	2.24E-5
	1.5	4.60E-6	6.17E-7	2.29E-6	8.51E-6
	2	2.10E-6	2.19E-7	9.02E-7	3.72E-6
	3	5.93E-7	4.17E-8	2.19E-7	1.00E-6
	5	8.95E-8	3.72E-9	2.40E-8	1.35E-7
	7	2.10E-8	5.56E-10	4.57E-9	3.06E-8
	10	3.75E-9	5.89E-11	6.17E-10	5.25E-9

Table 8.2.3-1
Mean and Select Fractiles for Rock Hazard at Houston: Digital Data for Figures 8.2-3a through 8.2-3c

Frequency	Spectral Accel. (g)	Mean	0.15	0.5	0.85
10 Hz	0.01	1.77E-3	5.01E-4	1.23E-3	3.24E-3
	0.015	1.13E-3	2.88E-4	7.08E-4	2.07E-3
	0.02	7.90E-4	1.91E-4	4.37E-4	1.41E-3
	0.03	4.49E-4	1.02E-4	2.34E-4	7.08E-4
	0.05	2.08E-4	4.47E-5	1.10E-4	2.51E-4
	0.07	1.22E-4	2.57E-5	6.31E-5	1.35E-4
	0.1	6.68E-5	1.43E-5	3.63E-5	7.24E-5
	0.15	3.19E-5	7.41E-6	1.95E-5	3.76E-5
	0.2	1.85E-5	4.57E-6	1.20E-5	2.40E-5
	0.3	8.74E-6	2.29E-6	6.92E-6	1.29E-5
	0.5	3.60E-6	9.02E-7	3.02E-6	6.03E-6
	0.7	2.03E-6	4.68E-7	1.74E-6	3.47E-6
	1	1.08E-6	2.34E-7	9.33E-7	1.86E-6
1 Hz	0.01	1.07E-3	1.26E-4	5.75E-4	2.14E-3
	0.015	6.30E-4	5.31E-5	2.51E-4	1.23E-3
	0.02	4.09E-4	2.95E-5	1.26E-4	7.08E-4
	0.03	2.07E-4	1.20E-5	4.79E-5	2.79E-4
	0.05	7.82E-5	3.72E-6	1.38E-5	6.76E-5
	0.07	3.82E-5	1.74E-6	6.46E-6	2.57E-5
	0.1	1.63E-5	7.59E-7	2.82E-6	1.01E-5
	0.15	5.45E-6	2.88E-7	1.15E-6	3.98E-6
	0.2	2.35E-6	1.45E-7	6.17E-7	2.14E-6
	0.3	6.92E-7	5.13E-8	2.51E-7	8.71E-7
	0.5	1.59E-7	1.20E-8	7.24E-8	2.69E-7
	0.7	6.42E-8	3.98E-9	3.16E-8	1.26E-7
	1	2.47E-8	1.15E-9	1.12E-8	5.13E-8

Frequency	Spectral Accel. (g)	Mean	0.15	0.5	0.85
PGA	0.01	7.82E-4	1.55E-4	3.80E-4	1.41E-3
	0.015	4.35E-4	8.32E-5	1.91E-4	6.61E-4
	0.02	2.77E-4	5.13E-5	1.26E-4	3.80E-4
	0.03	1.45E-4	2.66E-5	6.31E-5	1.78E-4
	0.05	6.17E-5	1.12E-5	2.95E-5	6.76E-5
	0.07	3.33E-5	6.92E-6	1.82E-5	3.89E-5
	0.1	1.70E-5	3.85E-6	1.12E-5	2.32E-5
	0.15	8.35E-6	2.00E-6	6.46E-6	1.29E-5
	0.2	5.26E-6	1.27E-6	4.27E-6	8.51E-6
	0.3	2.82E-6	6.61E-7	2.29E-6	4.90E-6
	0.5	1.26E-6	2.34E-7	1.00E-6	2.29E-6
	0.7	7.03E-7	1.06E-7	5.01E-7	1.32E-6
	1	3.56E-7	4.17E-8	2.27E-7	6.61E-7

Table 8.2.4-1
Mean and Select Fractiles for Rock Hazard at Jackson: Digital Data for Figures 8.2-4a through 8.2-4c

Frequency	Spectral Accel. (g)	Mean	0.15	0.5	0.85
10 Hz	0.1	4.85E-4	8.32E-5	2.69E-4	8.71E-4
	0.15	2.27E-4	3.89E-5	1.10E-4	3.55E-4
	0.2	1.25E-4	2.16E-5	5.89E-5	1.78E-4
	0.3	5.06E-5	9.77E-6	2.57E-5	6.31E-5
	0.5	1.54E-5	3.47E-6	9.77E-6	2.02E-5
	0.7	7.21E-6	1.68E-6	5.25E-6	1.05E-5
	1	3.35E-6	7.59E-7	2.63E-6	5.25E-6
	1.5	1.42E-6	2.88E-7	1.15E-6	2.46E-6
	2	7.51E-7	1.35E-7	6.17E-7	1.32E-6
	3	2.82E-7	4.32E-8	2.04E-7	5.01E-7
	5	6.80E-8	7.41E-9	4.47E-8	1.26E-7
	7	2.34E-8	2.00E-9	1.38E-8	4.32E-8
	10	6.62E-9	3.94E-10	3.47E-9	1.29E-8
1 Hz	0.01	2.51E-3	8.13E-4	2.14E-3	4.27E-3
	0.015	1.80E-3	4.37E-4	1.41E-3	3.24E-3
	0.02	1.35E-3	2.51E-4	9.33E-4	2.63E-3
	0.03	8.18E-4	1.10E-4	4.68E-4	1.62E-3
	0.05	3.56E-4	3.06E-5	1.45E-4	6.61E-4
	0.07	1.82E-4	1.25E-5	5.89E-5	2.99E-4
	0.1	8.04E-5	4.57E-6	2.16E-5	1.10E-4
	0.15	2.79E-5	1.51E-6	6.92E-6	3.06E-5
	0.2	1.21E-5	7.08E-7	3.02E-6	1.20E-5
	0.3	3.40E-6	2.19E-7	9.33E-7	3.47E-6
	0.5	6.42E-7	4.17E-8	2.34E-7	8.71E-7
	0.7	2.22E-7	1.25E-8	9.55E-8	3.67E-7
	1	7.58E-8	3.35E-9	3.16E-8	1.45E-7

Frequency	Spectral Accel. (g)	Mean	0.15	0.5	0.85
PGA	0.01	3.35E-3	1.23E-3	2.82E-3	5.25E-3
	0.015	2.34E-3	7.08E-4	1.86E-3	3.98E-3
	0.02	1.74E-3	4.37E-4	1.23E-3	3.24E-3
	0.03	1.05E-3	2.04E-4	6.38E-4	2.00E-3
	0.05	4.64E-4	6.76E-5	2.19E-4	8.71E-4
	0.07	2.43E-4	3.63E-5	1.02E-4	4.07E-4
	0.1	1.14E-4	1.76E-5	4.79E-5	1.66E-4
	0.15	4.54E-5	7.94E-6	2.24E-5	5.89E-5
	0.2	2.35E-5	4.73E-6	1.38E-5	2.95E-5
	0.3	9.78E-6	2.14E-6	6.92E-6	1.38E-5
	0.5	3.69E-6	7.33E-7	2.82E-6	6.46E-6
	0.7	2.00E-6	3.55E-7	1.41E-6	3.72E-6
	1	1.00E-6	1.45E-7	6.61E-7	1.86E-6

Table 8.2.5-1
Mean and Select Fractiles for Rock Hazard at Manchester: Digital Data for Figures 8.2-5a through 8.2-5c

Frequency	Spectral Accel. (g)	Mean	0.15	0.5	0.85
10 Hz	0.1	9.79E-4	5.19E-4	8.71E-4	1.41E-3
	0.15	5.46E-4	2.69E-4	5.01E-4	8.13E-4
	0.2	3.56E-4	1.78E-4	3.09E-4	5.37E-4
	0.3	1.92E-4	8.91E-5	1.66E-4	2.88E-4
	0.5	8.50E-5	3.39E-5	7.24E-5	1.35E-4
	0.7	4.80E-5	1.82E-5	4.17E-5	7.76E-5
	1	2.51E-5	8.51E-6	2.09E-5	4.17E-5
	1.5	1.11E-5	3.47E-6	8.51E-6	1.95E-5
	2	5.84E-6	1.62E-6	4.57E-6	1.01E-5
	3	2.14E-6	5.19E-7	1.51E-6	3.72E-6
	5	4.96E-7	9.55E-8	3.20E-7	8.71E-7
	7	1.66E-7	2.57E-8	9.89E-8	2.99E-7
	10	4.57E-8	5.62E-9	2.40E-8	8.32E-8
1 Hz	0.01	2.62E-3	9.33E-4	1.86E-3	4.42E-3
	0.015	1.43E-3	4.68E-4	1.00E-3	2.37E-3
	0.02	9.02E-4	2.88E-4	6.38E-4	1.51E-3
	0.03	4.54E-4	1.35E-4	3.09E-4	7.59E-4
	0.05	1.79E-4	4.79E-5	1.26E-4	2.88E-4
	0.07	9.45E-5	2.40E-5	6.76E-5	1.55E-4
	0.1	4.69E-5	1.05E-5	3.27E-5	8.04E-5
	0.15	2.08E-5	4.27E-6	1.38E-5	3.63E-5
	0.2	1.15E-5	2.14E-6	7.94E-6	2.09E-5
	0.3	4.89E-6	7.59E-7	3.13E-6	9.77E-6
	0.5	1.56E-6	1.78E-7	8.71E-7	3.13E-6
	0.7	6.91E-7	5.89E-8	3.55E-7	1.41E-6
	1	2.72E-7	1.59E-8	1.26E-7	5.37E-7

Frequency	Spectral Accel. (g)	Mean	0.15	0.5	0.85
PGA	0.1	3.73E-4	1.55E-4	3.09E-4	5.75E-4
	0.15	2.05E-4	8.32E-5	1.66E-4	3.31E-4
	0.2	1.33E-4	5.13E-5	1.10E-4	2.19E-4
	0.3	7.06E-5	2.40E-5	5.69E-5	1.18E-4
	0.5	2.99E-5	8.51E-6	2.24E-5	5.50E-5
	0.7	1.60E-5	3.98E-6	1.12E-5	2.95E-5
	1	7.66E-6	1.62E-6	4.90E-6	1.38E-5
	1.5	2.96E-6	4.68E-7	1.62E-6	5.25E-6
	2	1.37E-6	1.78E-7	7.08E-7	2.46E-6
	3	4.00E-7	3.63E-8	1.72E-7	6.61E-7
	5	6.31E-8	3.47E-9	2.09E-8	1.02E-7
	7	1.53E-8	5.75E-10	4.27E-9	2.32E-8
	10	2.84E-9	6.76E-11	6.17E-10	4.27E-9

Table 8.2.6-1
Mean and Select Fractiles for Rock Hazard at Savannah: Digital Data for Figures 8.2-6a through 8.2-6c

Frequency	Spectral Accel. (g)	Mean	0.15	0.5	0.85
10 Hz	0.1	1.71E-3	7.08E-4	1.51E-3	2.82E-3
	0.15	1.13E-3	4.07E-4	9.66E-4	1.86E-3
	0.2	7.99E-4	2.51E-4	6.61E-4	1.32E-3
	0.3	4.46E-4	1.18E-4	3.31E-4	8.13E-4
	0.5	1.81E-4	3.89E-5	1.18E-4	3.31E-4
	0.7	9.06E-5	1.70E-5	5.13E-5	1.66E-4
	1	4.08E-5	6.46E-6	2.09E-5	7.00E-5
	1.5	1.53E-5	1.86E-6	6.92E-6	2.57E-5
	2	7.23E-6	7.59E-7	3.02E-6	1.12E-5
	3	2.30E-6	2.04E-7	9.33E-7	3.47E-6
	5	4.44E-7	3.16E-8	1.66E-7	6.84E-7
	7	1.31E-7	8.51E-9	4.79E-8	2.04E-7
	10	3.17E-8	1.74E-9	1.12E-8	5.13E-8
1 Hz	0.01	2.88E-3	1.32E-3	2.63E-3	4.57E-3
	0.015	2.10E-3	8.41E-4	1.86E-3	3.47E-3
	0.02	1.68E-3	5.75E-4	1.51E-3	2.82E-3
	0.03	1.18E-3	3.31E-4	1.00E-3	2.00E-3
	0.05	6.82E-4	1.26E-4	5.01E-4	1.27E-3
	0.07	4.37E-4	5.89E-5	2.88E-4	8.41E-4
	0.1	2.50E-4	2.40E-5	1.35E-4	5.01E-4
	0.15	1.19E-4	7.94E-6	5.13E-5	2.34E-4
	0.2	6.51E-5	3.24E-6	2.24E-5	1.26E-4
	0.3	2.53E-5	9.02E-7	6.46E-6	4.47E-5
	0.5	6.52E-6	1.55E-7	1.23E-6	9.44E-6
	0.7	2.41E-6	4.17E-8	3.80E-7	3.02E-6
	1	7.64E-7	9.77E-9	1.10E-7	8.13E-7

Frequency	Spectral Accel. (g)	Mean	0.15	0.5	0.85
PGA	0.1	8.13E-4	2.34E-4	6.17E-4	1.41E-3
	0.15	4.46E-4	1.02E-4	3.09E-4	8.13E-4
	0.2	2.70E-4	5.50E-5	1.66E-4	5.01E-4
	0.3	1.22E-4	1.95E-5	6.76E-5	2.19E-4
	0.5	3.99E-5	4.90E-6	1.95E-5	7.00E-5
	0.7	1.81E-5	1.86E-6	7.94E-6	2.95E-5
	1	7.37E-6	6.61E-7	2.92E-6	1.25E-5
	1.5	2.40E-6	1.72E-7	8.71E-7	3.98E-6
	2	9.94E-7	6.10E-8	3.55E-7	1.62E-6
	3	2.50E-7	1.20E-8	7.76E-8	3.80E-7
	5	3.40E-8	1.04E-9	8.51E-9	5.13E-8
	7	7.66E-9	1.66E-10	1.68E-9	1.08E-8
	10	1.34E-9	1.82E-11	2.34E-10	1.86E-9

Table 8.2.7-1
Mean and Select Fractiles for Rock Hazard at Topeka: Digital Data for Figures 8.2-7a through 8.2-7c

Frequency	Spectral Accel. (g)	Mean	0.15	0.5	0.85
10 Hz	0.1	4.11E-4	1.45E-4	2.88E-4	5.75E-4
	0.15	2.13E-4	7.24E-5	1.55E-4	3.09E-4
	0.2	1.32E-4	4.47E-5	1.02E-4	1.91E-4
	0.3	6.67E-5	2.24E-5	5.13E-5	1.02E-4
	0.5	2.81E-5	9.12E-6	2.24E-5	4.47E-5
	0.7	1.56E-5	4.57E-6	1.29E-5	2.57E-5
	1	8.08E-6	2.14E-6	6.24E-6	1.38E-5
	1.5	3.55E-6	8.13E-7	2.63E-6	6.46E-6
	2	1.85E-6	3.55E-7	1.32E-6	3.24E-6
	3	6.66E-7	1.02E-7	4.37E-7	1.23E-6
	5	1.49E-7	1.48E-8	8.32E-8	2.69E-7
	7	4.84E-8	3.24E-9	2.48E-8	8.91E-8
	10	1.29E-8	5.19E-10	5.62E-9	2.40E-8
1 Hz	0.01	2.32E-3	6.17E-4	1.74E-3	4.12E-3
	0.015	1.42E-3	2.69E-4	9.33E-4	2.63E-3
	0.02	9.55E-4	1.50E-4	5.37E-4	1.86E-3
	0.03	5.00E-4	5.89E-5	2.19E-4	9.02E-4
	0.05	1.92E-4	1.59E-5	6.31E-5	2.69E-4
	0.07	9.44E-5	6.68E-6	2.75E-5	1.10E-4
	0.1	4.13E-5	2.63E-6	1.12E-5	4.47E-5
	0.15	1.46E-5	8.13E-7	3.98E-6	1.59E-5
	0.2	6.63E-6	3.09E-7	1.86E-6	7.94E-6
	0.3	2.08E-6	6.76E-8	6.61E-7	3.02E-6
	0.5	4.85E-7	6.68E-9	1.55E-7	8.71E-7
	0.7	1.89E-7	1.37E-9	5.31E-8	3.67E-7
	1	6.87E-8	2.19E-10	1.59E-8	1.35E-7

Frequency	Spectral Accel. (g)	Mean	0.15	0.5	0.85
PGA	0.01	4.03E-3	1.51E-3	3.02E-3	6.46E-3
	0.015	2.46E-3	8.71E-4	1.74E-3	4.27E-3
	0.02	1.67E-3	5.37E-4	1.11E-3	2.82E-3
	0.03	9.14E-4	2.88E-4	5.75E-4	1.51E-3
	0.05	4.10E-4	1.18E-4	2.69E-4	6.17E-4
	0.07	2.40E-4	6.76E-5	1.66E-4	3.55E-4
	0.1	1.35E-4	3.89E-5	9.55E-5	2.04E-4
	0.15	6.97E-5	2.09E-5	5.13E-5	1.10E-4
	0.2	4.40E-5	1.29E-5	3.39E-5	7.24E-5
	0.3	2.31E-5	6.24E-6	1.82E-5	3.89E-5
	0.5	9.77E-6	2.14E-6	6.92E-6	1.76E-5
	0.7	5.24E-6	9.33E-7	3.47E-6	9.77E-6
	1	2.51E-6	3.43E-7	1.41E-6	4.57E-6

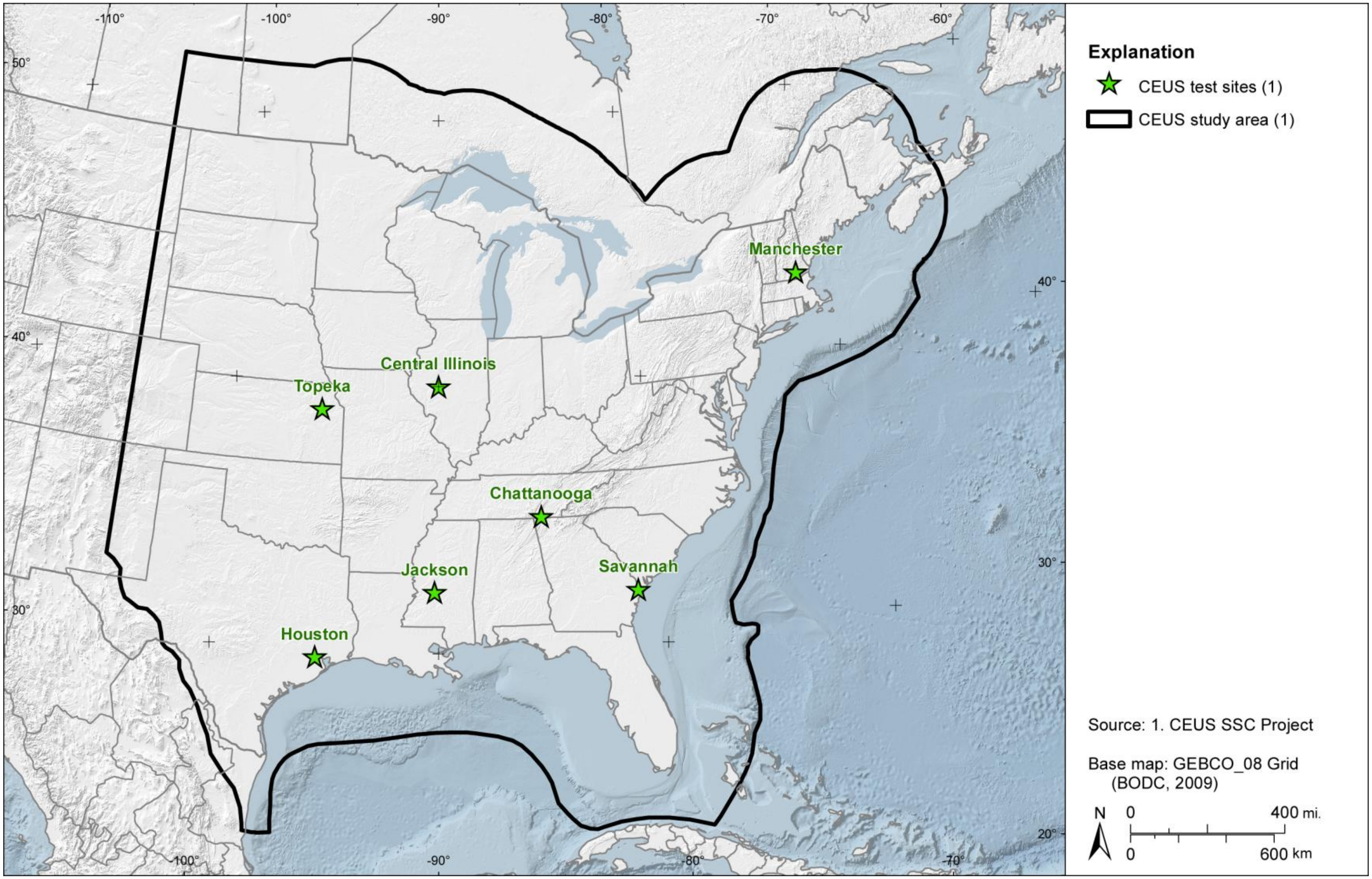

Figure 8.1-1
Map showing the study area and seven test sites for the CEUS SSC Project

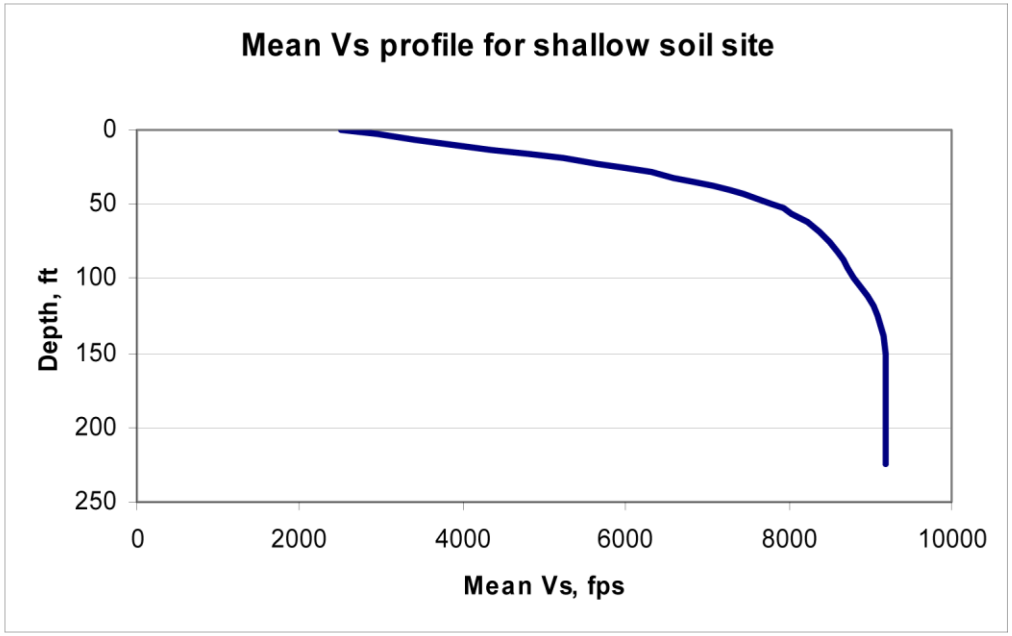

Figure 8.1-2
Mean V_S profile for shallow soil site

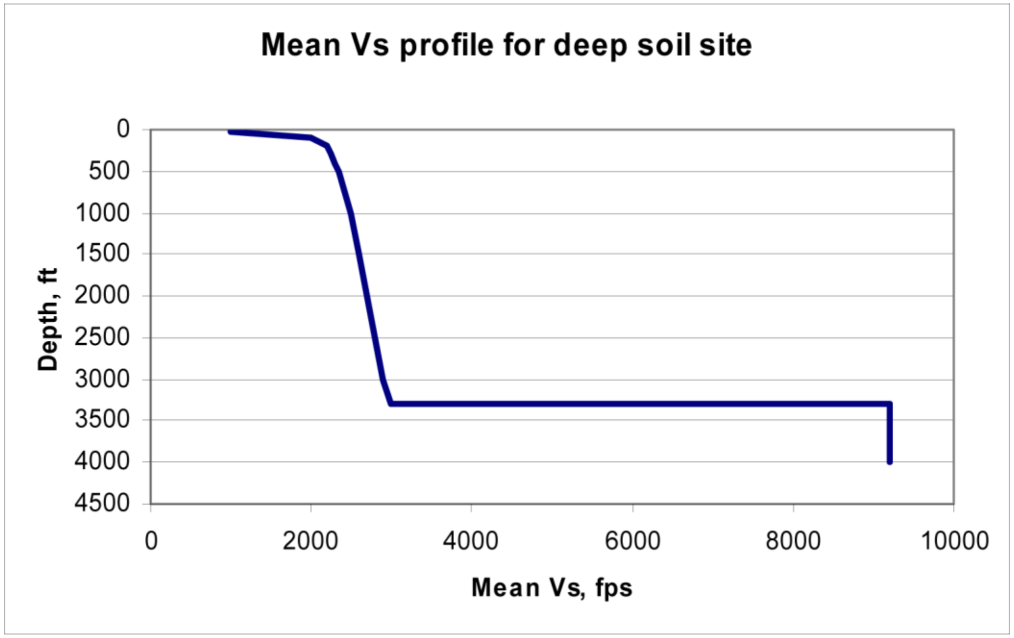

Figure 8.1-3
Mean V_S profile for deep soil site

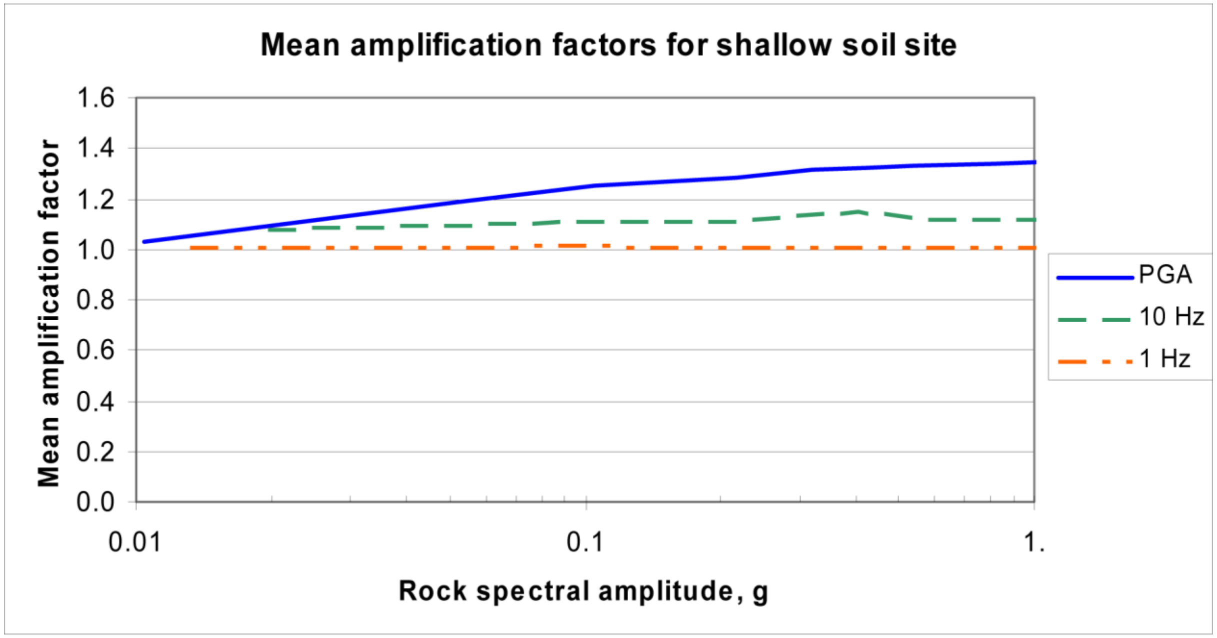

Figure 8.1-4
Mean amplification factors for shallow soil site

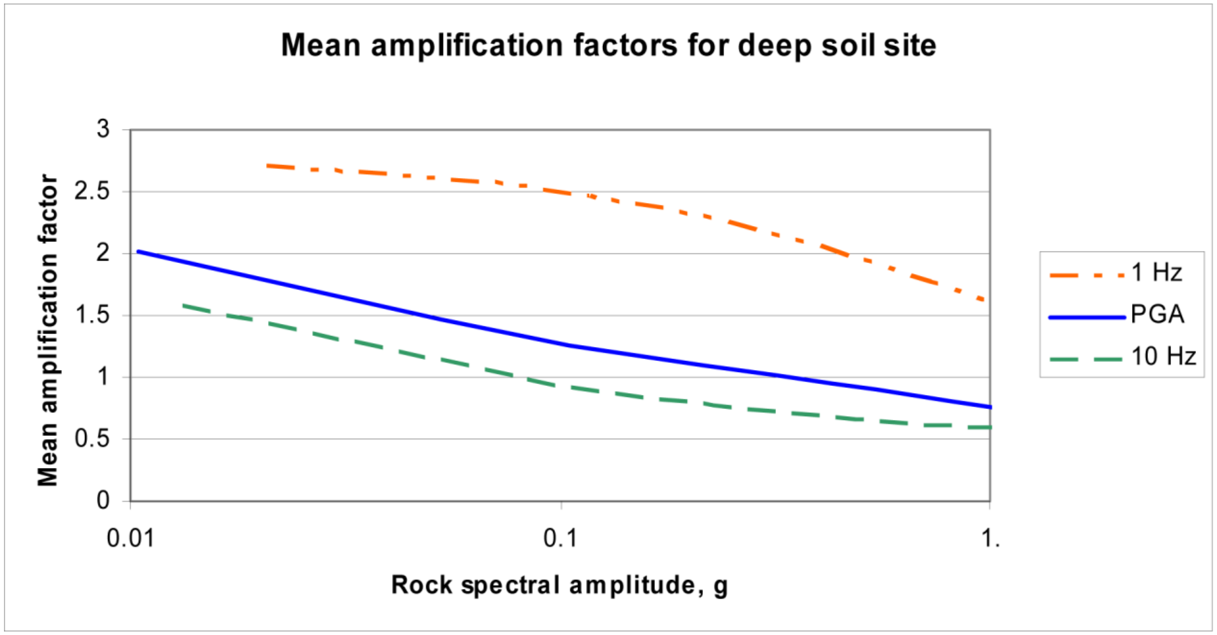

Figure 8.1-5
Mean amplification factors for deep soil site

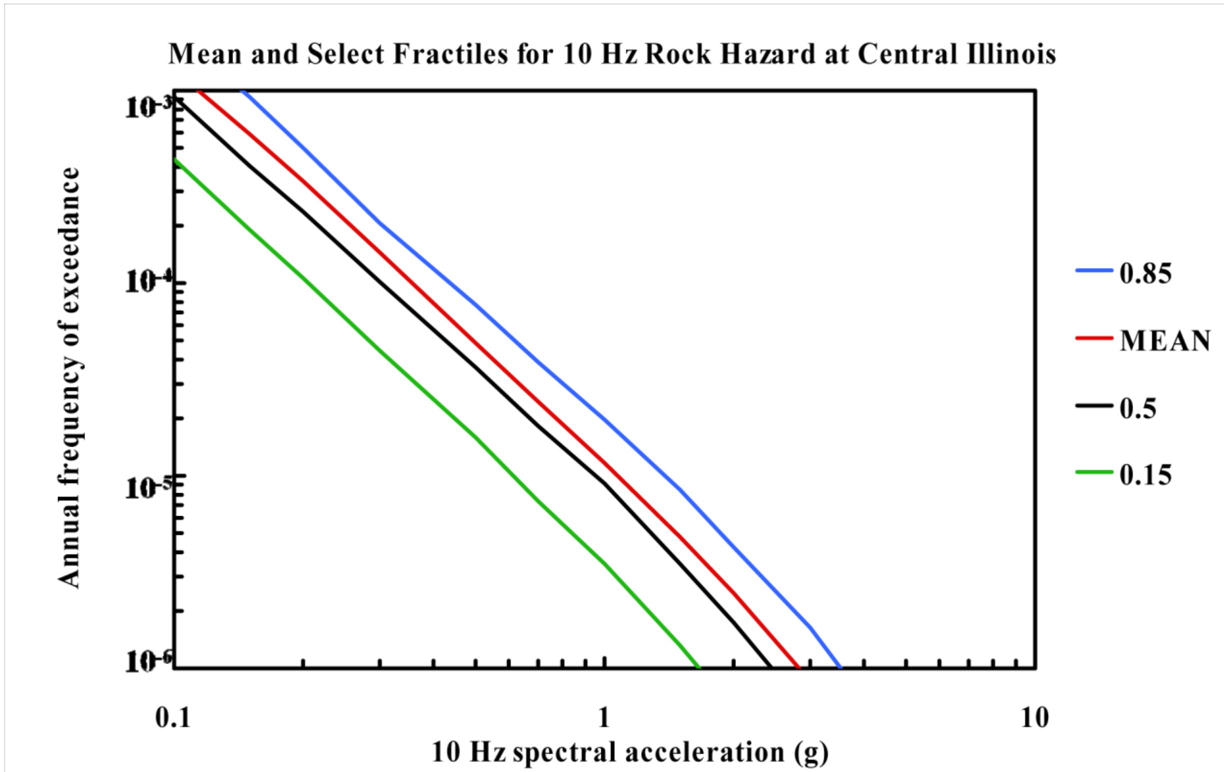

Figure 8.2-1a
Central Illinois 10 Hz rock hazard: mean and fractile total hazard

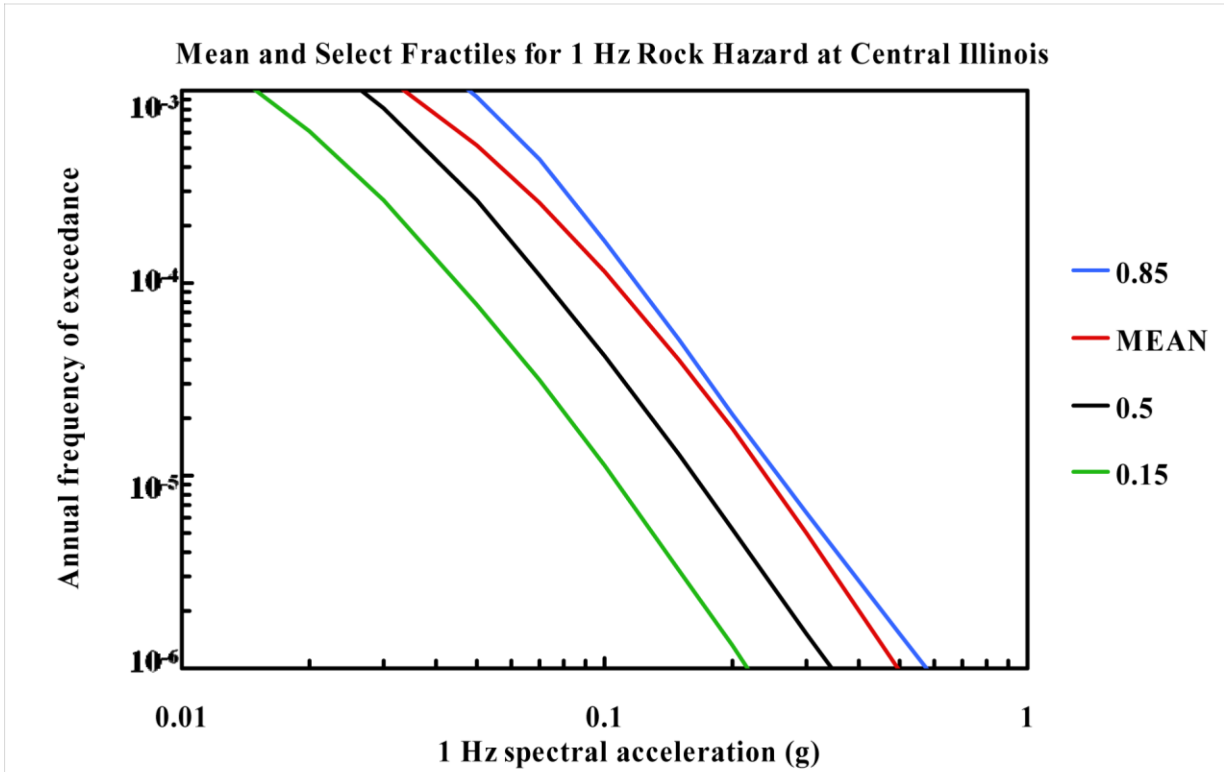

Figure 8.2-1b
Central Illinois 1 Hz rock hazard: mean and fractile total hazard

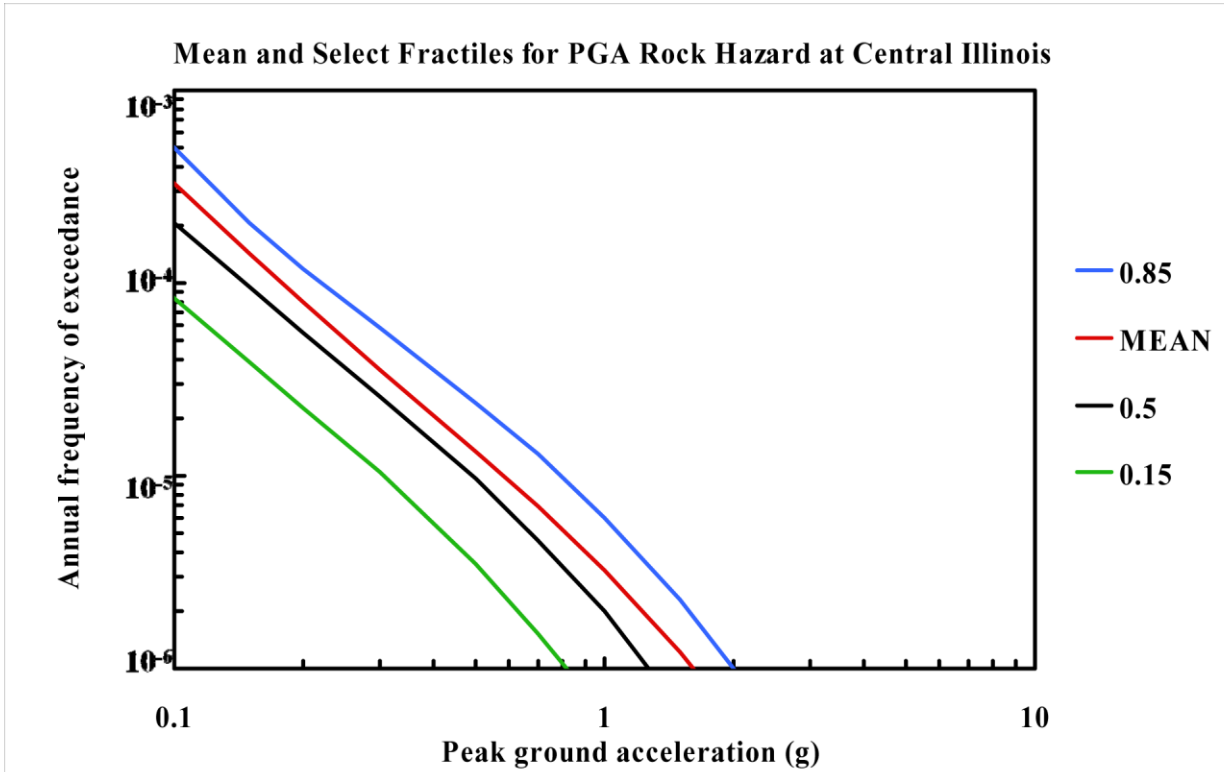

Figure 8.2-1c
Central Illinois PGA rock hazard: mean and fractile total hazard

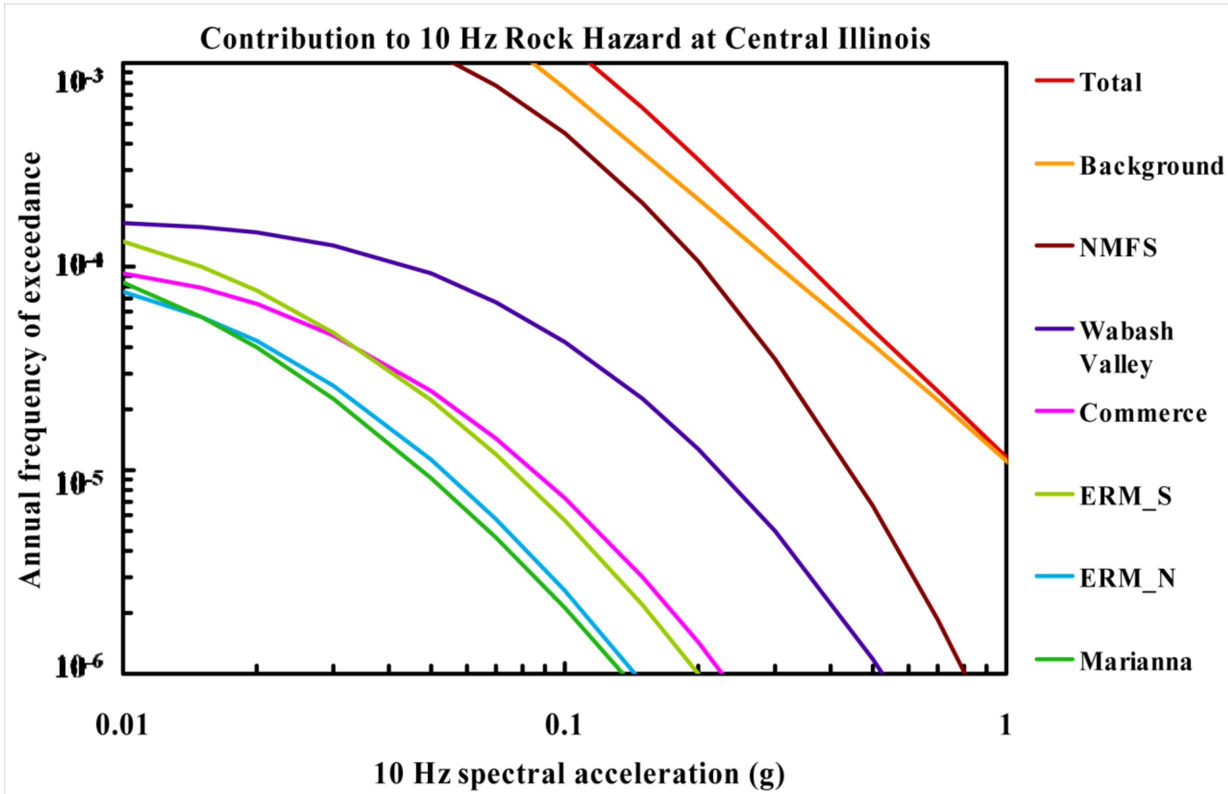

Figure 8.2-1d
Central Illinois 10 Hz rock hazard: total and contribution by RLME and background

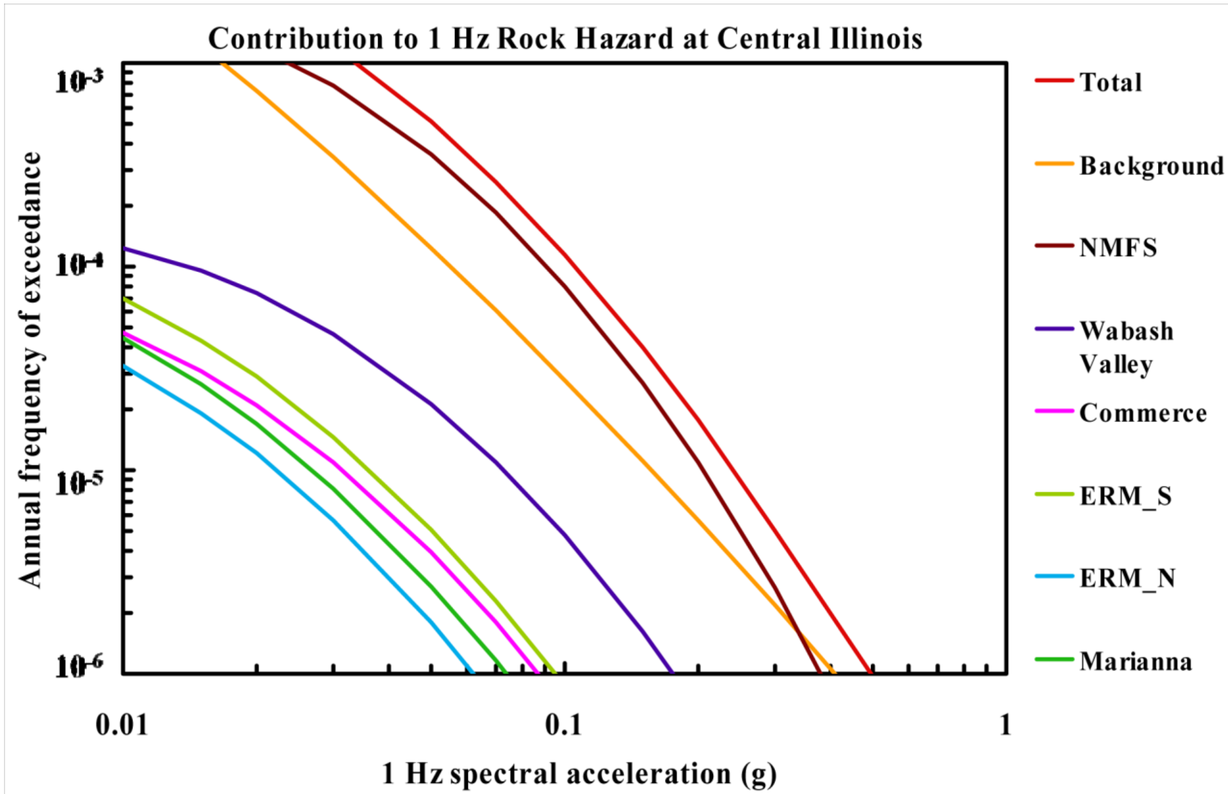

Figure 8.2-1e
Central Illinois 1 Hz rock hazard: total and contribution by RLME and background

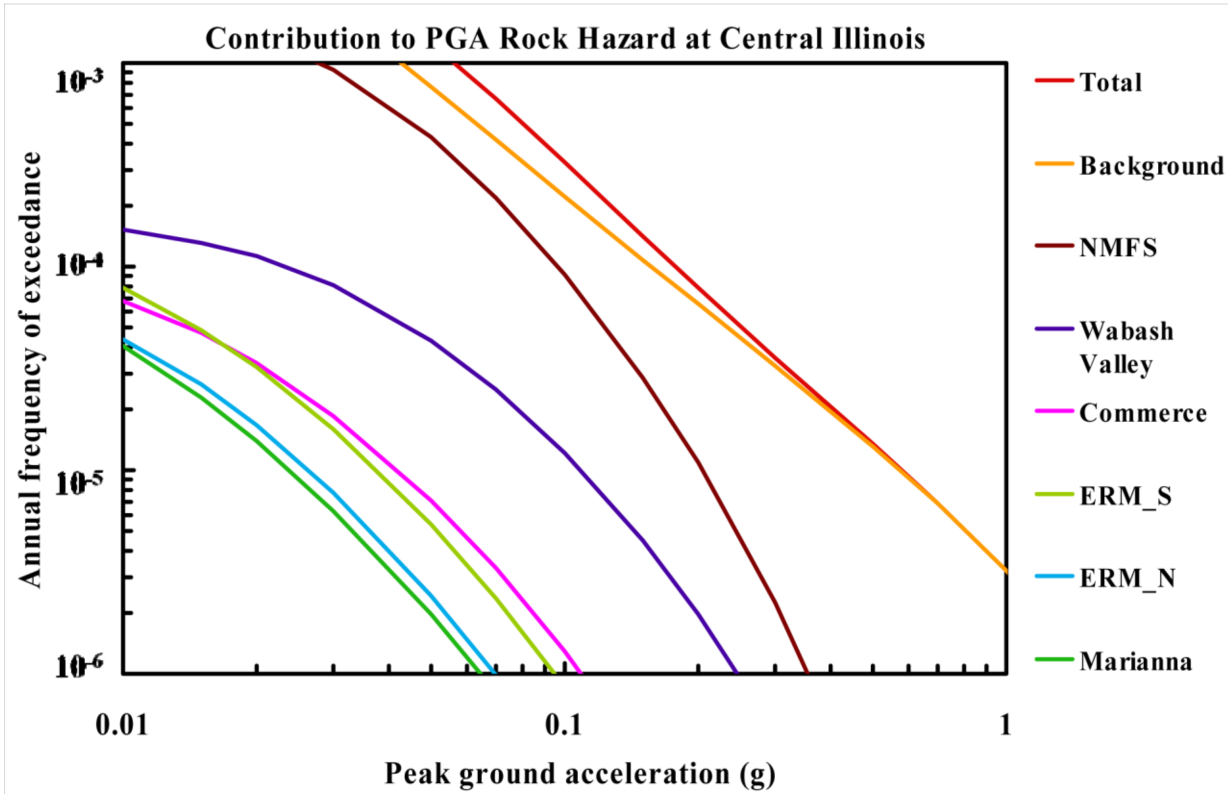

Figure 8.2-1f
Central Illinois PGA rock hazard: total and contribution by RLME and background

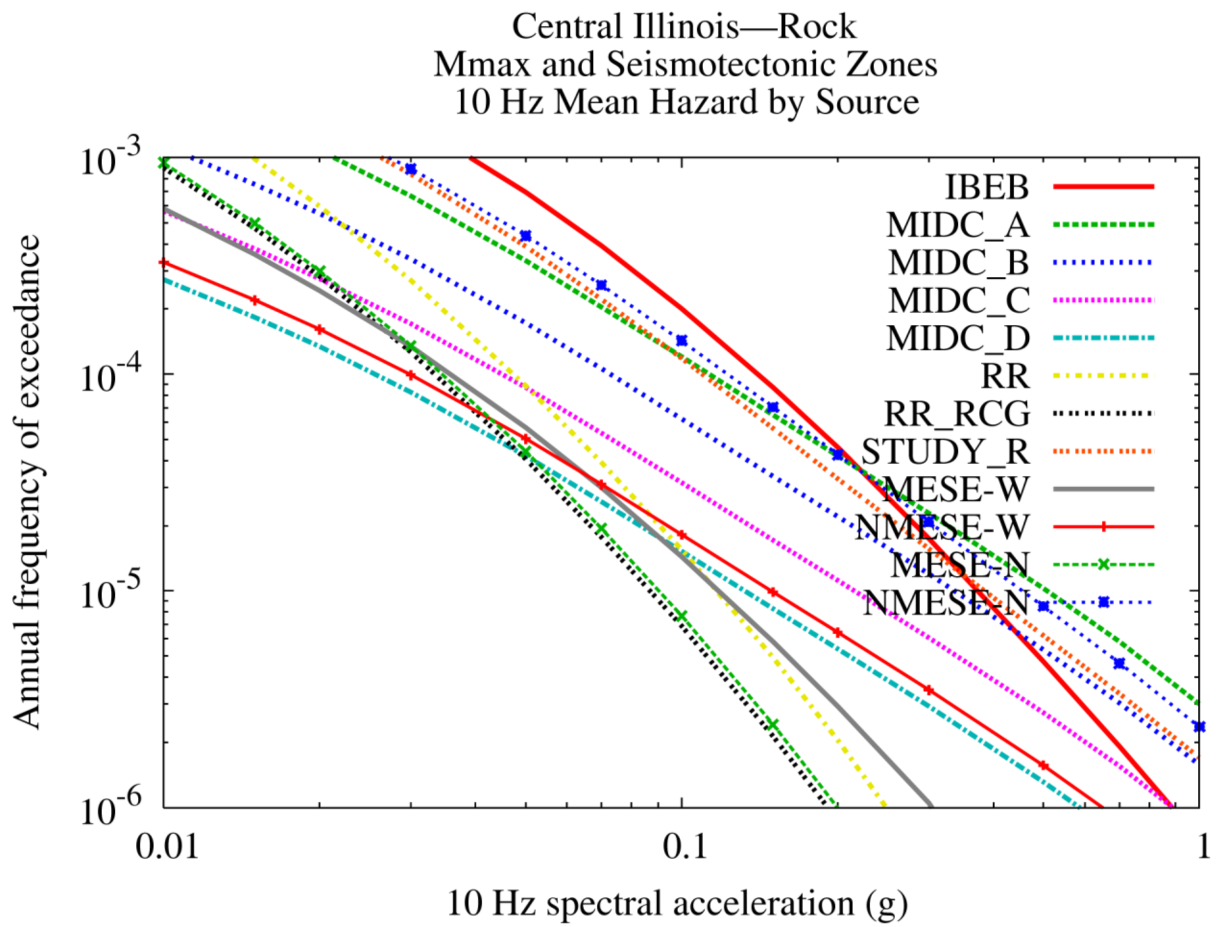

Figure 8.2-1g
Central Illinois 10 Hz rock hazard: contribution by background source

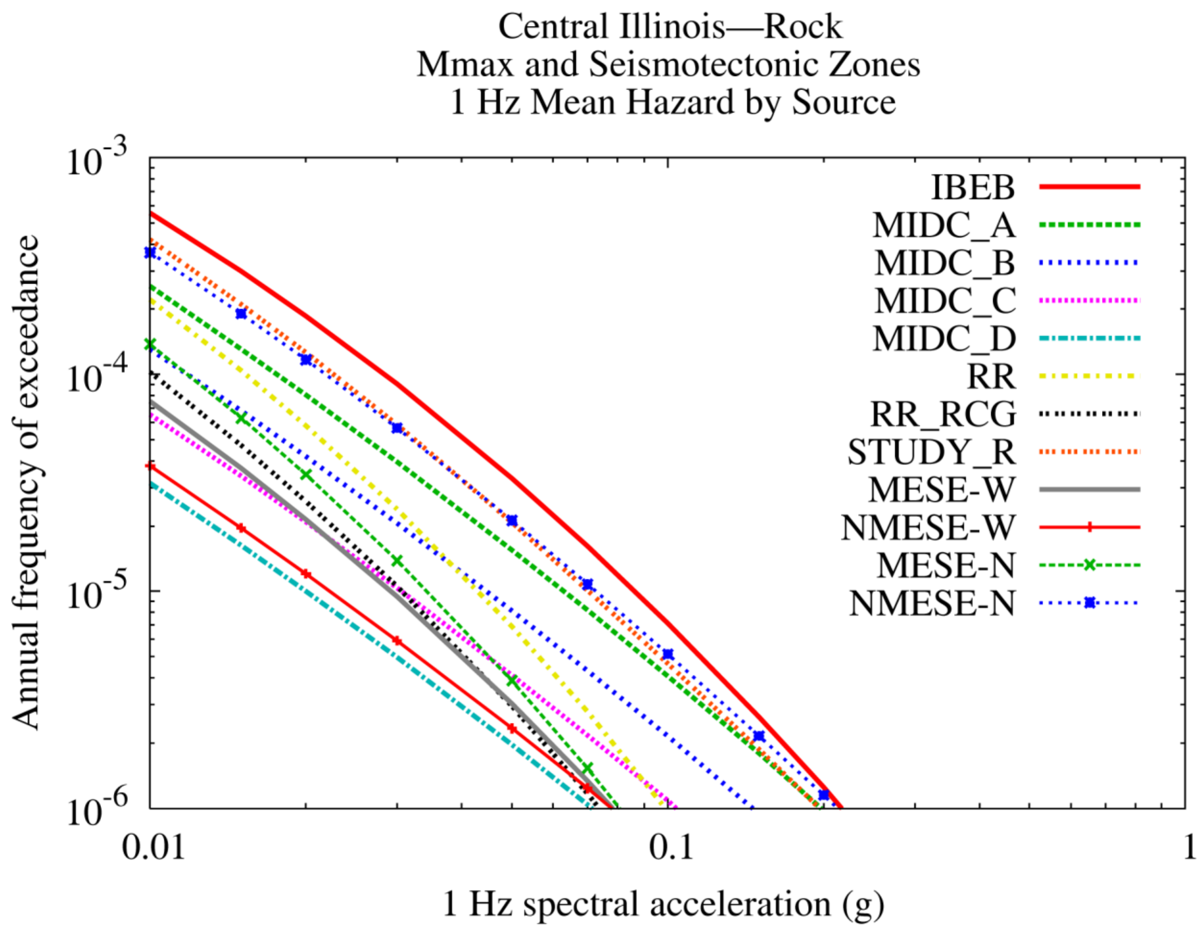

Figure 8.2-1h
Central Illinois 1 Hz rock hazard: contribution by background source

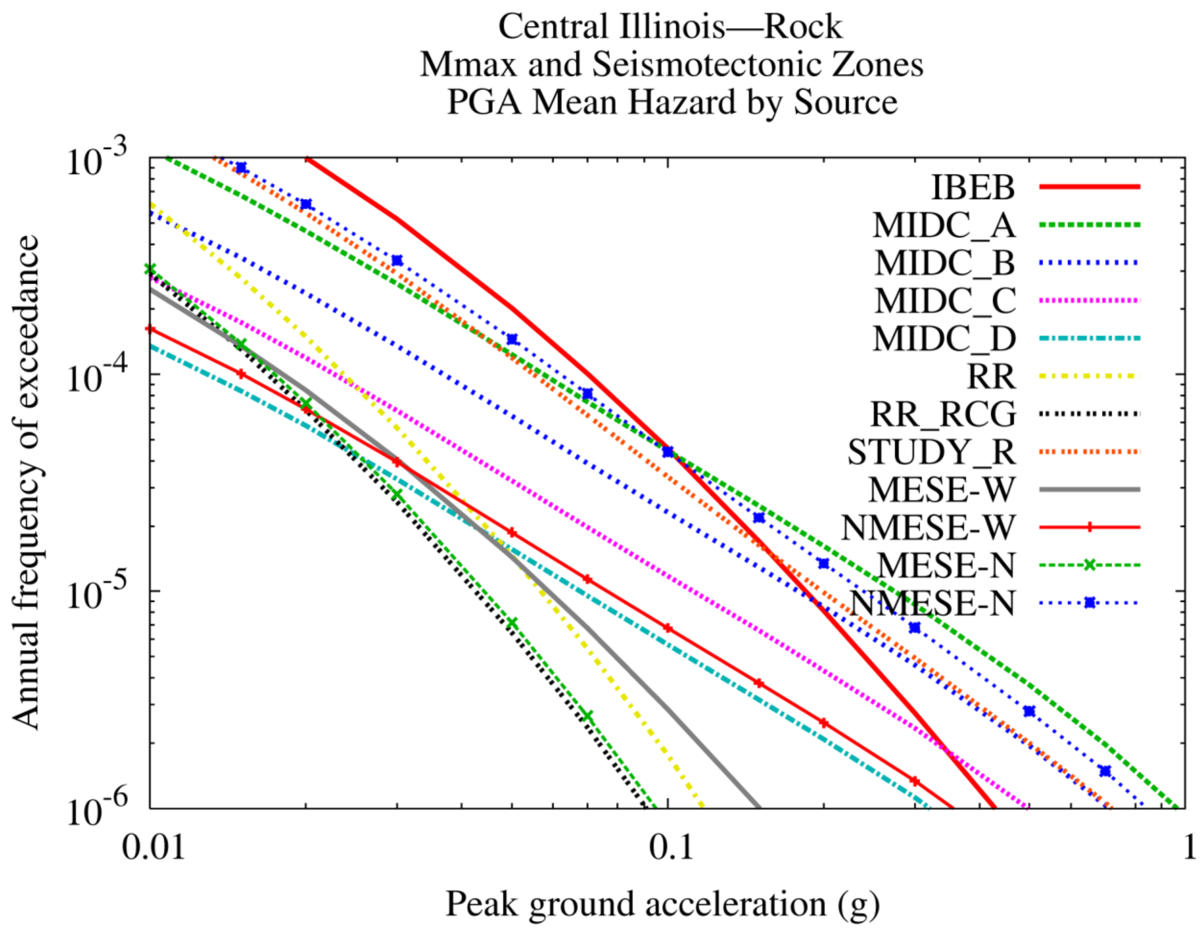

Figure 8.2-1i
Central Illinois PGA rock hazard: contribution by background source

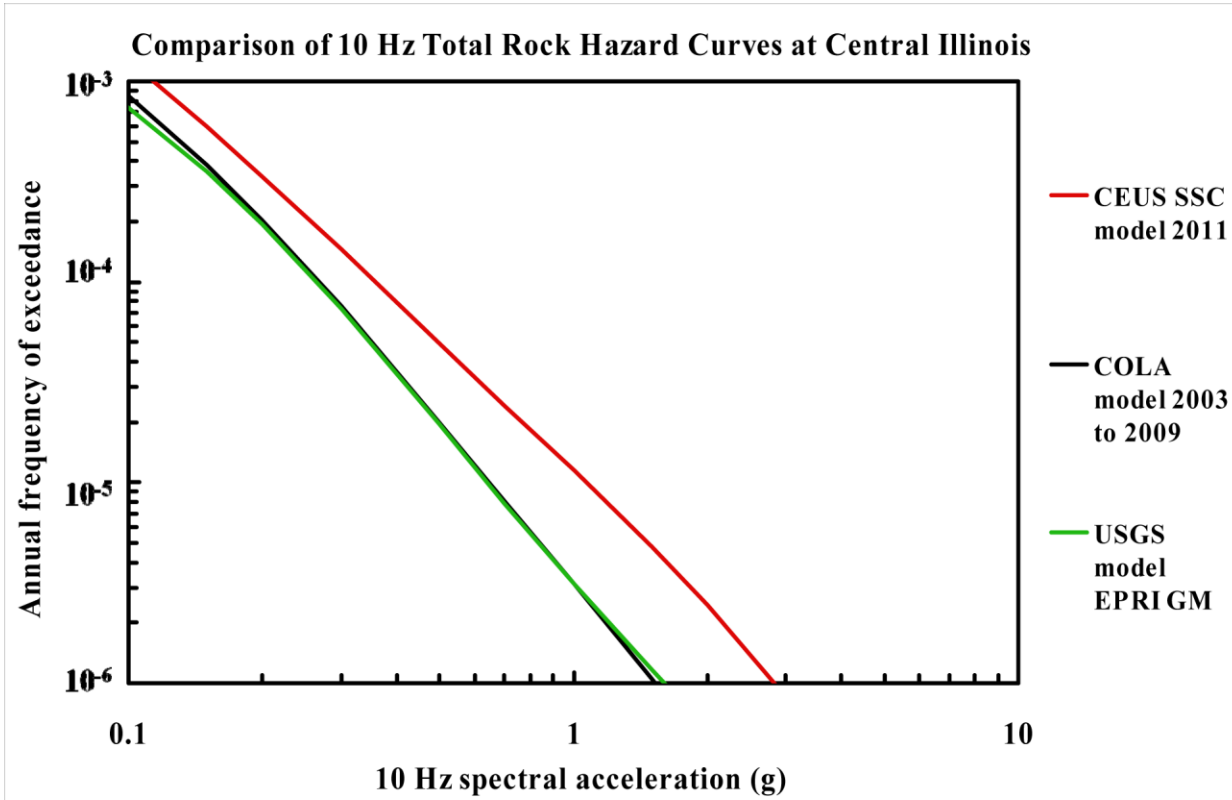

Figure 8.2-1j
Central Illinois 10 Hz rock hazard: comparison of three source models

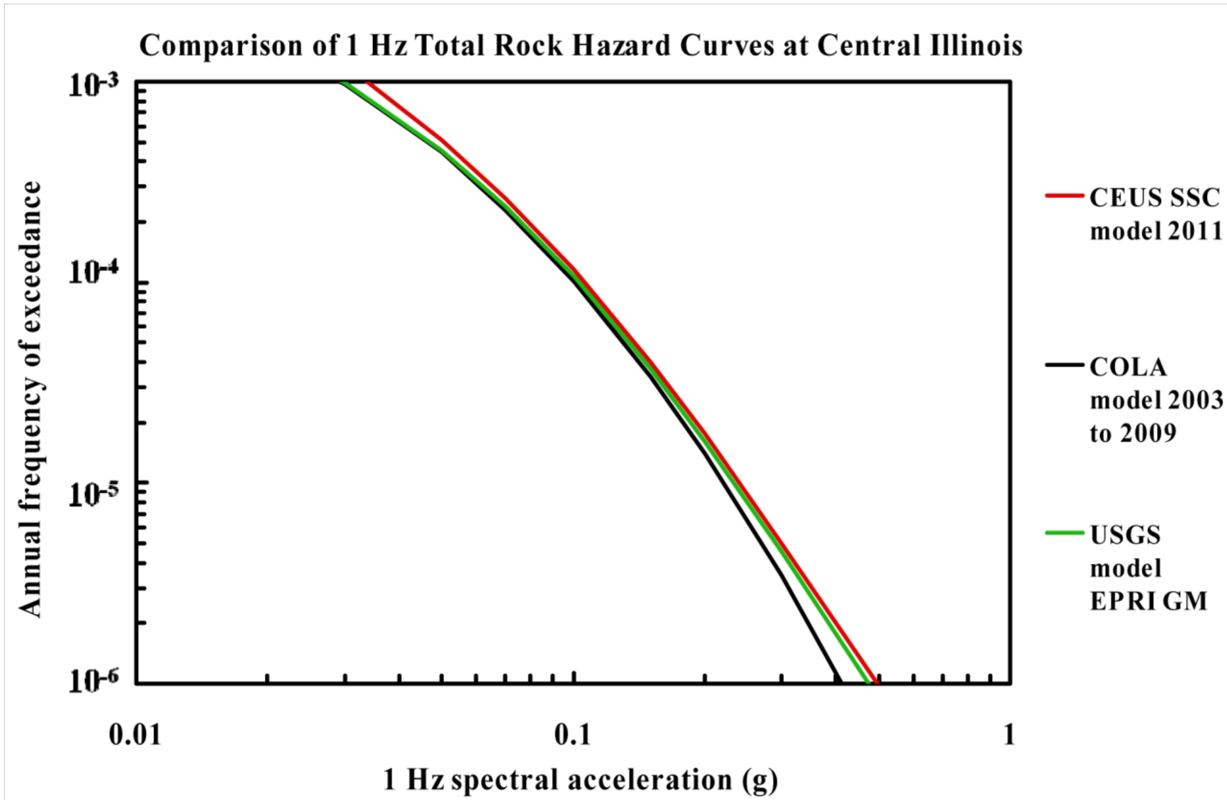

Figure 8.2-1k
Central Illinois 1 Hz rock hazard: comparison of three source models

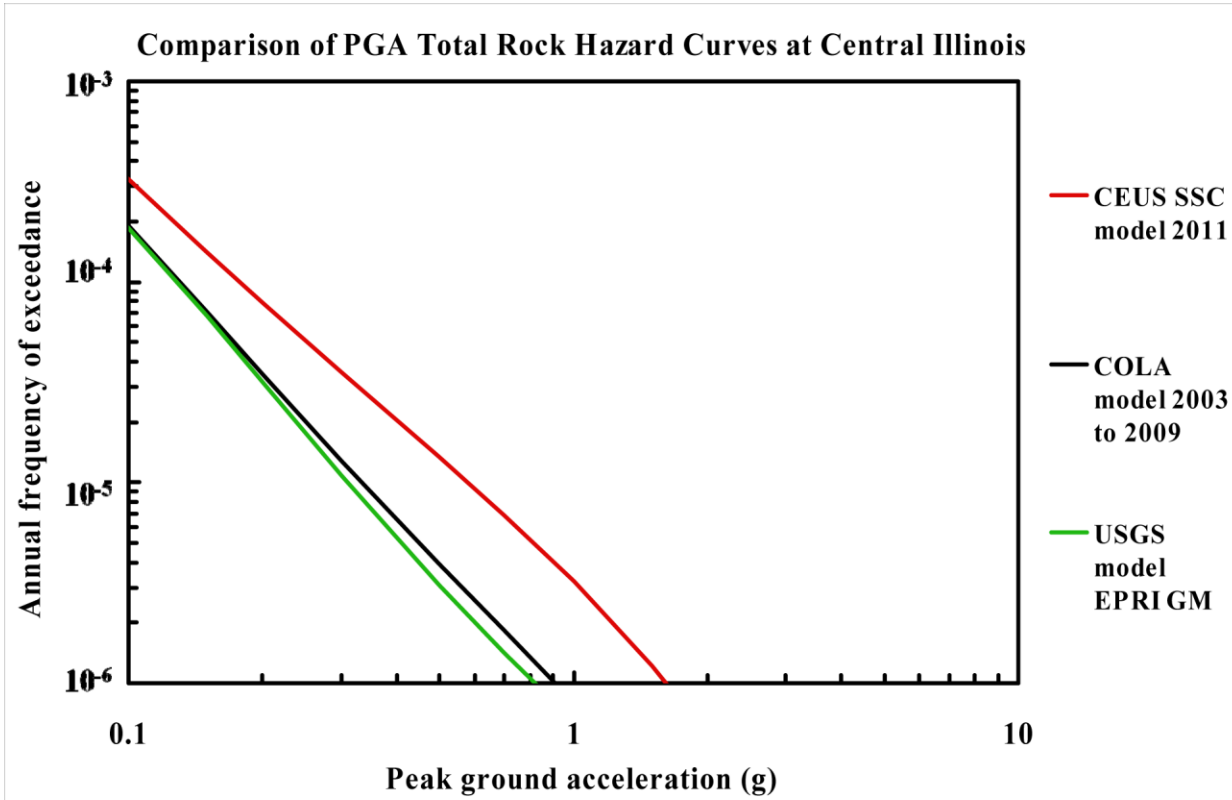

Figure 8.2-1l
Central Illinois PGA rock hazard: comparison of three source models

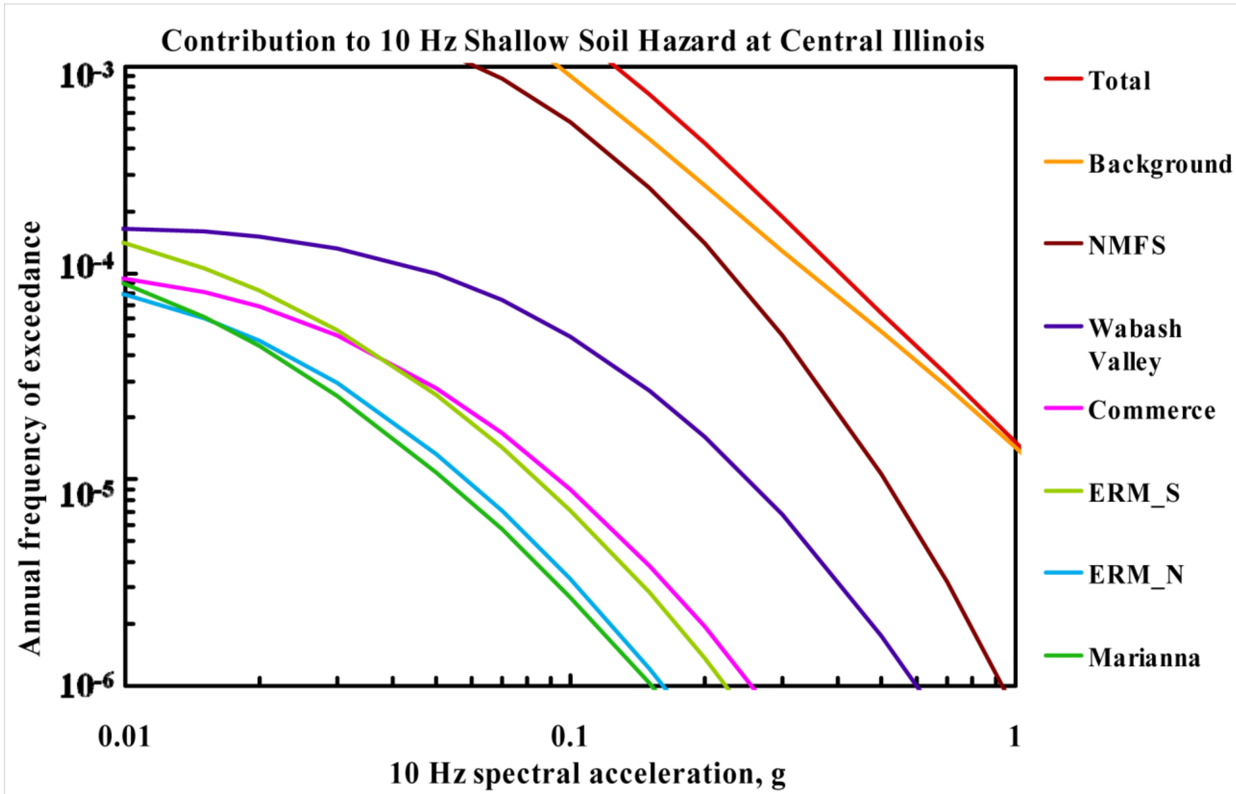

Figure 8.2-1m
Central Illinois 10 Hz shallow soil hazard: total and total and contribution by RLME and background

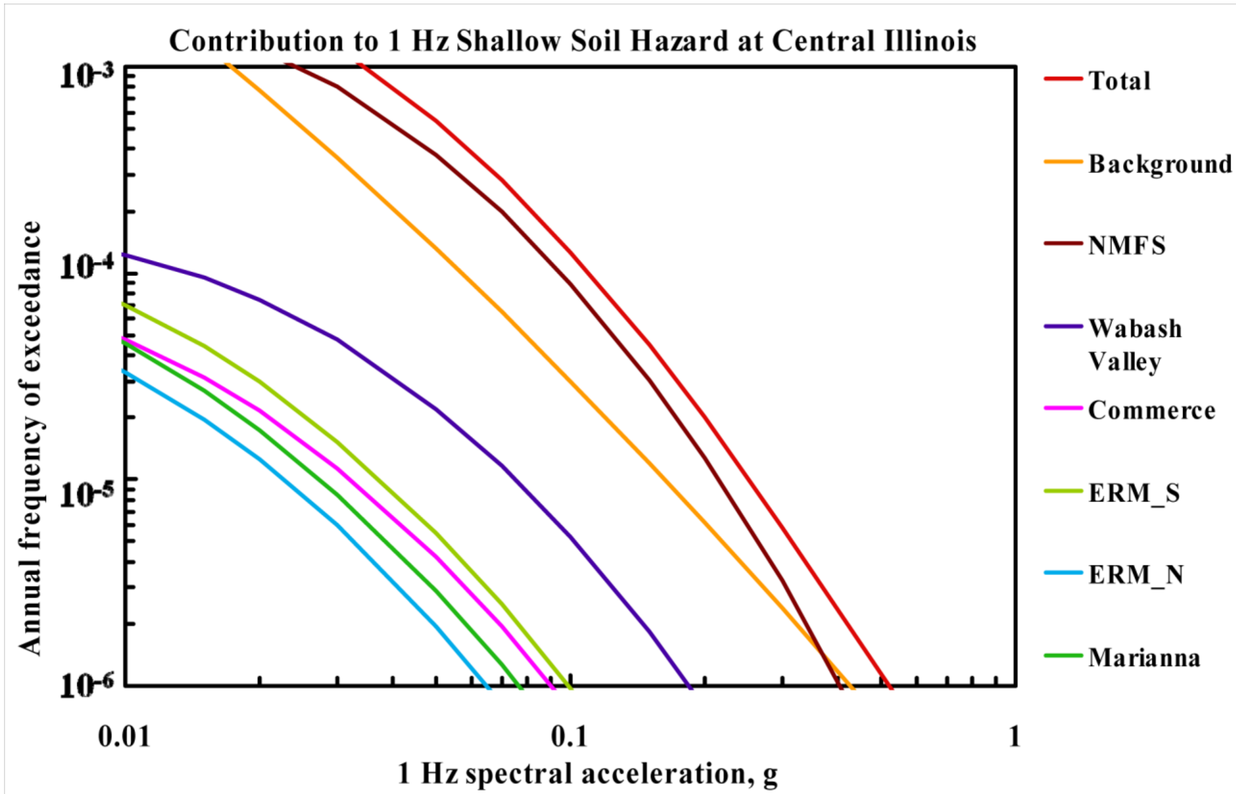

Figure 8.2-1n
Central Illinois 1 Hz shallow soil hazard: total and contribution by RLME and background

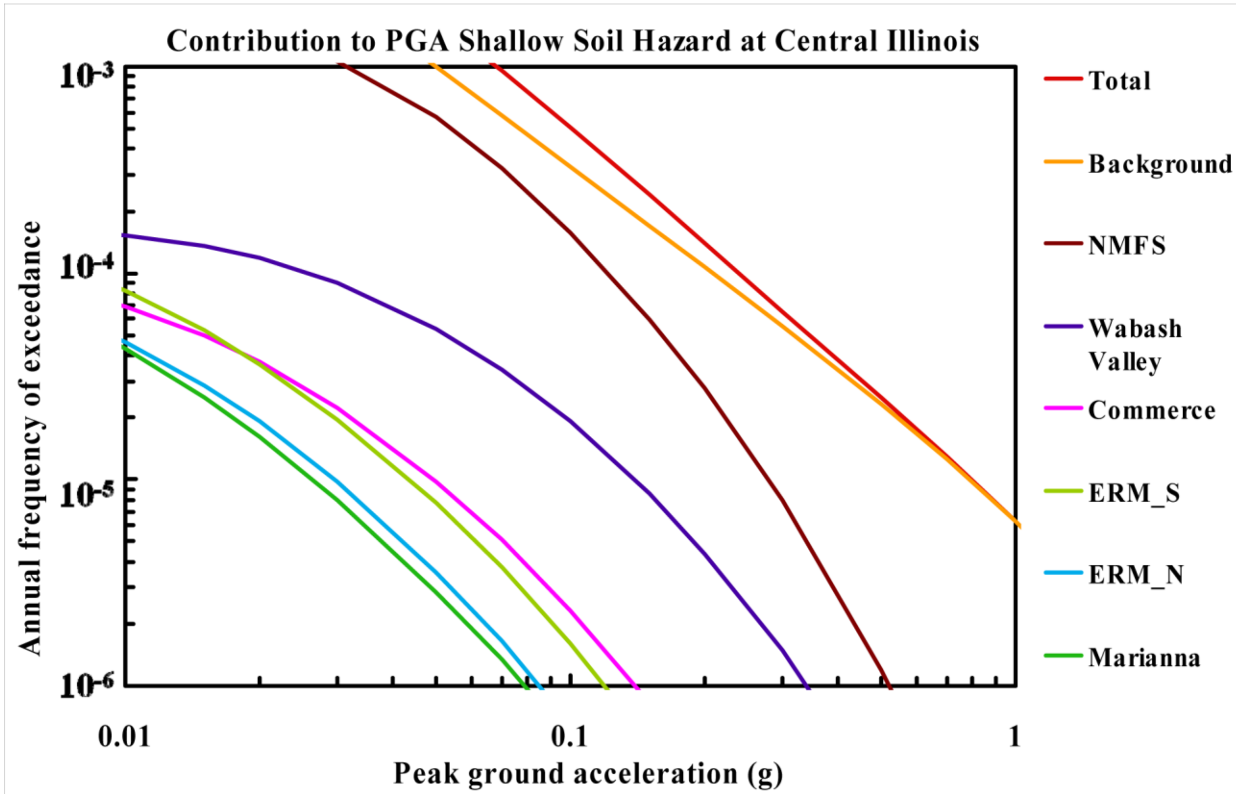

Figure 8.2-1o
Central Illinois PGA shallow soil hazard: total and contribution by RLME and background

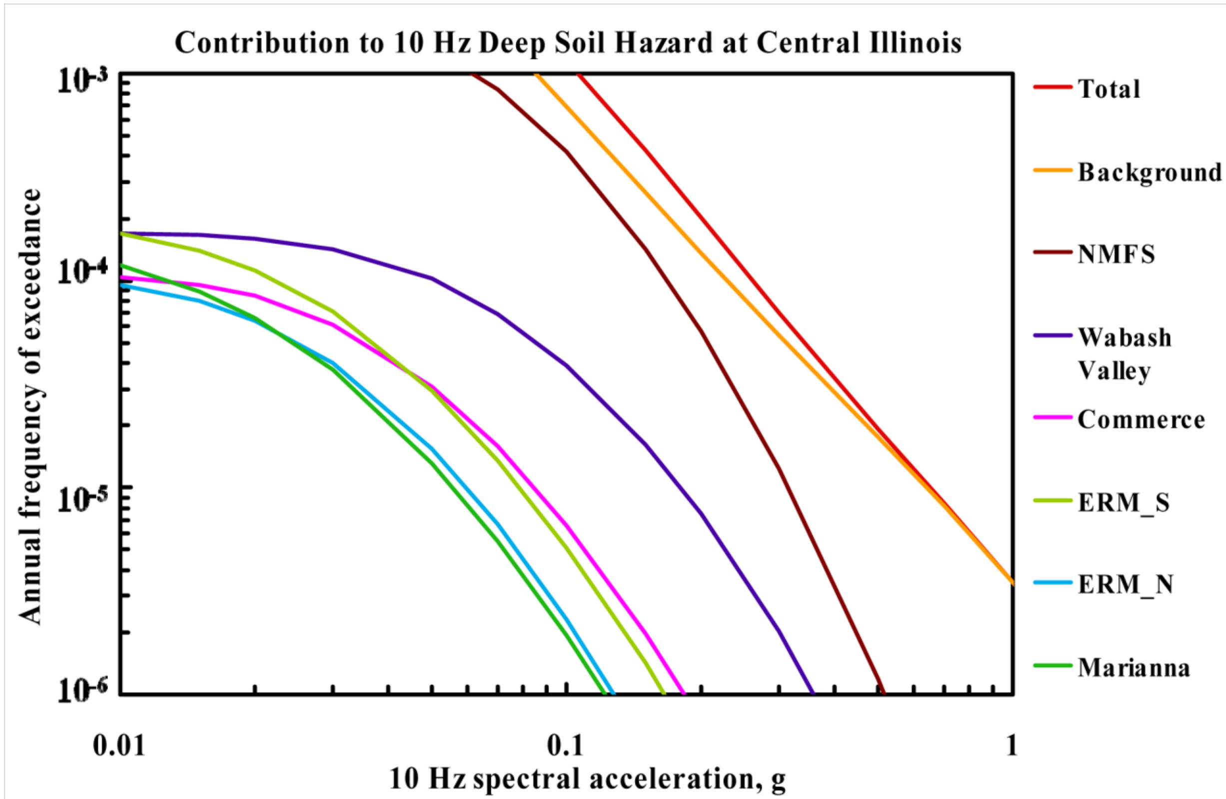

Figure 8.2-1p
Central Illinois 10 Hz deep soil hazard: total and contribution by RLME and background

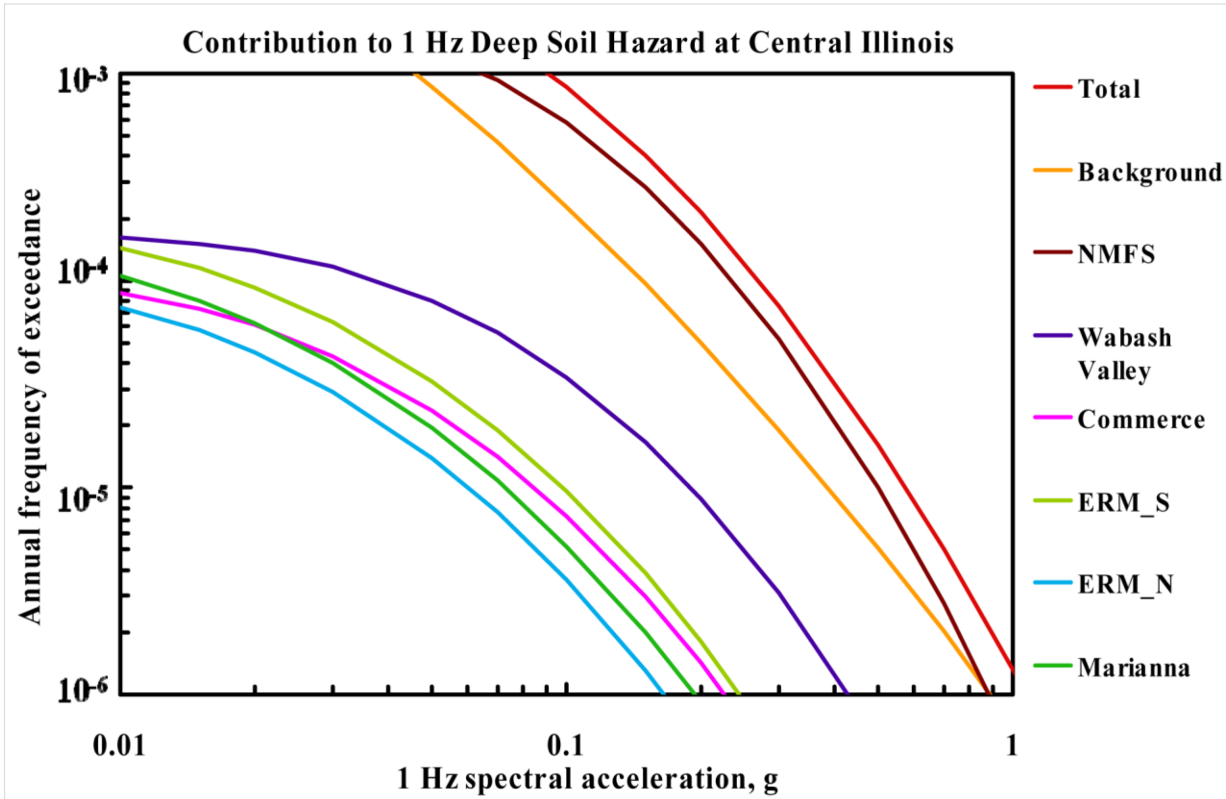

Figure 8.2-1q
Central Illinois 1 Hz deep soil hazard: total and contribution by RLME and background

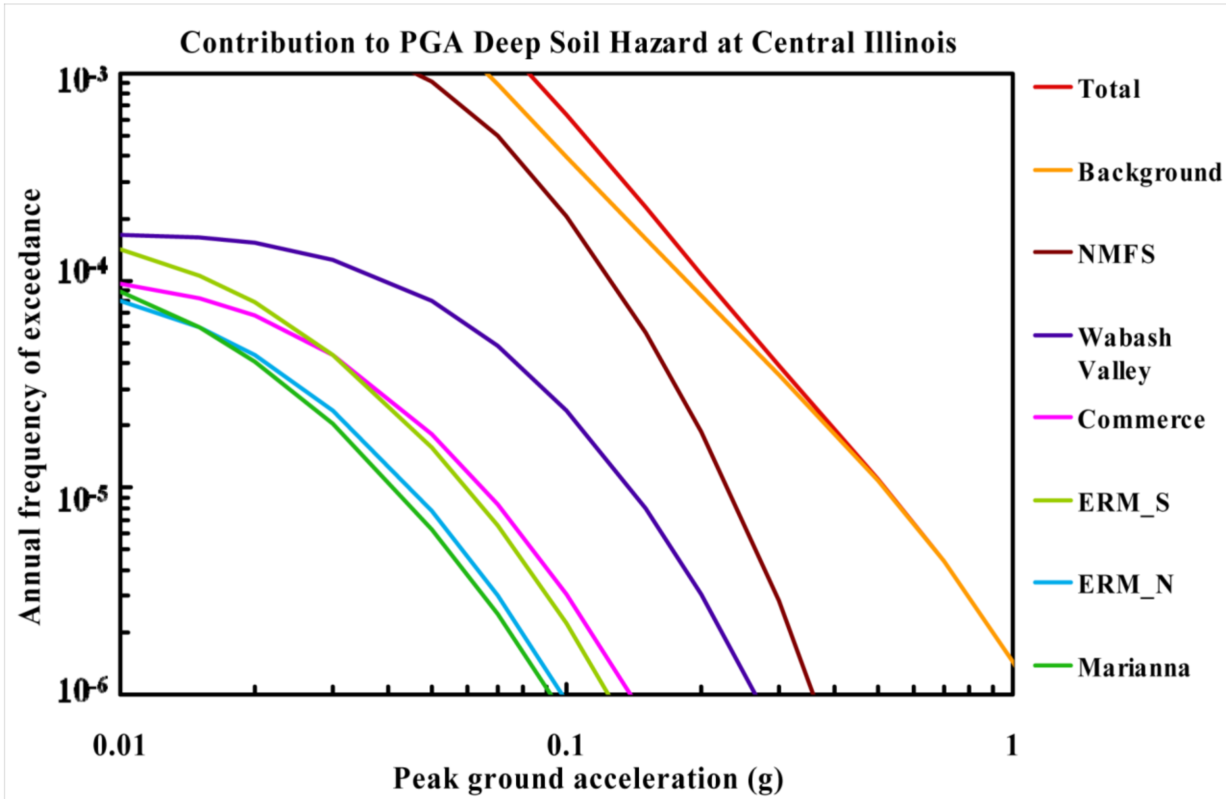

Figure 8.2-1r
Central Illinois PGA deep soil hazard: total and contribution by RLME and background

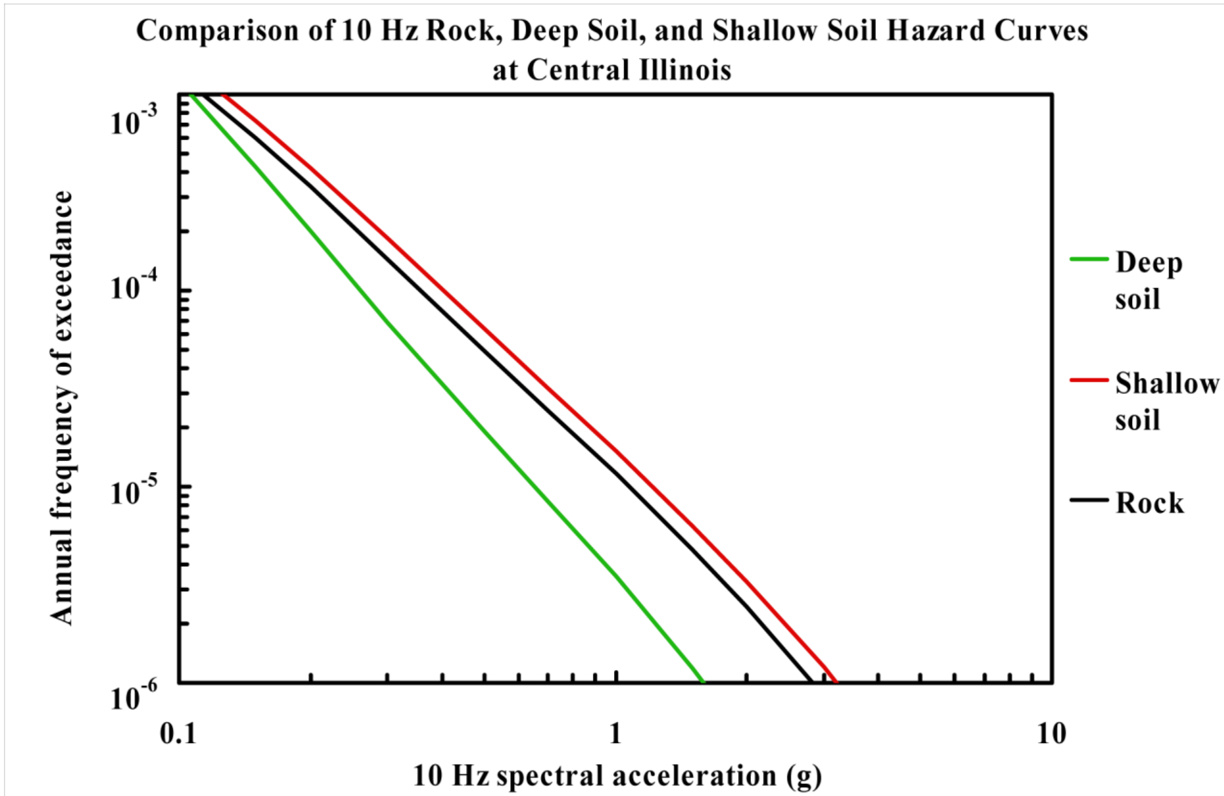

Figure 8.2-1s
Central Illinois 10 Hz hazard: comparison of three site conditions

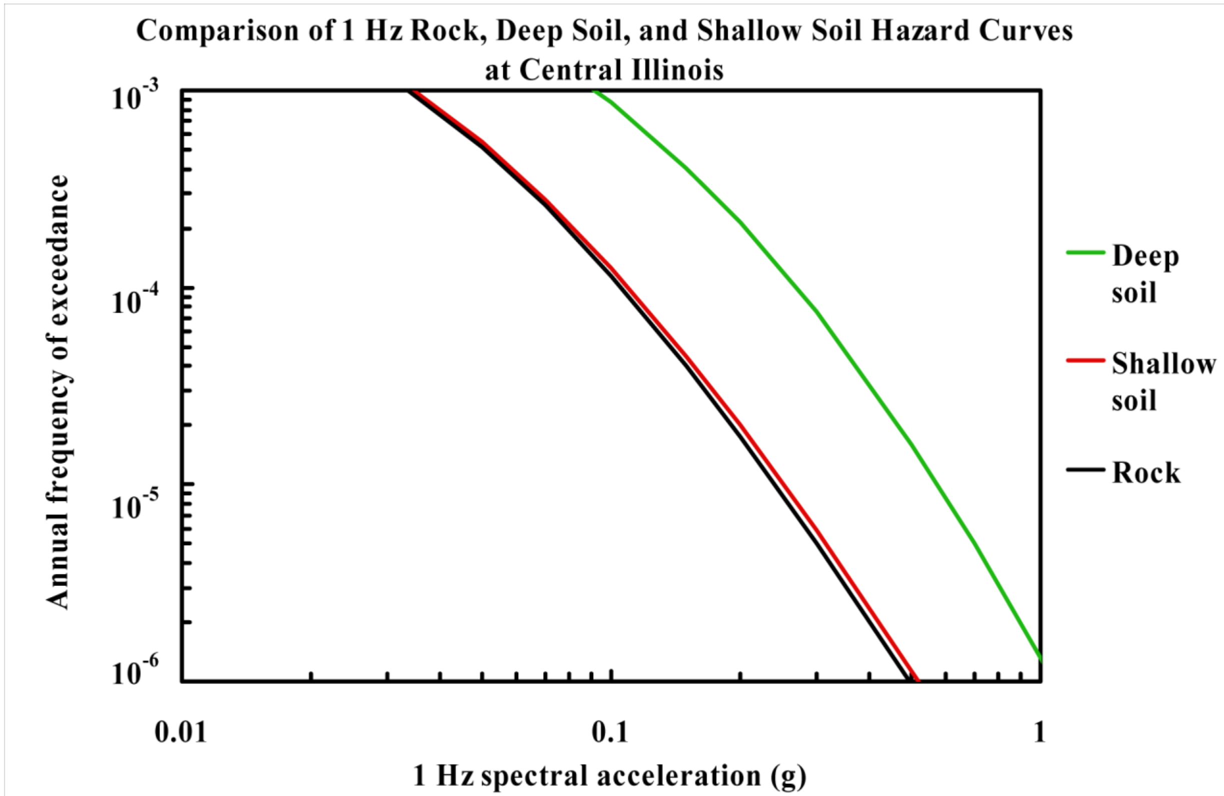

Figure 8.2-1t
Central Illinois 1 Hz hazard: comparison of three site conditions

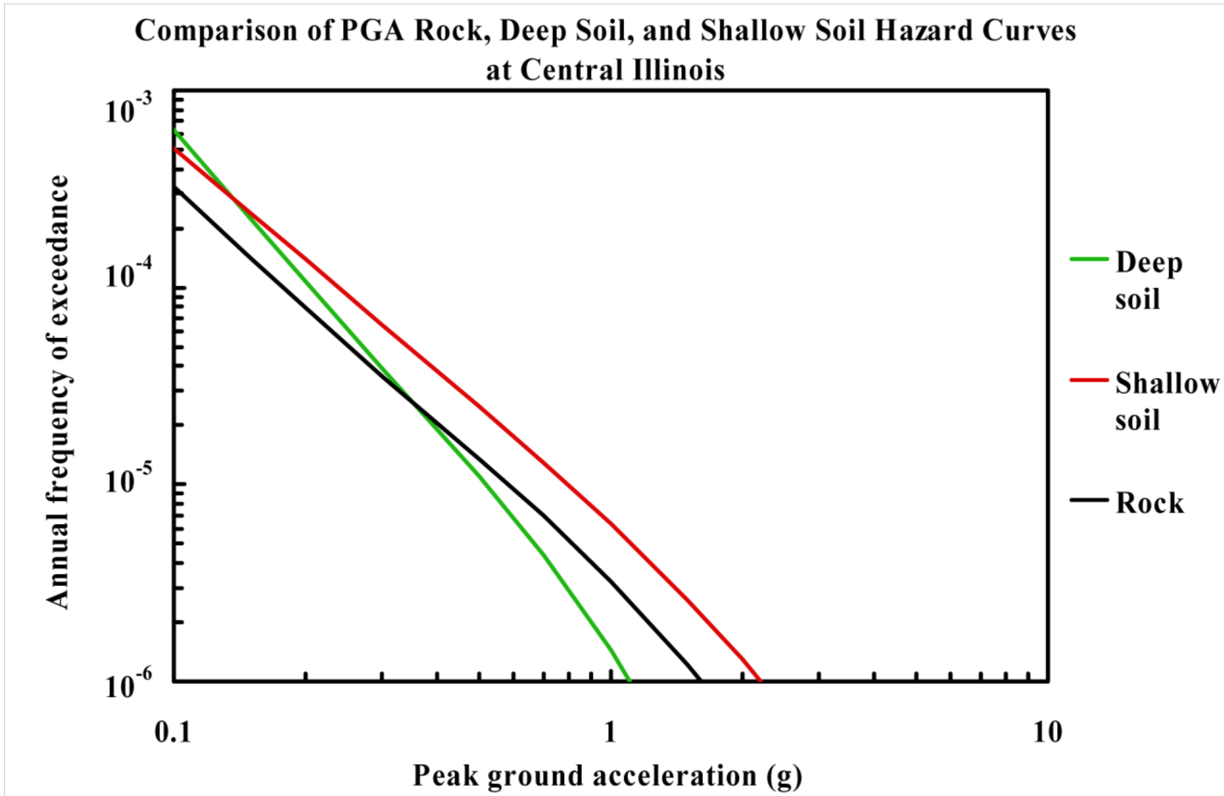

Figure 8.2-1u
Central Illinois PGA hazard: comparison of three site conditions

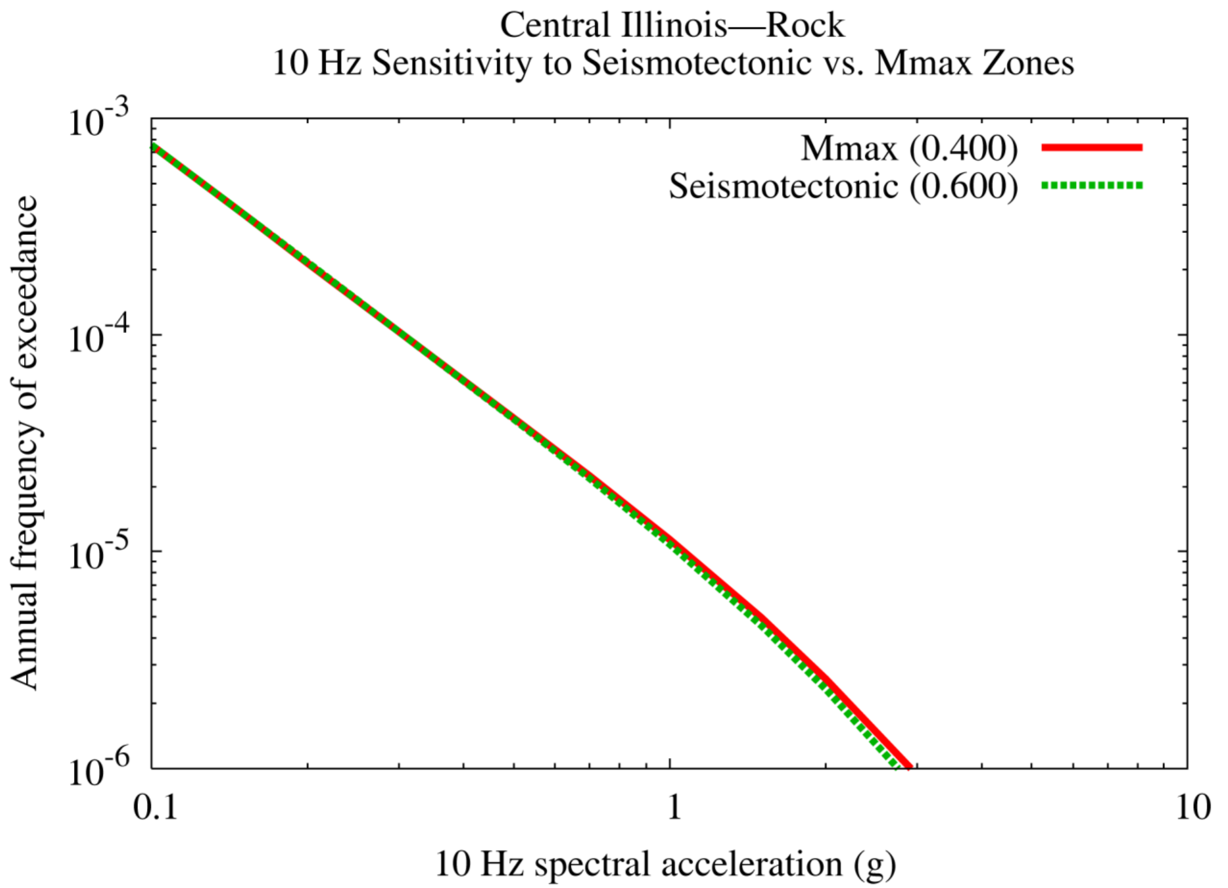

Figure 8.2-1v
Central Illinois 10 Hz rock hazard: sensitivity to seismotectonic vs. Mmax zones

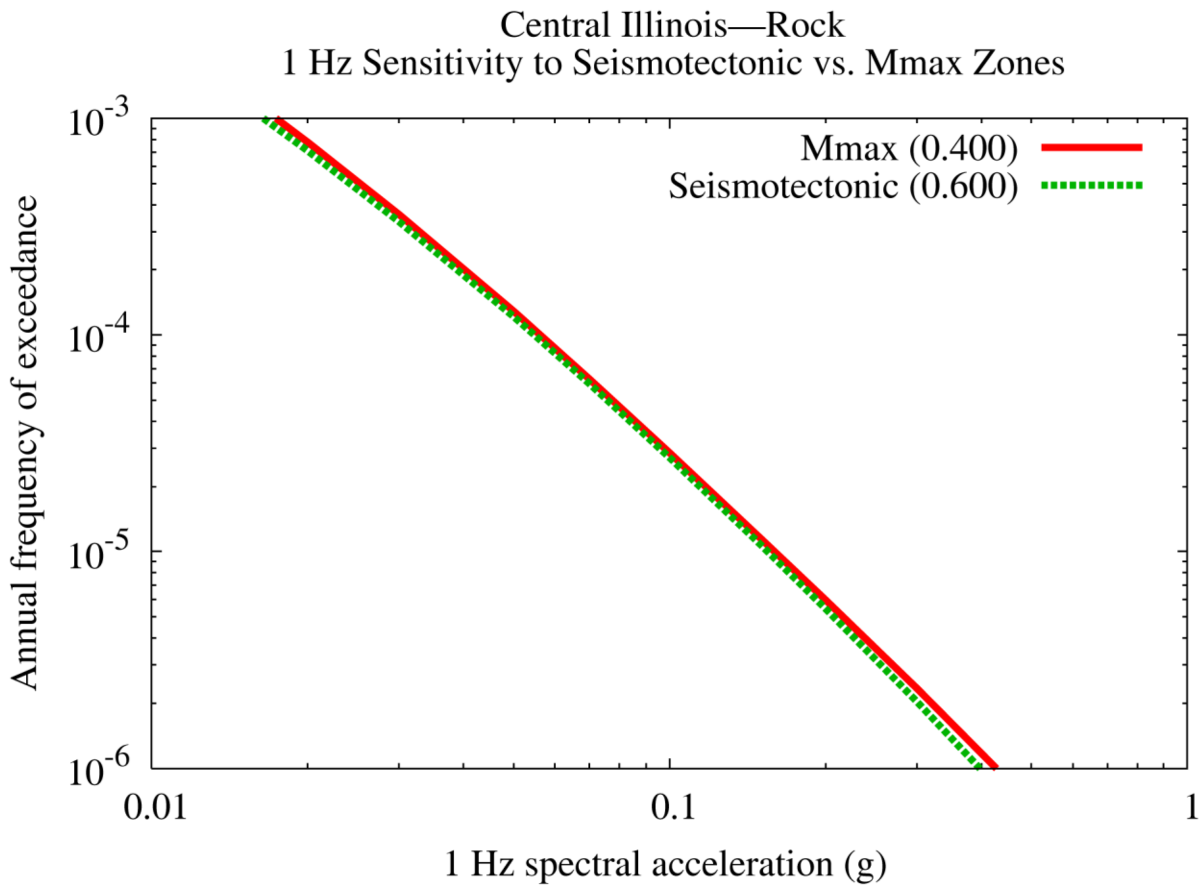

Figure 8.2-1w
Central Illinois 1 Hz rock hazard: sensitivity to seismotectonic vs. Mmax zones

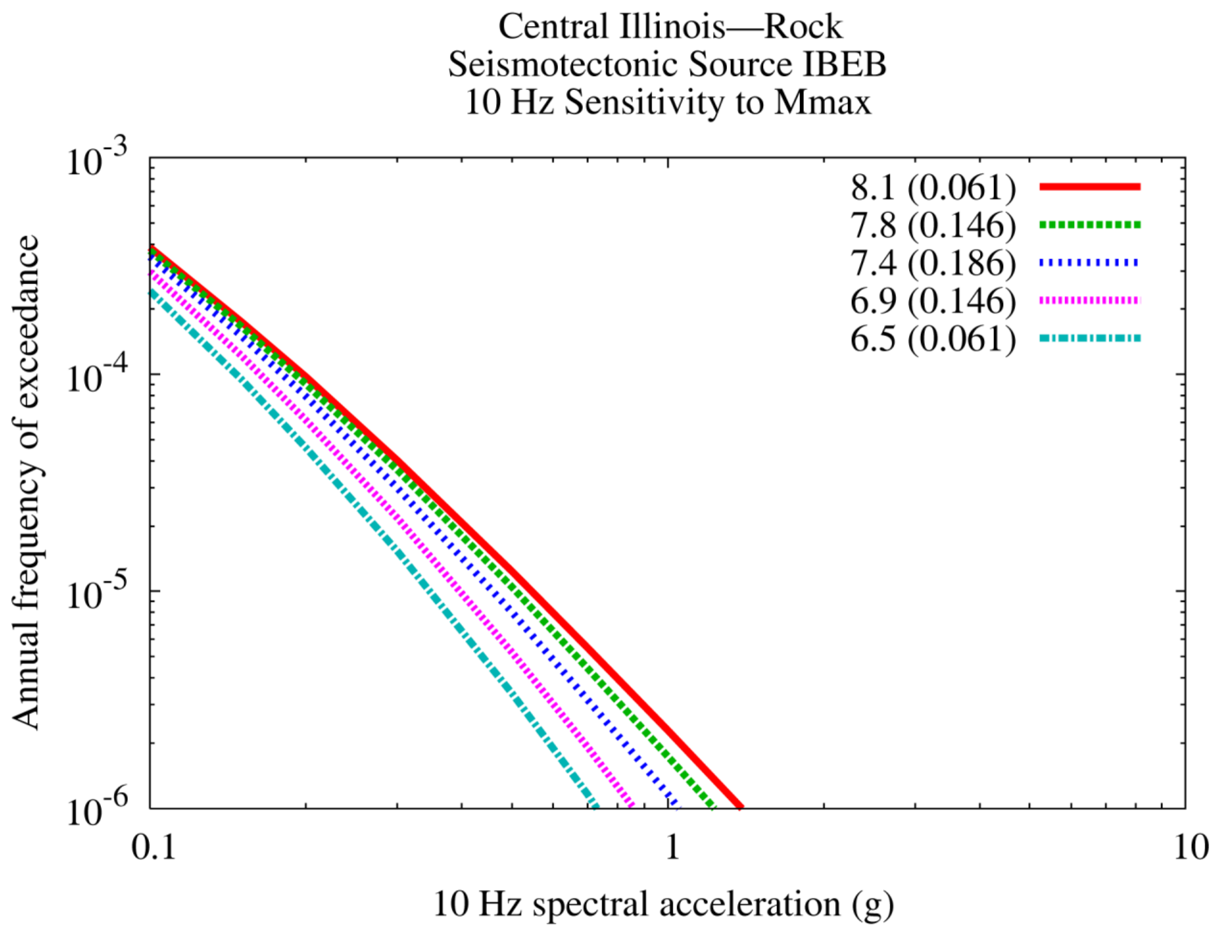

Figure 8.2-1x
Central Illinois 10 Hz rock hazard: sensitivity to Mmax for source IBEB

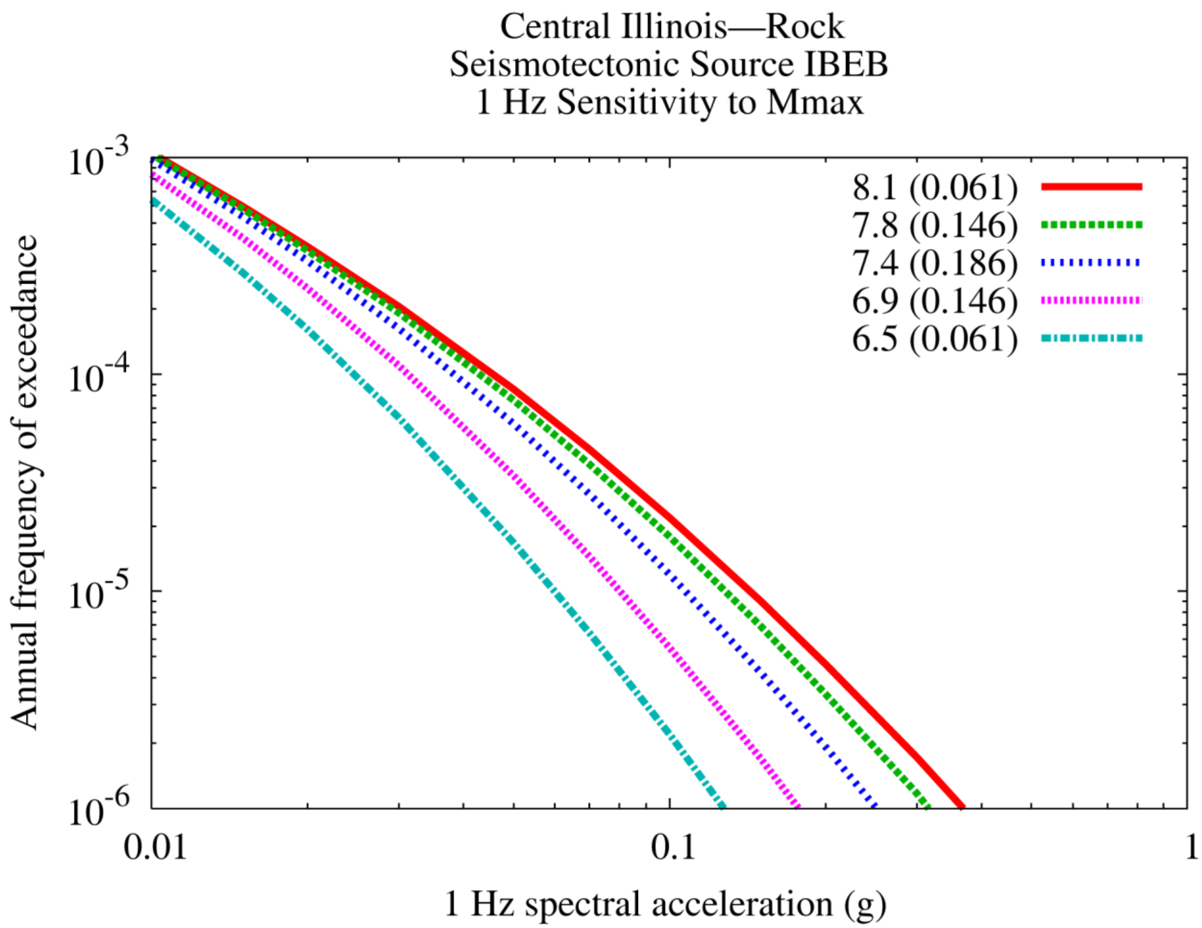

Figure 8.2-1y
Central Illinois 1 Hz rock hazard: sensitivity to Mmax for source IBEB

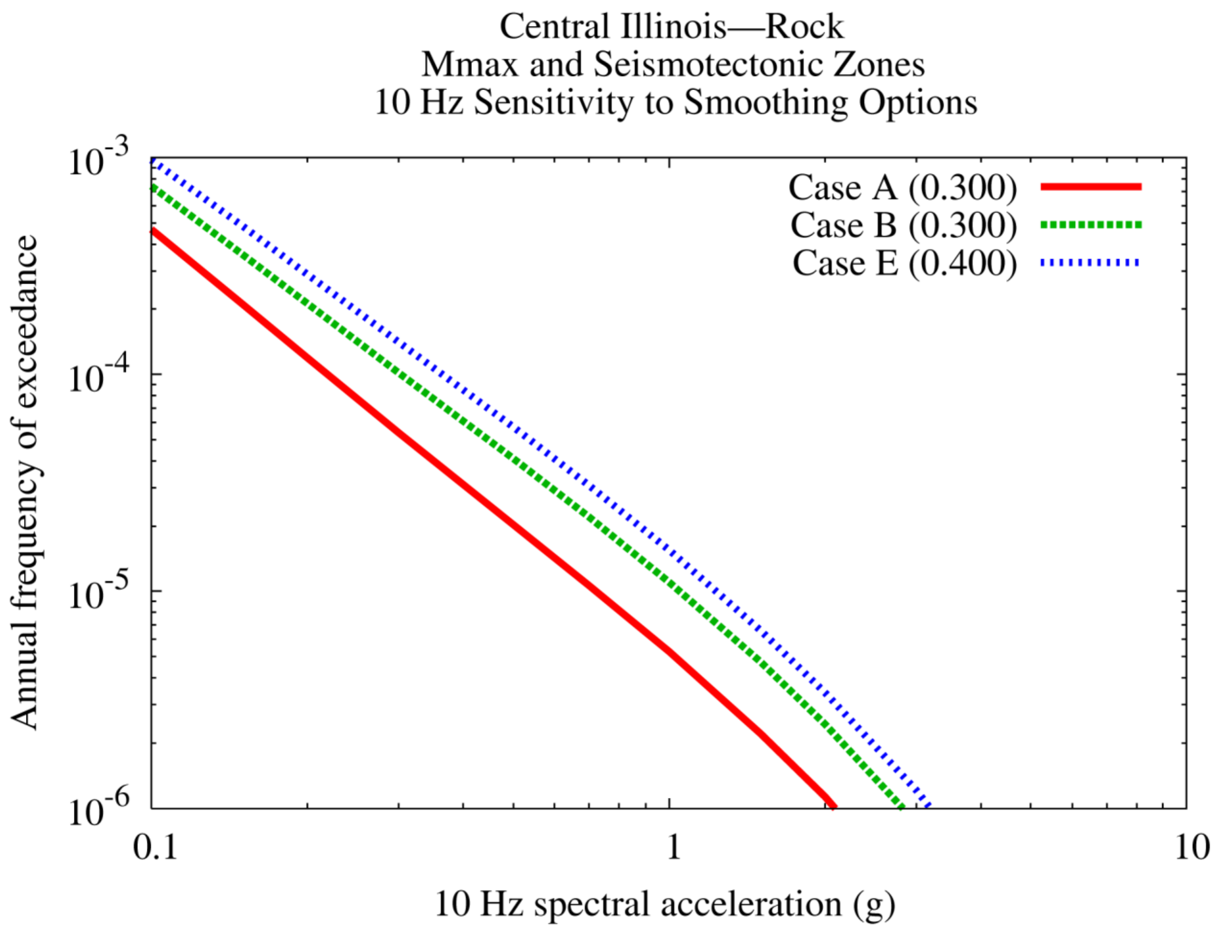

Figure 8.2-1z
Central Illinois 10 Hz rock hazard: sensitivity to smoothing options

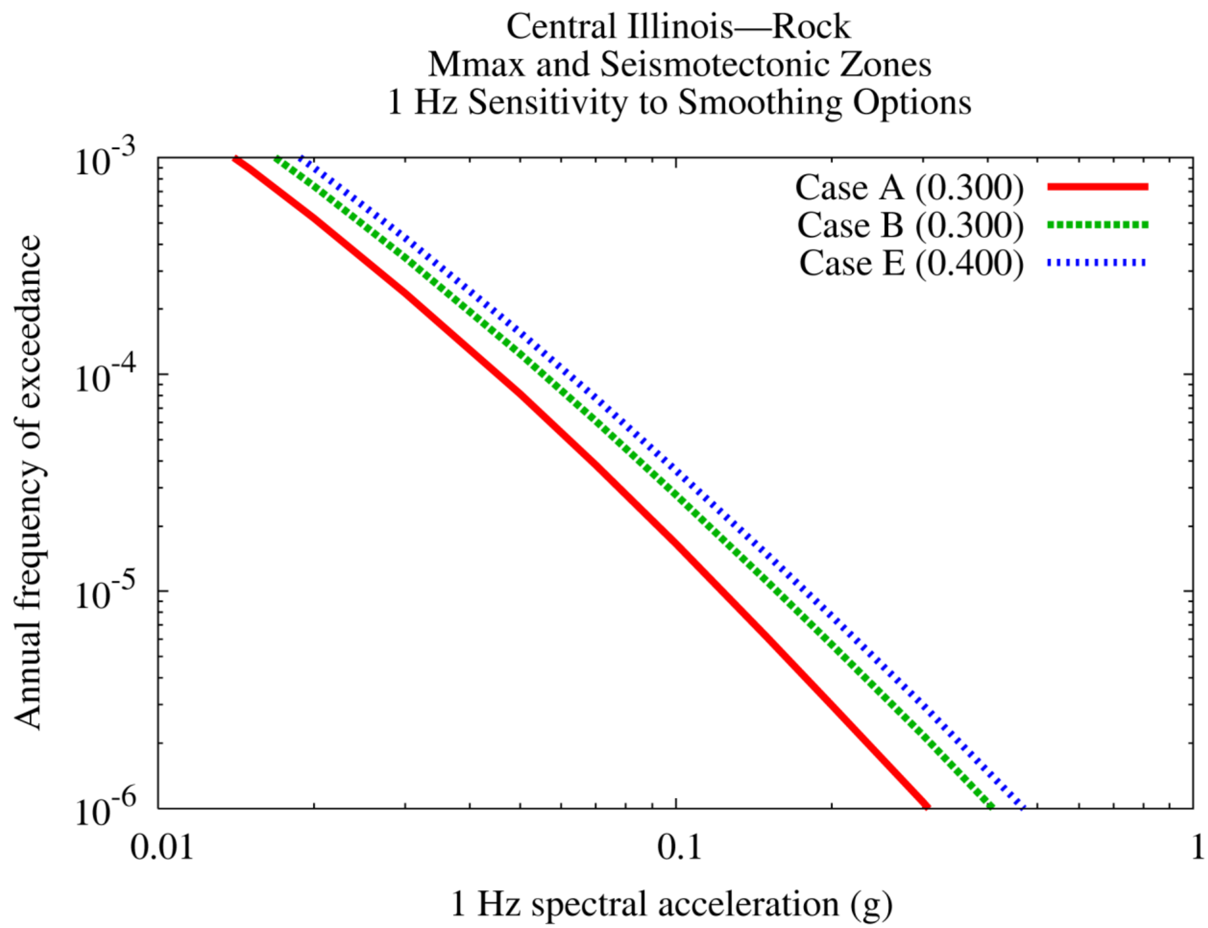

Figure 8.2-1aa
Central Illinois 1 Hz rock hazard: sensitivity to smoothing options

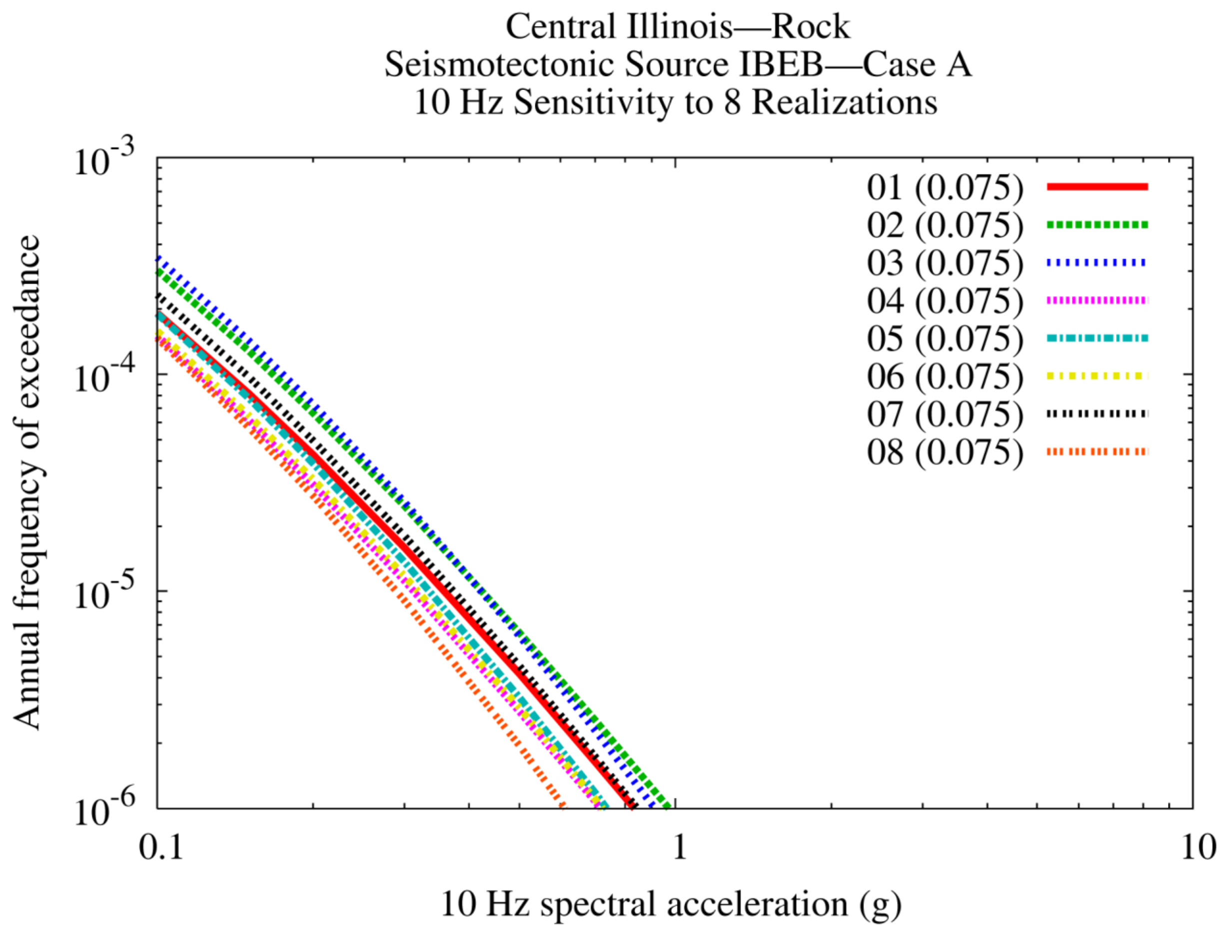

Figure 8.2-1bb
Central Illinois 10 Hz rock hazard: sensitivity to eight realizations for source IBEB, Case A

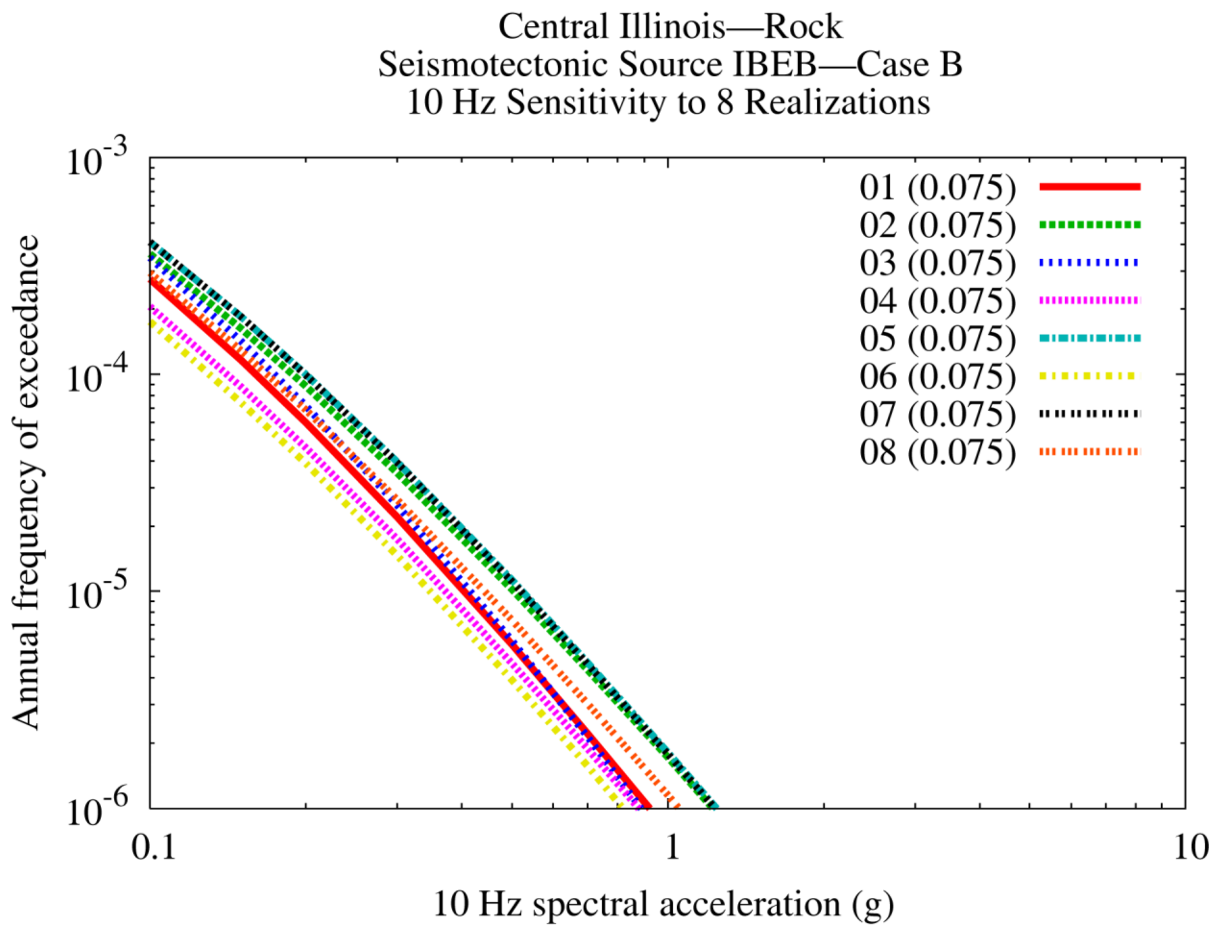

Figure 8.2-1cc
Central Illinois 10 Hz rock hazard: sensitivity to eight realizations for source IBEB, Case B

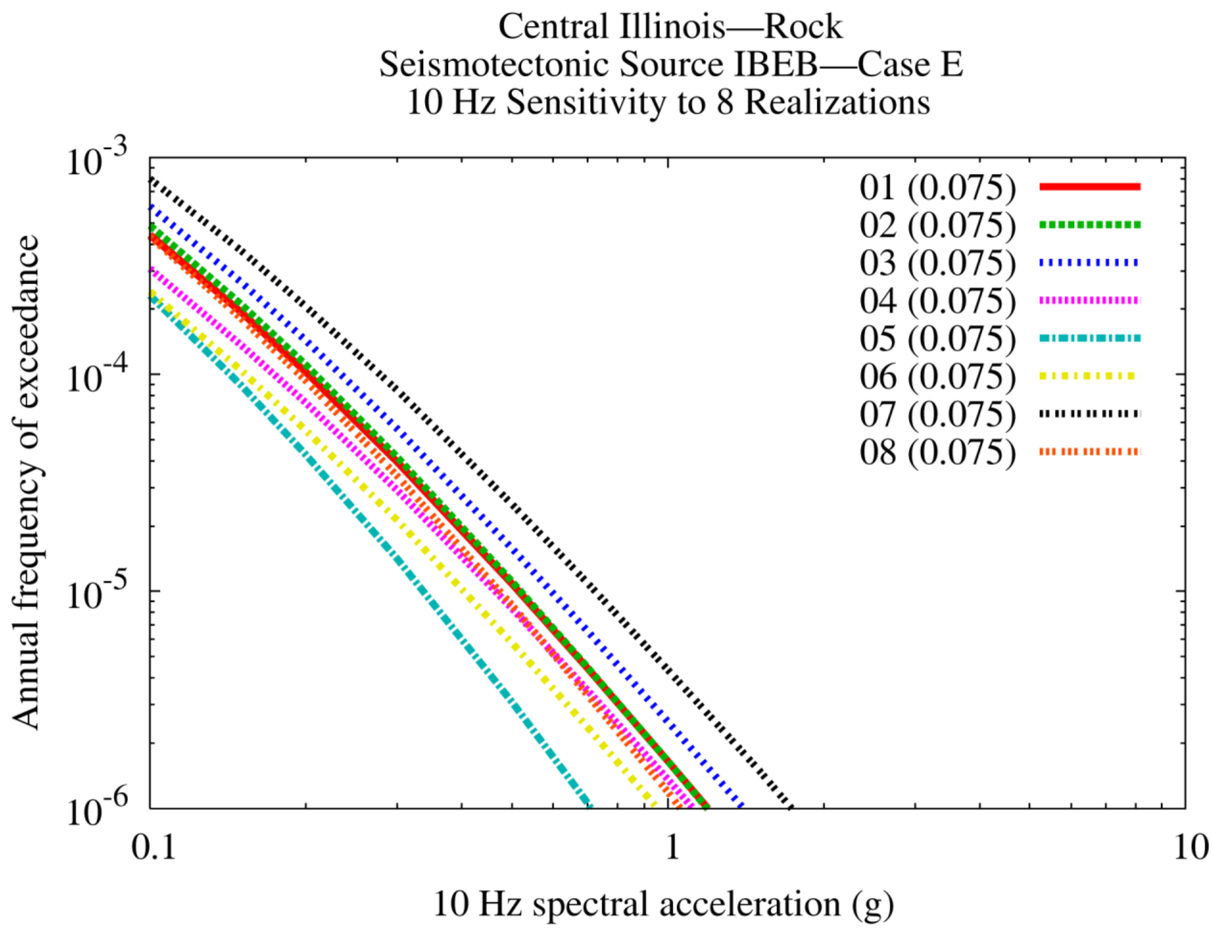

Figure 8.2-1dd
Central Illinois 10 Hz rock hazard: sensitivity to eight realizations for source IBEB, Case E

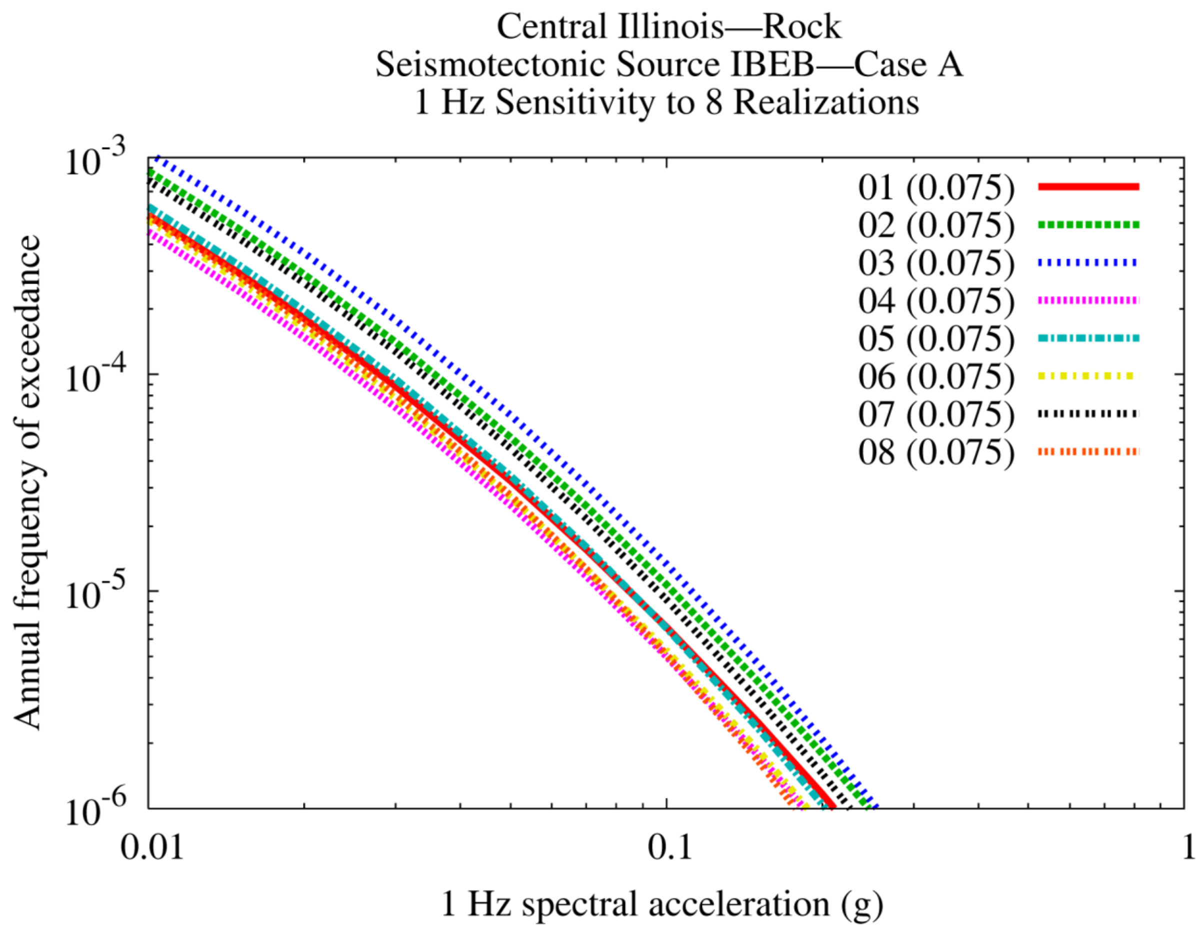

Figure 8.2-1ee
Central Illinois 1 Hz rock hazard: sensitivity to eight realizations for source IBEB, Case A

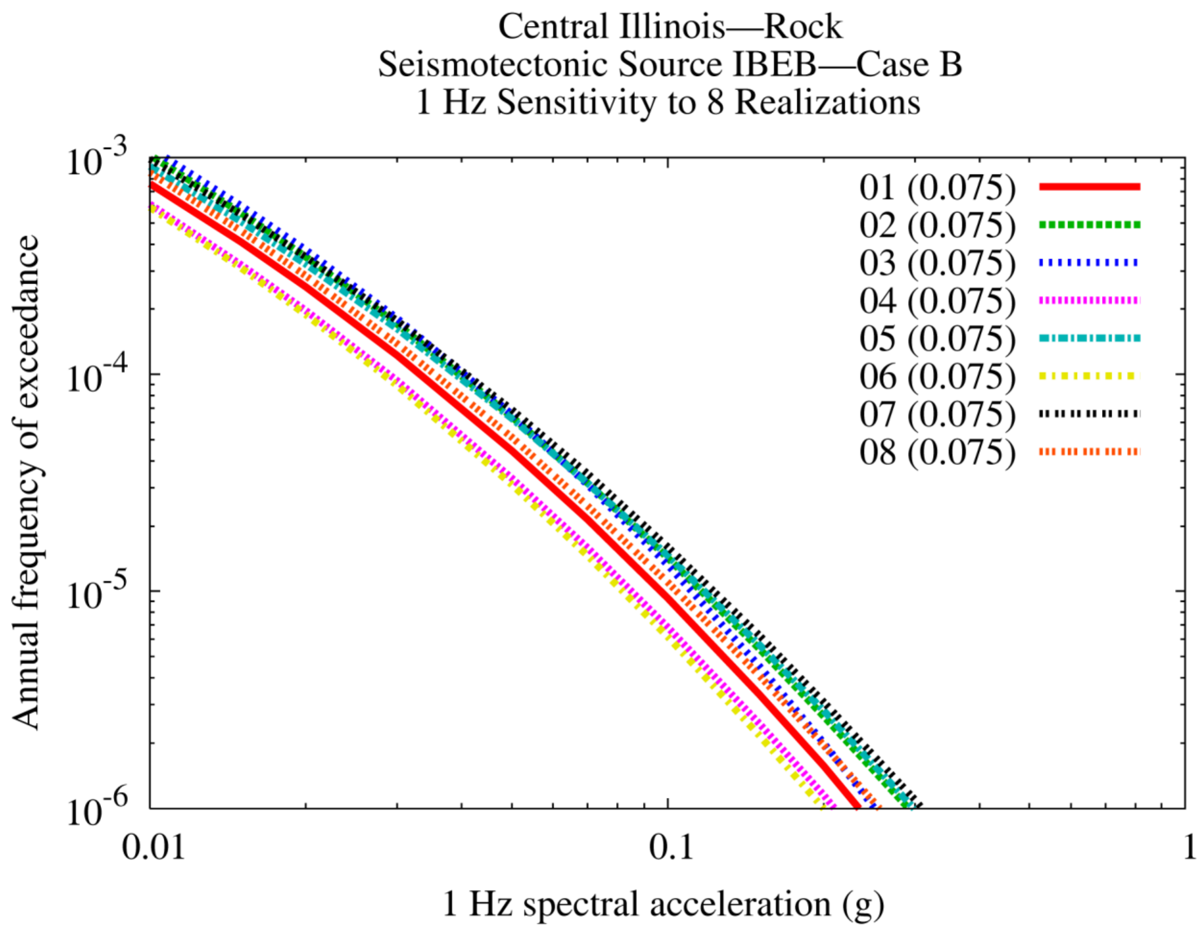

Figure 8.2-1ff
Central Illinois 1 Hz rock hazard: sensitivity to eight realizations for source IBEB, Case B

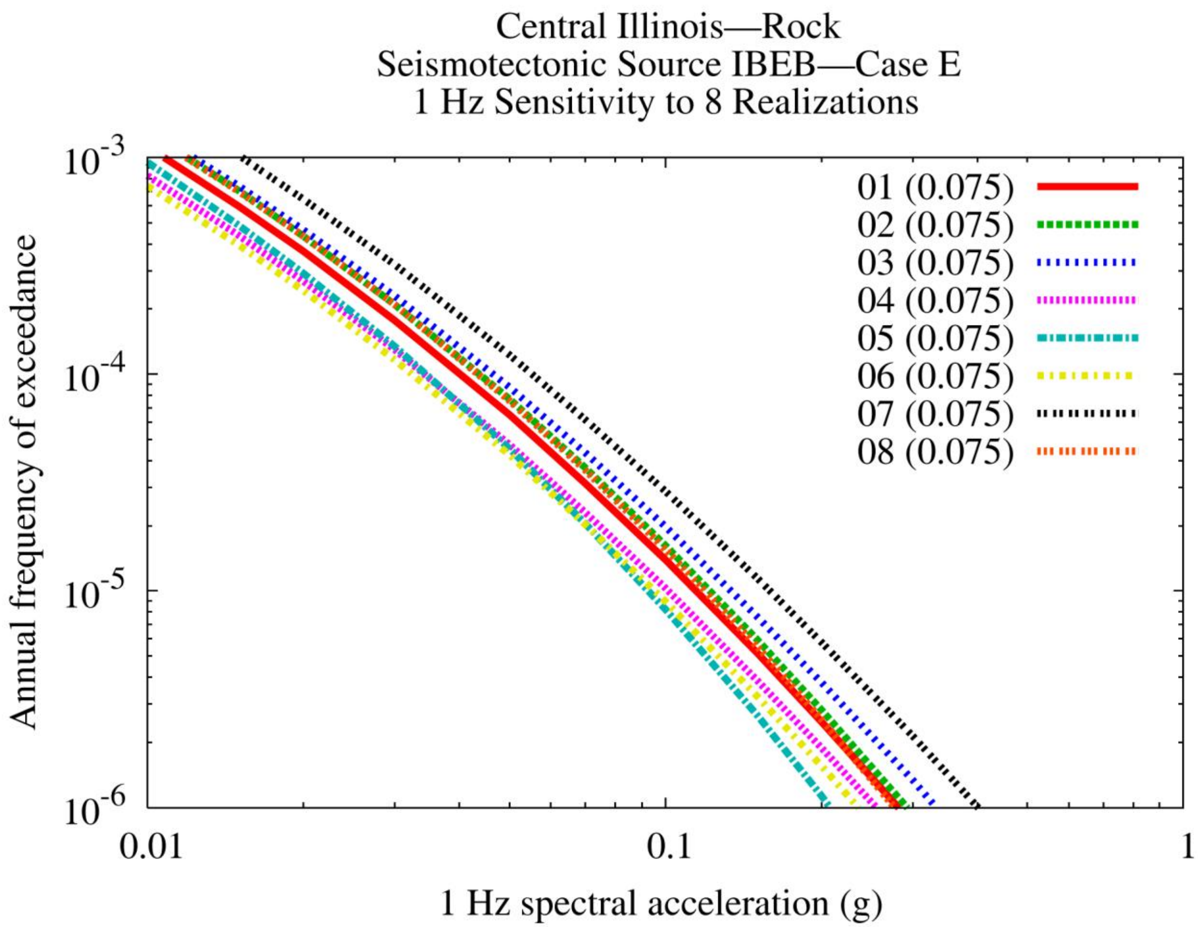

Figure 8.2-1gg
Central Illinois 1 Hz rock hazard: sensitivity to eight realizations for source IBEB, Case E

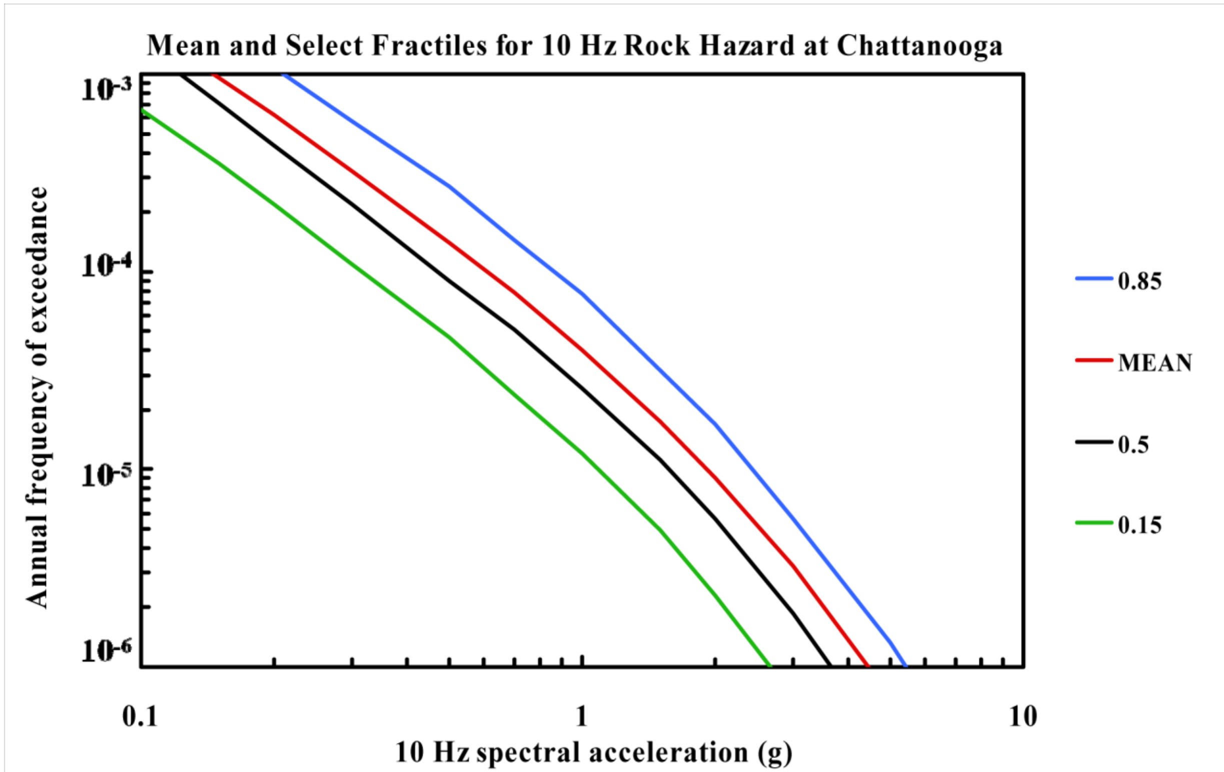

Figure 8.2-2a
Chattanooga 10 Hz rock hazard: mean and fractile total hazard

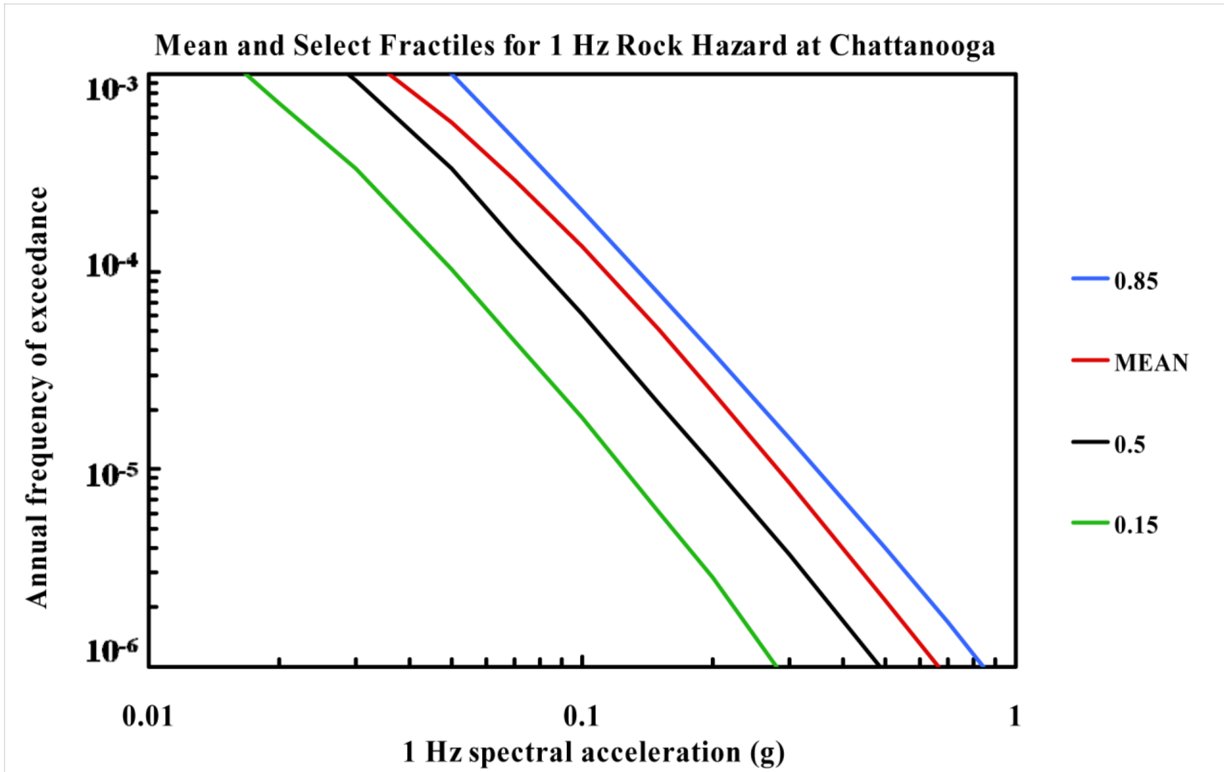

Figure 8.2-2b
Chattanooga 1 Hz rock hazard: mean and fractile total hazard

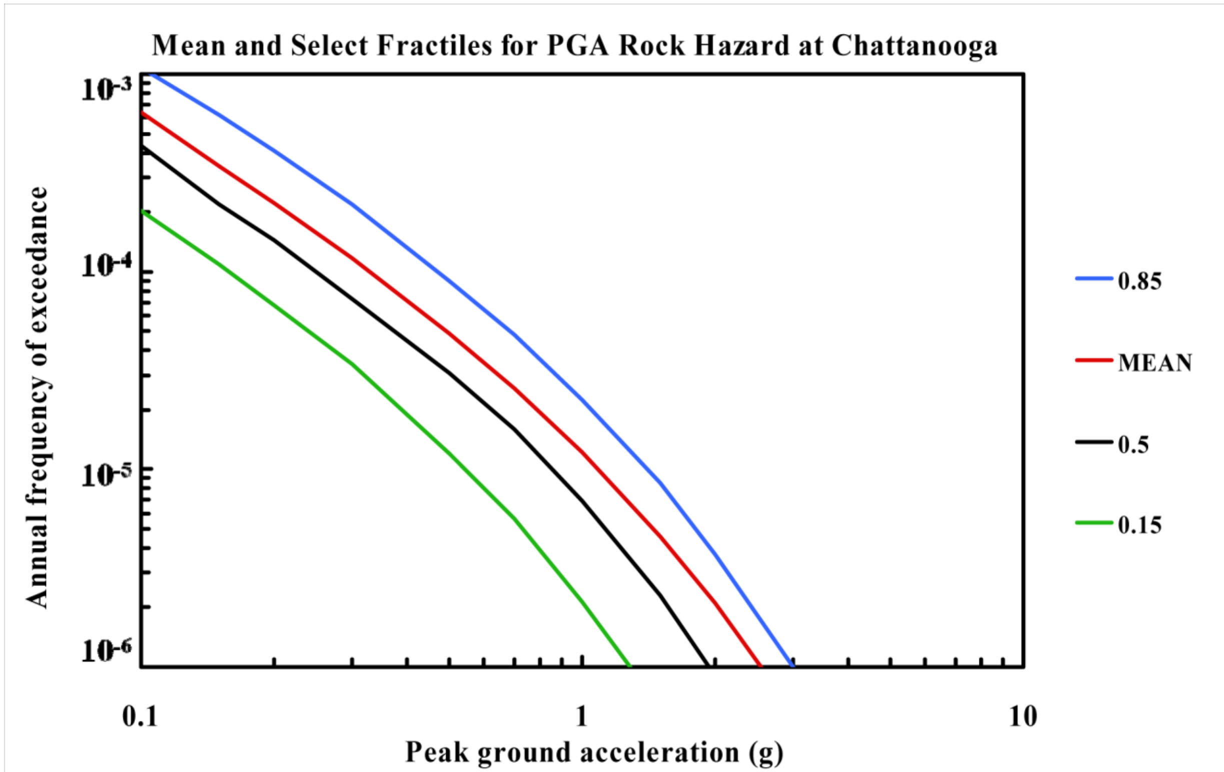

Figure 8.2-2c
Chattanooga PGA rock hazard: mean and fractile total hazard

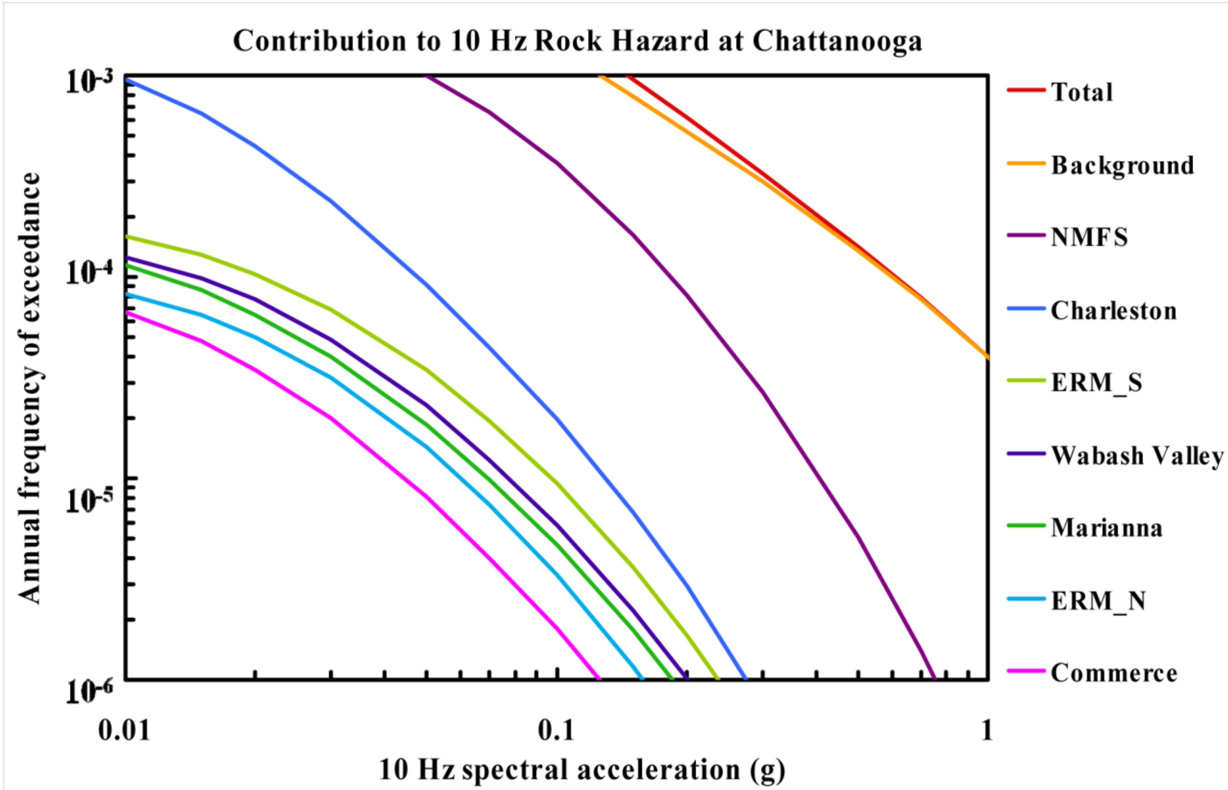

Figure 8.2-2d
Chattanooga 10 Hz rock hazard: total and contribution by RLME and background

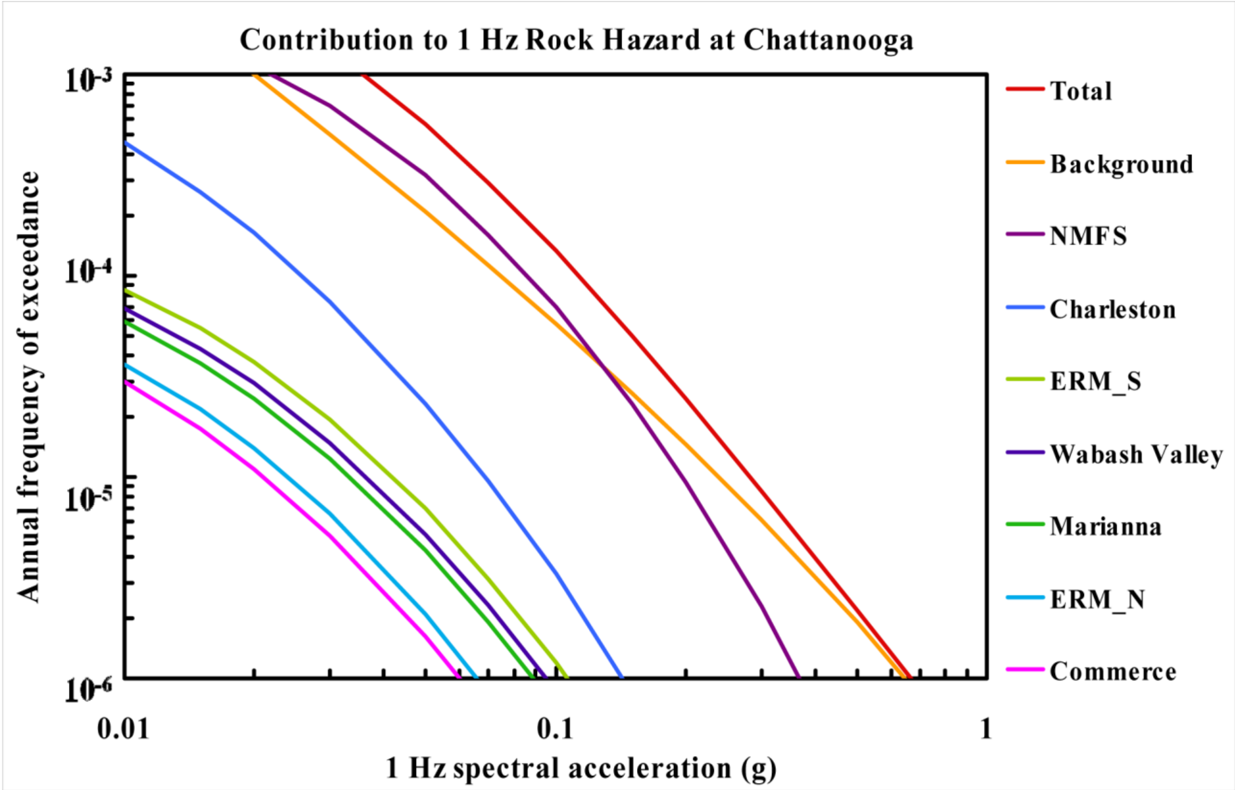

Figure 8.2-2e
Chattanooga 1 Hz rock hazard: total and contribution by RLME and background

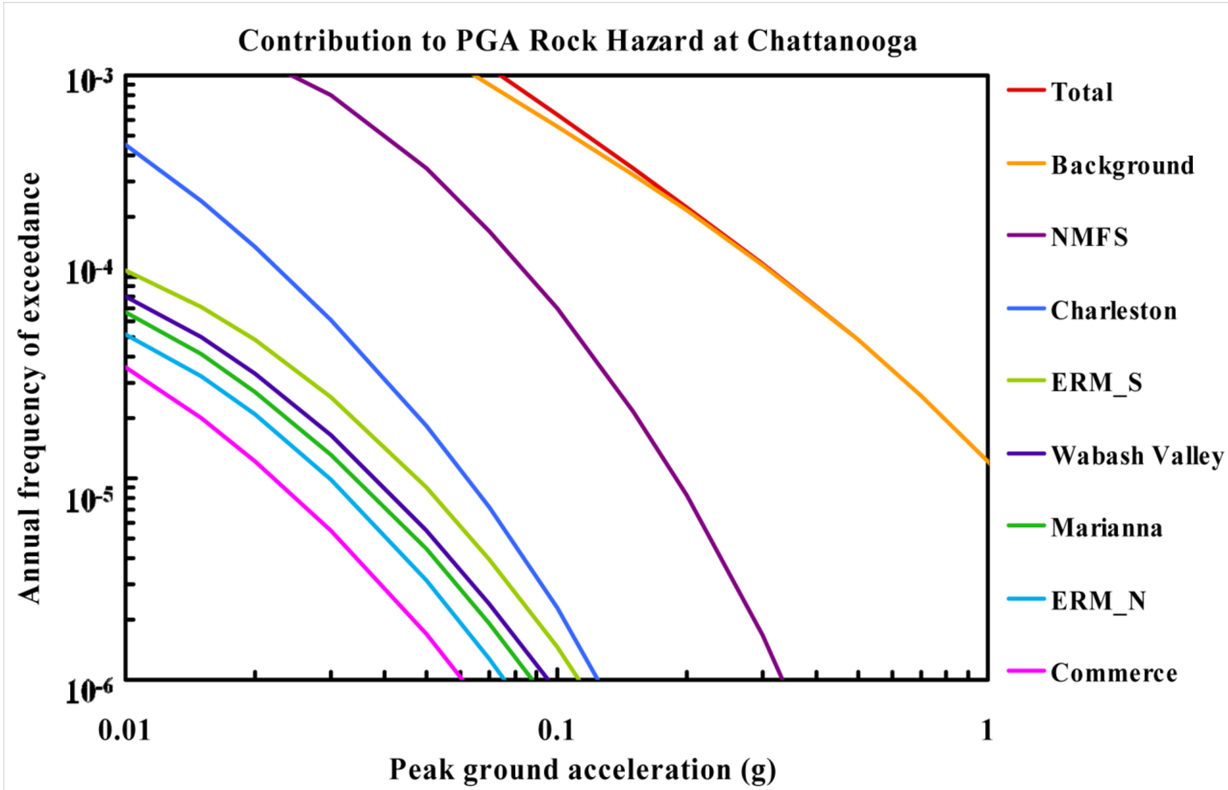

Figure 8.2-2f
Chattanooga PGA rock hazard: total and contribution by RLME and background

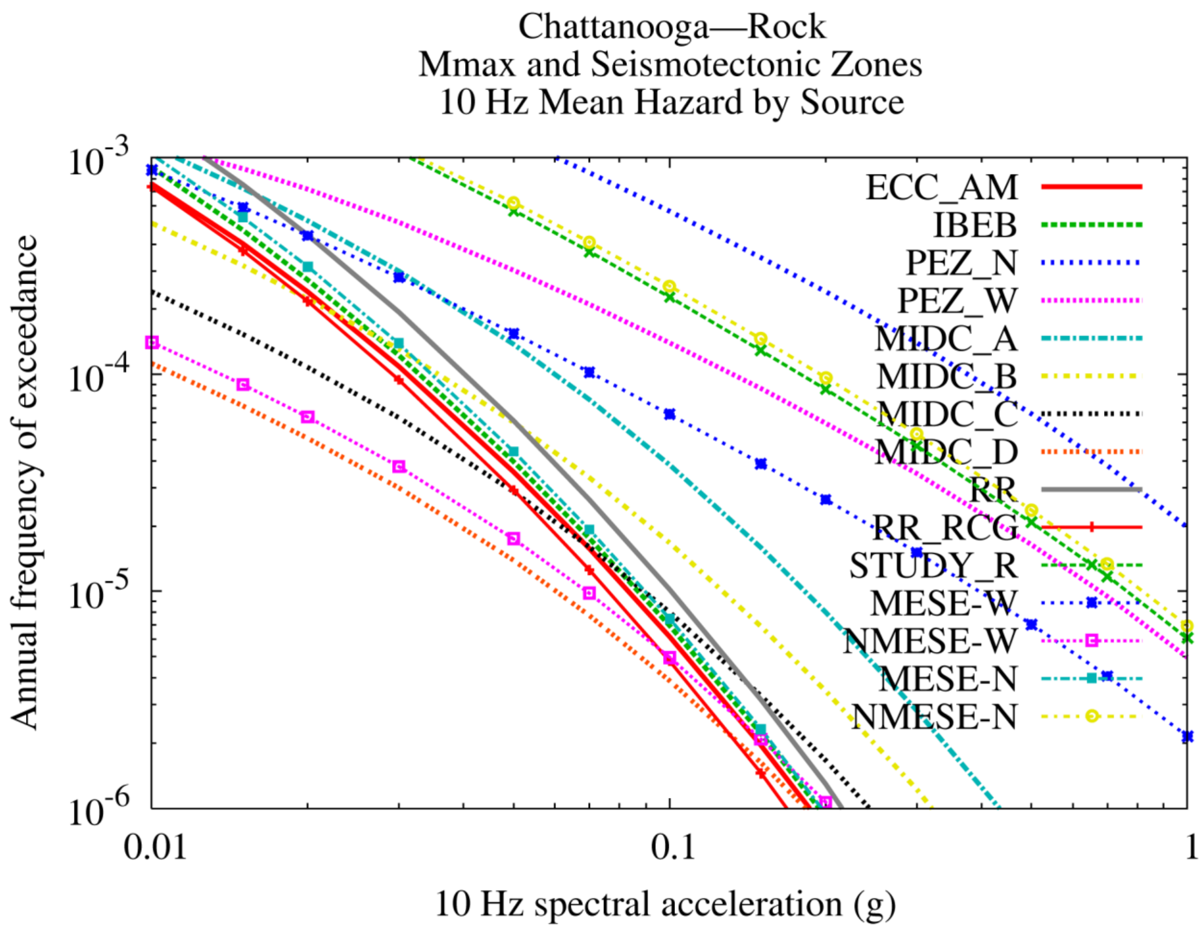

Figure 8.2-2g
Chattanooga 10 Hz rock hazard: contribution by background source

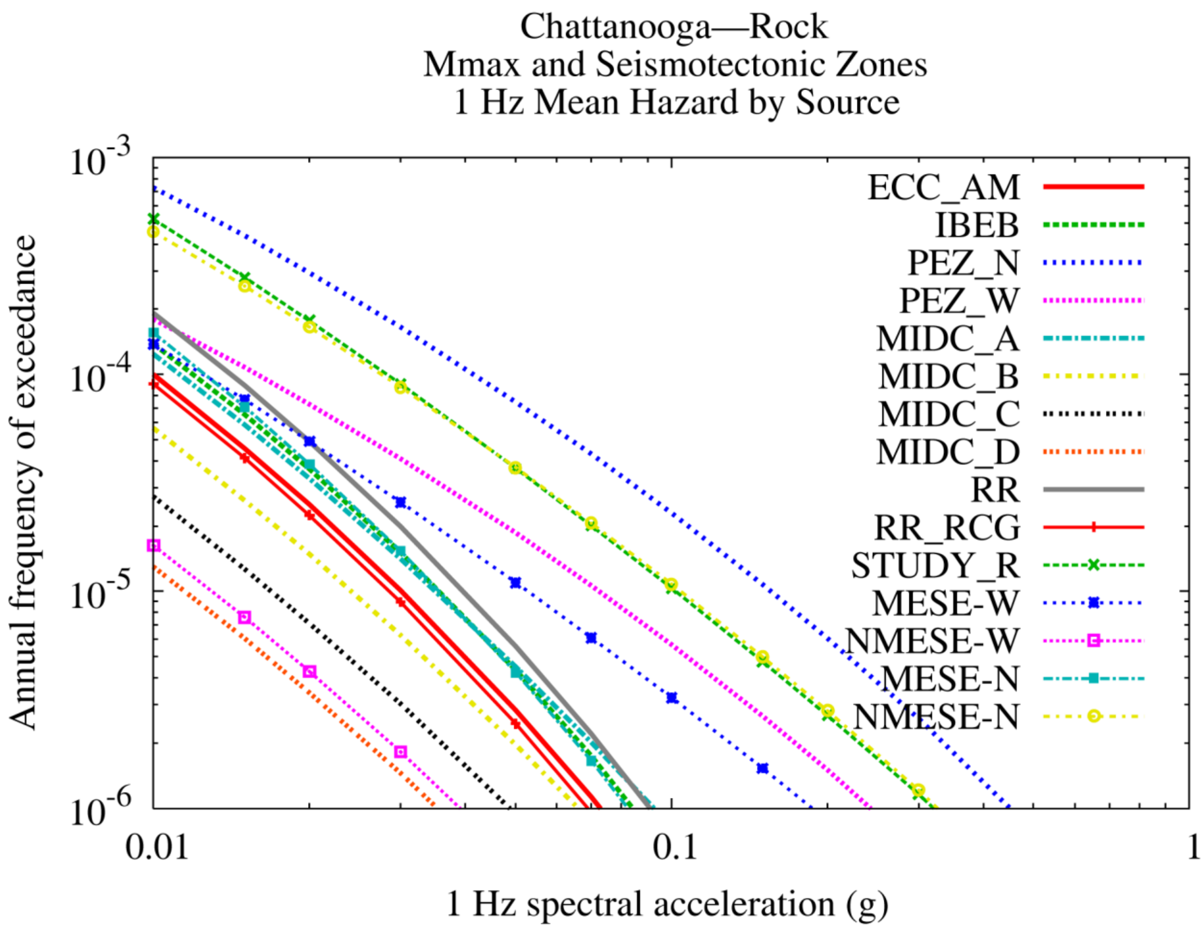

Figure 8.2-2h
Chattanooga 1 Hz rock hazard: contribution by background source

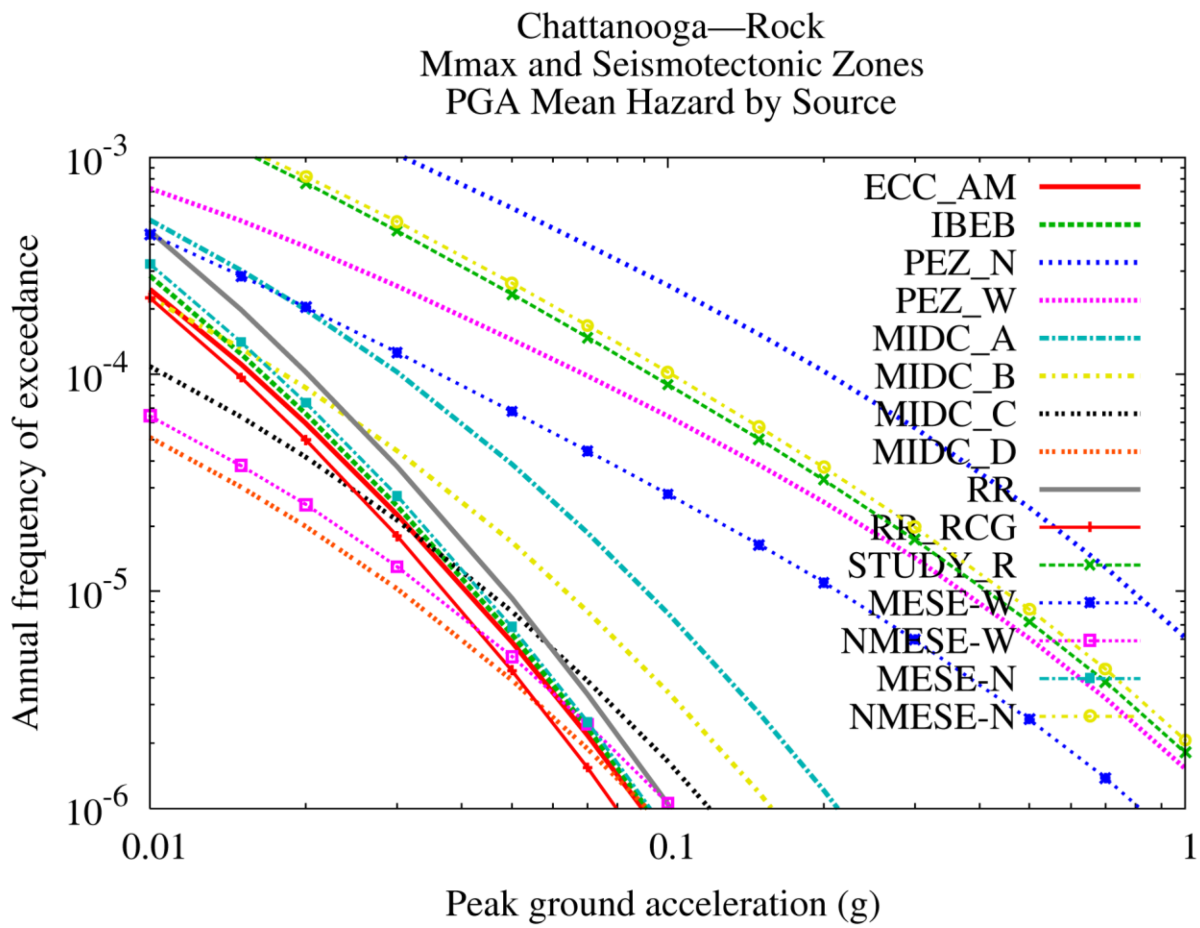

Figure 8.2-2i
Chattanooga PGA rock hazard: contribution by background source

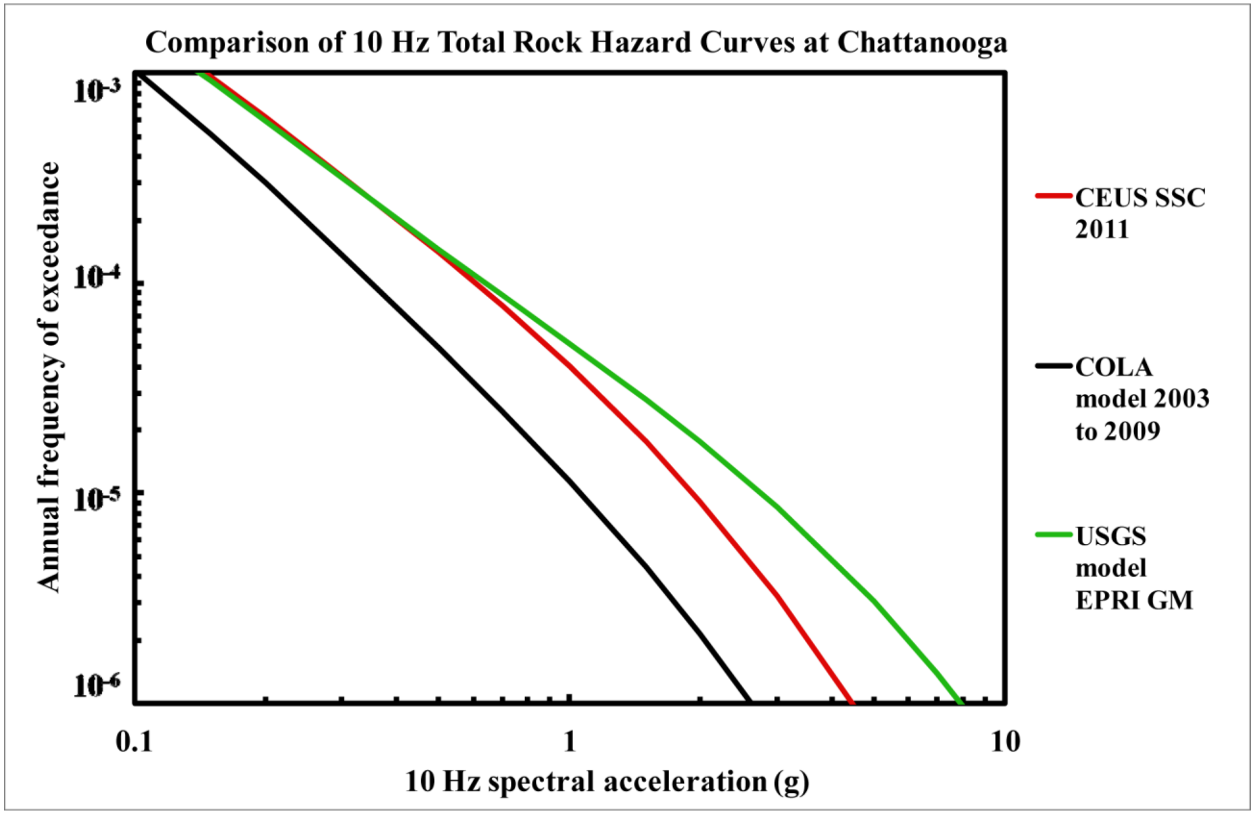

Figure 8.2-2j
Chattanooga 10 Hz rock hazard: comparison of three source models

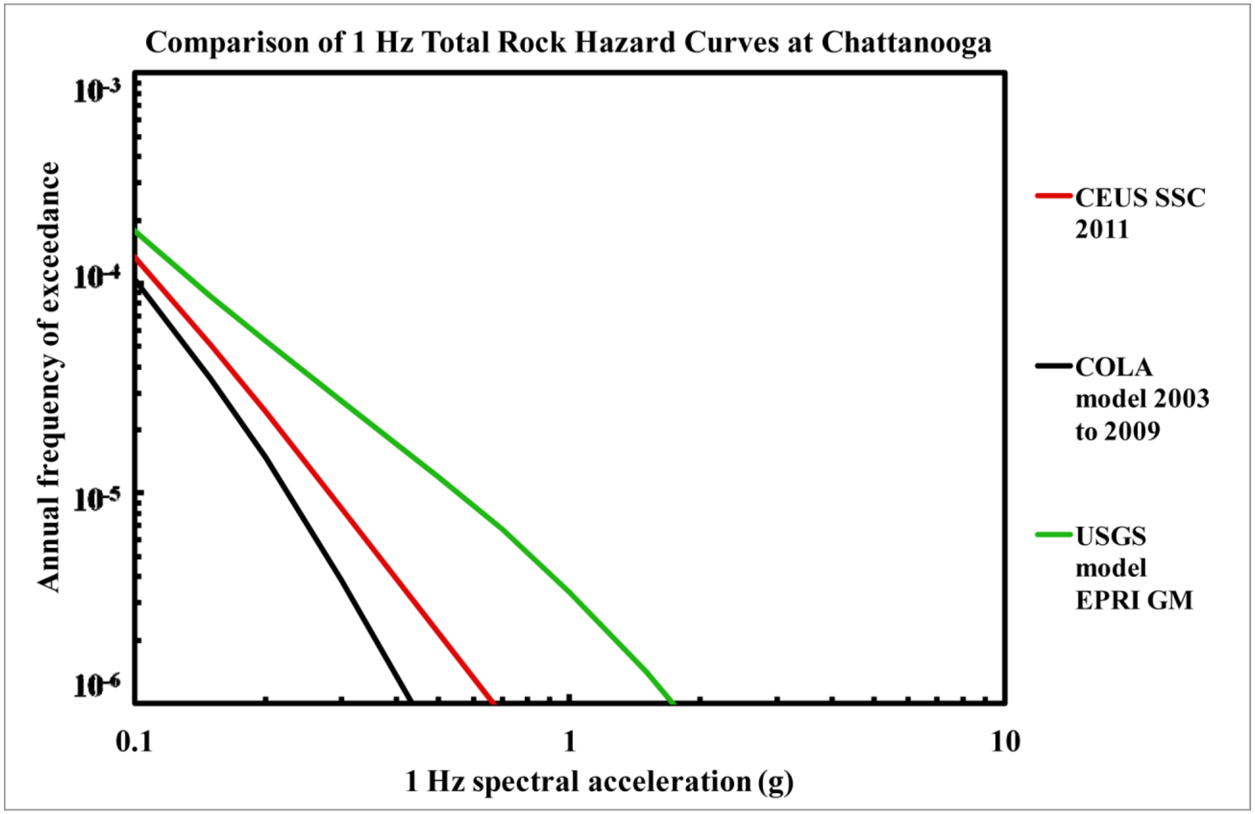

Figure 8.2-2k
Chattanooga is 1 Hz rock hazard: comparison of three source models

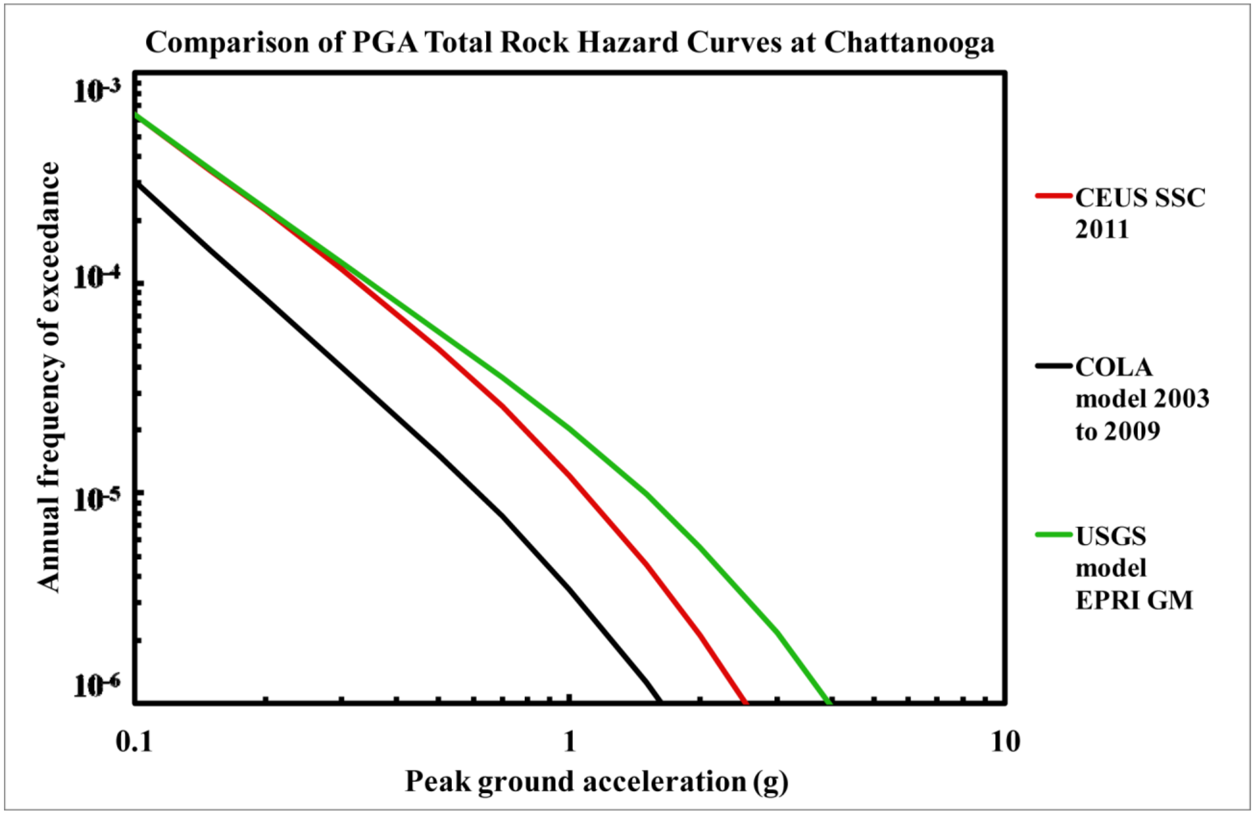

Figure 8.2-2l
Chattanooga PGA rock hazard: comparison of three source models

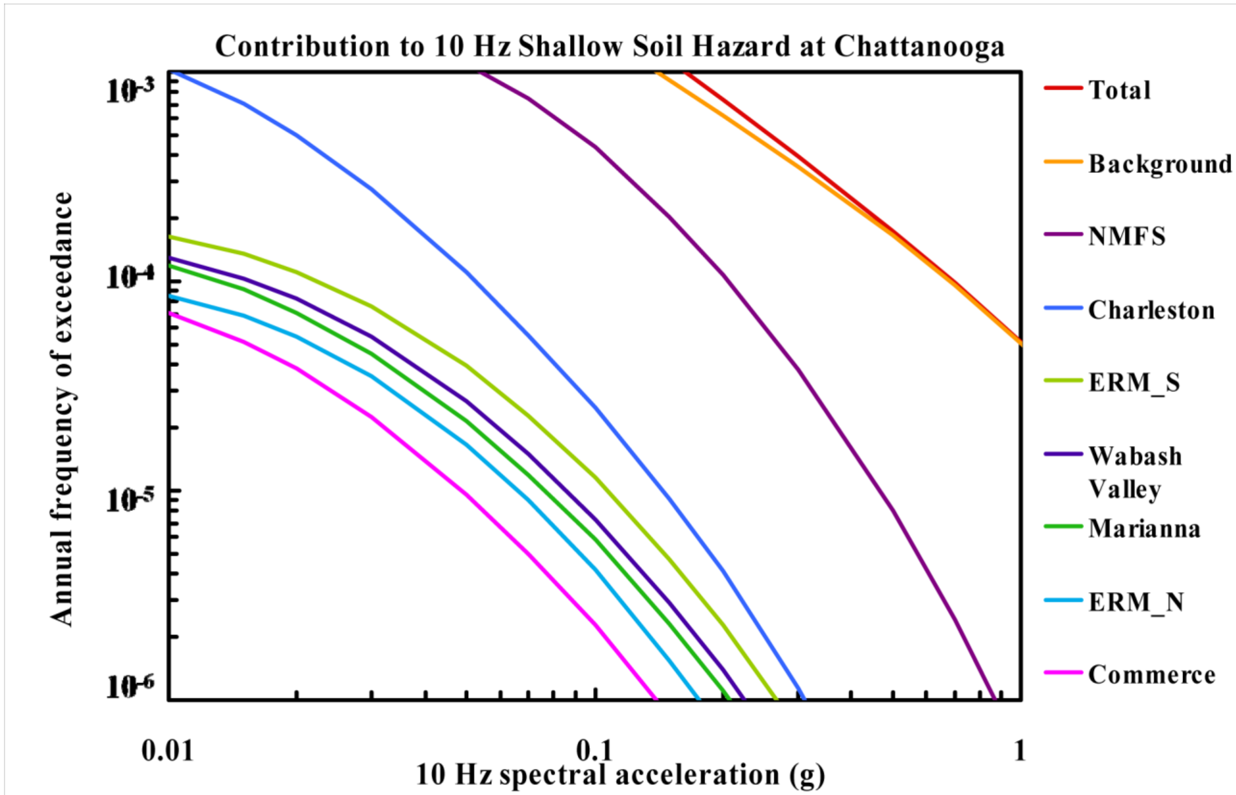

Figure 8.2-2m
Chattanooga 10 Hz shallow soil hazard: total and contribution by RLME and background

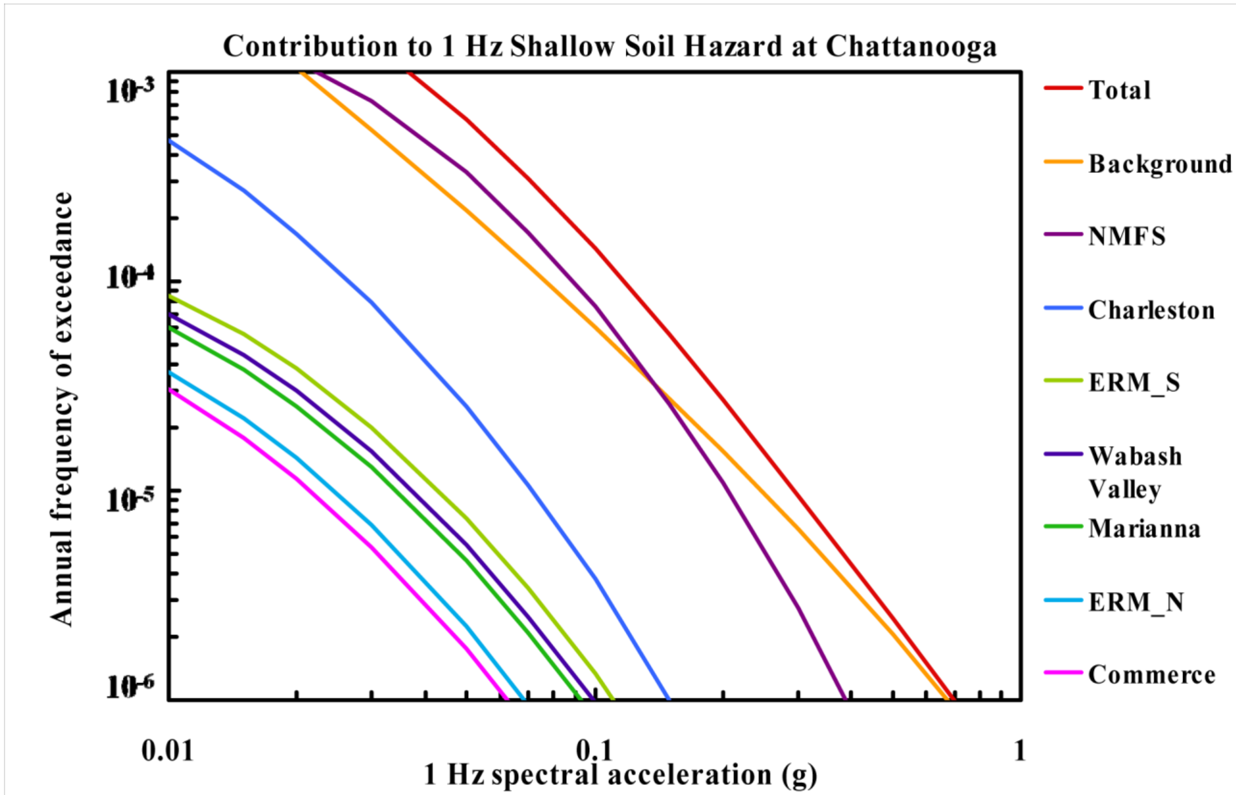

Figure 8.2-2n
Chattanooga 1 Hz shallow soil hazard: total and contribution by RLME and background

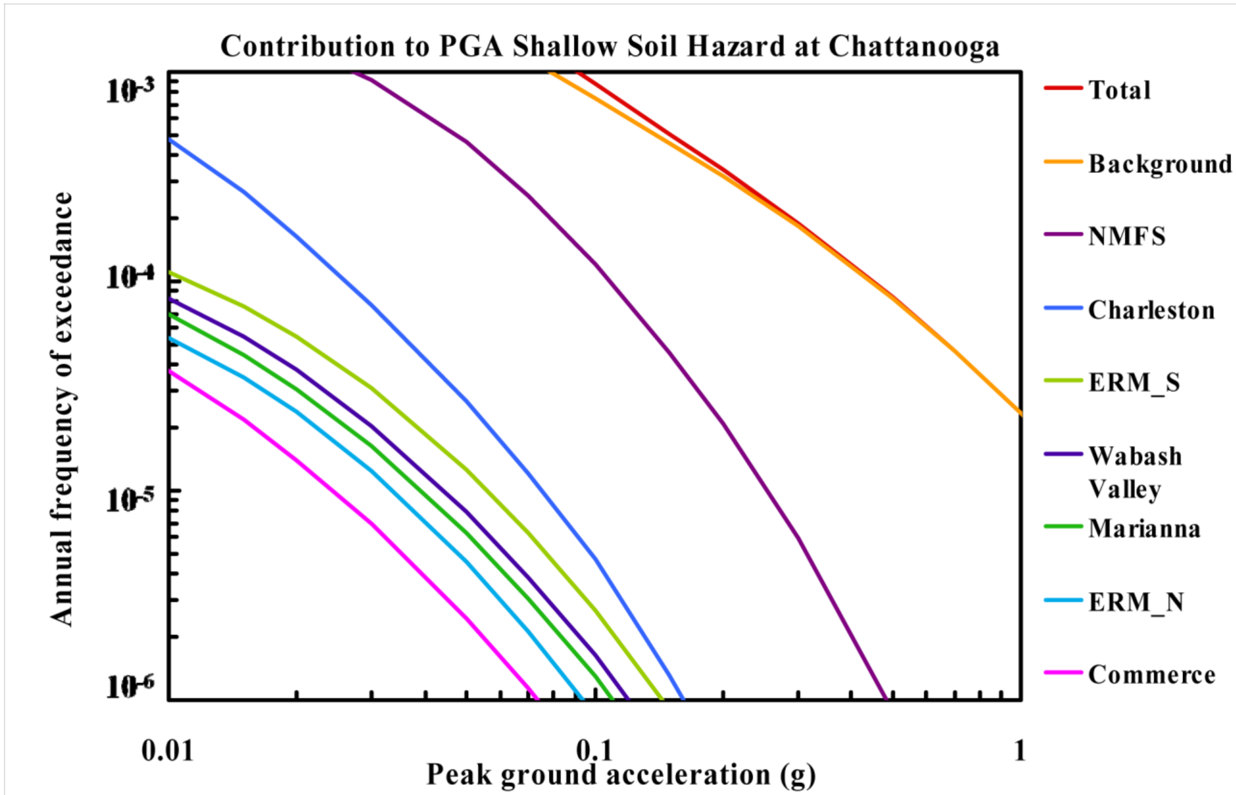

Figure 8.2-2o
Chattanooga PGA shallow soil hazard: total and contribution by RLME and background

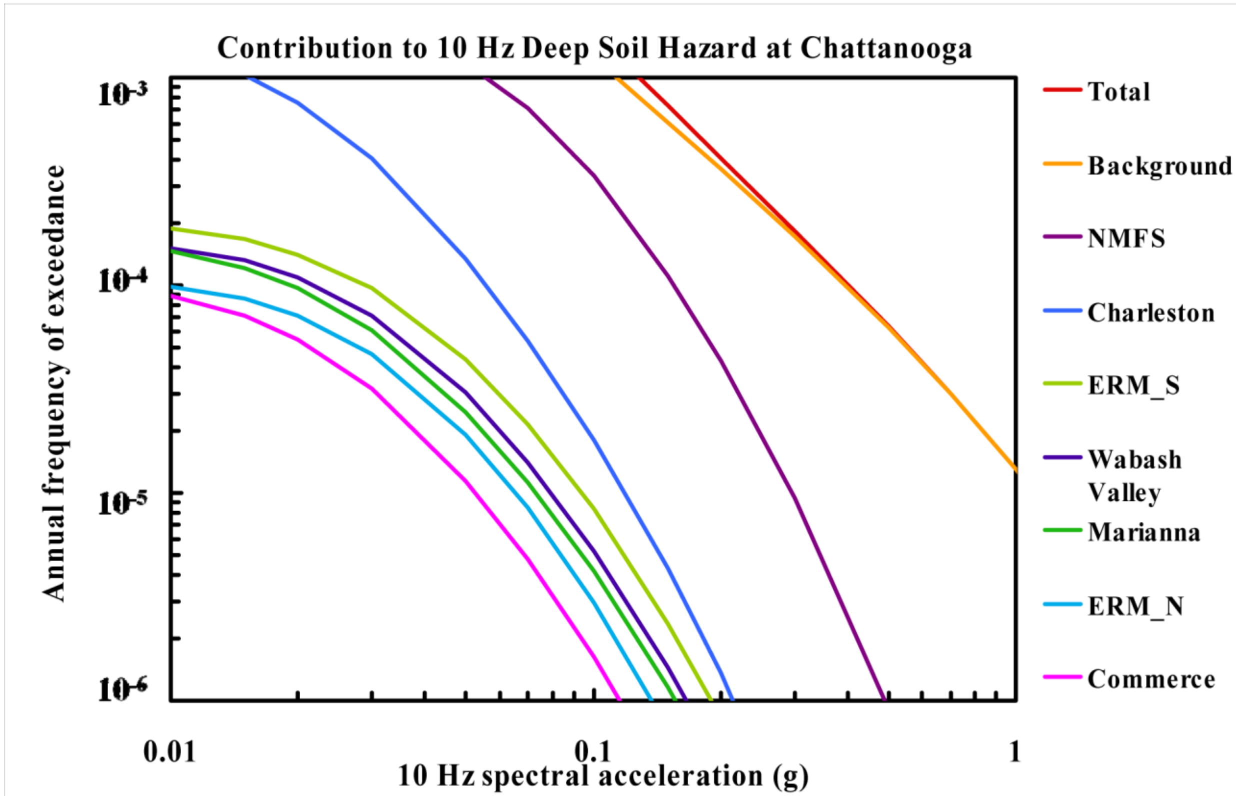

Figure 8.2-2p
Chattanooga 10 Hz deep soil hazard: total and contribution by RLME and background

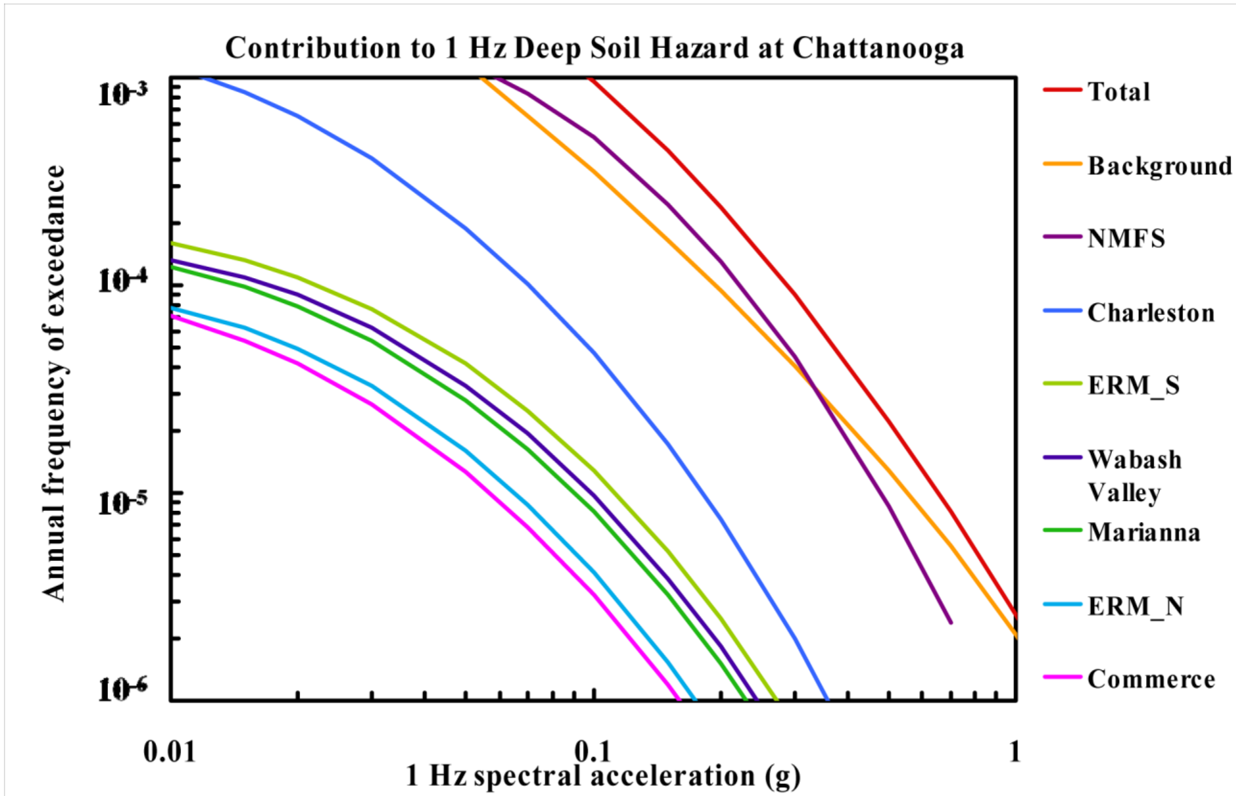

Figure 8.2-2q
Chattanooga 1 Hz deep soil hazard: total and contribution by RLME and background

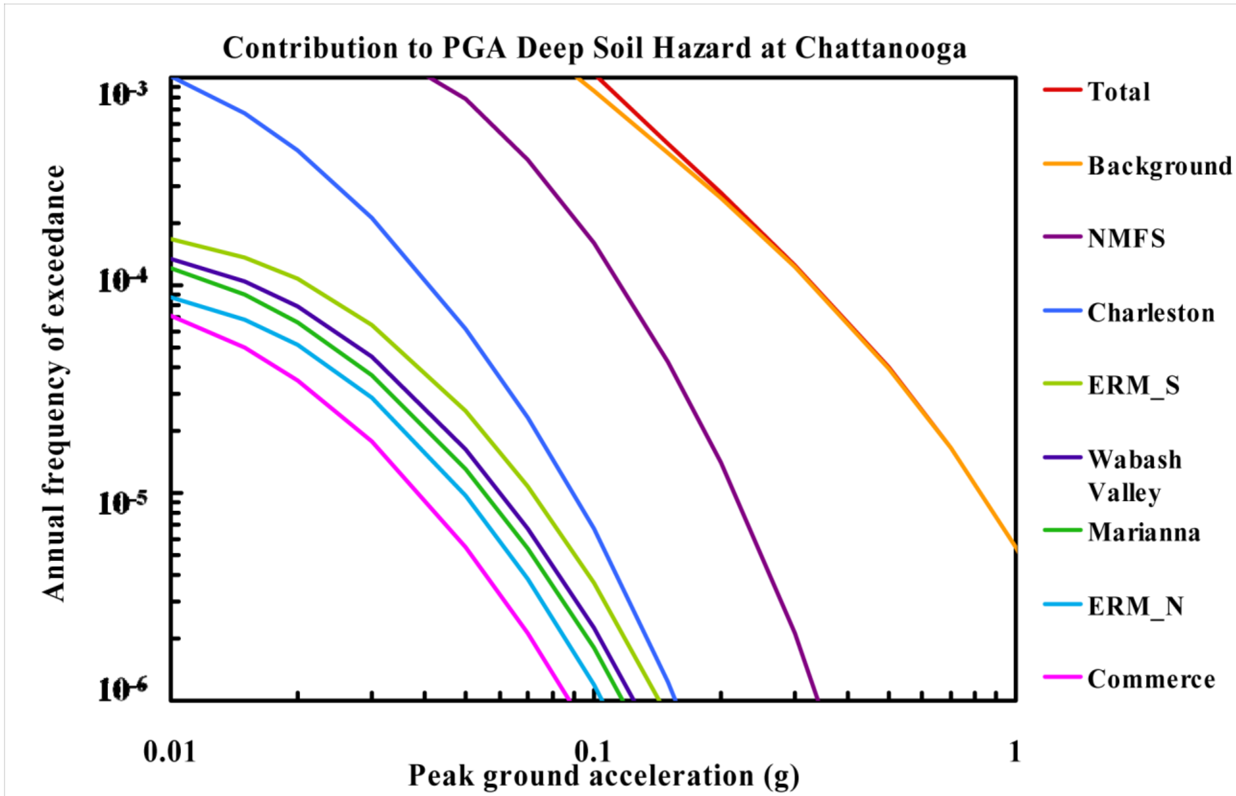

Figure 8.2-2r
Chattanooga PGA deep soil hazard: total and contribution by RLME and background

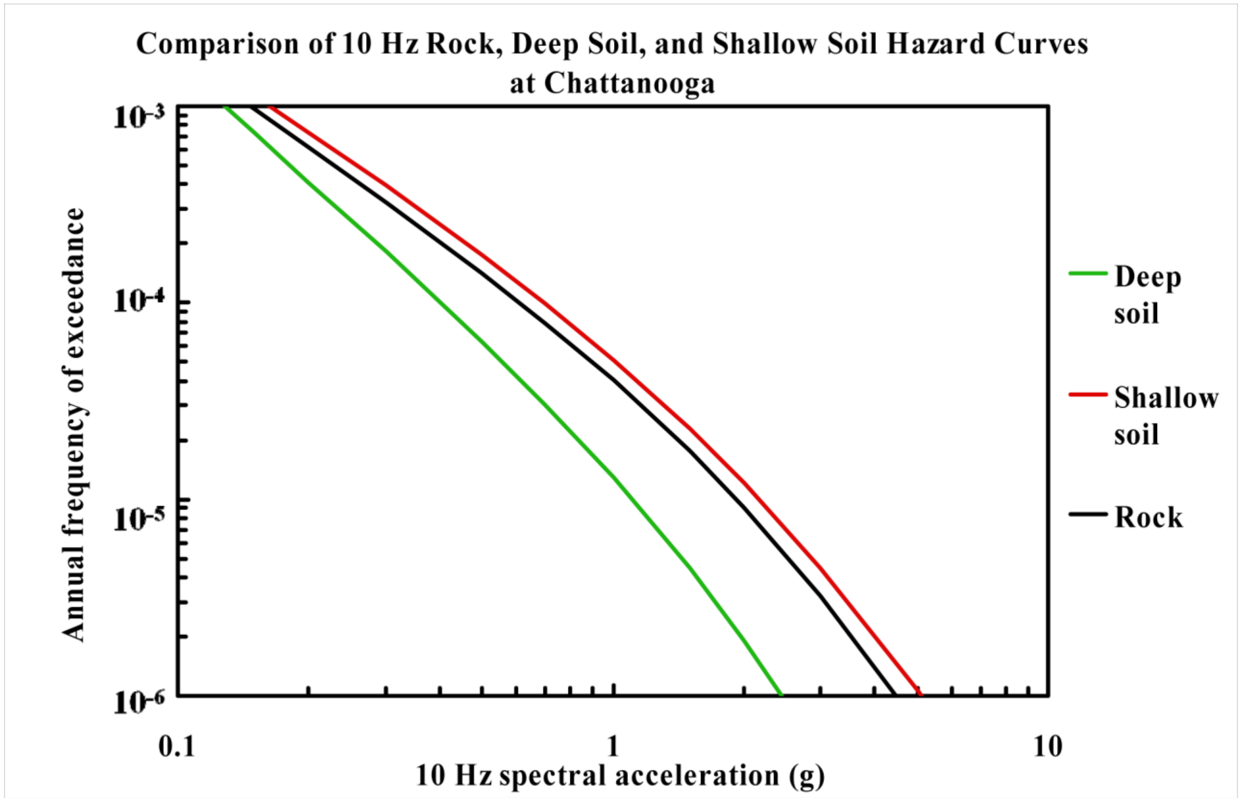

Figure 8.2-2s
Chattanooga 10 Hz hazard: comparison of three site conditions

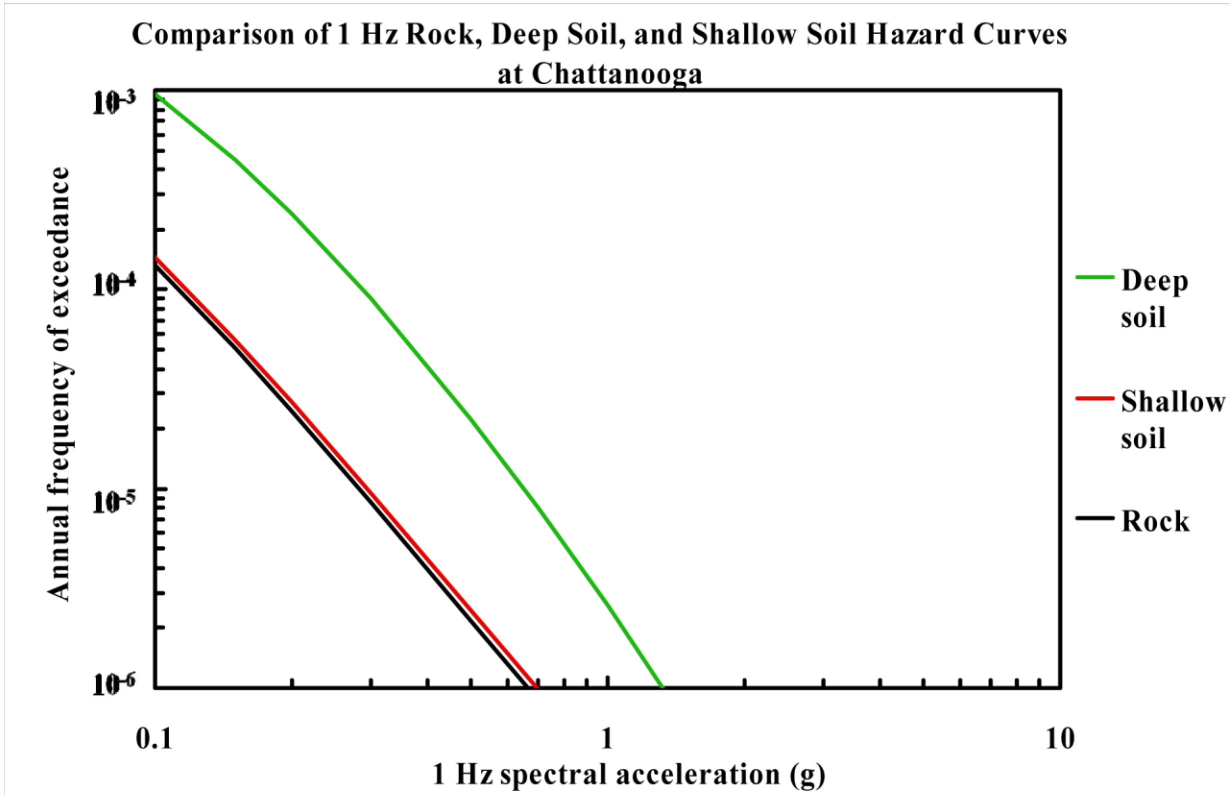

Figure 8.2-2t
Chattanooga 1 Hz hazard: comparison of three site conditions

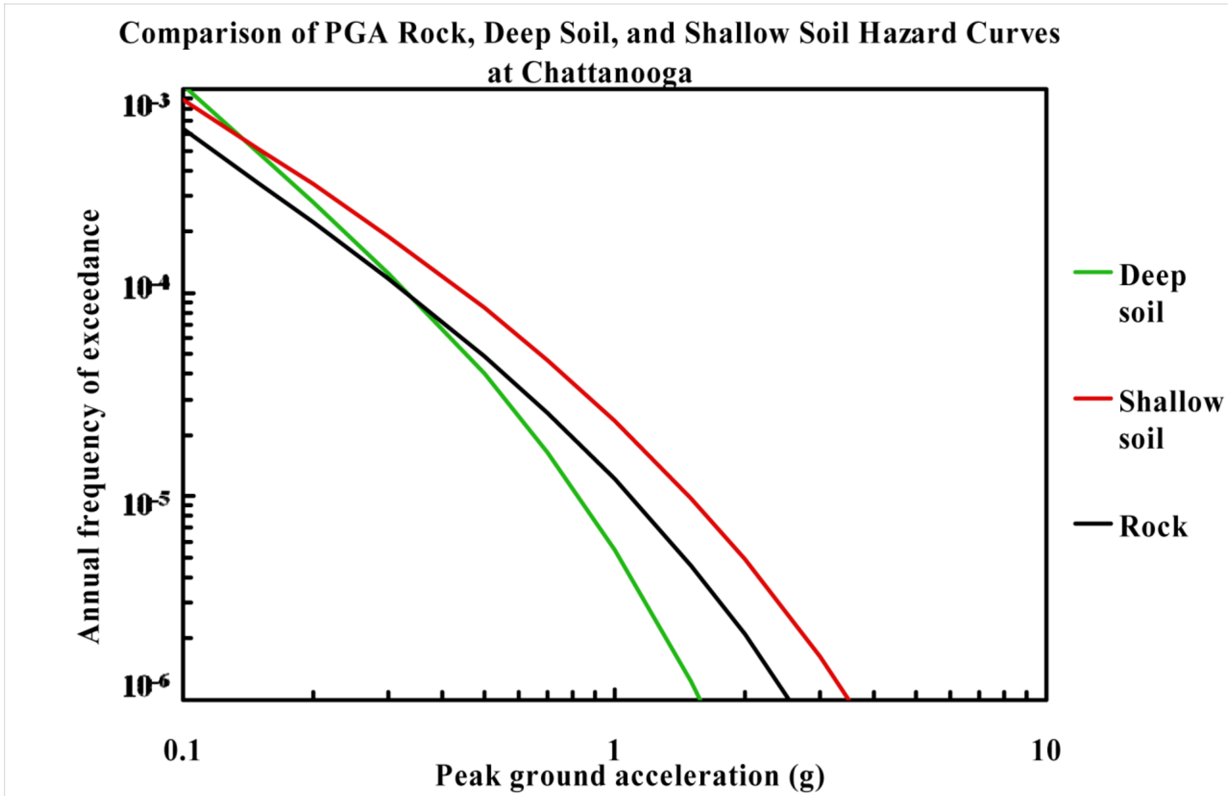

Figure 8.2-2u
Chattanooga PGA hazard: comparison of three site conditions

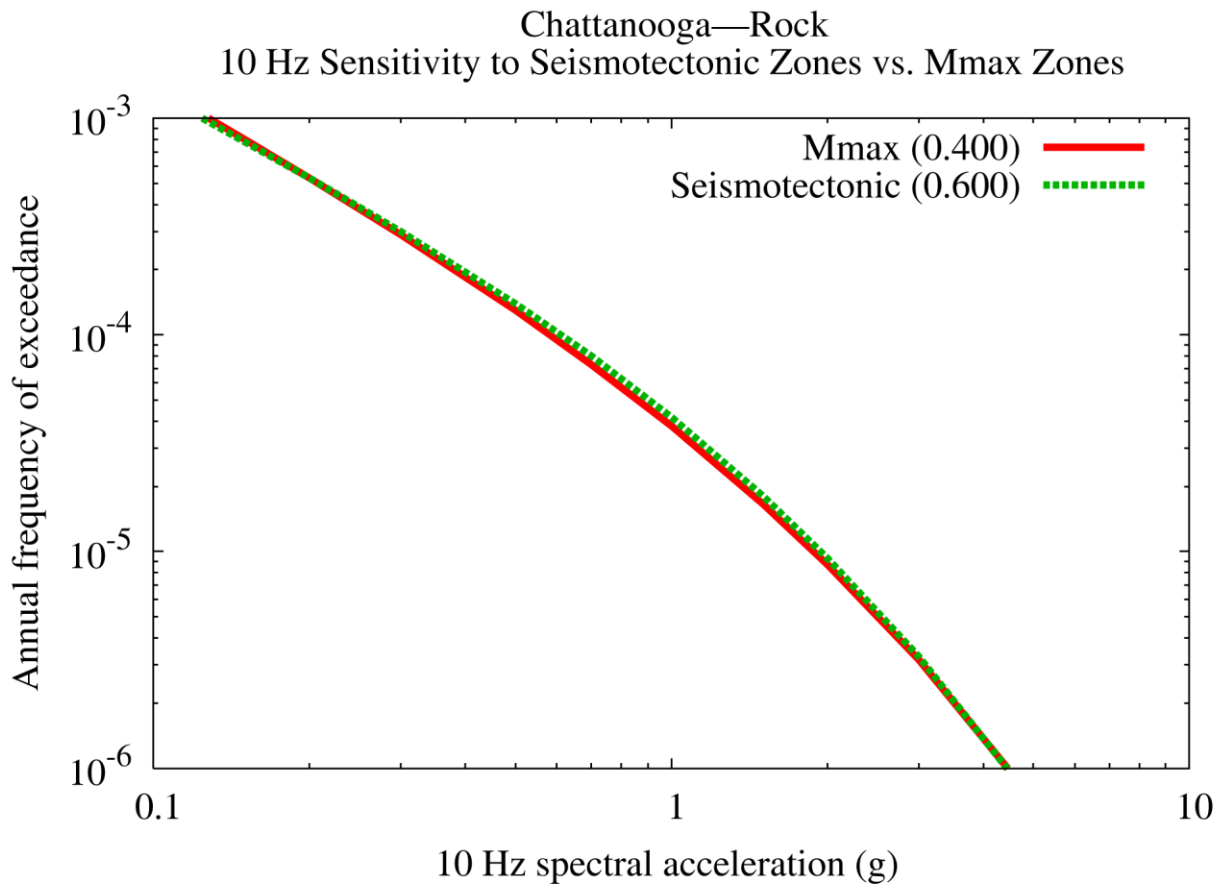

Figure 8.2-2v
Chattanooga 10 Hz rock hazard: sensitivity to seismotectonic vs. Mmax zones

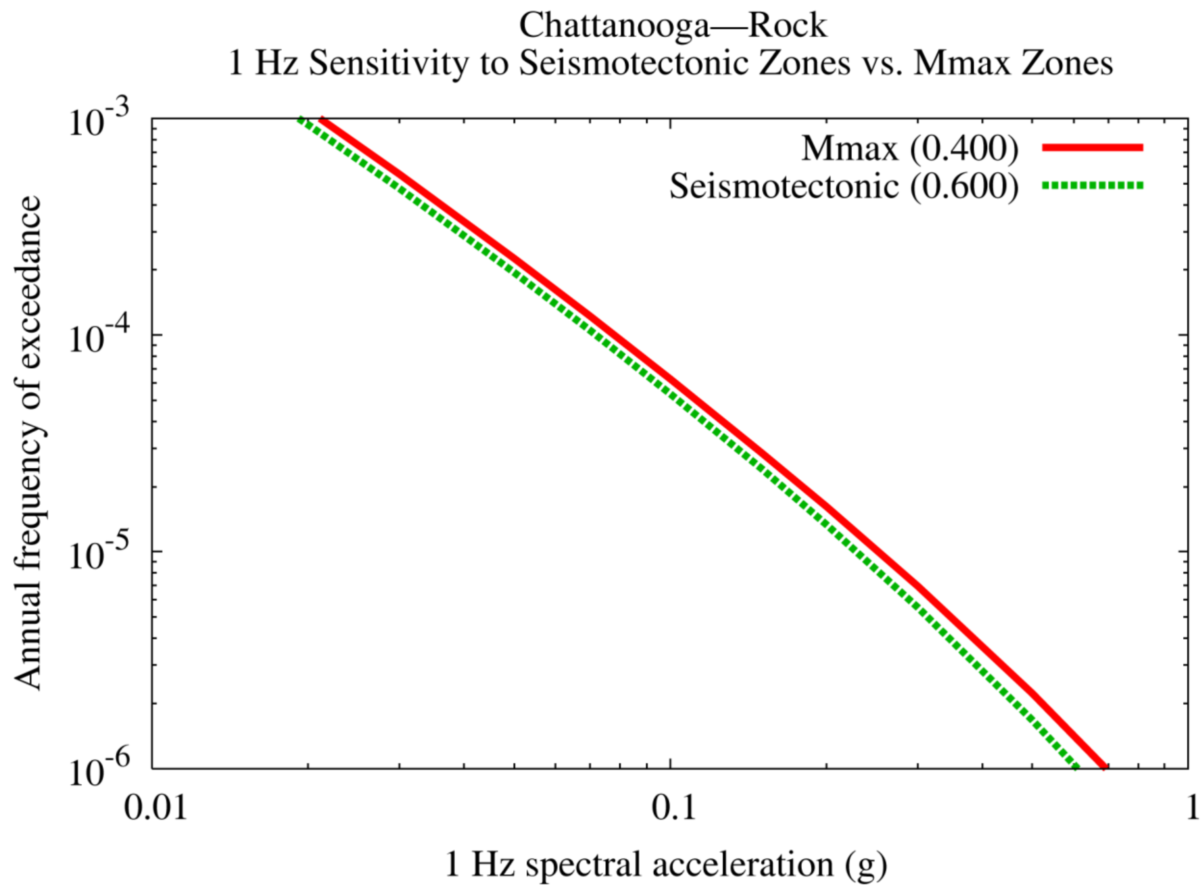

Figure 8.2-2w
Chattanooga 1 Hz rock hazard: sensitivity to seismotectonic vs. Mmax zones

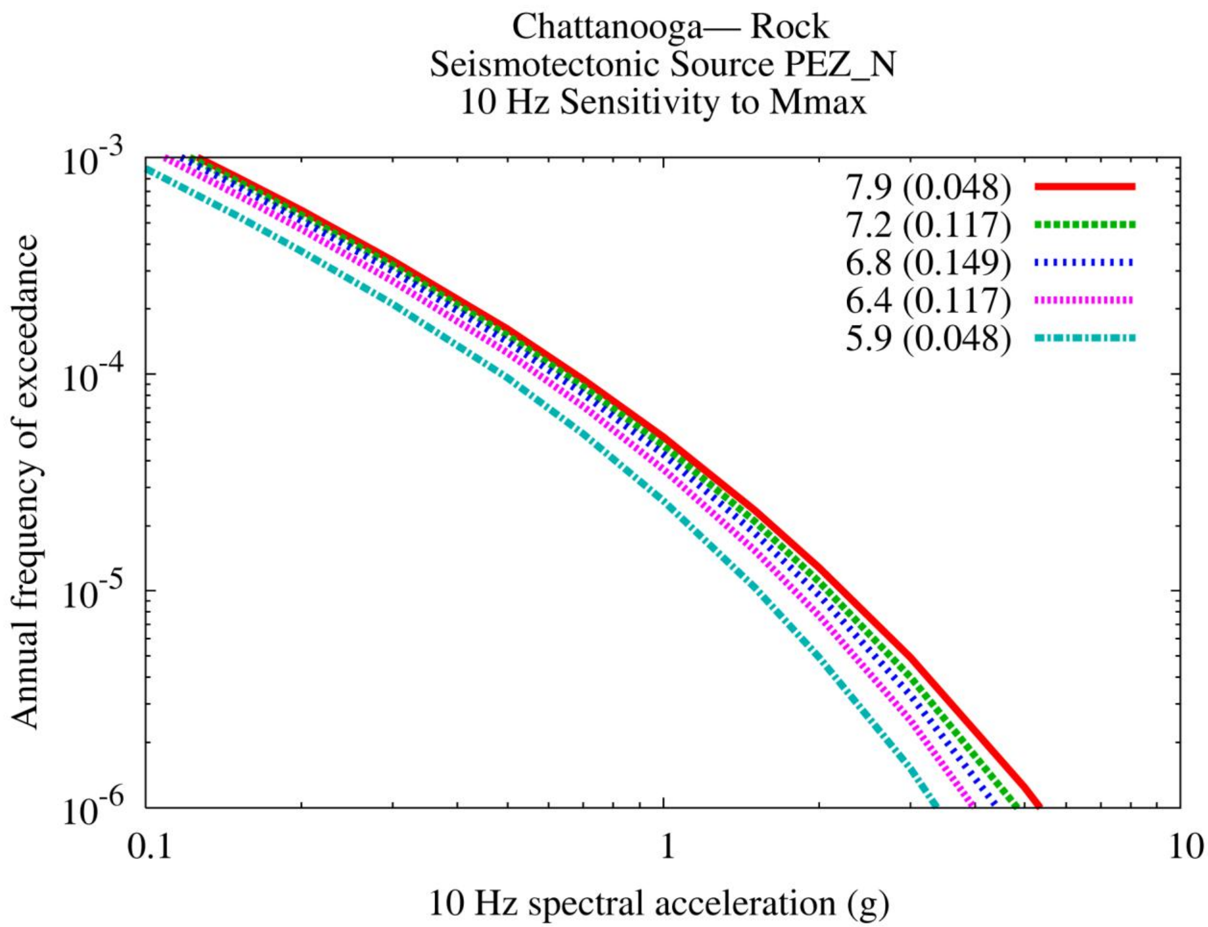

Figure 8.2-2x
Chattanooga 10 Hz rock hazard: sensitivity to Mmax for source PEZ-N

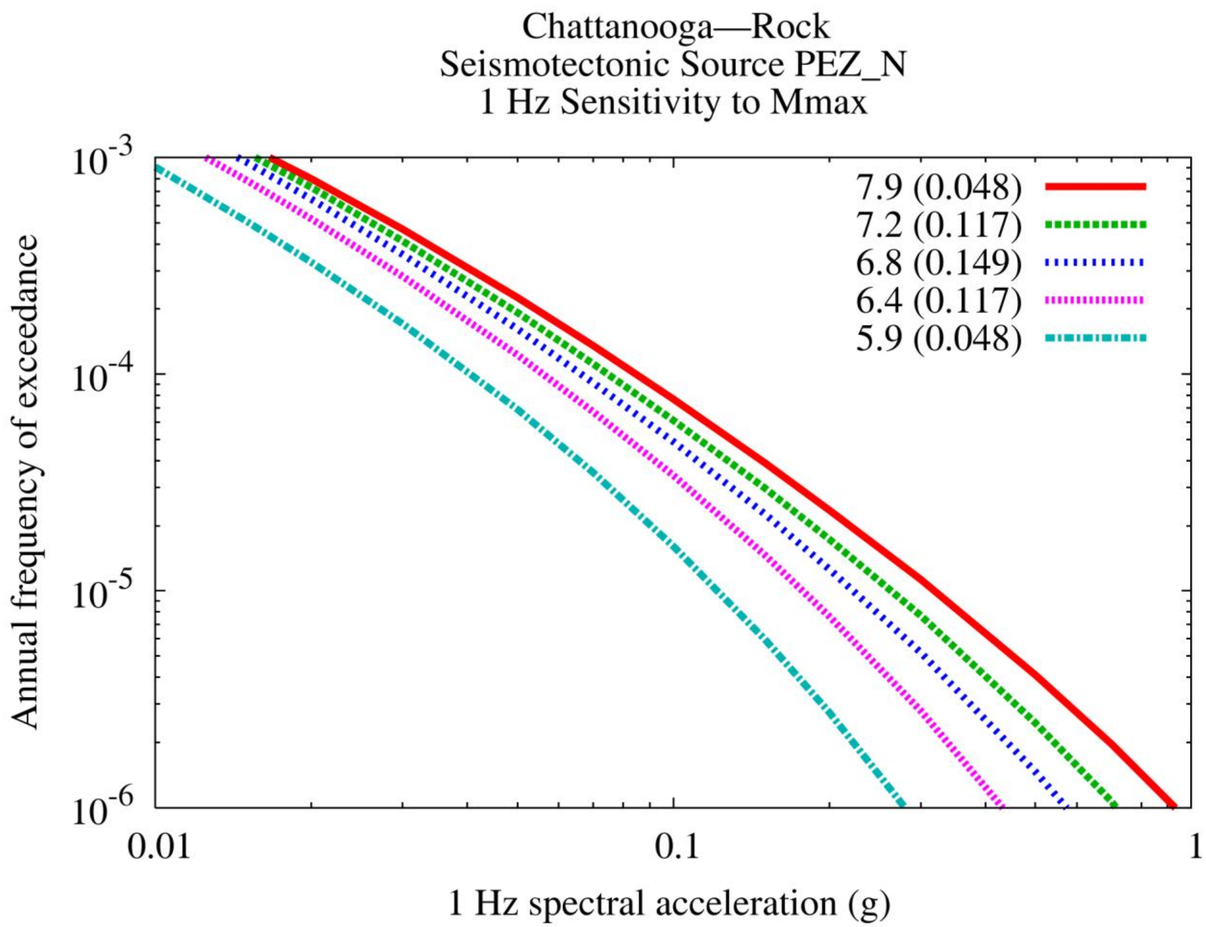

Figure 8.2-2y
Chattanooga 1 Hz rock hazard: sensitivity to Mmax for source PEZ-N

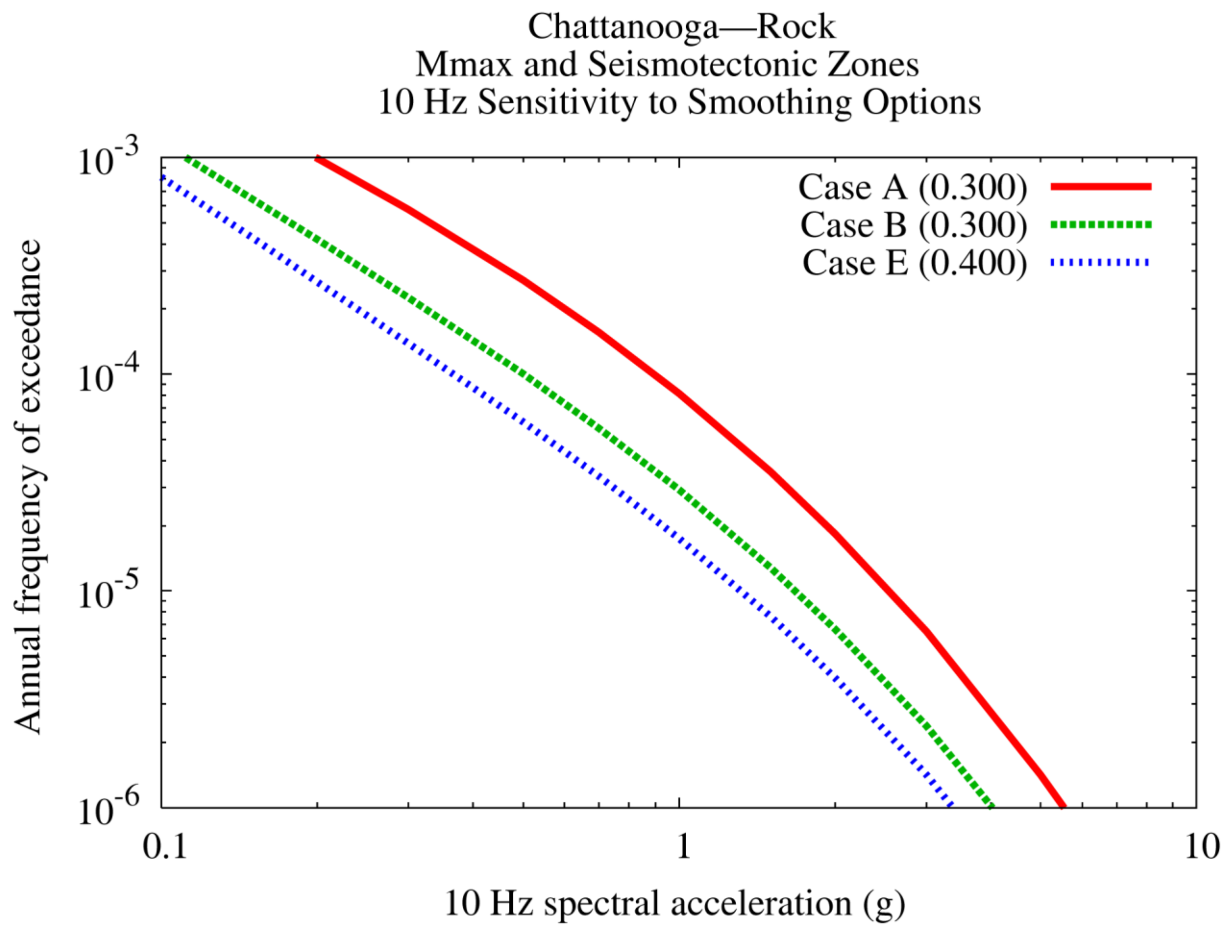

Figure 8.2-2z
Chattanooga 10 Hz rock hazard: sensitivity to smoothing options

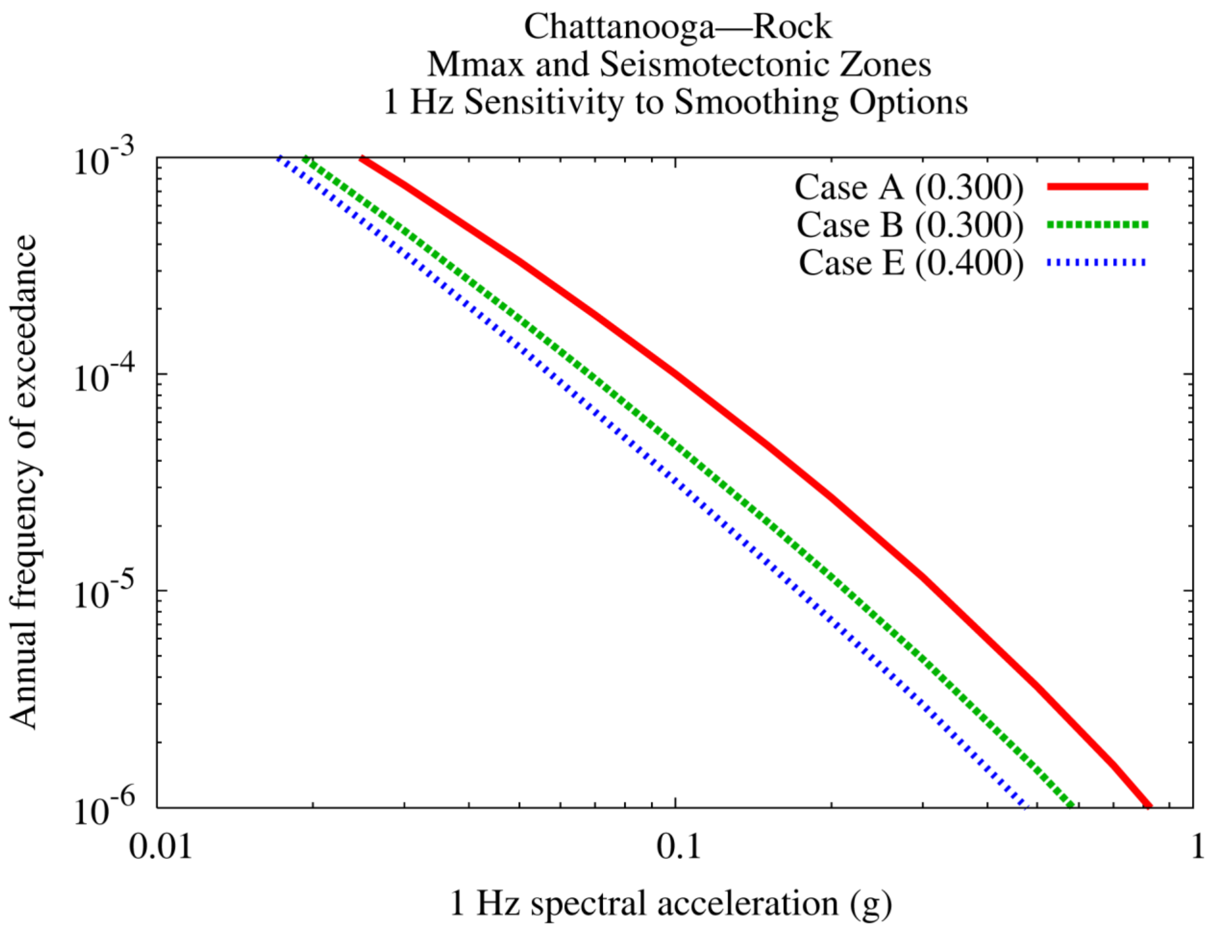

Figure 8.2-2aa
Chattanooga 1 Hz rock hazard: sensitivity to smoothing options

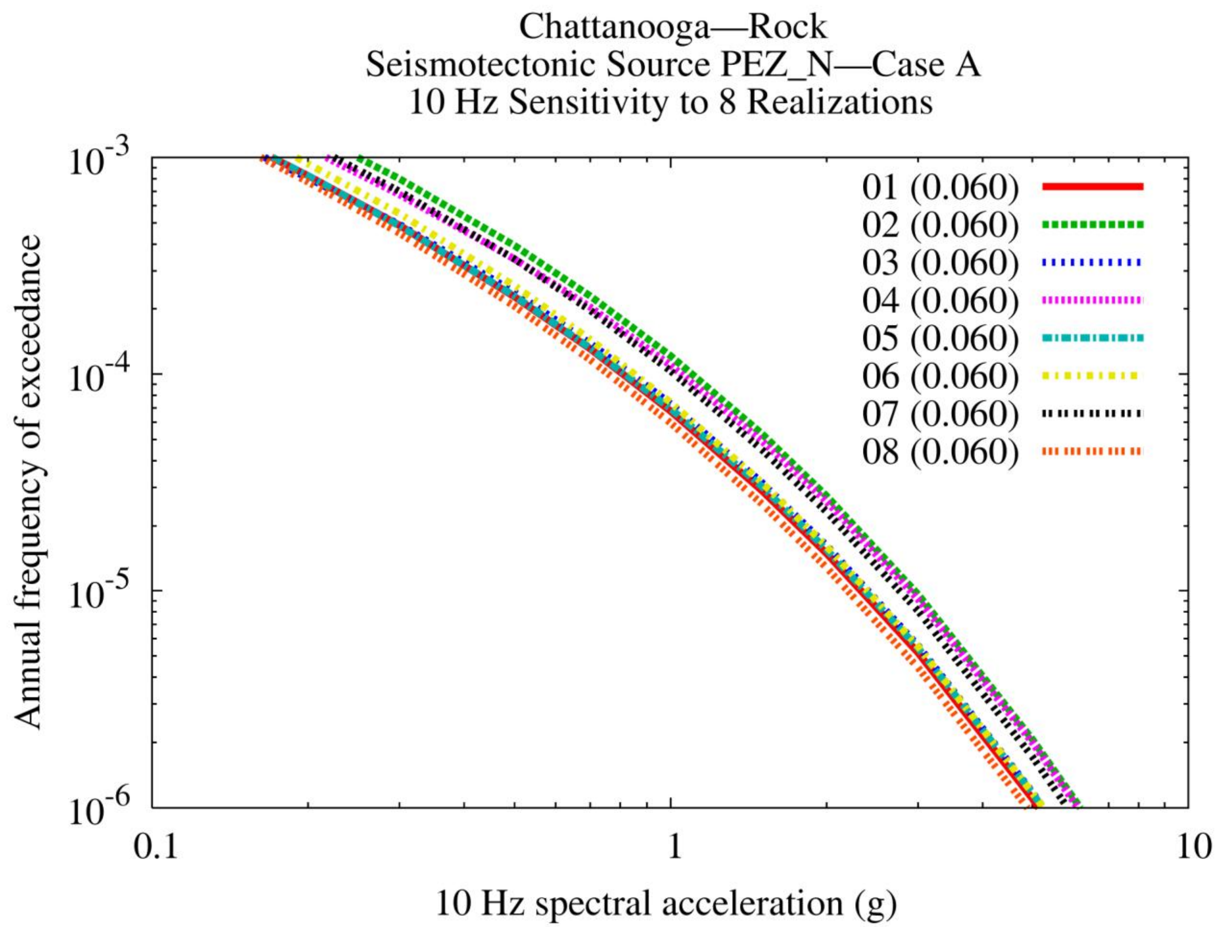

Figure 8.2-2bb
Chattanooga 10 Hz rock hazard: sensitivity to eight realizations for source PEZ-N, Case A

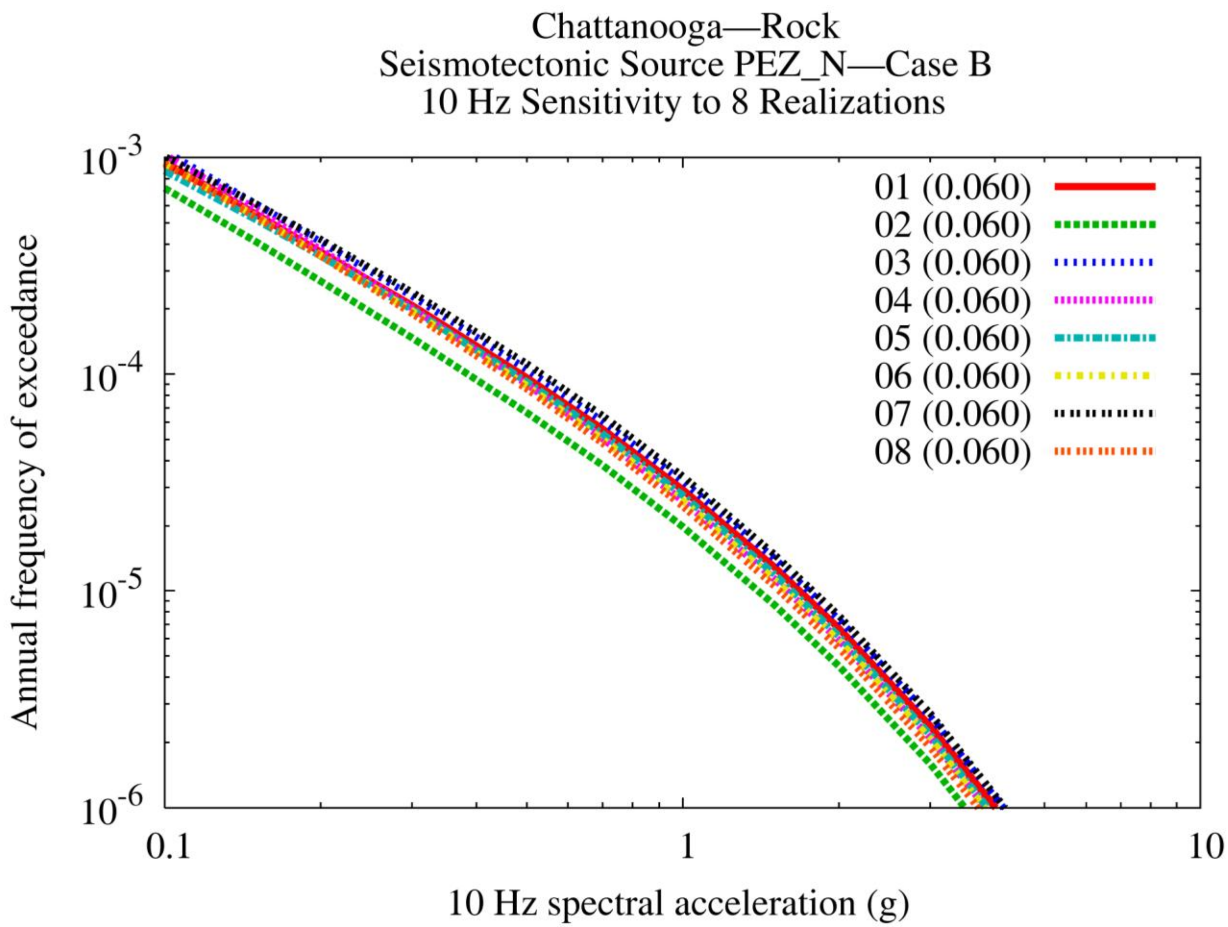

Figure 8.2-2cc
Chattanooga 10 Hz rock hazard: sensitivity to eight realizations for source PEZ-N, Case B

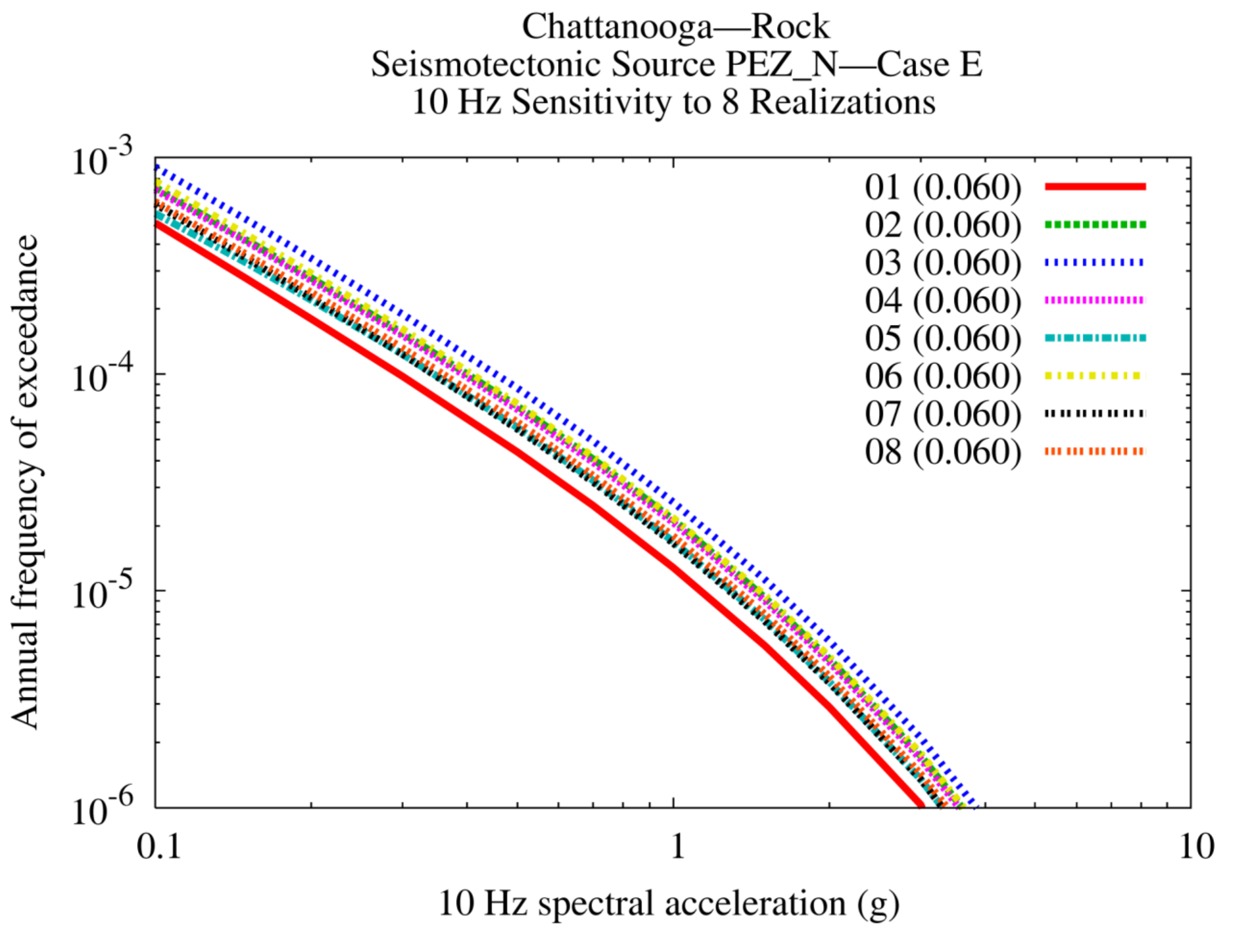

Figure 8.2-2dd
Chattanooga 10 Hz rock hazard: sensitivity to eight realizations for source PEZ-N, Case E

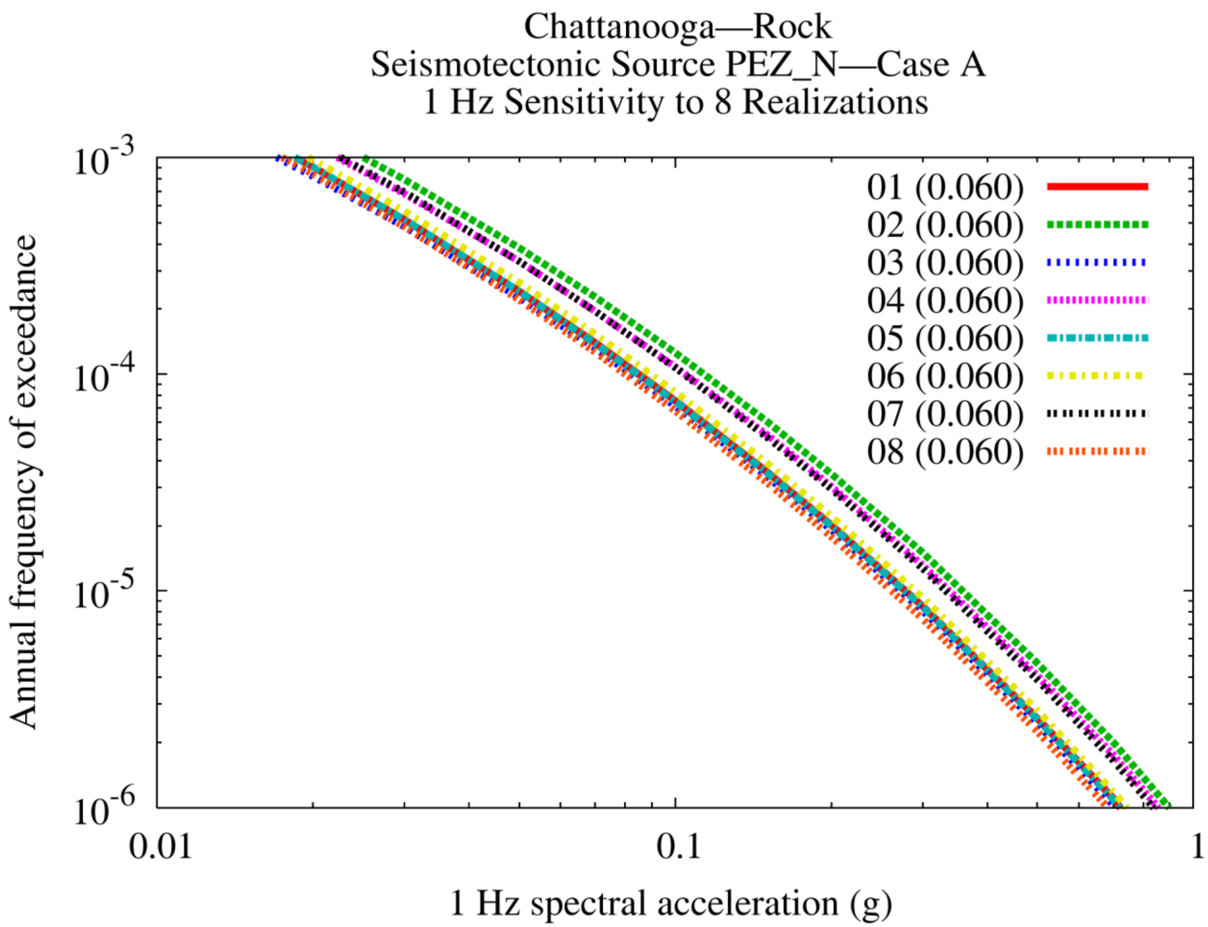

Figure 8.2-2ee
Chattanooga 1 Hz rock hazard: sensitivity to eight realizations for source PEZ-N, Case A

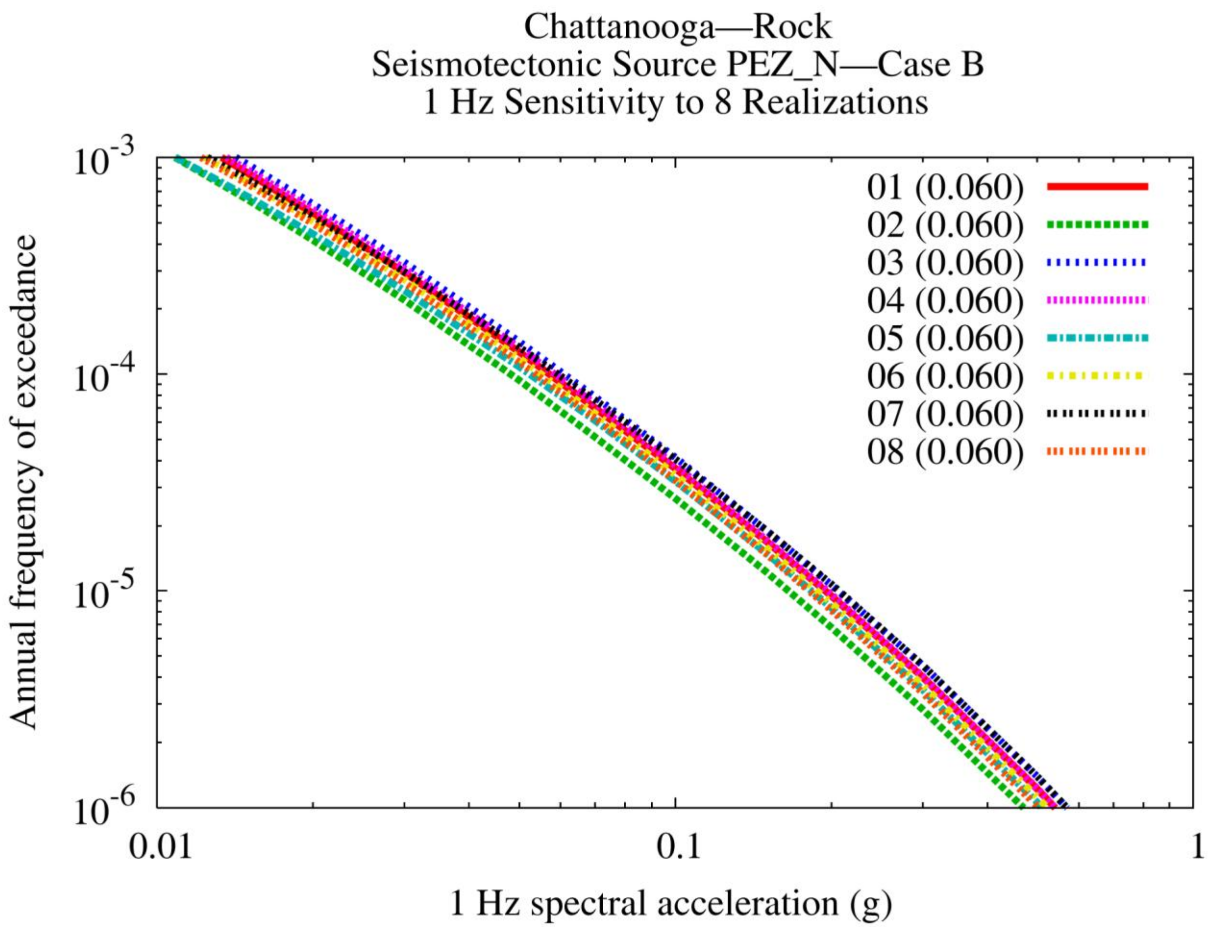

Figure 8.2-2ff
Chattanooga 1 Hz rock hazard: sensitivity to eight realizations for source PEZ-N, Case B

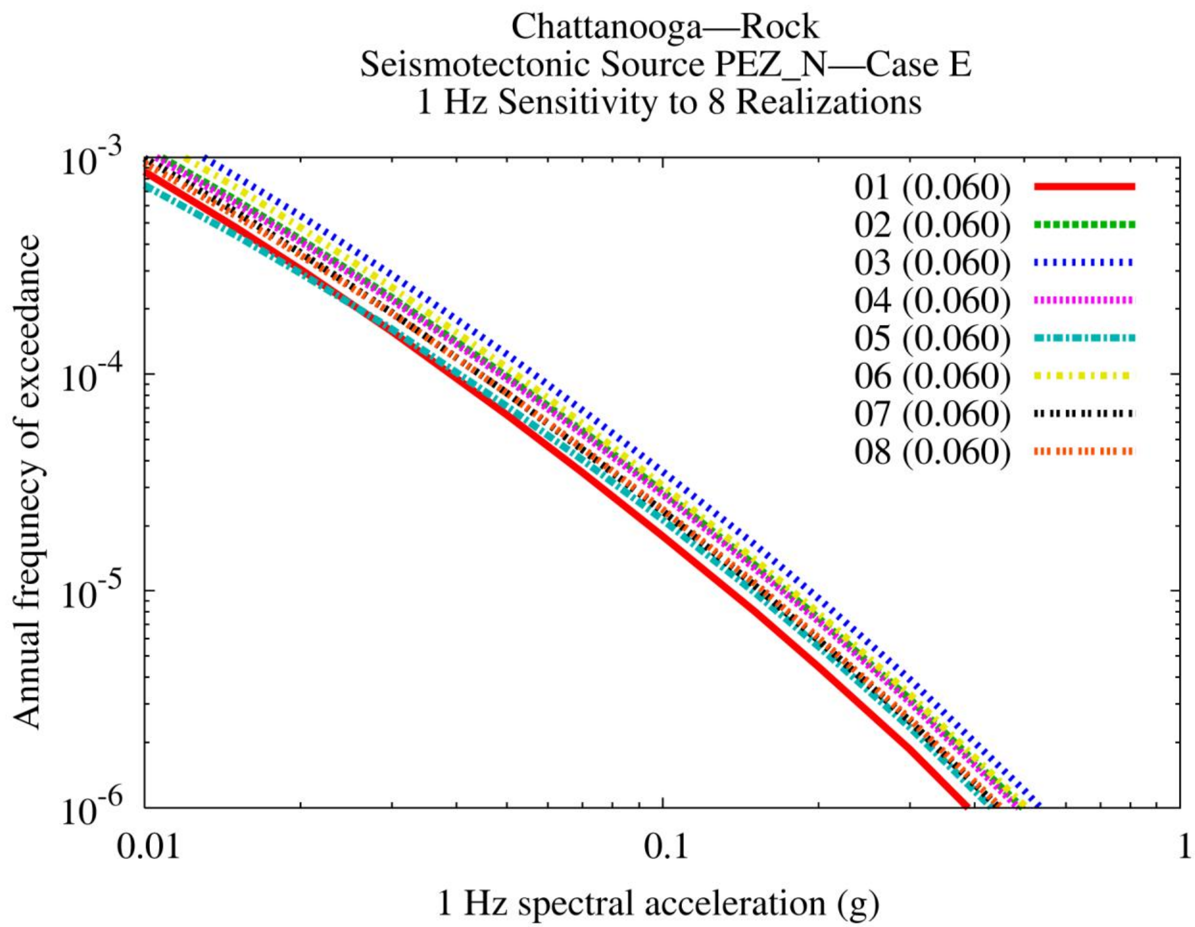

Figure 8.2-2gg
Chattanooga 1 Hz rock hazard: sensitivity to eight realizations for source PEZ-N, Case E

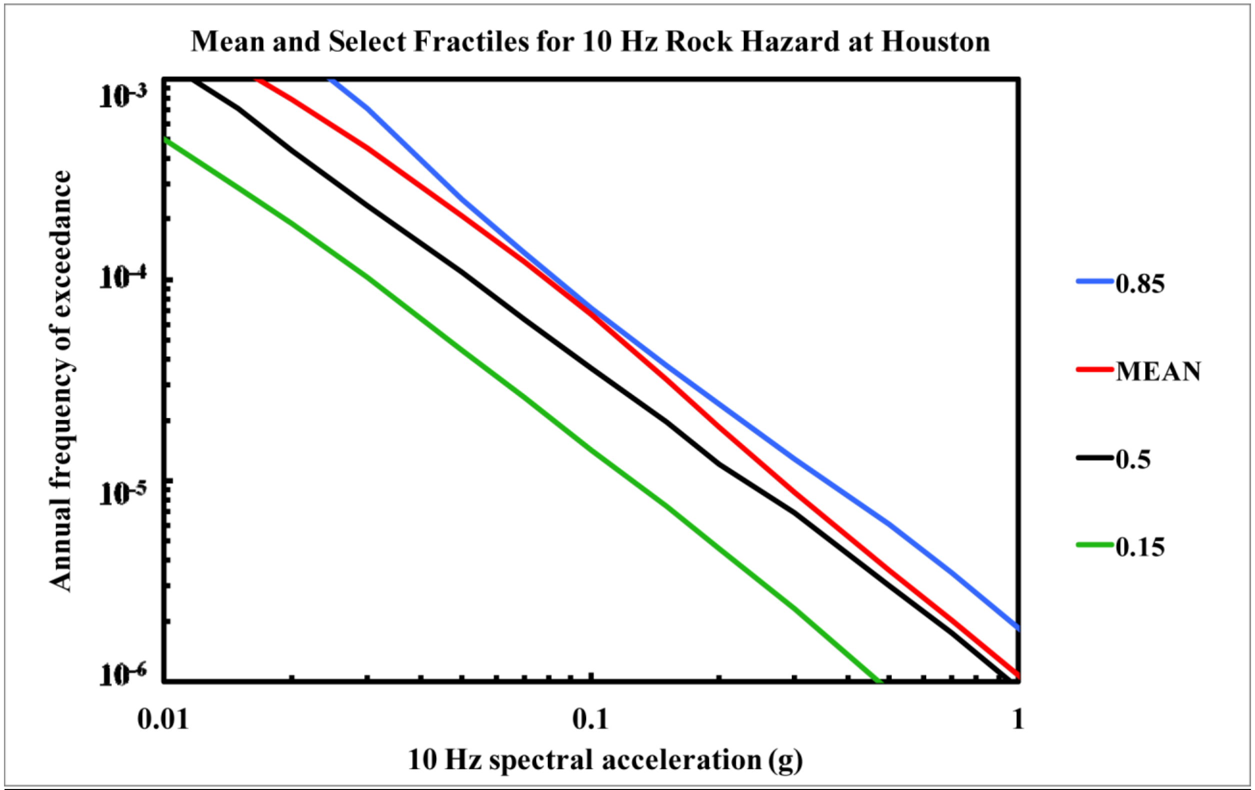

Figure 8.2-3a
Houston 10 Hz rock hazard: mean and fractile total hazard

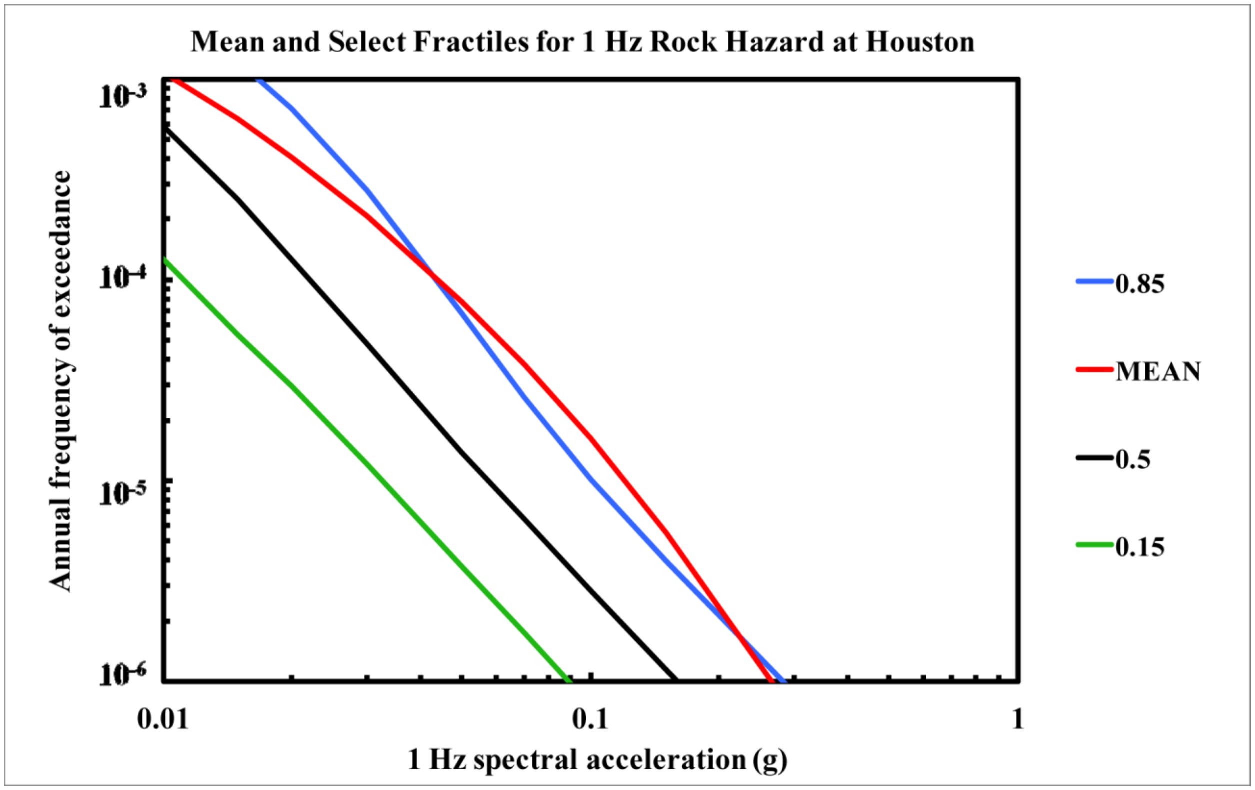

Figure 8.2-3b
Houston 1 Hz rock hazard: mean and fractile total hazard

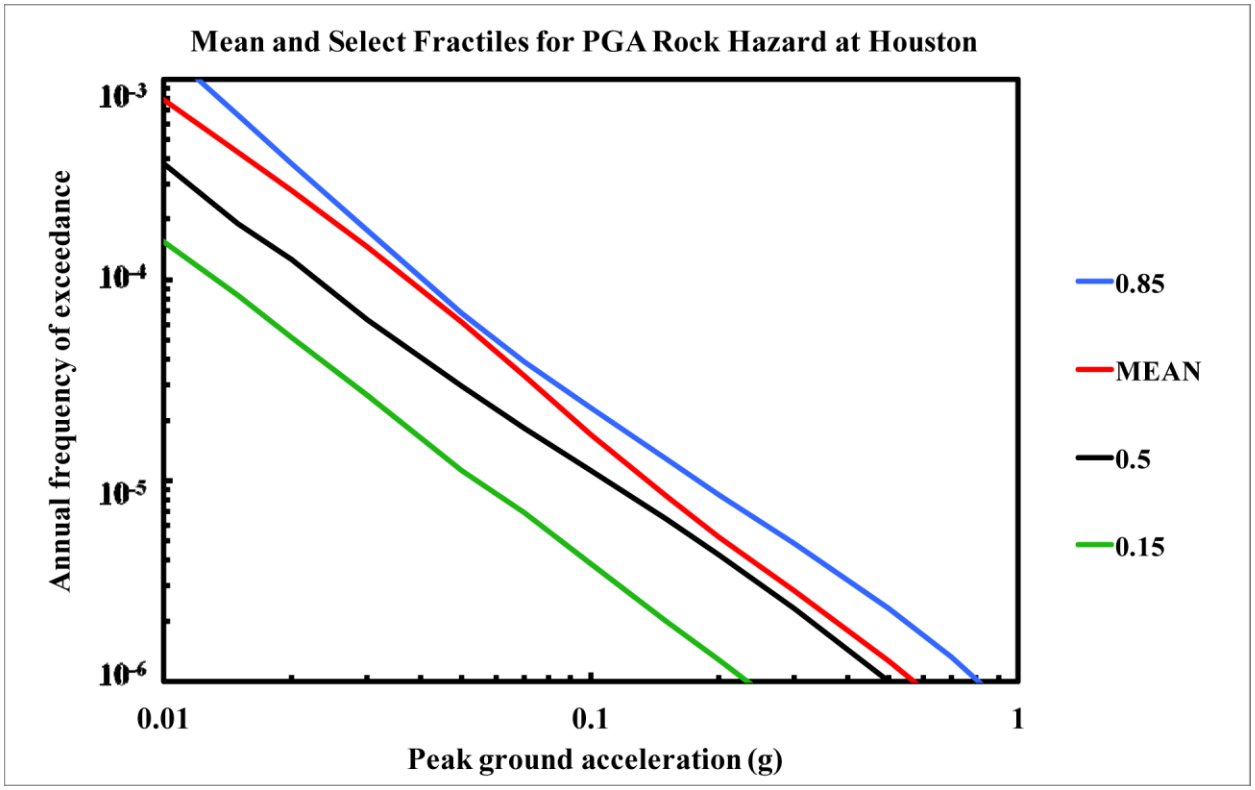

Figure 8.2-3c
Houston PGA rock hazard: mean and fractile total hazard

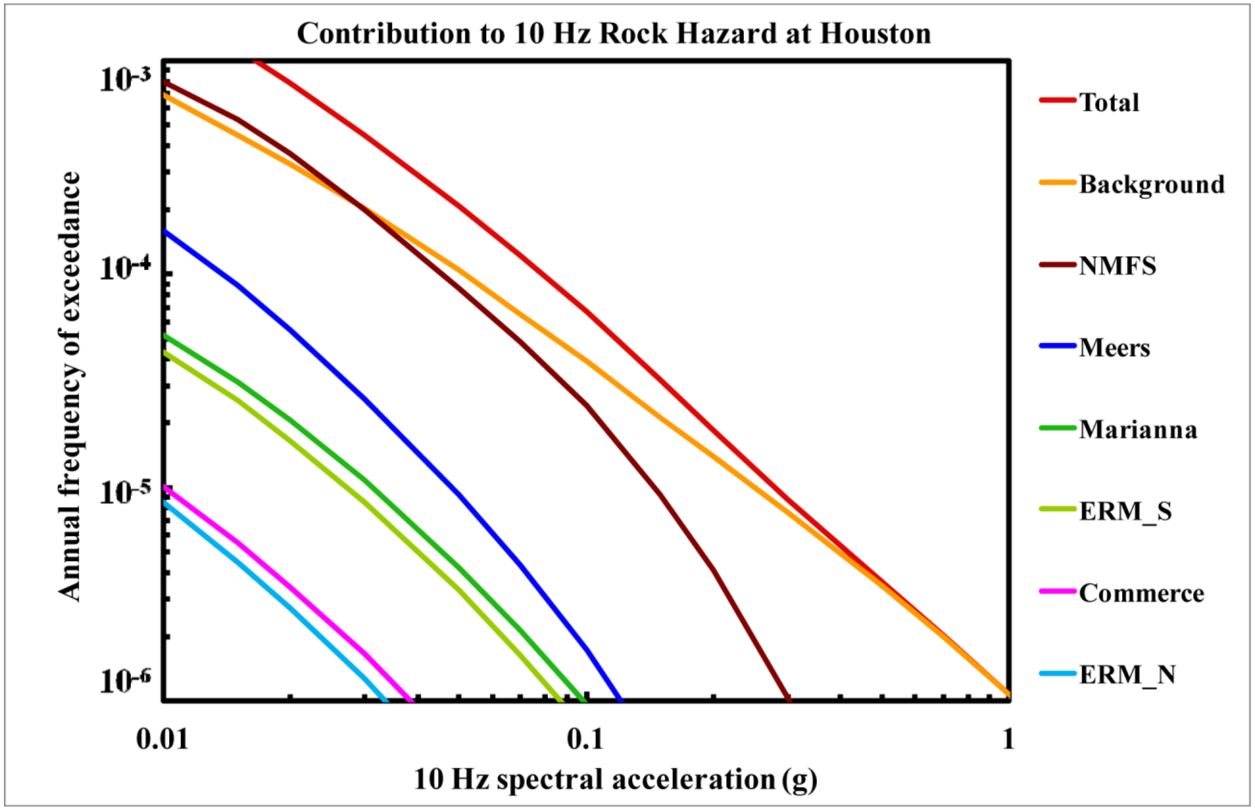

Figure 8.2-3d
Houston 10 Hz rock hazard: total and contribution by RLME and background

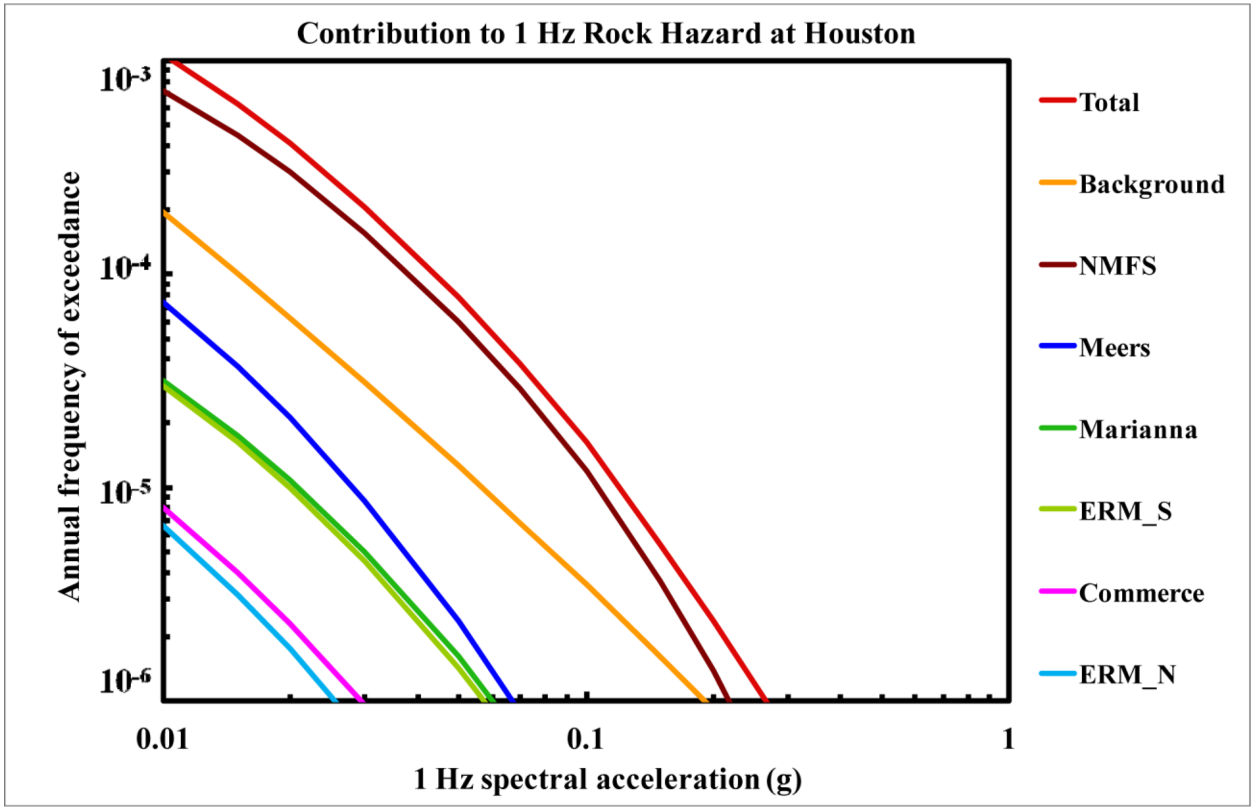

Figure 8.2-3e
Houston 1 Hz rock hazard: total and contribution by RLME and background

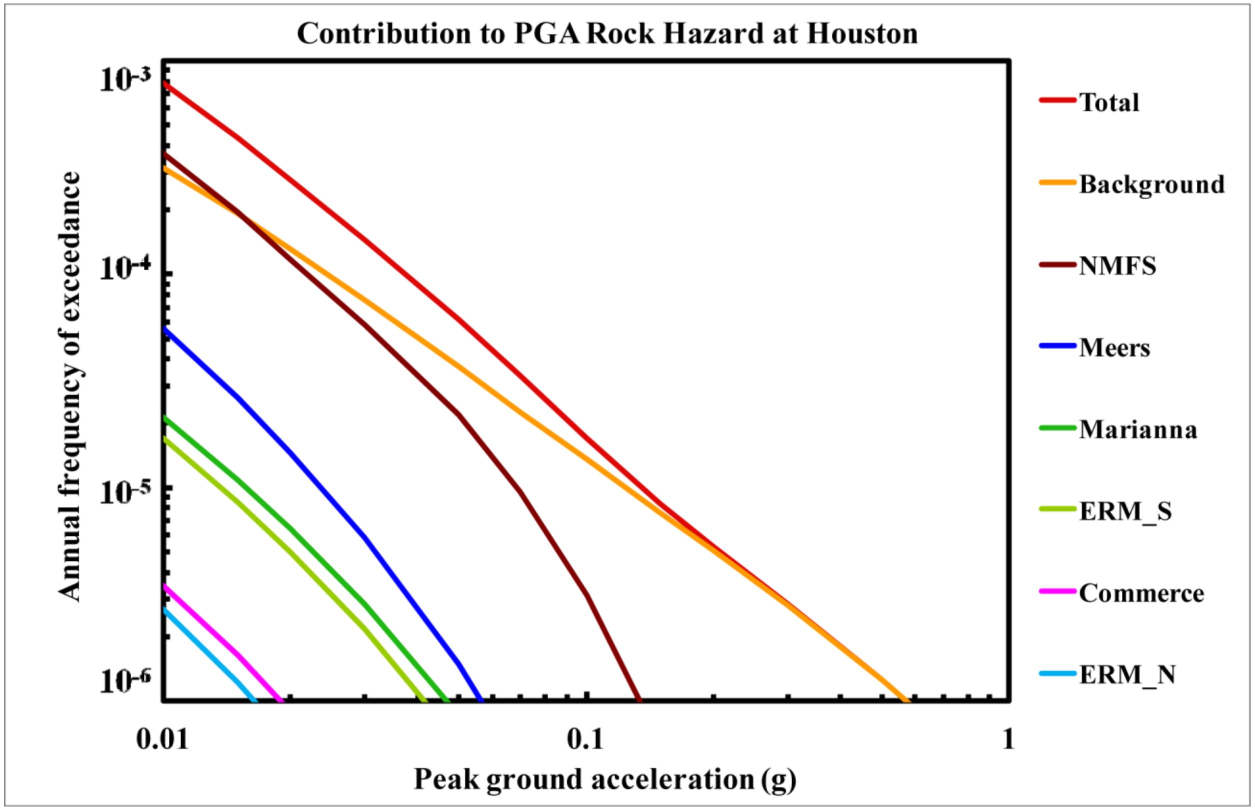

Figure 8.2-3f
Houston PGA rock hazard: total and contribution by RLME and background

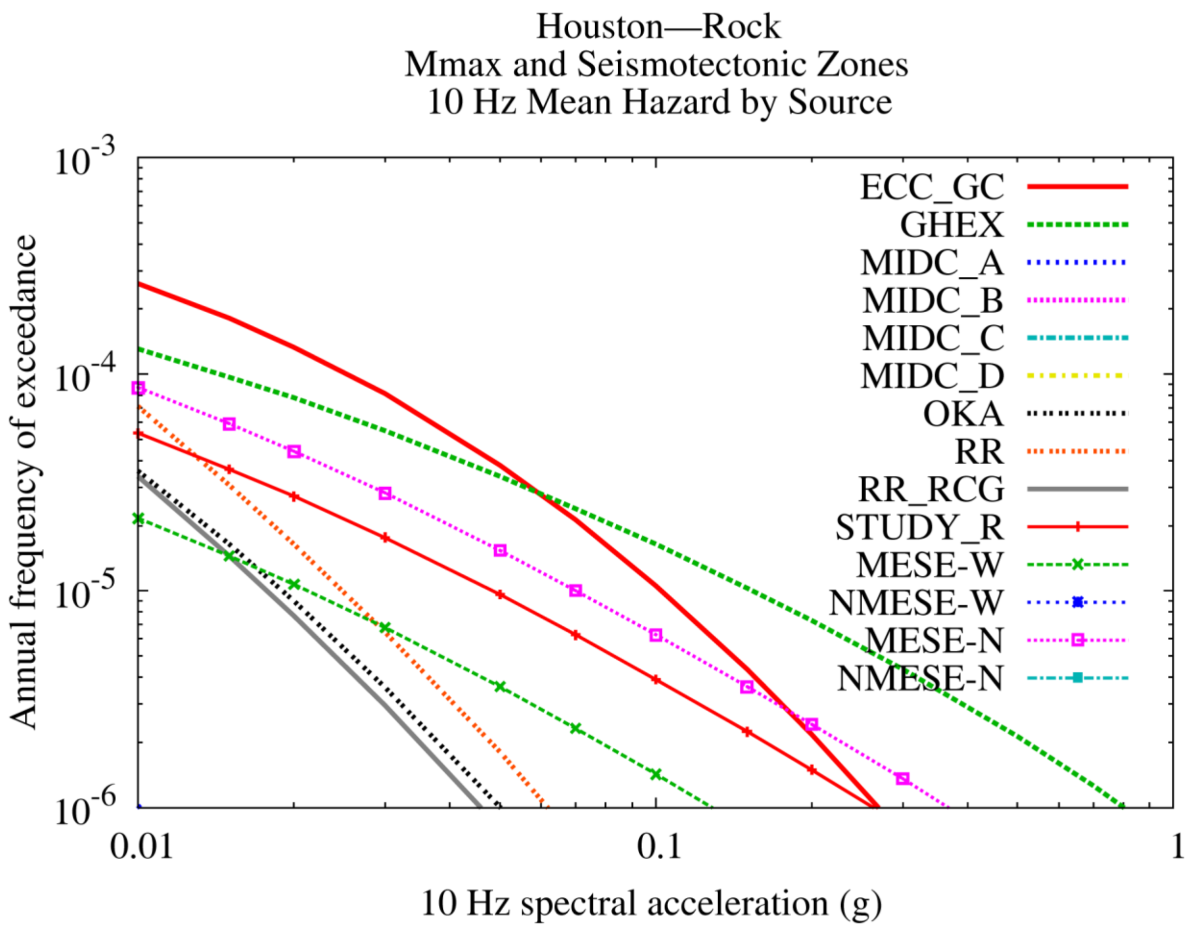

Figure 8.2-3g
Houston 10 Hz rock hazard: contribution by background source

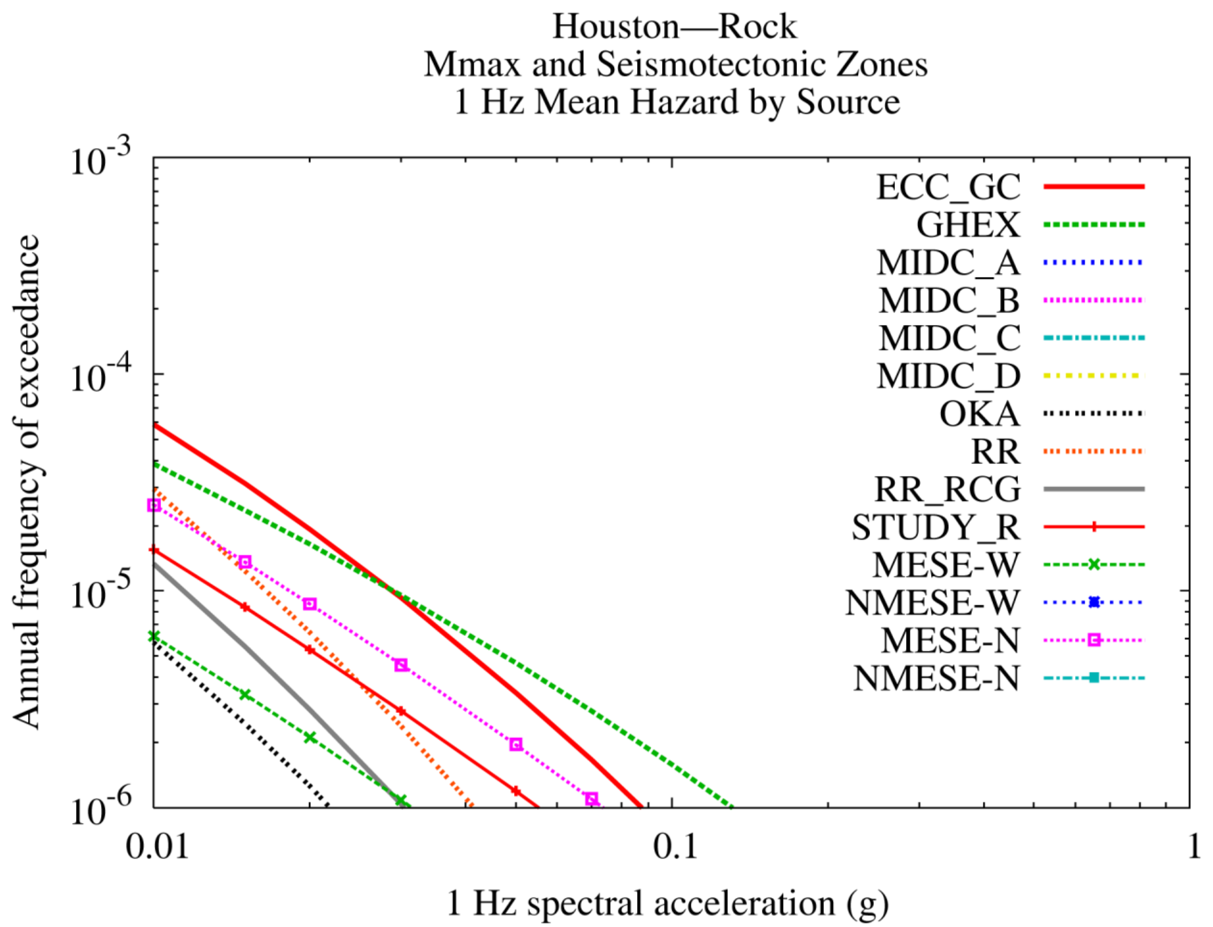

Figure 8.2-3h
Houston 1 Hz rock hazard: contribution by background source

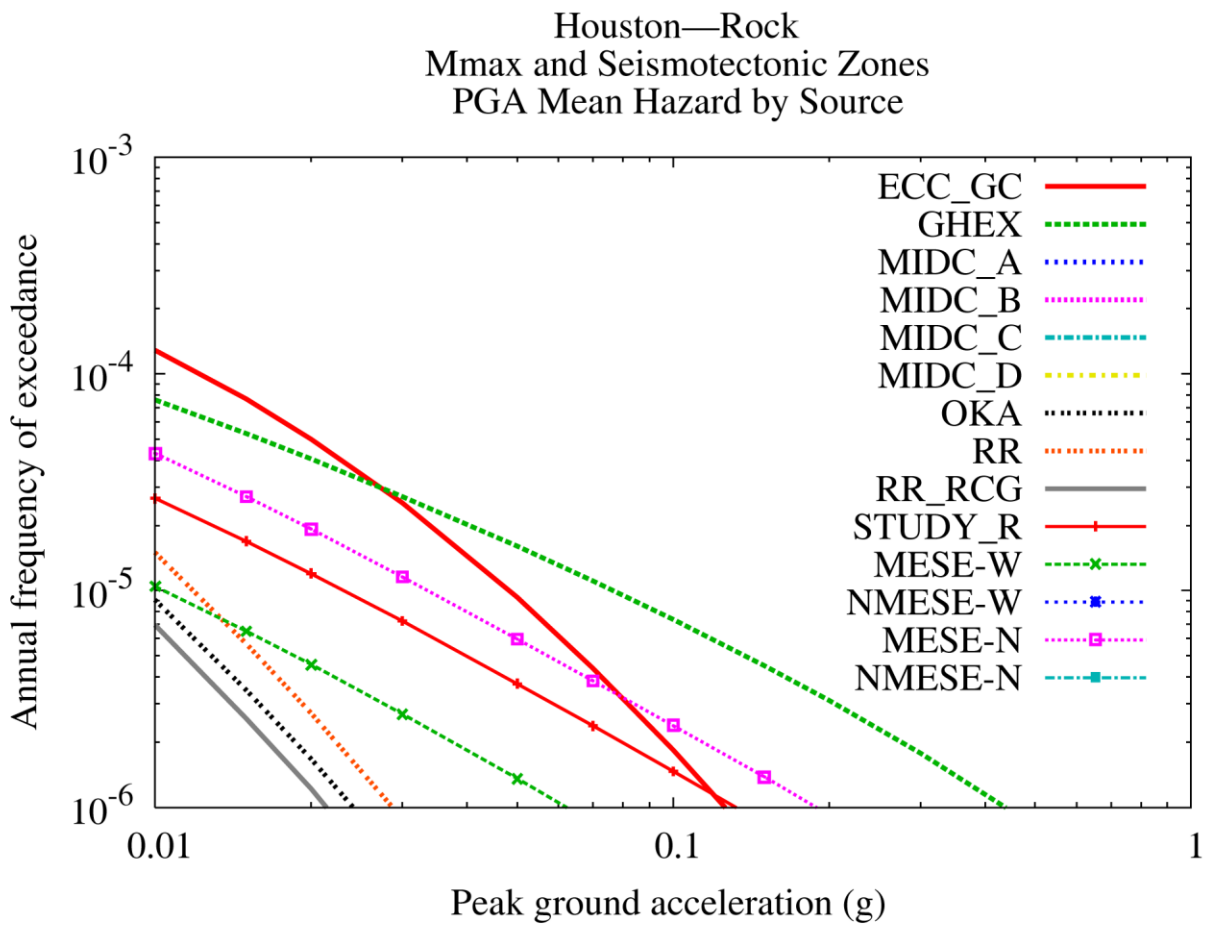

Figure 8.2-3i
Houston PGA rock hazard: contribution by background source

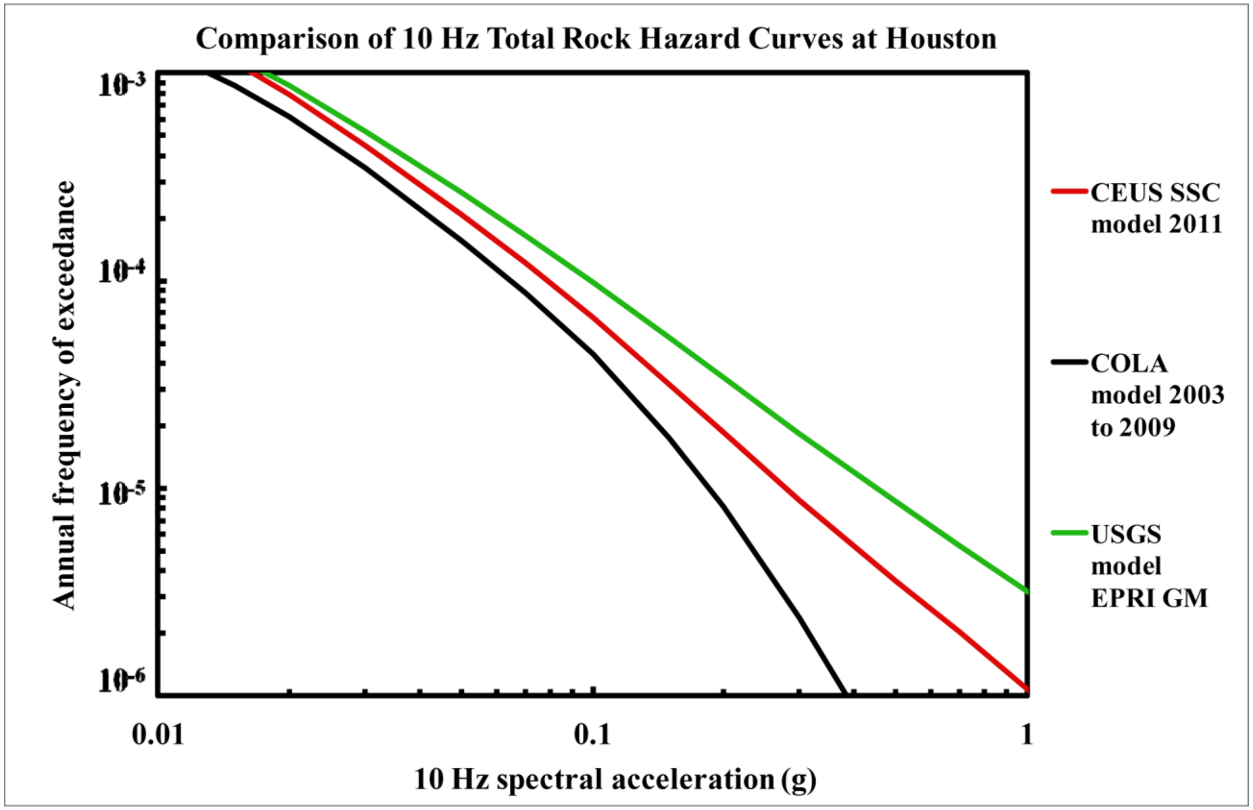

Figure 8.2-3j
Houston 10 Hz rock hazard: comparison of three source models

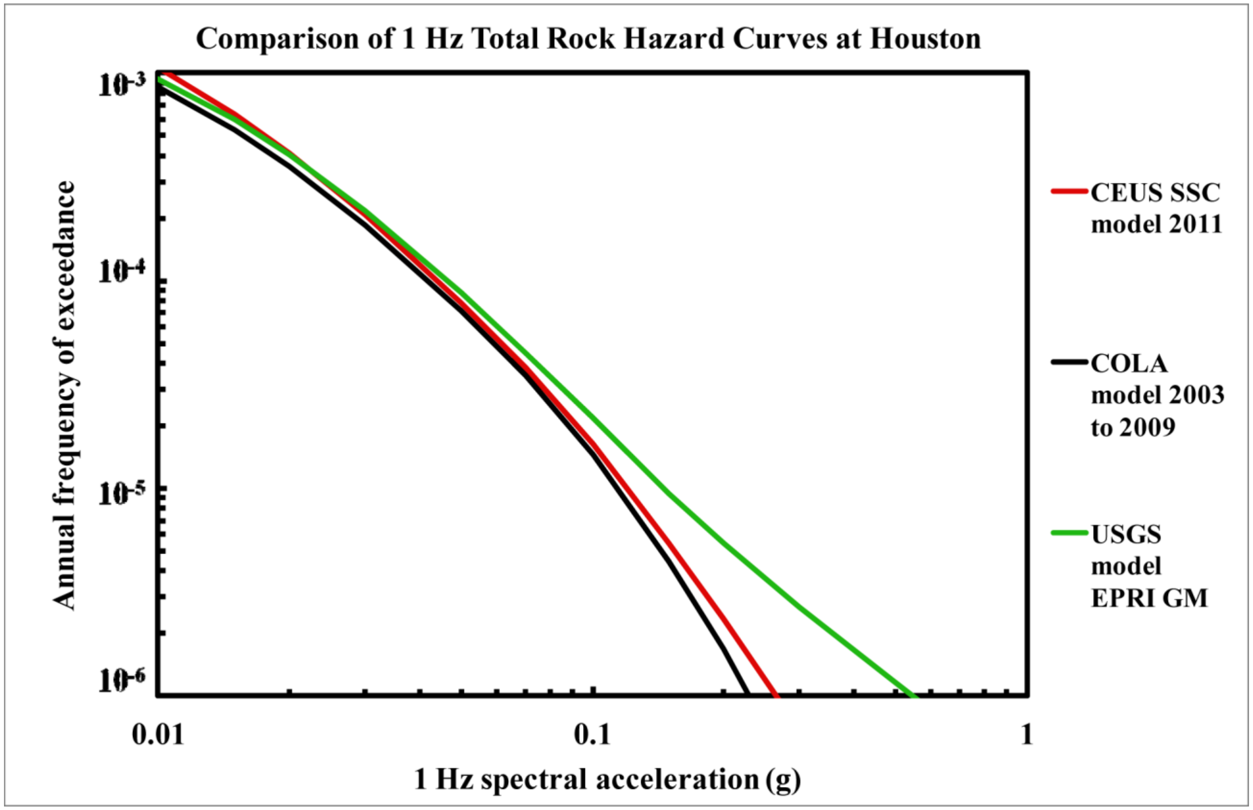

Figure 8.2-3k
Houston is 1 Hz rock hazard: comparison of three source models

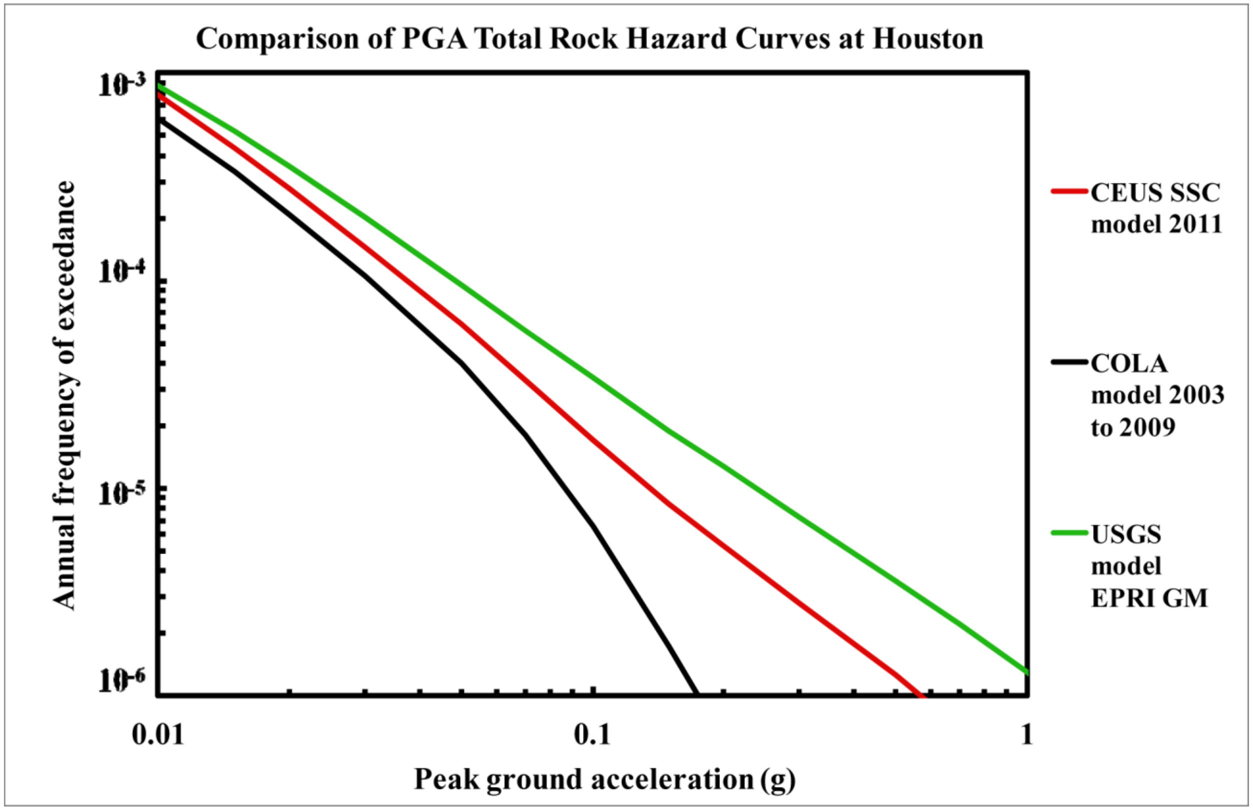

Figure 8.2-3l
Houston PGA rock hazard: comparison of three source models

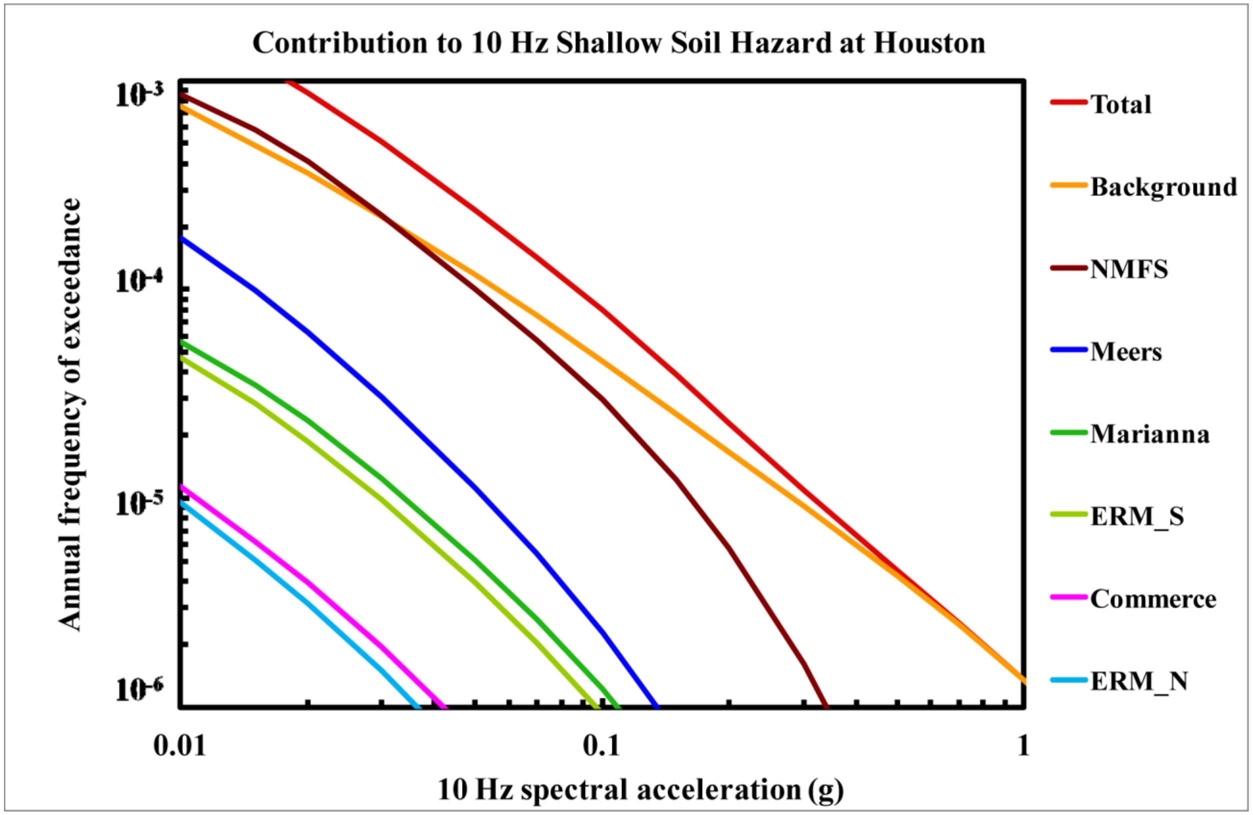

Figure 8.2-3m
Houston 10 Hz shallow soil hazard: total and contribution by RLME and background

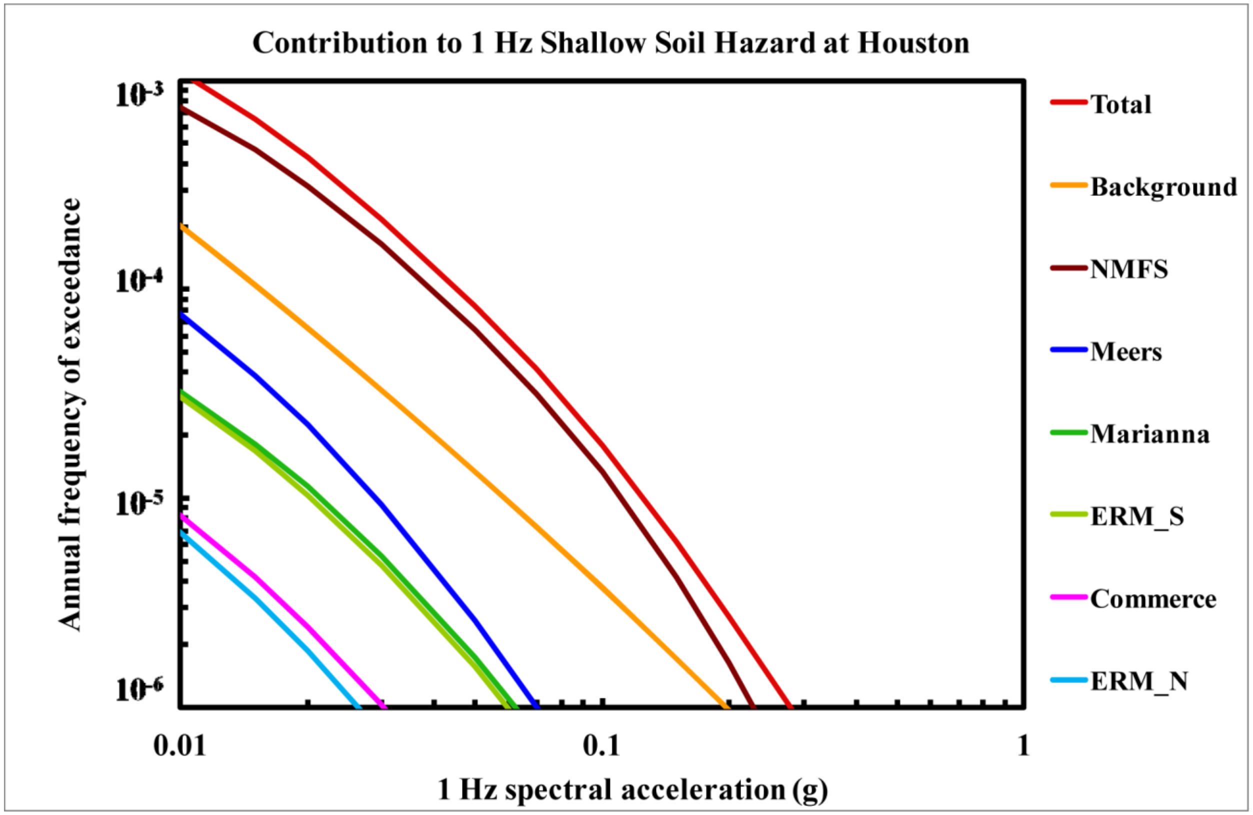

Figure 8.2-3n
Houston 1 Hz shallow soil hazard: total and contribution by RLME and background

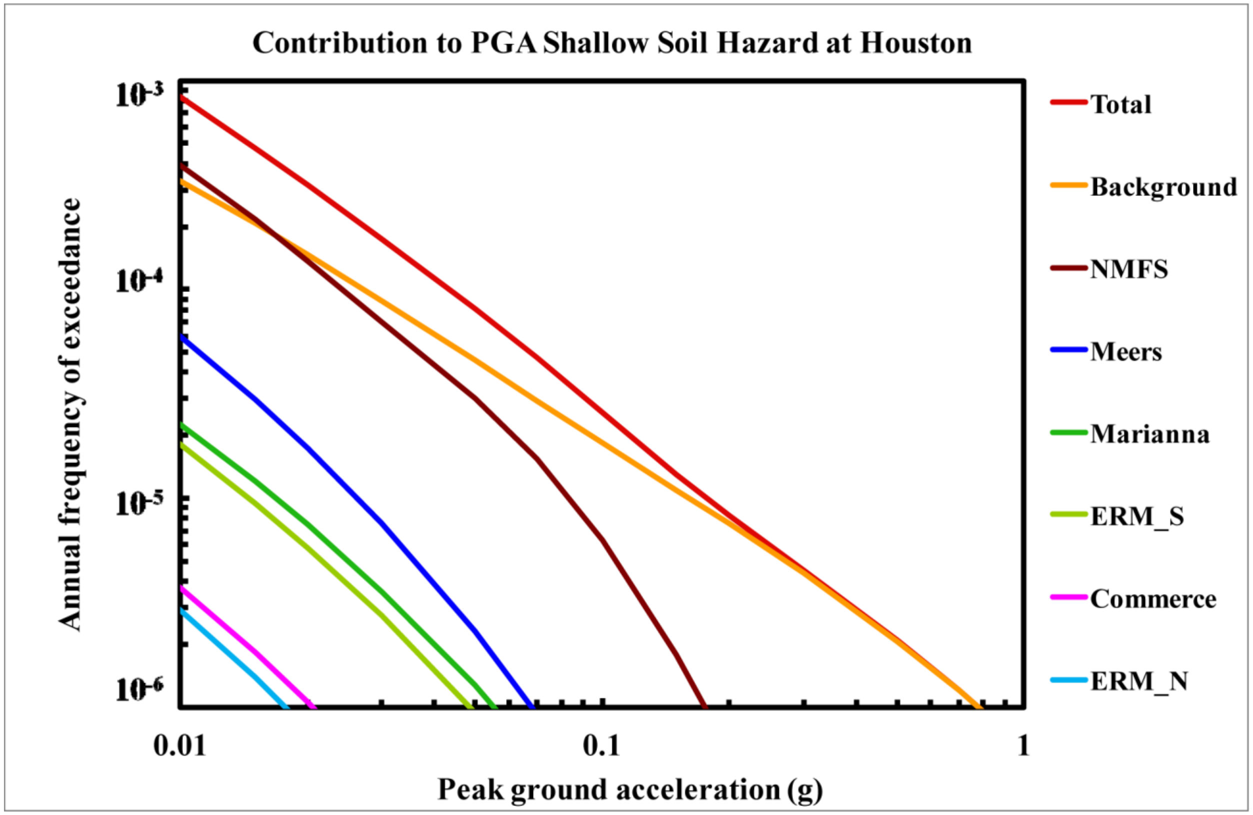

Figure 8.2-3o
Houston PGA shallow soil hazard: total and contribution by RLME and background

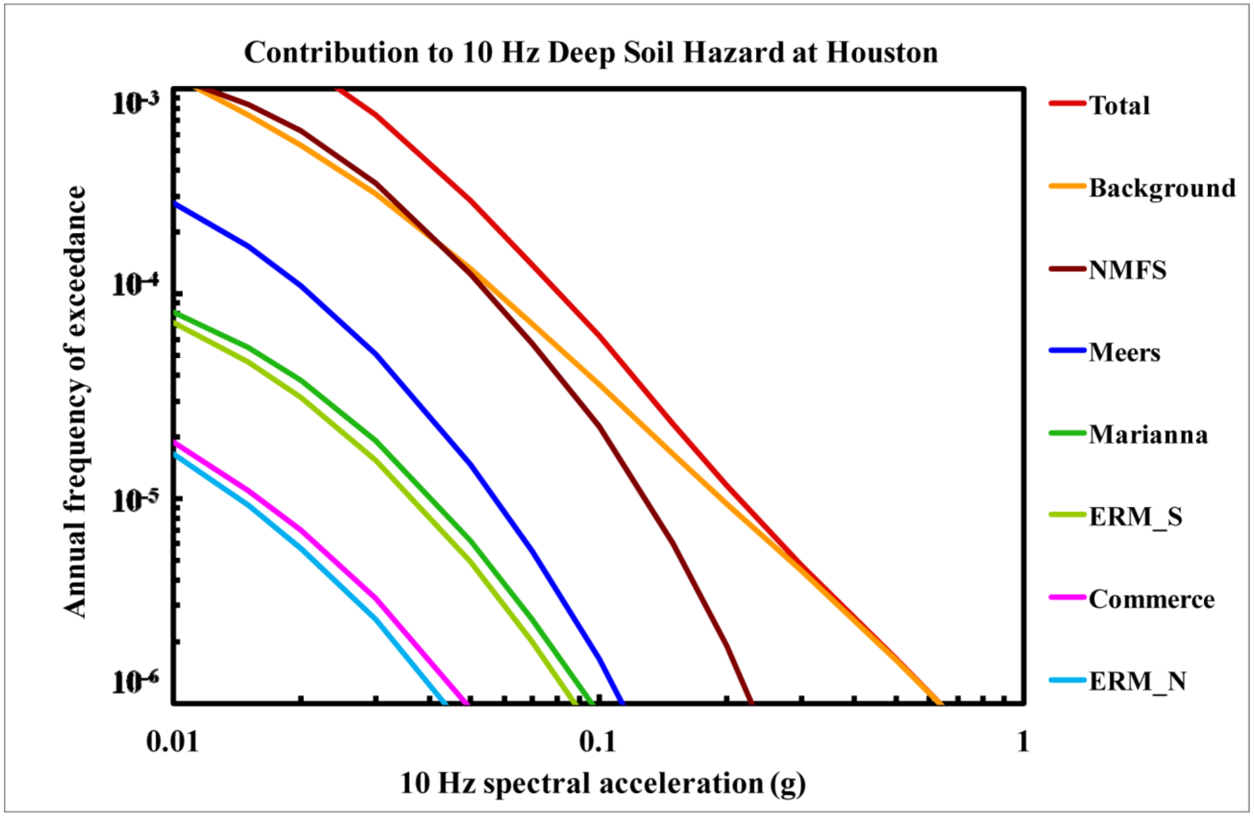

Figure 8.2-3p
Houston 10 Hz deep soil hazard: total and contribution by RLME and background

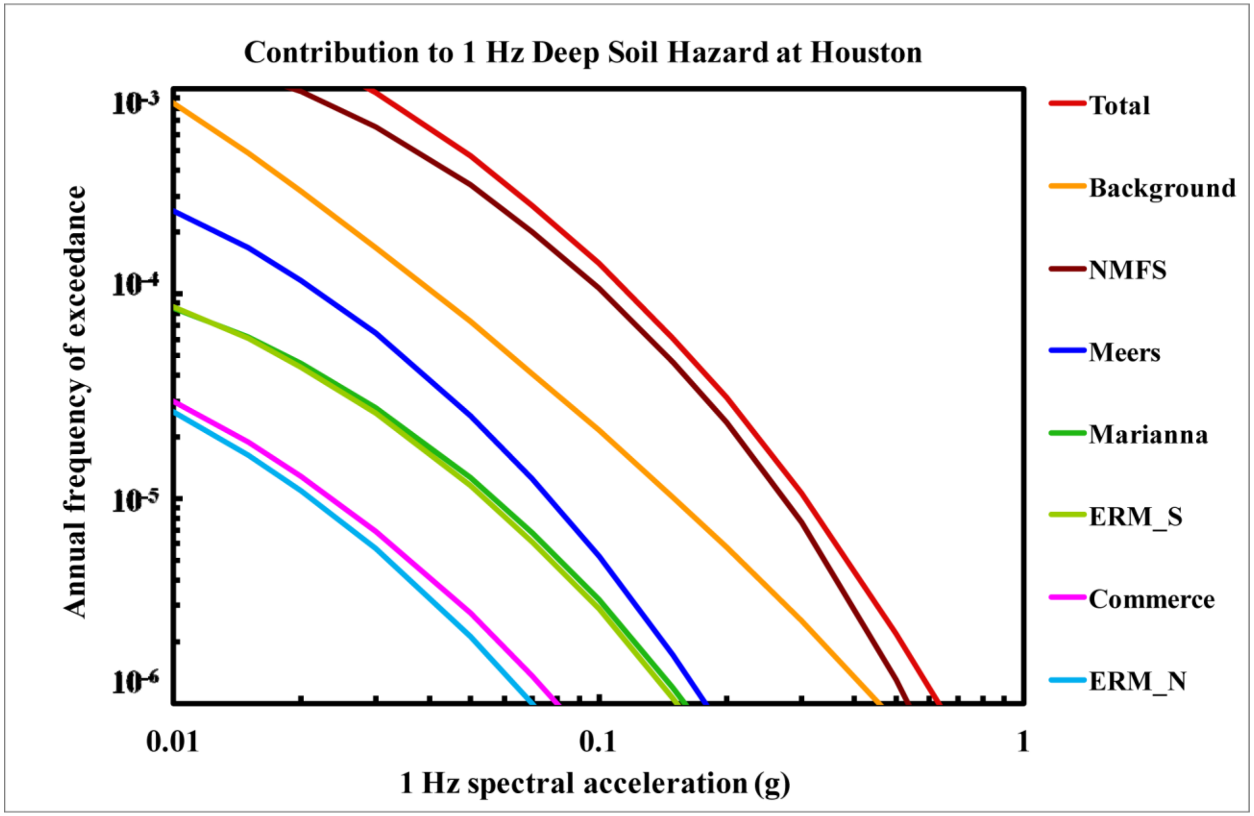

Figure 8.2-3q
Houston 1 Hz deep soil hazard: total and contribution by RLME and background

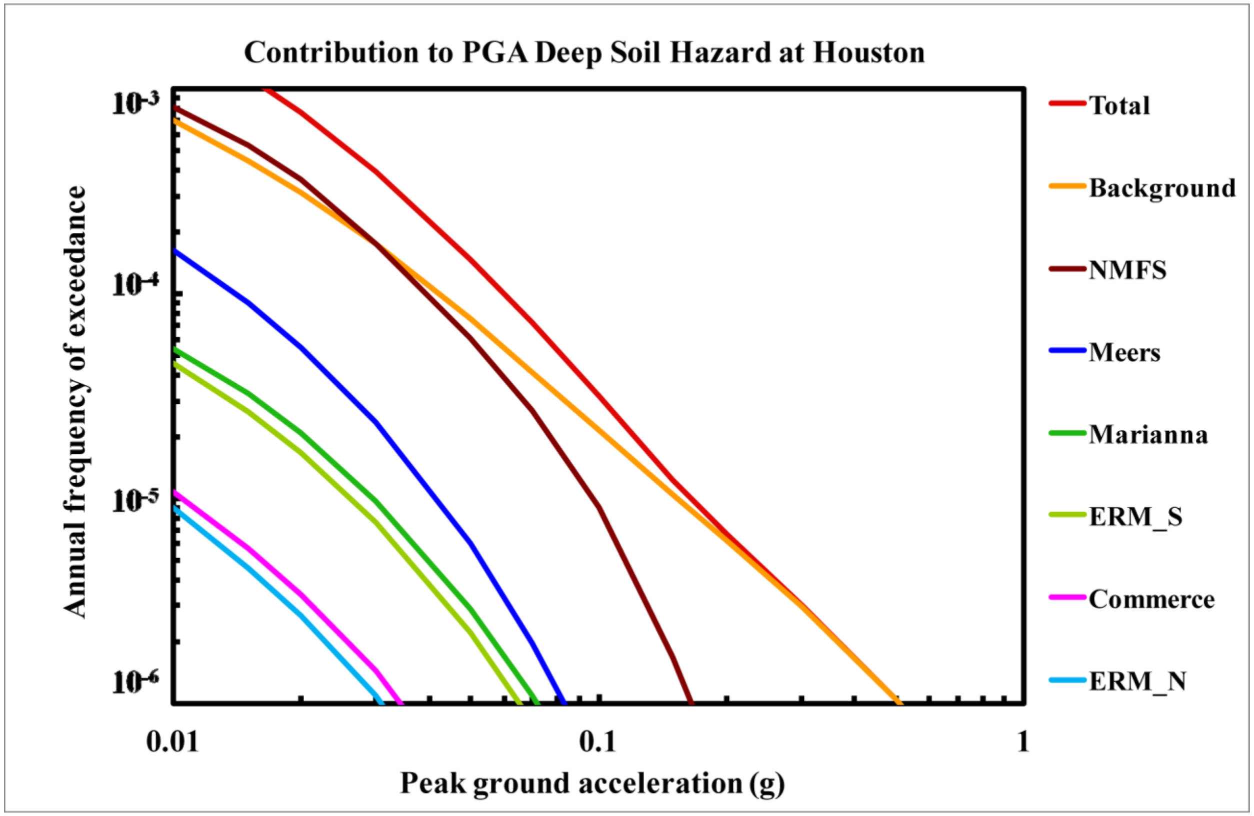

Figure 8.2-3r
Houston PGA deep soil hazard: total and contribution by RLME and background

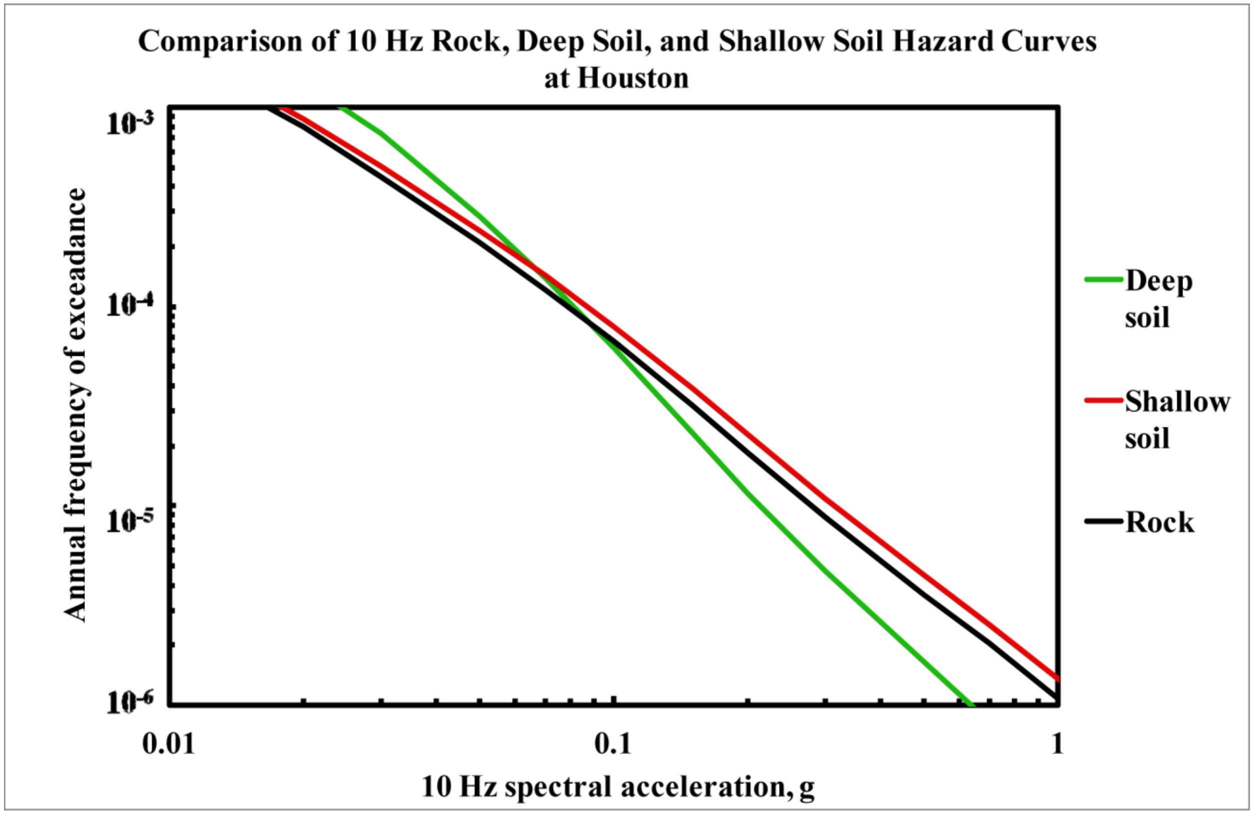

Figure 8.2-3s
Houston 10 Hz hazard: comparison of three site conditions

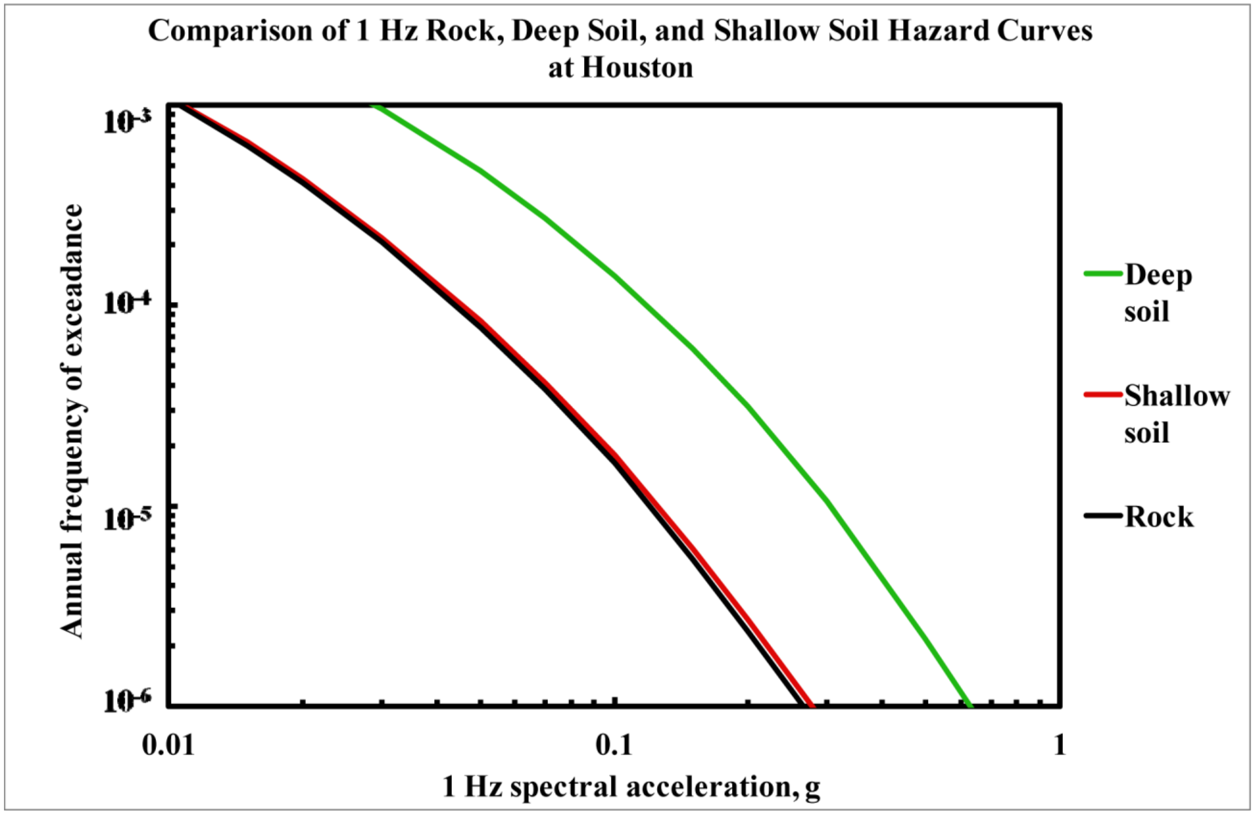

Figure 8.2-3t
Houston 1 Hz hazard: comparison of three site conditions

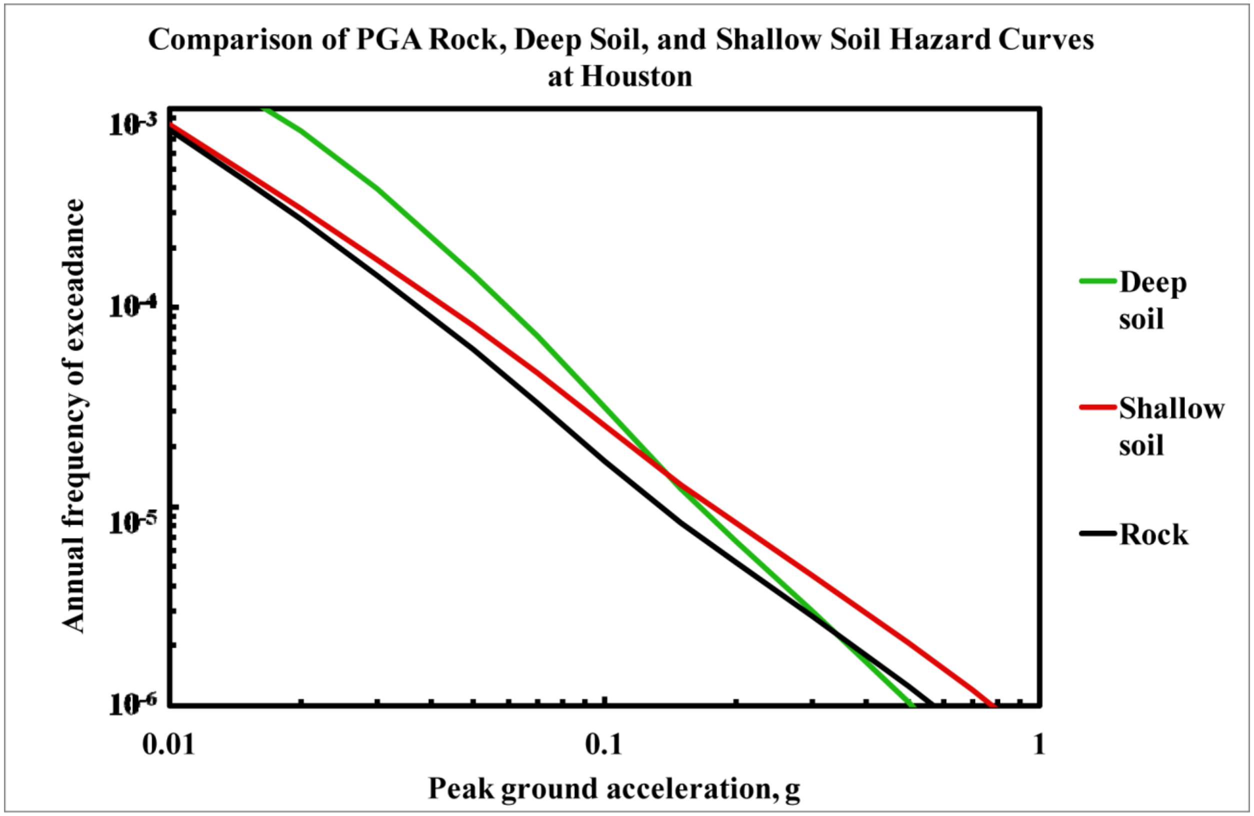

Figure 8.2-3u
Houston PGA hazard: comparison of three site conditions

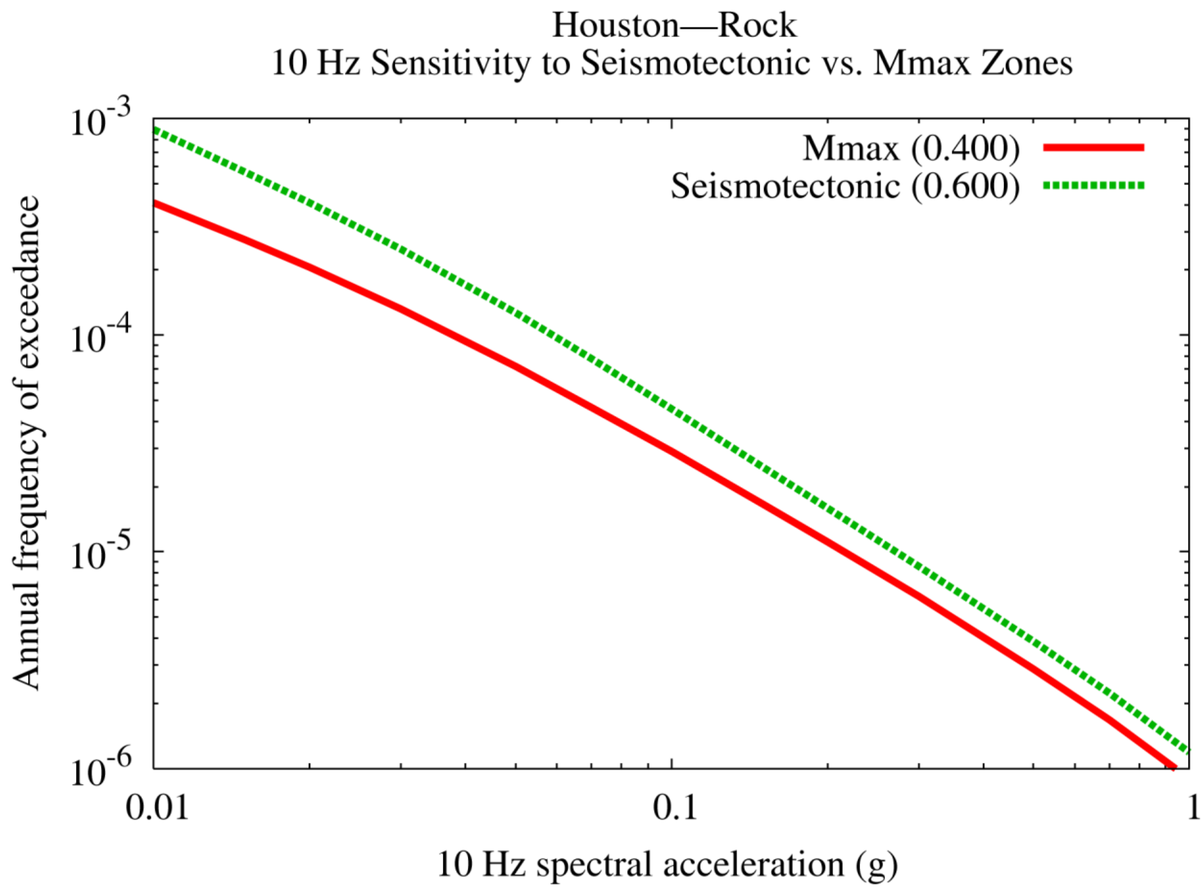

Figure 8.2-3v
Houston 10 Hz rock hazard: sensitivity to seismotectonic vs. Mmax zones

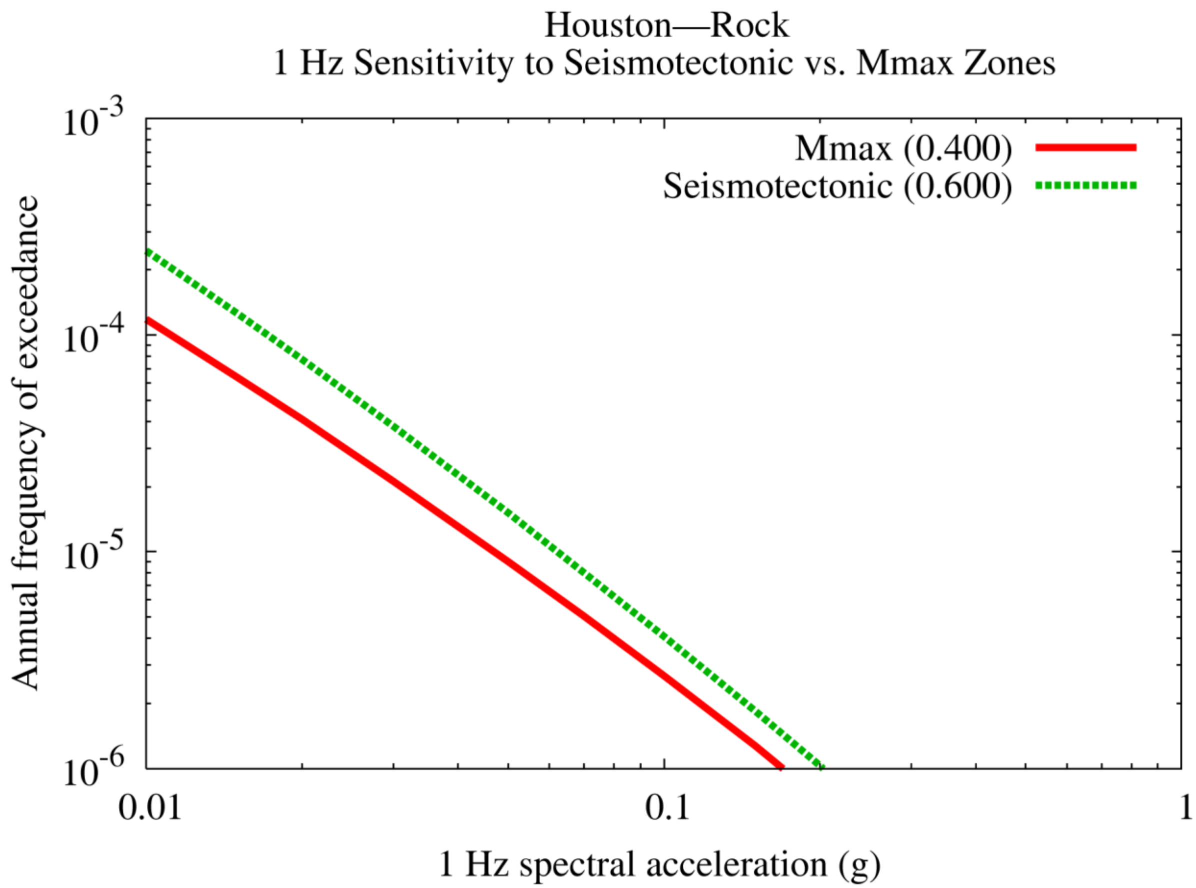

Figure 8.2-3w
Houston 1 Hz rock hazard: sensitivity to seismotectonic vs. Mmax zones

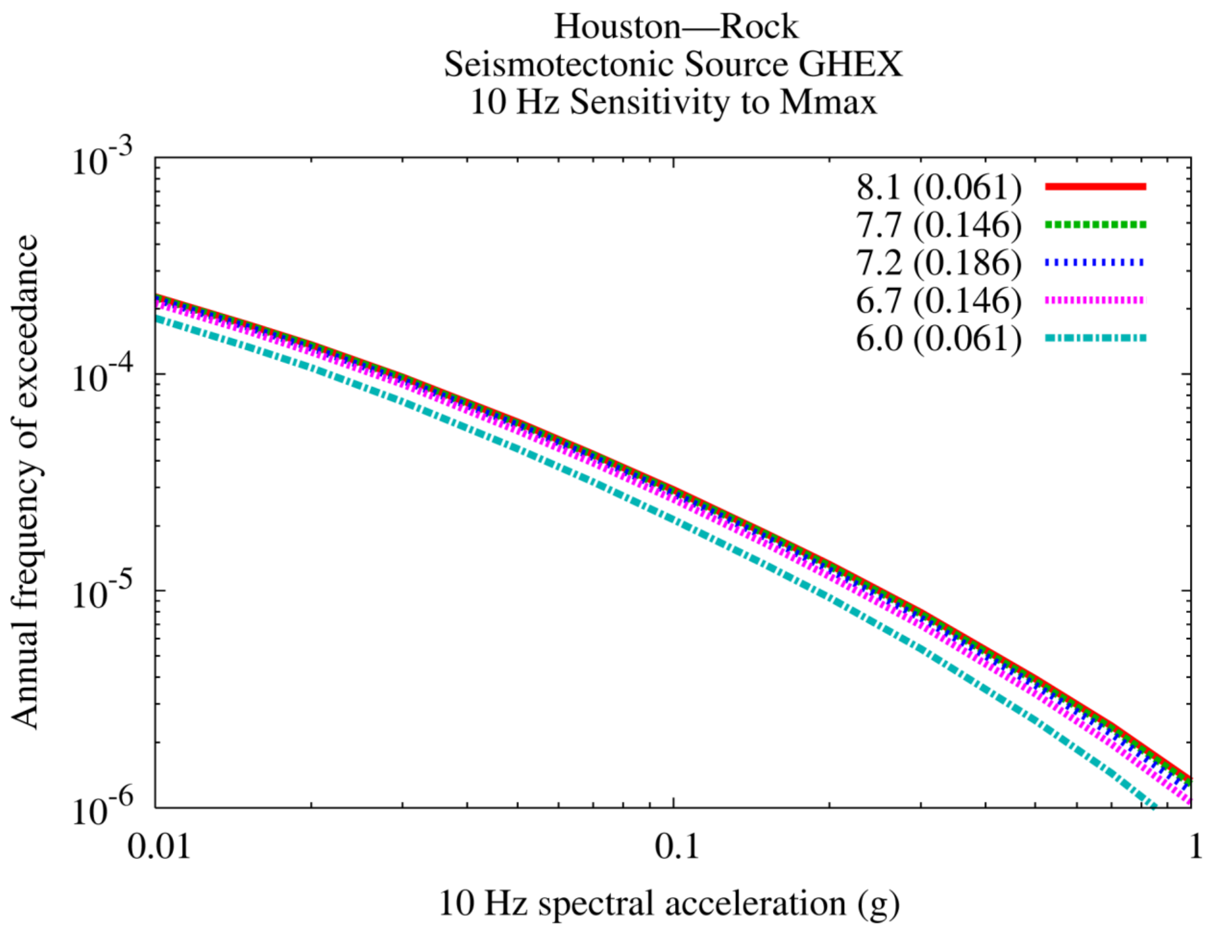

Figure 8.2-3x
Houston 10 Hz rock hazard: sensitivity to Mmax for source GHEX

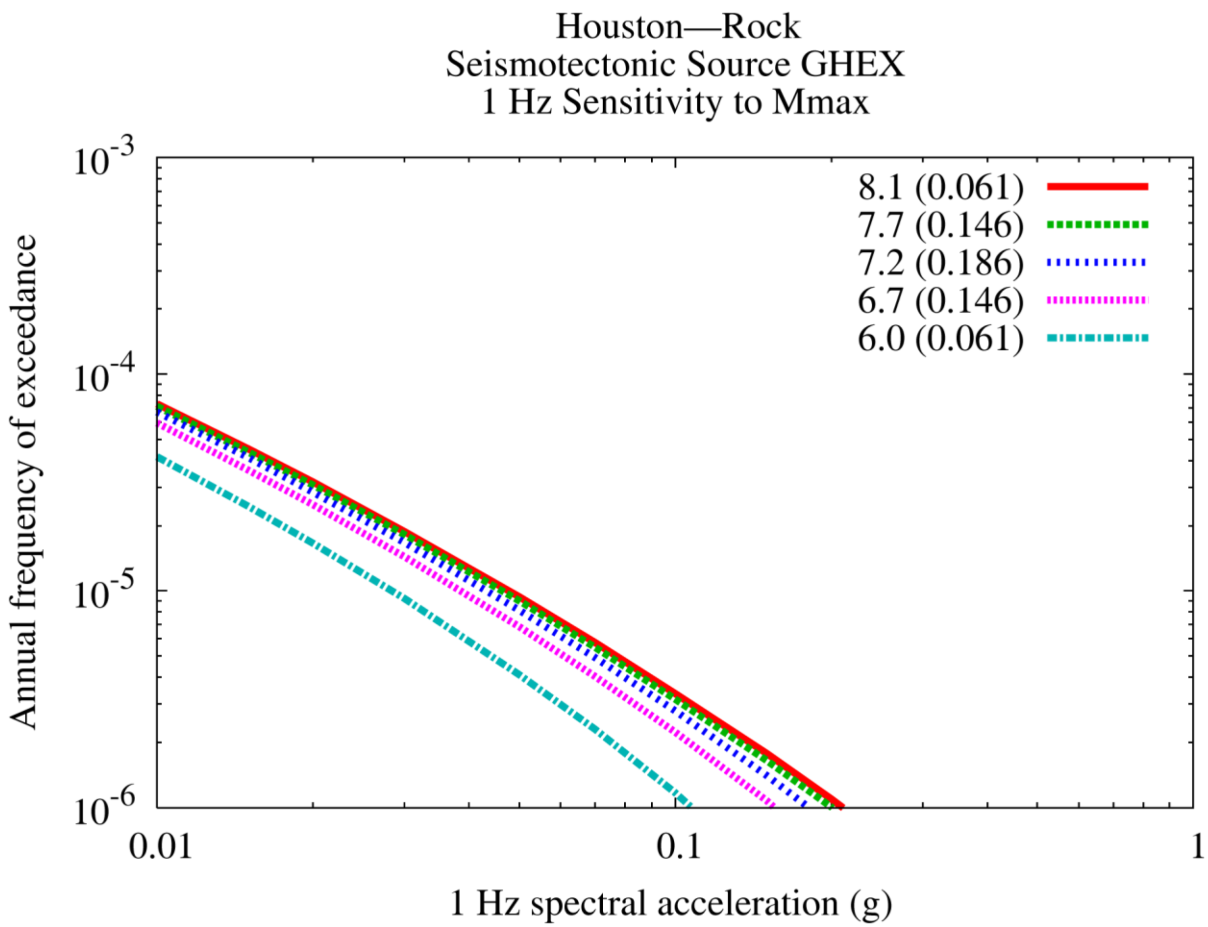

Figure 8.2-3y
Houston 1 Hz rock hazard: sensitivity to Mmax for source GHEX

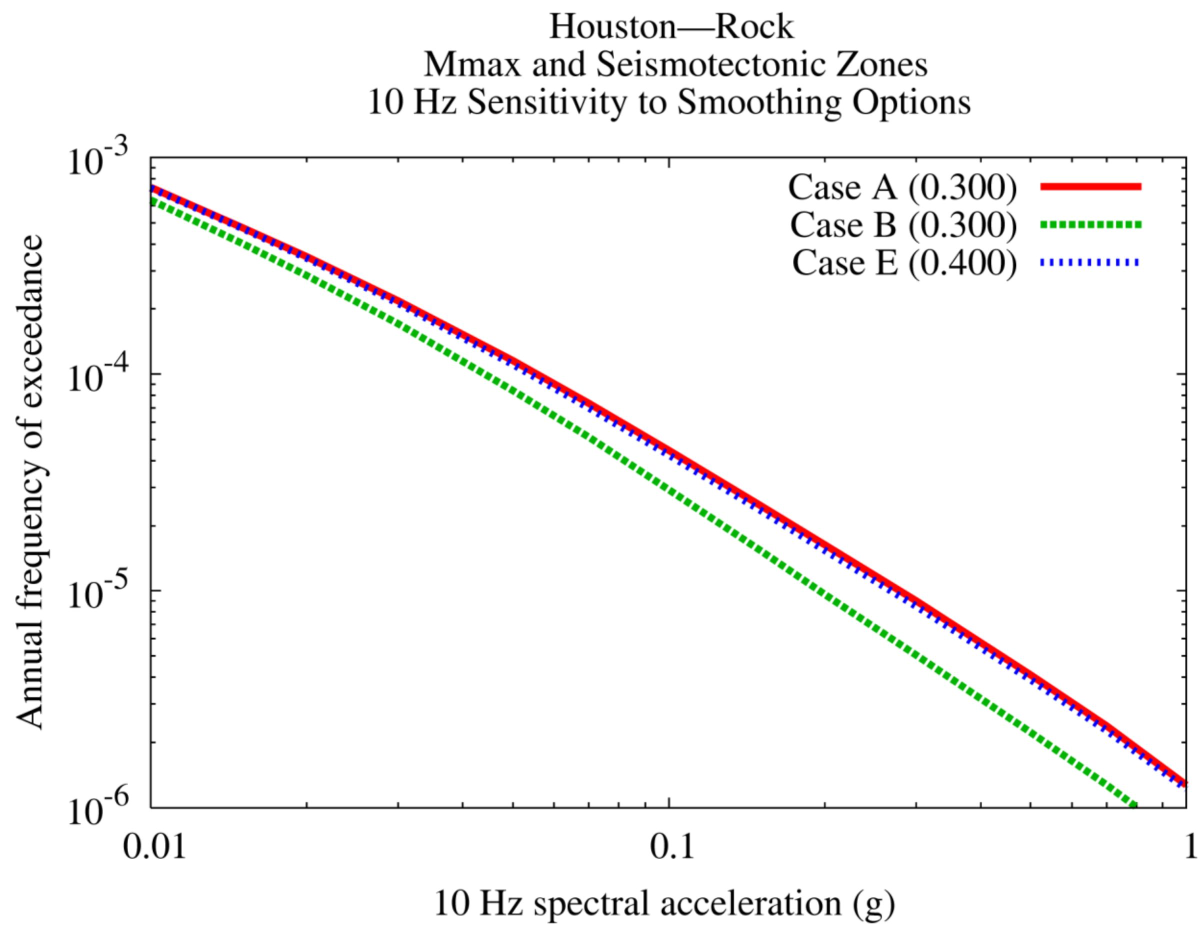

Figure 8.2-3z
Houston 10 Hz rock hazard: sensitivity to smoothing options

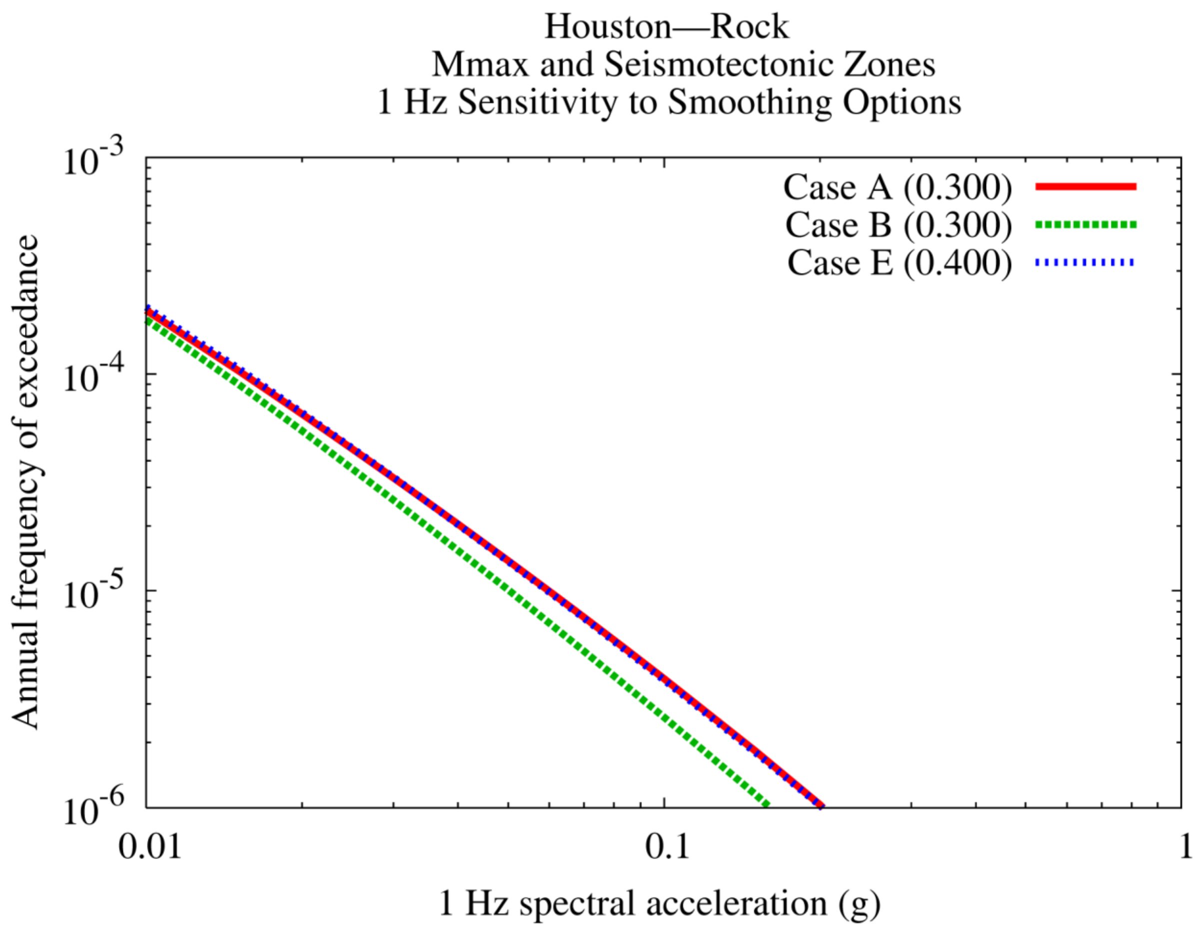

Figure 8.2-3aa
Houston 1 Hz rock hazard: sensitivity to smoothing options

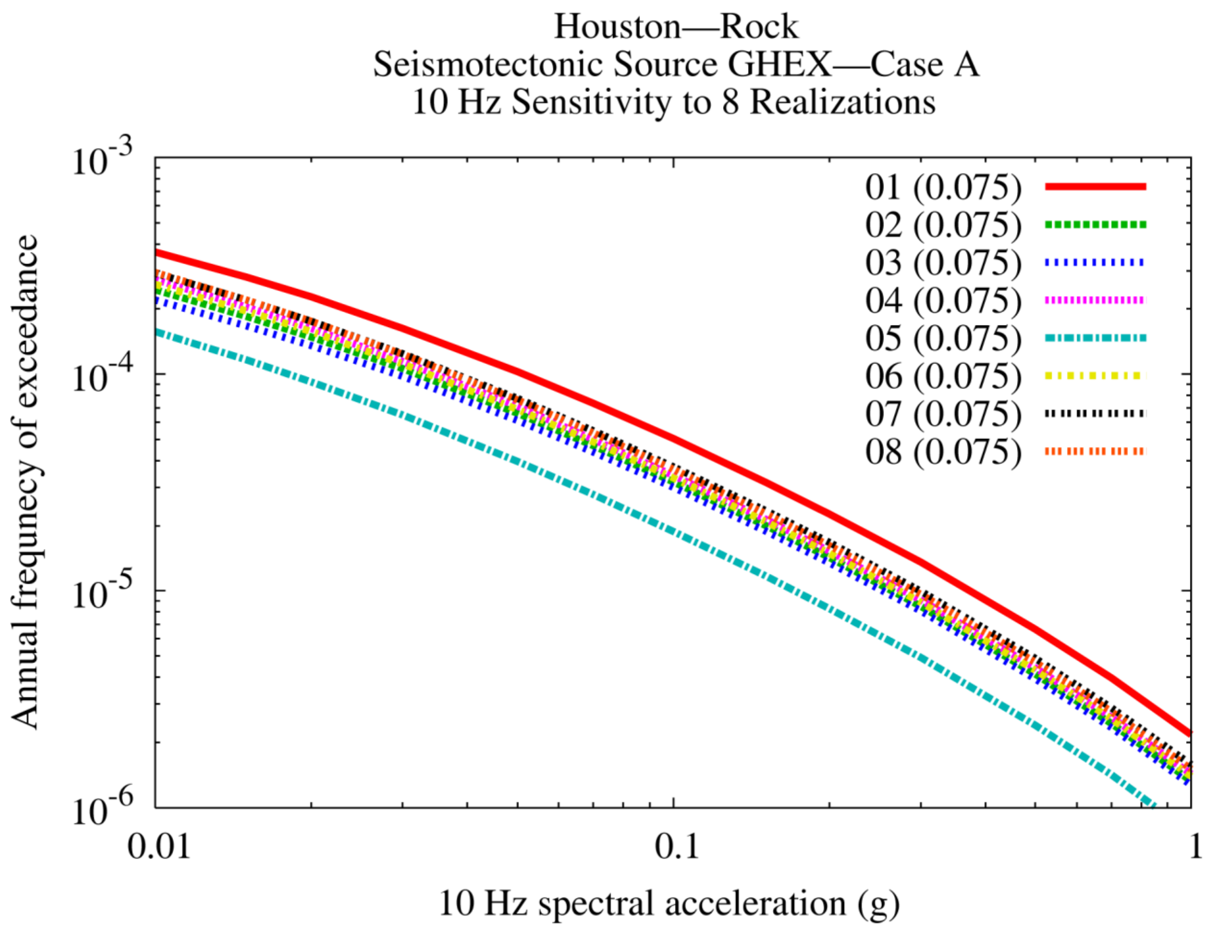

Figure 8.2-3bb
Houston 10 Hz rock hazard: sensitivity to eight realizations for source GHEX, Case A

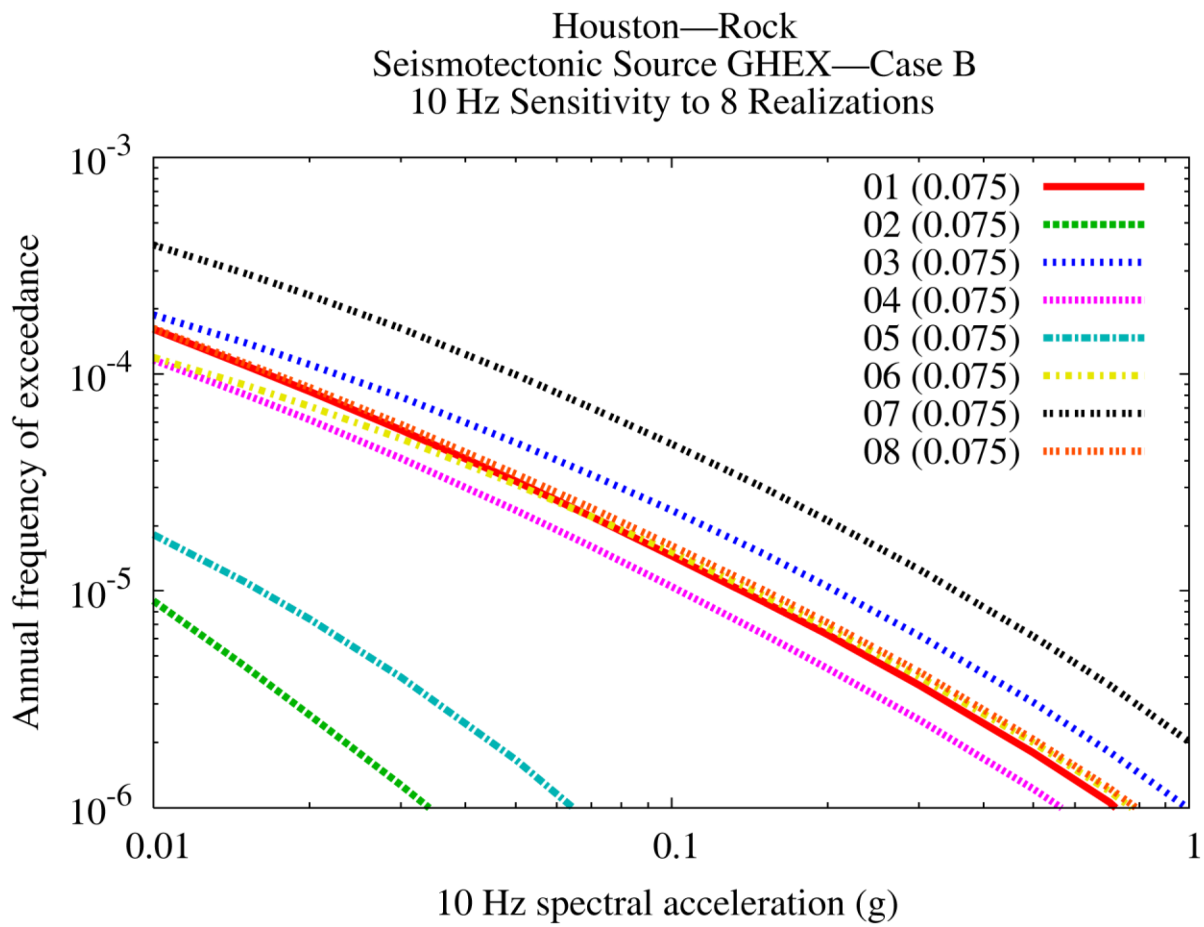

Figure 8.2-3cc
Houston 10 Hz rock hazard: sensitivity to eight realizations for source GHEX, Case B

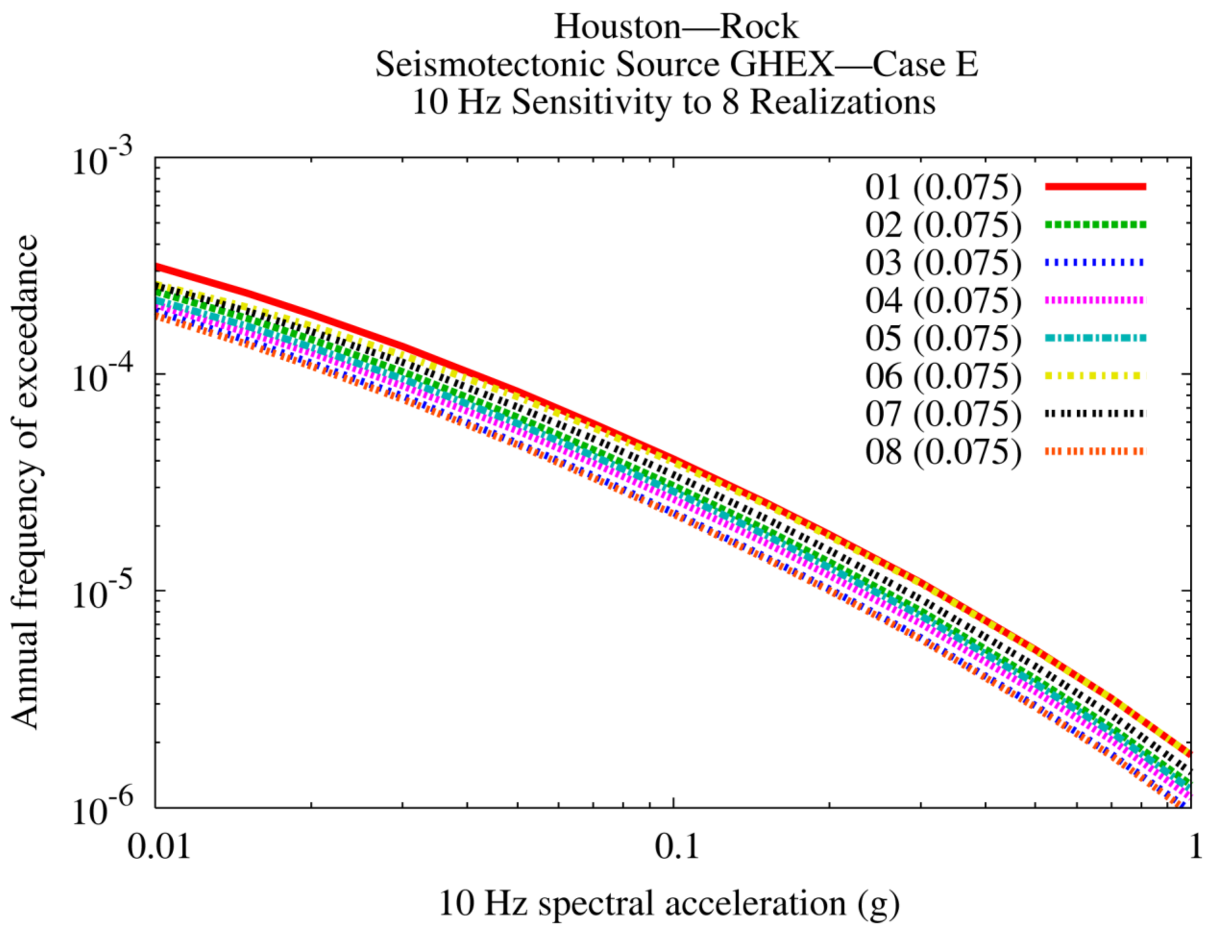

Figure 8.2-3dd
Houston 10 Hz rock hazard: sensitivity to eight realizations for source GHEX, Case E

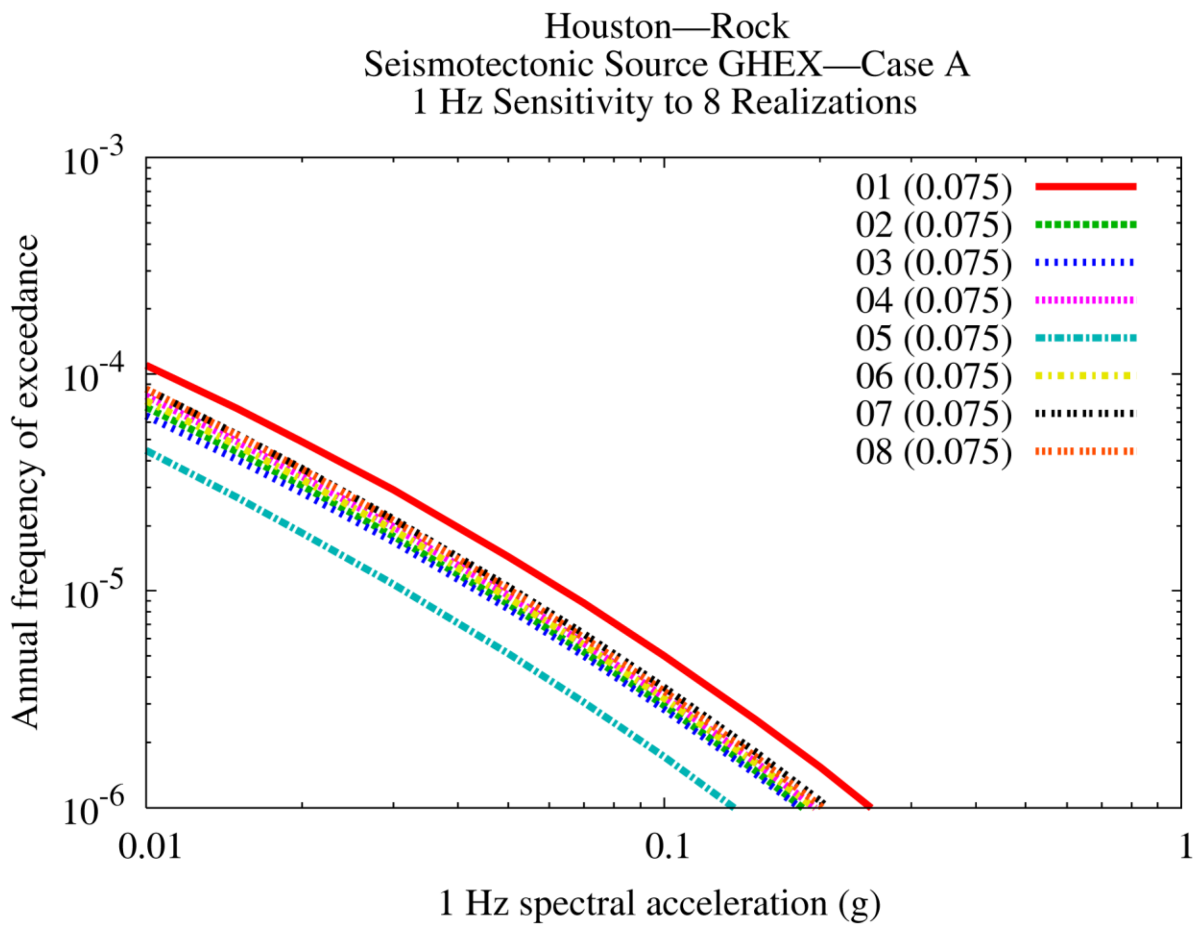

Figure 8.2-3ee
Houston 1 Hz rock hazard: sensitivity to eight realizations for source GHEX, Case A

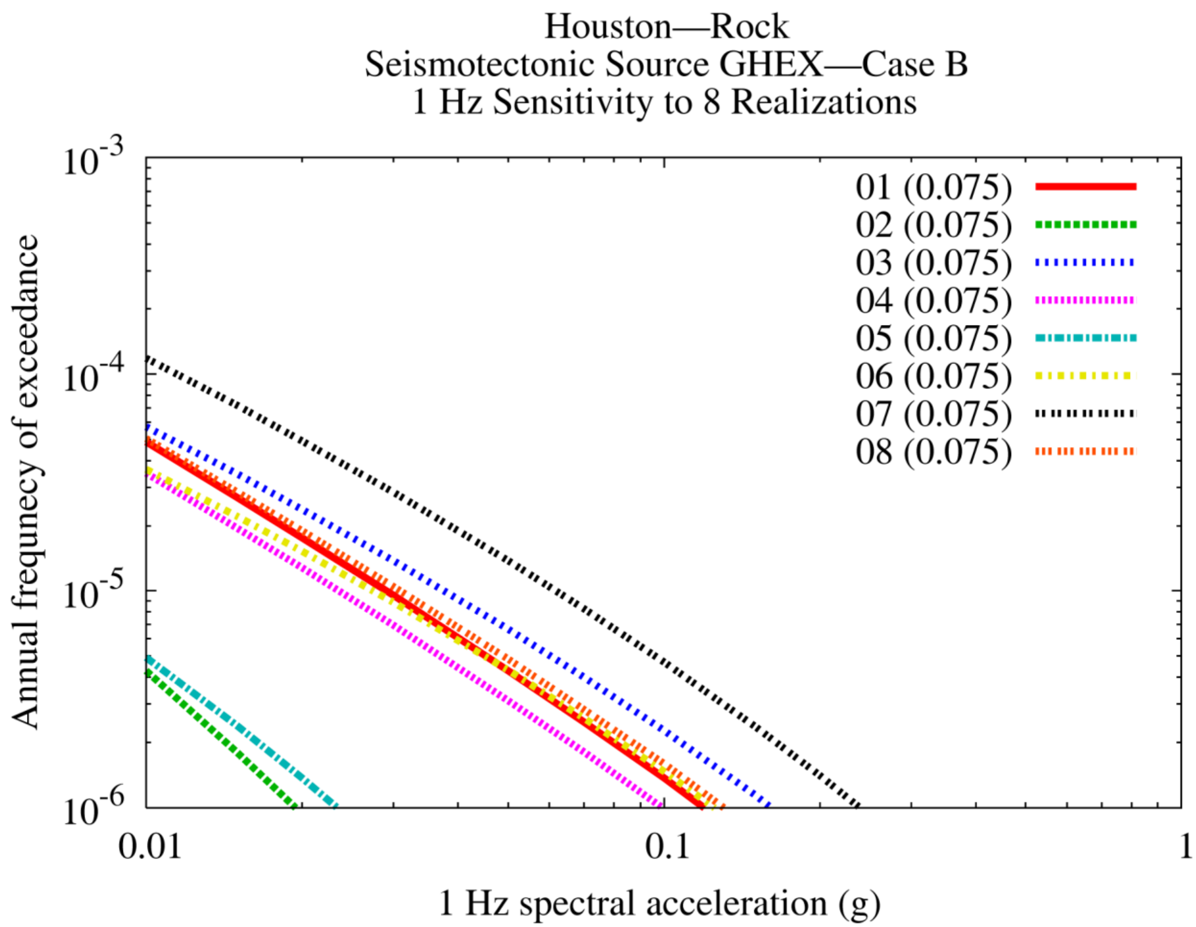

Figure 8.2-3ff
Houston 1 Hz rock hazard: sensitivity to eight realizations for source GHEX, Case B

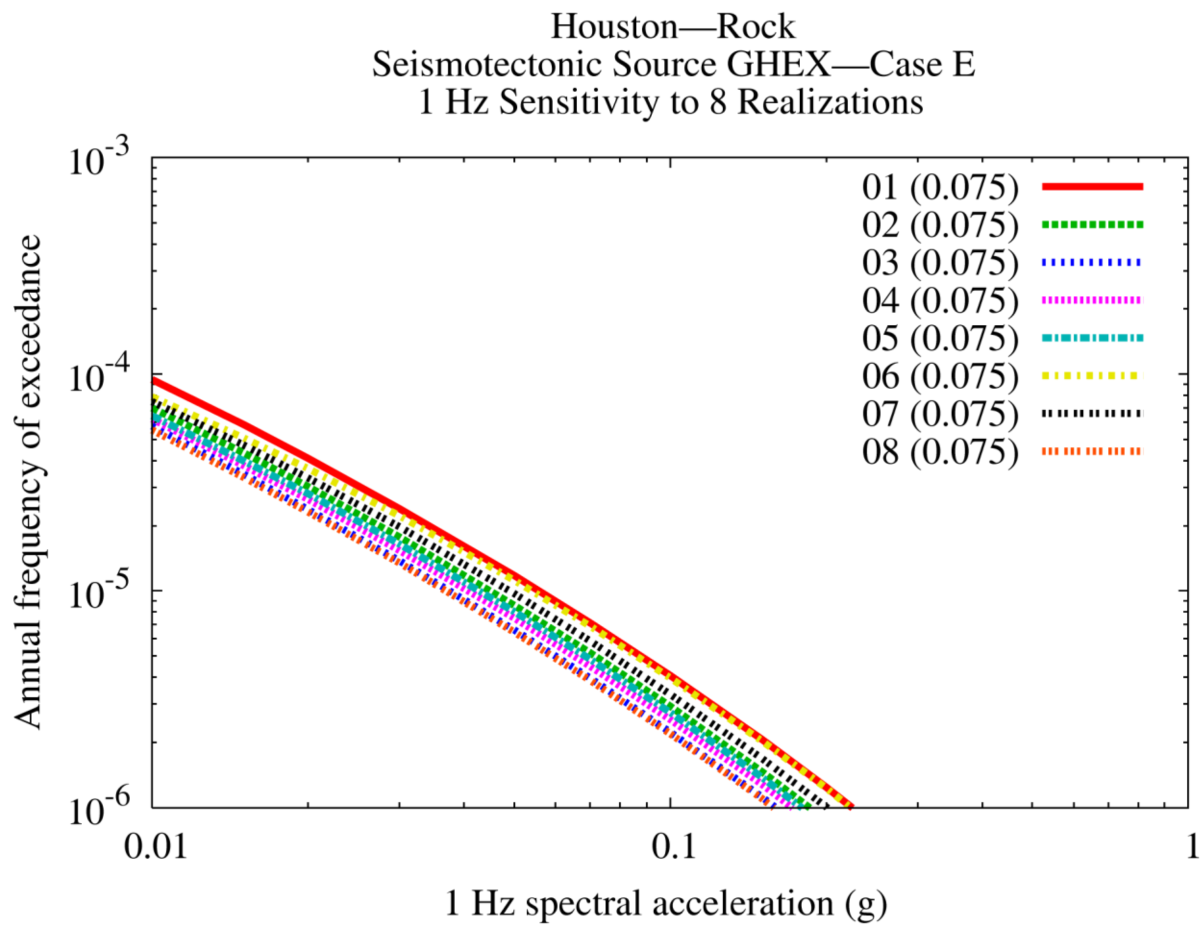

Figure 8.2-3gg
Houston 1 Hz rock hazard: sensitivity to eight realizations for source GHEX, Case E

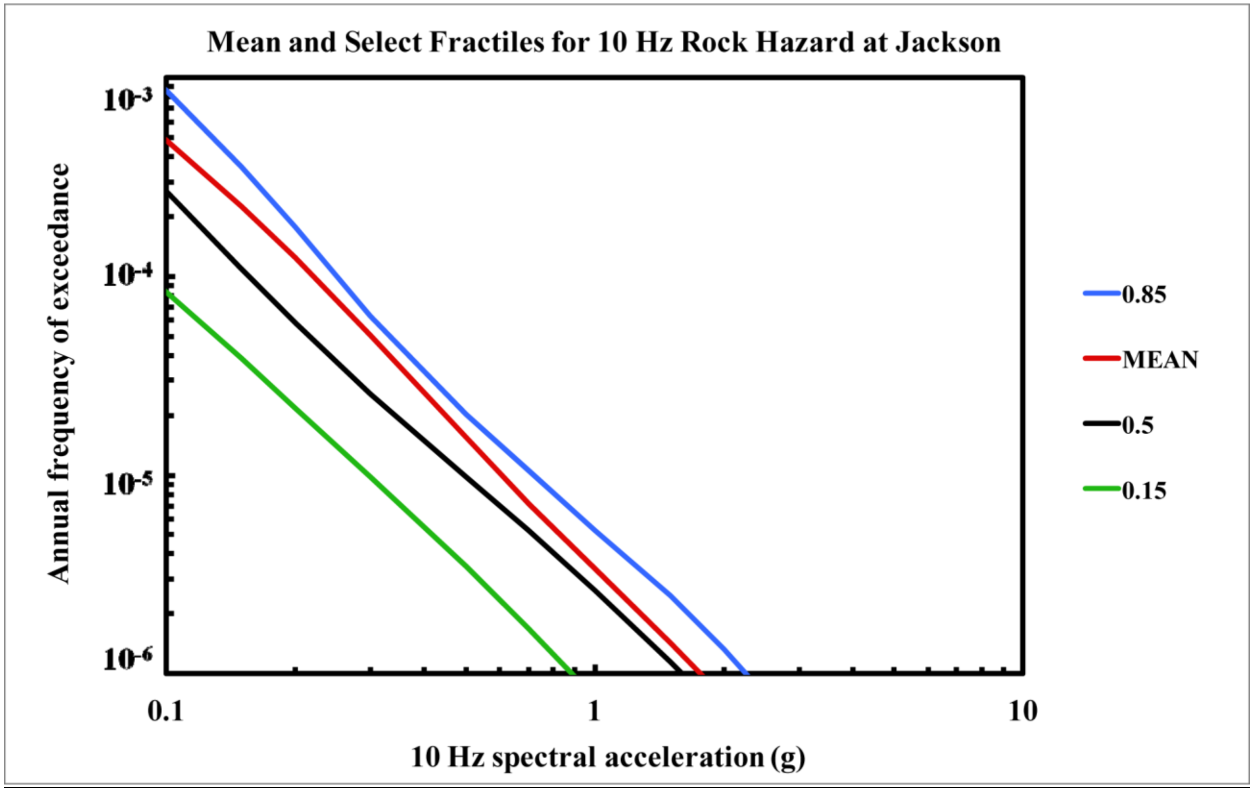

Figure 8.2-4a
Jackson 10 Hz rock hazard: mean and fractile total hazard

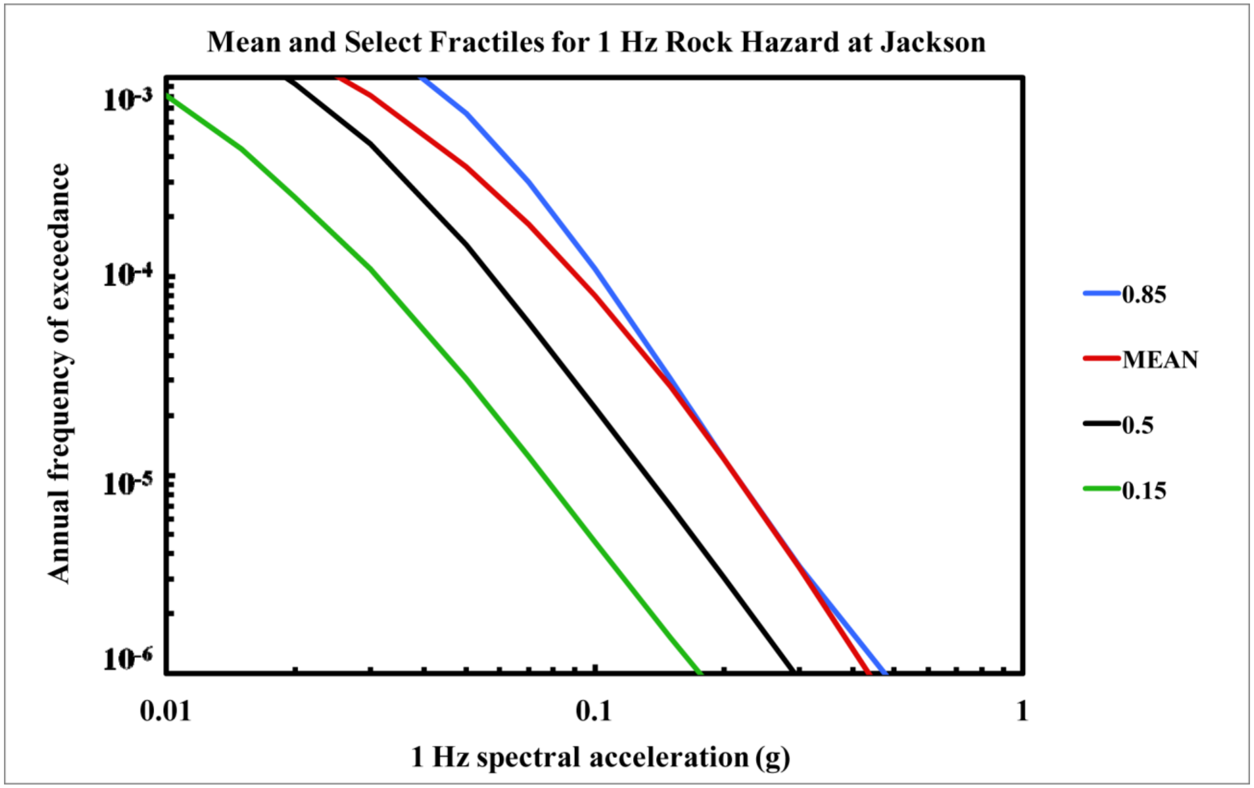

Figure 8.2-4b
Jackson 1 Hz rock hazard: mean and fractile total hazard

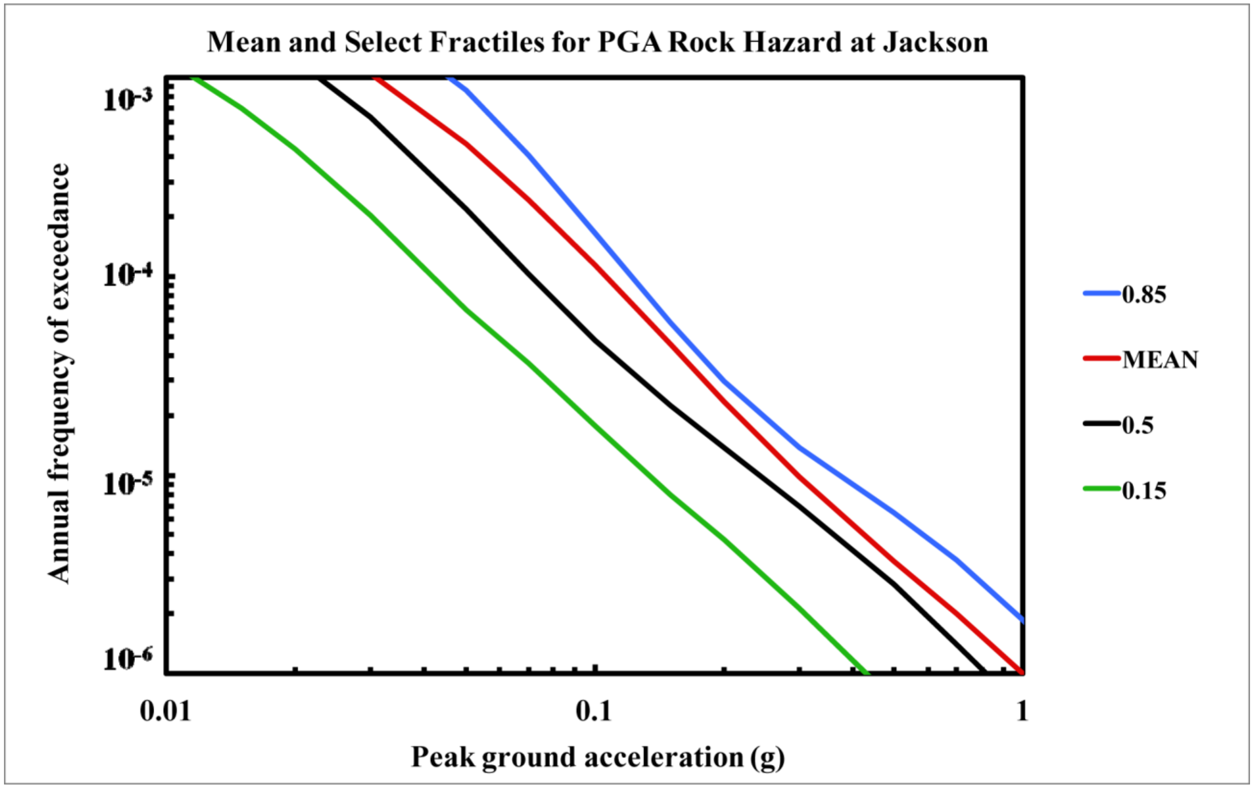

Figure 8.2-4c
Jackson PGA rock hazard: mean and fractile total hazard

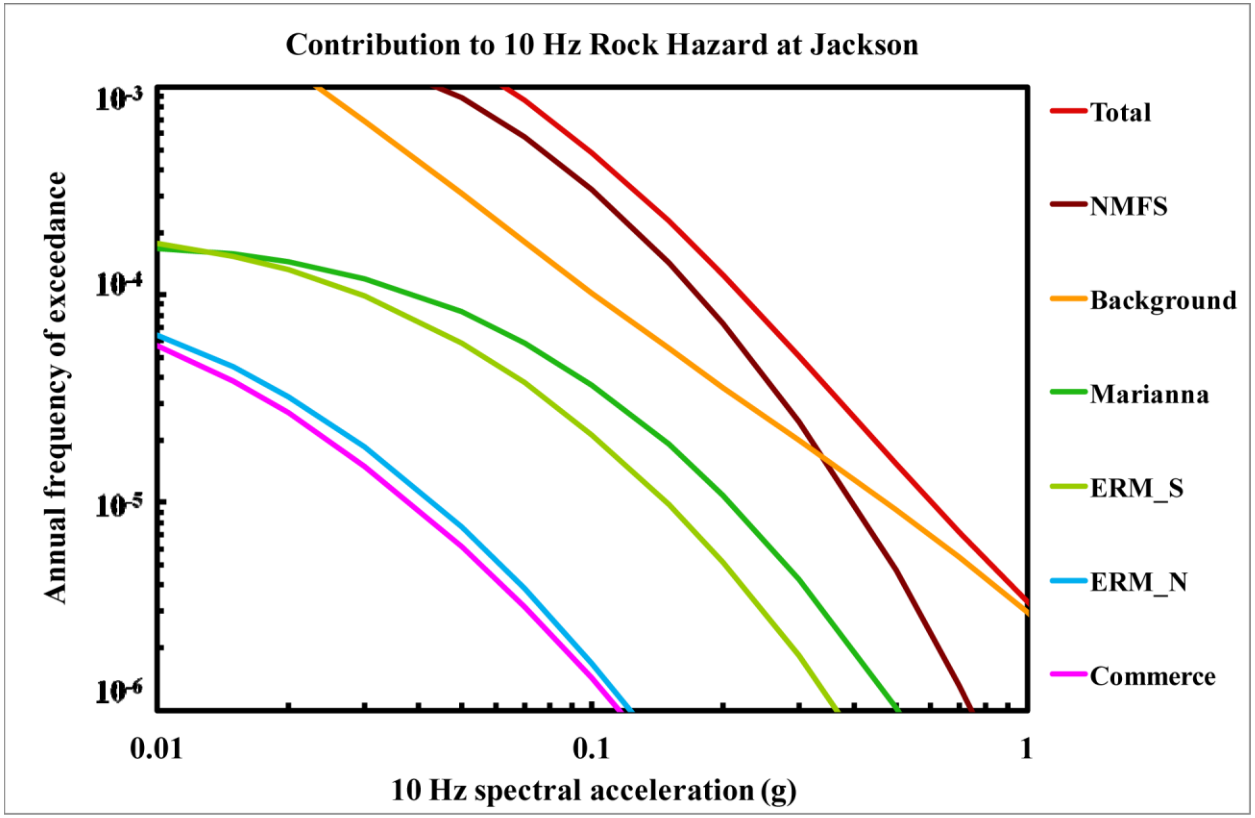

Figure 8.2-4d
Jackson 10 Hz rock hazard: total and contribution by RLME and background

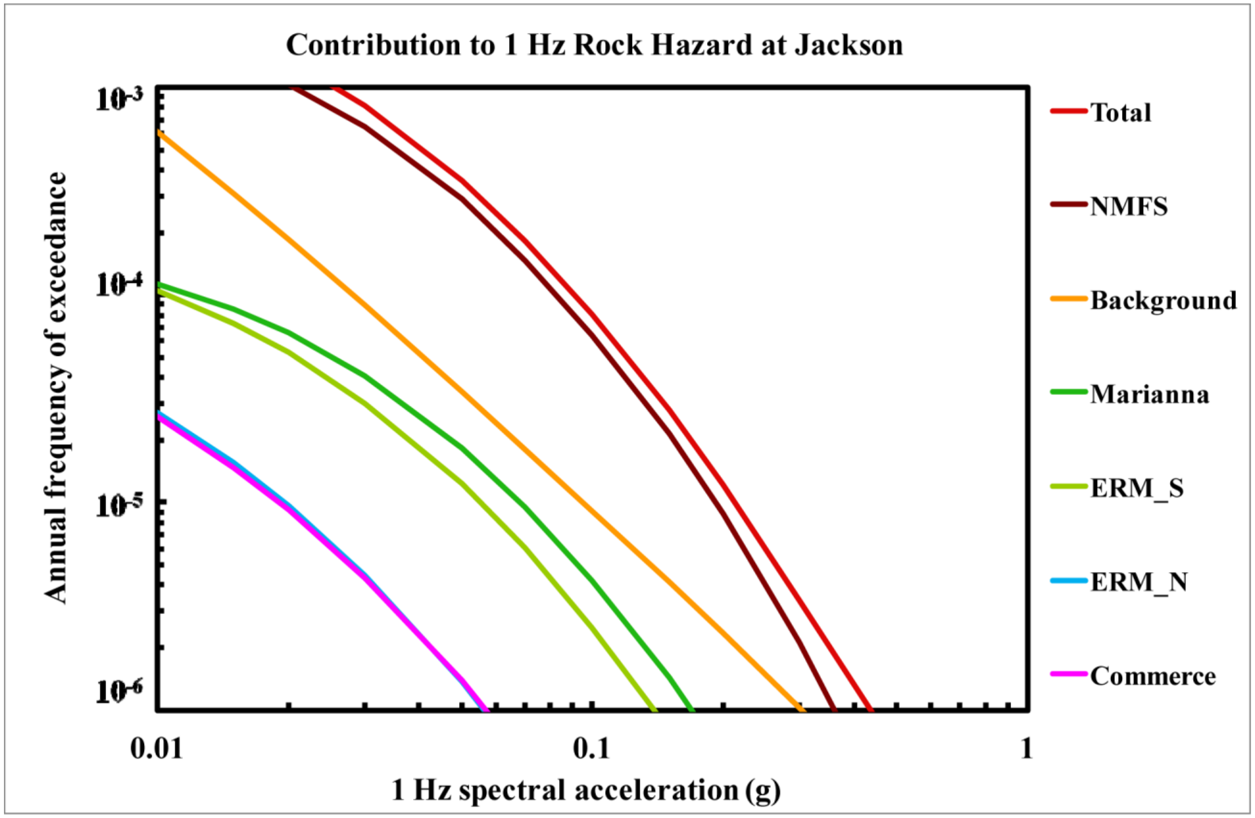

Figure 8.2-4e
Jackson 1 Hz rock hazard: total and contribution by RLME and background

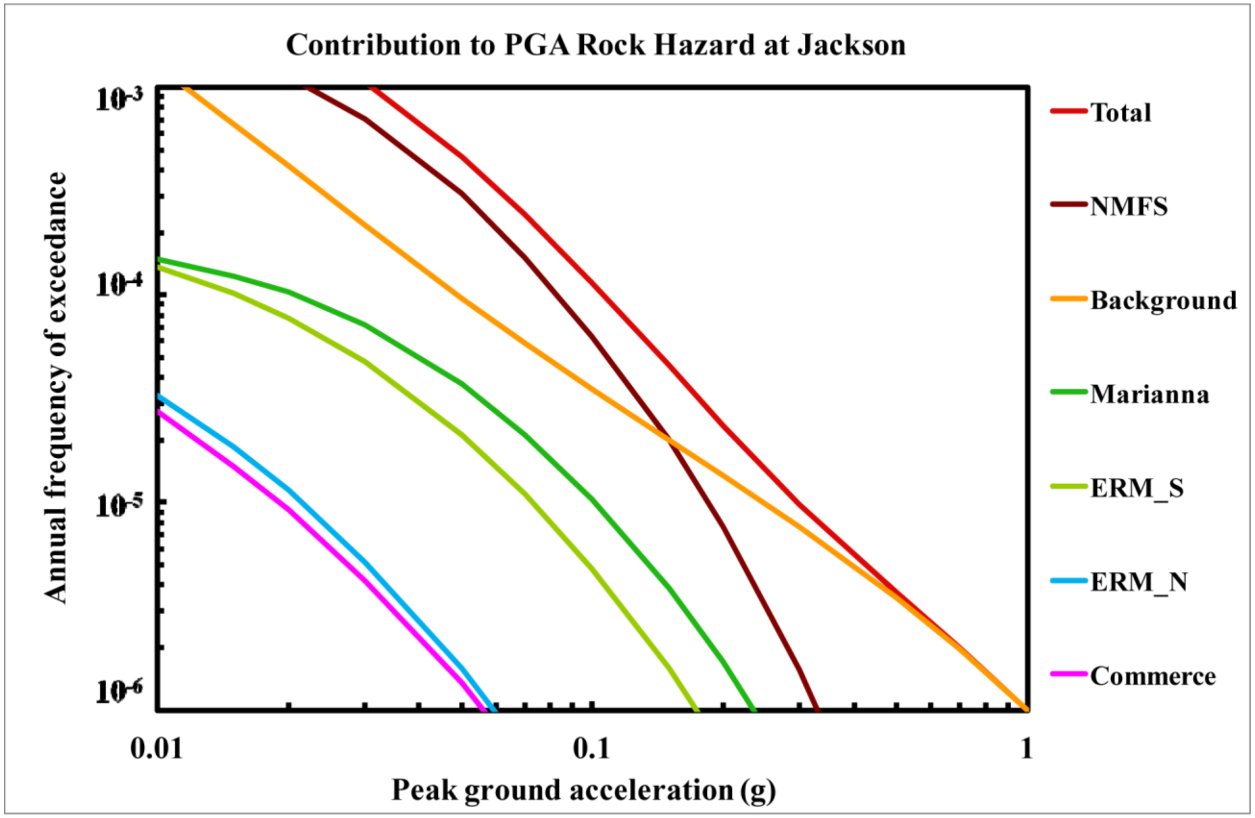

Figure 8.2-4f
Jackson PGA rock hazard: total and contribution by RLME and background

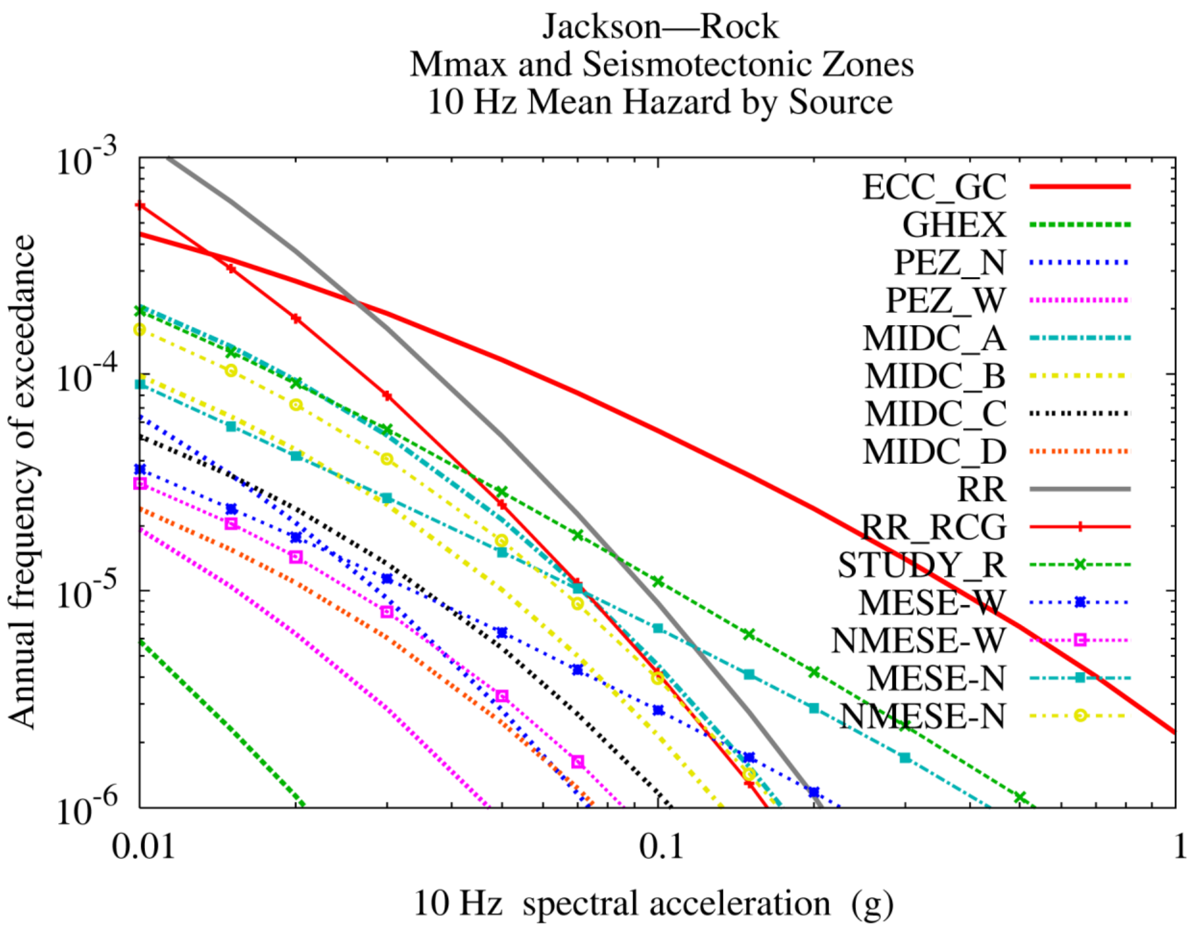

Figure 8.2-4g
Jackson 10 Hz rock hazard: contribution by background source

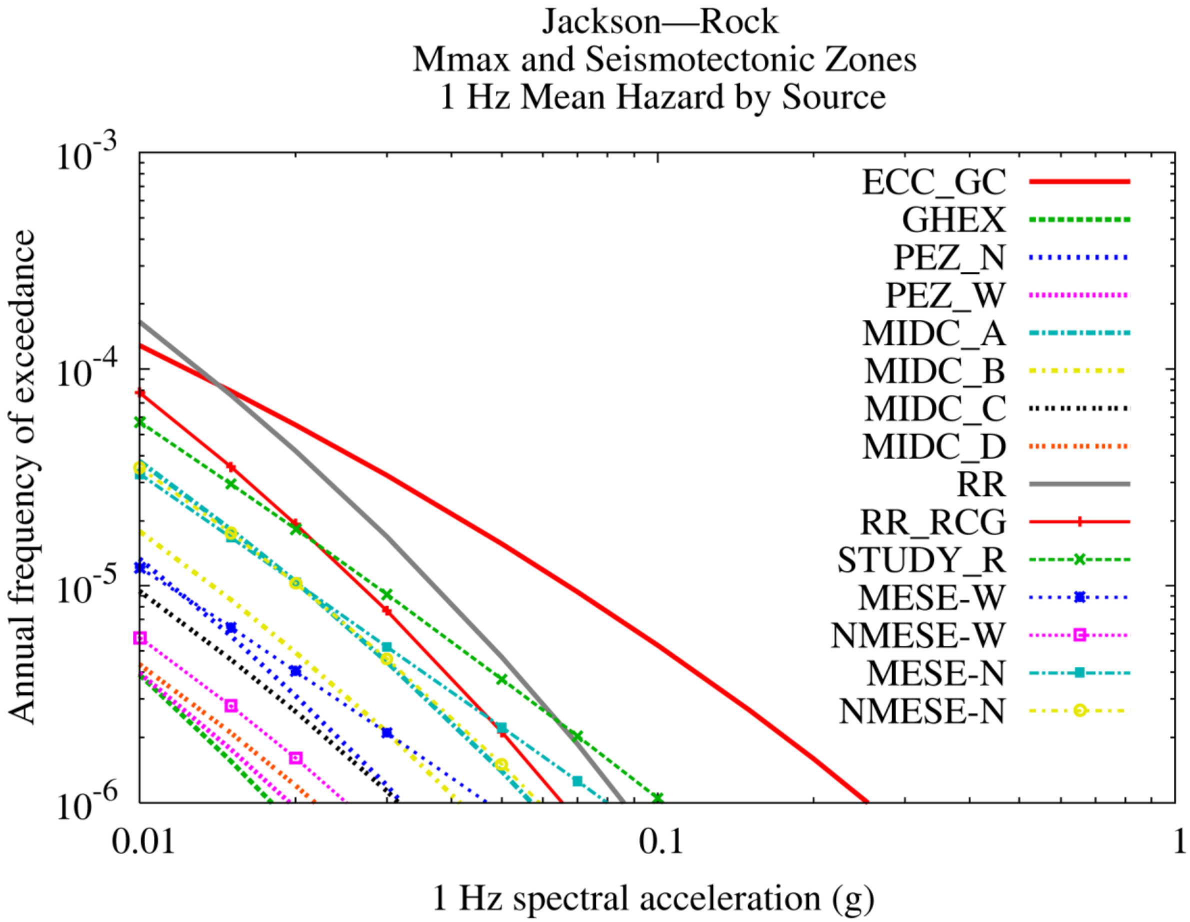

Figure 8.2-4h
Jackson 1 Hz rock hazard: contribution by background source

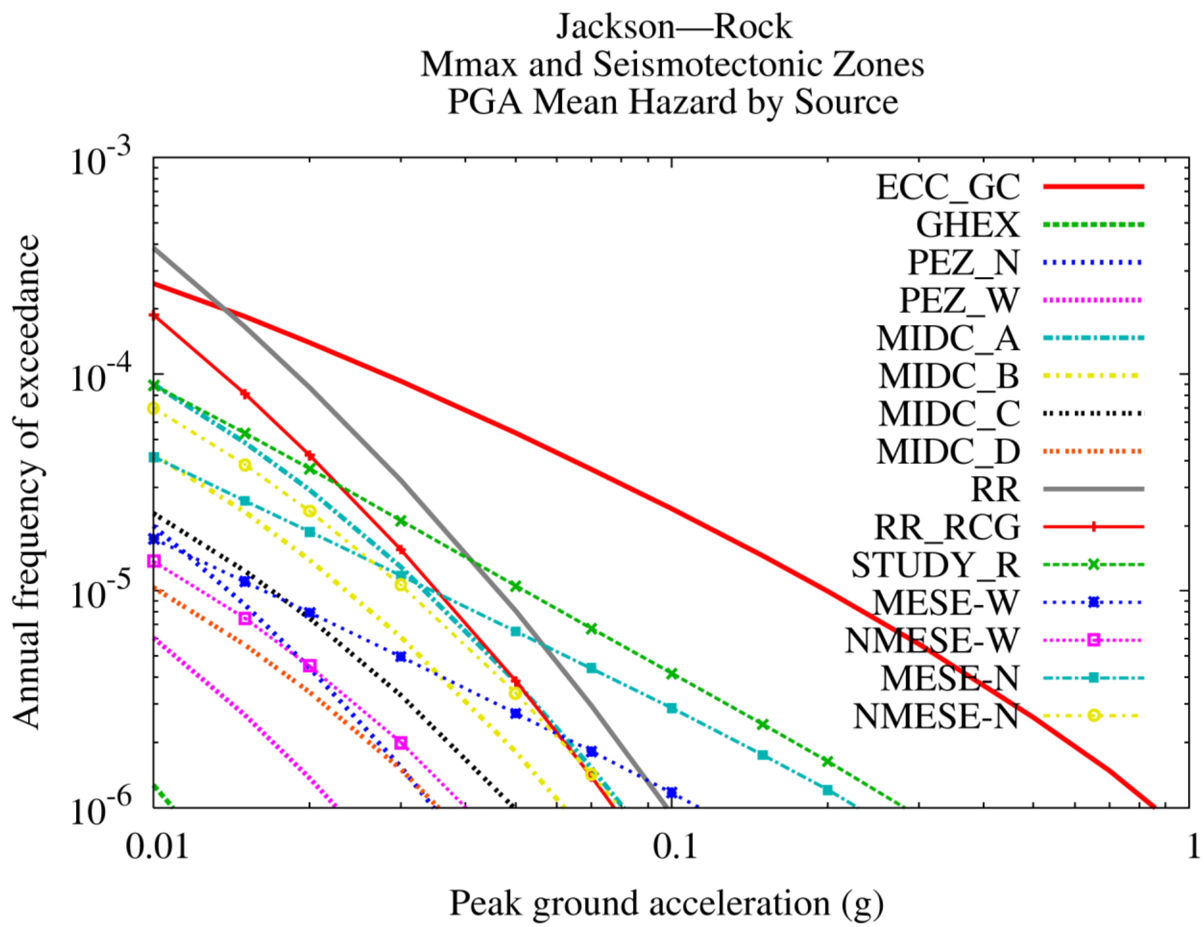

Figure 8.2-4i
Jackson PGA rock hazard: contribution by background source

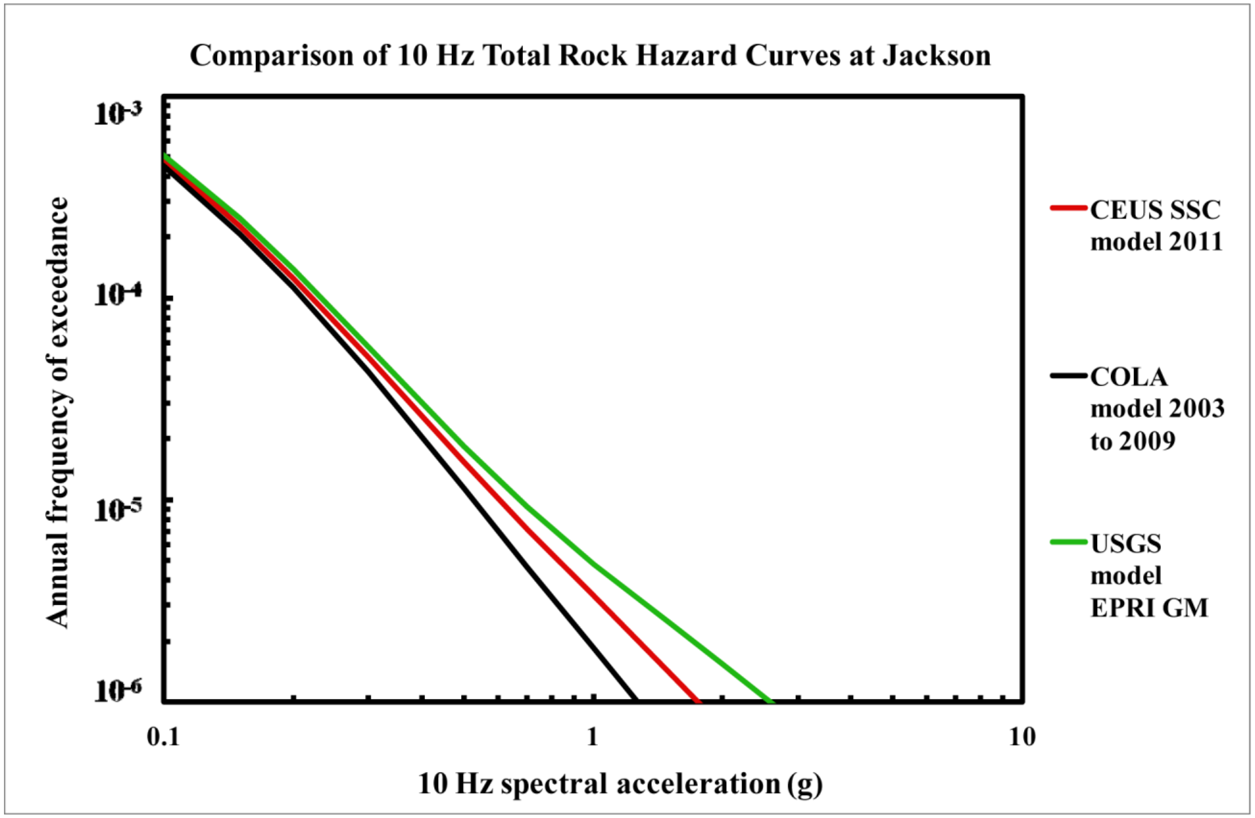

Figure 8.2-4j
Jackson 10 Hz rock hazard: comparison of three source models

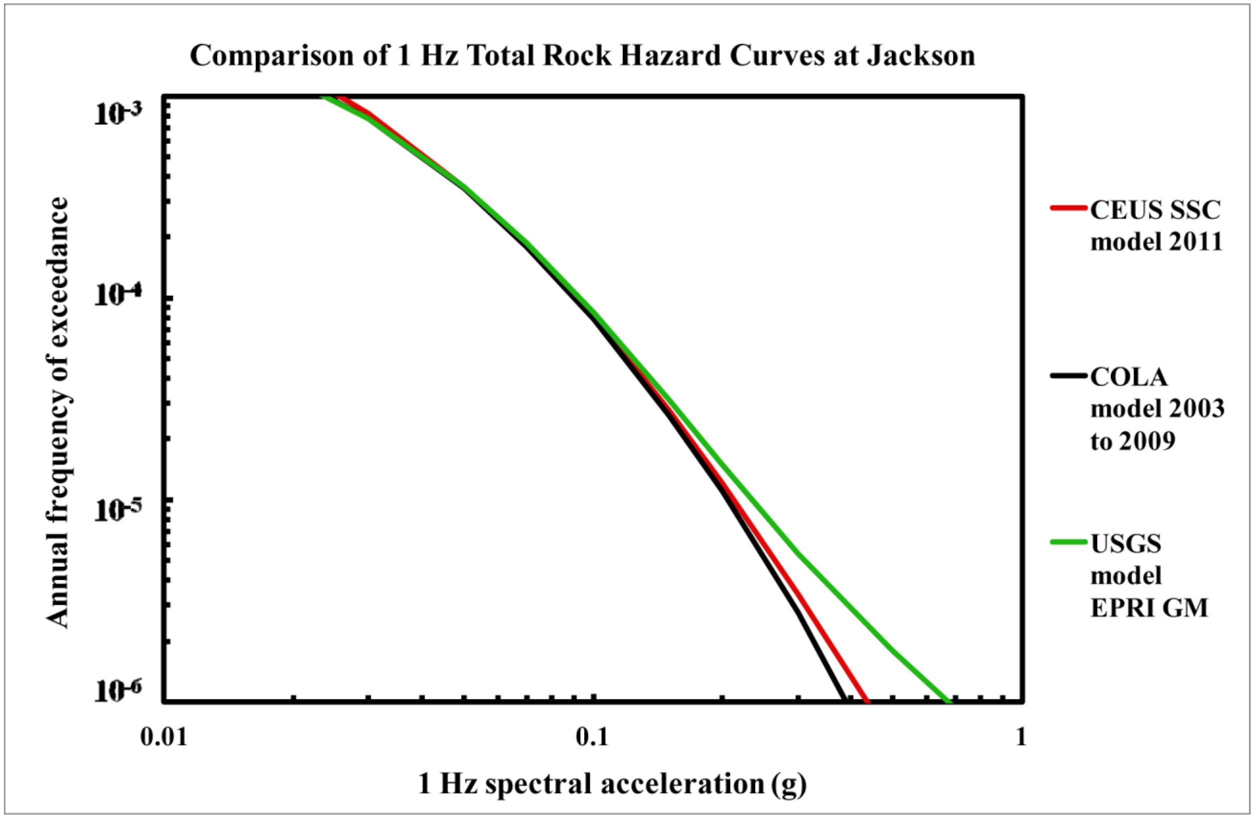

Figure 8.2-4k
Jackson is 1 Hz rock hazard: comparison of three source models

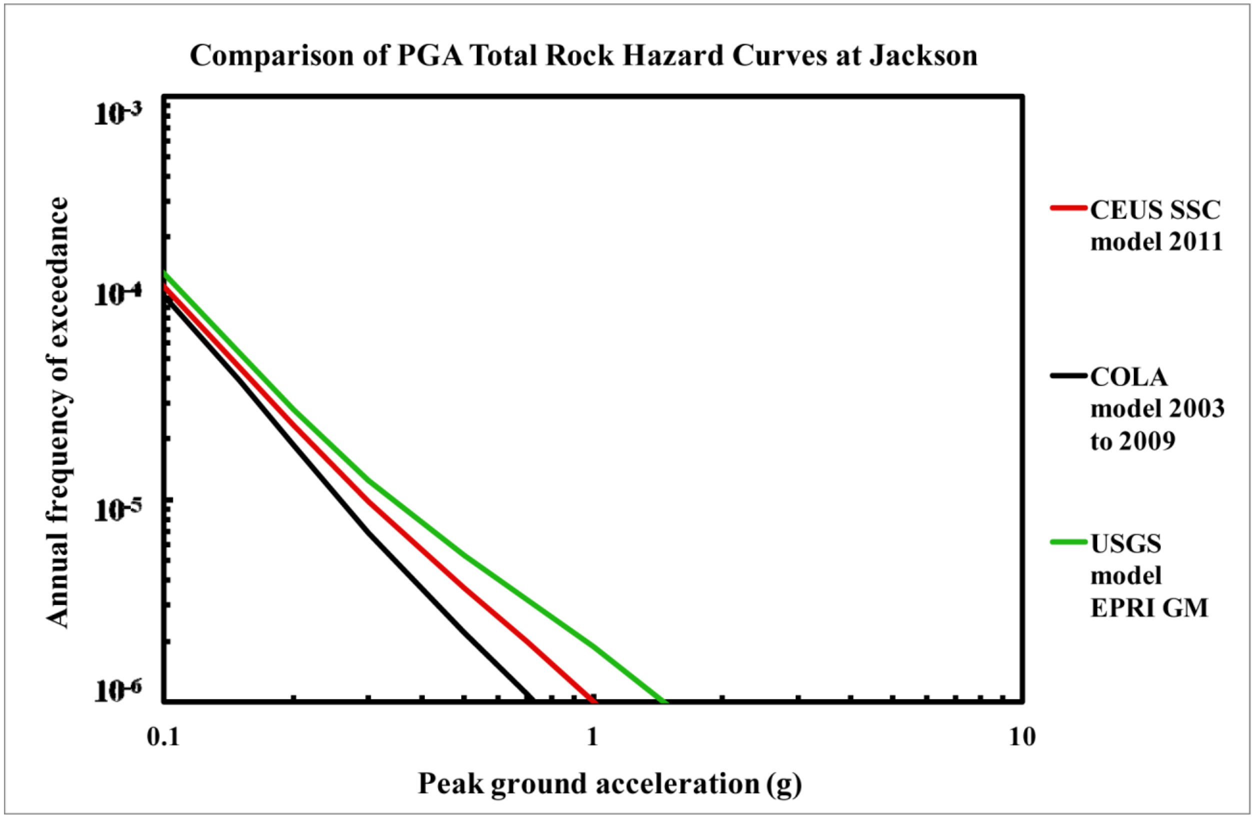

Figure 8.2-4l
Jackson PGA rock hazard: comparison of three source models

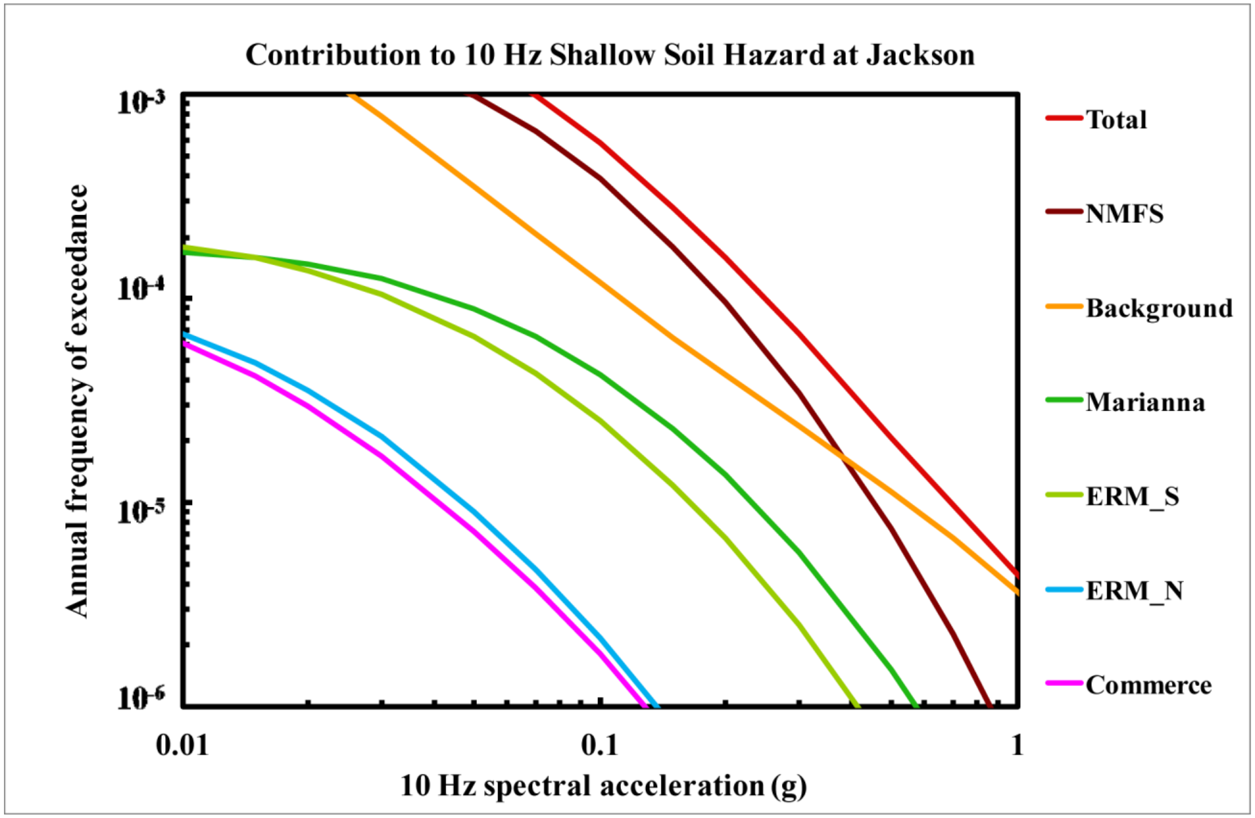

Figure 8.2-4m
Jackson 10 Hz shallow soil hazard: total and contribution by RLME and background

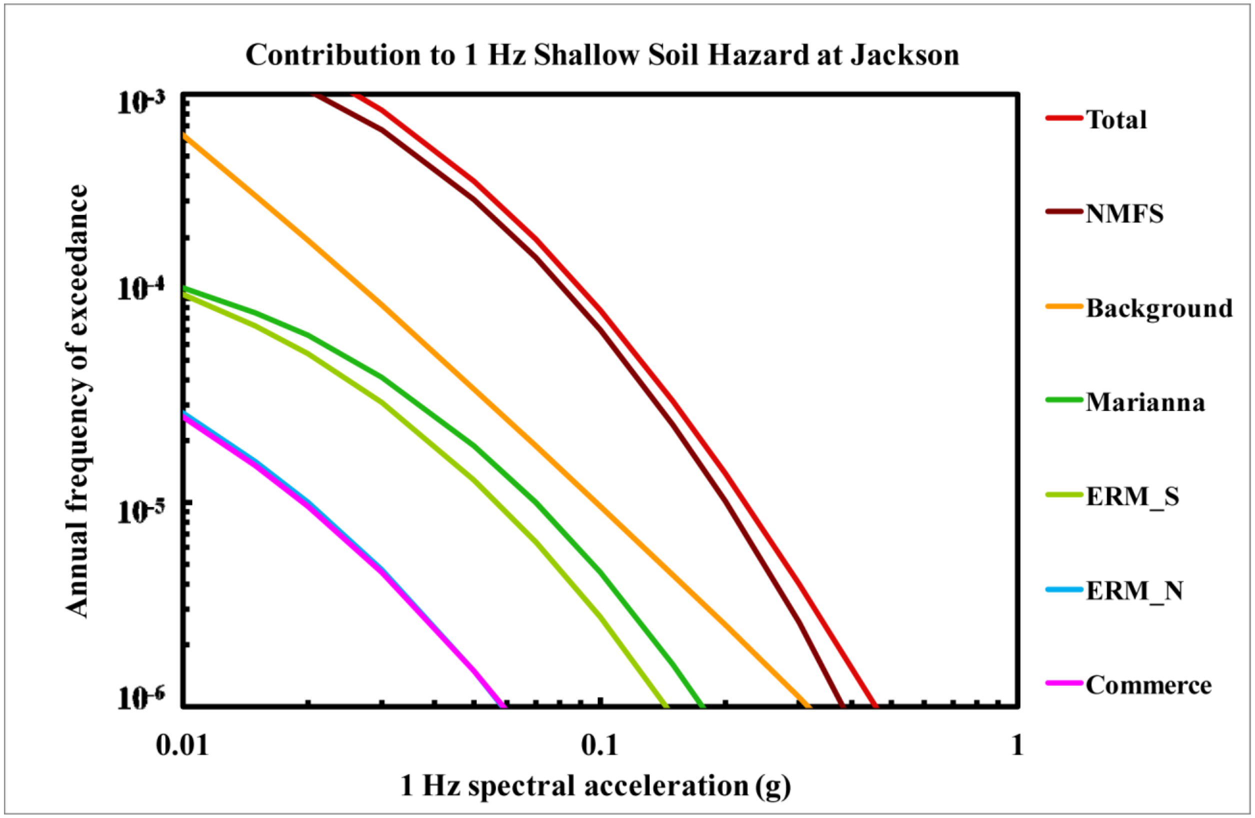

Figure 8.2-4n
Jackson 1 Hz shallow soil hazard: total and contribution by RLME and background

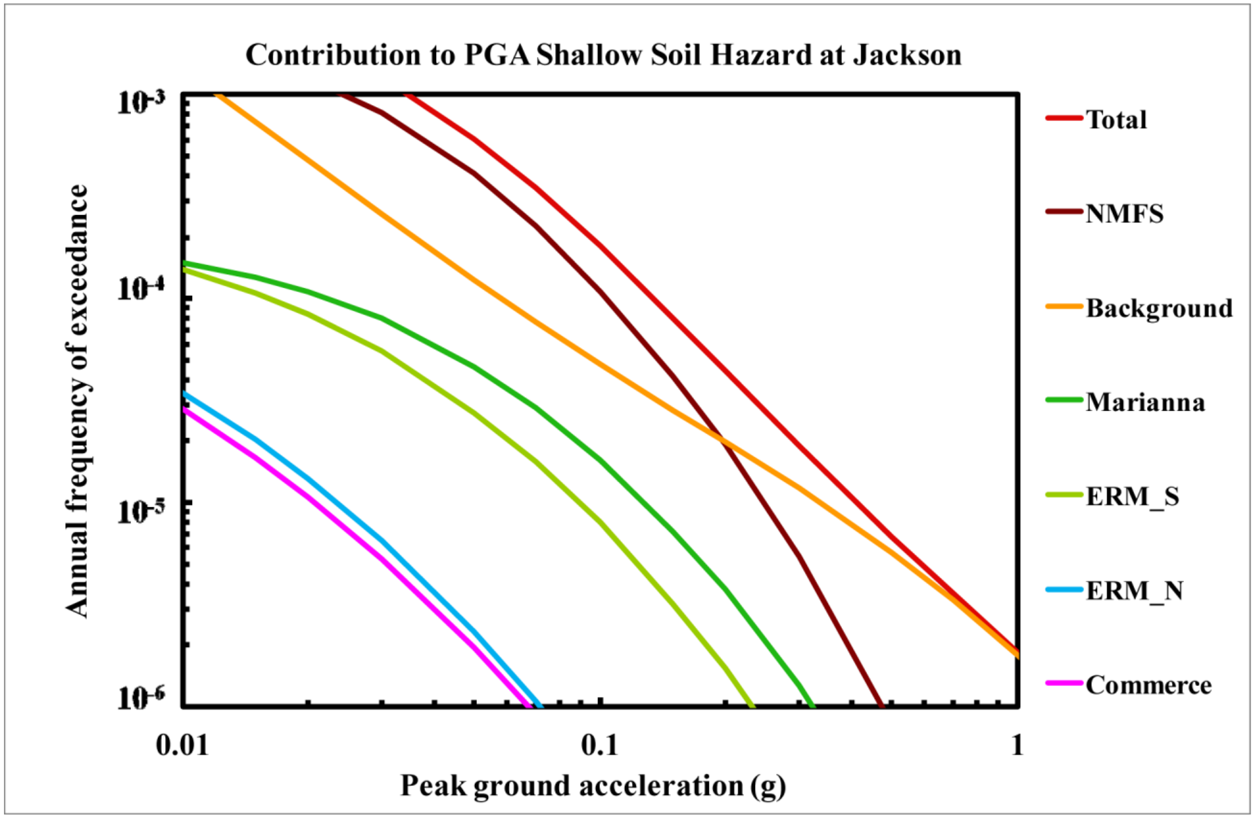

Figure 8.2-4o
Jackson PGA shallow soil hazard: total and contribution by RLME and background

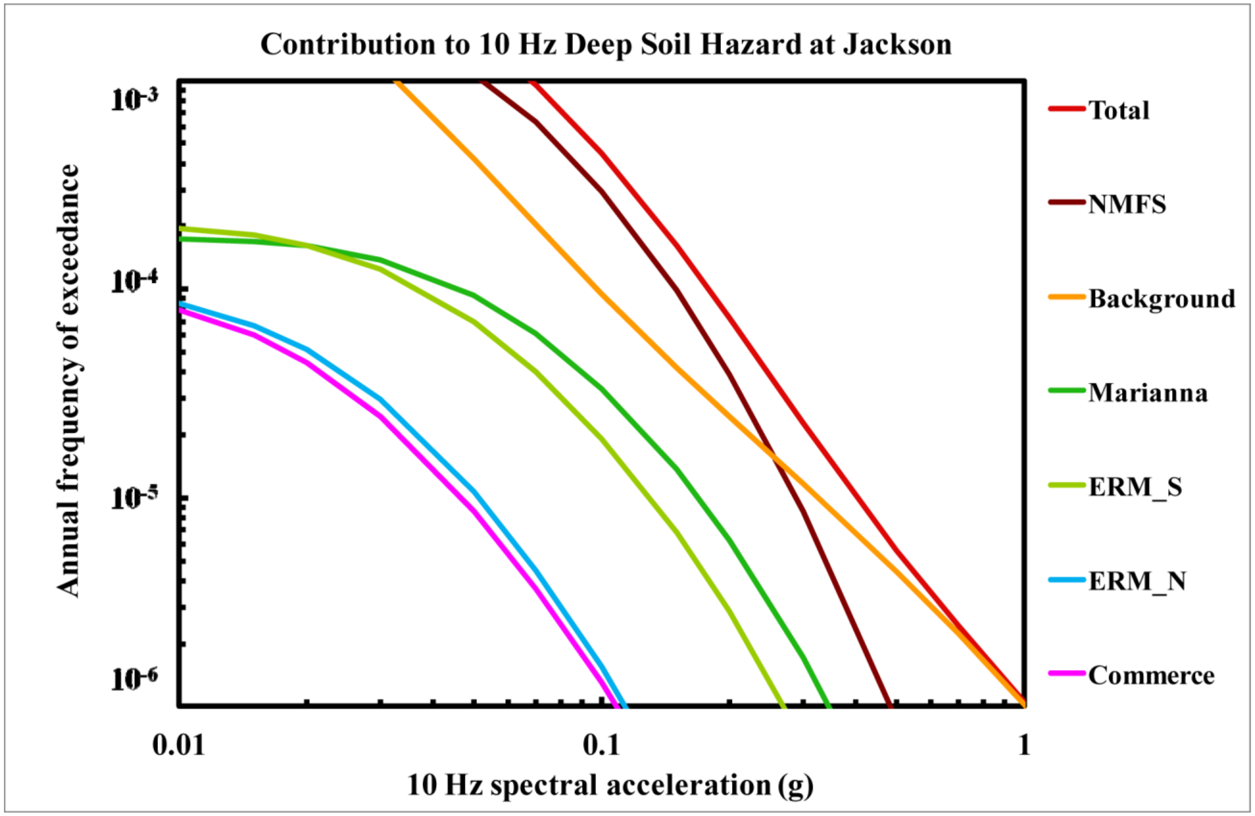

Figure 8.2-4p
Jackson 10 Hz deep soil hazard: total and contribution by RLME and background

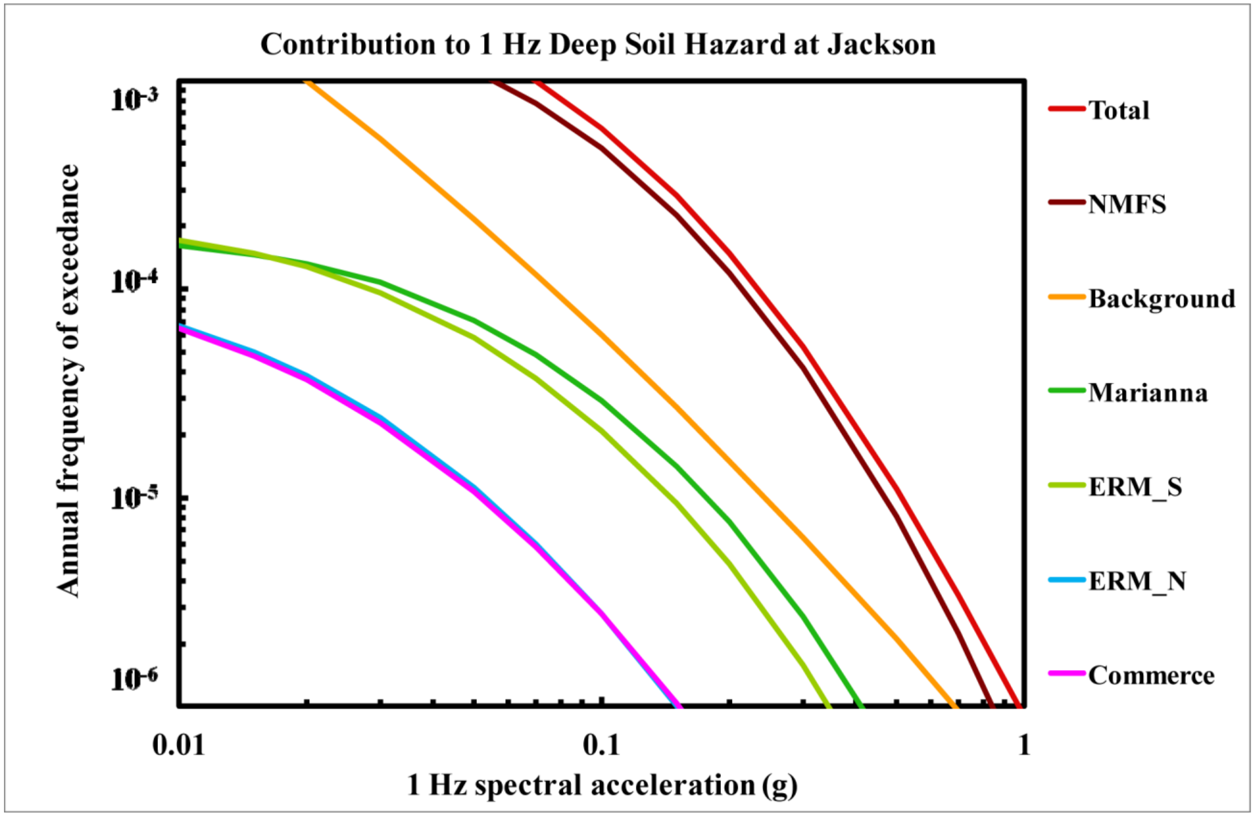

Figure 8.2-4q
Jackson 1 Hz deep soil hazard: total and contribution by RLME and background

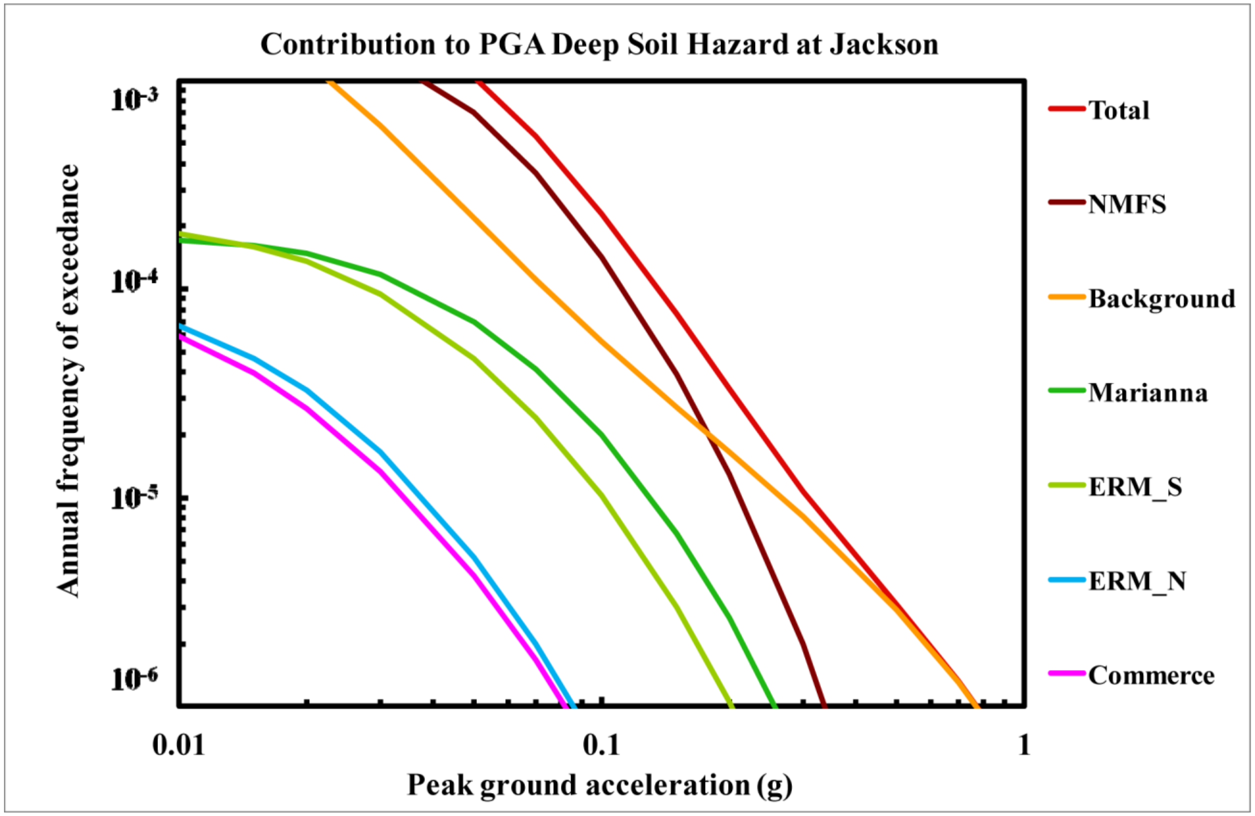

Figure 8.2-4r
Jackson PGA deep soil hazard: total and contribution by RLME and background

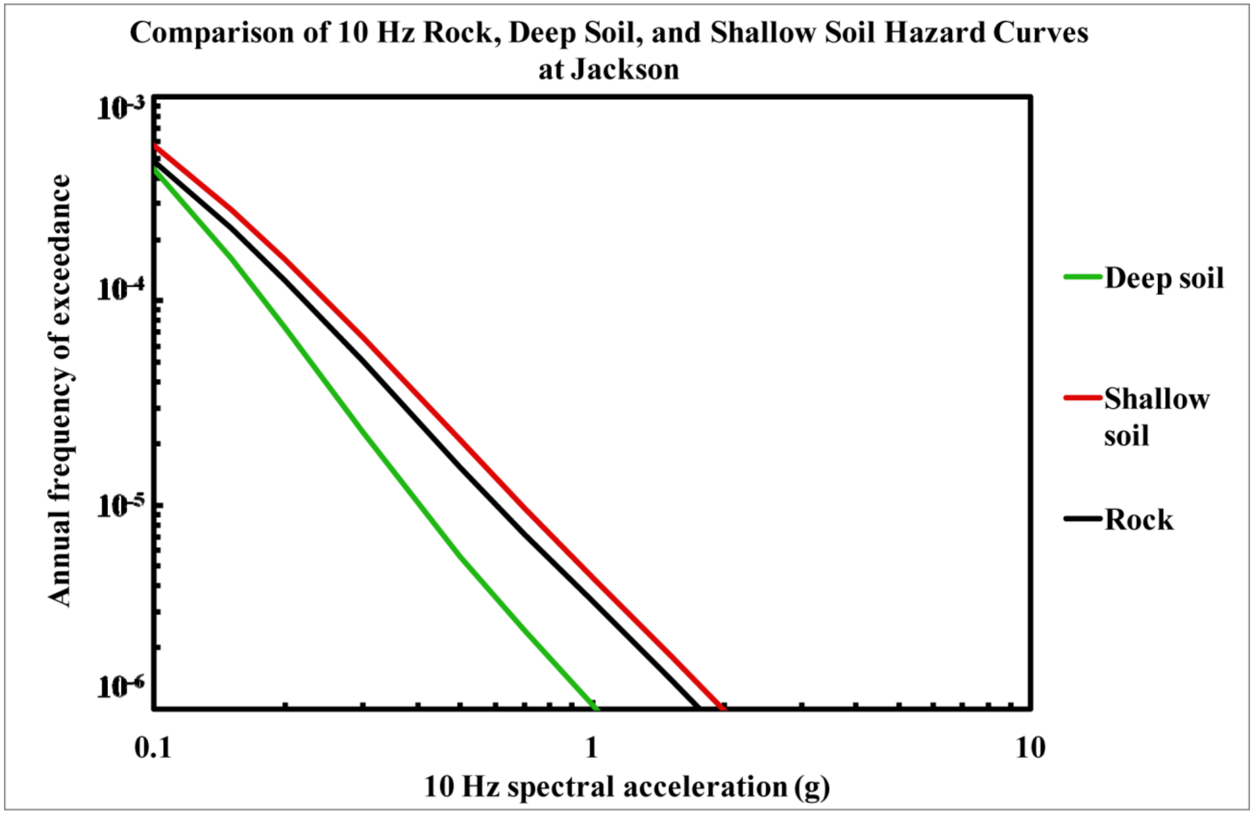

Figure 8.2-4s
Jackson 10 Hz hazard: comparison of three site conditions

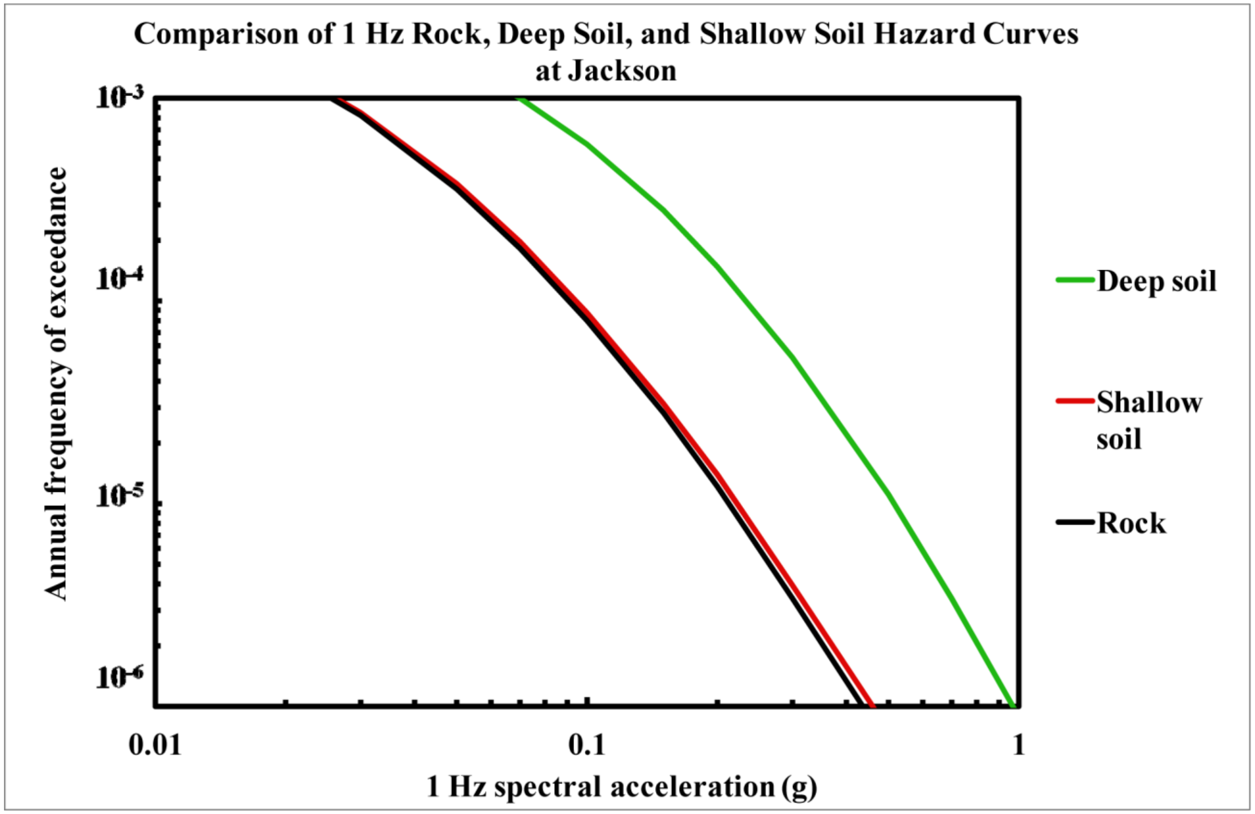

Figure 8.2-4t
Jackson 1 Hz hazard: comparison of three site conditions

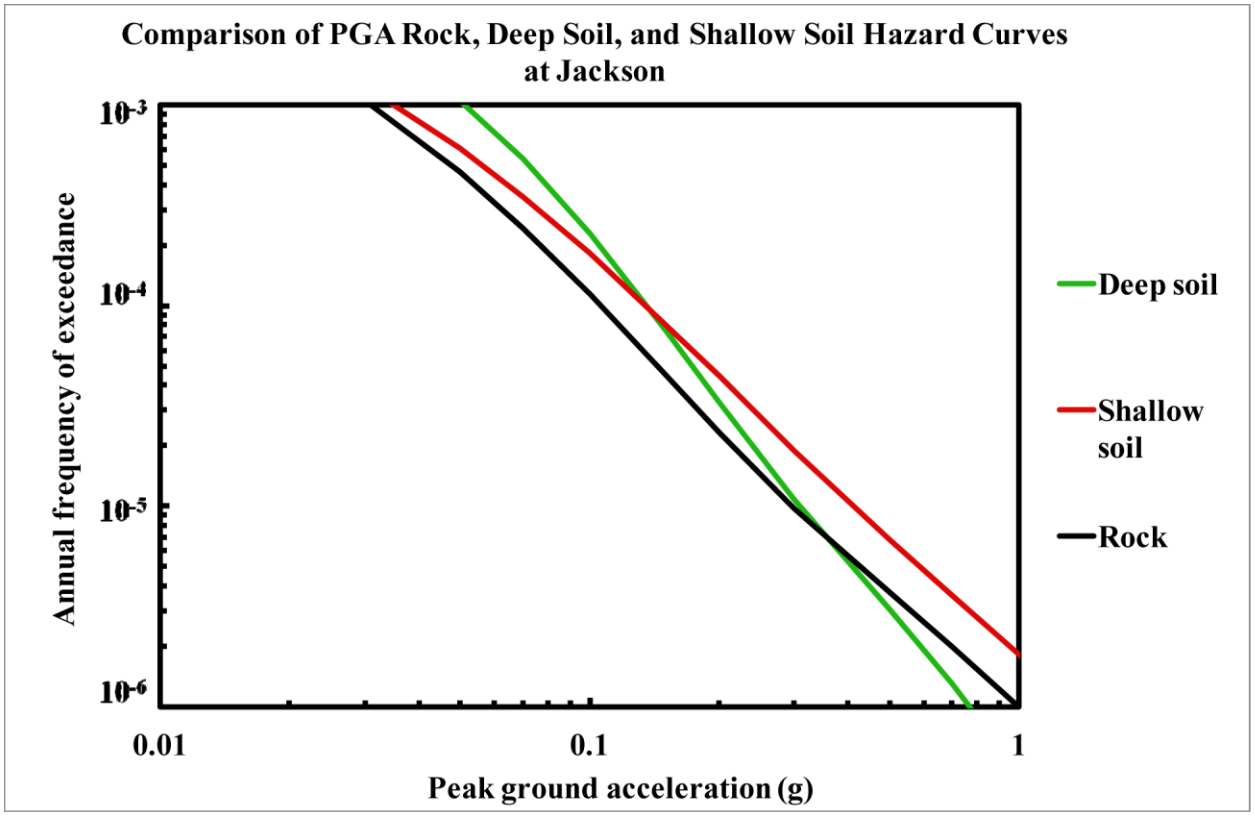

Figure 8.2-4u
Jackson PGA hazard: comparison of three site conditions

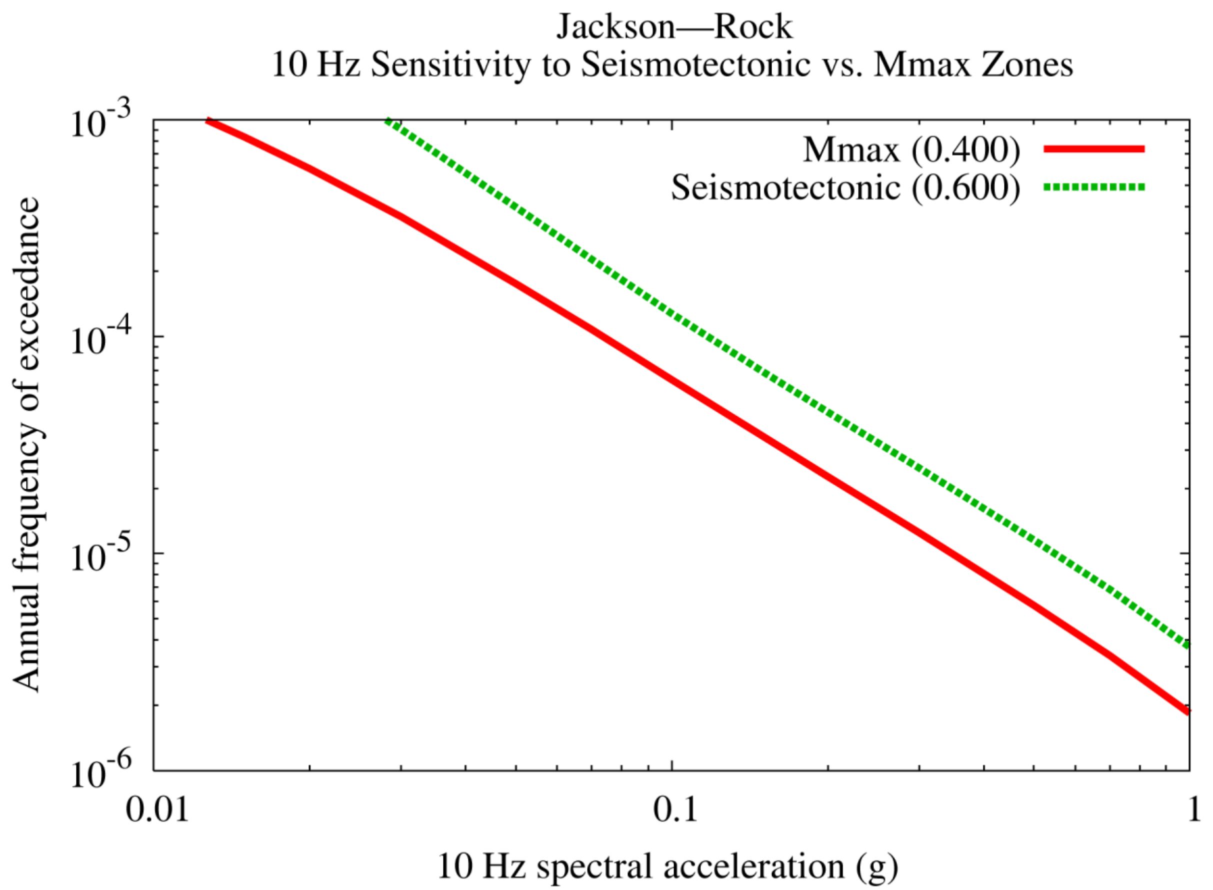

Figure 8.2-4v
Jackson 10 Hz rock hazard: sensitivity to seismotectonic vs. Mmax zones

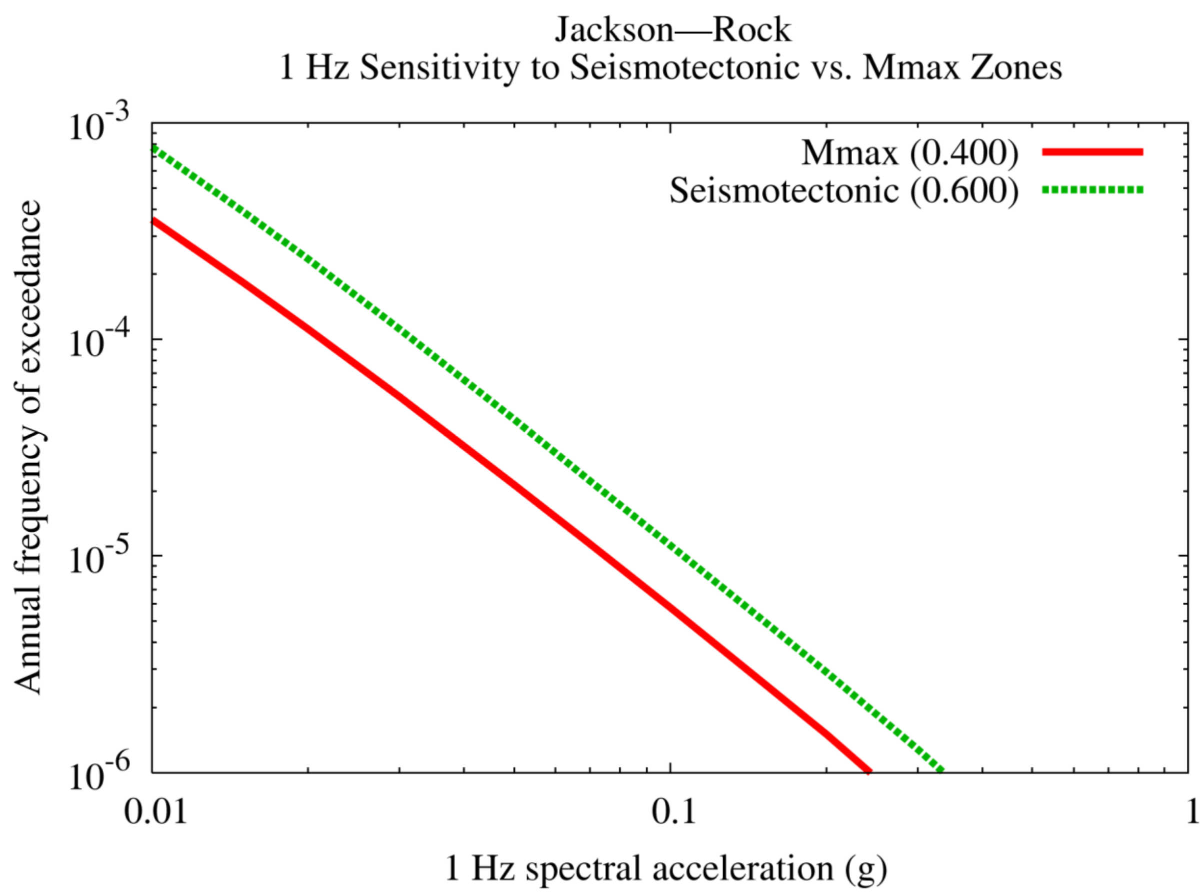

Figure 8.2-4w
Jackson 1 Hz rock hazard: sensitivity to seismotectonic vs. Mmax zones

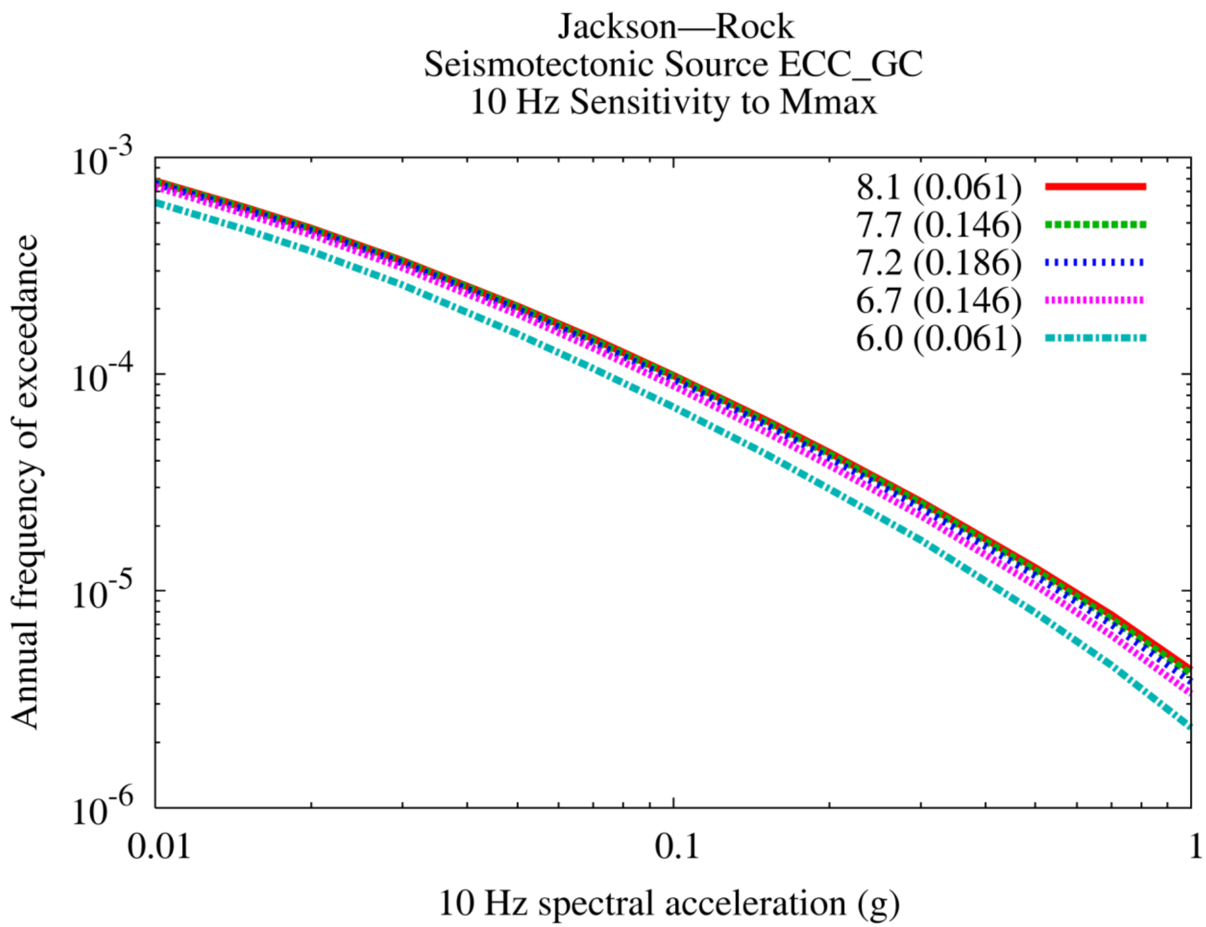

Figure 8.2-4x
Jackson 10 Hz rock hazard: sensitivity to Mmax for source ECC-GC

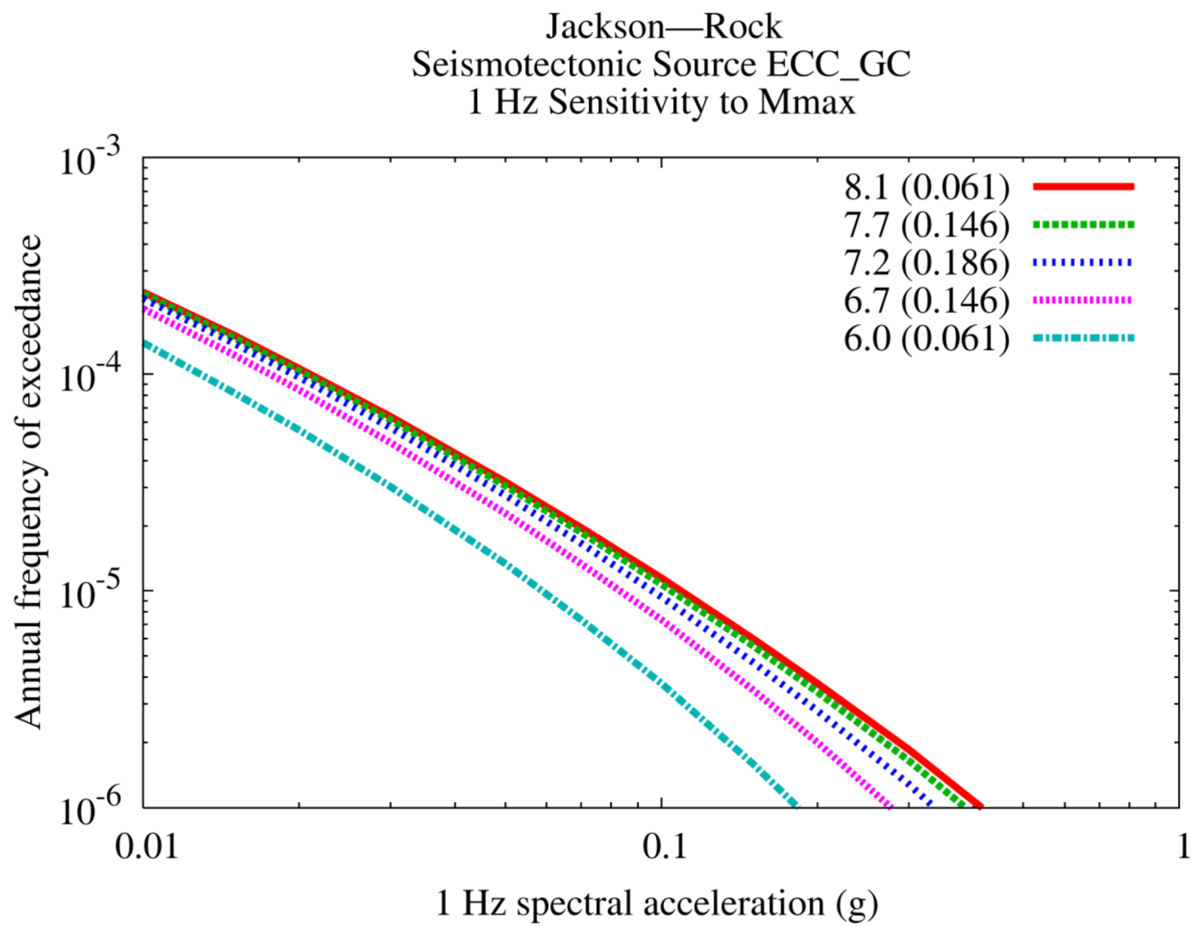

Figure 8.2-4y
Jackson 1 Hz rock hazard: sensitivity to Mmax for source ECC-GC

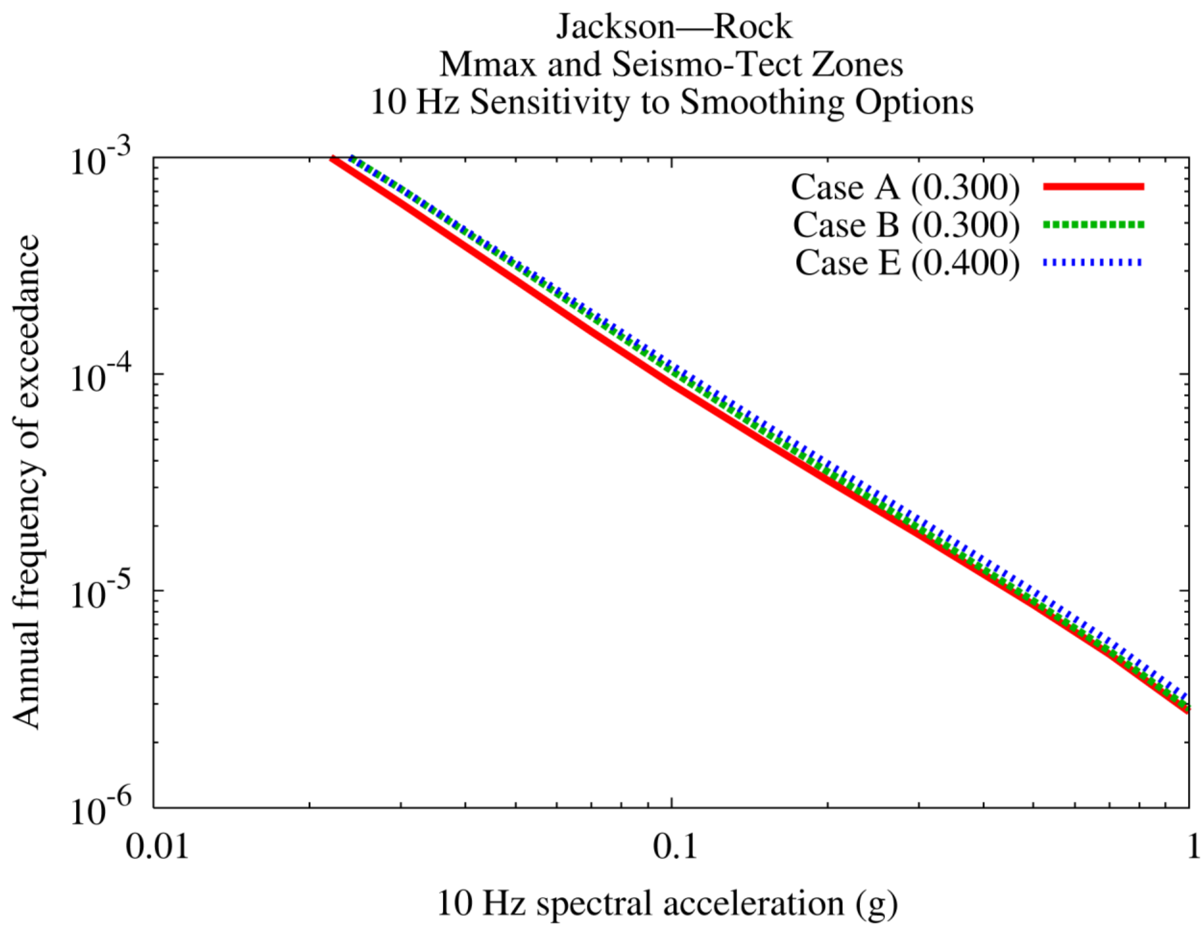

Figure 8.2-4z
Jackson 10 Hz rock hazard: sensitivity to smoothing options

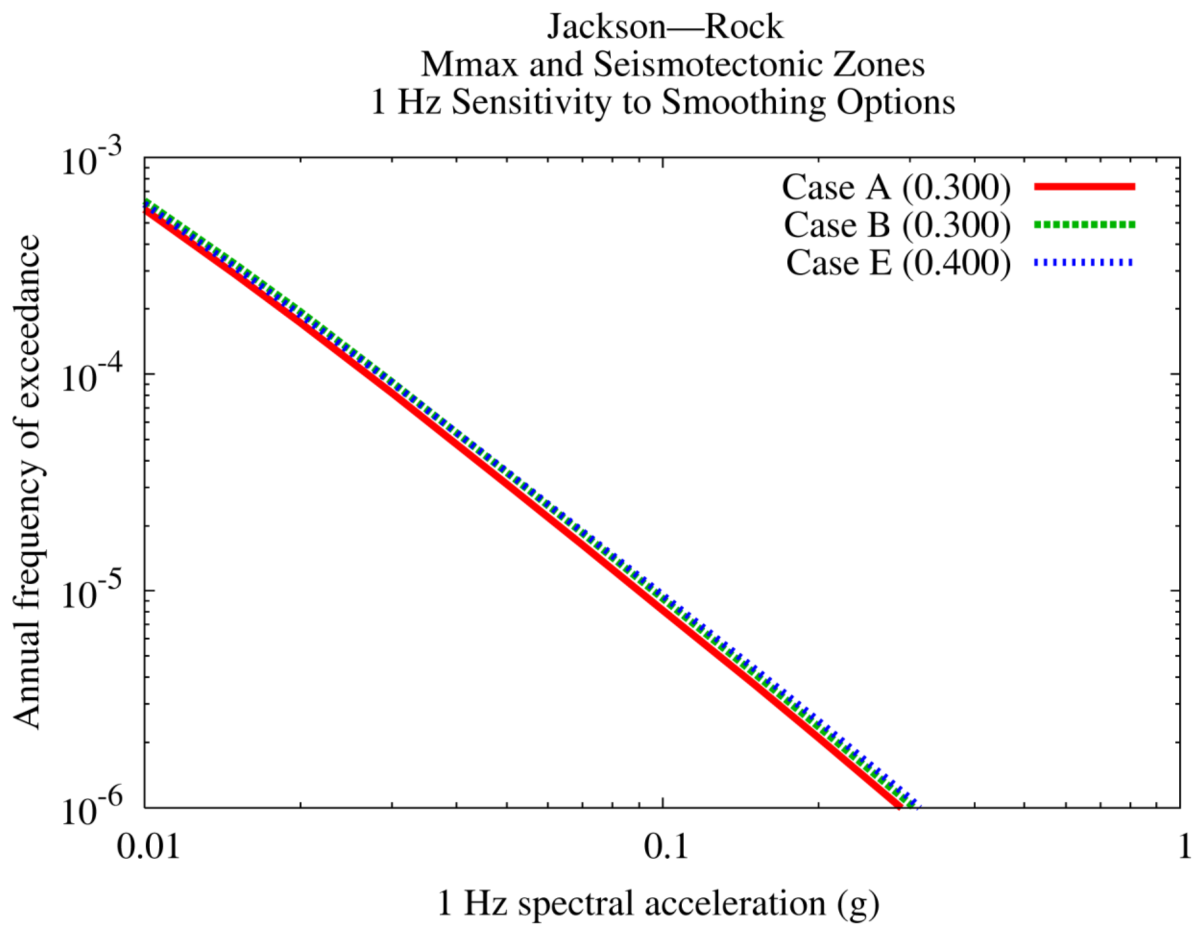

Figure 8.2-4aa
Jackson 1 Hz rock hazard: sensitivity to smoothing options

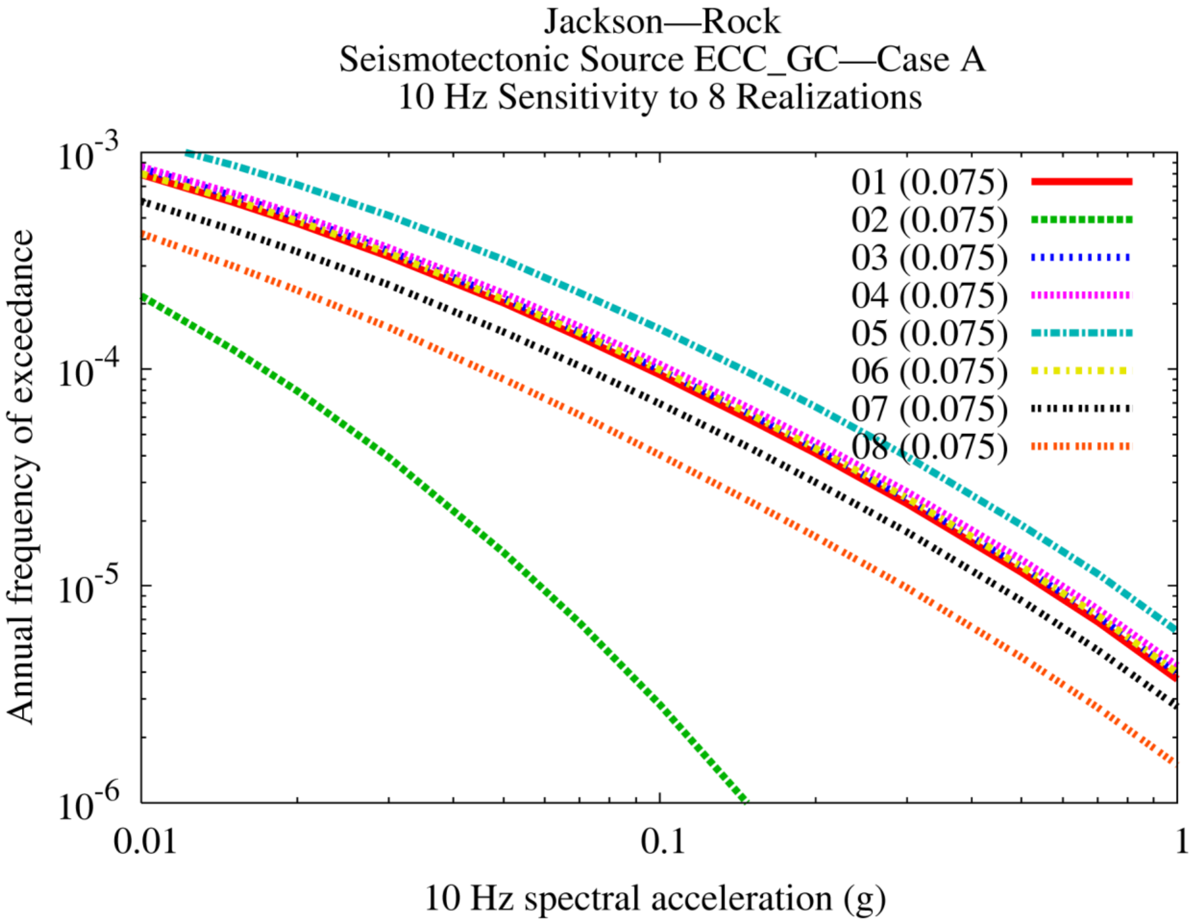

Figure 8.2-4bb
Jackson 10 Hz rock hazard: sensitivity to eight realizations for source ECC-GC, Case A

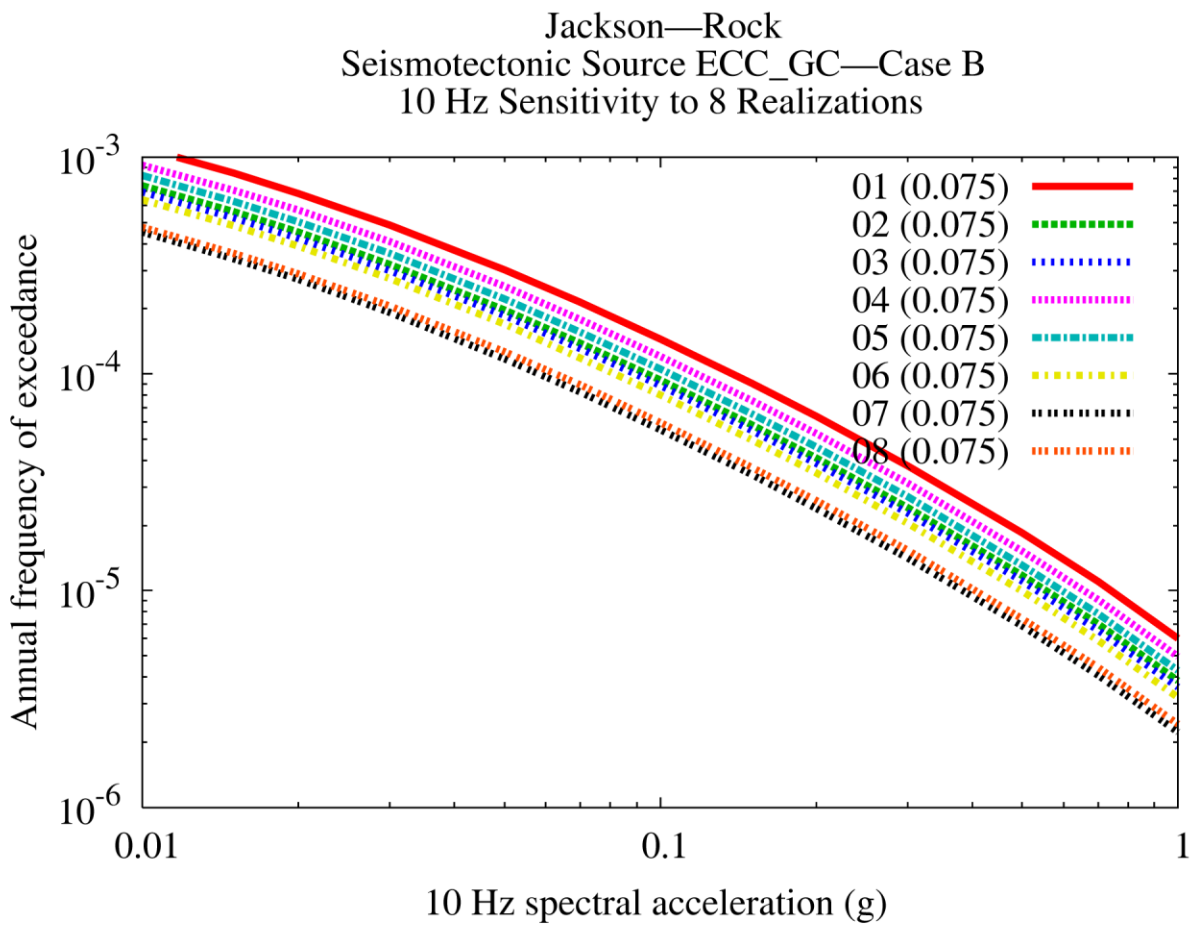

Figure 8.2-4cc
Jackson 10 Hz rock hazard: sensitivity to eight realizations for source ECC-GC, Case B

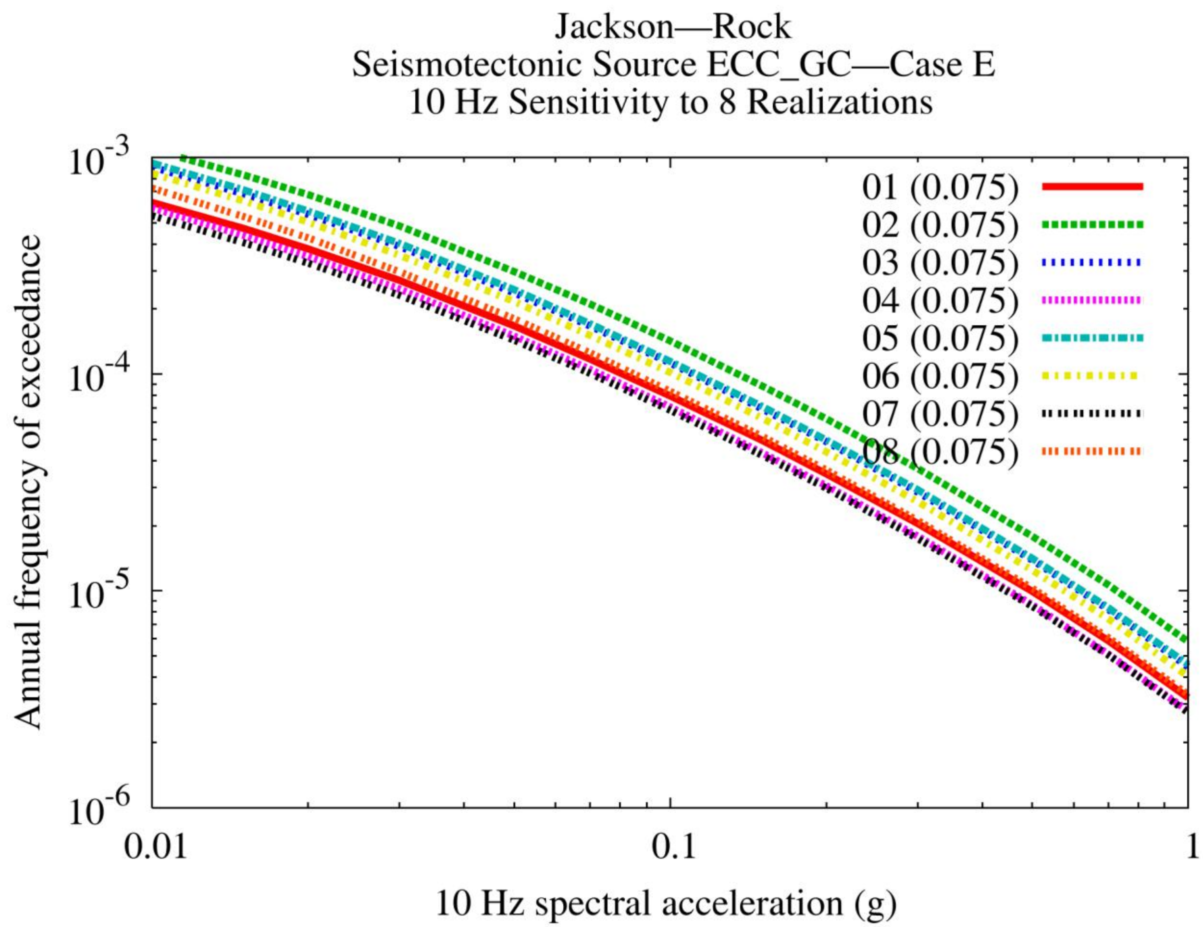

Figure 8.2-4dd
Jackson 10 Hz rock hazard: sensitivity to eight realizations for source ECC-GC, Case E

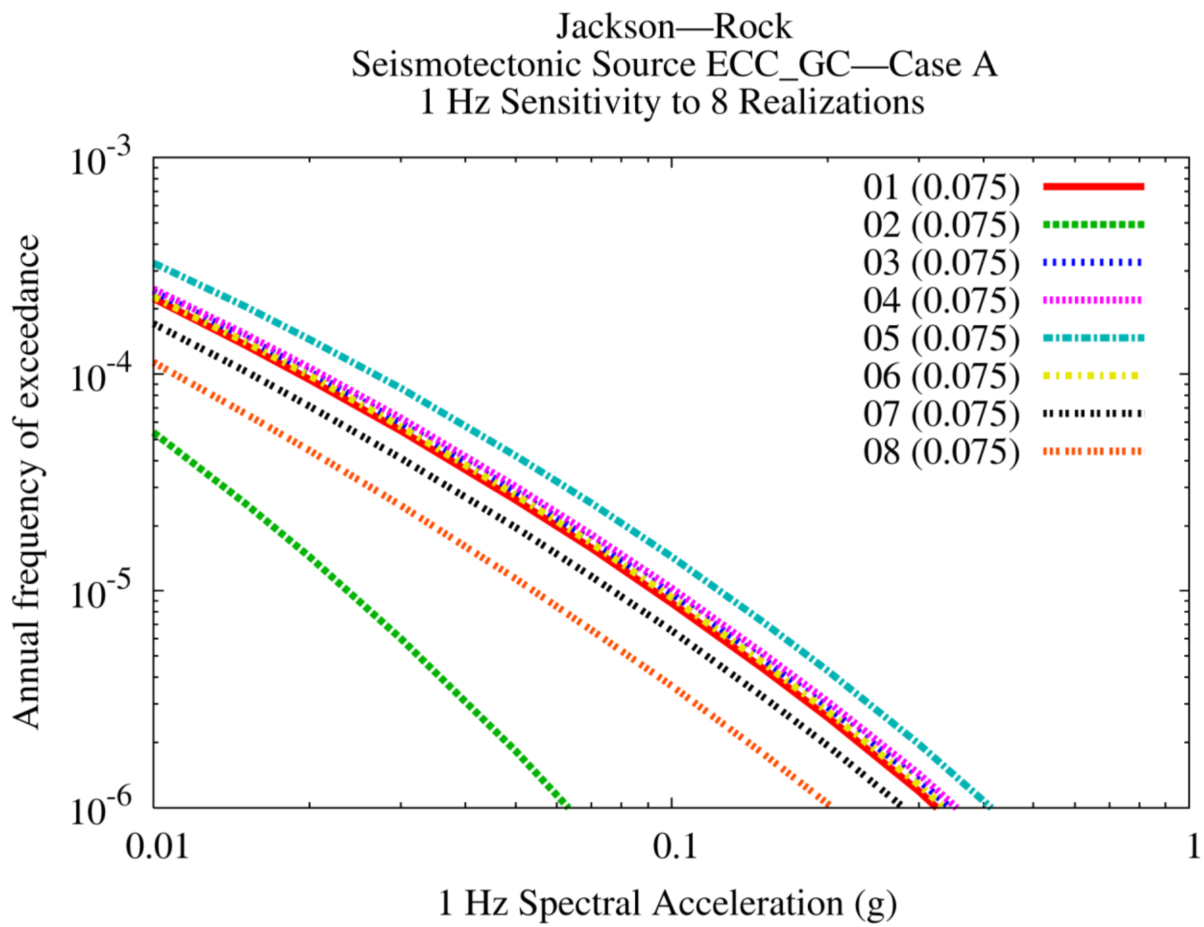

Figure 8.2-4ee
Jackson 1 Hz rock hazard: sensitivity to eight realizations for source ECC-GC, Case A

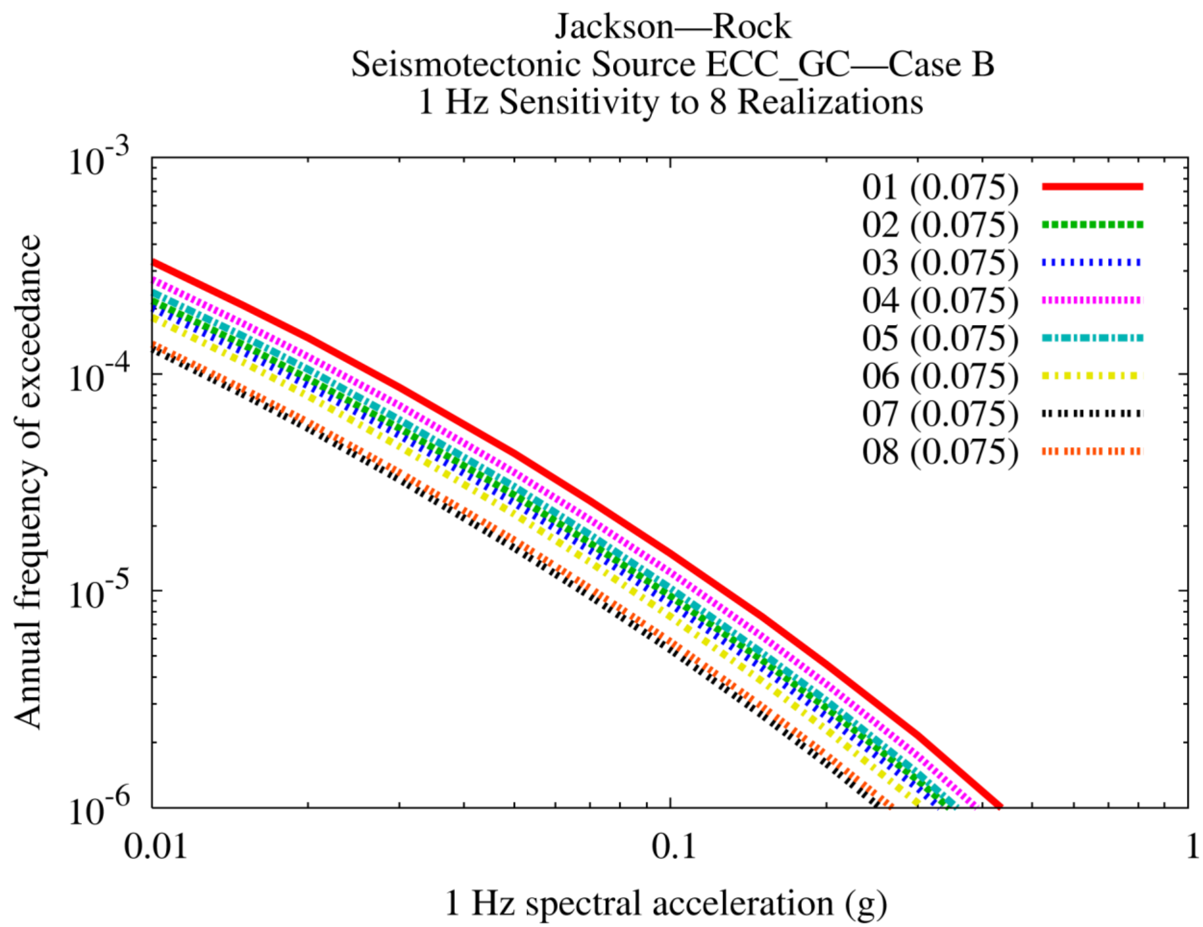

Figure 8.2-4ff
Jackson 1 Hz rock hazard: sensitivity to eight realizations for source ECC-GC, Case B

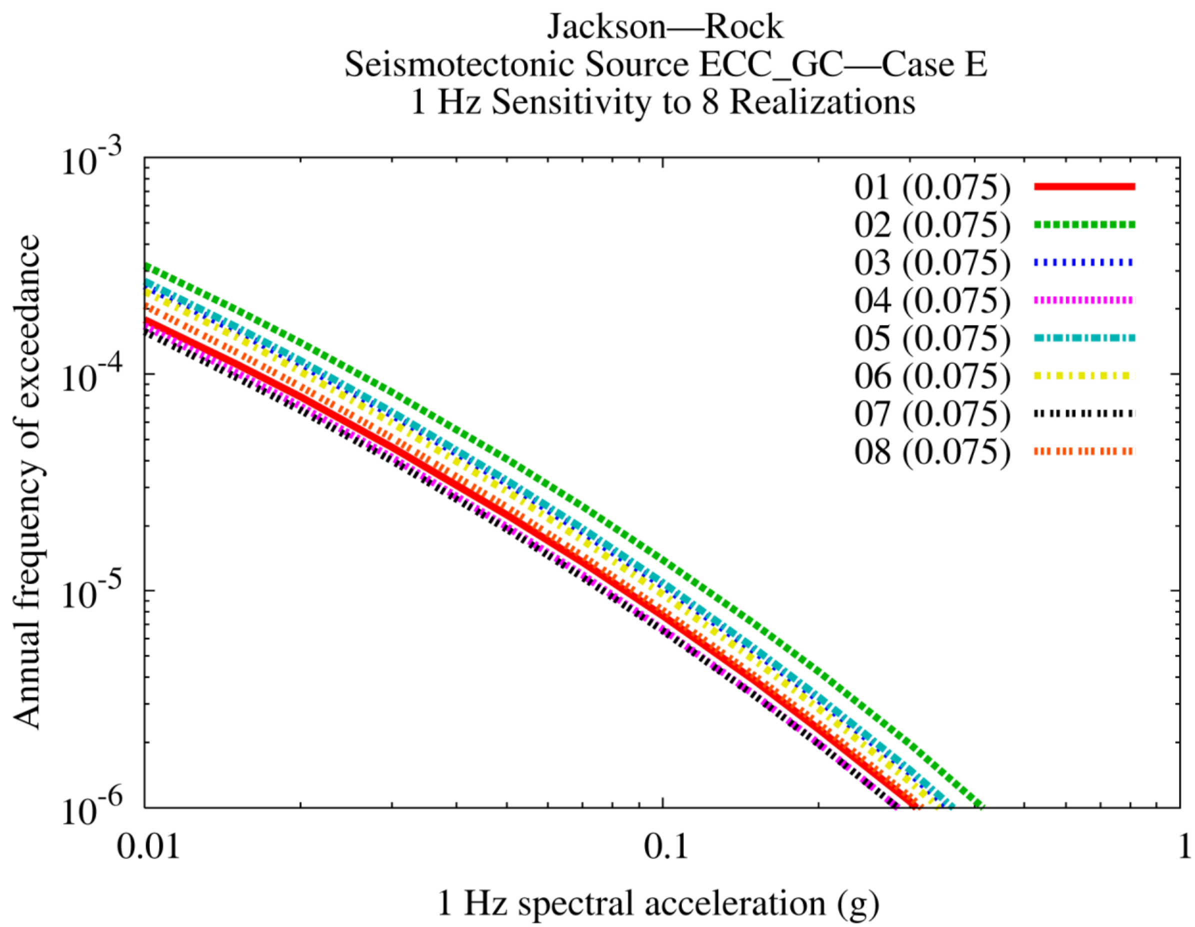

Figure 8.2-4gg
Jackson 1 Hz rock hazard: sensitivity to eight realizations for source ECC-GC, Case E

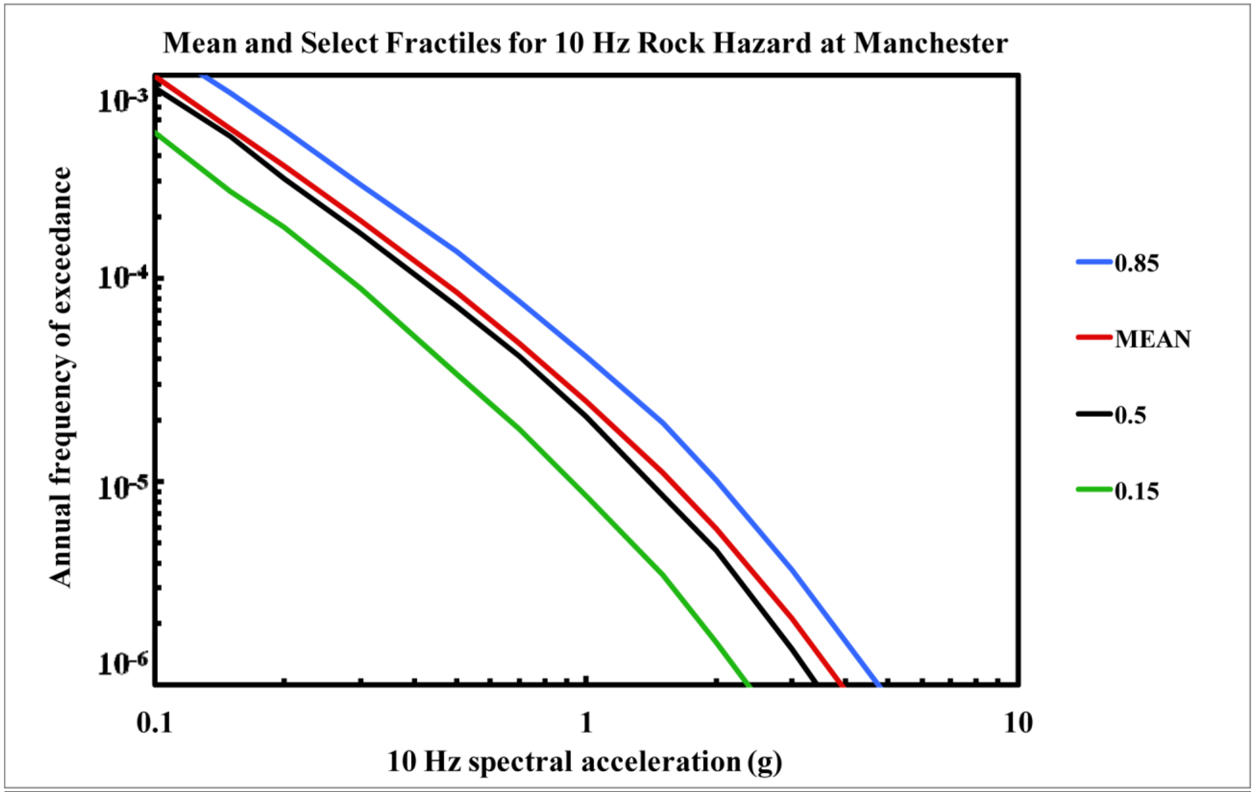

Figure 8.2-5a
Manchester 10 Hz rock hazard: mean and fractile total hazard

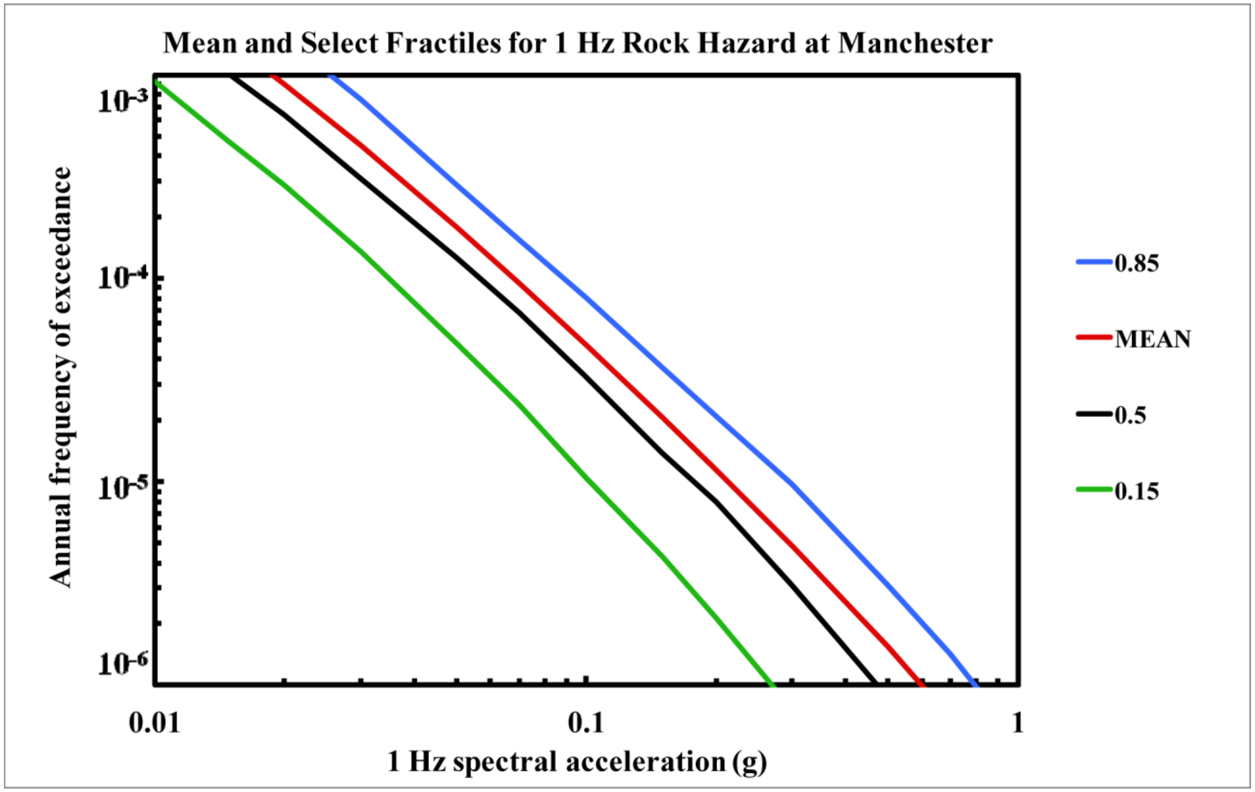

Figure 8.2-5b
Manchester 1 Hz rock hazard: mean and fractile total hazard

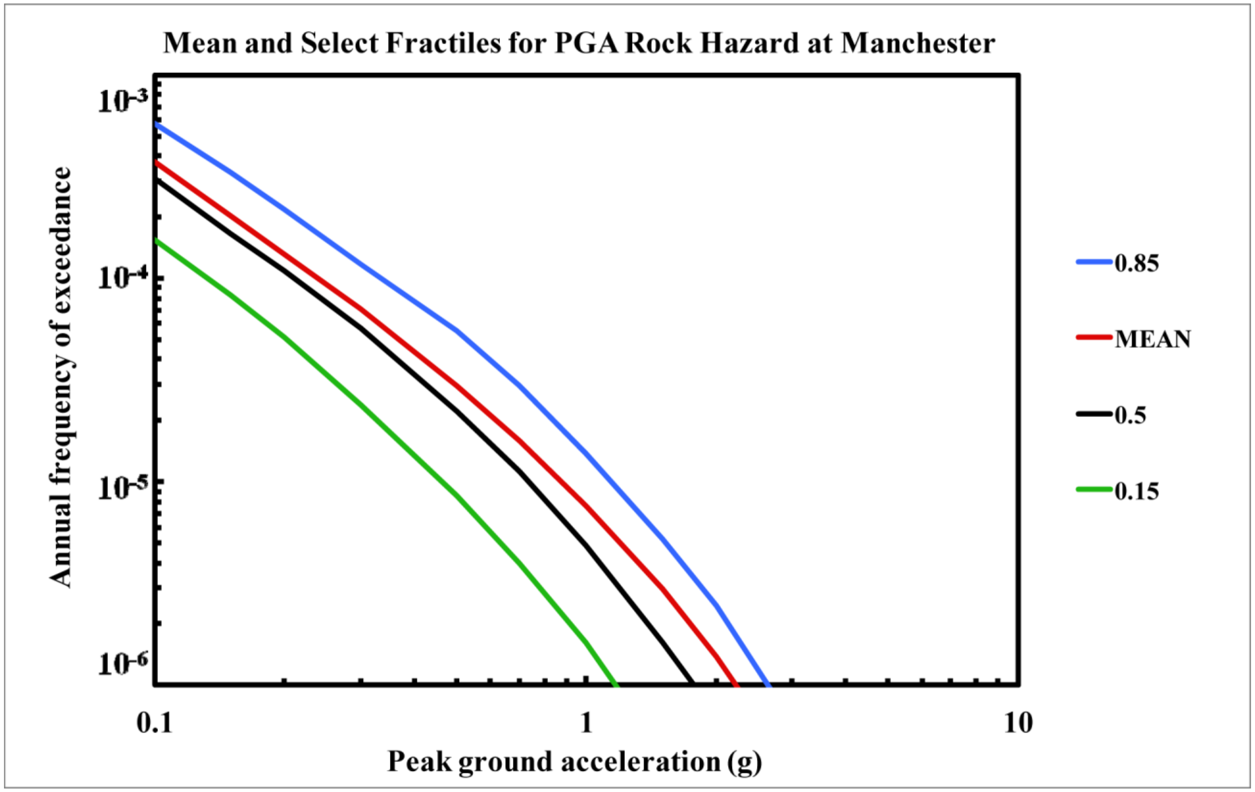

Figure 8.2-5c
Manchester PGA rock hazard: mean and fractile total hazard

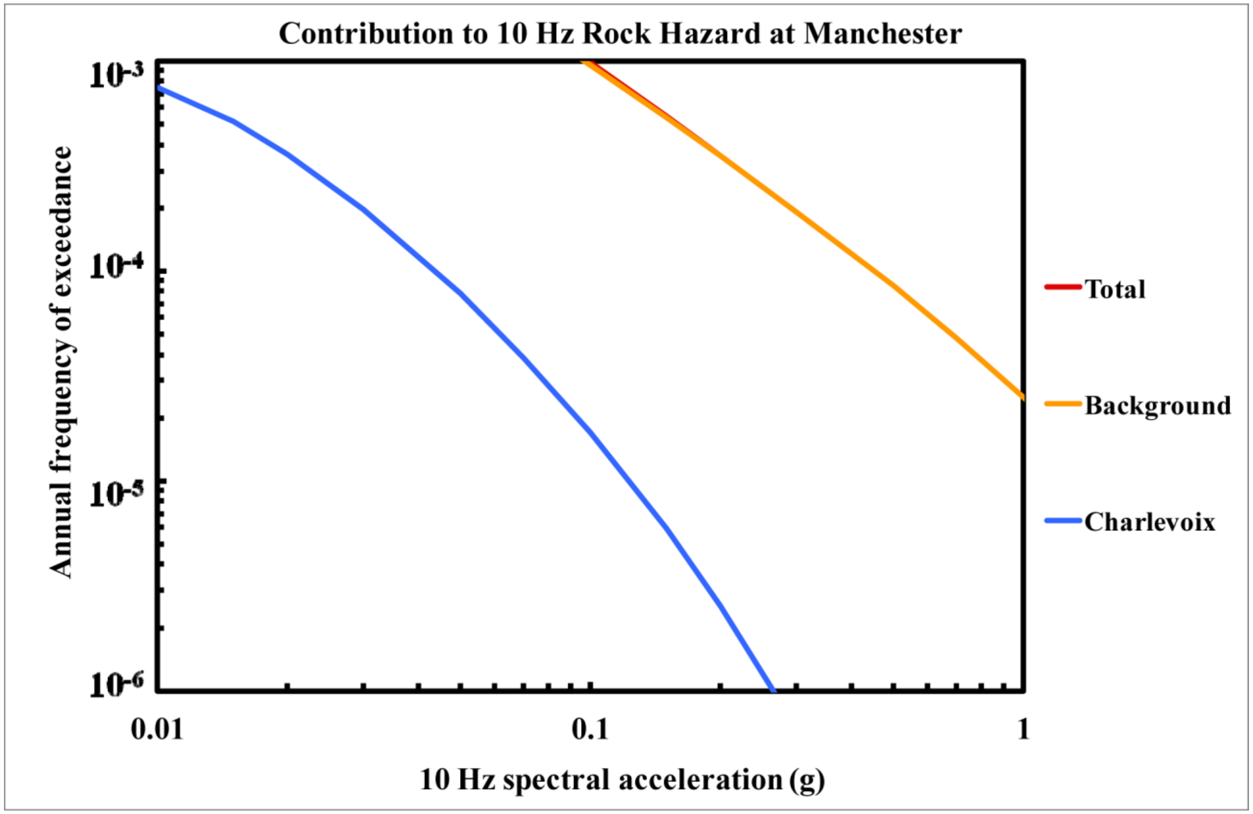

Figure 8.2-5d
Manchester 10 Hz rock hazard: total and contribution by RLME and background

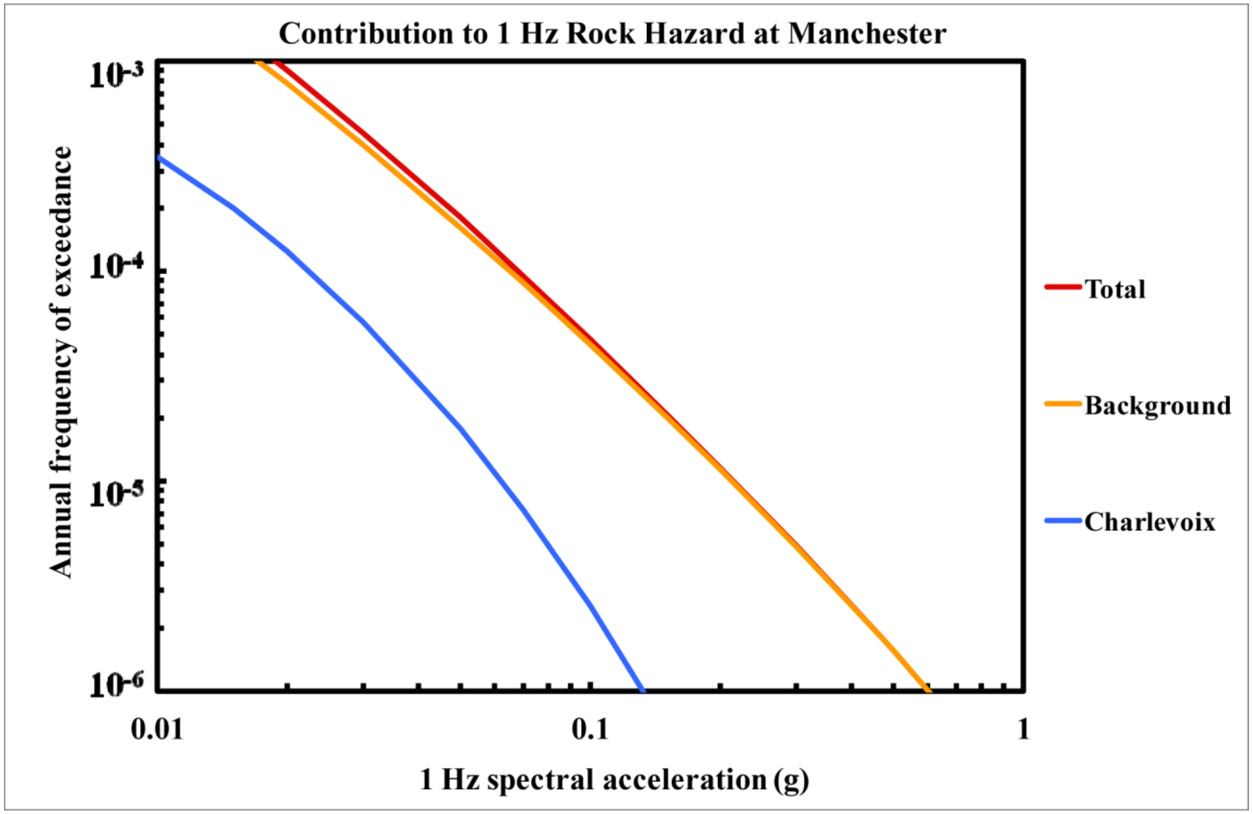

Figure 8.2-5e
Manchester 1 Hz rock hazard: total and contribution by RLME and background

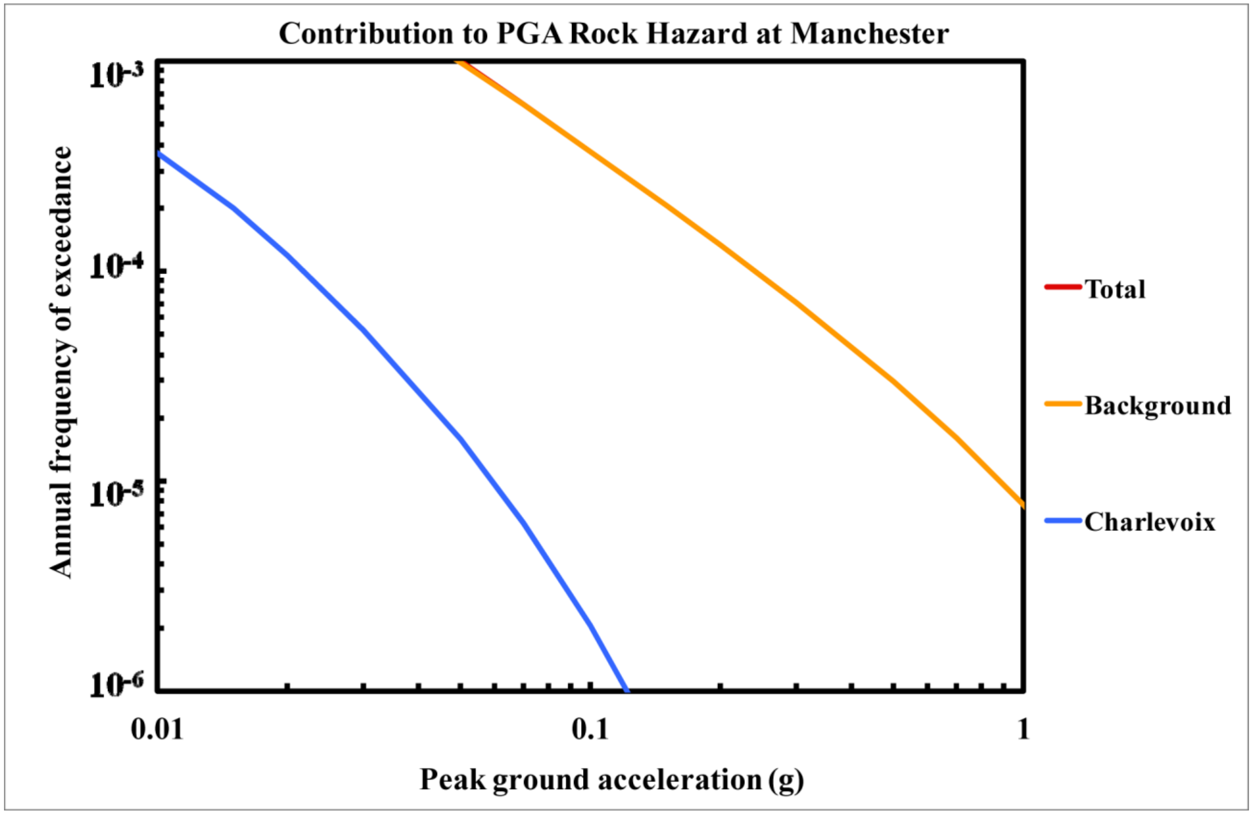

Figure 8.2-5f
Manchester PGA rock hazard: total and contribution by RLME and background

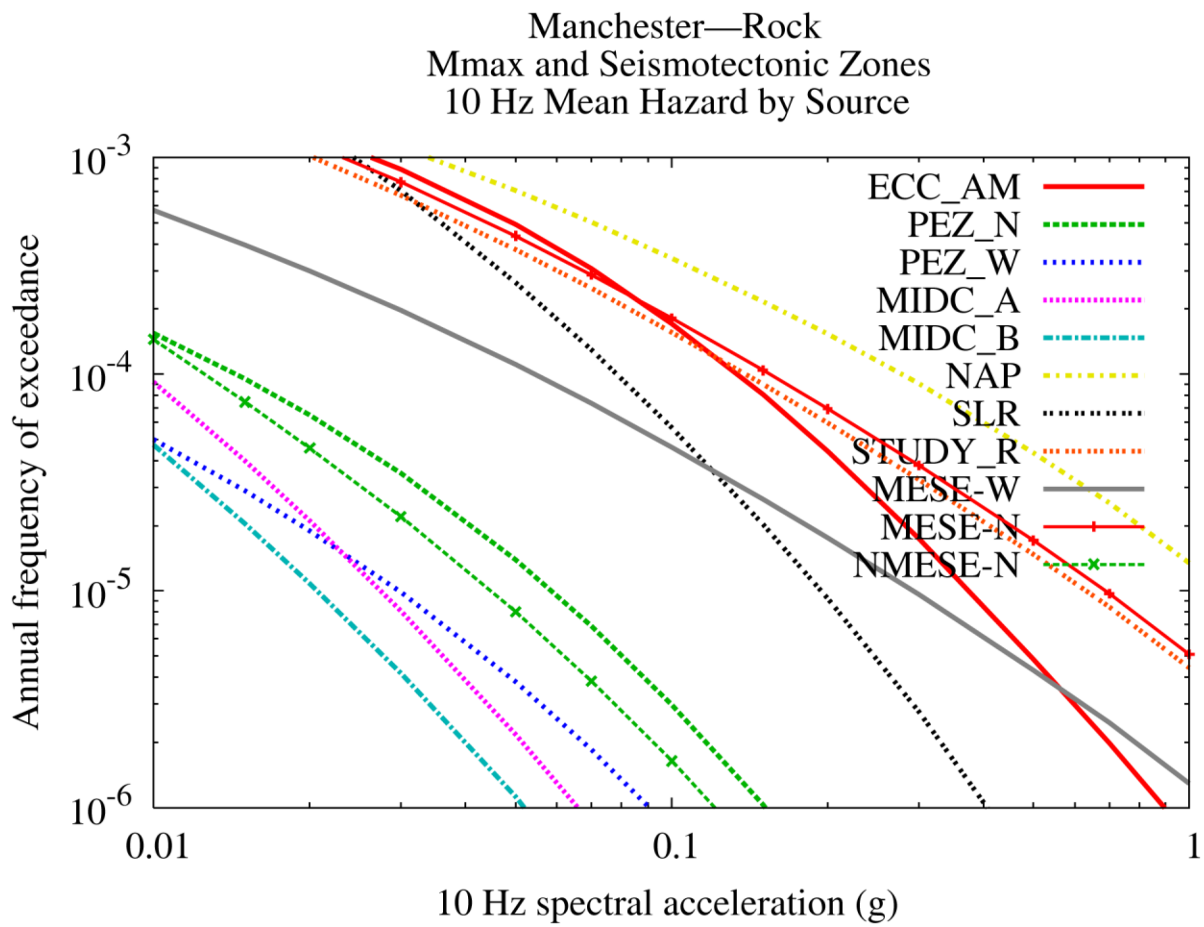

Figure 8.2-5g
Manchester 10 Hz rock hazard: contribution by background source

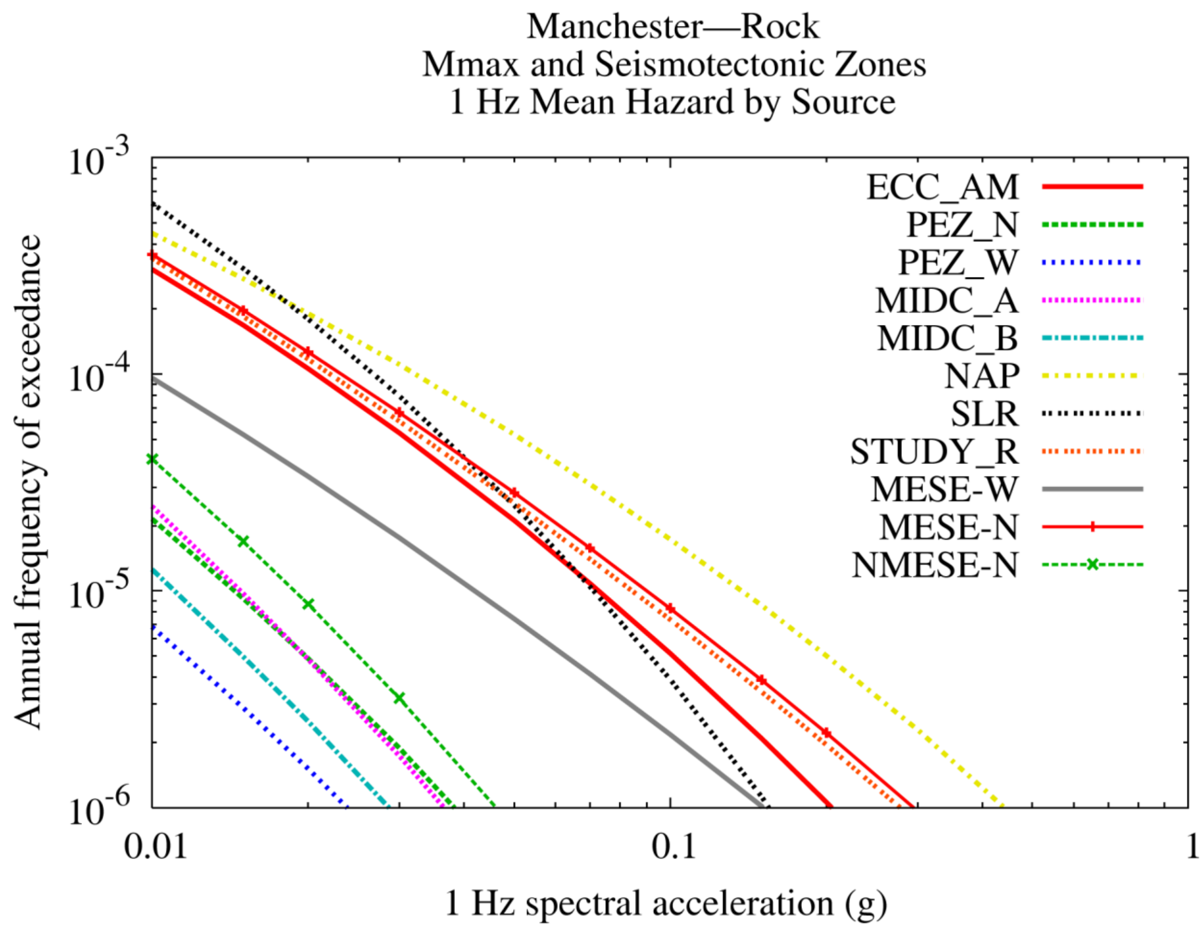

Figure 8.2-5h
Manchester 1 Hz rock hazard: contribution by background source

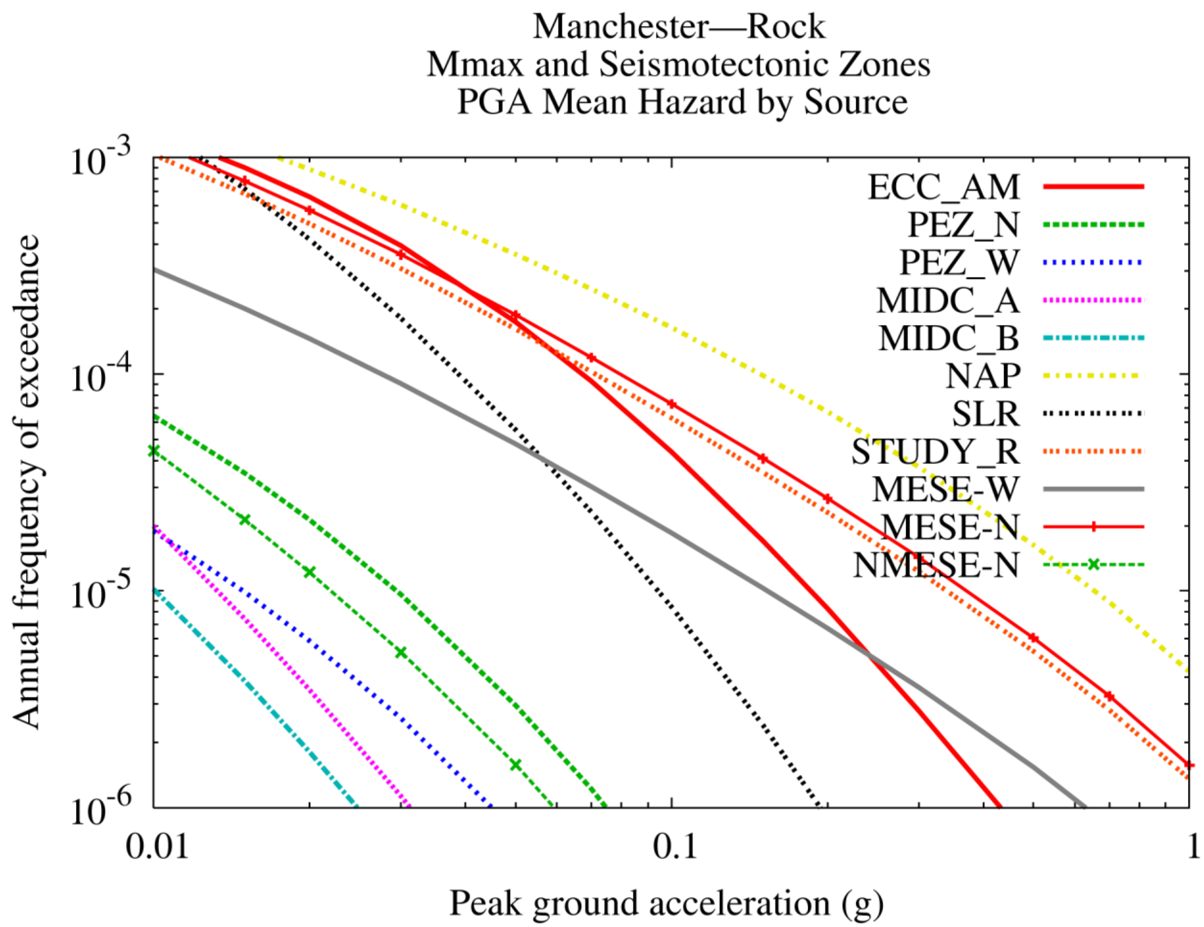

Figure 8.2-5i
Manchester PGA rock hazard: contribution by background source

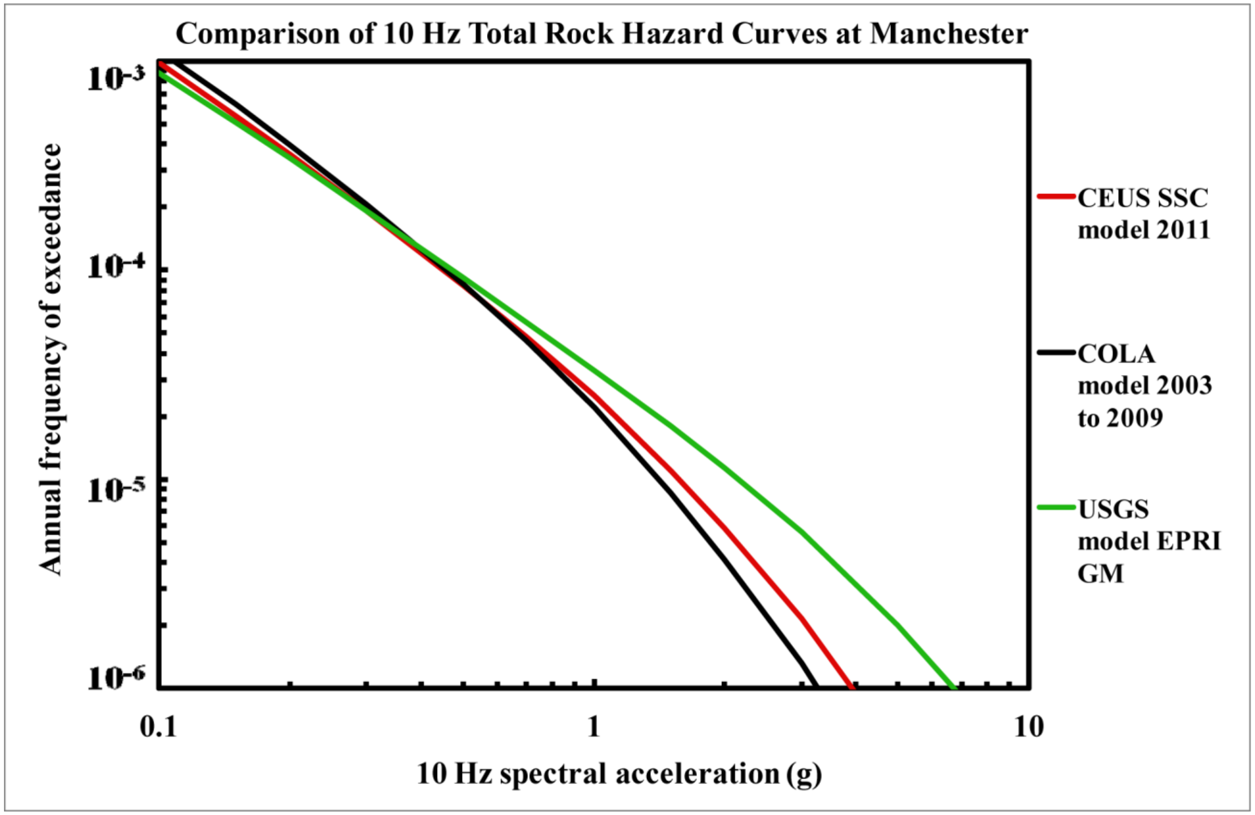

Figure 8.2-5j
Manchester 10 Hz rock hazard: comparison of three source models

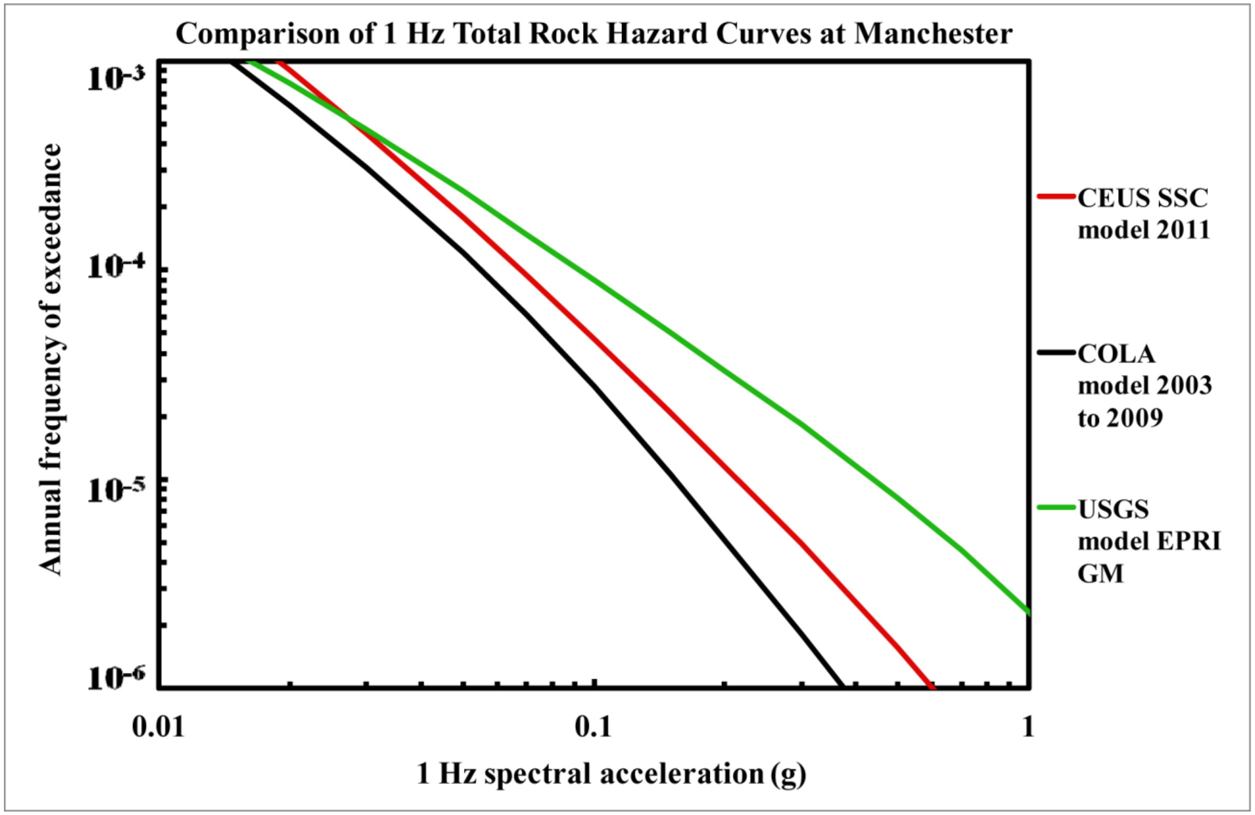

Figure 8.2-5k
Manchester is 1 Hz rock hazard: comparison of three source models

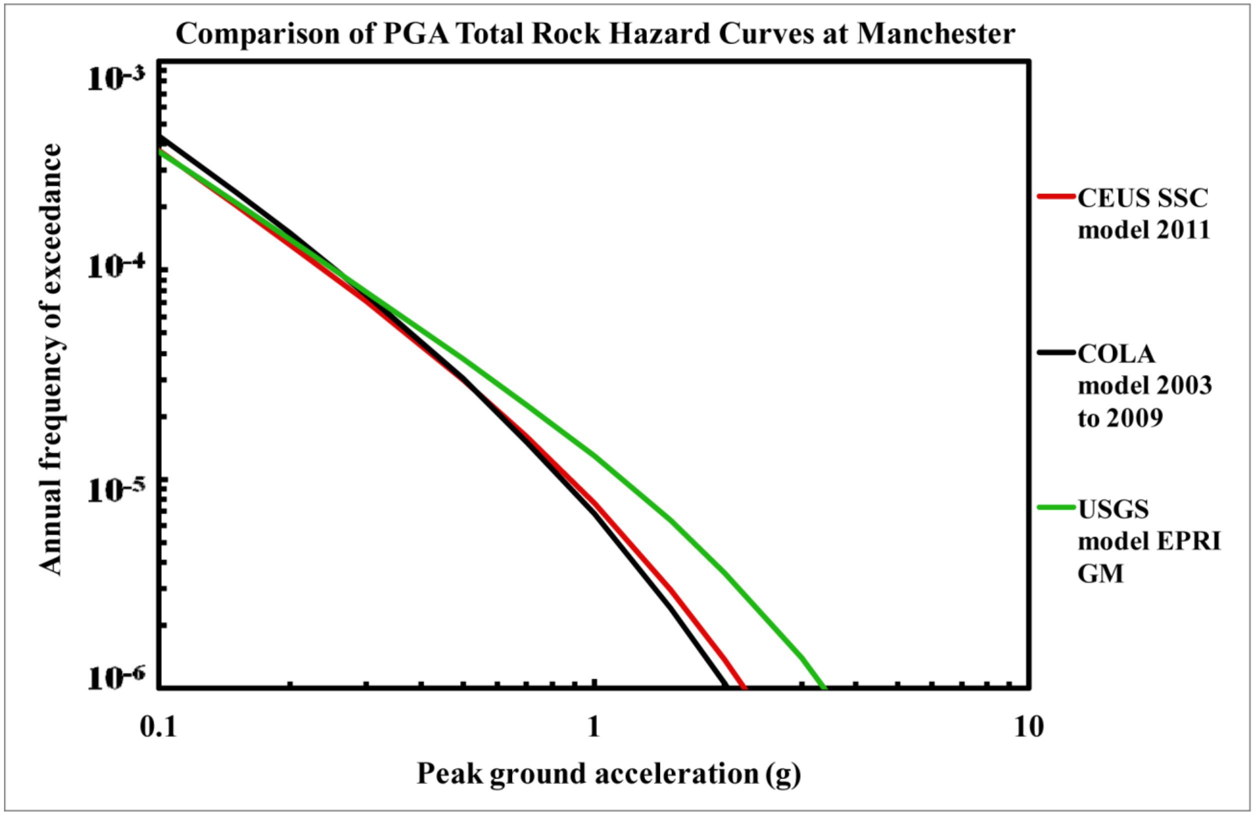

Figure 8.2-5l
Manchester PGA rock hazard: comparison of three source models

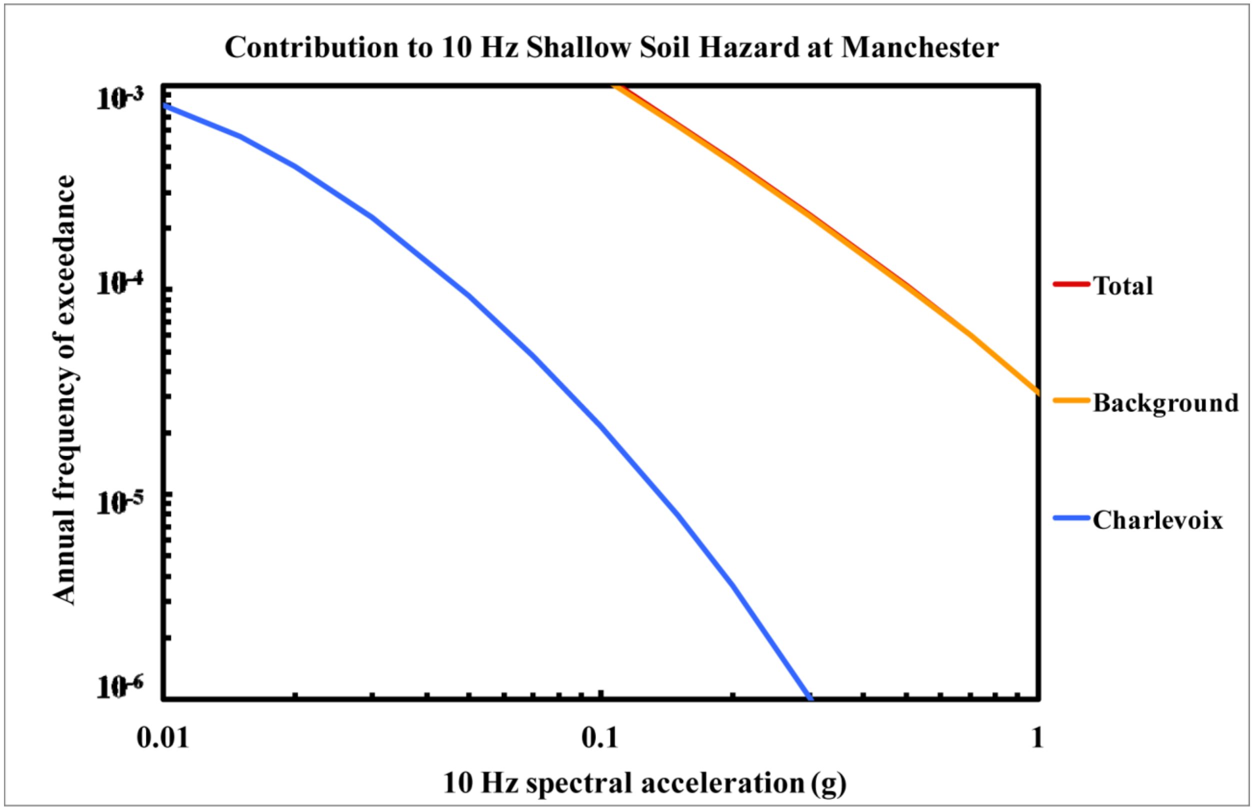

Figure 8.2-5m
Manchester 10 Hz shallow soil hazard: total and contribution by RLME and background

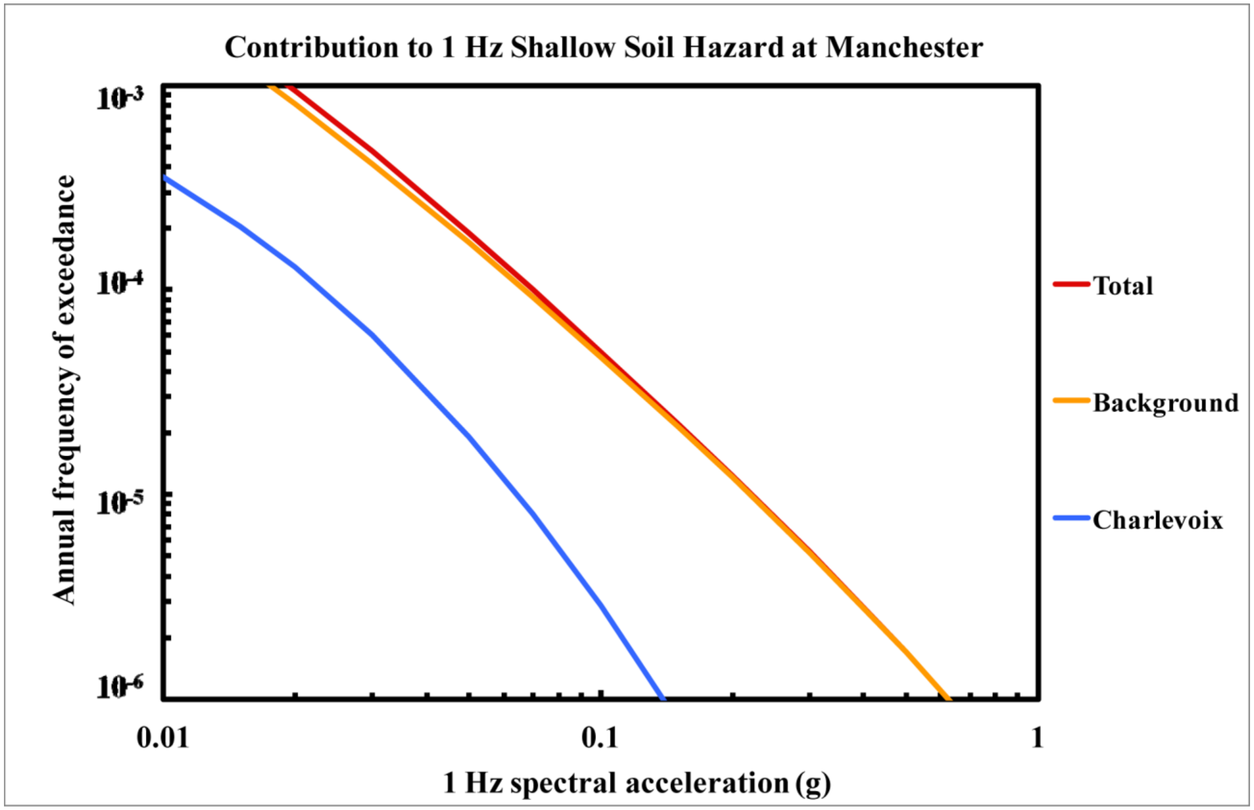

Figure 8.2-5n
Manchester 1 Hz shallow soil hazard: total and contribution by RLME and background

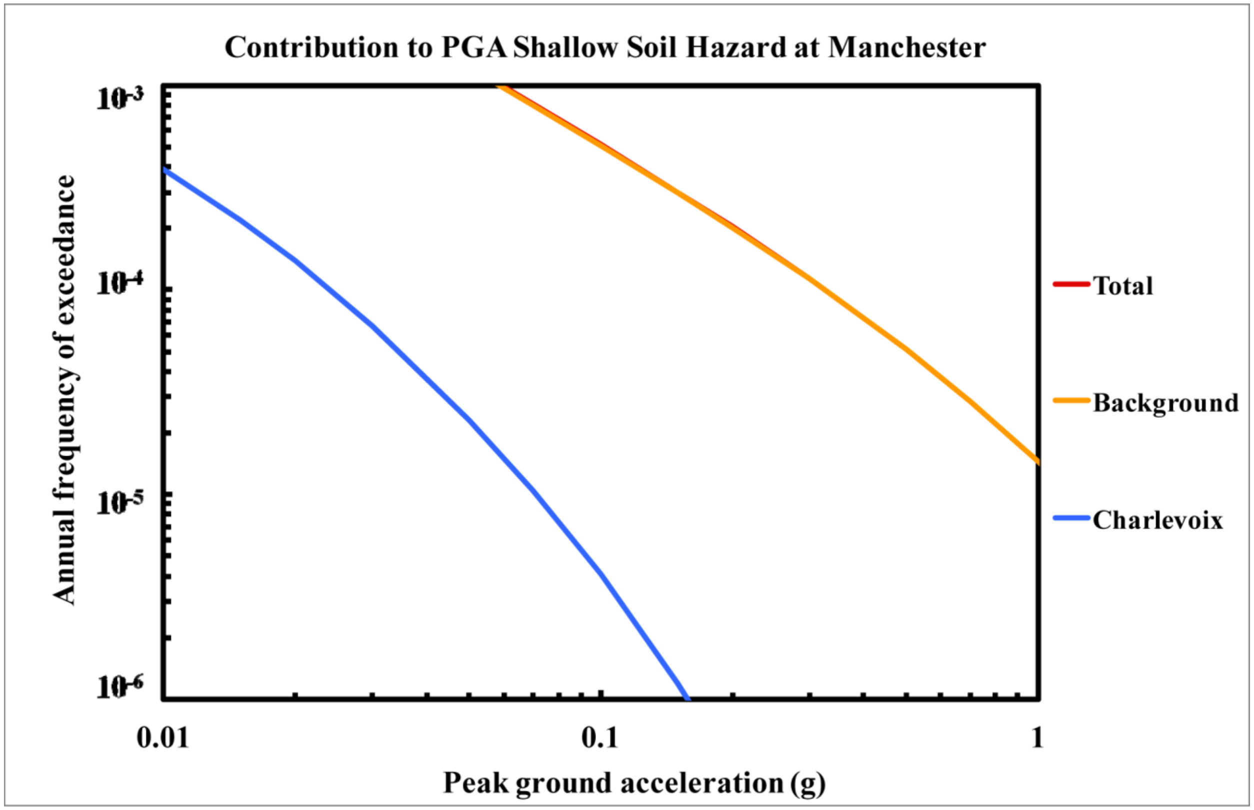

Figure 8.2-5o
Manchester PGA shallow soil hazard: total and contribution by RLME and background

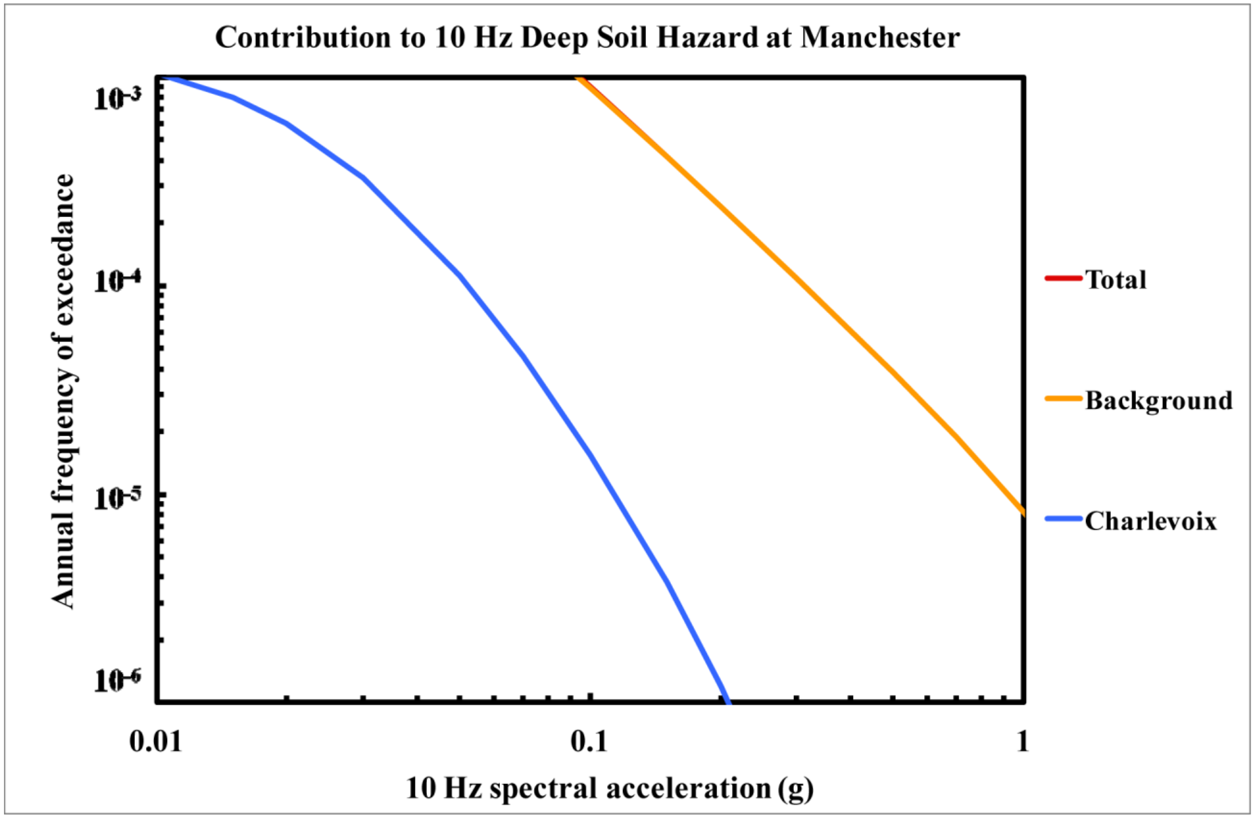

Figure 8.2-5p
Manchester 10 Hz deep soil hazard: total and contribution by RLME and background

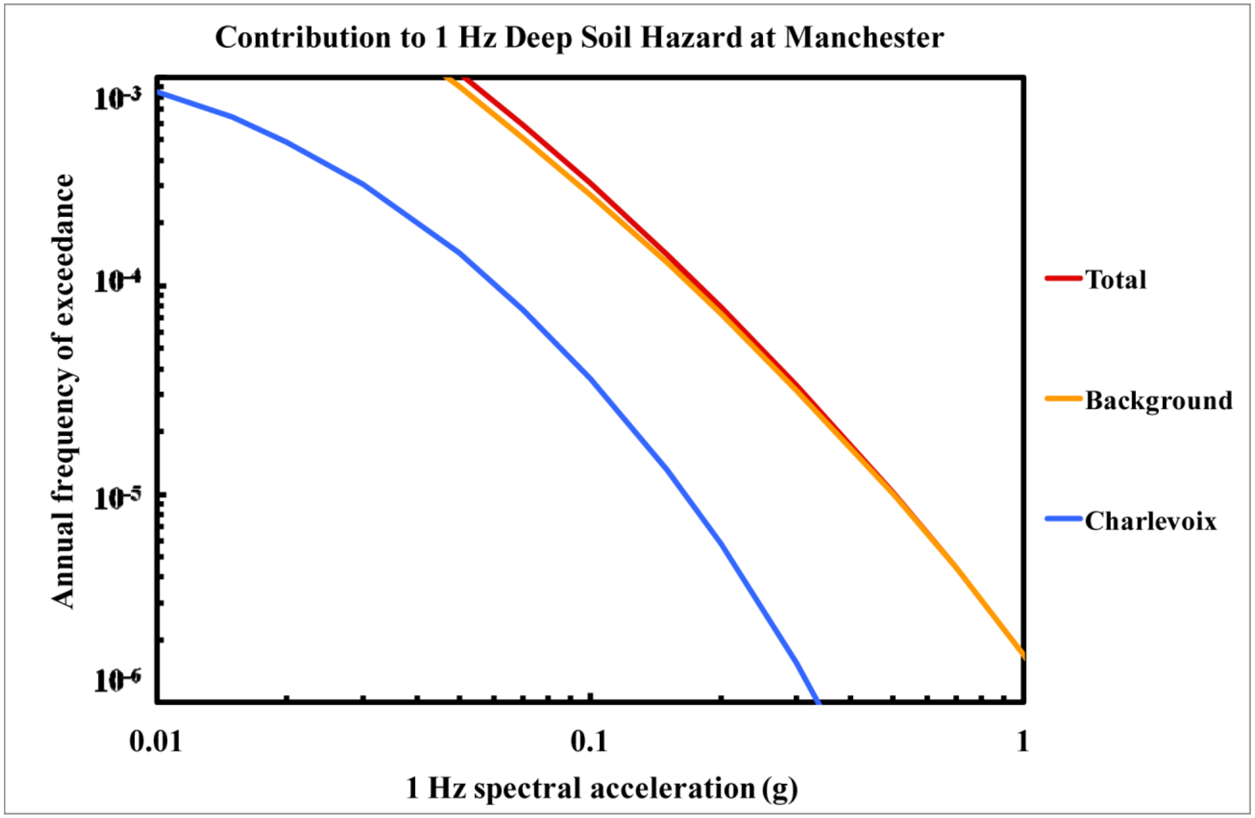

Figure 8.2-5q
Manchester 1 Hz deep soil hazard: total and contribution by RLME and background

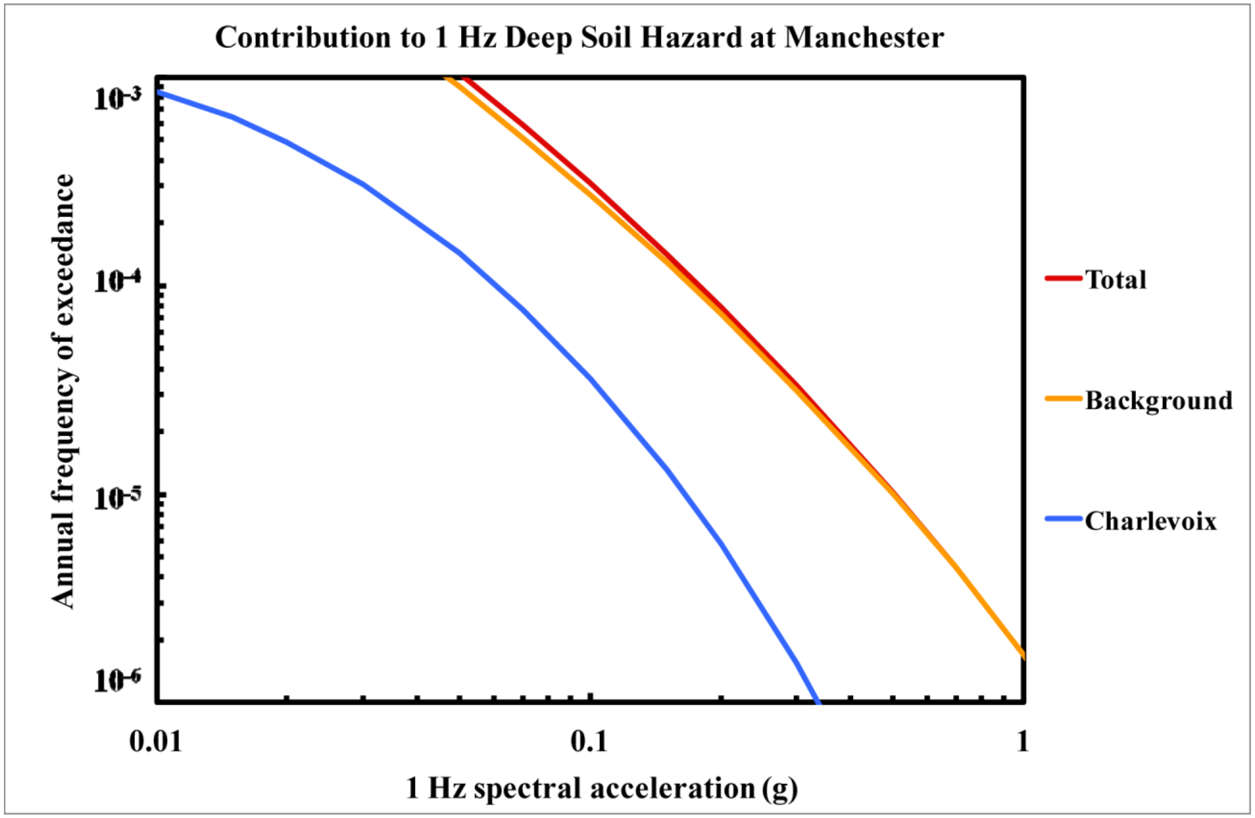

Figure 8.2-5r
Manchester PGA deep soil hazard: total and contribution by RLME and background

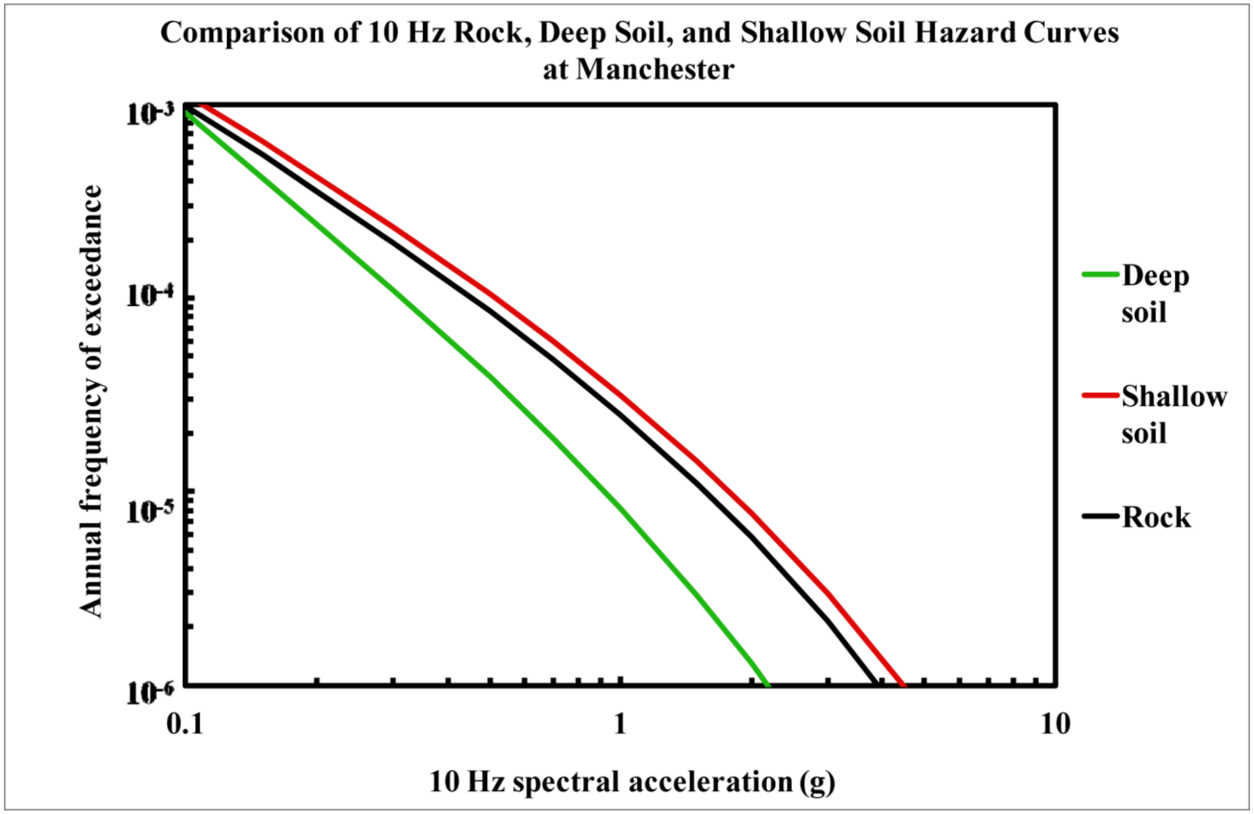

Figure 8.2-5s
Manchester 10 Hz hazard: comparison of three site conditions

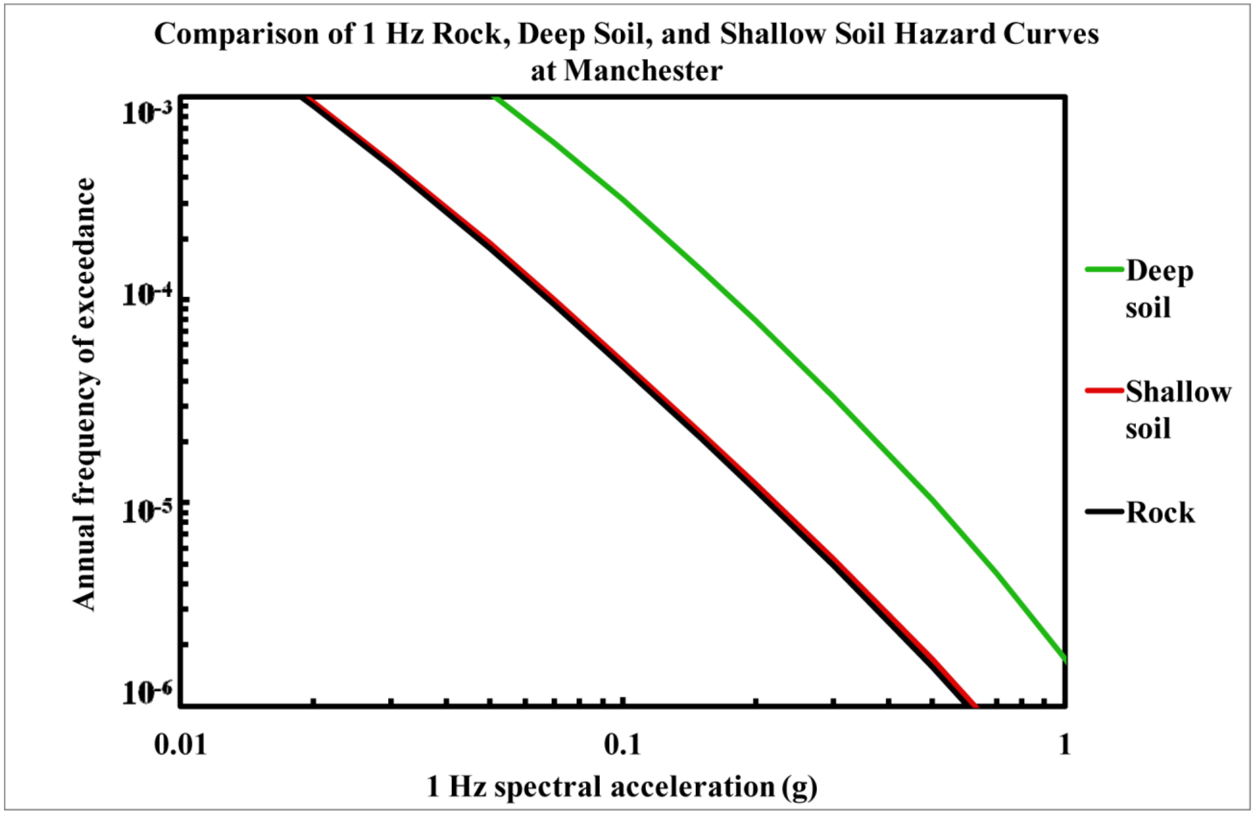

Figure 8.2-5t
Manchester 1 Hz hazard: comparison of three site conditions

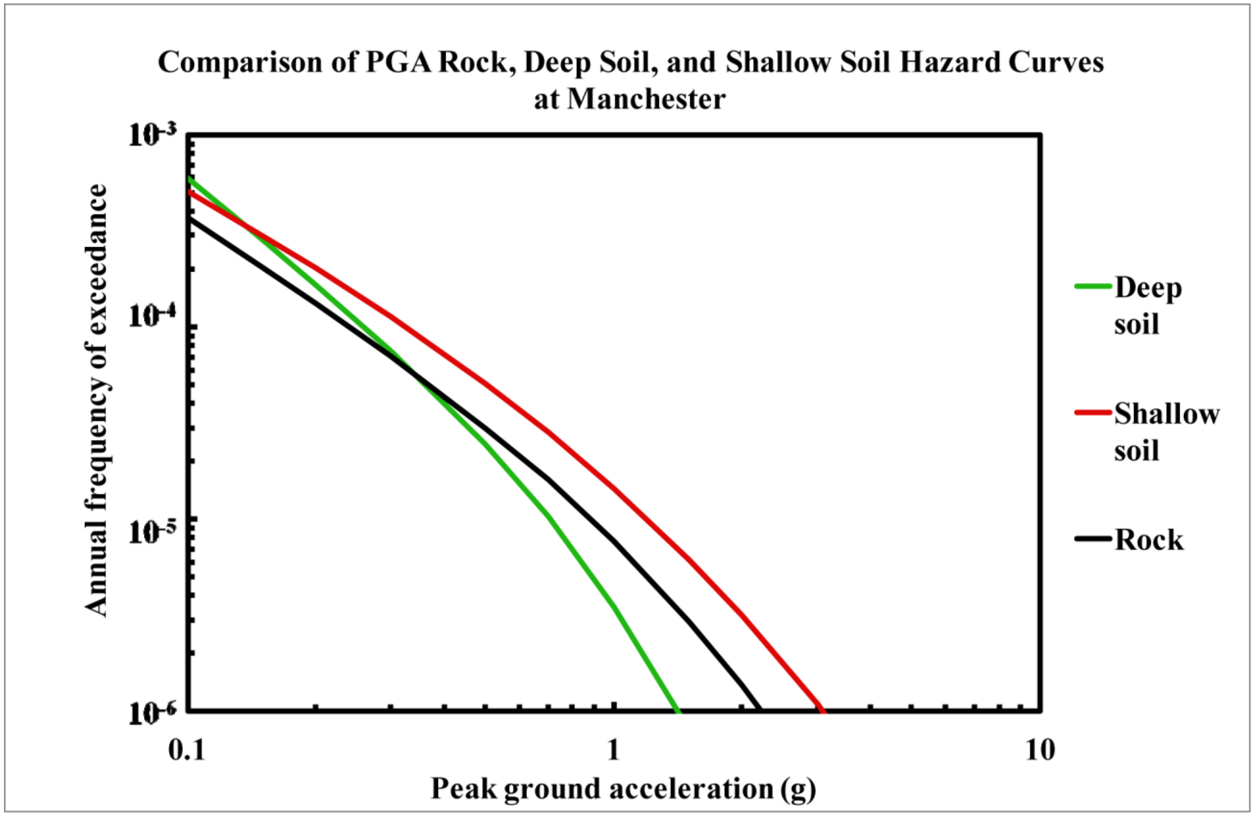

Figure 8.2-5u
Manchester PGA hazard: comparison of three site conditions

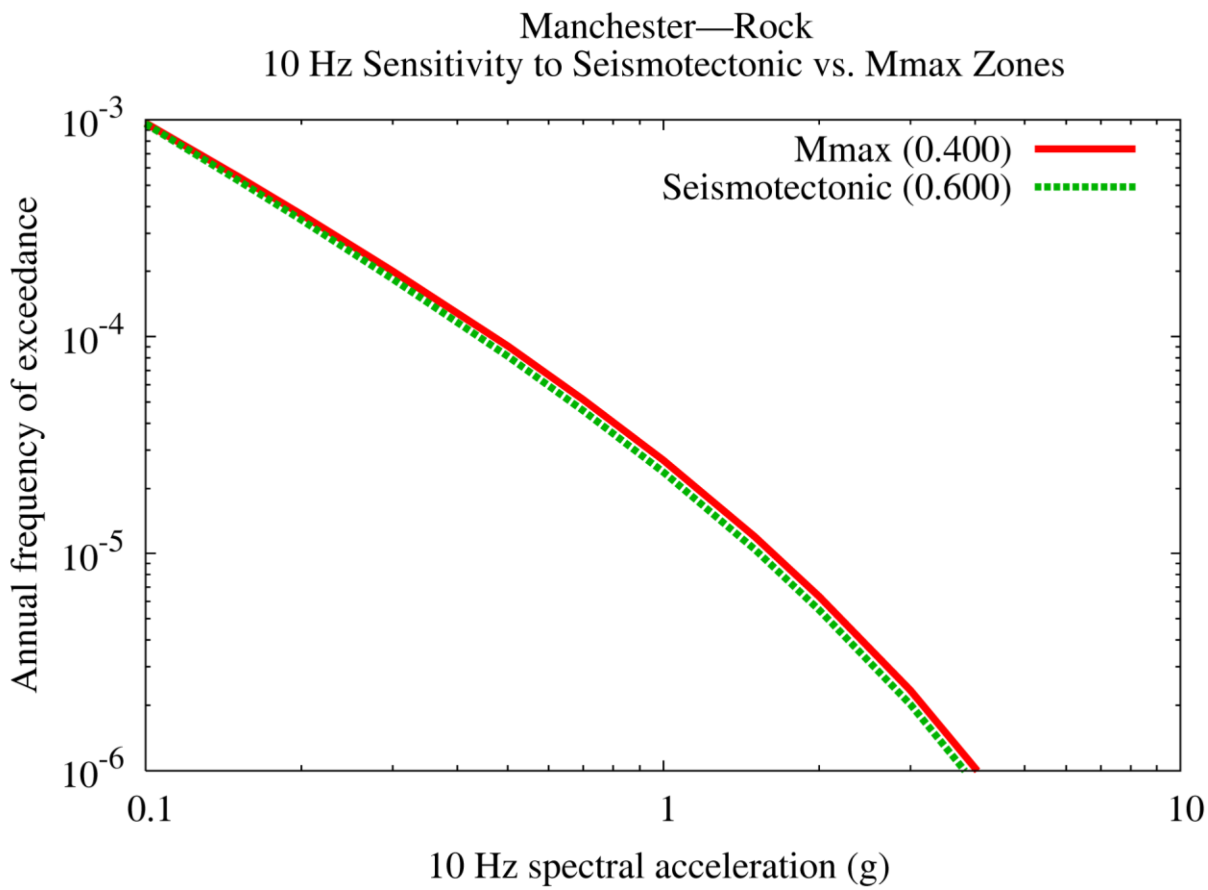

Figure 8.2-5v
Manchester 10 Hz rock hazard: sensitivity to seismotectonic vs. Mmax zones

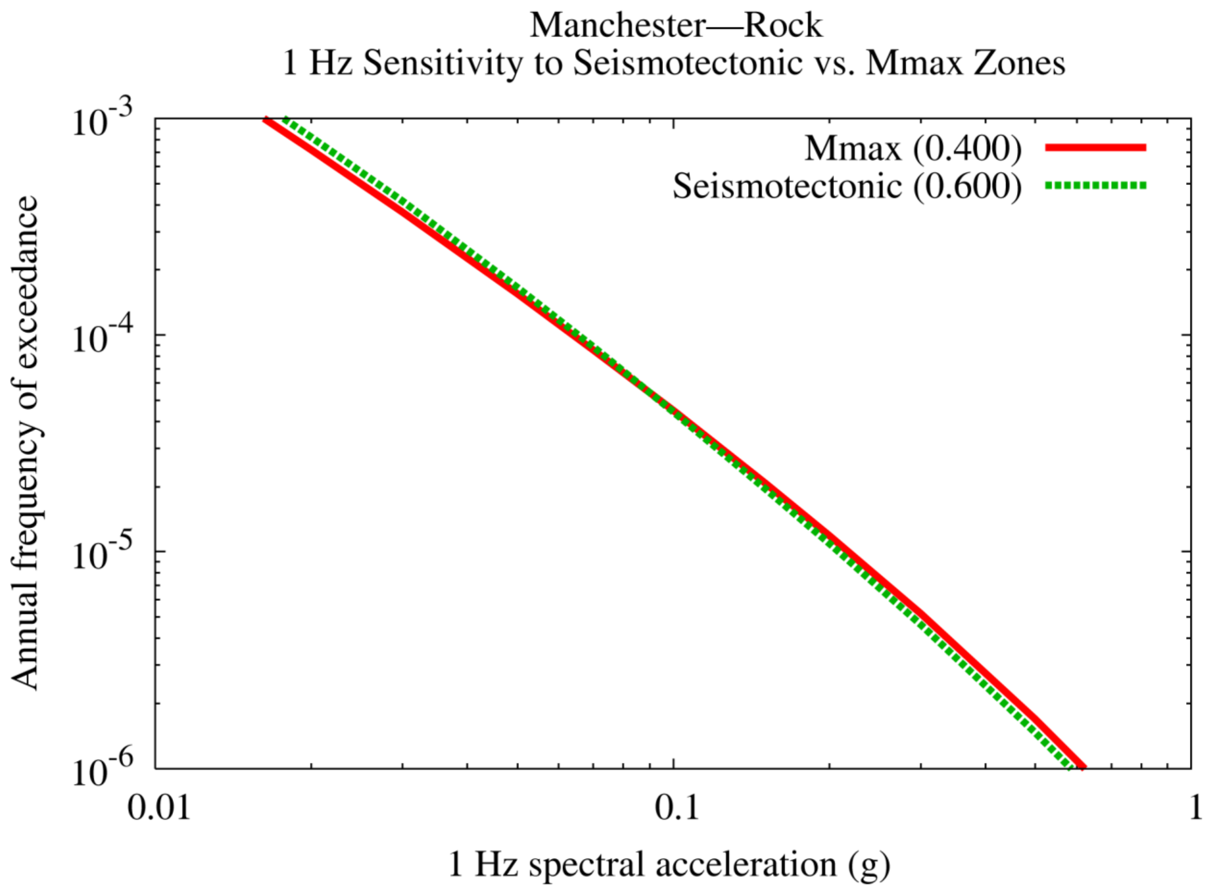

Figure 8.2-5w
Manchester 1 Hz rock hazard: sensitivity to seismotectonic vs. Mmax zones

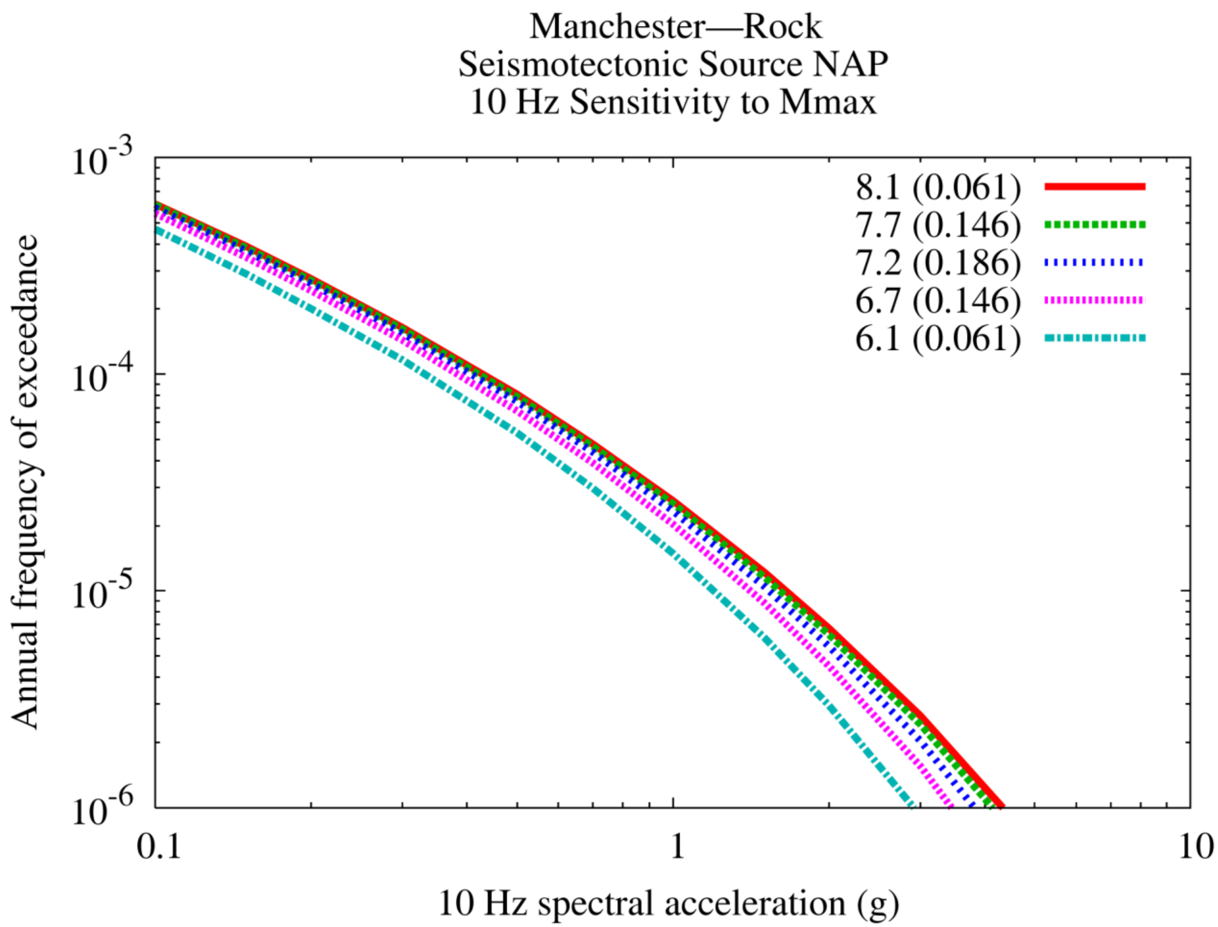

Figure 8.2-5x
Manchester 10 Hz rock hazard: sensitivity to Mmax for source NAP

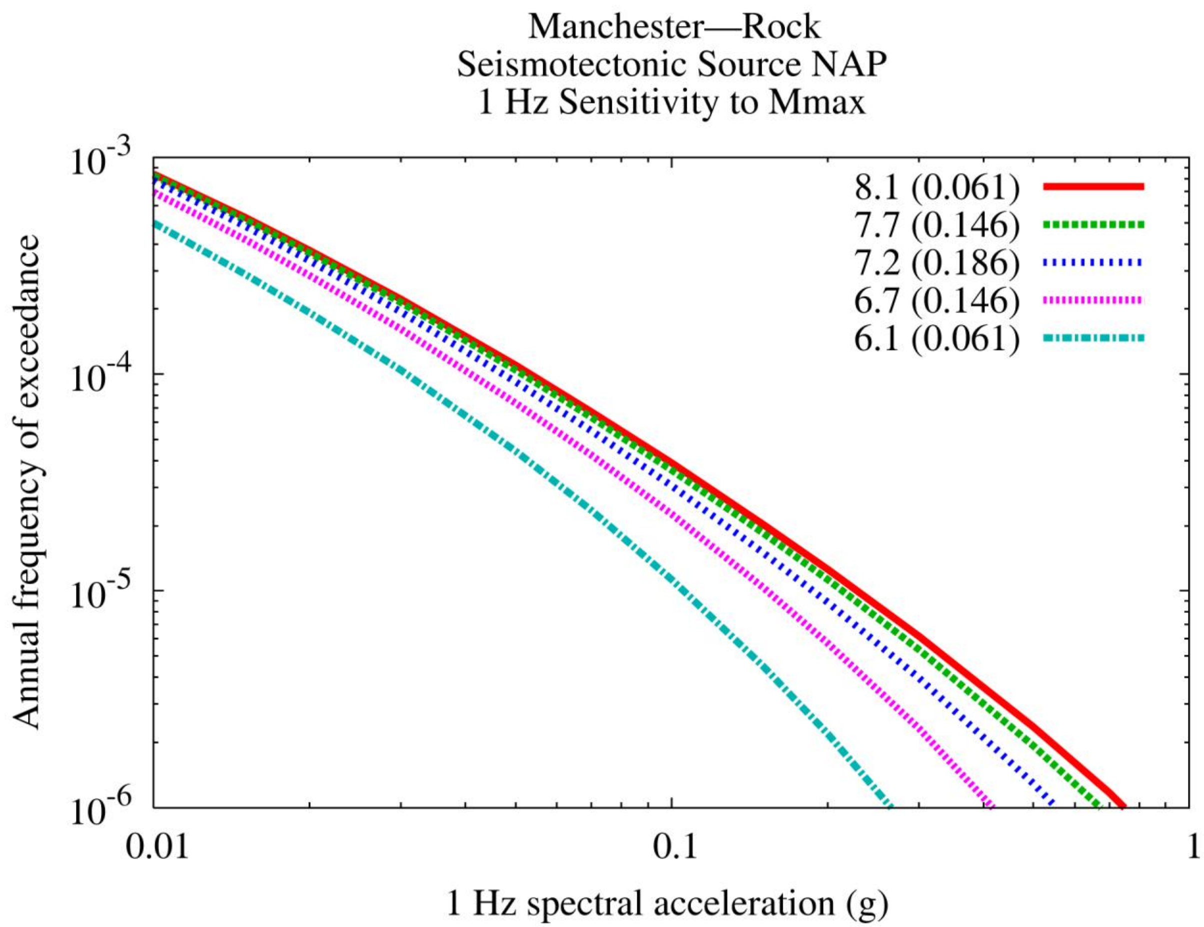

Figure 8.2-5y
Manchester 1 Hz rock hazard: sensitivity to Mmax for source NAP

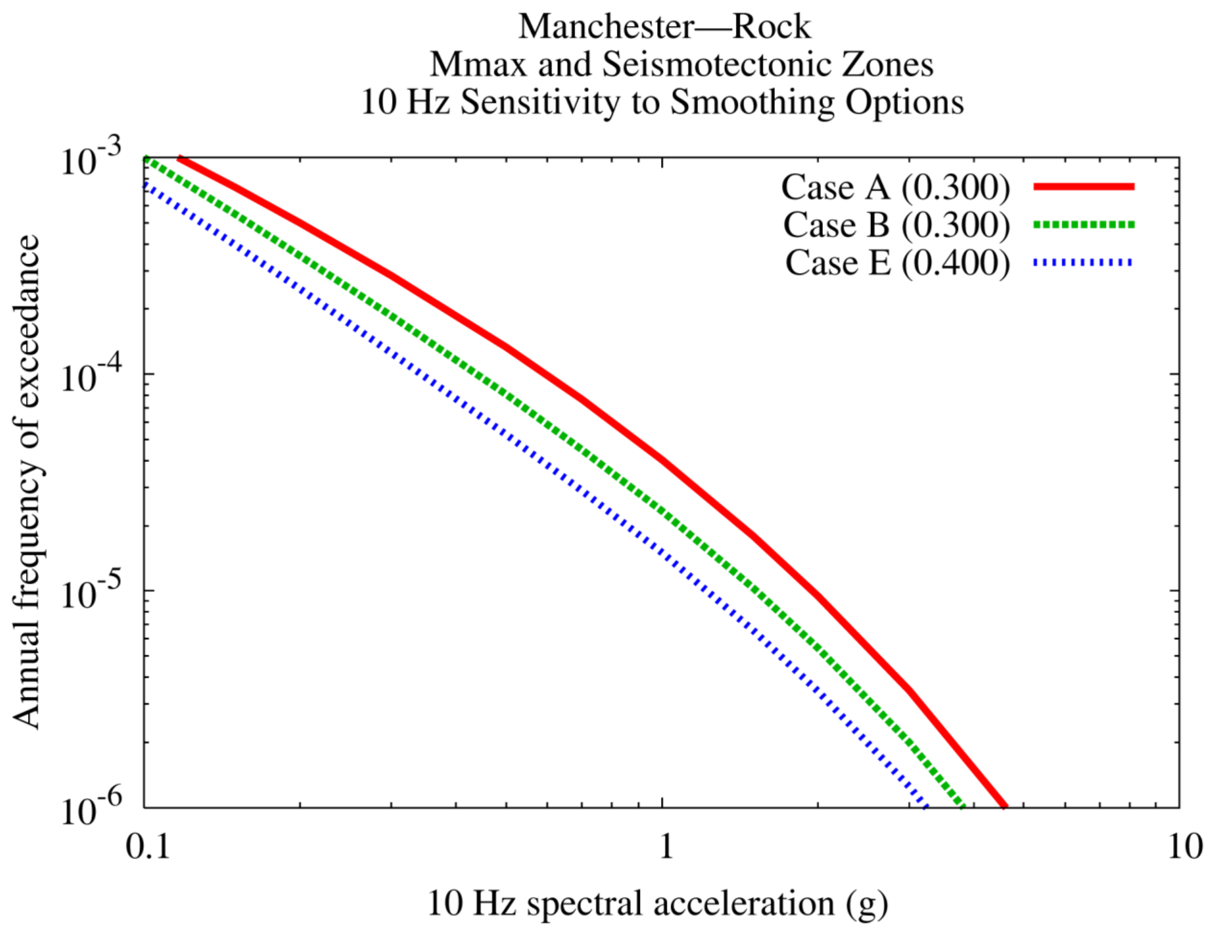

Figure 8.2-5z
Manchester 10 Hz rock hazard: sensitivity to smoothing options

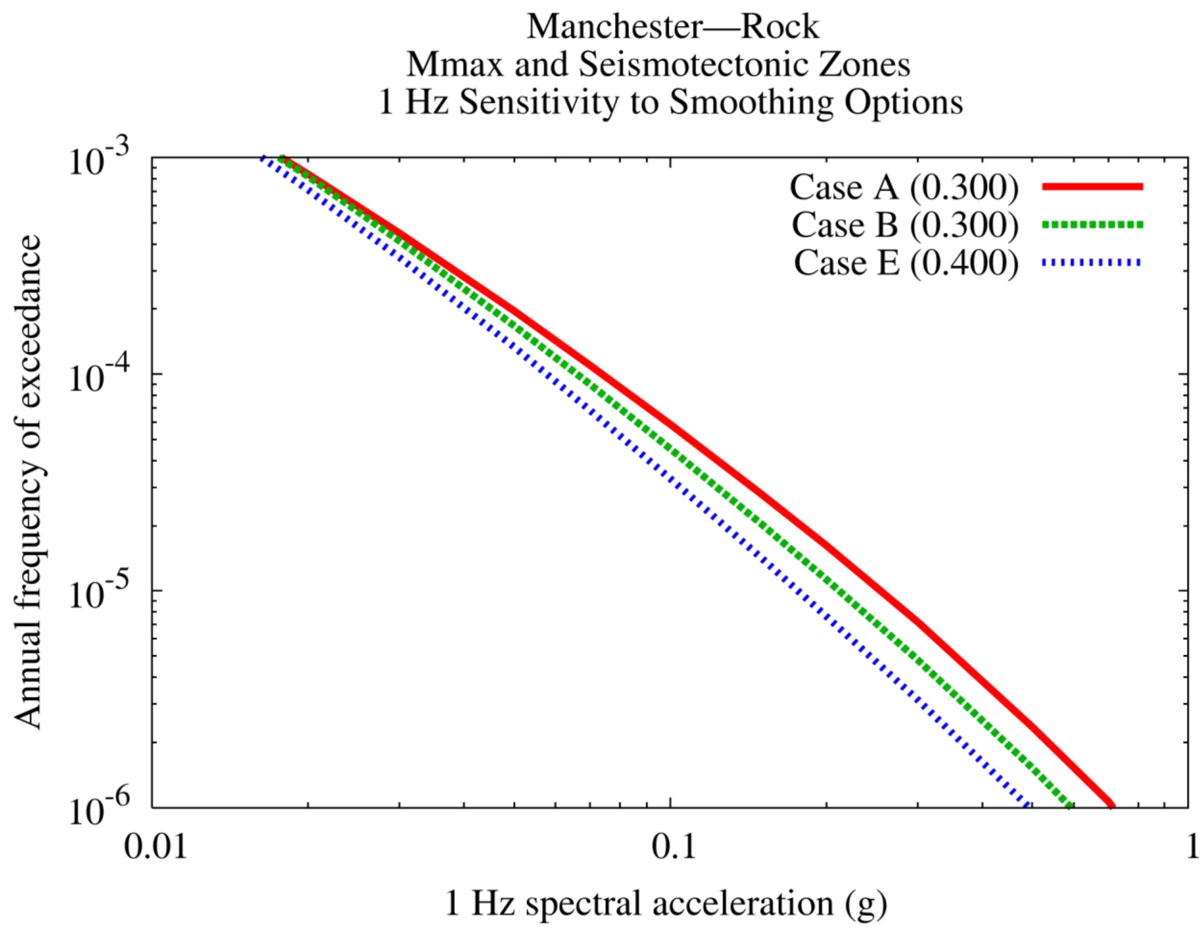

Figure 8.2-5aa
Manchester 1 Hz rock hazard: sensitivity to smoothing options

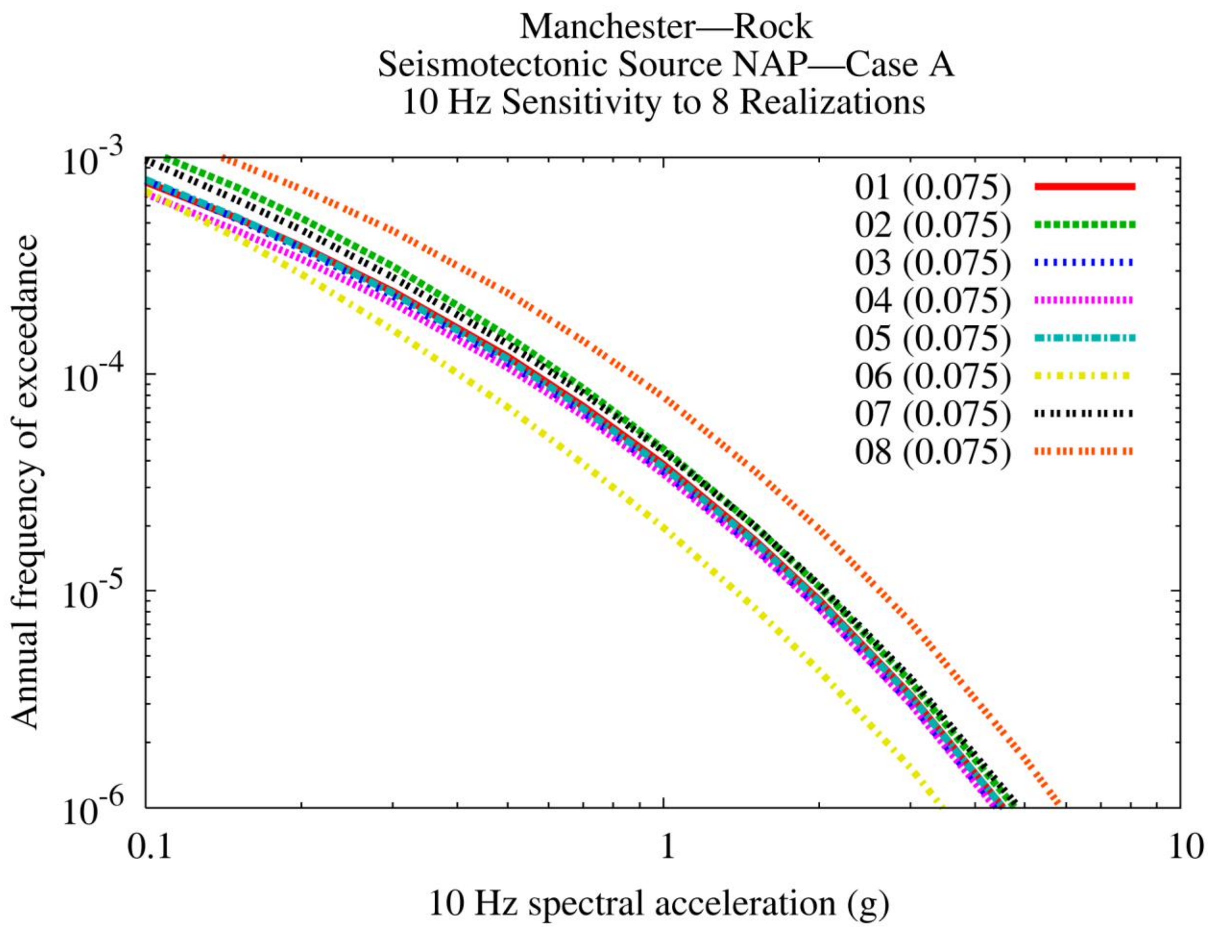

Figure 8.2-5bb
Manchester 10 Hz rock hazard: sensitivity to eight realizations for source NAP, Case A

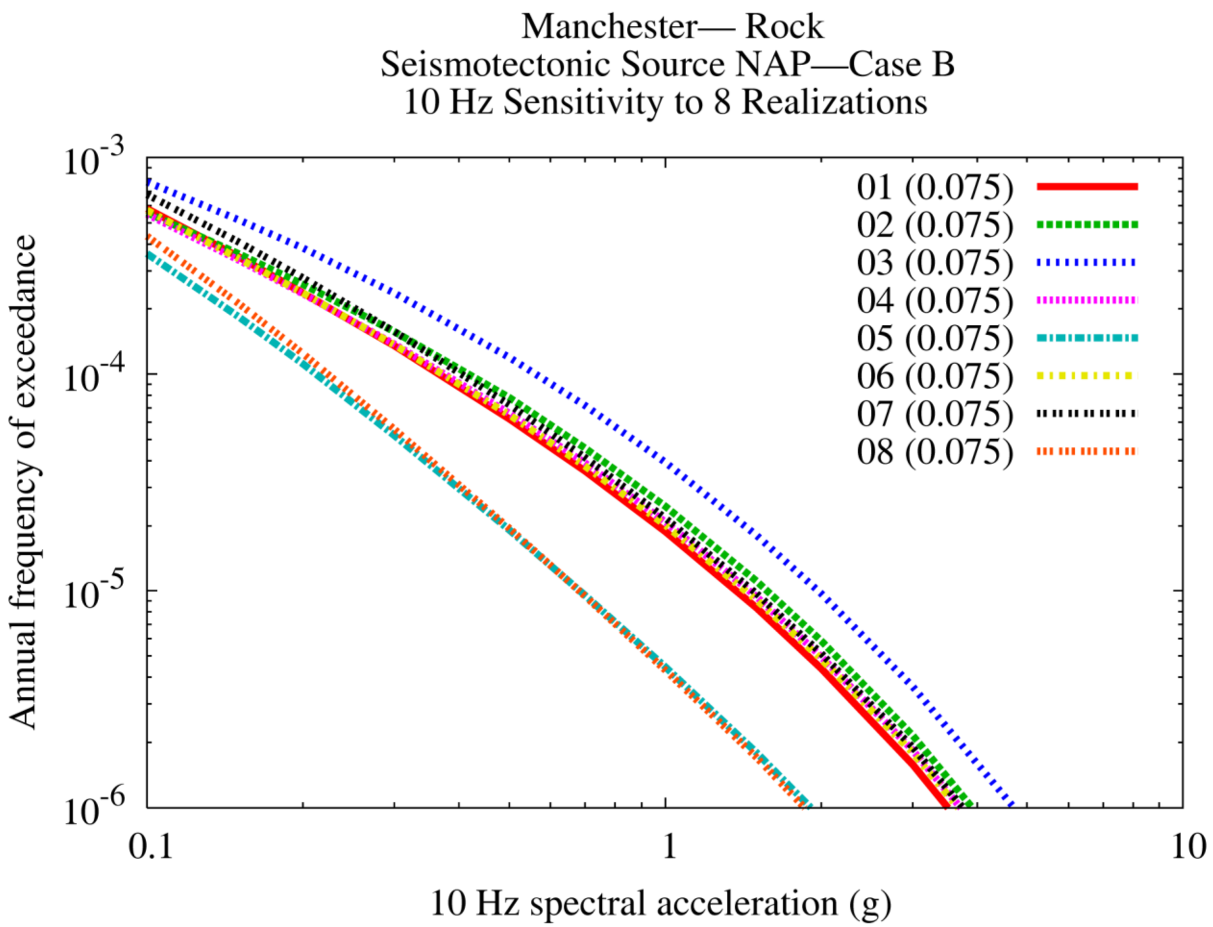

Figure 8.2-5cc
Manchester 10 Hz rock hazard: sensitivity to eight realizations for source NAP, Case B

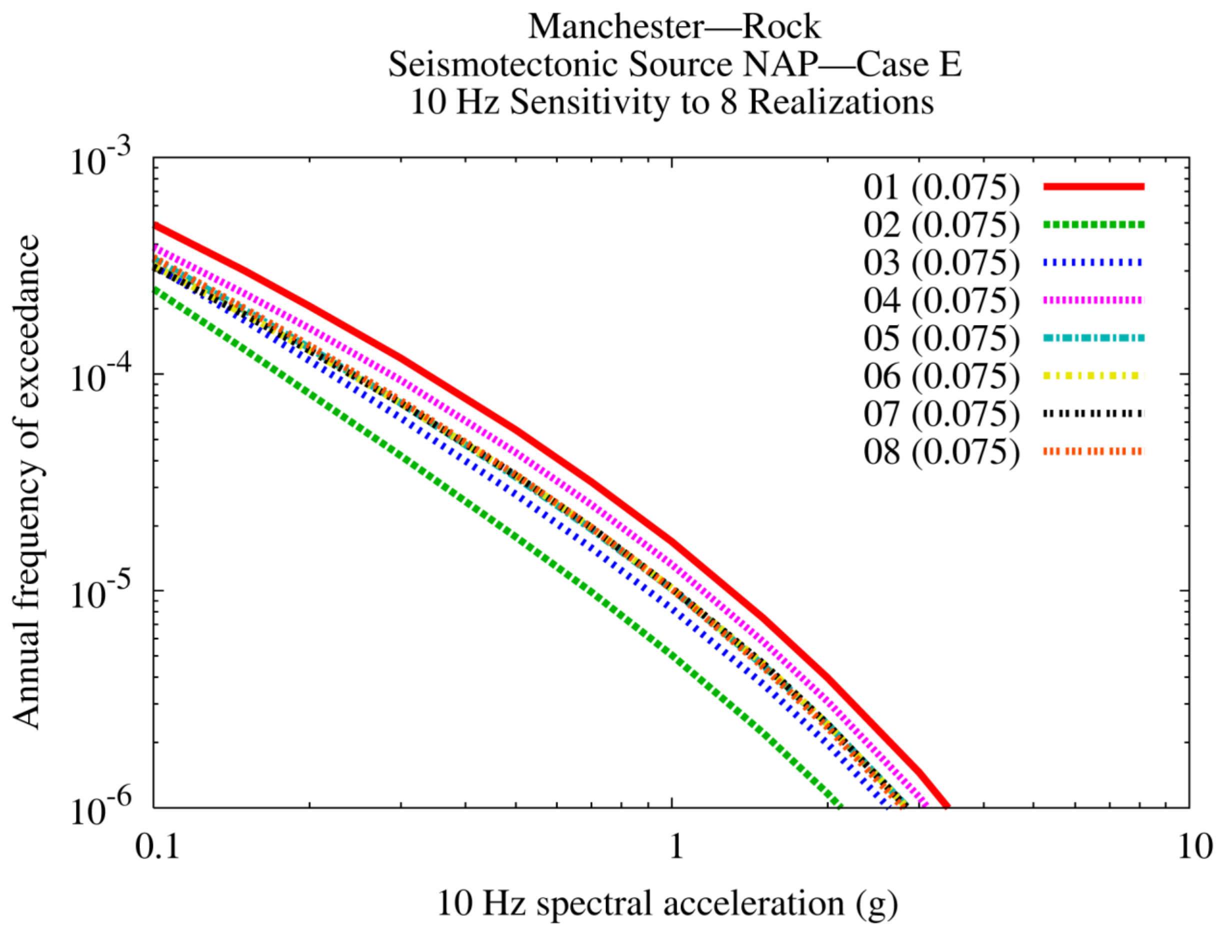

Figure 8.2-5dd
Manchester 10 Hz rock hazard: sensitivity to eight realizations for source NAP, Case E

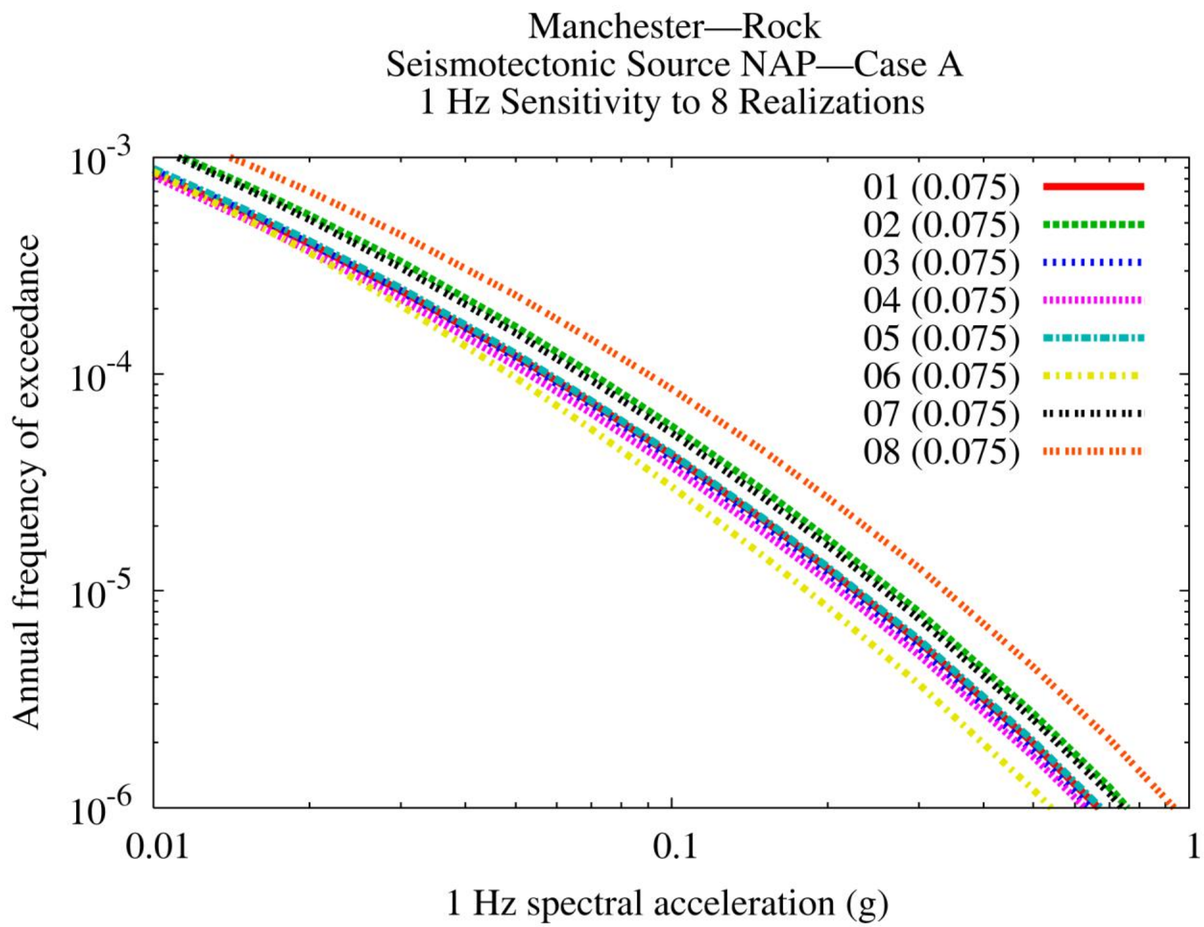

Figure 8.2-5ee
Manchester 1 Hz rock hazard: sensitivity to eight realizations for source NAP, Case A

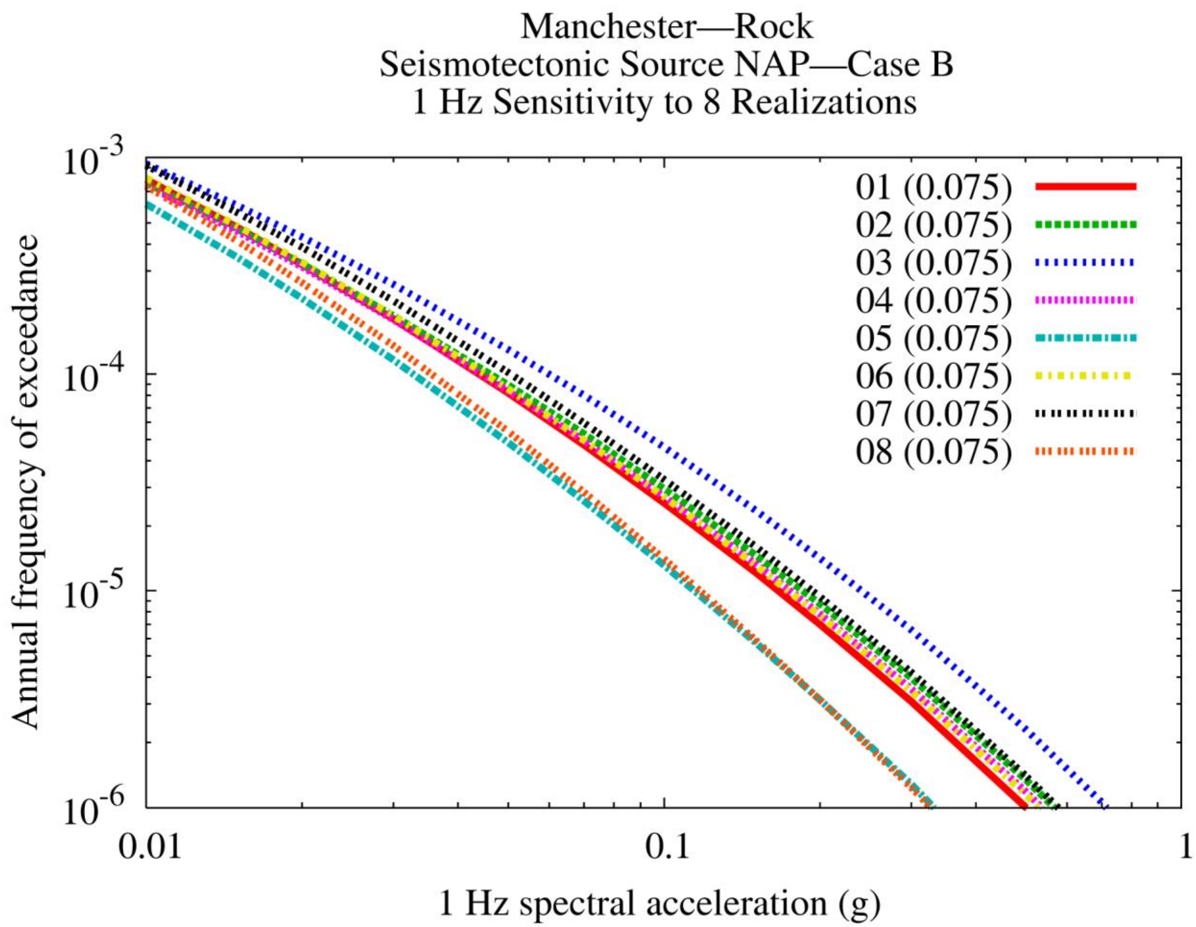

Figure 8.2-5ff
Manchester 1 Hz rock hazard: sensitivity to eight realizations for source NAP, Case B

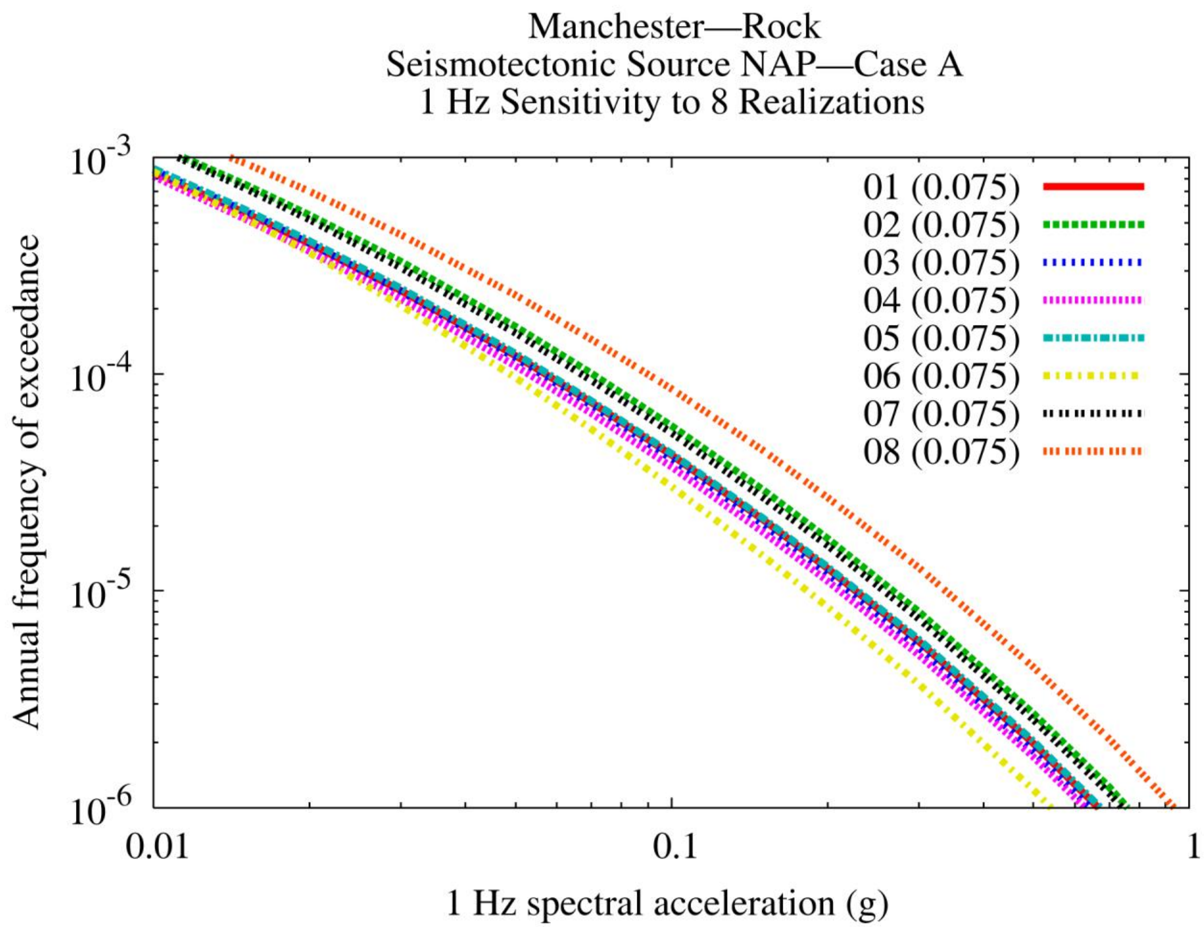

Figure 8.2-5gg
Manchester 1 Hz rock hazard: sensitivity to eight realizations for source NAP, Case E

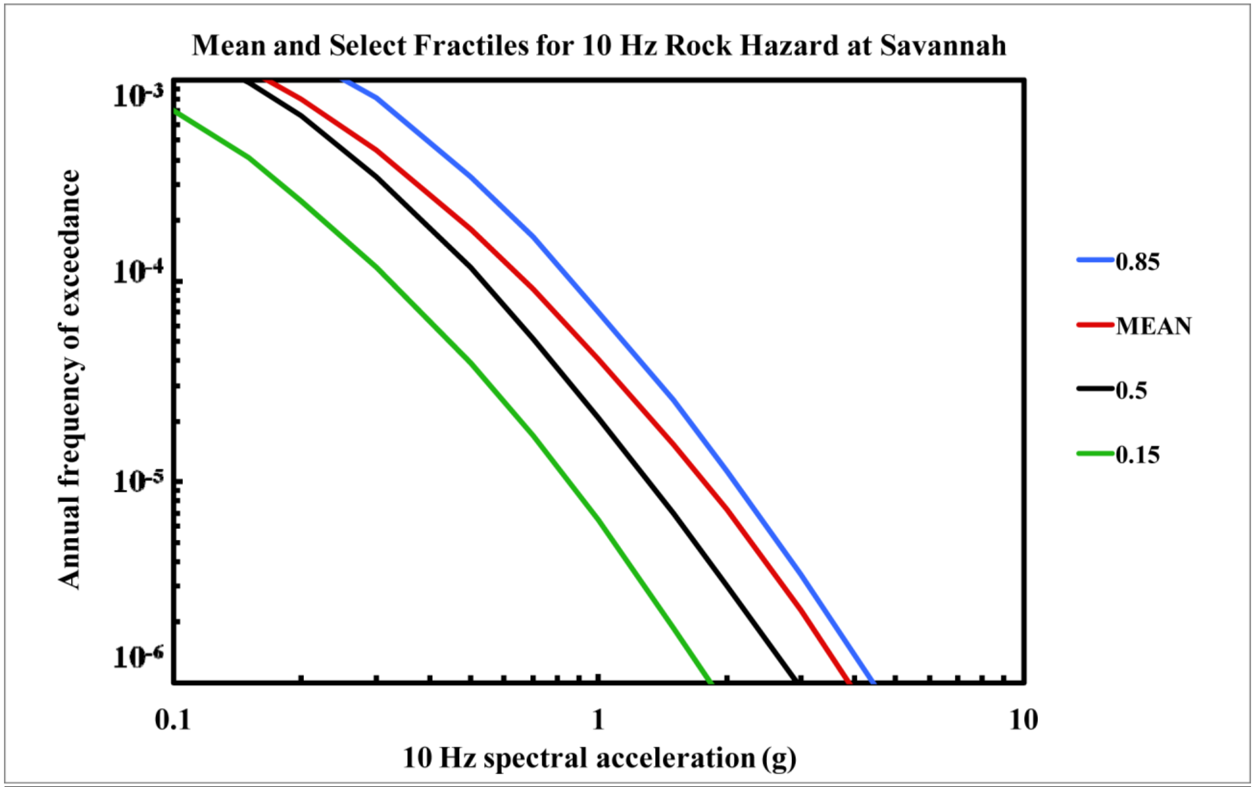

Figure 8.2-6a
Savannah 10 Hz rock hazard: mean and fractile total hazard

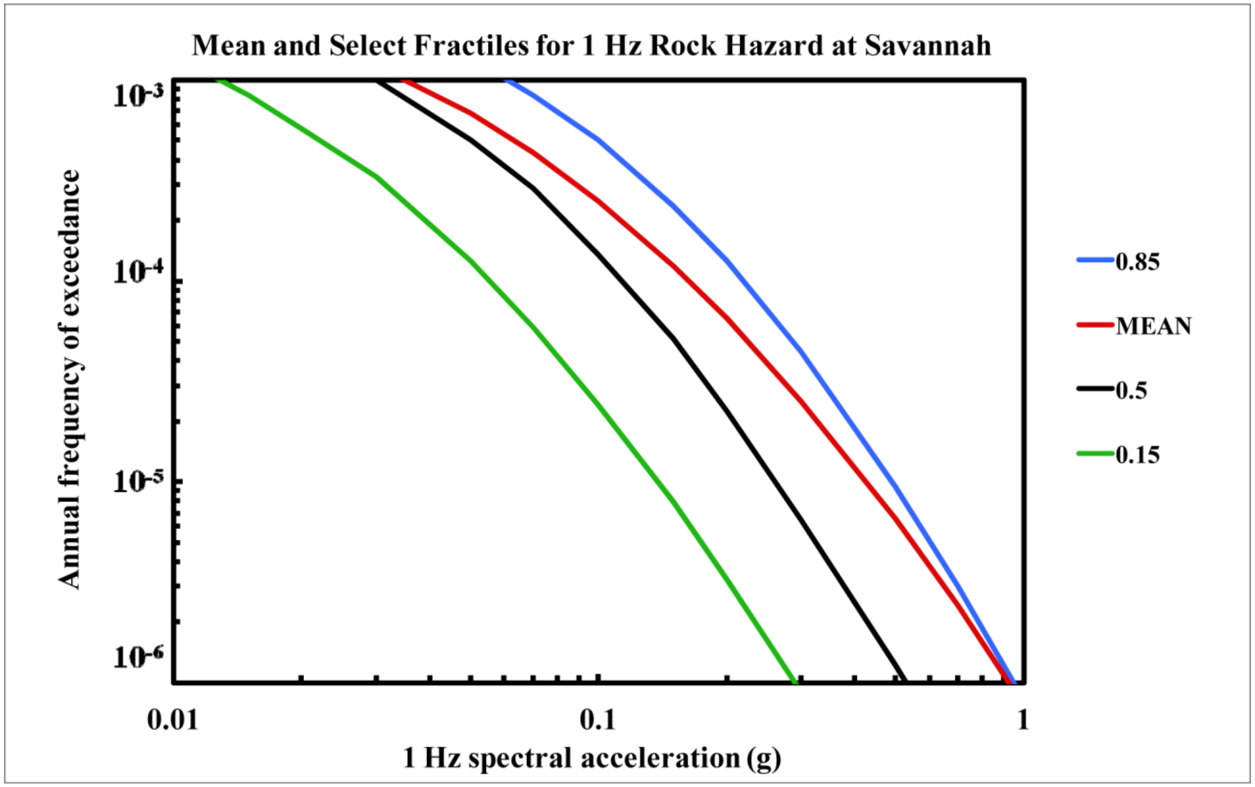

Figure 8.2-6b
Savannah 1 Hz rock hazard: mean and fractile total hazard

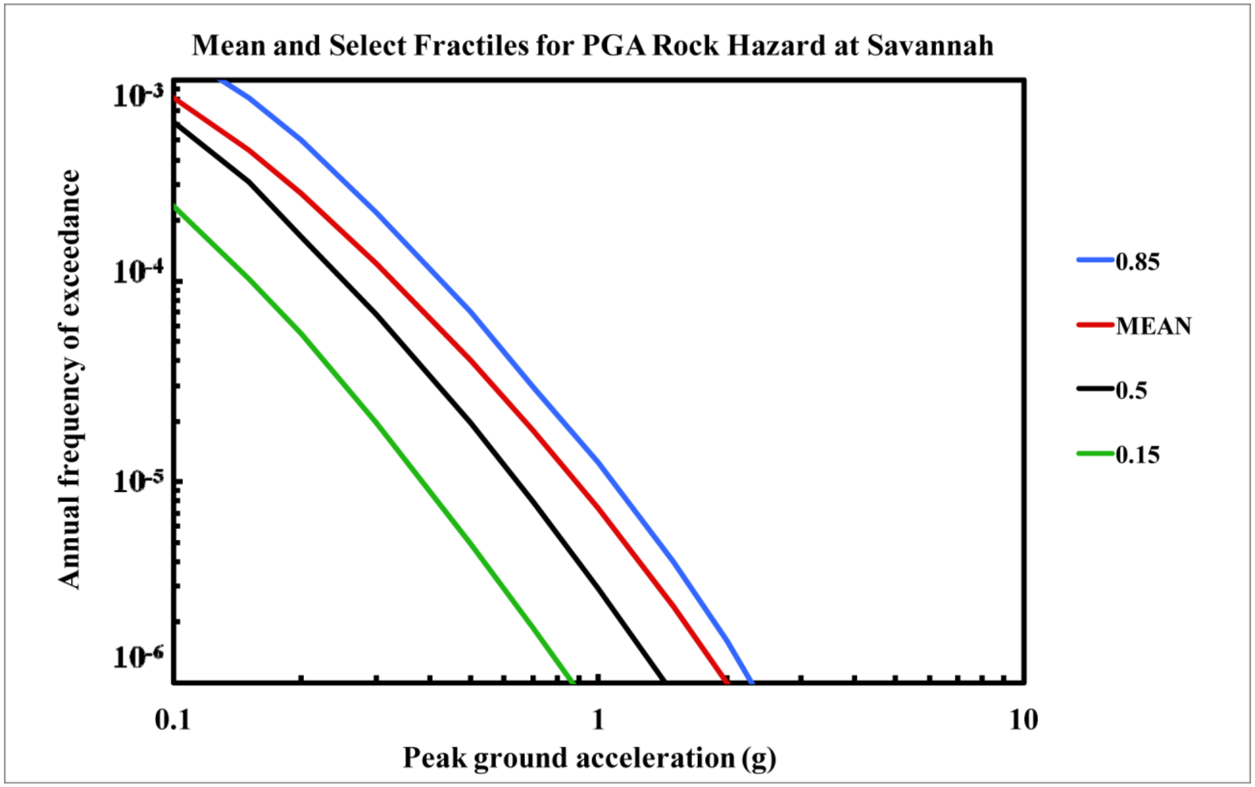

Figure 8.2-6c
Savannah PGA rock hazard: mean and fractile total hazard

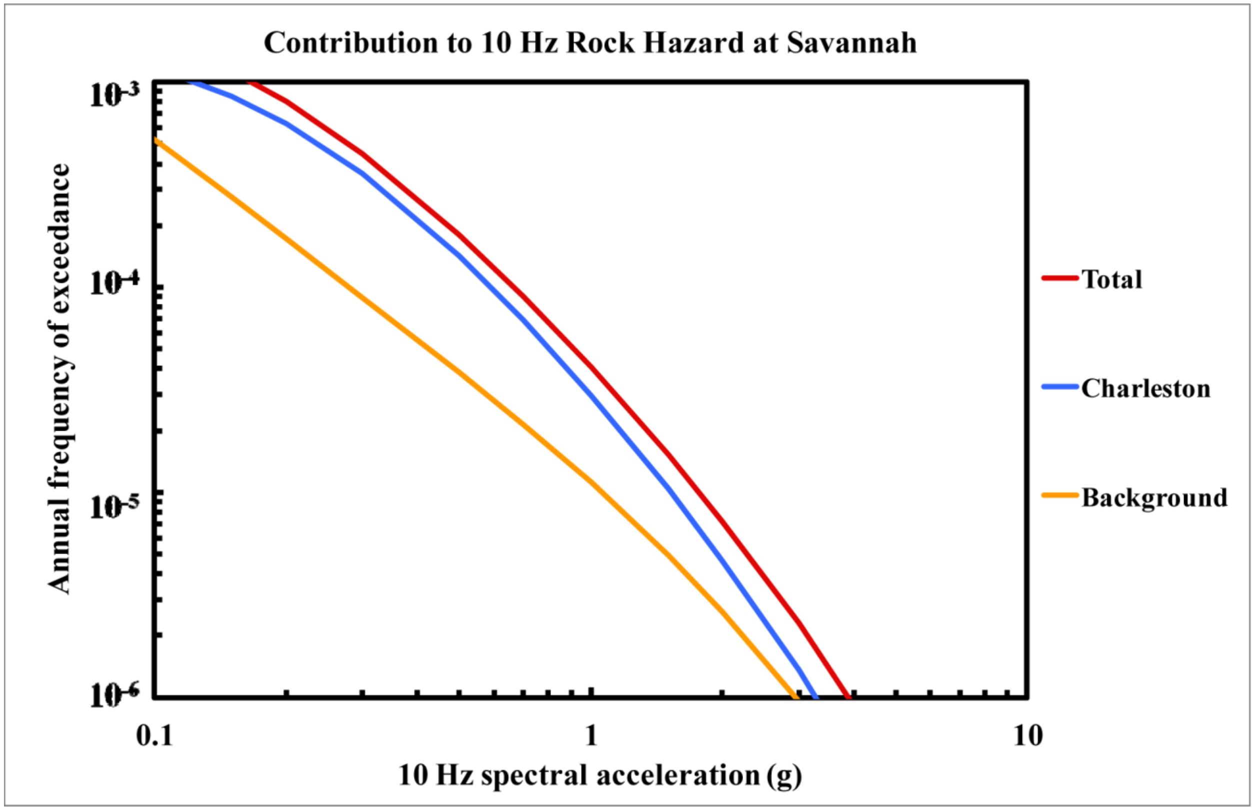

Figure 8.2-6d
Savannah 10 Hz rock hazard: total and contribution by RLME and background

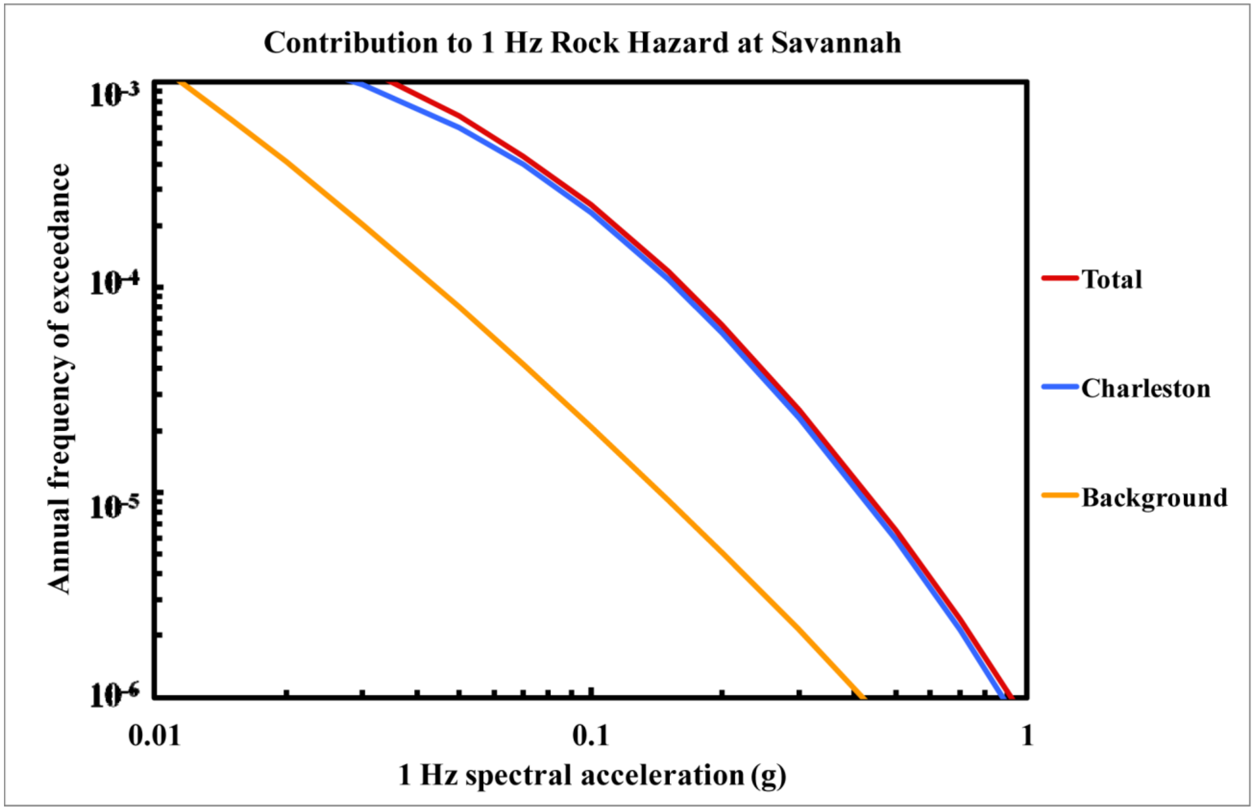

Figure 8.2-6e
Savannah 1 Hz rock hazard: total and contribution by RLME and background

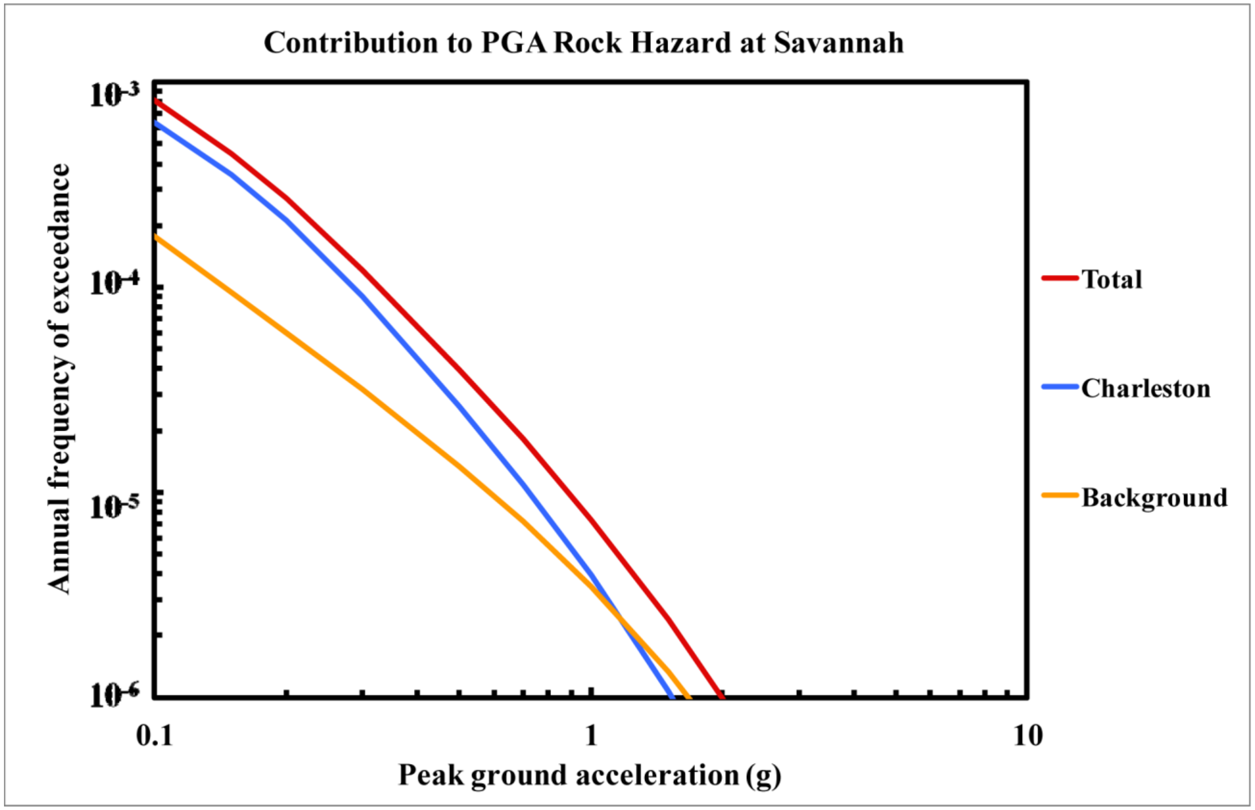

Figure 8.2-6f
Savannah PGA rock hazard: total and contribution by RLME and background

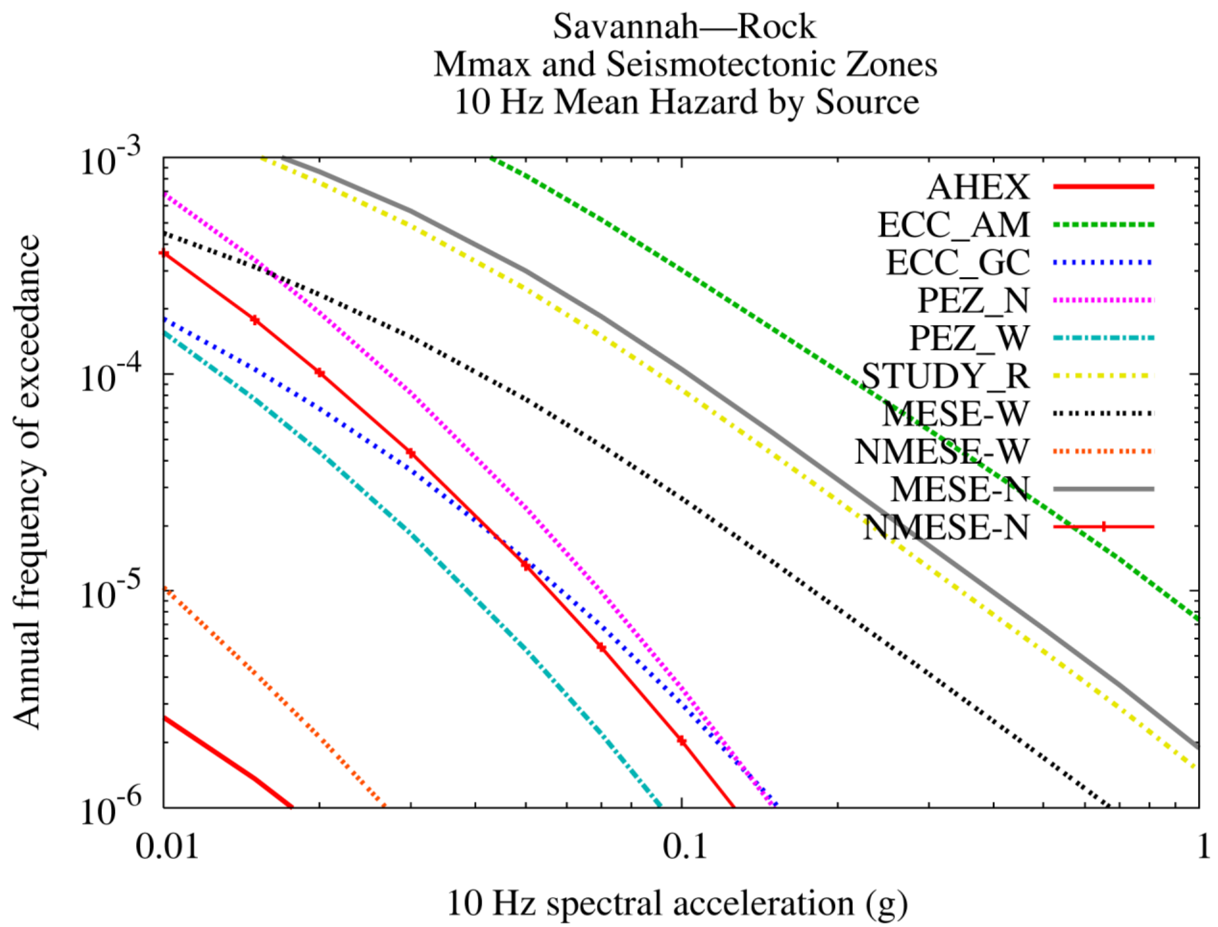

Figure 8.2-6g
Savannah 10 Hz rock hazard: contribution by background source

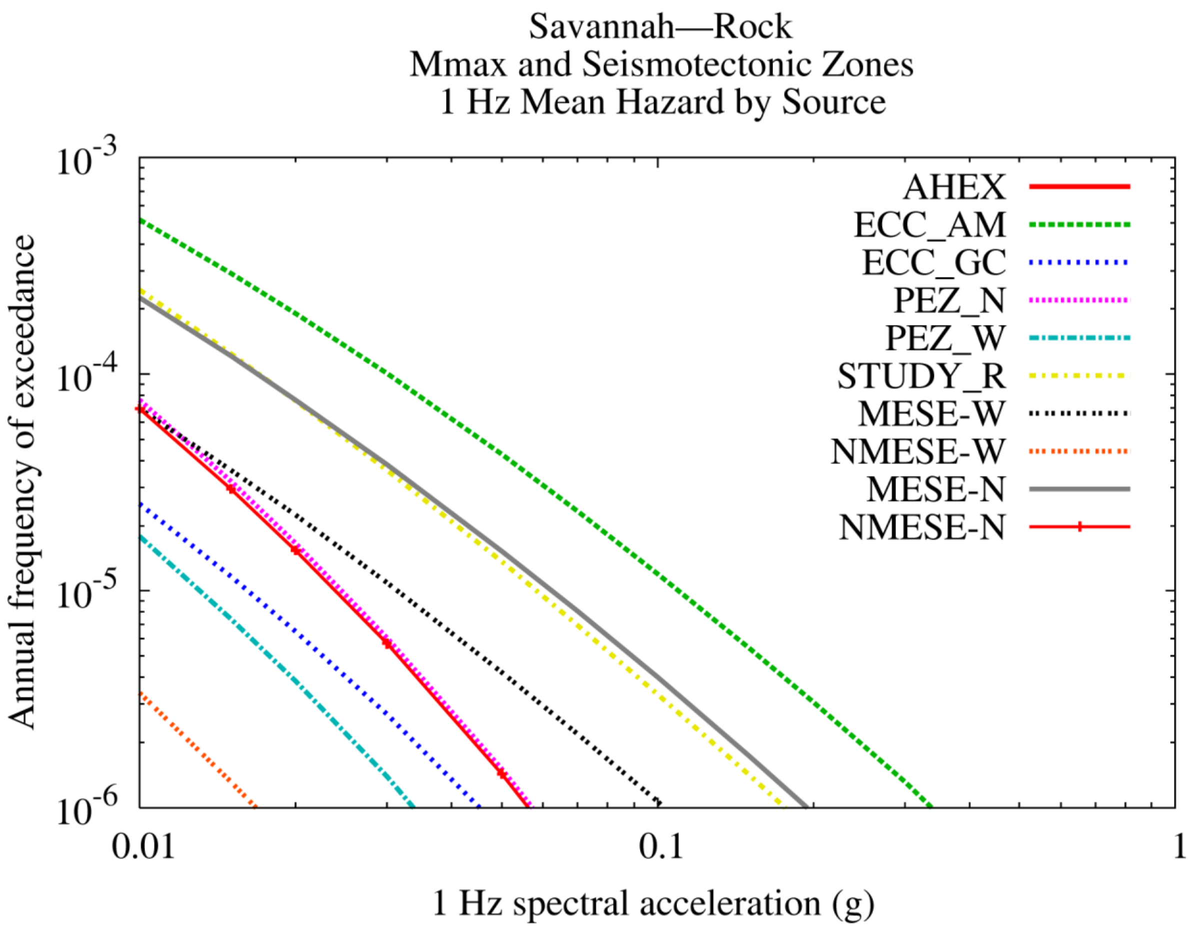

Figure 8.2-6h
Savannah 1 Hz rock hazard: contribution by background source

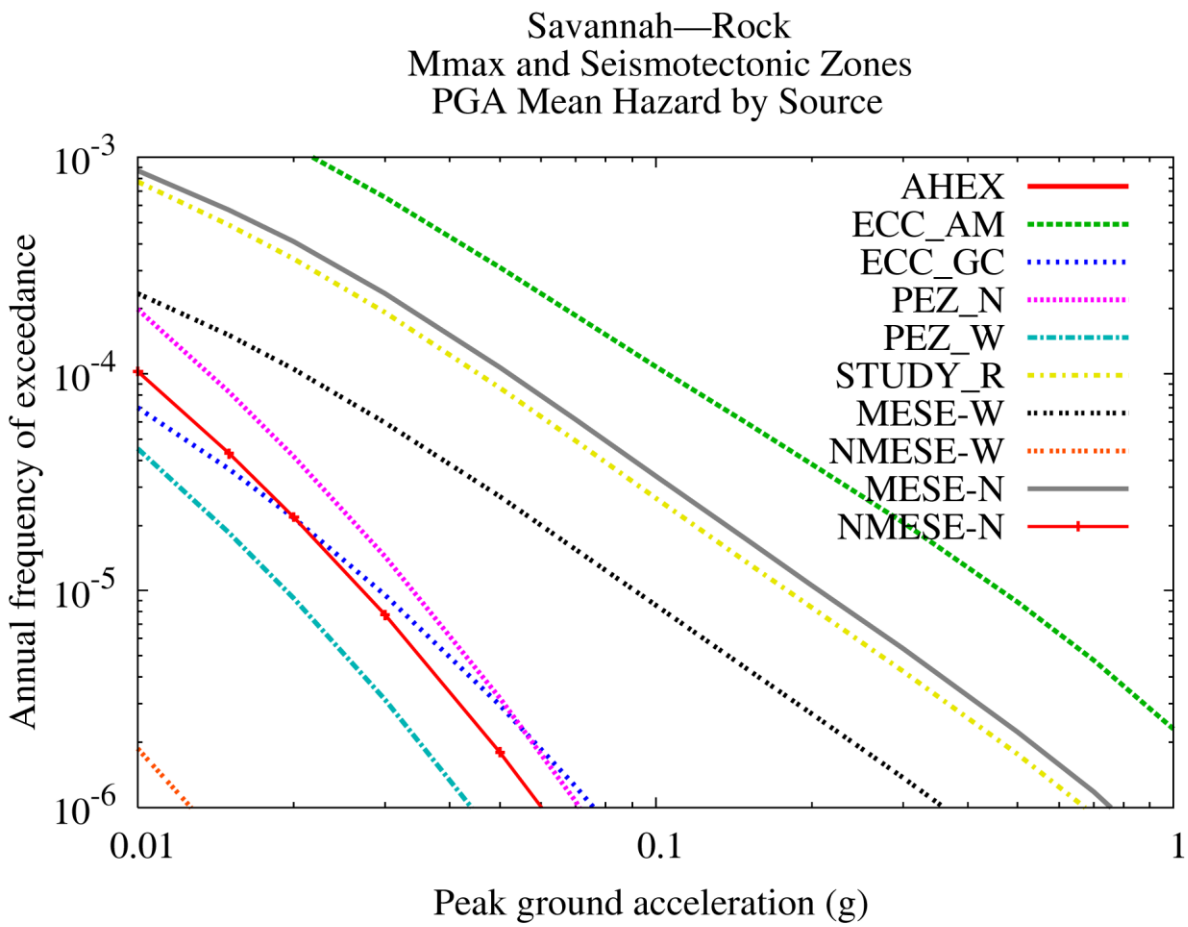

Figure 8.2-6i
Savannah PGA rock hazard: contribution by background source

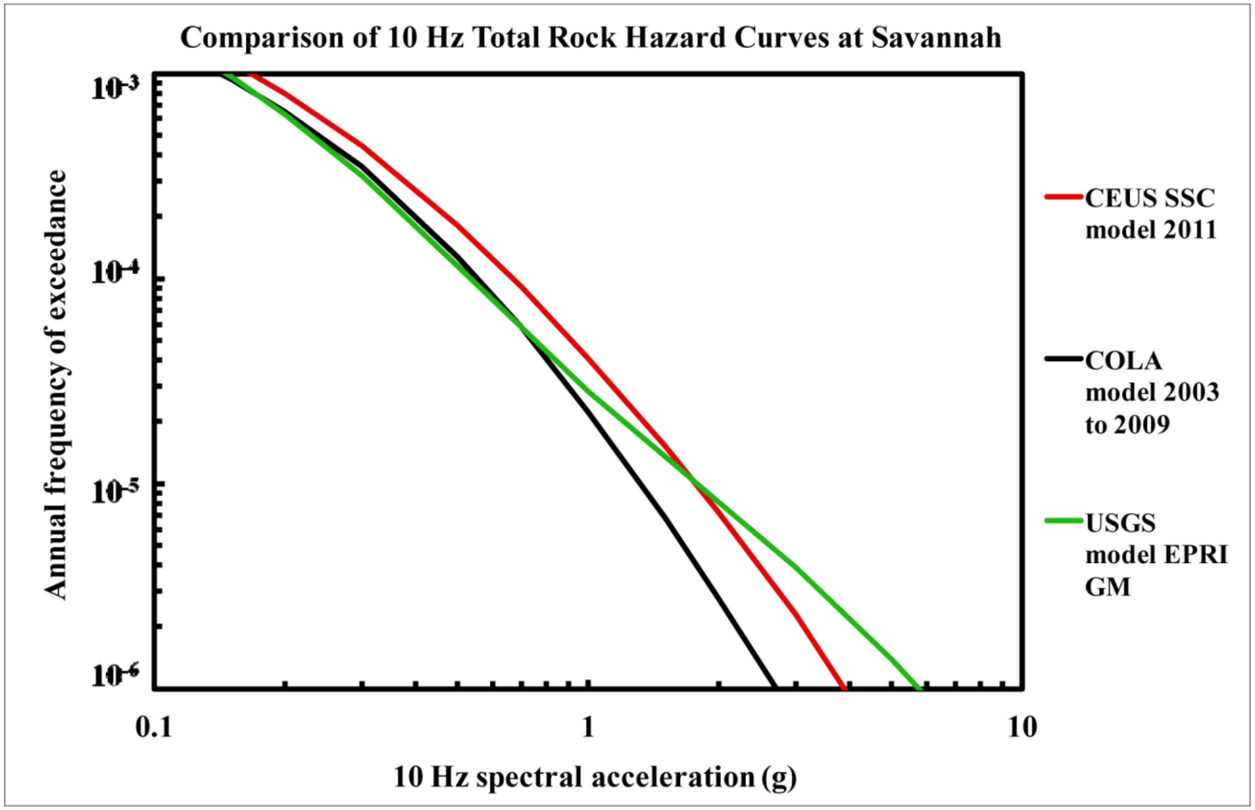

Figure 8.2-6j
Savannah 10 Hz rock hazard: comparison of three source models

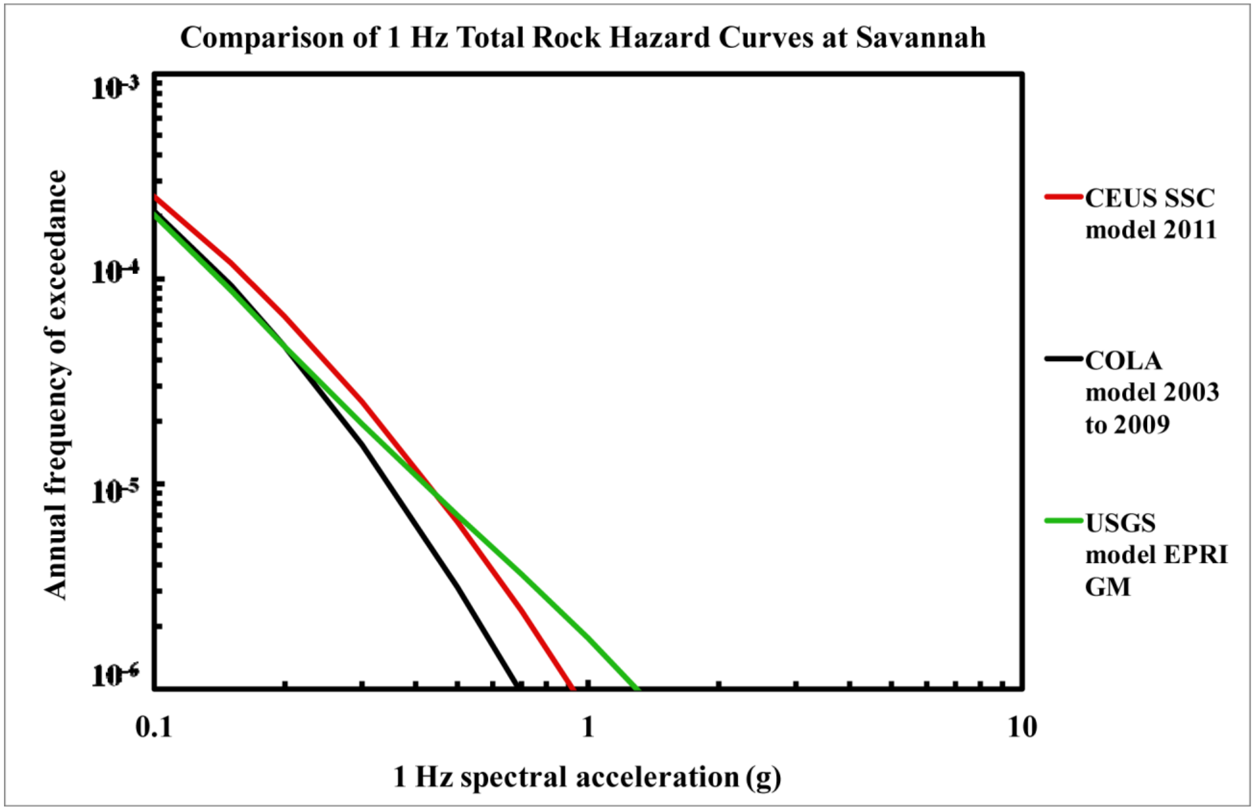

Figure 8.2-6k
Savannah is 1 Hz rock hazard: comparison of three source models

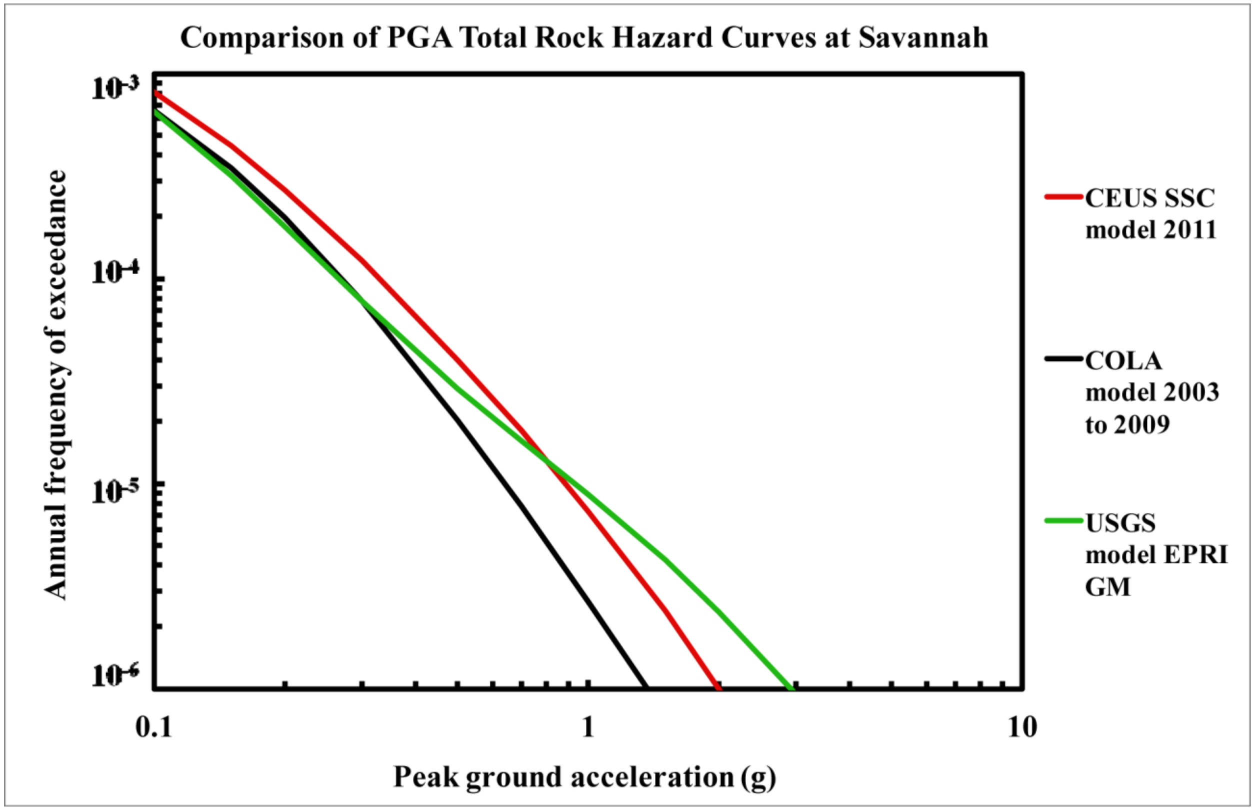

Figure 8.2-6l
Savannah PGA rock hazard: comparison of three source models

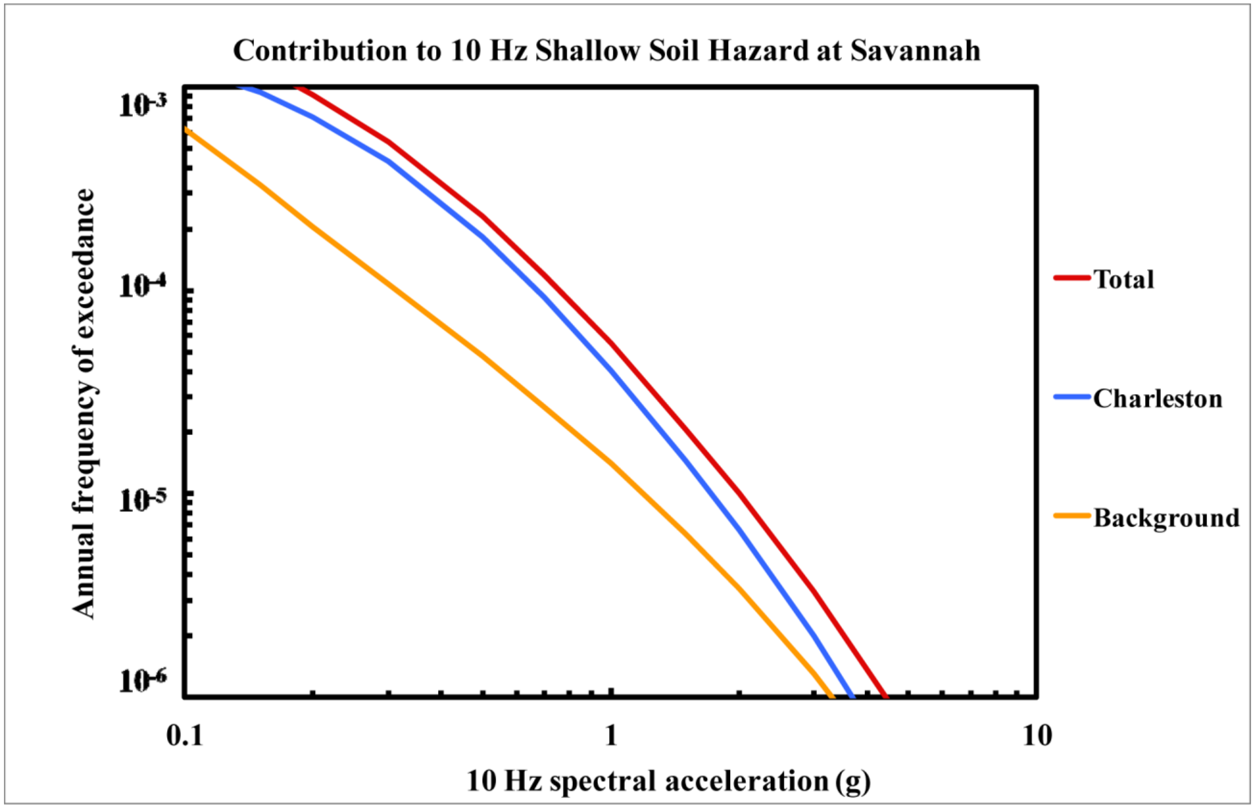

Figure 8.2-6m
Savannah 10 Hz shallow soil hazard: total and contribution by RLME and background

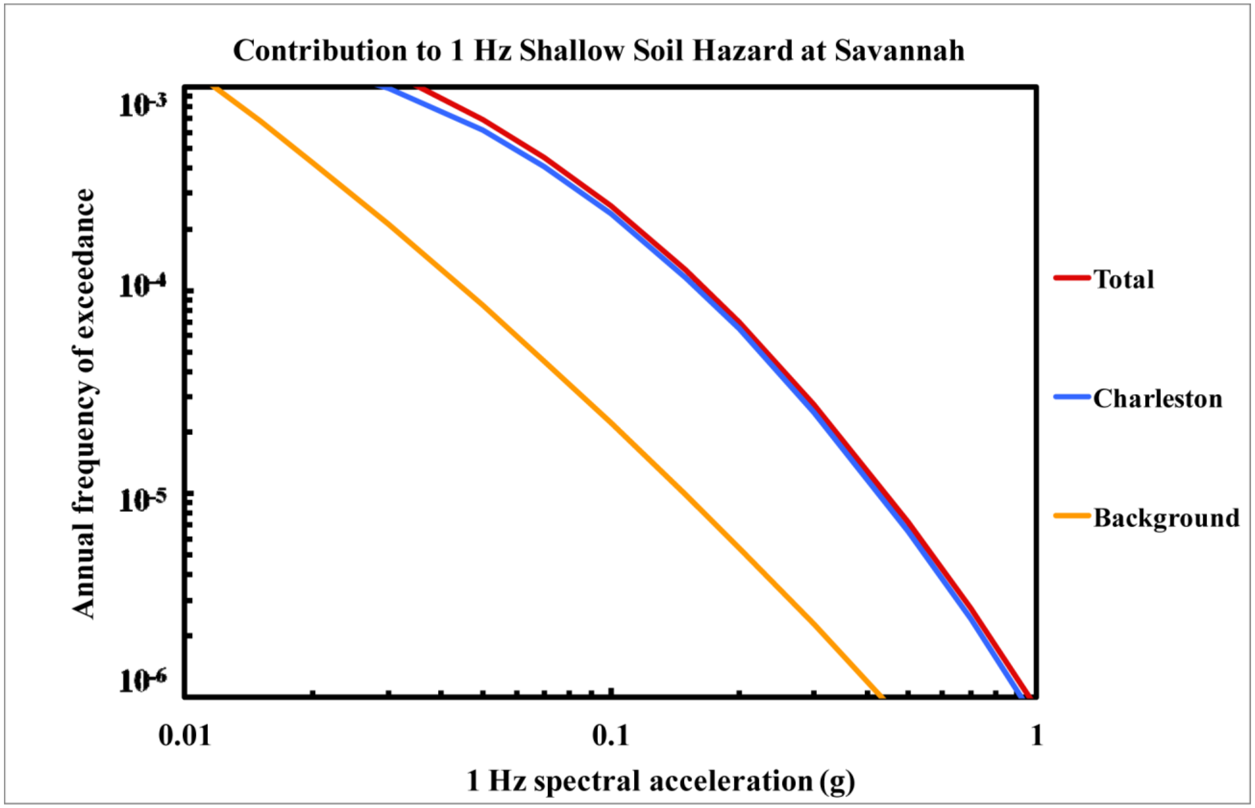

Figure 8.2-6n
Savannah 1 Hz shallow soil hazard: total and contribution by RLME and background

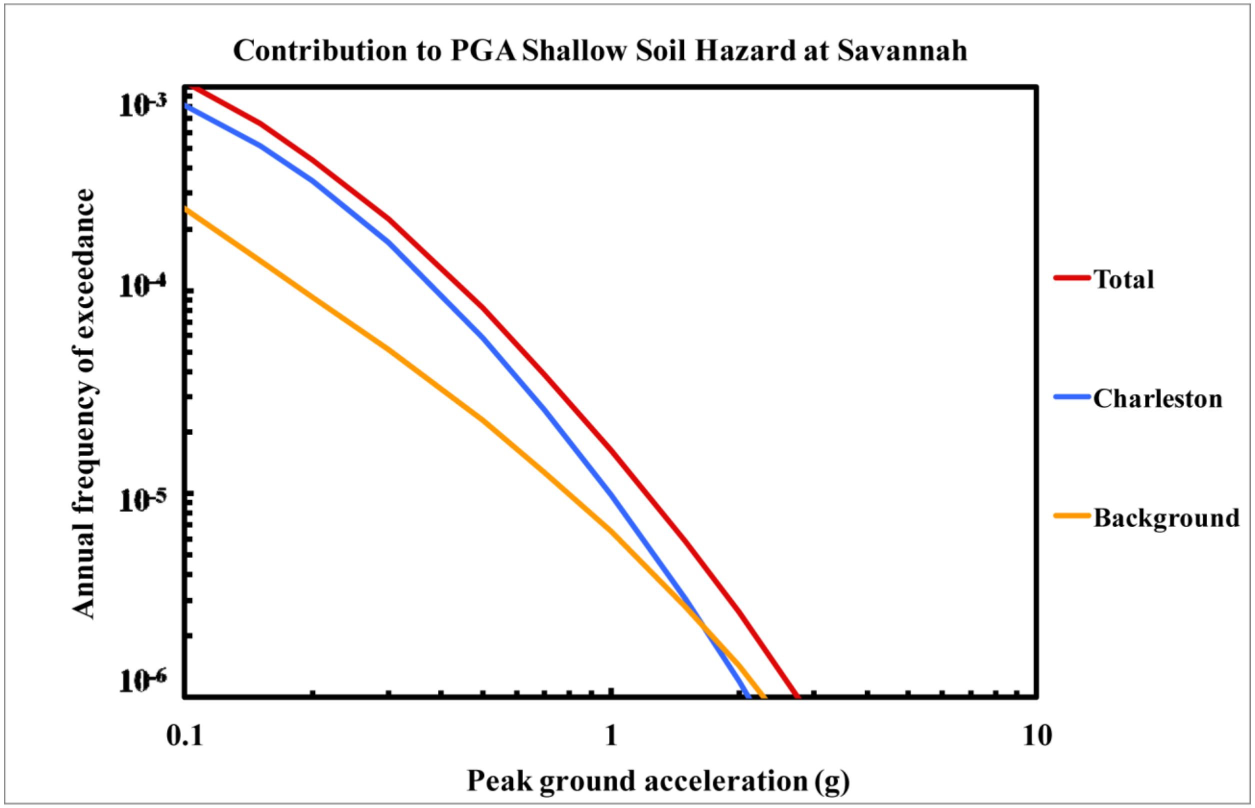

Figure 8.2-6o
Savannah PGA shallow soil hazard: total and contribution by RLME and background

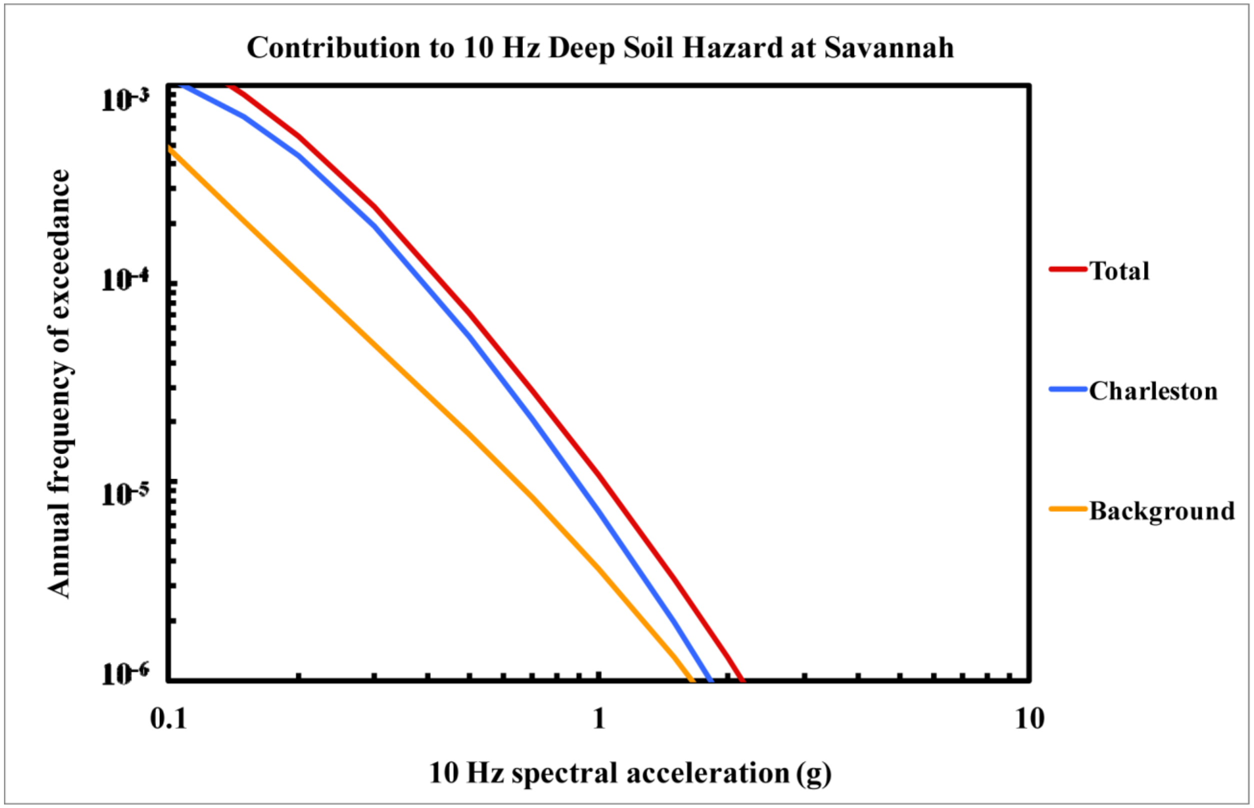

Figure 8.2-6p
Savannah 10 Hz deep soil hazard: total and contribution by RLME and background

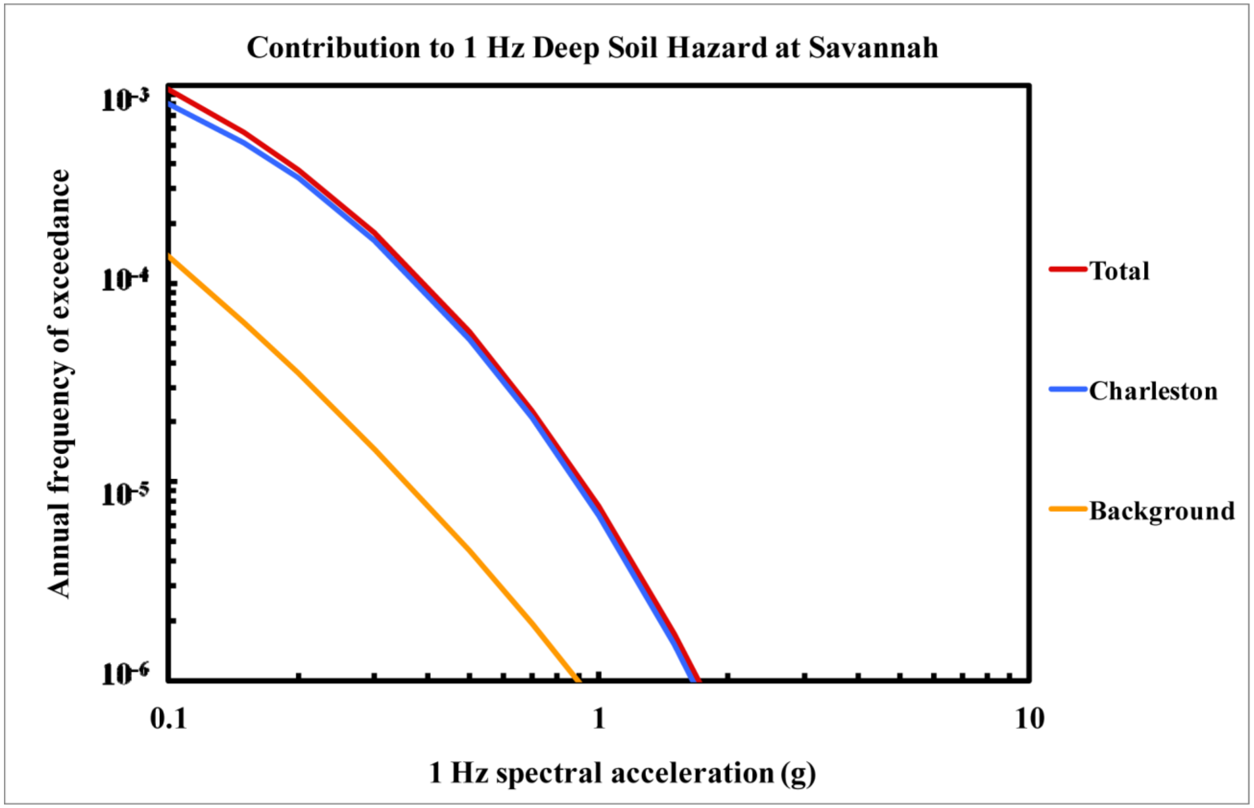

Figure 8.2-6q
Savannah 1 Hz deep soil hazard: total and contribution by RLME and background

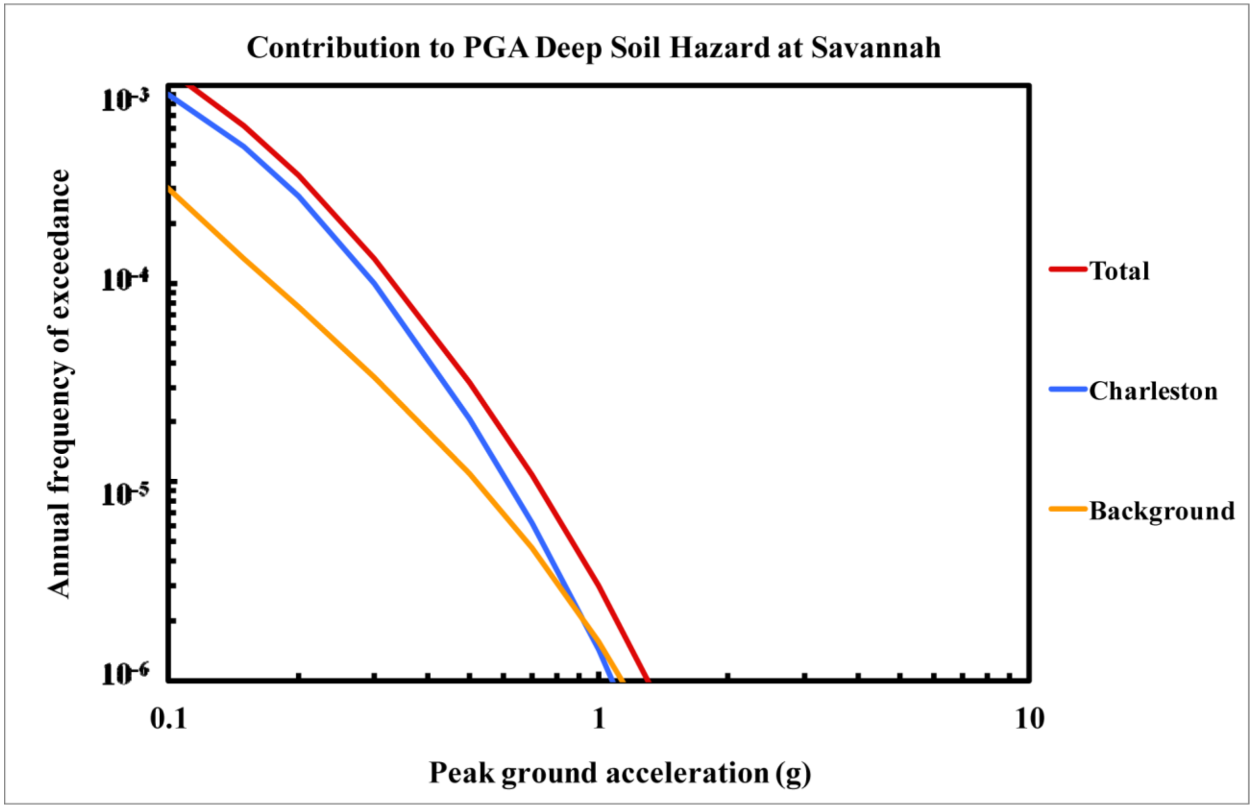

Figure 8.2-6r
Savannah PGA deep soil hazard: total and contribution by RLME and background

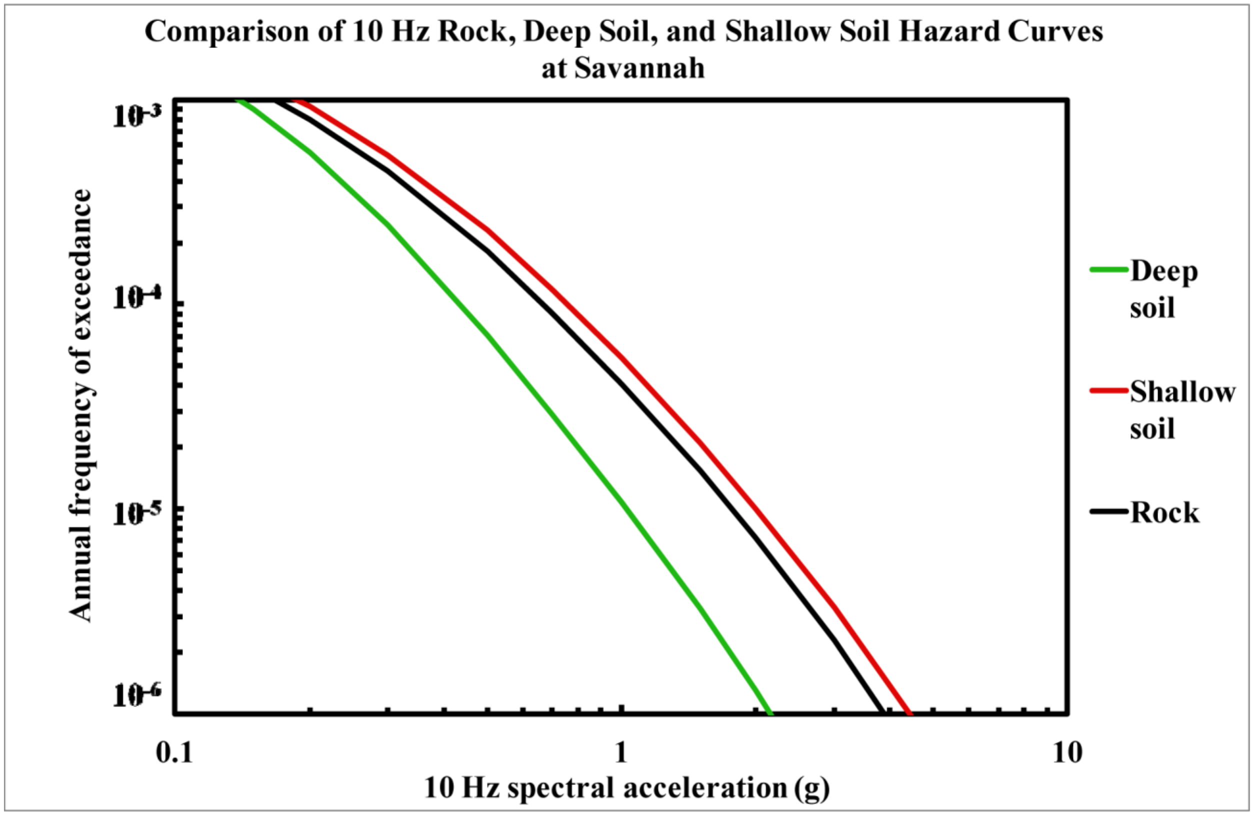

Figure 8.2-6s
Savannah 10 Hz hazard: comparison of three site conditions

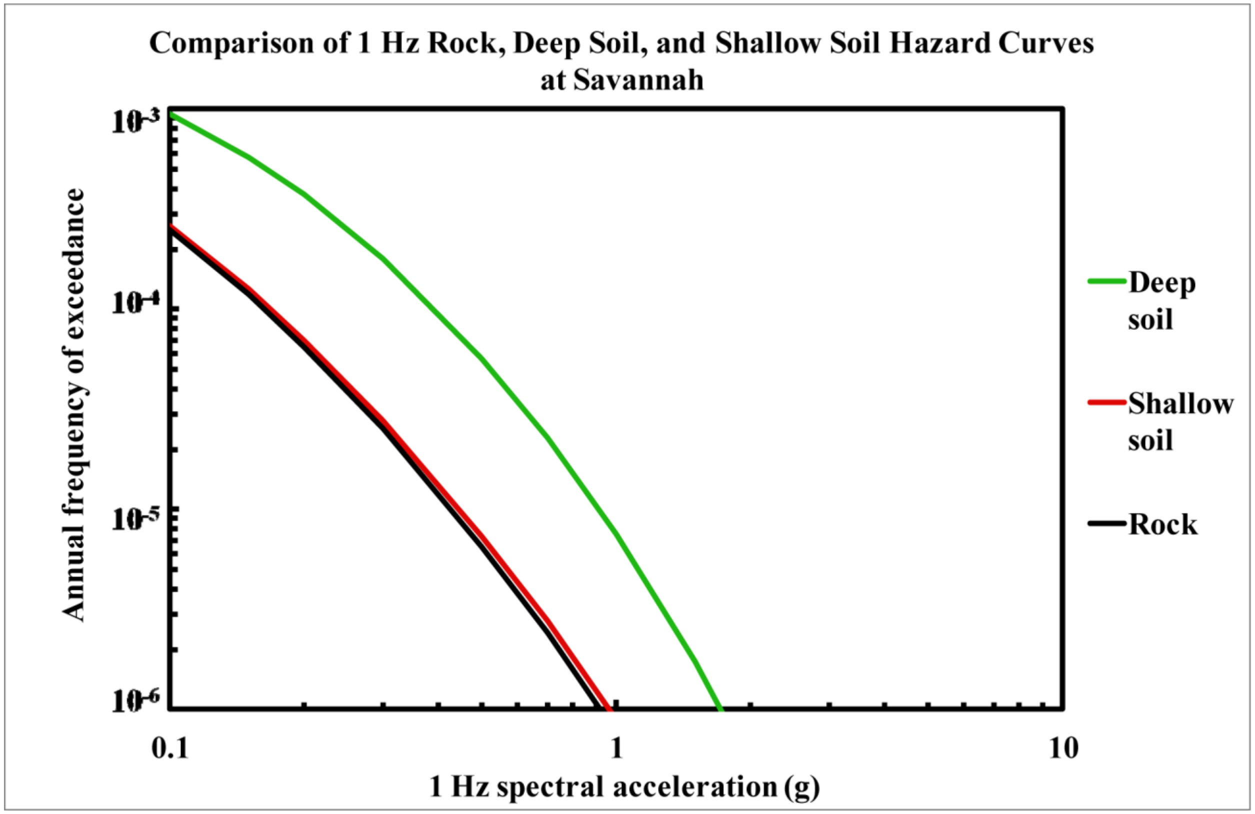

Figure 8.2-6t
Savannah 1 Hz hazard: comparison of three site conditions

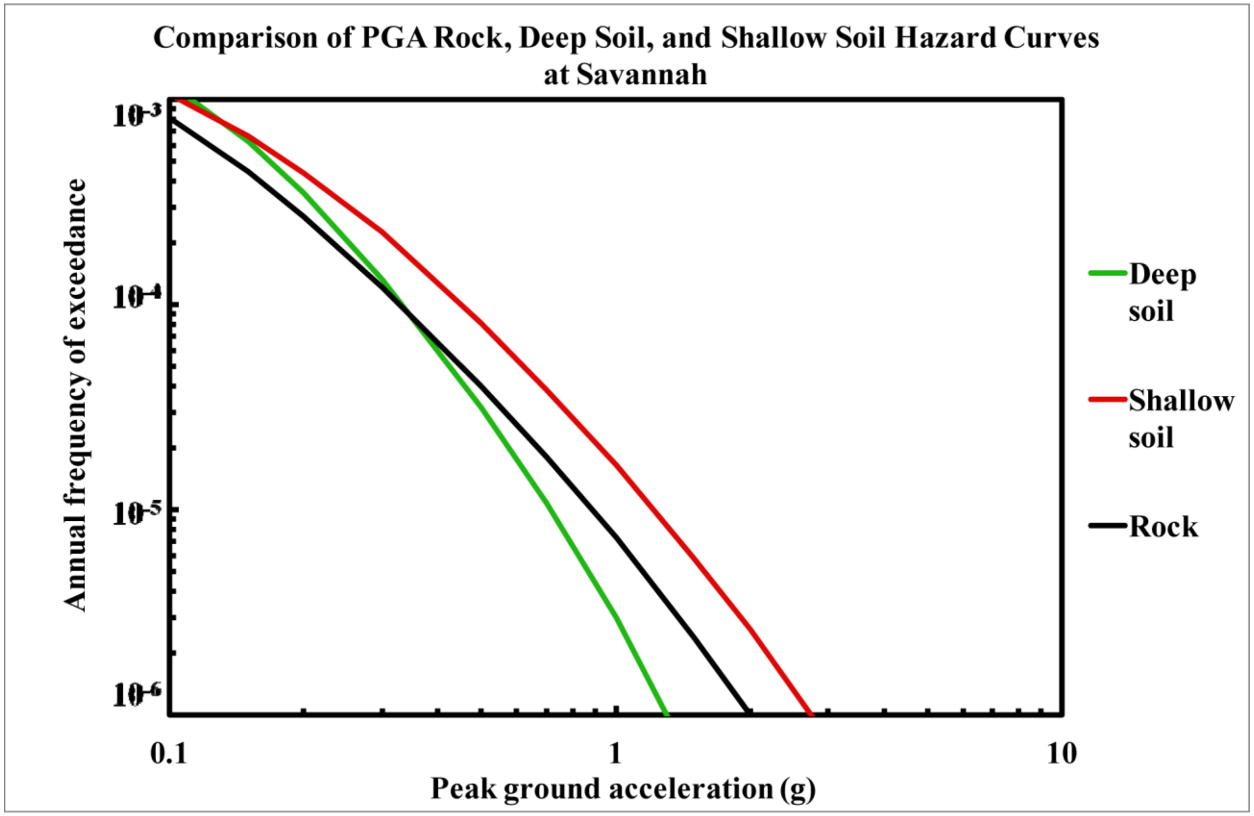

Figure 8.2-6u
Savannah PGA hazard: comparison of three site conditions

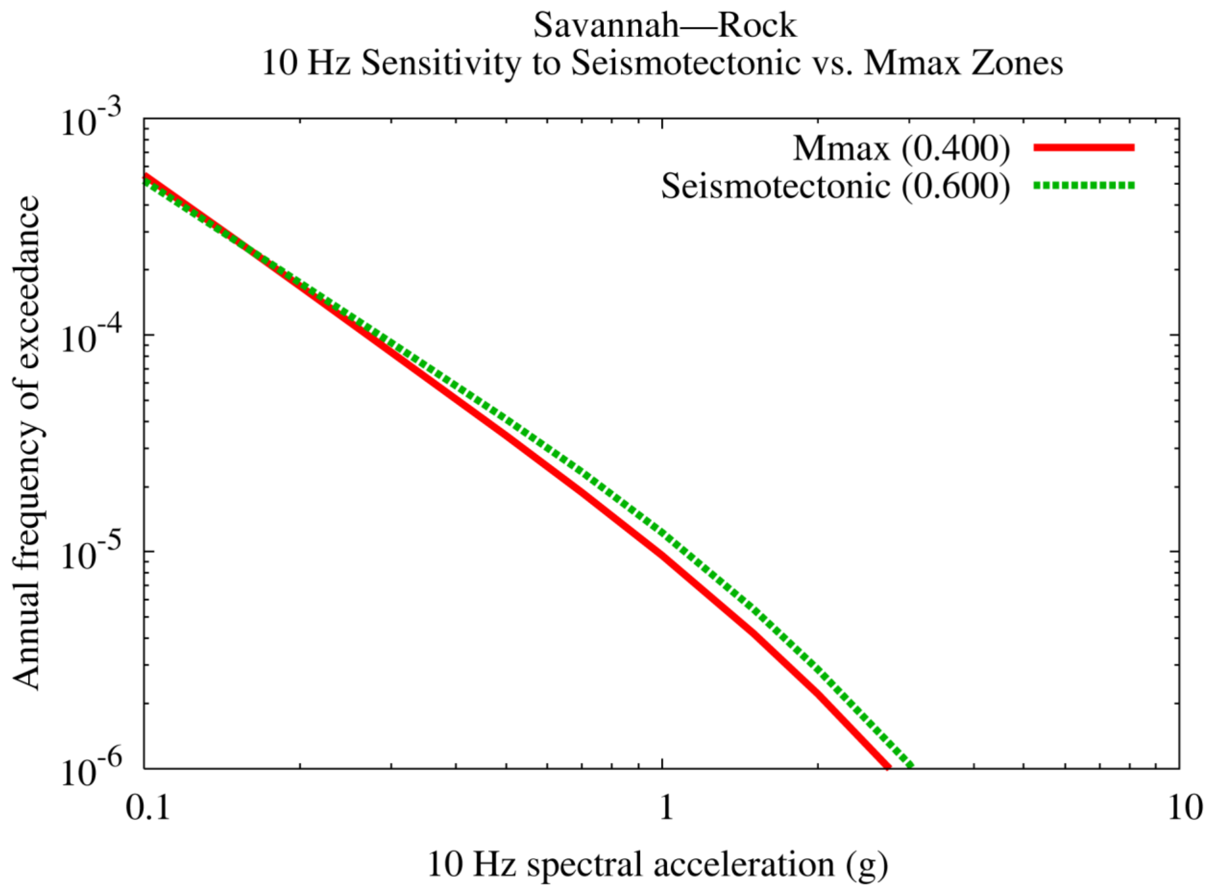

Figure 8.2-6v
Savannah 10 Hz rock hazard: sensitivity to seismotectonic vs. Mmax zones

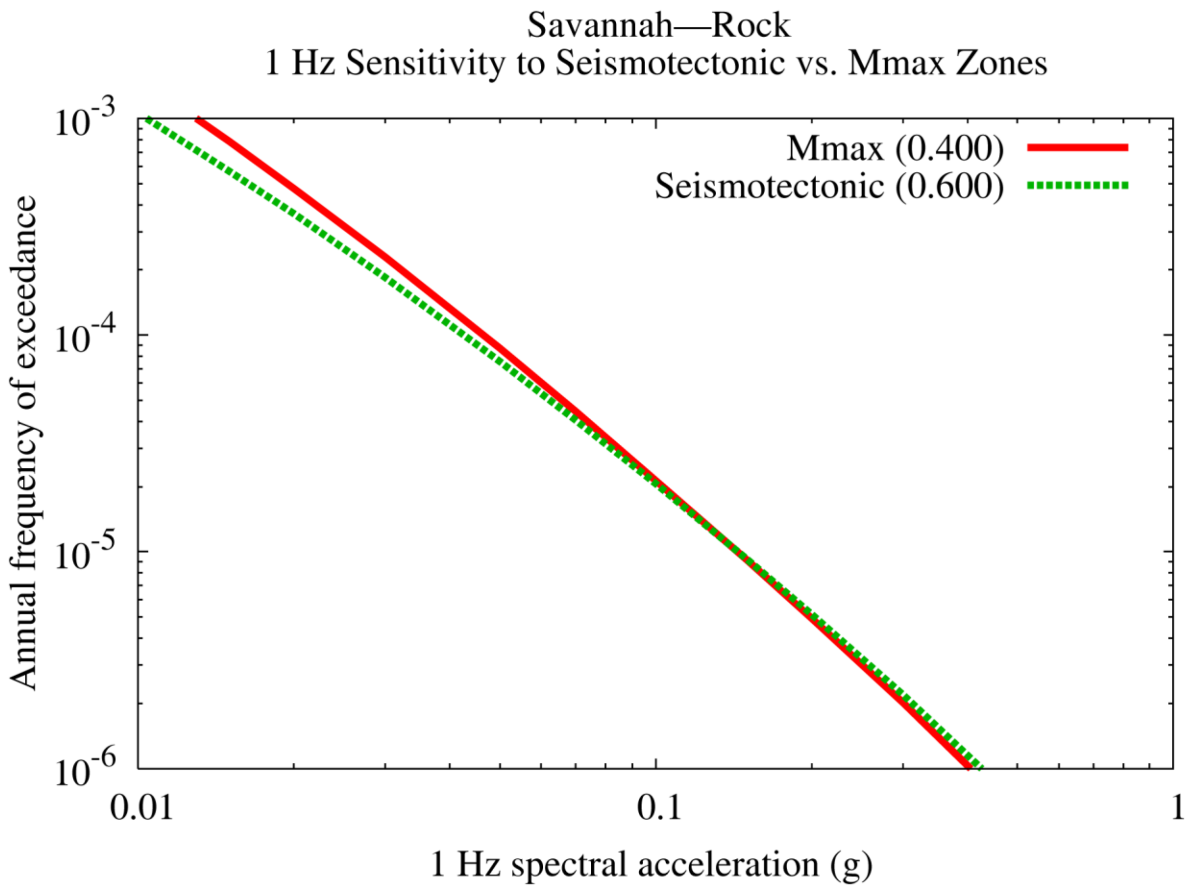

Figure 8.2-6w
Savannah 1 Hz rock hazard: sensitivity to seismotectonic vs. Mmax zones

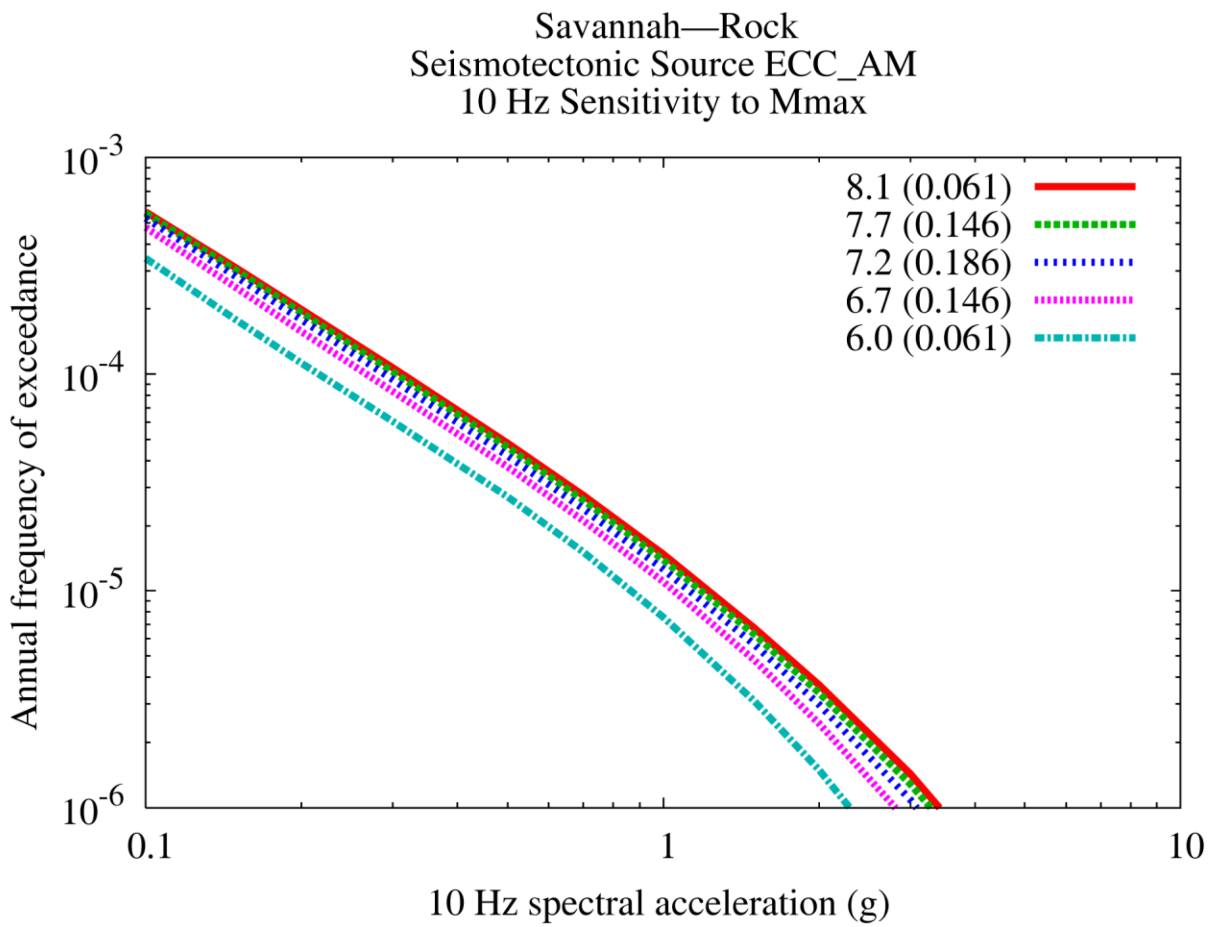

Figure 8.2-6x
Savannah 10 Hz rock hazard: sensitivity to Mmax for source ECC-AM

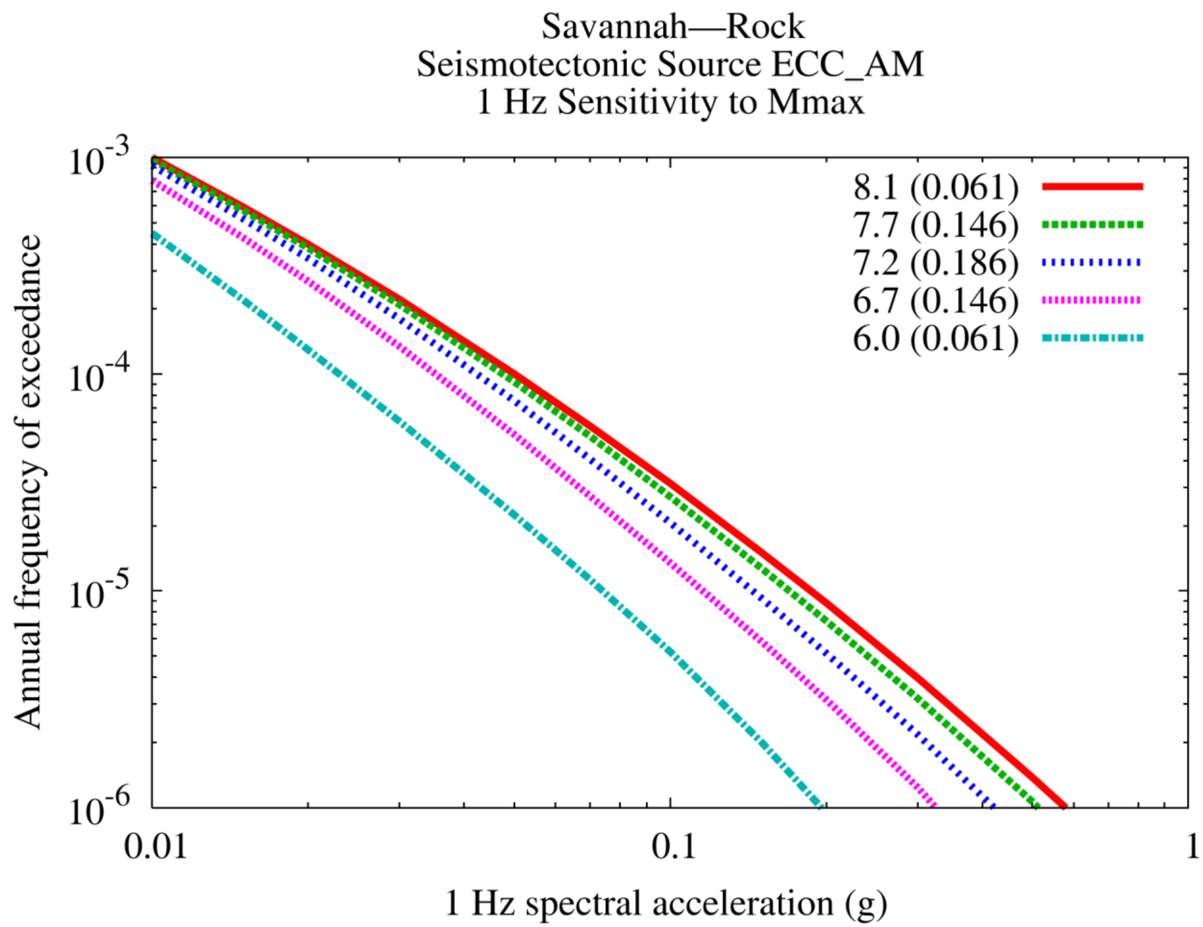

Figure 8.2-6y
Savannah 1 Hz rock hazard: sensitivity to Mmax for source ECC-AM

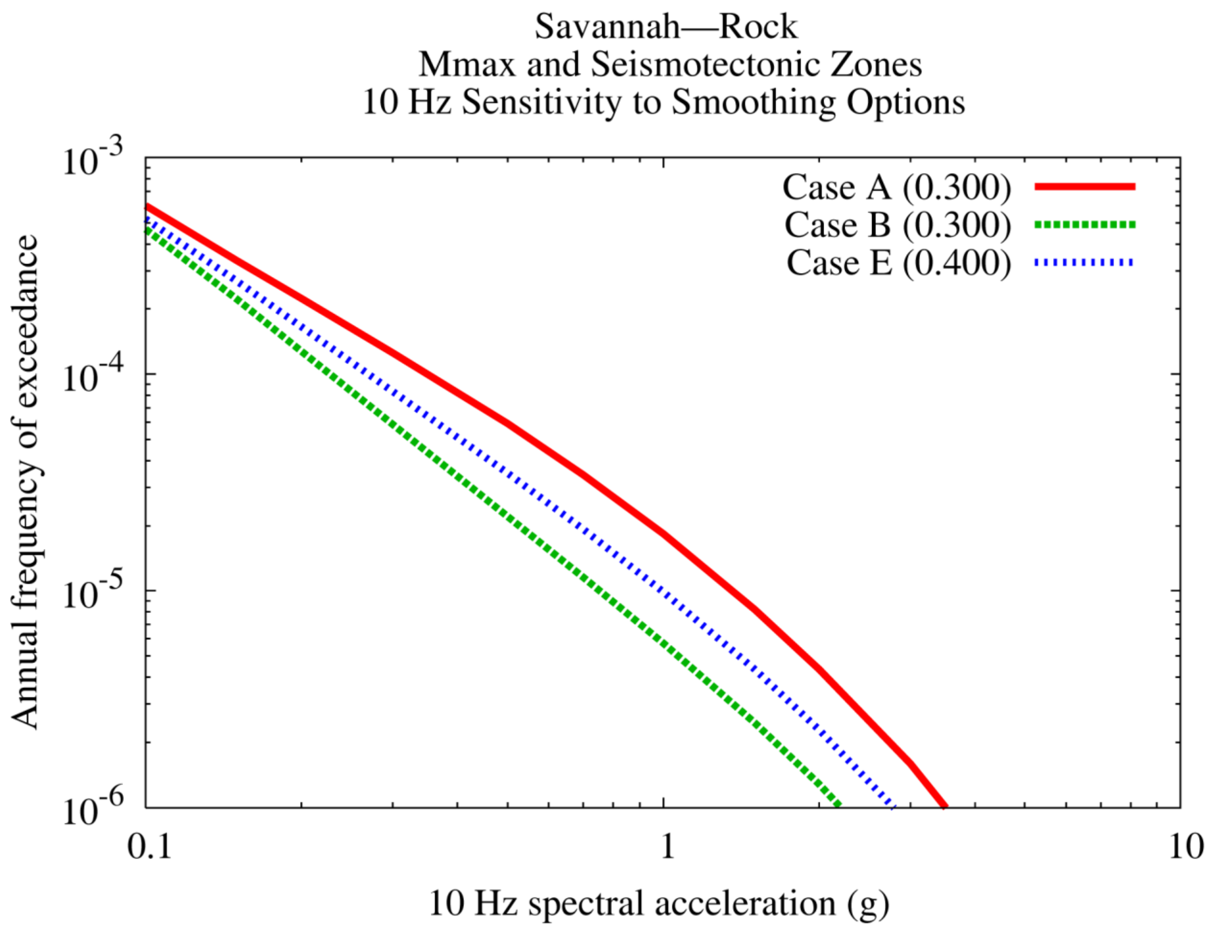

Figure 8.2-6z
Savannah 10 Hz rock hazard: sensitivity to smoothing options

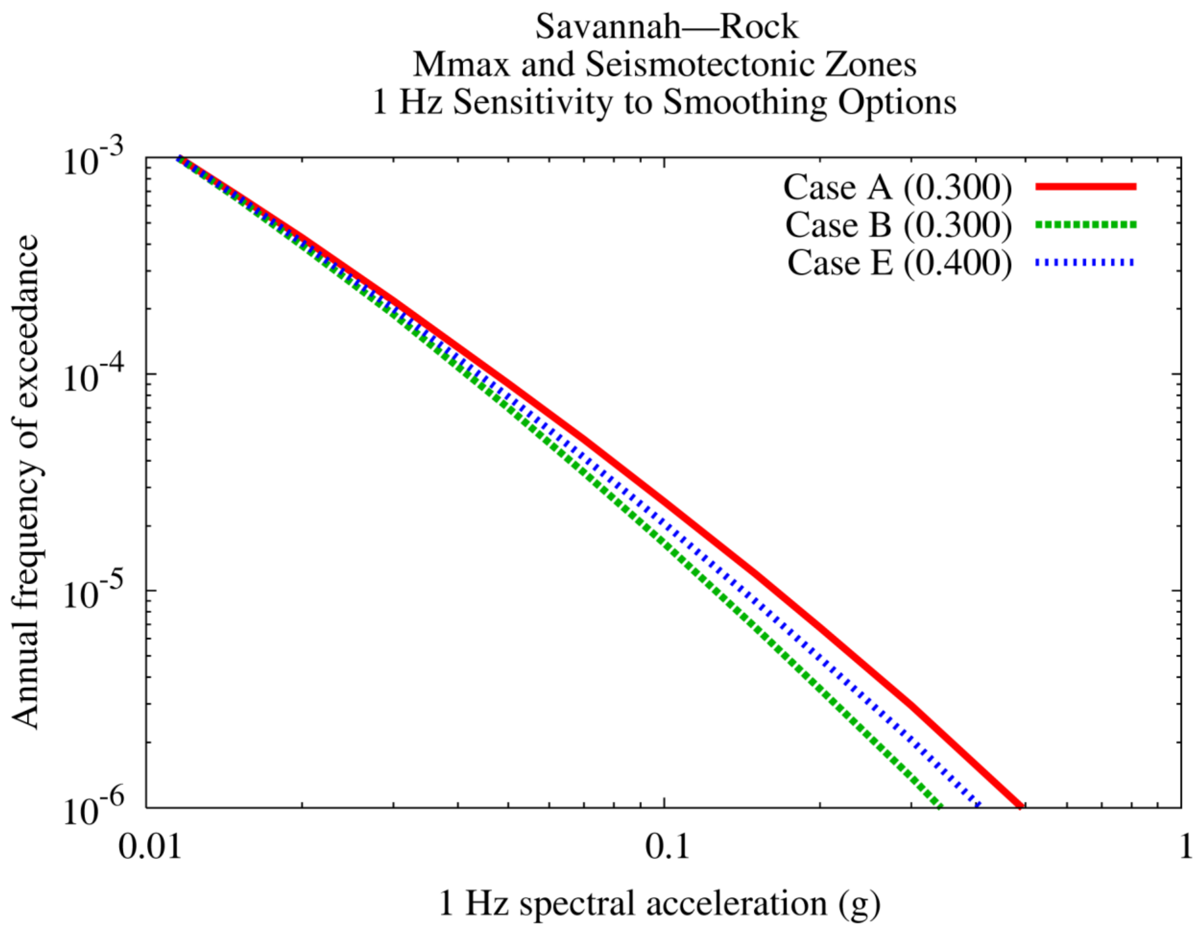

Figure 8.2-6aa
Savannah 1 Hz rock hazard: sensitivity to smoothing options

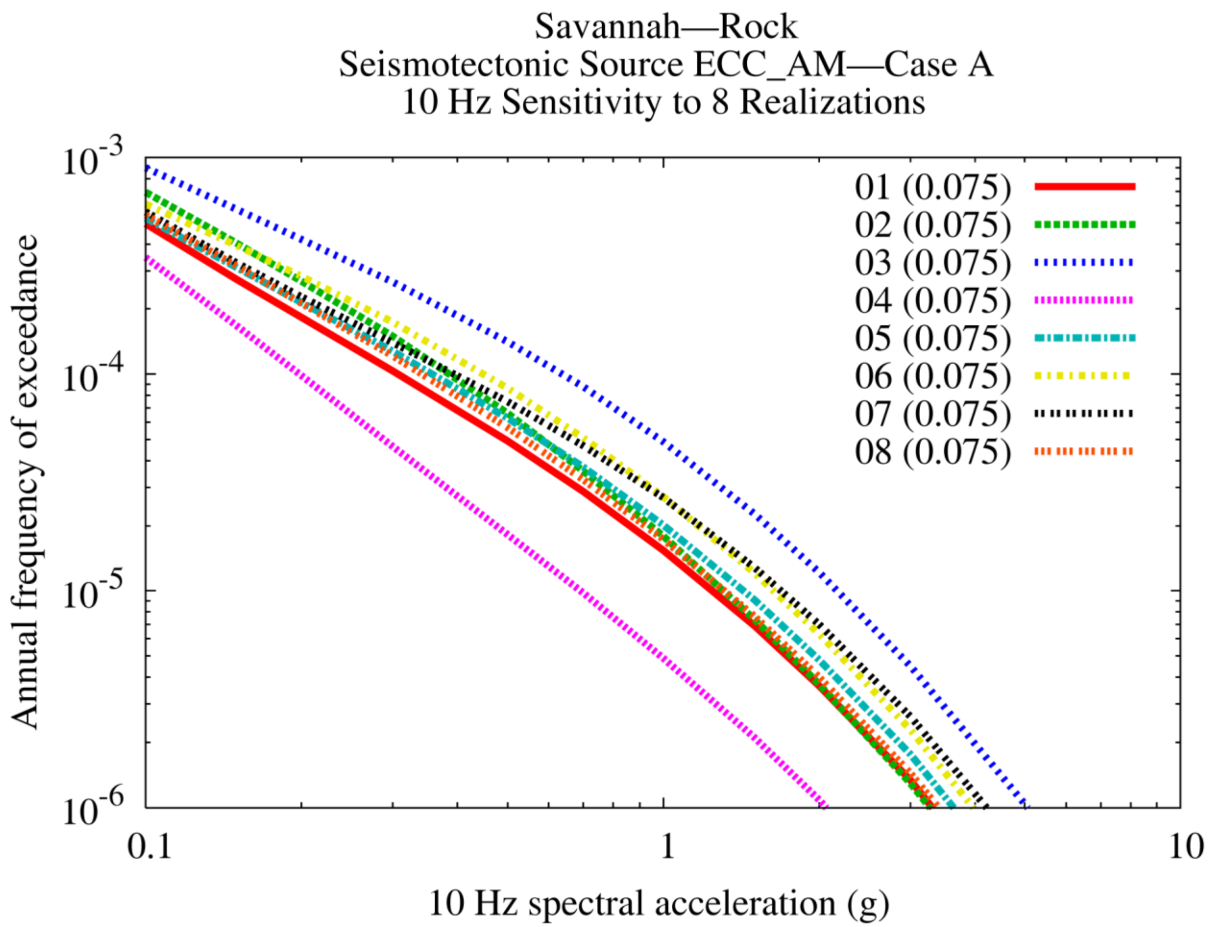

Figure 8.2-6bb
Savannah 10 Hz rock hazard: sensitivity to eight realizations for source ECC-AM, Case A

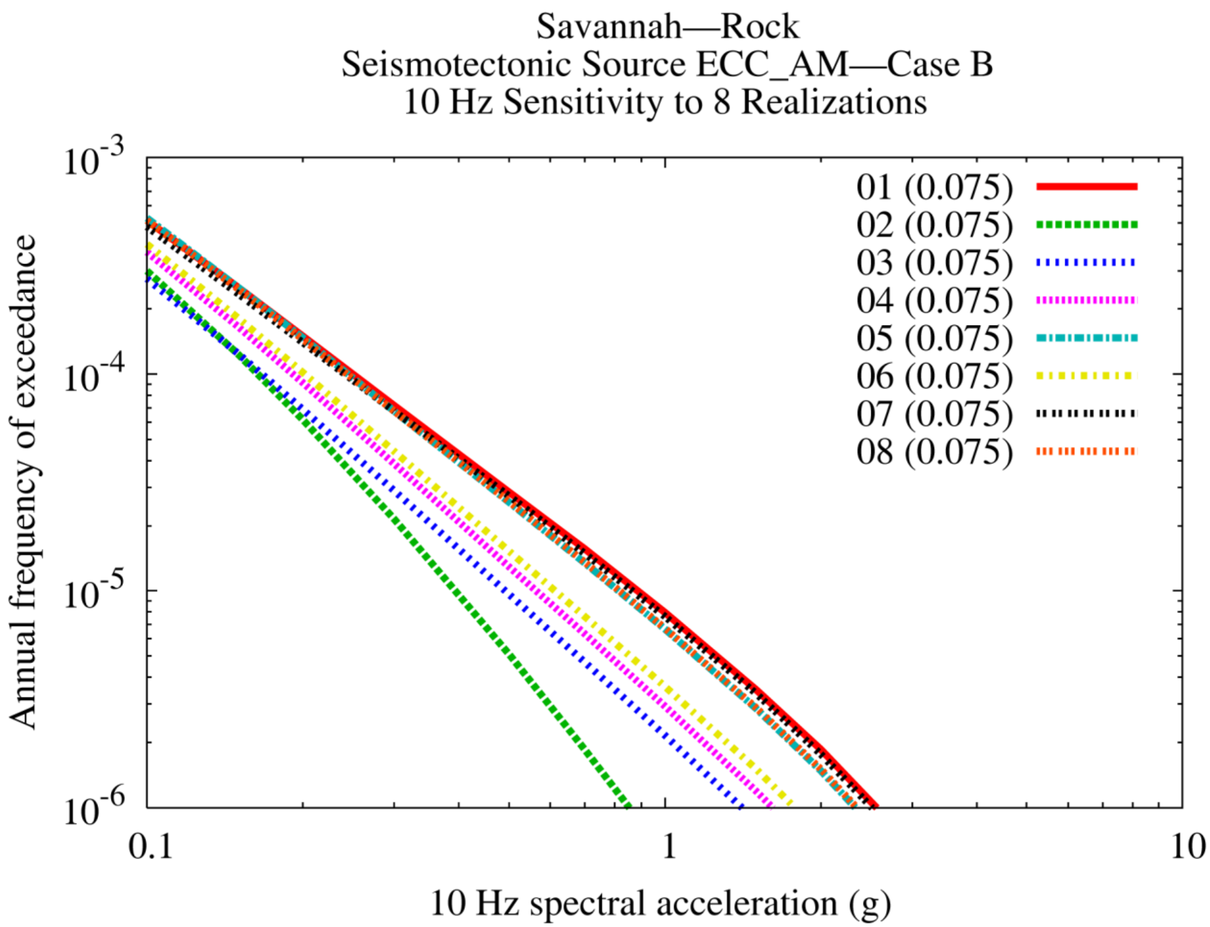

Figure 8.2-6cc
Savannah 10 Hz rock hazard: sensitivity to eight realizations for source ECC-AM, Case B

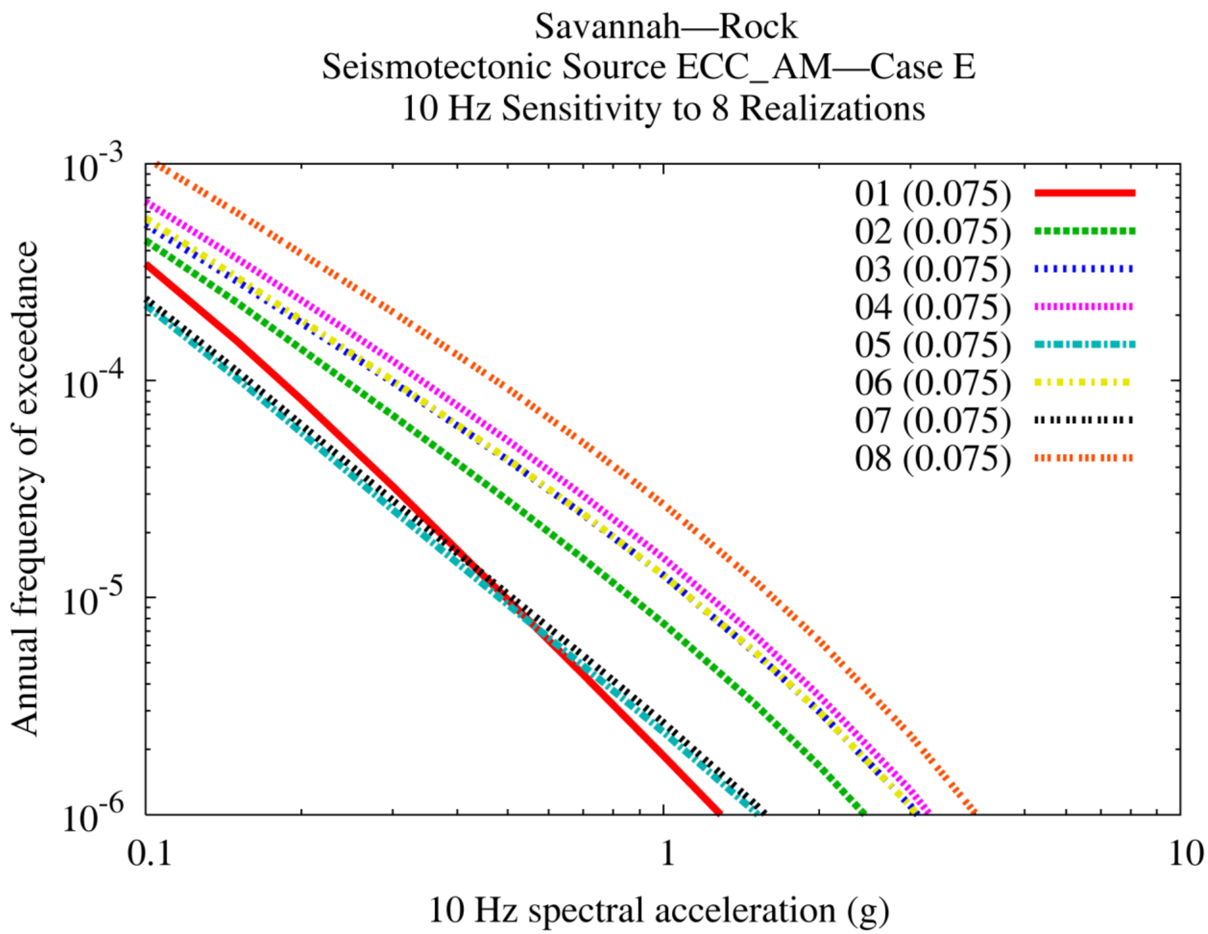

Figure 8.2-6dd
Savannah 10 Hz rock hazard: sensitivity to eight realizations for source ECC-AM, Case E

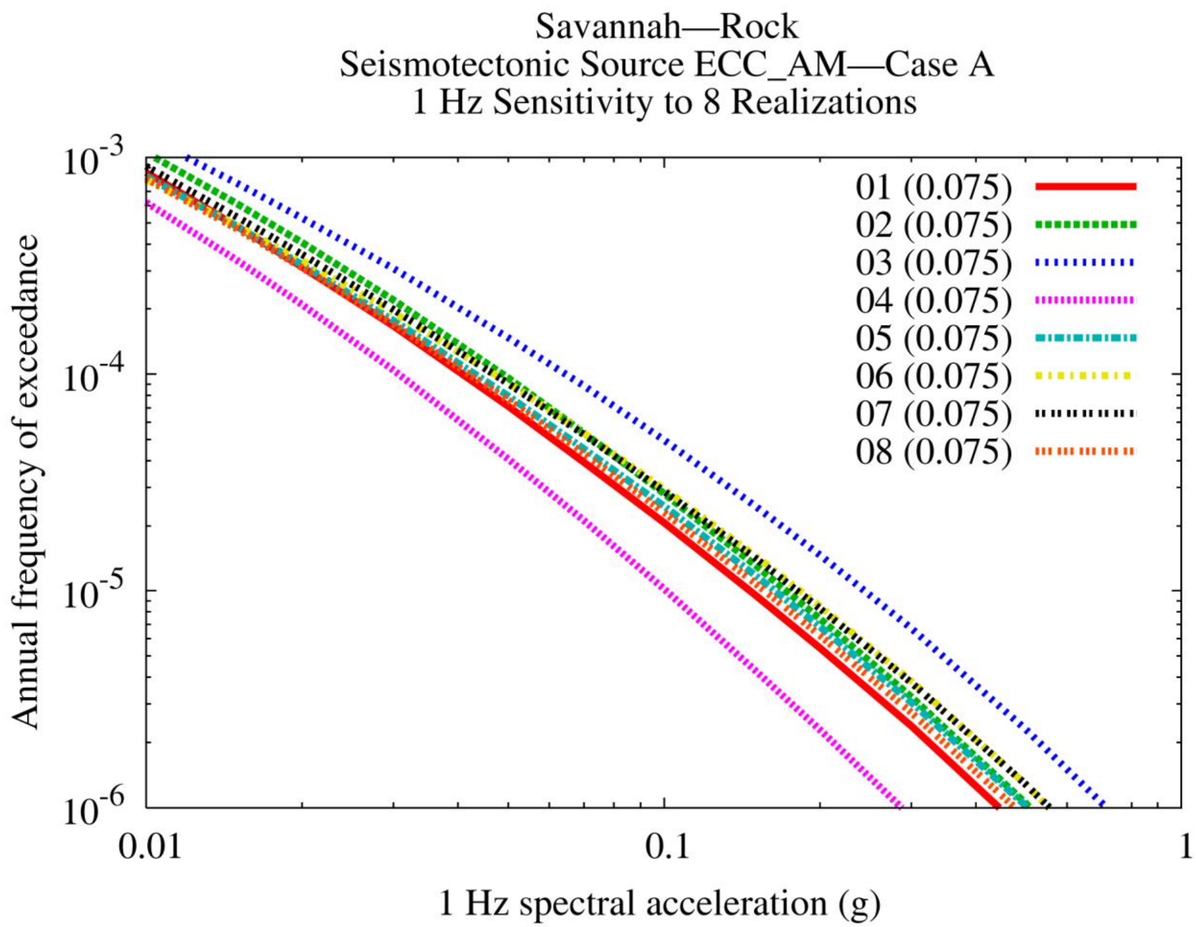

Figure 8.2-6ee
Savannah 1 Hz rock hazard: sensitivity to eight realizations for source ECC-AM, Case A

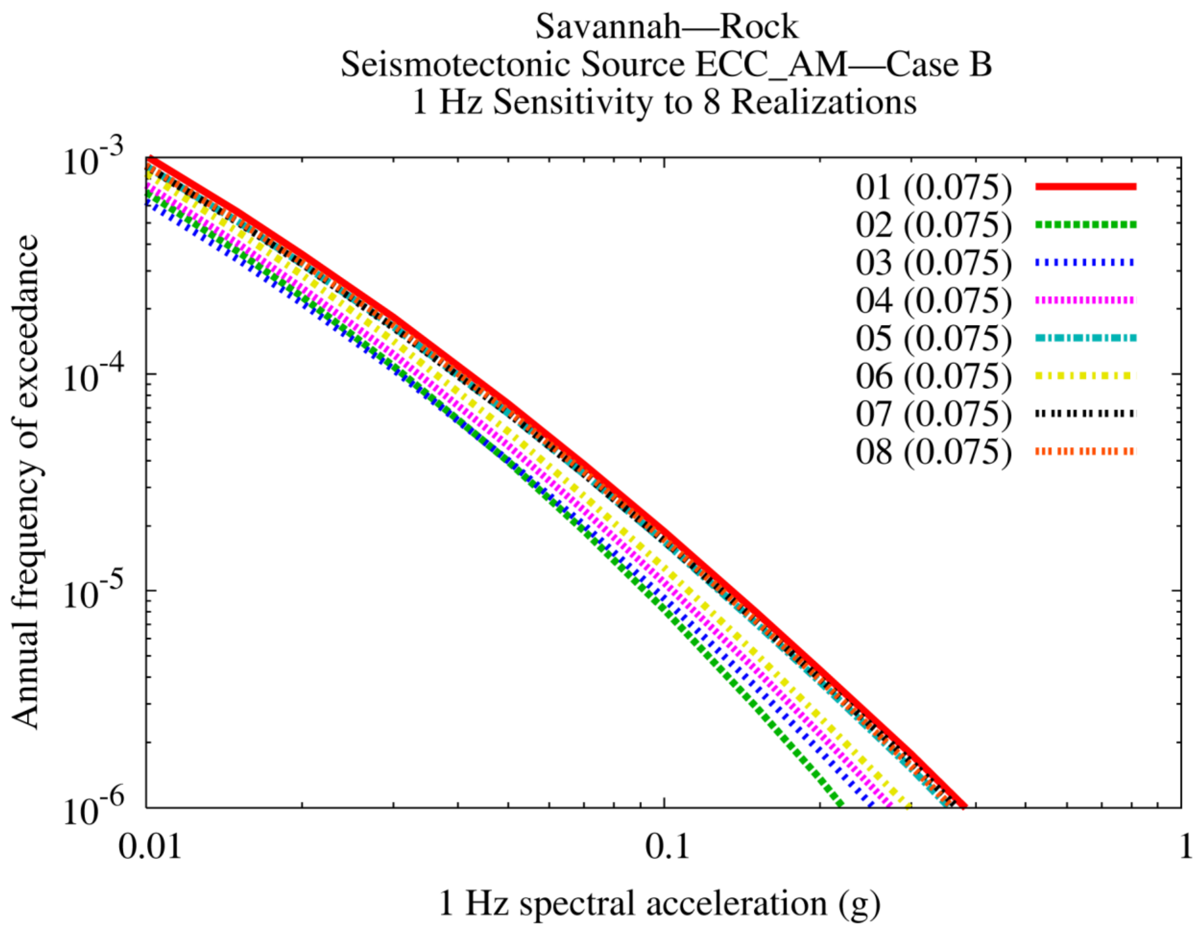

Figure 8.2-6ff
Savannah 1 Hz rock hazard: sensitivity to eight realizations for source ECC-AM, Case B

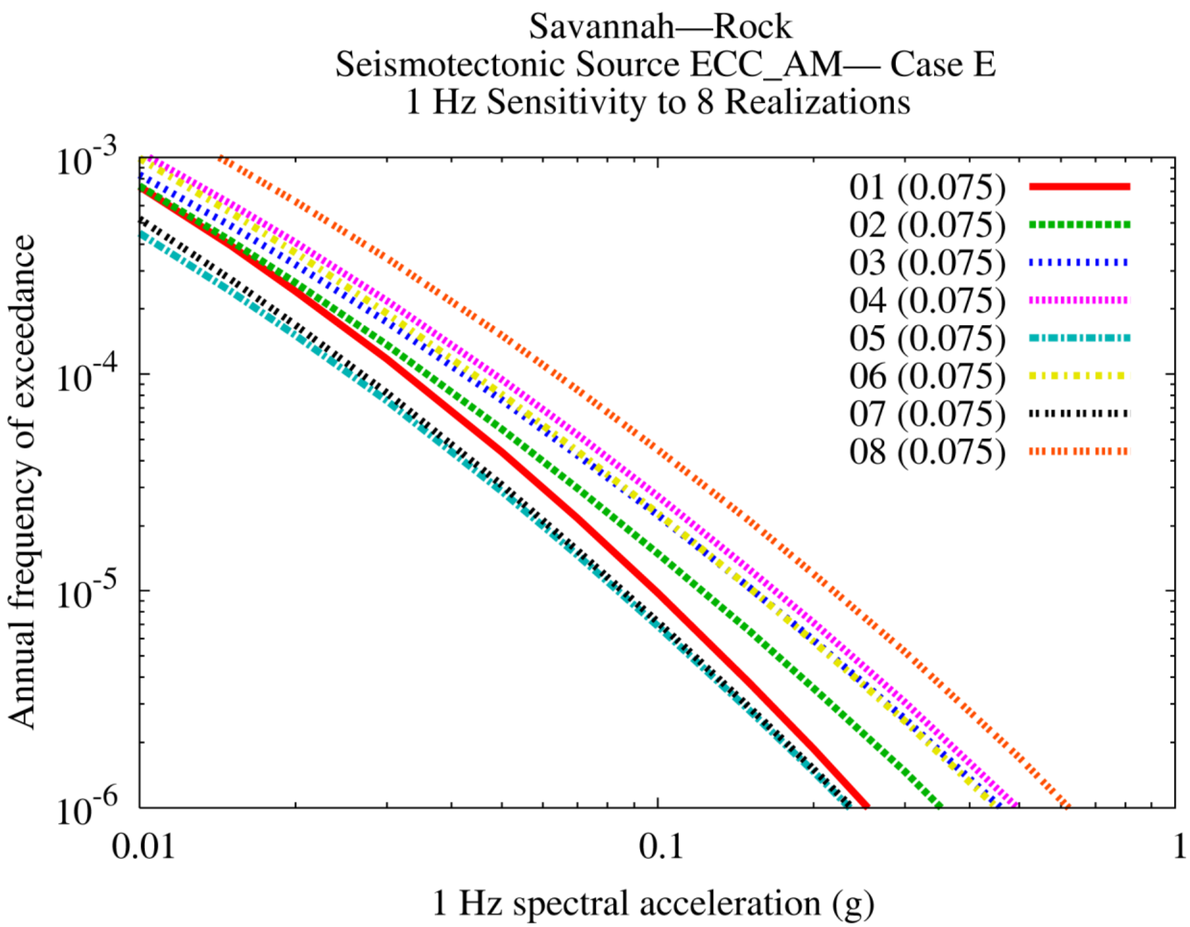

Figure 8.2-6gg
Savannah 1 Hz rock hazard: sensitivity to eight realizations for source ECC-AM, Case E

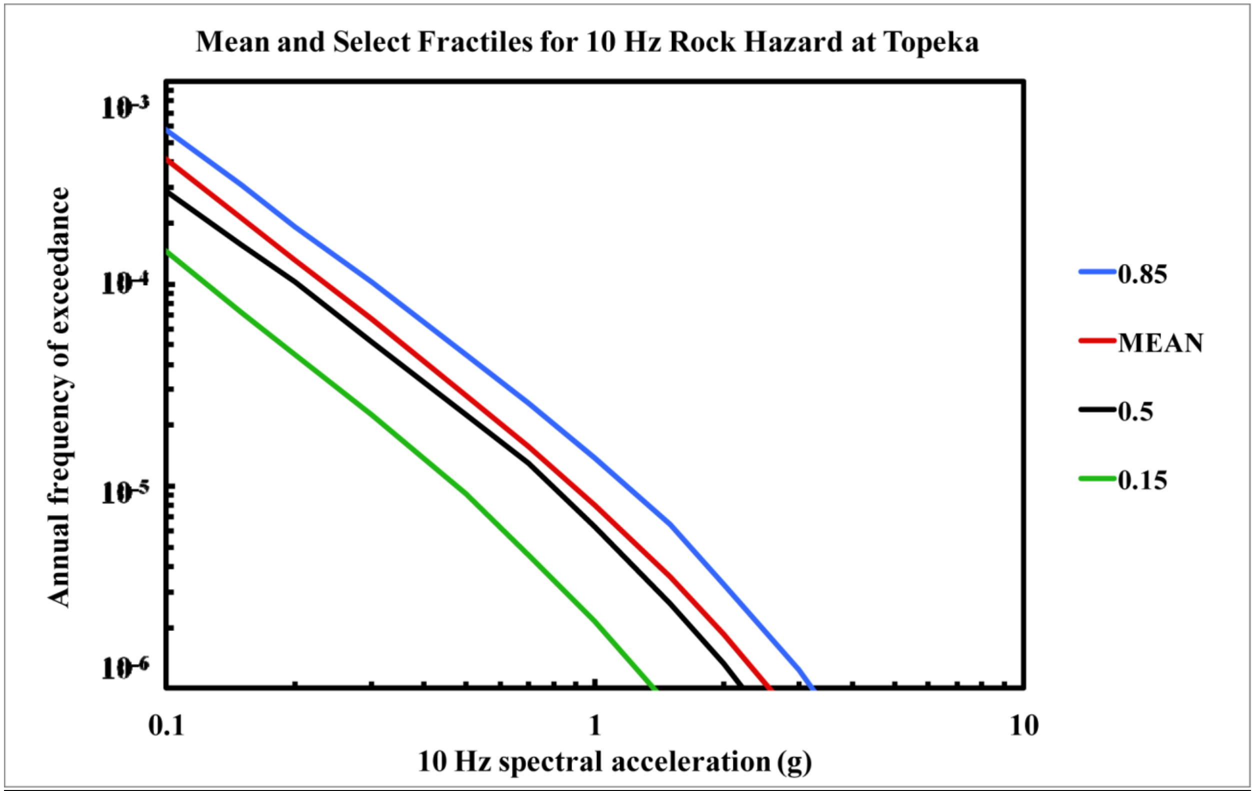

Figure 8.2-7a
Topeka 10 Hz rock hazard: mean and fractile total hazard

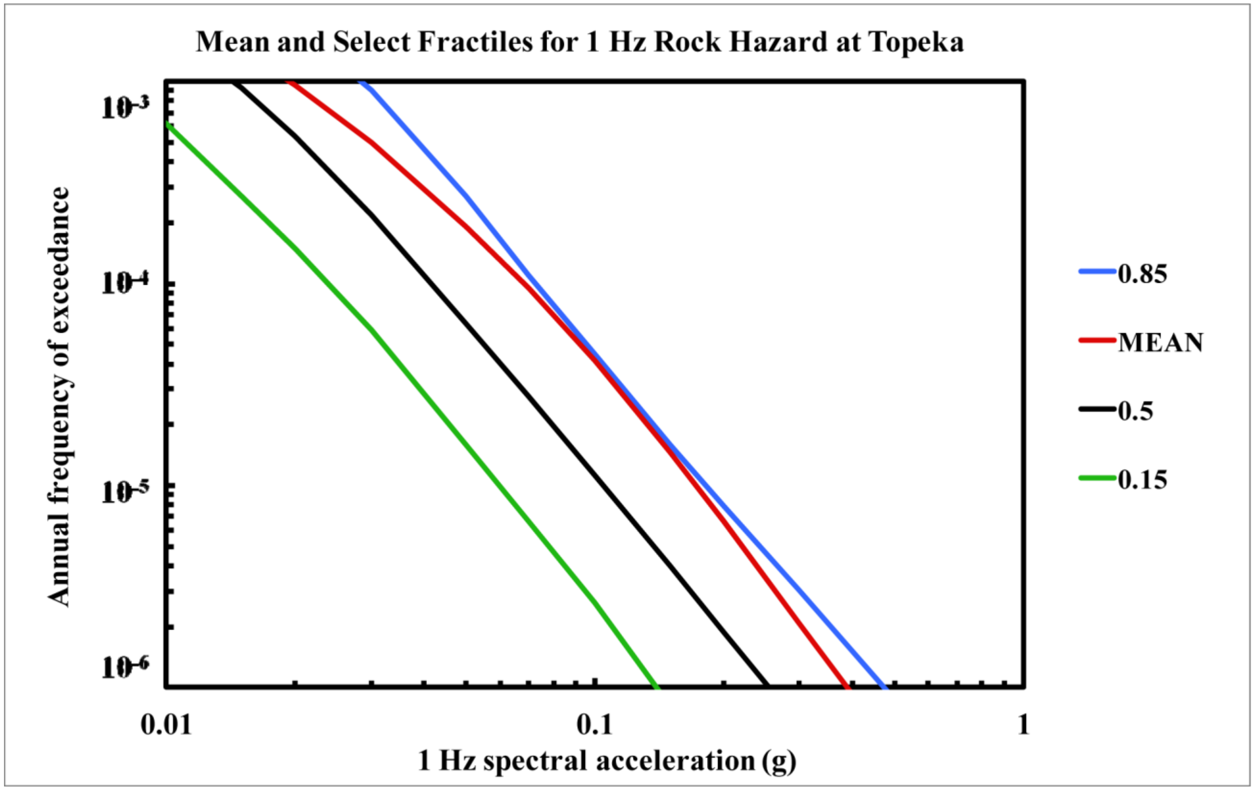

Figure 8.2-7b
Topeka 1 Hz rock hazard: mean and fractile total hazard

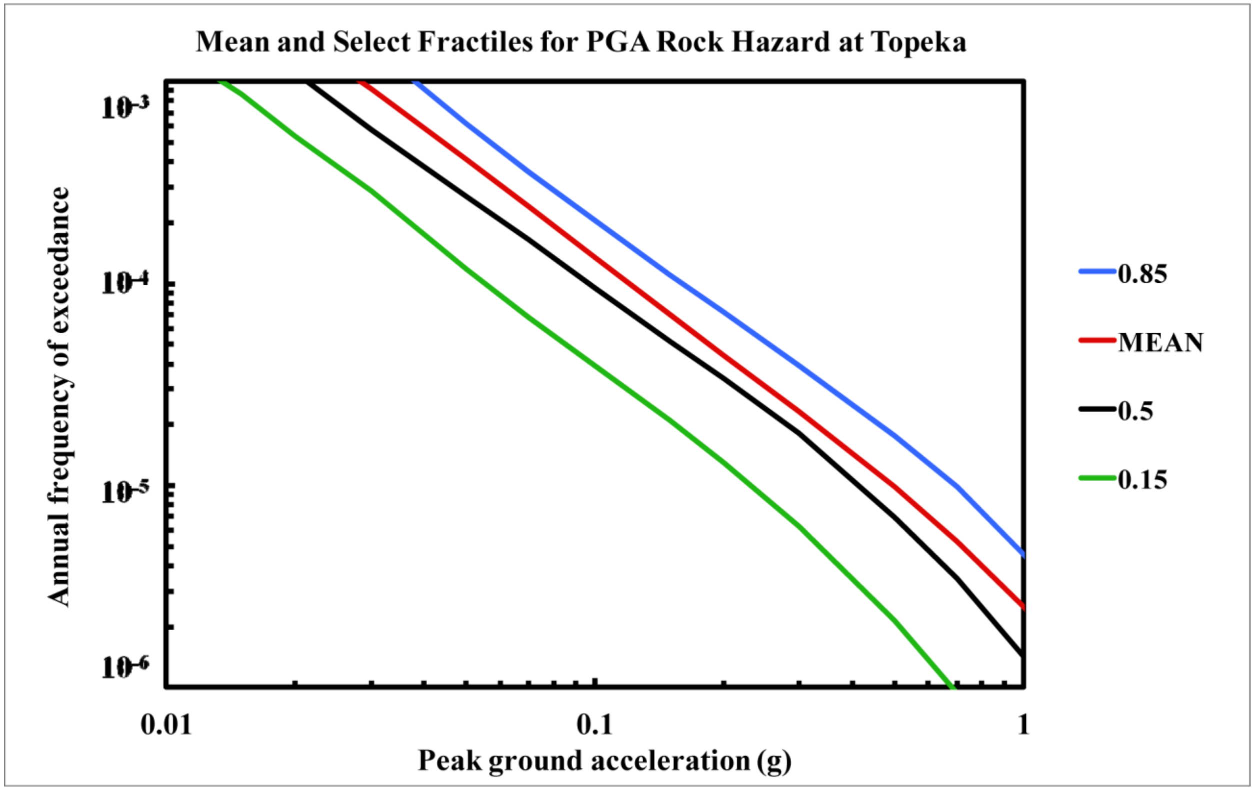

Figure 8.2-7c
Topeka PGA rock hazard: mean and fractile total hazard

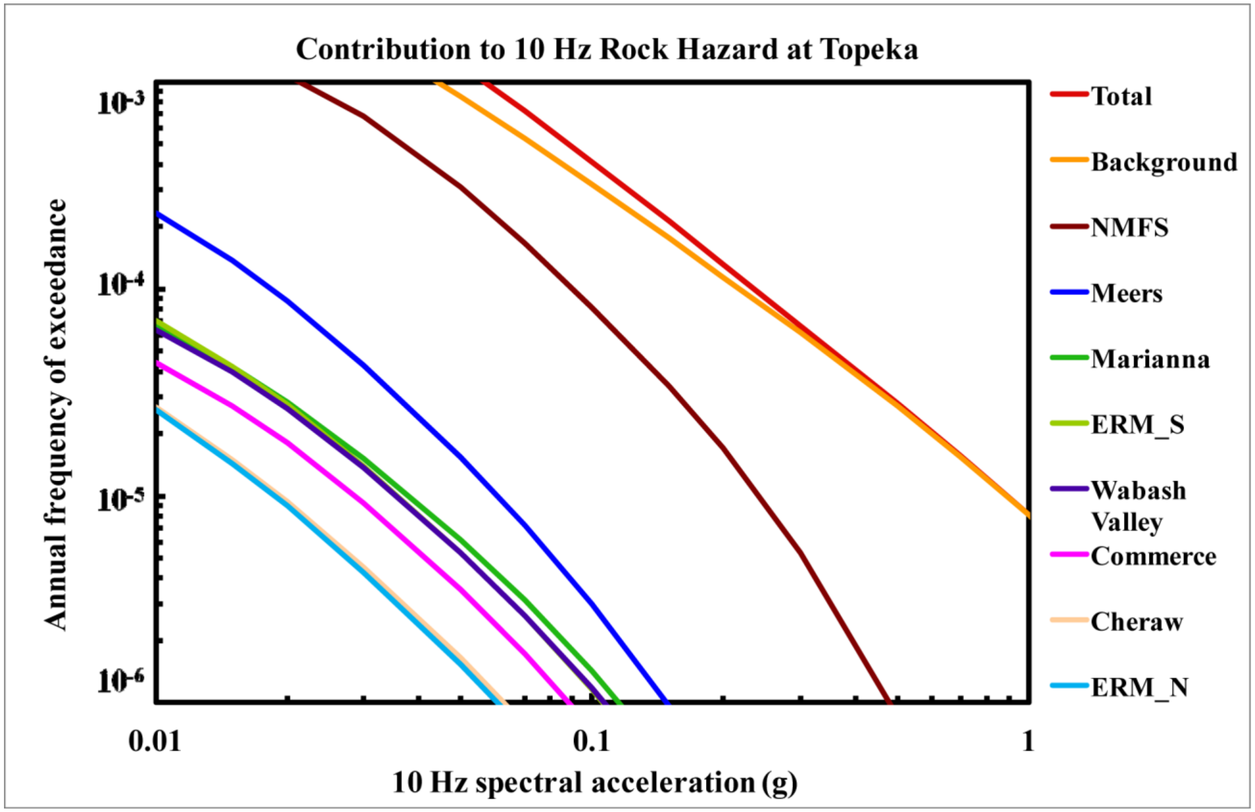

Figure 8.2-7d
Topeka 10 Hz rock hazard: total and contribution by RLME and background

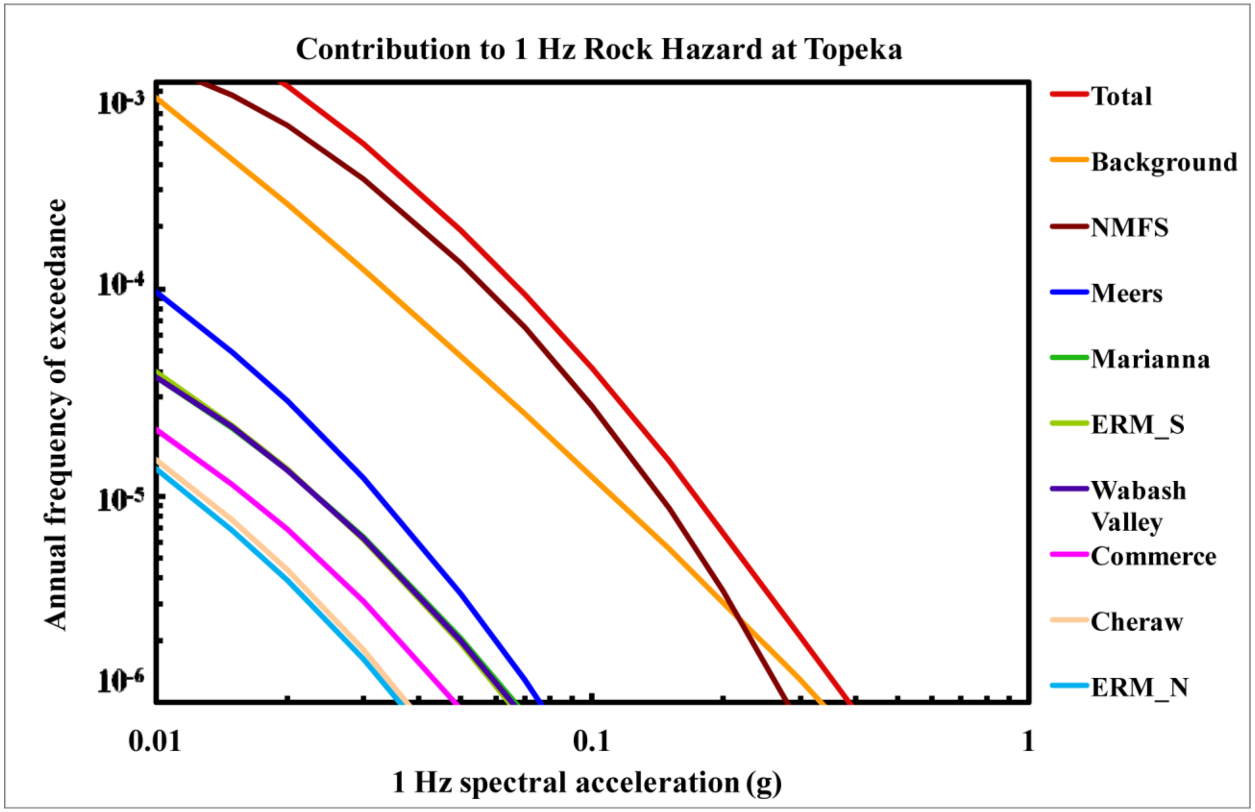

Figure 8.2-7e
Topeka 1 Hz rock hazard: total and contribution by RLME and background

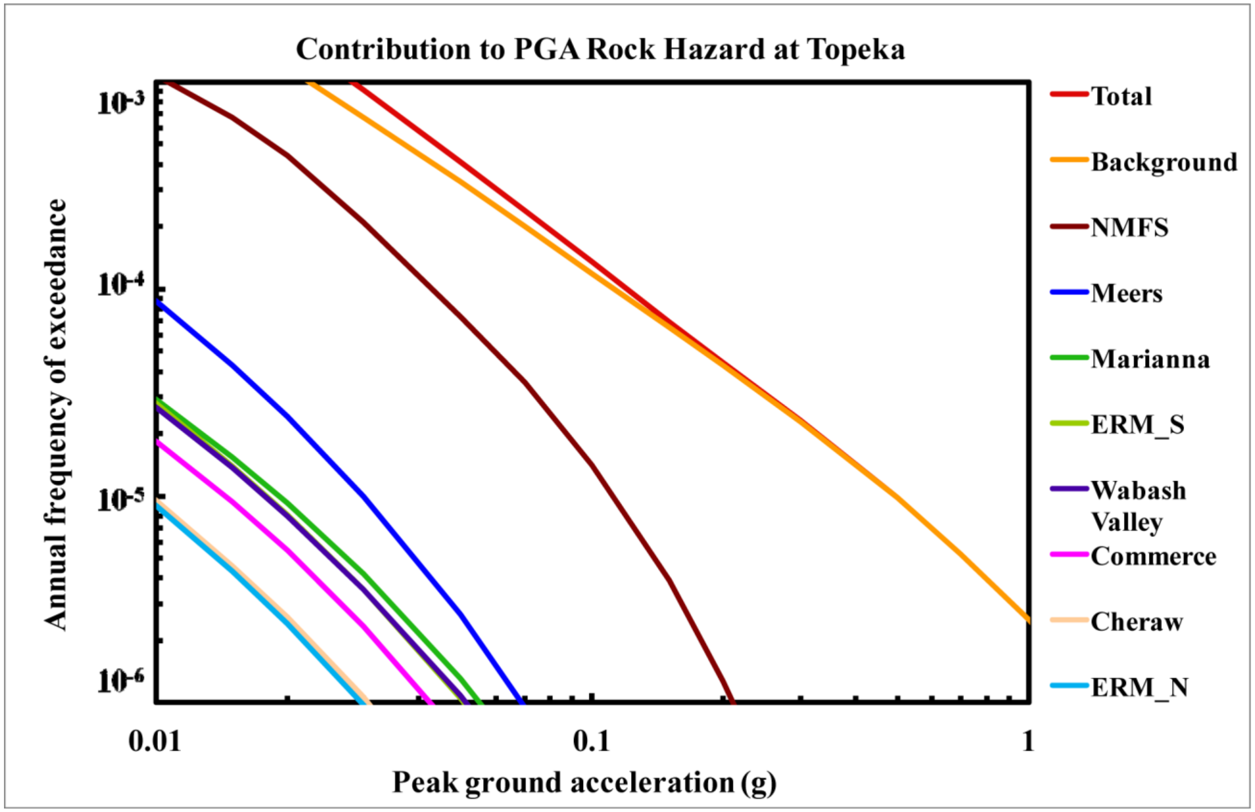

Figure 8.2-7f
Topeka PGA rock hazard: total and contribution by RLME and background

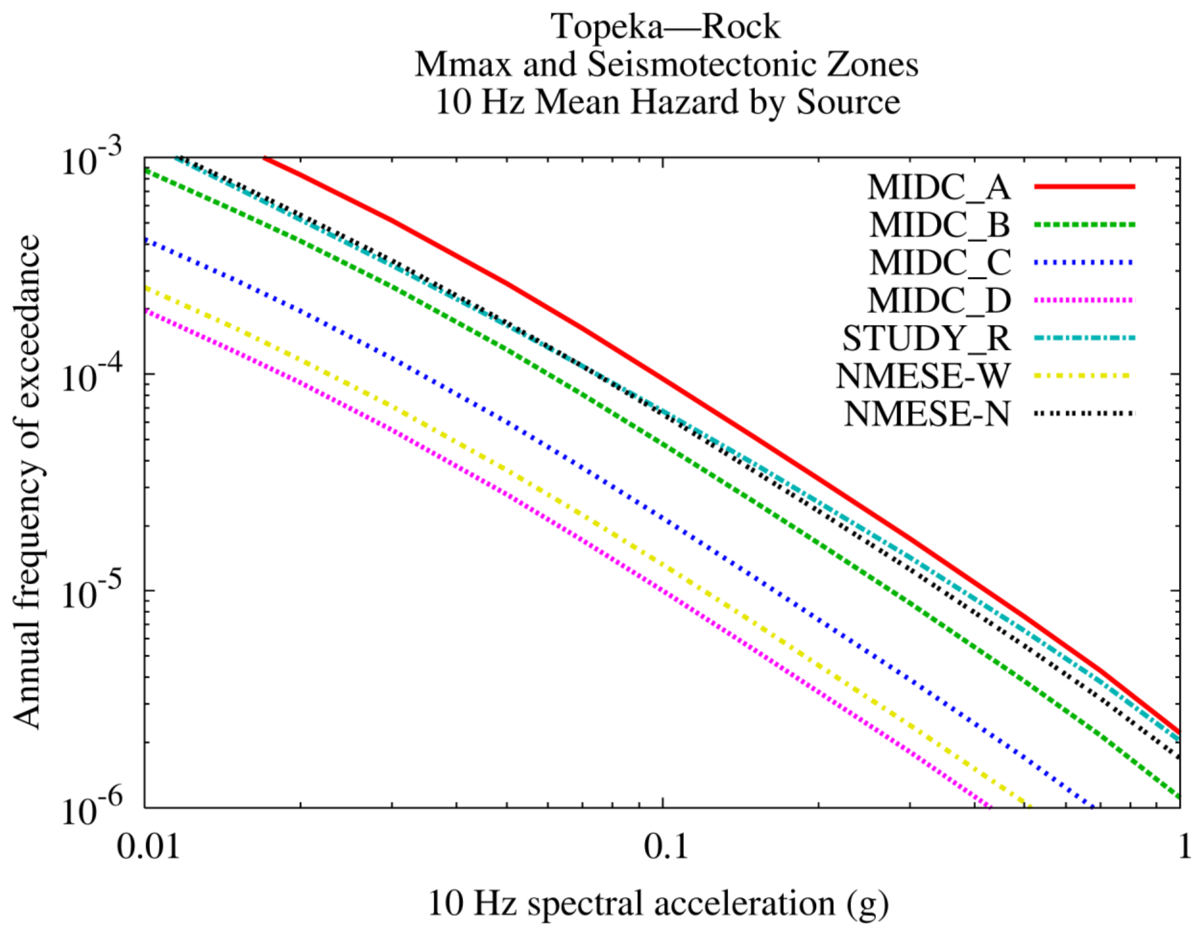

Figure 8.2-7g
Topeka 10 Hz rock hazard: contribution by background source

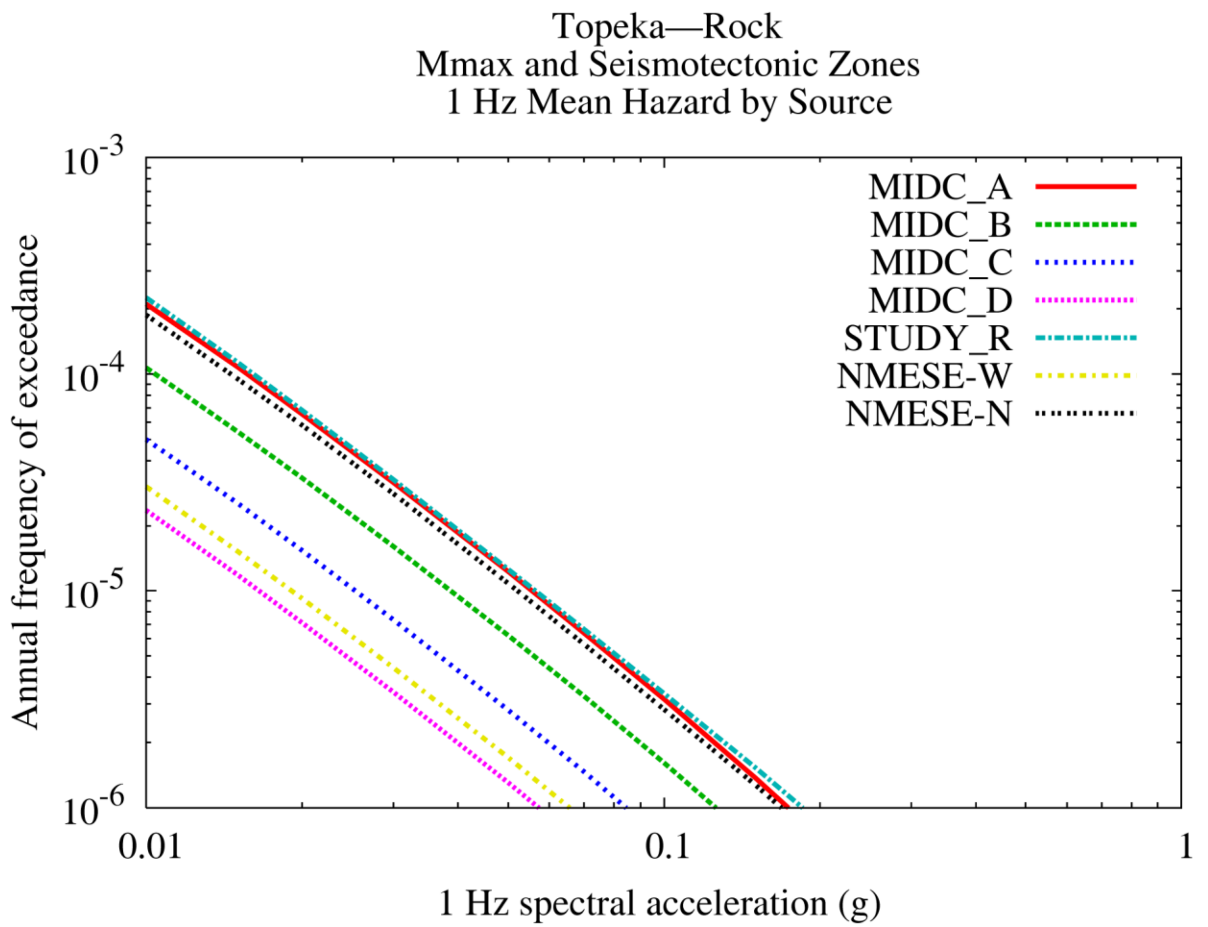

Figure 8.2-7h
Topeka 1 Hz rock hazard: contribution by background source

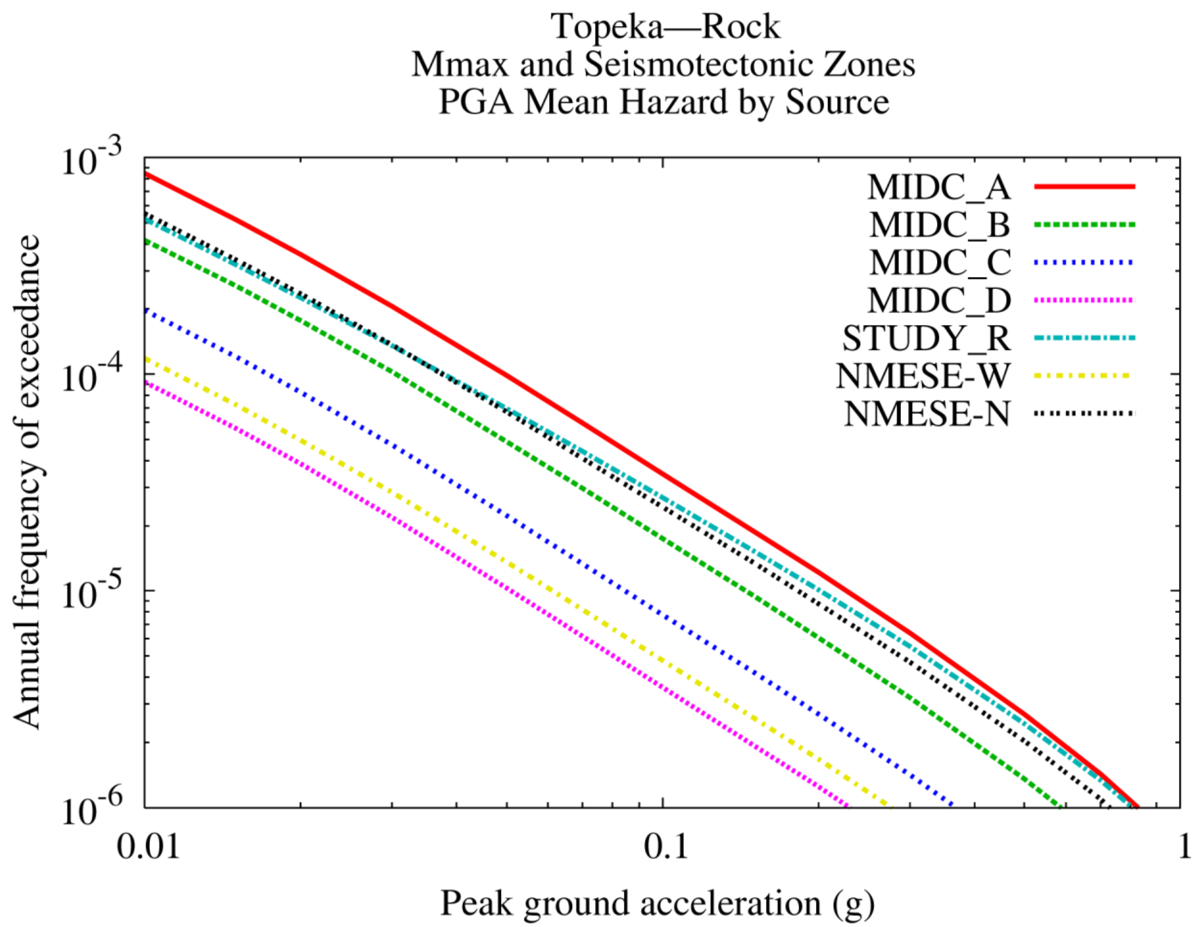

Figure 8.2-7i
Topeka PGA rock hazard: contribution by background source

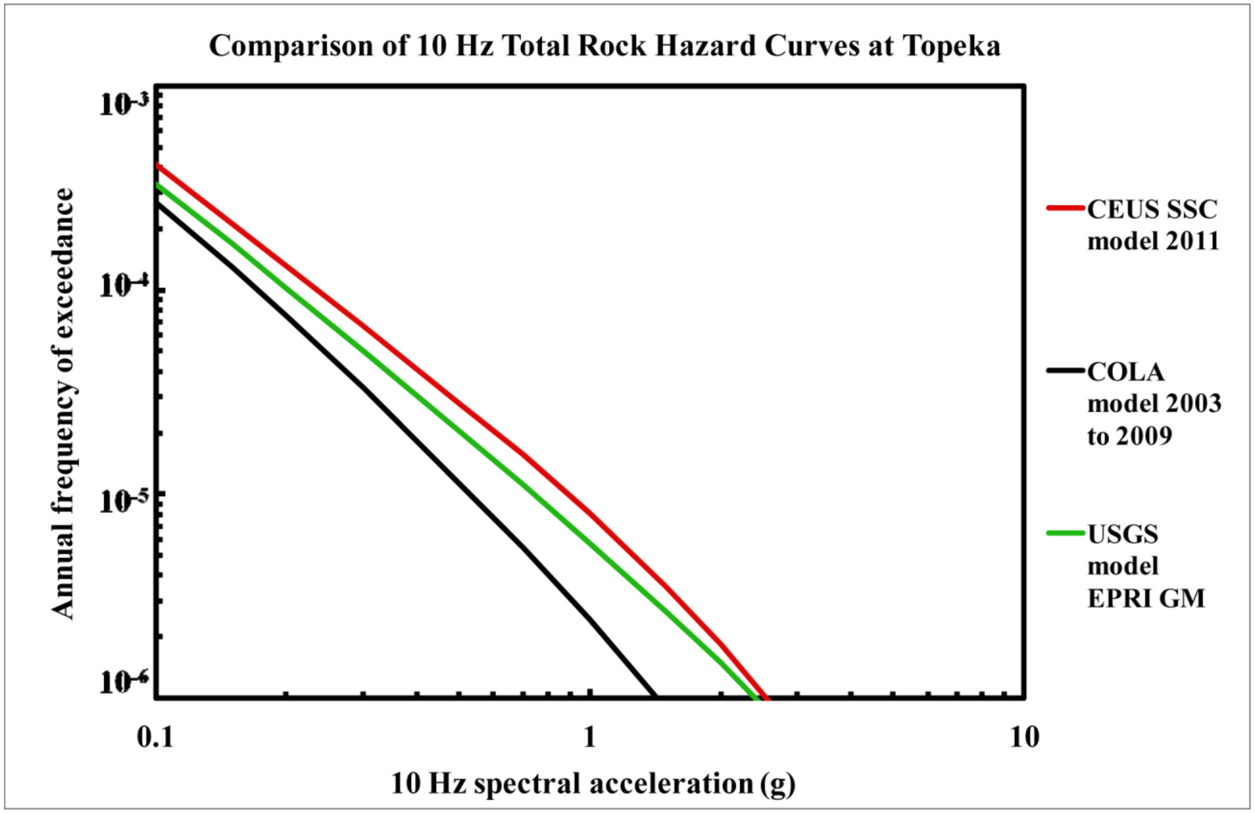

Figure 8.2-7j
Topeka 10 Hz rock hazard: comparison of three source models

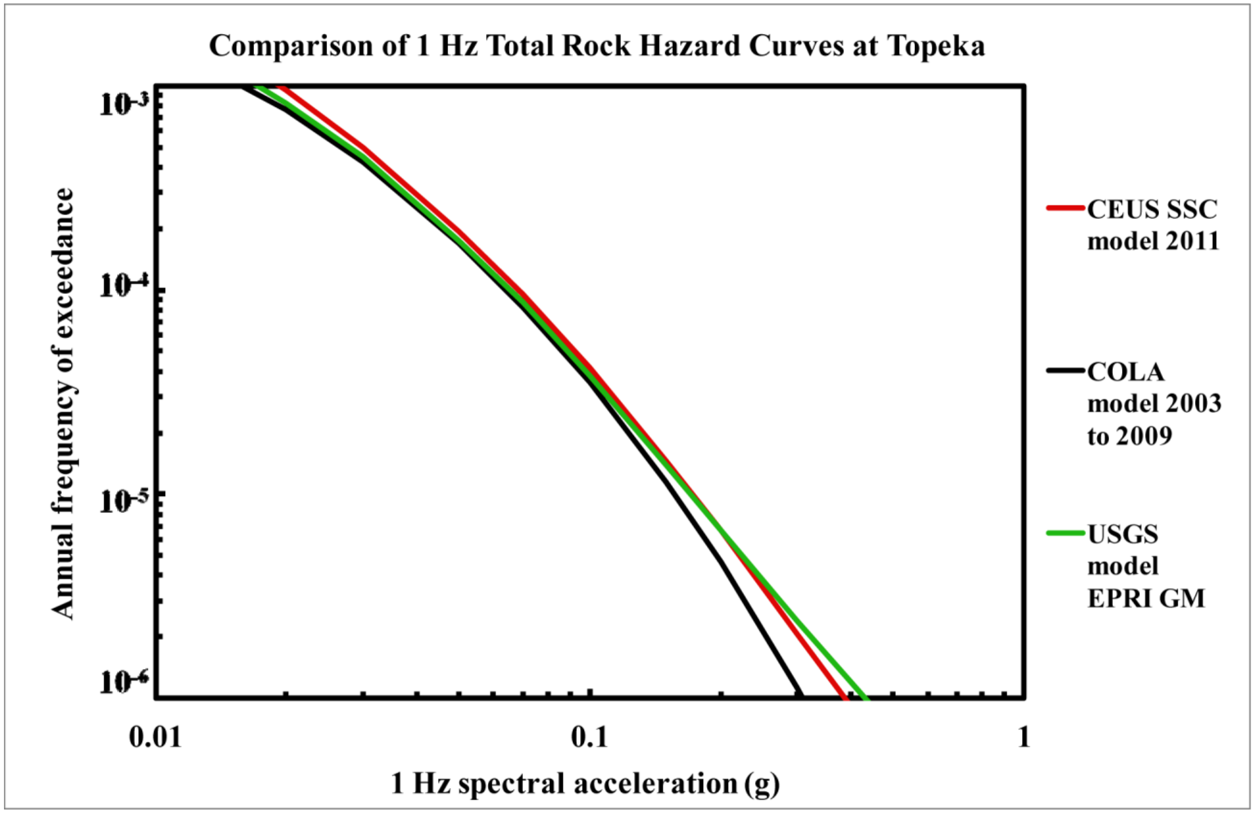

Figure 8.2-7k
Topeka is 1 Hz rock hazard: comparison of three source models

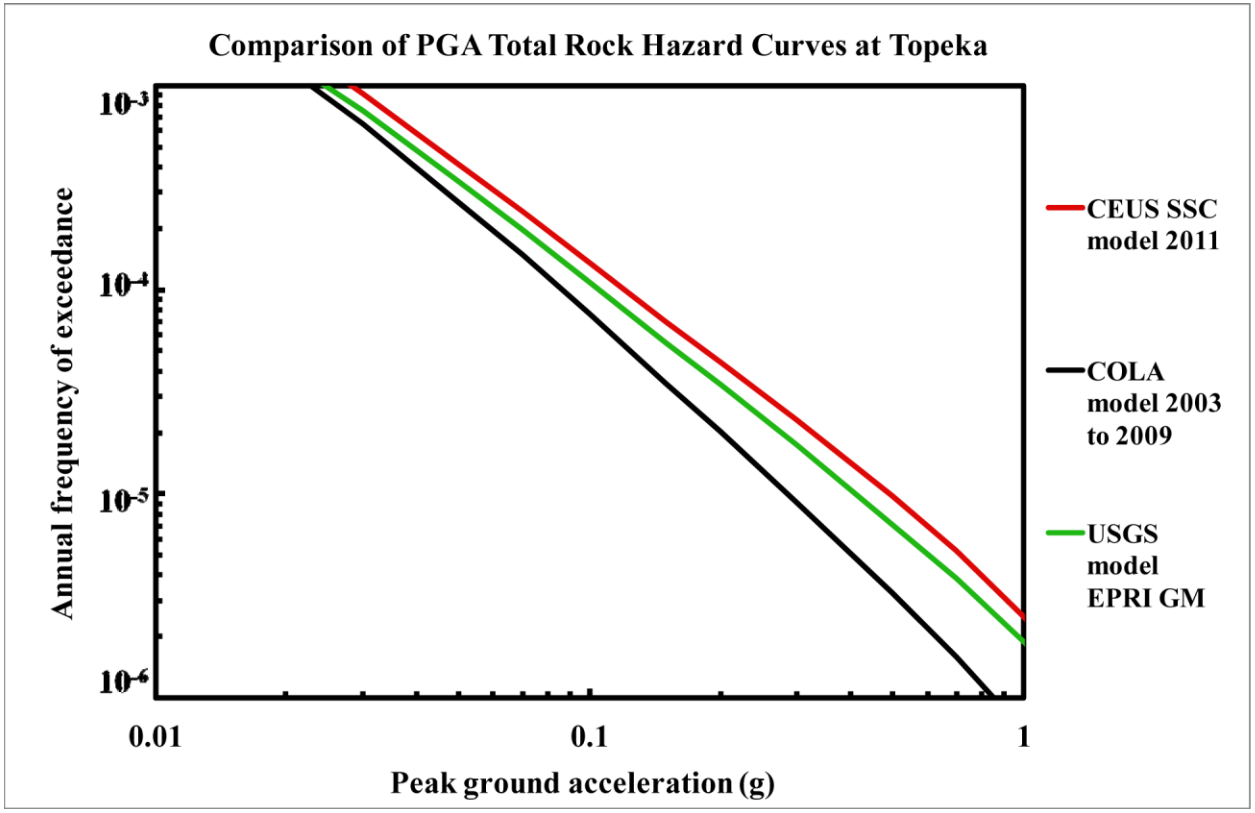

Figure 8.2-7l
Topeka PGA rock hazard: comparison of three source models

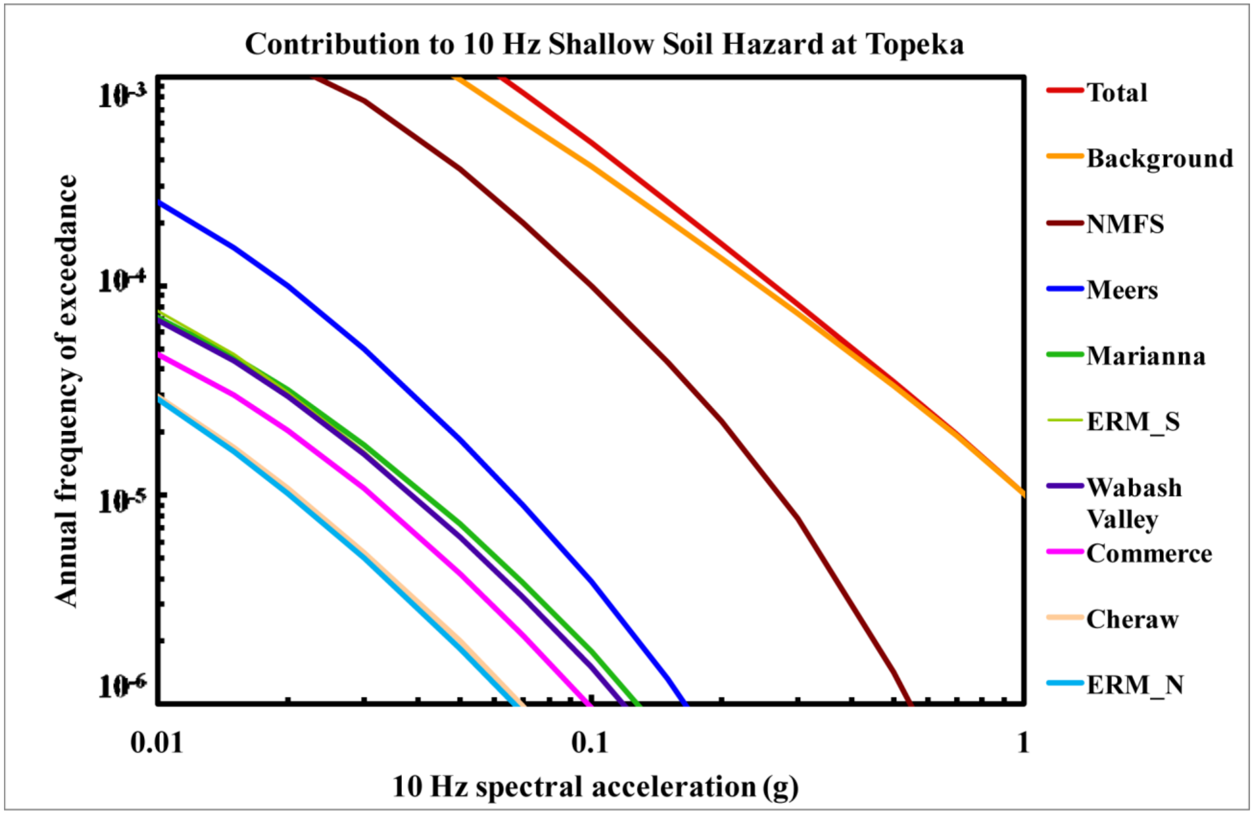

Figure 8.2-7m
Topeka 10 Hz shallow soil hazard: total and contribution by RLME and background

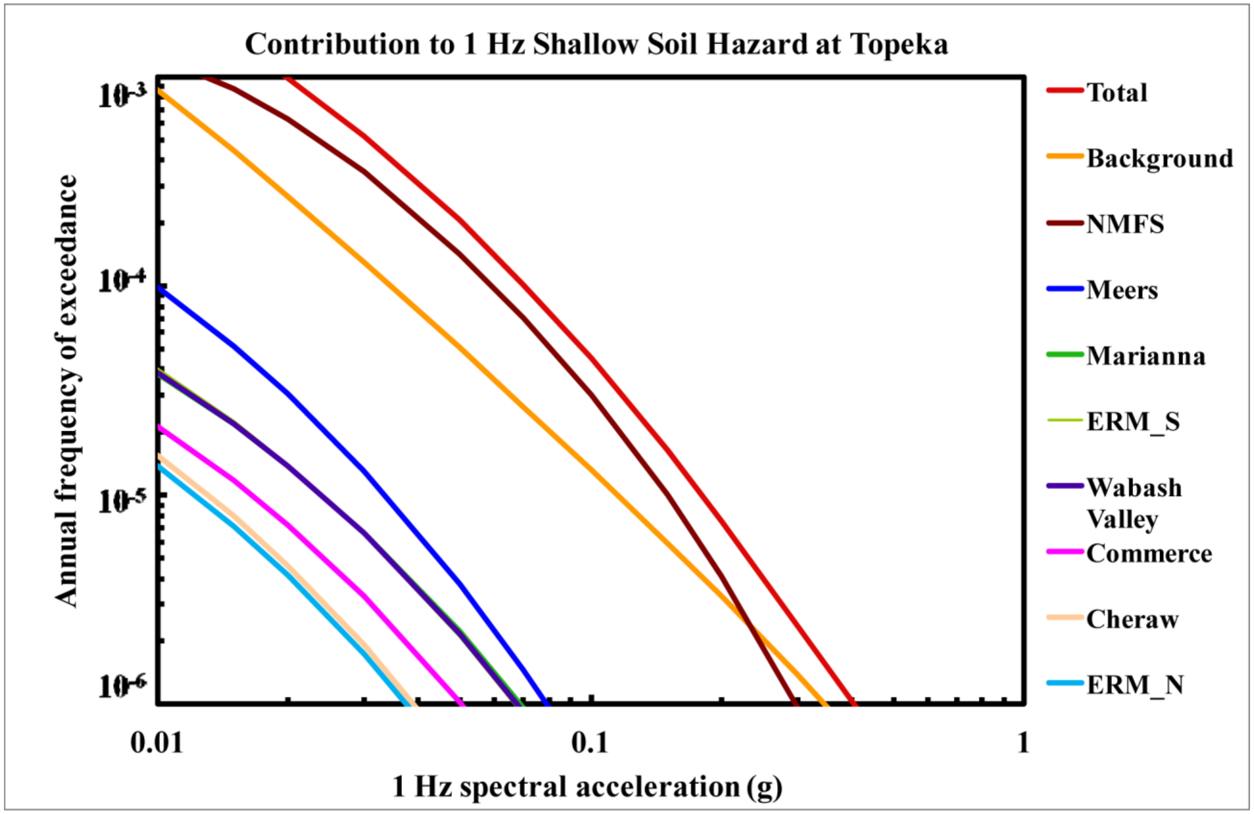

Figure 8.2-7n
Topeka 1 Hz shallow soil hazard: total and contribution by RLME and background

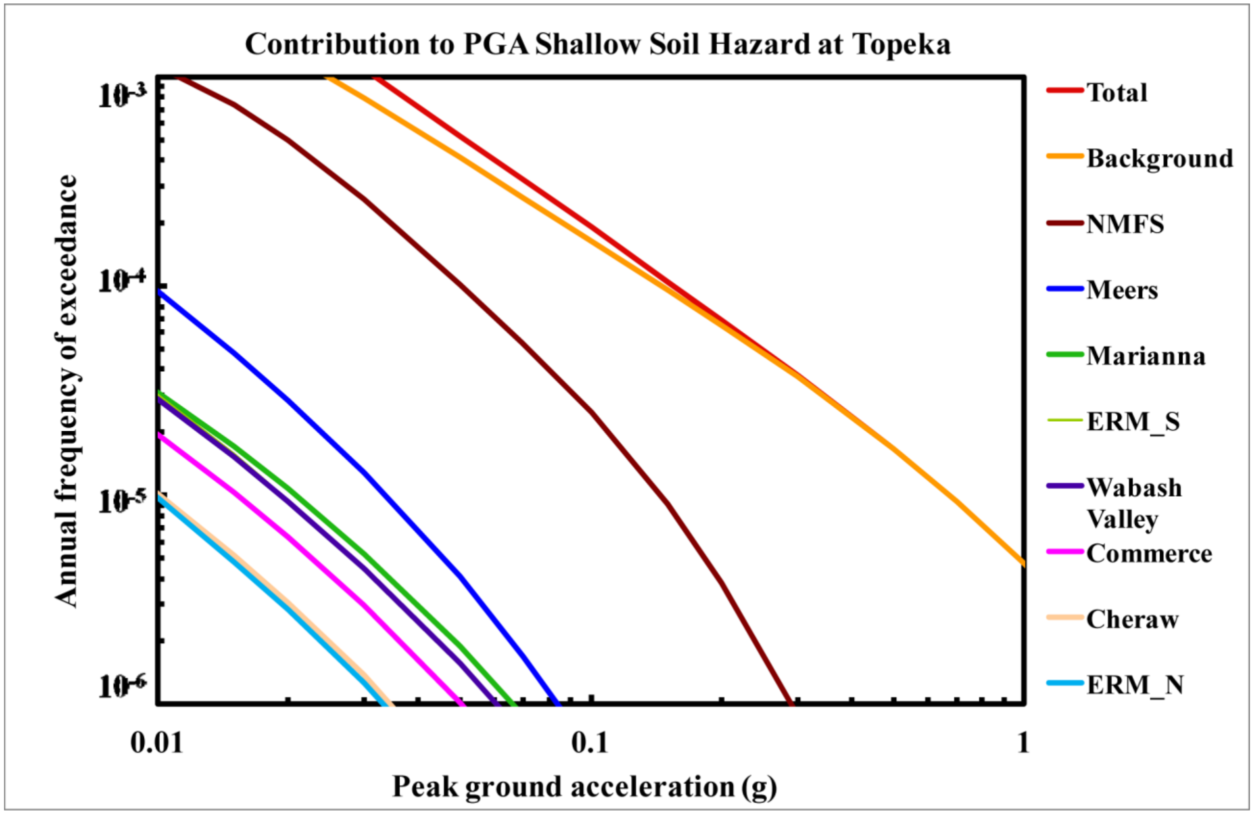

Figure 8.2-7o
Topeka PGA shallow soil hazard: total and contribution by RLME and background

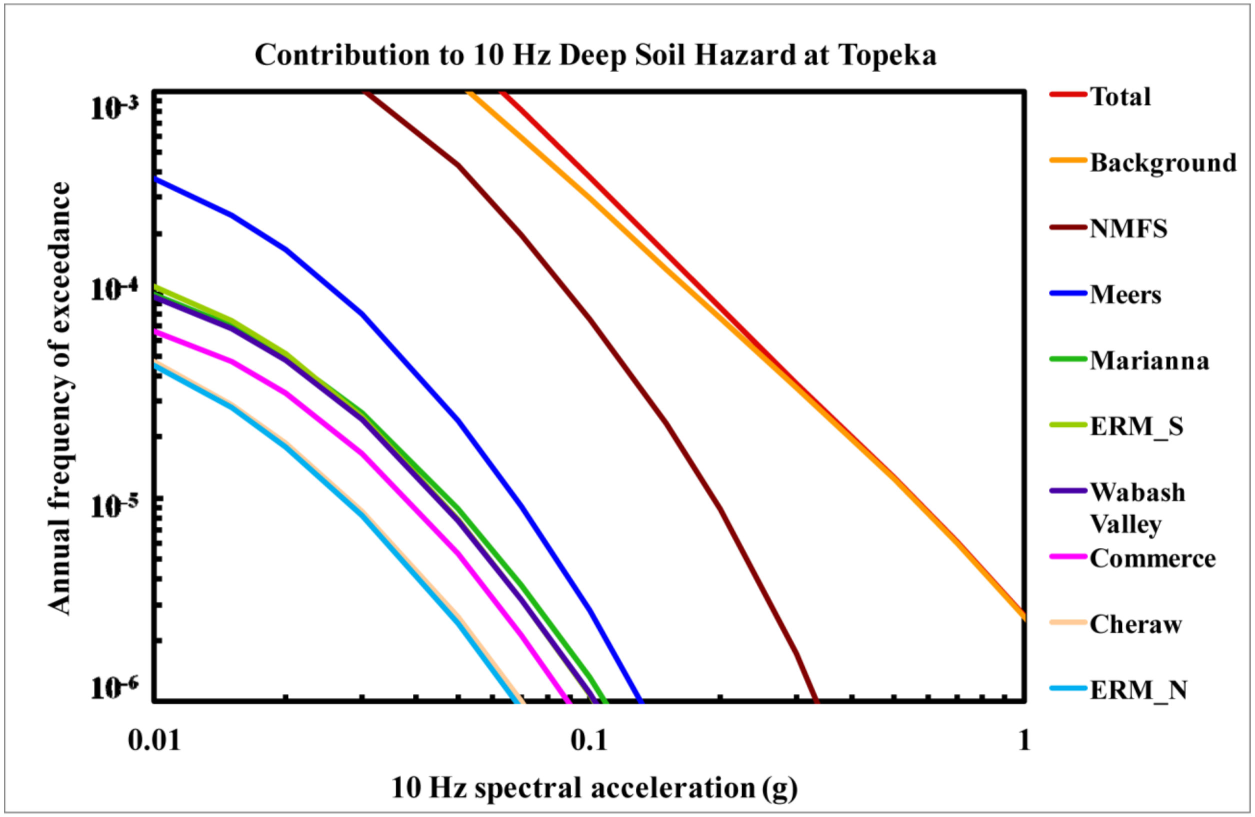

Figure 8.2-7p
Topeka 10 Hz deep soil hazard: total and contribution by RLME and background

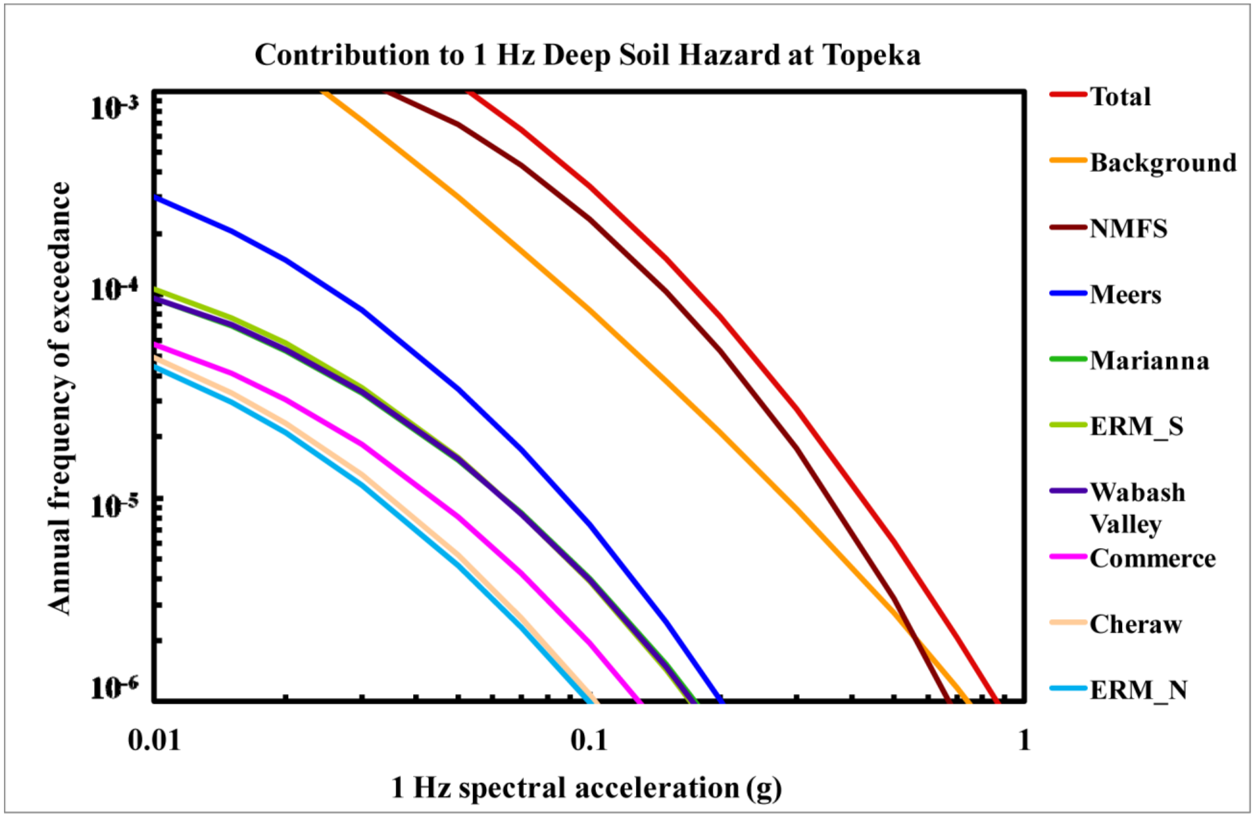

Figure 8.2-7q
Topeka 1 Hz deep soil hazard: total and contribution by RLME and background

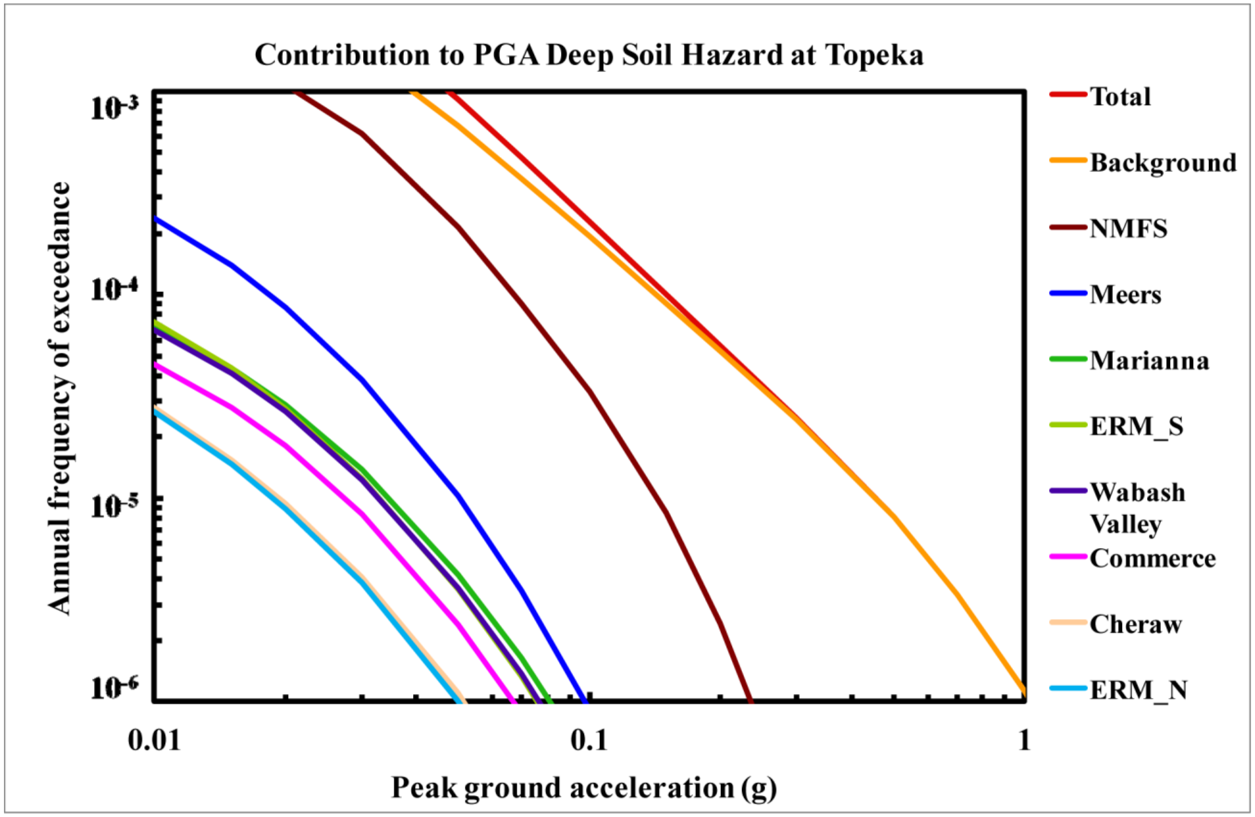

Figure 8.2-7r
Topeka PGA deep soil hazard: total and contribution by RLME and background

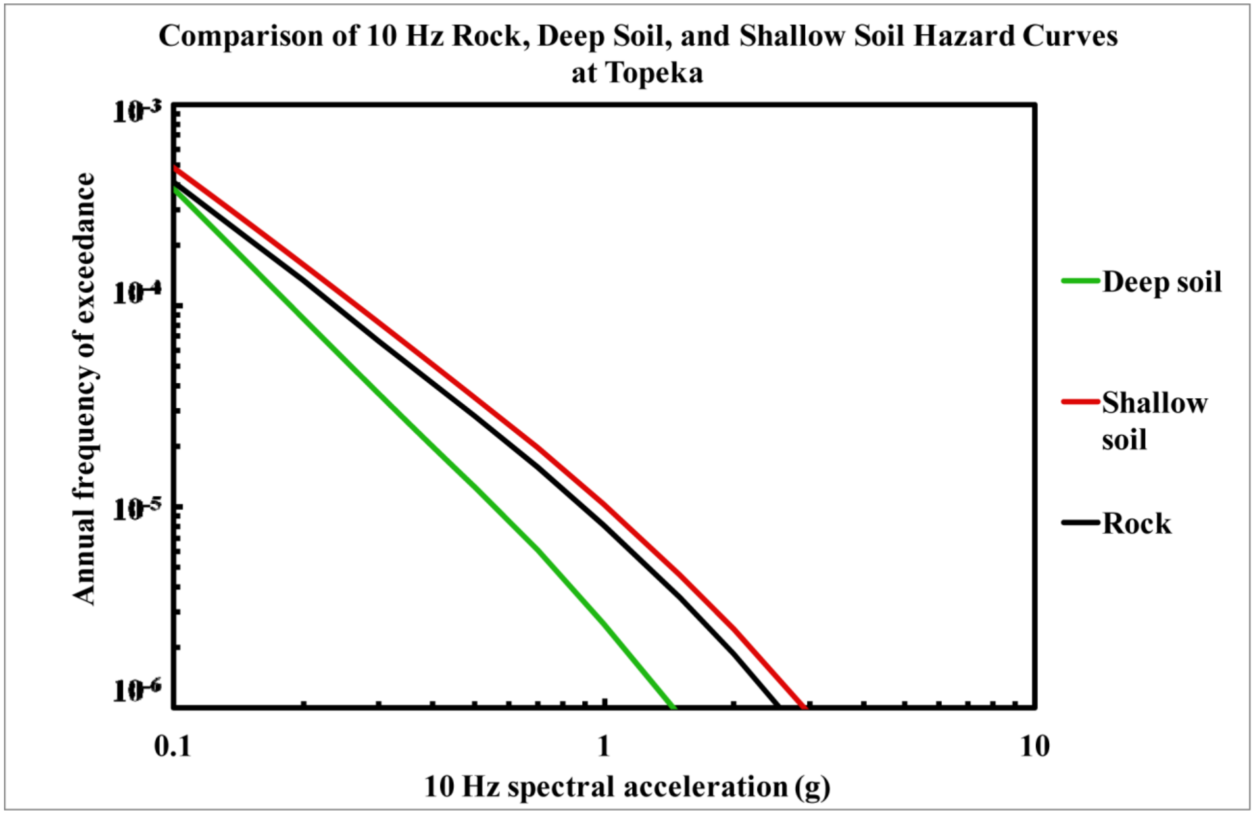

Figure 8.2-7s
Topeka 10 Hz hazard: comparison of three site conditions

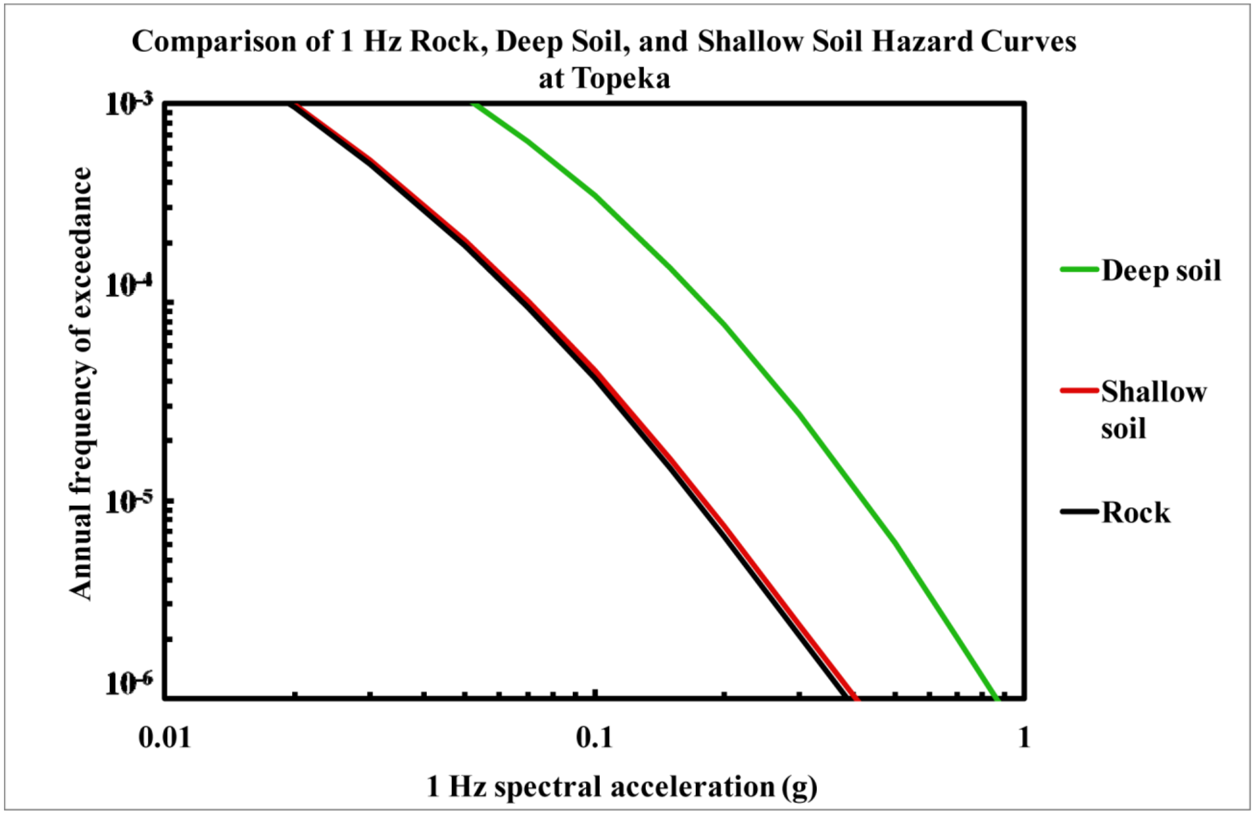

Figure 8.2-7t
Topeka 1 Hz hazard: comparison of three site conditions

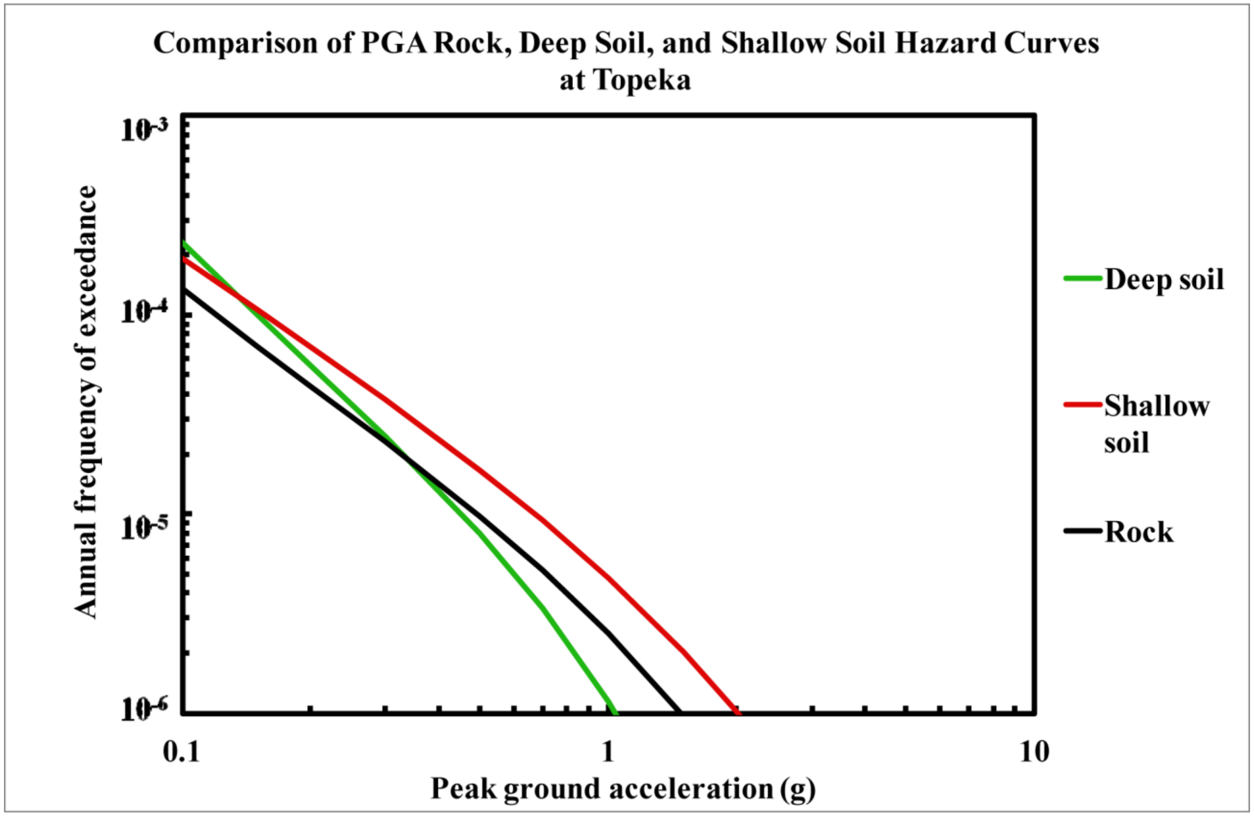

Figure 8.2-7u
Topeka PGA hazard: comparison of three site conditions

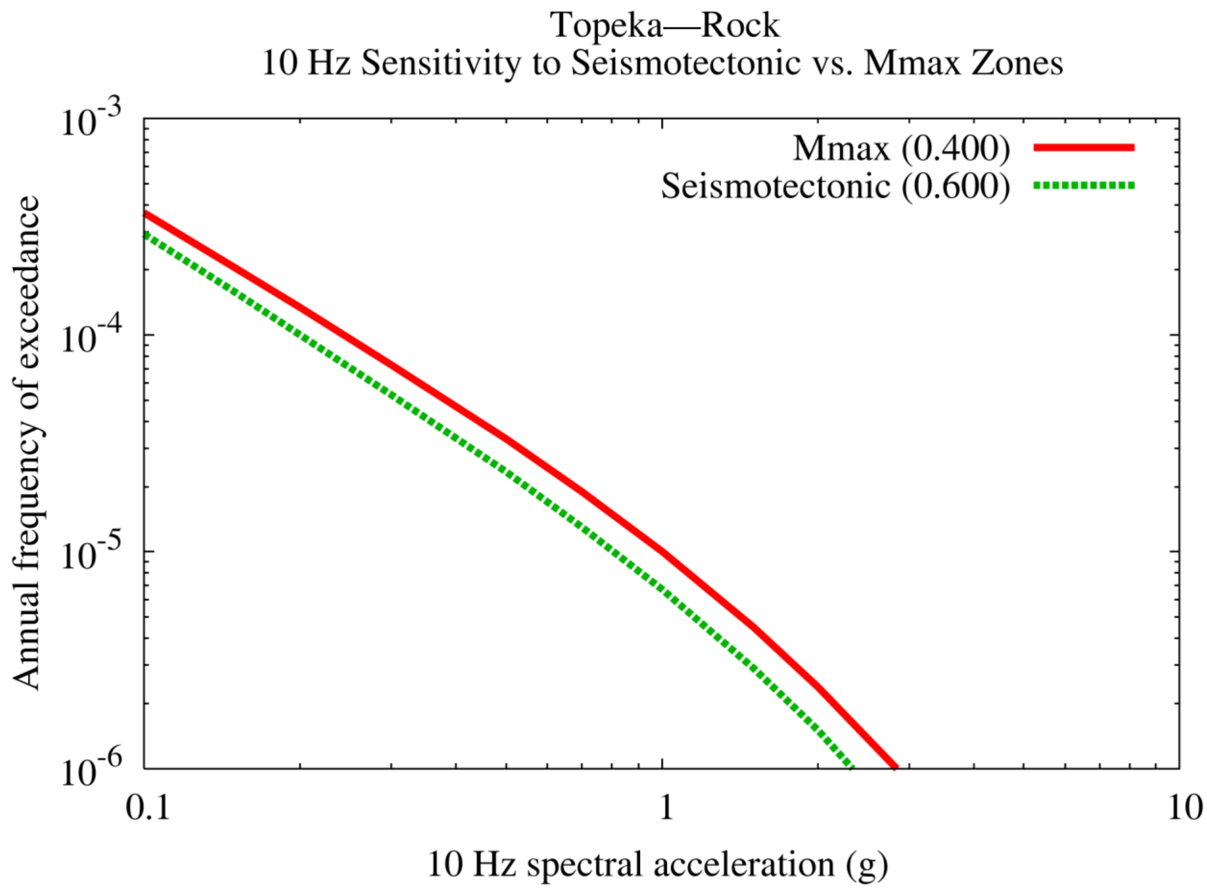

Figure 8.2-7v
Topeka 10 Hz rock hazard: sensitivity to seismotectonic vs. Mmax zones

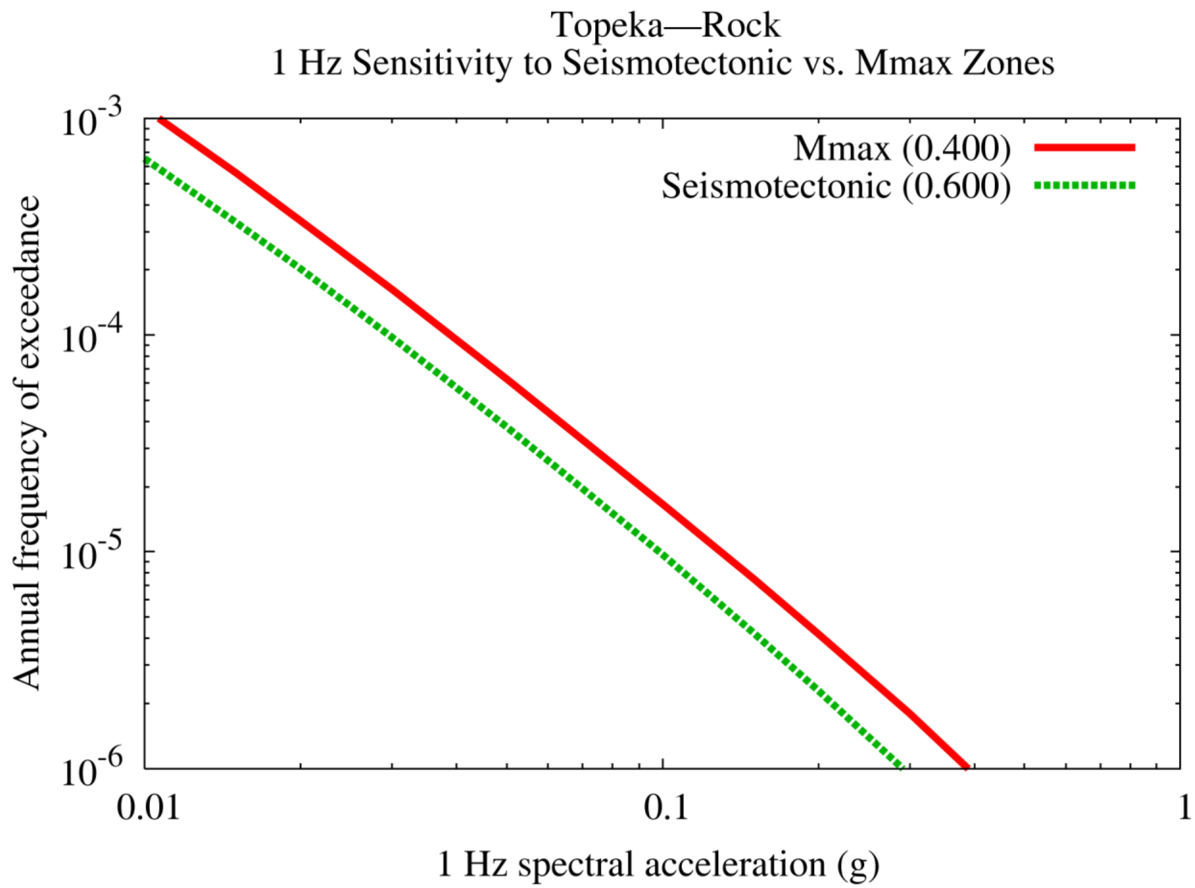

Figure 8.2-7w
Topeka 1 Hz rock hazard: sensitivity to seismotectonic vs. Mmax zones

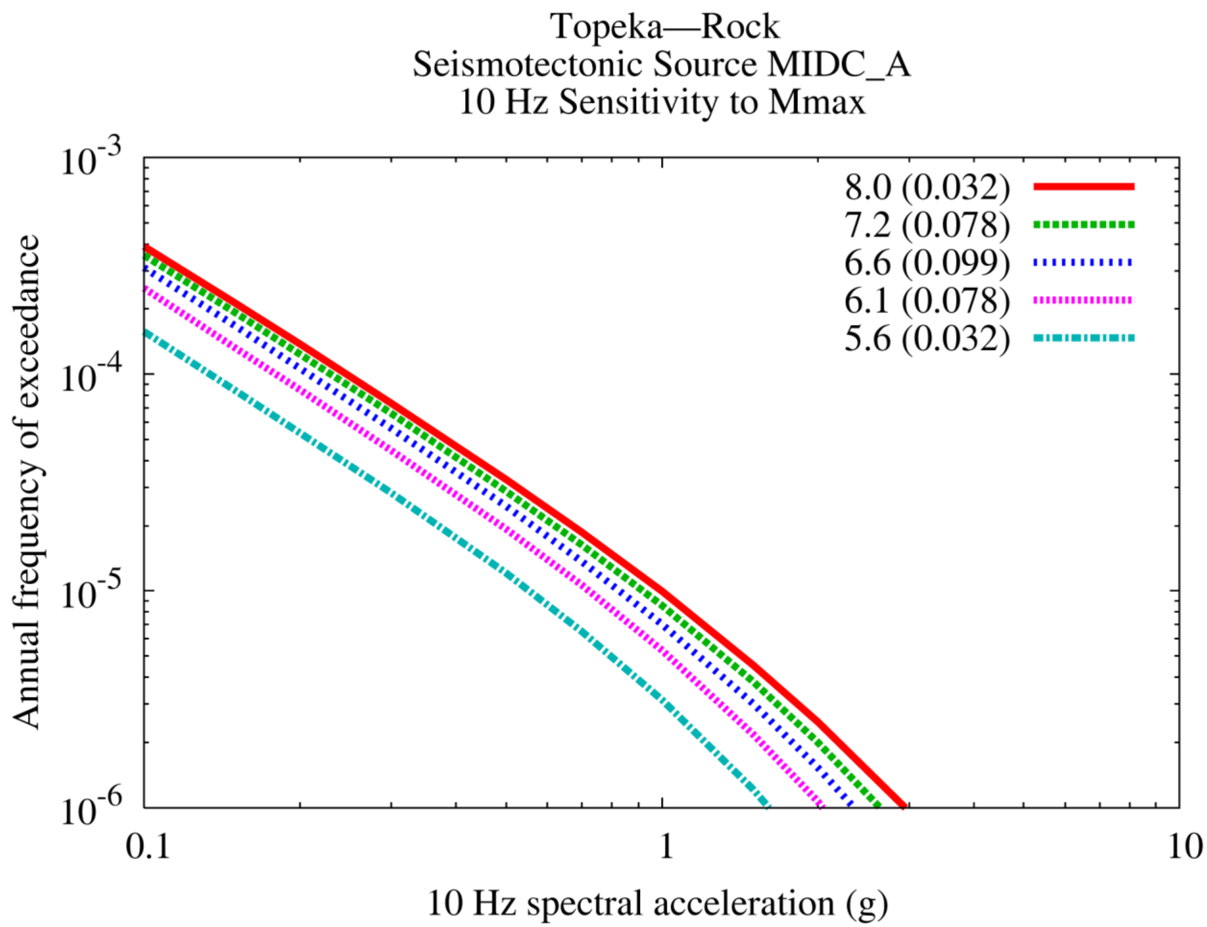

Figure 8.2-7x
Topeka 10 Hz rock hazard: sensitivity to Mmax for source MidC-A

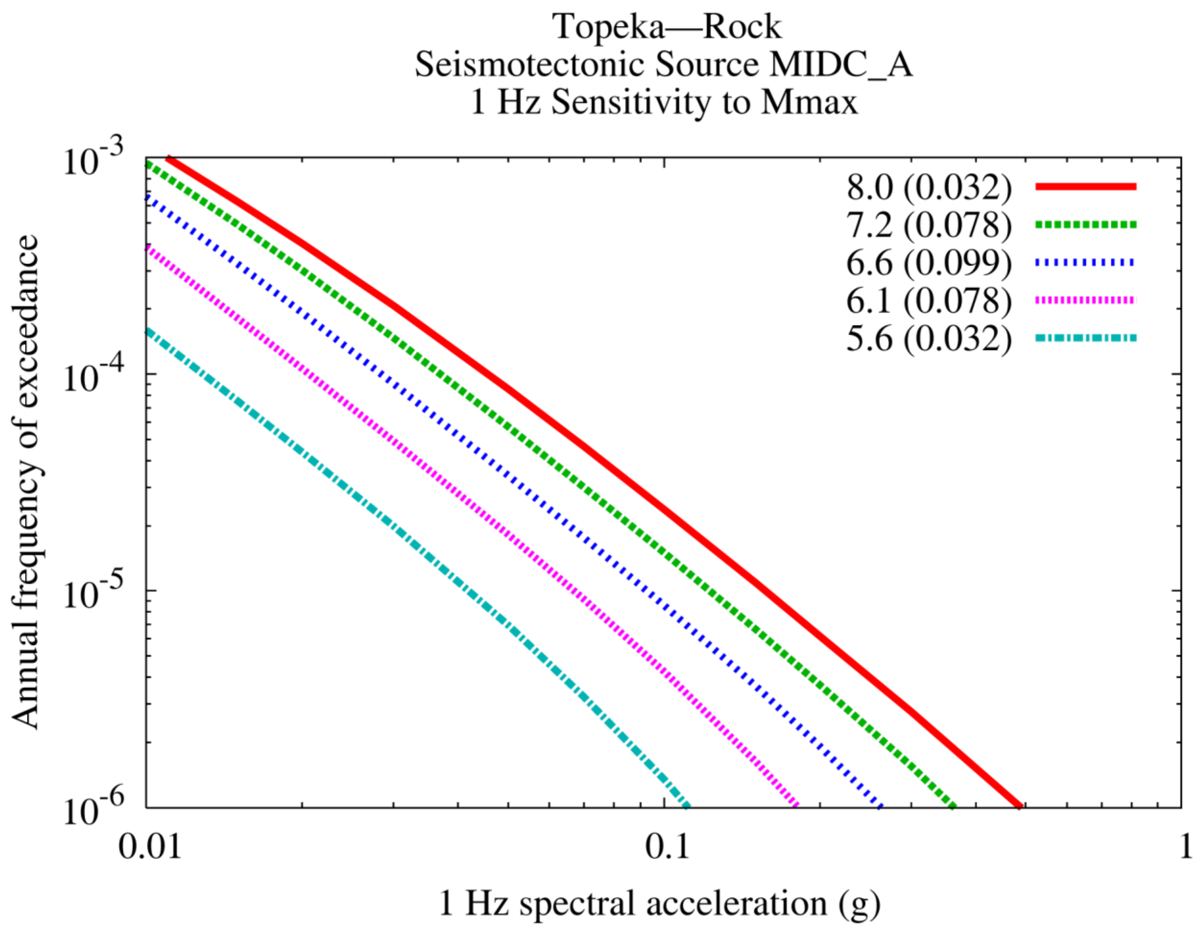

Figure 8.2-7y
Topeka 1 Hz rock hazard: sensitivity to Mmax for source MidC-A

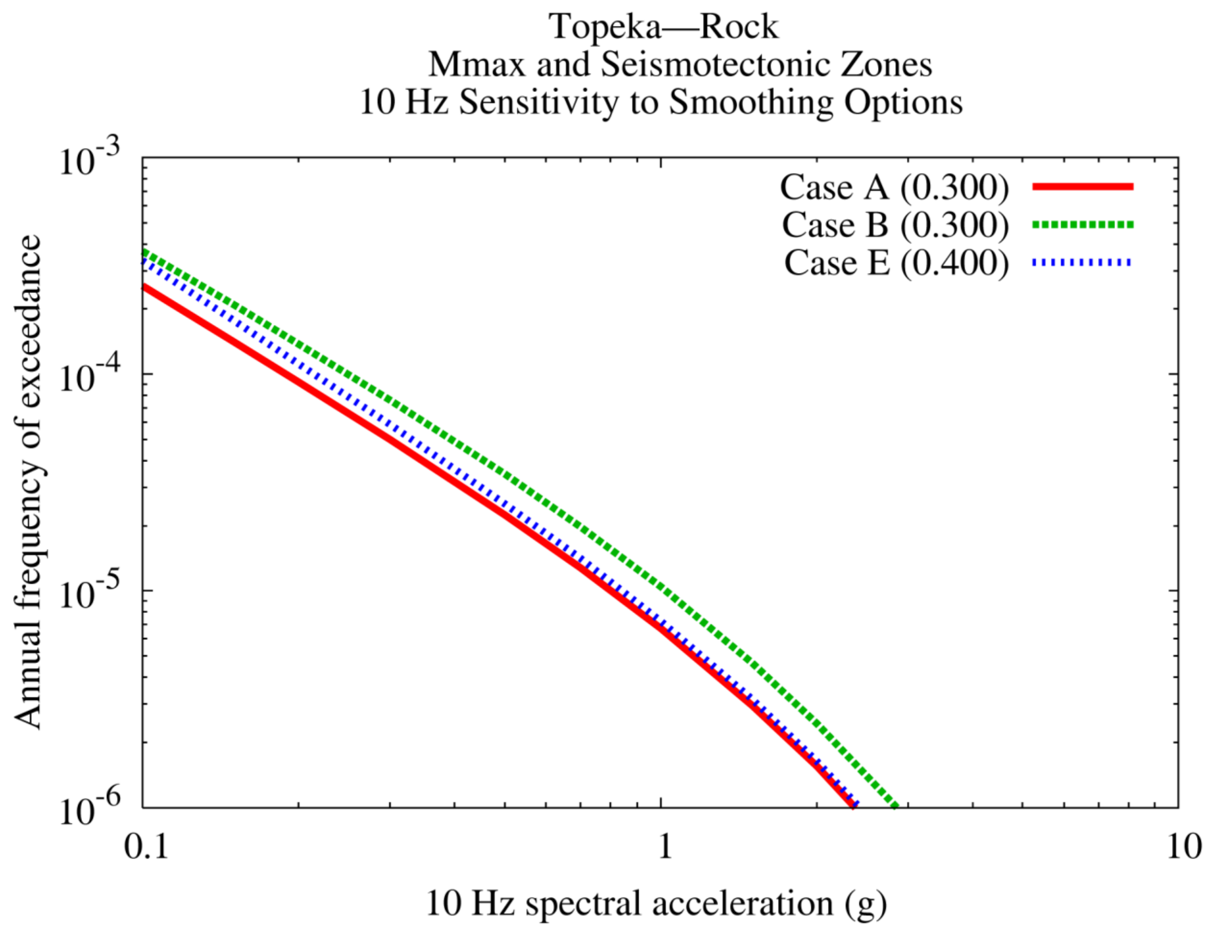

Figure 8.2-7z
Topeka 10 Hz rock hazard: sensitivity to smoothing options

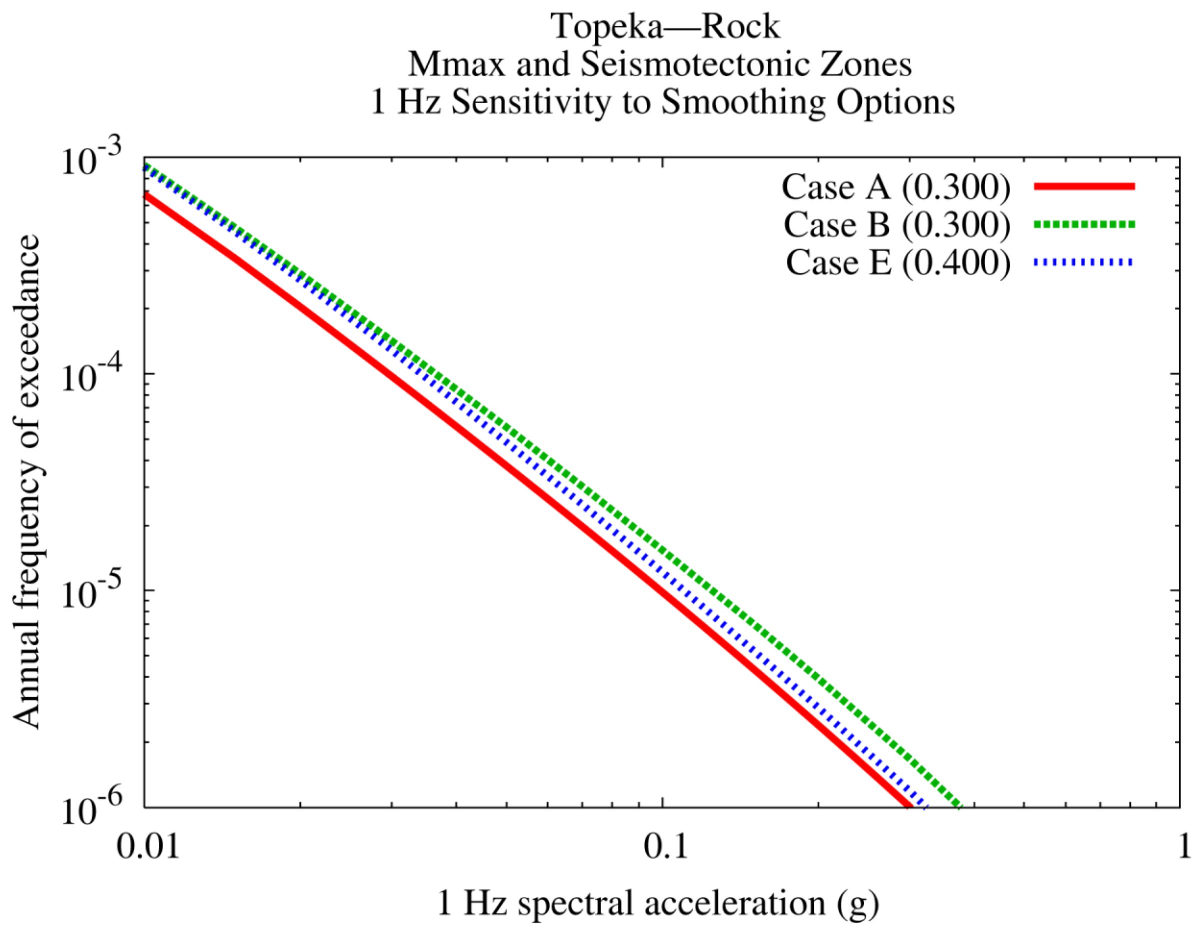

Figure 8.2-7aa
Topeka 1 Hz rock hazard: sensitivity to smoothing options

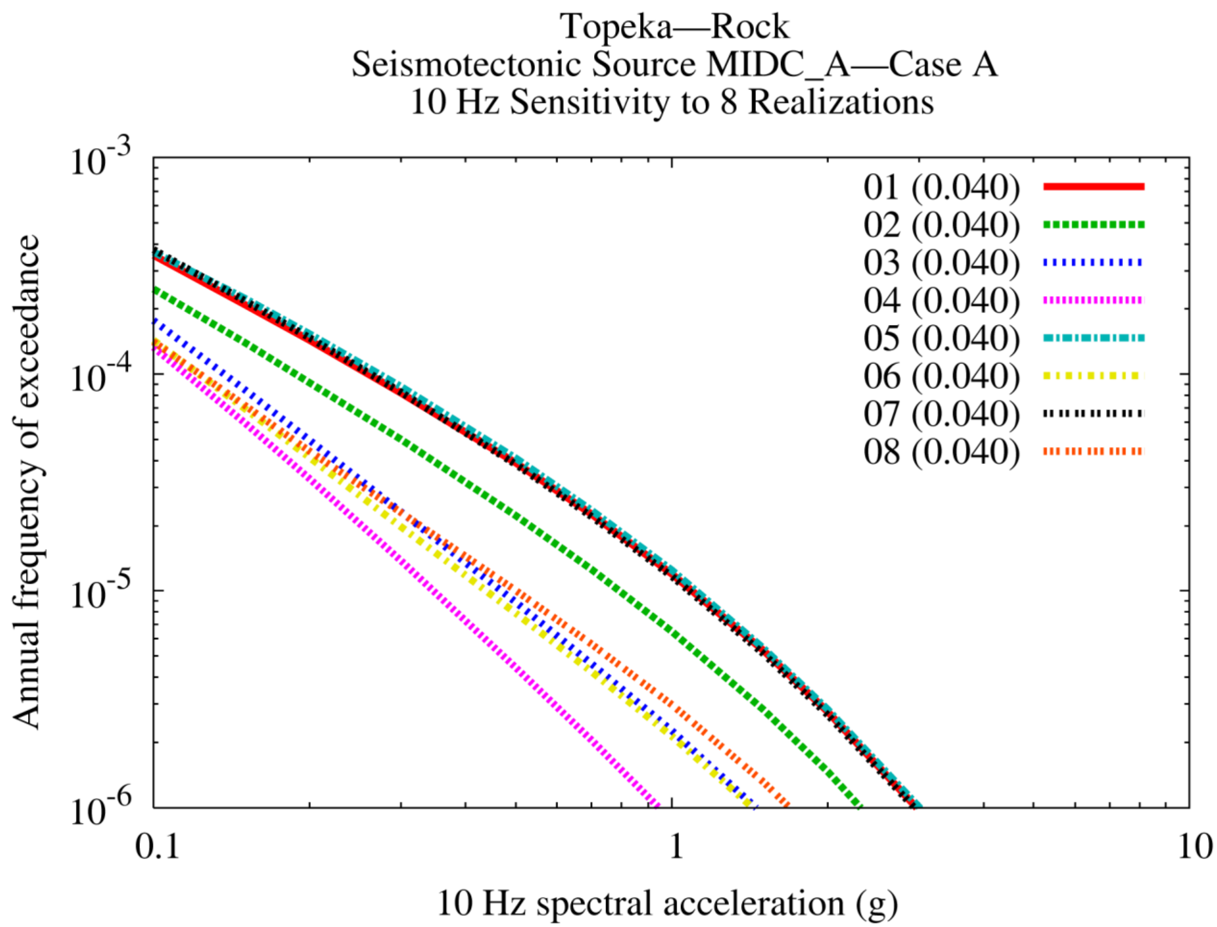

Figure 8.2-7bb
Topeka 10 Hz rock hazard: sensitivity to eight realizations for source MidC-A, Case A

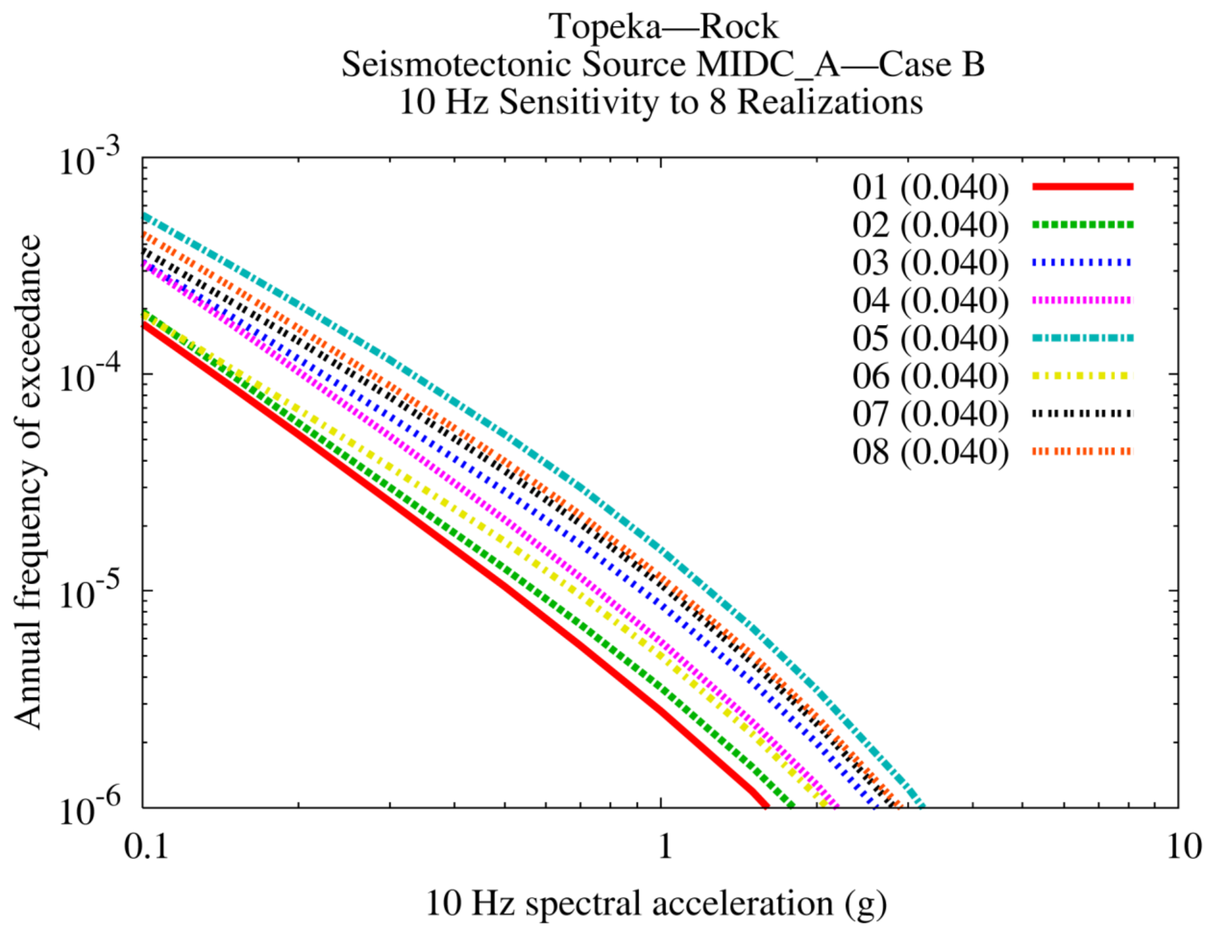

Figure 8.2-7cc
Topeka 10 Hz rock hazard: sensitivity to eight realizations for source MidC-A, Case B

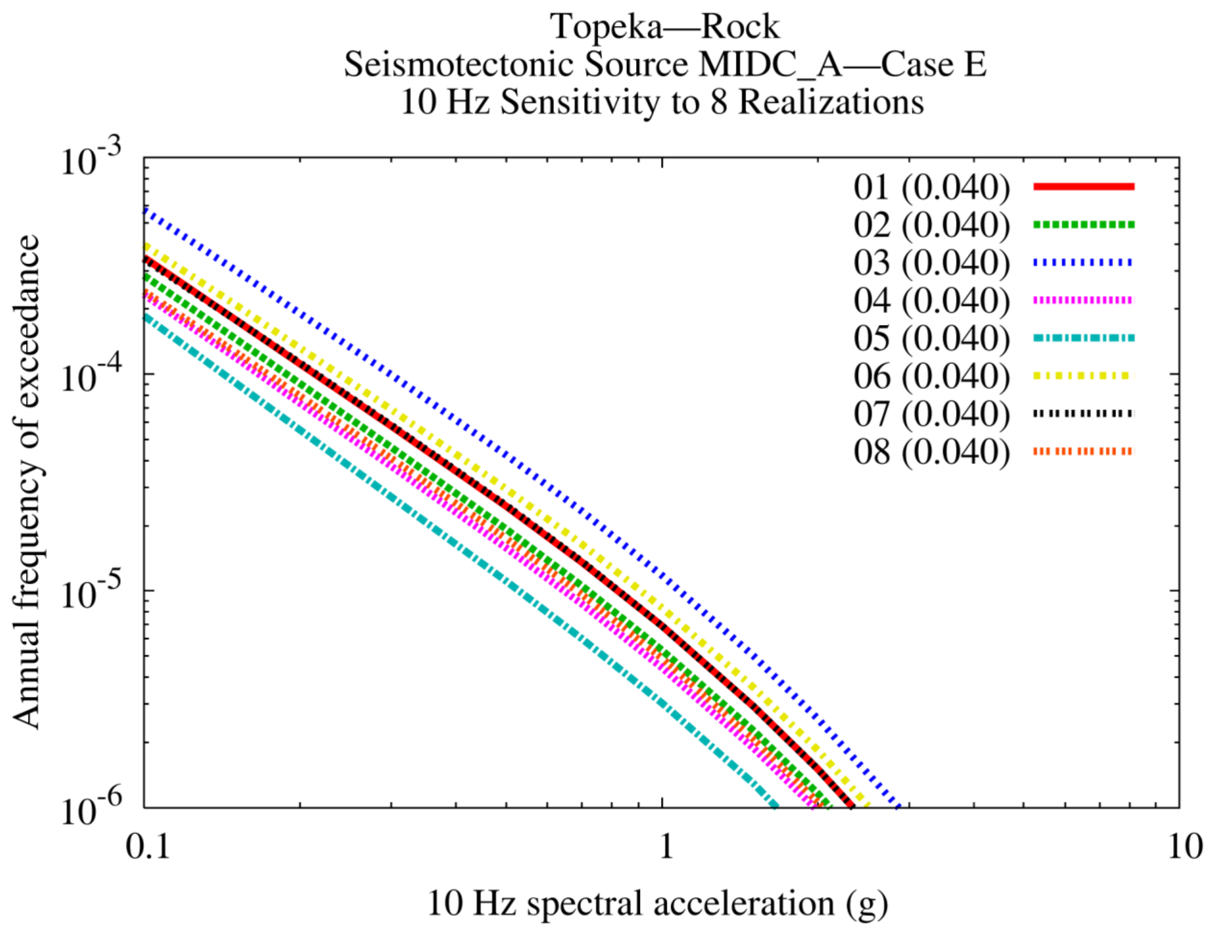

Figure 8.2-7dd
Topeka 10 Hz rock hazard: sensitivity to eight realizations for source MidC-A, Case E

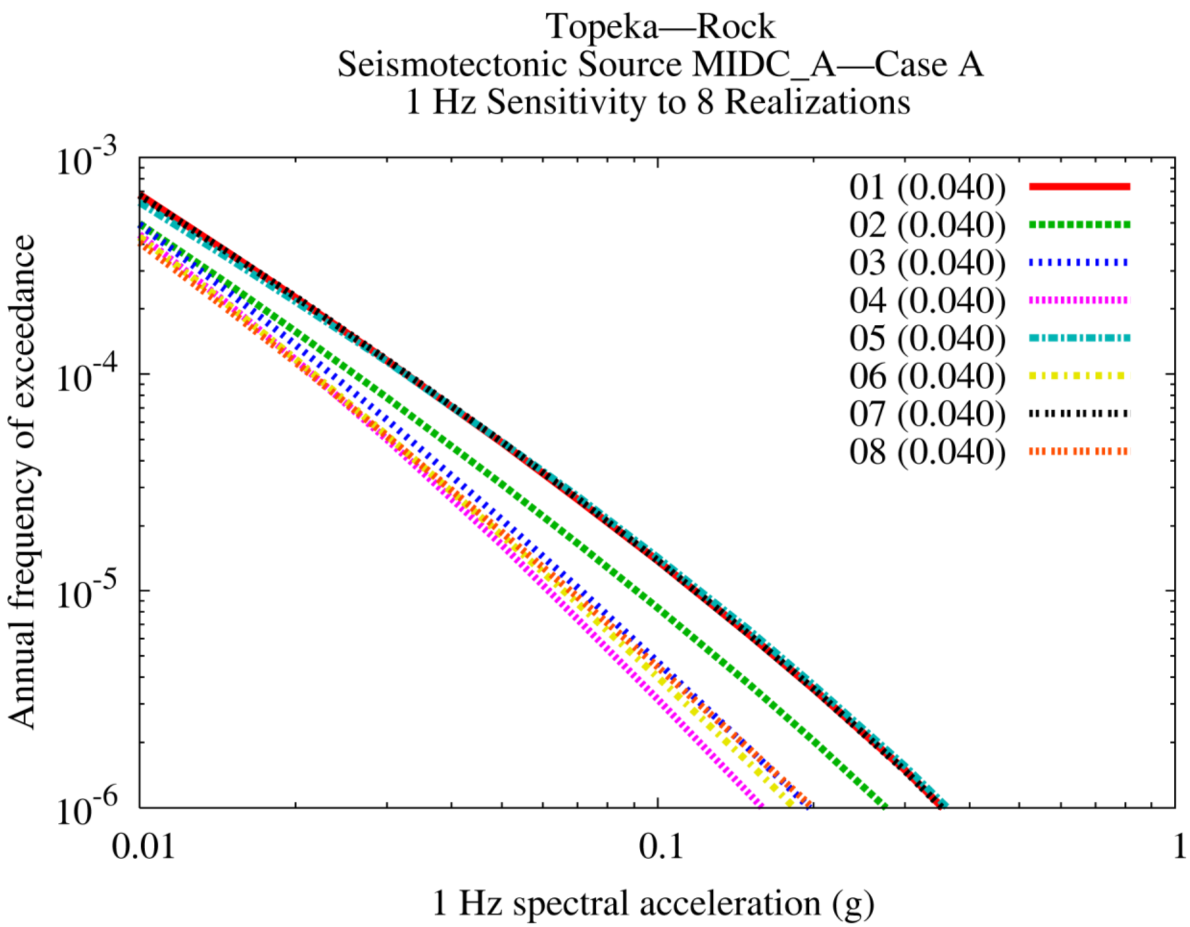

Figure 8.2-7ee
Topeka 1 Hz rock hazard: sensitivity to eight realizations for source MidC-A, Case A

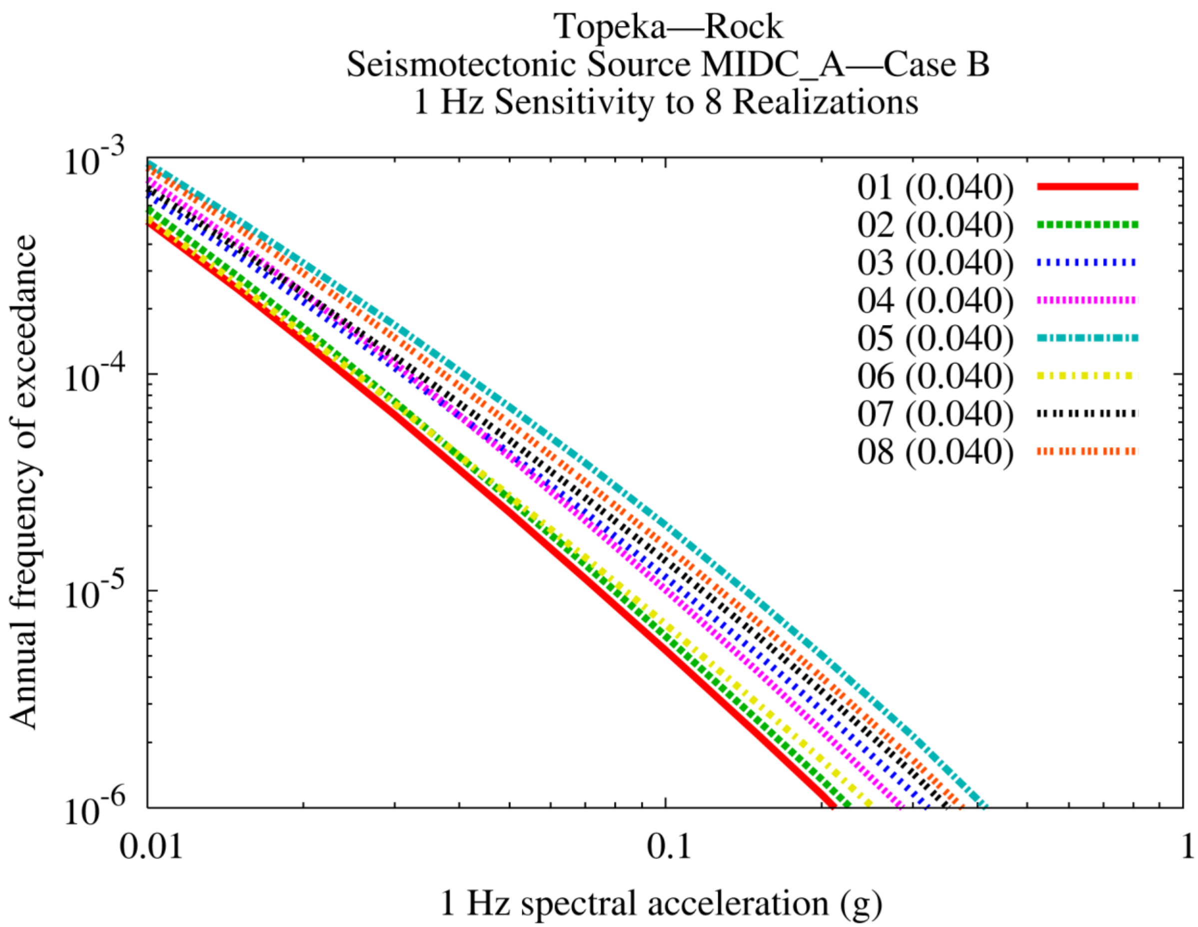

Figure 8.2-7ff
Topeka 1 Hz rock hazard: sensitivity to eight realizations for source MidC-A, Case B

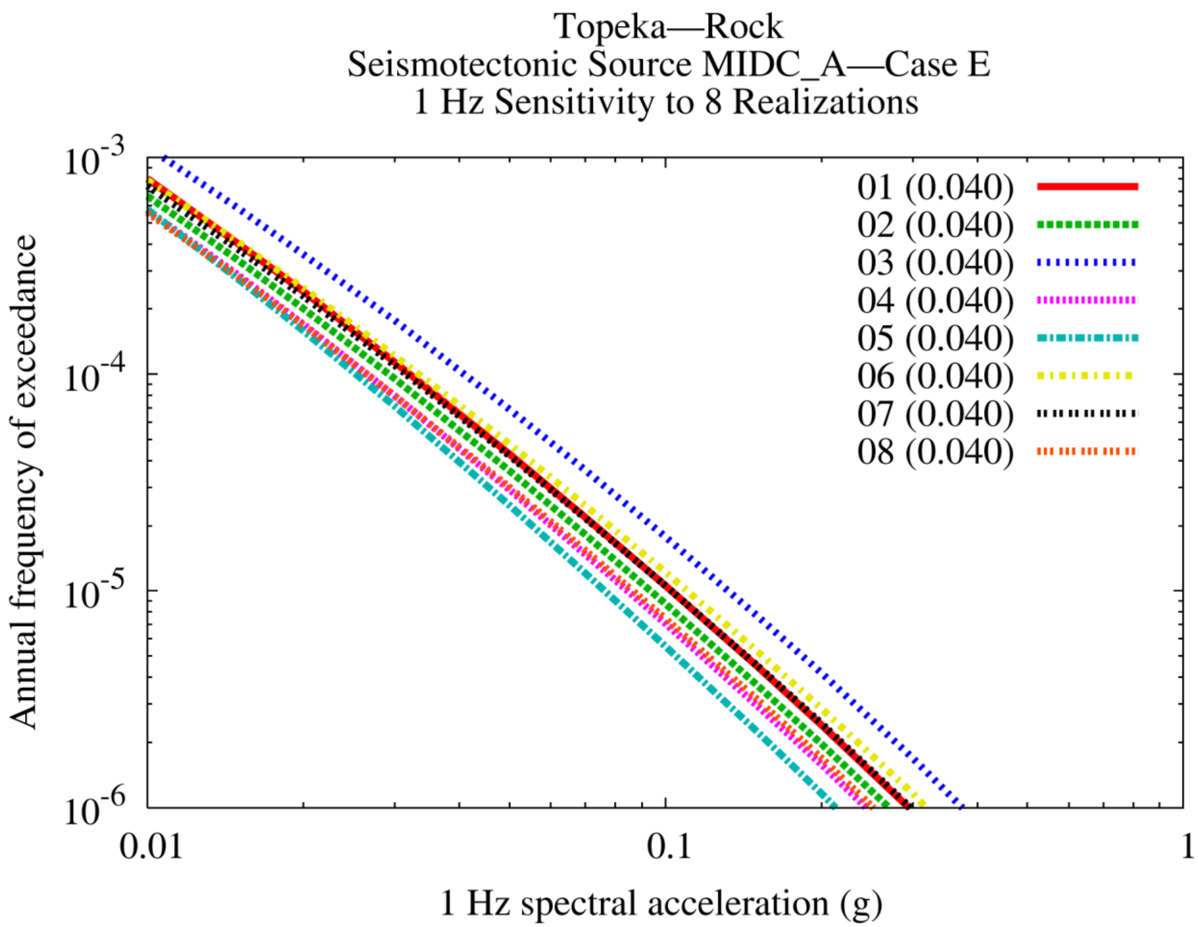

Figure 8.2-7gg
Topeka 1 Hz rock hazard: sensitivity to eight realizations for source MidC-A, Case E

9

CHAPTER 9
USE OF THE CEUS SSC MODEL IN PSHA

9.1 Overview

This section is intended to provide the reader with information about the future use of the CEUS SSC model for purposes of PSHA. Much of the guidance provided in this section is pragmatic and aimed at assisting the user such that the subsequent calculational process is optimized but the accuracy of the SSC model is maintained. The CEUS SSC model was developed within the framework of a SSHAC Level 3 process, and all the required steps were taken to implement the letter and the spirit of the SSHAC guidelines (Budnitz et al., 1997). Chapter 2 describes those process steps in some detail. A key step in achieving this goal has been the careful consideration of alternative data, models, and methods, and—using the hazard-informed approach discussed in Section 4.1.3.1—incorporating the center, body, and range of technically defensible interpretations into the SSC model. In this sense, the SSC model has been "optimized" to include only those assessments that capture present knowledge and uncertainties and are believed to be significant to hazard. Once this level of uncertainty treatment was reached, there was no further attempt to optimize or reduce the complexity of the model for purposes of subsequent calculational efficiency.

The CEUS SSC model is a regional model, developed explicitly to calculate seismic hazard at nuclear facilities. For site-specific applications—consistent with the applicable regulatory guidance for the nuclear facility of interest—local data sets will need to be reviewed and possible site-specific refinements made to the model to account for local information. This could include consideration of local geologic structures or local seismic sources that were not considered in this regional SSC model. In addition, the SSC model will need to be paired with a comparable ground-motion characterization (GMC) model to perform hazard calculations. The SSC model was developed with due consideration of the likely types of information that would be needed for these GMC models (see Section 5.4). For example, each seismic source is characterized by its style of faulting and likely future rupture geometries.

The end product of the SSHAC process—and the deliverable for PSHA calculations—is the hazard input document (HID), which is discussed below in Section 9.2 and is provided in Appendix H. Instructions for implementing the HID are given in Section 9.3, with an eye toward simplifications that can be made for future applications without sacrificing accuracy. Section 9.4 discusses approaches to define the level of precision incorporated into a hazard analysis. The purpose of this analysis is to identify the changes in hazard that can be considered significant. One application of this concept would be to provide a basis for assessing whether future changes to the model would lead to significant changes in hazard, which in turn would require that the model be updated.

9.2 Hazard Input Document (HID)

The seismic source characterization of the CEUS presented in this report consists of a large and complex model. The report has been structured to give the reader an understanding of the reasoning for the structure of the model and the basis for all the model components. When the time comes for a hazard analysis to implement the model, there is a tremendous amount of material to go through in order to obtain all the model components and link them together for a hazard calculation. One of the innovations of the PEGASOS project (NAGRA, 2004) was creation of the concept of the HID. The purpose of the HID is to provide the analyst with a complete description of how to build the source model and a listing of all the model components in one place. The HID does not contain any discussion of the bases for the model structure and model components (that is, the purpose of the entire report). Rather, the intent of the HID is to provide a clear and unambiguous description of how to implement all the SSC model components that are described in this report.

The HID for the CEUS SSC model is presented in Appendix H. This version of the HID includes references to data files for aspects such as seismic source coordinates, gridded seismicity parameters, and the like. These components of the HID will be made part of the CEUS SSC Project website and will be provided in a suitable structure to provide the analyst access to the volumes of data that constitute these model components.

9.3 Implementation Instructions

The seismic source model developed in this project is based on interpretations over a broad region of eastern North America. Implementation for a specific site in that region, as an input to a PSHA, requires that the local region around the site be examined for additional or alternative interpretations. These might show, for example, evidence for a small geologic feature near the site that might be tectonically active. As another example, a site located near the boundary of two seismic sources described here might be affected by the uncertainty in that boundary, to ensure that its effect on seismic hazard has been properly characterized. This section gives guidance on what simplifications might be made, and on what additional studies might be undertaken, to properly represent seismic hazard.

9.3.1 Simplifications to Seismic Sources

In the HID for seismic sources (Appendix H), the specification includes ranges for thickness of the seismogenic crust, fault dip, orientation of fault strike, geometry of the source, and so on. For example, to calculate seismic hazard, hypocenters are distributed uniformly over the specified seismogenic crustal thickness. Ranges in the above parameters have been included to ensure a complete description of uncertainties in parameters. However, not all variations of parameters for a given source will be influential on seismic hazard at every site. For example, for a site located a great distance from a source, small variations in source geometry (including the extent of the source vertically in the crust) will have a small influence on seismic hazard, compared with other sites.

This section describes several simplifications to seismic sources that can be made to increase efficiency in seismic hazard calculations. These simplifications are recommended on the basis of sensitivity studies of alternative hazard curves that represent a range of assumptions on a parameter's value. Sensitivities are presented using the test sites in the CEUS SSC Project (see

Figure 8.1-1 for a map of these test sites). For applications of the seismic sources from the CEUS SSC Project, similar sensitivity studies should be conducted for the particular site of interest to confirm these results and to identify additional simplifications that might be appropriate. For the seismic sources below, only parameters that can be simplified are discussed and presented graphically.

The sensitivity studies consisted of determining the sensitivity of hazard to logic tree branches for each node of the logic tree describing that source. The purpose was to determine which nodes of the logic tree could be collapsed to a single branch, to achieve more efficient hazard calculations without compromising the accuracy of overall hazard results. The sensitivity calculations were performed at the project test sites for 1 Hz, 10 Hz, and PGA; the results for 1 Hz and 10 Hz are shown below.

For many comparisons in this section, a difference in hazard of 25% is mentioned as a threshold. Many comparisons show less sensitivity of less than 25%. Section 9.4 gives a more detailed and quantitative description of what constitutes a significant difference in hazard.

9.3.1.1 Charleston RLME

A sensitivity study was performed at the Savannah test site using Appendix H. Note that any sensitivities to alternative geometries in the Charleston RLME source model will be accentuated at Savannah because it lies close to the Charleston RLME source. Sites more distant to this source will show less sensitivity to alternative geometries.

Level: Rupture Orientation

For the regional source, there are two rupture orientations outlined in the Charleston RLME source model HID logic tree. Ruptures are oriented either parallel to the long axis of the source (northeast) or parallel to the short axis of the source (northwest), with weights of 0.8 and 0.2, respectively. The results from the sensitivity analysis show that, at the 10^{-5} ground motion, the difference in hazard between the two curves representing these two orientations is less than 25% (Figures 9.3-1 and 9.3-2). At the 10^{-5} ground motion, the percent difference between the weighted mean average hazard and the selected northeast orientation is less than 5%, indicating that mean hazard at Savannah is not significantly affected by having two alternative rupture orientations for the regional source. The northeast rupture orientation was selected as the orientation that will represent this level of the logic tree for three reasons: it was assigned the highest weight, the two other alternative geometries in the Charleston RLME source model also have northeast rupture orientations, and the northeast rupture orientation gives slightly more conservative hazard than the northwest rupture orientation, at least for the Savannah site.

9.3.1.2 Charlevoix RLME

A sensitivity study was performed at the Manchester test site using Appendix H.

Level: Seismogenic Thickness

For the Charlevoix area source, there are two seismogenic thicknesses outlined in the Charlevoix RLME source model HID logic tree. The seismogenic thicknesses are 25 and 30 km (15.5 and 18.6 mi.), with weights of 0.8 and 0.2, respectively. The results from the sensitivity analysis show that, at the 10^{-5} ground motion, the difference in hazard between the two curves representing the seismogenic thicknesses is less than 10% (Figures 9.3-3 and 9.3-4), indicating that hazard at Manchester is not significantly affected by having two alternative seismogenic thicknesses for the area source. A thickness of 25 km (15.5 mi.) was selected as the seismogenic thickness that will represent this level of the logic tree because it has the highest weight and is the more conservative of the two thicknesses.

Level: Rupture Orientation

For the Charlevoix area source, there is a range of fault dips outlined in the Charlevoix RLME source model HID logic tree. The dips of the faults range from 40° to 60° (modeled as 40°, 50°, and 60°, with weights of 0.333, 0.334, and 0.333, respectively, in the sensitivity analysis). The results from the sensitivity analysis show that, at the 10^{-5} ground motion, the difference in hazard between the three curves representing the three fault dips is less than 10% (Figures 9.3-5 and 9.3-6), indicating that mean hazard at Manchester is not significantly affected by having three alternative fault dips for the area source. The 50° dip was selected as the orientation that will represent this level of the logic tree because it is the average of the three dips.

9.3.1.3 Cheraw RLME

A sensitivity study was performed at the Topeka test site using Appendix H.

Level: Seismogenic Thickness

For the fault source, there are three seismogenic thicknesses outlined in the Cheraw RLME source model HID logic tree. The seismogenic thicknesses are 13, 17, and 22 km (8, 10.6, and 13.7 mi.), with weights of 0.4, 0.4, and 0.2, respectively. The results from the sensitivity analysis show that, at the 10^{-5} ground motion, the total range in hazard among the three curves representing these three seismogenic thicknesses is less than $\pm$20% (Figures 9.3-7 and 9.3-8). The weighted mean average hazard, at the 10^{-5} ground motion, from these three hazard curves is within 2% of the central curve (17 km, or 10.6 mi.), indicating that the mean hazard at Topeka (using three alternative seismogenic thicknesses) is not significantly different from the hazard using the central curve only. Therefore, the thickness of 17 km (10.6 mi.) was selected as the seismogenic thickness that will represent this level of the logic tree. It is worth pointing out that the thickest crustal assumption indicates the highest hazard because some specifications of fault activity for the Cheraw fault are made using fault slip rate. For a given slip rate, a thicker seismogenic crust implies more fault area, which results in more seismic activity and higher seismic hazard.

Level: Rupture Orientation

For the fault source, there are two rupture orientations outlined in the Cheraw RLME source model HID logic tree. The dip of the fault is either 50°NW or 65°NW, with weights of 0.6 and 0.4, respectively. The results from the sensitivity analysis show that, at the 10^{-5} ground motion, the difference in hazard between the two curves representing these two orientations is less than 10% (Figures 9.3-9 and 9.3-10), indicating that hazard at Topeka is not significantly affected by having two alternative rupture orientations for the fault source. The 50°NW dip was selected as the orientation that will represent this level of the logic tree because it was assigned the highest weight and is the more conservative of the two dips.

9.3.1.4 Commerce Fault Zone RLME

A sensitivity study was performed at the Jackson test site using Appendix H.

Level: Seismogenic Thickness

For the area source, there are three seismogenic thicknesses outlined in the Commerce Fault Zone RLME source model HID logic tree. The seismogenic thicknesses are 13, 15, and 17 km (8, 9.3, and 10.6 mi.), with weights of 0.2, 0.5, and 0.3, respectively. The results from the sensitivity analysis show that, at the 10^{-5} ground motion, the difference in hazard between the three curves representing these three seismogenic thicknesses is less than 10% (Figures 9.3-11 and 9.3-12), indicating that mean hazard at Jackson is not significantly affected by having three alternative seismogenic thicknesses for the area source. A thickness of 15 km (9.3 mi.) was selected as the seismogenic thickness that will represent this level of the logic tree because it is approximately the average of the three thicknesses.

9.3.1.5 Eastern Rift Margin North RLME

A sensitivity study was performed at the Jackson test site using Appendix H.

Level: Seismogenic Thickness

For the area source, there are three seismogenic thicknesses outlined in the ERM-N RLME source model HID logic tree. The seismogenic thicknesses are 13, 15, and 17 km (8, 9.3, and 10.6 mi.), with weights of 0.2, 0.5, and 0.3, respectively. The results from the sensitivity analysis show that, at the 10^{-5} ground motion, the difference in hazard between the three curves representing these three seismogenic thicknesses is less than 10% (Figures 9.3-13 and 9.3-14), indicating that mean hazard at Jackson is not significantly affected by having three alternative seismogenic thicknesses for the area source. A thickness of 15 km (9.3 mi.) was selected as the seismogenic thickness that will represent this level of the logic tree because it is approximately the average of the three thicknesses.

9.3.1.6 Eastern Rift Margin South RLME

A sensitivity study was performed at the Jackson test site using Appendix H.

Level: Seismogenic Thickness

For the area source, there are three seismogenic thicknesses outlined in the ERM-S RLME source model HID logic tree. The seismogenic thicknesses are 13, 15, and 17 km (8, 9.3, and 10.6 mi.), with weights of 0.2, 0.5, and 0.3, respectively. The results from the sensitivity analysis show that, at the 10^{-5} ground motion, the difference in hazard between the three curves representing these three seismogenic thicknesses is less than 20% (Figures 9.3-15 and 9.3-16). At the 10^{-5} ground motion, the percent difference between the weighted mean average hazard and the central value (15 km, or 9.3 mi.) is less than 1%, indicating that mean hazard at Jackson is not significantly affected by having three alternative seismogenic thicknesses for the area source. A thickness of 15 km (9.3 mi.) was selected as the seismogenic thickness that will represent this level of the logic tree because it is approximately the average of the three thicknesses.

9.3.1.7 Marianna RLME

A sensitivity study was performed at the Jackson test site using Appendix H.

Level: Seismogenic Thickness

For the area source, there are three seismogenic thicknesses outlined in the Marianna RLME source model HID logic tree. The seismogenic thicknesses are 13, 15, and 17 km (8, 9.3, and 10.6 mi.), with weights of 0.2, 0.5, and 0.3, respectively. The results from the sensitivity analysis show that, at the 10^{-5} ground motion, the difference in hazard between the three curves representing these three seismogenic thicknesses is less than 20% (Figures 9.3-17 and 9.3-18). At the 10^{-5} ground motion, the percent difference between the weighted mean average hazard and the central value (15 km, or 9.3 mi.) is less than 1%, indicating that mean hazard at Jackson is not significantly affected by having three alternative seismogenic thicknesses for the area source. A thickness of 15 km (9.3 mi.) was selected as the seismogenic thickness that will represent this level of the logic tree because it is approximately the average of the three thicknesses.

9.3.1.8 Meers RLME

A sensitivity study was performed at the Topeka and Houston test sites using Appendix H.

Level: Seismogenic Thickness

For both the Meers fault source and Oklahoma Aulacogen (OKA) area source that make up the Meers RLME source, there are two seismogenic thicknesses outlined in the Meers RLME source model HID logic tree. The seismogenic thicknesses are 15 and 20 km (9.3 and 12.4 mi.), each with a weight of 0.5. The results from the sensitivity analysis show that, at the 10^{-5} ground motion, the difference in hazard between the two curves representing these two seismogenic thicknesses is less than 10% (Figures 9.3-19 through 9.3-22), indicating that mean hazards at Topeka and Houston are not significantly affected by having two alternative seismogenic thicknesses for the fault and area source. A thickness of 15 km (9.3 mi.) was selected as the seismogenic thickness that will represent this level of the logic tree because it is the more conservative value.

Level: Rupture Orientation

For the OKA area source, there is a range of rupture orientations outlined in the Meers RLME source model HID logic tree. Ruptures are oriented N60°W ± 15°, parallel with the long axis of the area source (modeled as N50°W, N60°W, and N70°W, with weights of 0.333, 0.334, and 0.333, respectively, for the sensitivity analysis at Houston). The results from the sensitivity analysis show that, at the 10^{-5} ground motion, the difference in hazard between the two curves (N60°W and N60°W ± 15°) representing these two orientations is less than 10% (Figures 9.3-23 and 9.3-24), indicating that mean hazard at Houston is not significantly affected by having two alternative rupture orientations for the OKA area source. An orientation of N60°W was selected as the value that will represent this level of the logic tree because it is the average value.

For the OKA area source, there is a range of fault dips outlined in the Meers RLME source model HID logic tree. The dips of the faults range from 40° to 90° (modeled as 40°, 50°, 60°, 65°, 70°, 80°, and 90°, with weights of 0.143 in the sensitivity analysis). The results from the sensitivity analysis show that, at the 10^{-5} ground motion, the difference in hazard between the seven curves representing the seven fault dips is less than 10% (Figures 9.3-25 through 9.3-28), indicating that mean hazards at Topeka and Houston are not significantly affected by having seven alternative fault dips for the OKA area source. The 65°SW dip was selected as the orientation that will represent this level of the logic tree because it is the average value.

For the Meers fault source, there are two rupture orientations outlined in the Meers RLME source model HID logic tree. The dip of the fault is either 90° (vertical) or 40°SW, both with weights of 0.5. The results from the sensitivity analysis show that, at the 10^{-5} ground motion, the difference in hazard between the two curves representing these two orientations is less than 10% (Figures 9.3-29 through 9.3-32), indicating that mean hazard at Topeka and Houston is not significantly affected by having two alternative rupture orientations for the fault source. The 90° dip was selected as the orientation that will represent this level of the logic tree because it is the simpler model.

9.3.1.9 New Madrid Fault System RLME

A sensitivity study was performed at the Jackson test site using Appendix H.

Level: Seismogenic Thickness

For all fault sources, there are three seismogenic thicknesses outlined in the NMFS RLME source model HID logic tree. The seismogenic thicknesses are 13, 15, and 17 km (8, 9.3, and 10.6 mi.), with weights of 0.2, 0.5, and 0.3, respectively. The results from the sensitivity analysis show that, at the 10^{-5} ground motion, the difference in hazard of the three curves representing these three seismogenic thicknesses is less than 10% (Figures 9.3-33 and 9.3-34), indicating that mean hazard at Jackson is not significantly affected by having three alternative seismogenic thicknesses for the fault sources. A thickness of 15 km (9.3 mi.) was selected as the seismogenic thickness that will represent this level of the logic tree because it is approximately the average of the three thicknesses.

9.3.1.10 Wabash Valley RLME

A sensitivity study was performed at the Central Illinois test site using Appendix H.

Level: Seismogenic Thickness

For the area source, there are two seismogenic thicknesses outlined in the Wabash Valley RLME source model HID logic tree. The seismogenic thicknesses are 17 and 22 km (10.6 and 13.7 mi.), with weights of 0.7 and 0.3, respectively. The results from the sensitivity analysis show that, at the 10^{-5} ground motion, the difference in hazard between the two curves representing these two seismogenic thicknesses is less than 10% (Figures 9.3-35 and 9.3-36), indicating that mean hazard at Central Illinois is not significantly affected by having two alternative seismogenic thicknesses for the area source. A thickness of 17 km (10.6 mi.) was selected as the seismogenic thickness that will represent this level of the logic tree because it has the highest weight and is the more conservative of the two thicknesses.

Level: Rupture Orientation

For the area source, there are multiple rupture orientations (outlined in e-mails from Kathryn Hanson on June 9 and 20, 2010) that replace the rupture orientations outlined in the Wabash Valley RLME source model HID logic tree. Ruptures in the area source are to be modeled in three ways: parallel to the long axis of the source zone (which is oriented N51°E); N50°W; and

N20°W, with weights of 0.8, 0.1, and 0.1, respectively. For the ruptures oriented parallel to the long axis, the dips of the faults are vertical or 40°NW to 60°NW (modeled as 40°NW, 50°NW, and 60°NW), with weights of 0.666, 0.111, 0.112, and 0.111, respectively. For ruptures oriented N50°W, the dips of the faults are vertical. For the ruptures oriented N20°W, the dips of the faults are oriented 40°SW to 60°SW (modeled as 40°SW, 50°SW, and 60°SW), with weights of 0.333, 0.334, and 0.333, respectively.

The results from the sensitivity analysis show that, at the 10^{-5} ground motion, the hazard at Central Illinois is sensitive to the three rupture orientations and, therefore, this level of the logic tree will not be collapsed. However, the results from the sensitivity analysis show that, at the 10^{-5} ground motion, the difference in hazard between dips for each fault orientation is less than 10% (Figures 9.3-37 and 9.3-38), indicating that mean hazard at Central Illinois is not significantly affected by having one dip for each of the fault orientations for the area source. Therefore, one dip can be selected for the two fault orientations that have multiple dips: ruptures oriented parallel to the long axis and ruptures oriented N20°W. For ruptures oriented parallel to the long axis, a dip of 90° was selected (vertical faults) because it was assigned the highest weight (0.666) and is the simpler model. For the ruptures oriented N20°W, a dip of 50°SW was selected because it is the average of the three dips.

9.3.1.11 Background Sources

A sensitivity study was performed at the Central Illinois test site using Midcontinent A as a background source. For this sensitivity study, the focus was on determining the influence of fault ruptures on seismic hazard vs. using point sources within background sources to represent earthquake energy release. For the fault rupture model, multiple fault orientations, dips, and seismogenic depths are used in each background source characterization. In the hazard calculations, ruptures are represented explicitly, and the appropriate distance to the rupture is calculated for the ground motion equations. For the point source model, earthquake occurrences are represented as point sources, and correction factors are used (as published in EPRI, 2004) to modify the distance from the point-source distance to an equivalent rupture distance, and to increase aleatory uncertainties in ground motion estimates to account for random rupture orientation.

Figures 9.3-39 and 9.3-40 compare seismic hazards at the Central Illinois test site for the two models. For ground motions with a frequency of exceedence greater than 10^{-5} per year, the difference is less than 10%. Given that background sources generally make up only a fraction of the total hazard, using the point source model for background sources is an acceptable approximation. The fault rupture model is fully documented and available if future ground motion equations require the fault rupture geometry to be specified explicitly.

9.3.2 Accessing the SSC Model and Components from the Website

A hazard input document (HID) was developed for the CEUS SSC Project that documents the SSC model, including logic trees, parameter distributions, and derived Mmax and recurrence parameters. The HID specifies the inputs provided by the SSC model to the hazard calculations, providing a clear and complete record of how the SSC model is translated into hazard calculations. The HID is presented in Appendix H of the CEUS SSC Report, which is available on the CEUS SSC website at www.ceus-ssc.com.

The HID provides sufficient documentation for users to implement the SSC model in PSHA calculations for future applications. Demonstration hazard calculations were made at seven test sites to illustrate the effects of seismic sources on calculated seismic hazard and to compare hazards calculated using other SSC models. The demonstration hazard calculations are provided in Chapter 8 of this report; these can be used to confirm the seismic hazard results calculated by other hazard analysts using their hazard calculation software.

9.3.3 Accessing Project Databases

The data for the CEUS SSC Project were managed and documented in accordance with a data management procedure developed specifically for the project; this procedure is discussed in Task 2 of the CEUS SSC Project Plan, *Develop a Database*, and is described in further detail in Appendix A of the CEUS SSC Report. The CEUS SSC Project Plan, the project databases, and the CEUS SSC Report are available on the CEUS SSC website, www.ceus-ssc.com.

The CEUS SSC Project databases were compiled to organize and store those data and resources that were carefully and thoroughly collected and described for the TI Team's use in characterizing potential seismic sources in the CEUS. Development of the project database began at the inception of the project, and continued throughout the project using new references and data collected by the TI Team and project subcontractors. These updates included information from several sources, including presentations at project workshops by resource experts and proponents and review documentation provided by the PPRP.

Listed below are the contents of the CEUS SSC website, all of which are accessible.

- CEUS SSC Report
- HID data necessary to implement the CEUS SSC model
- Project GIS database including magnetic, gravity and stress data compiled for the CEUS SSC Project
- Project paleoliquefaction database
- Complete CEUS SSC earthquake catalog
- Bibliography (master list of all references used during the project, also provided in Chapter 10 of the CEUS SSC report)
- New computer code used to smooth *a* and *b* values
- All stakeholder and non-PPRP reviewer comments and correspondence, including response tables (Note: PPRP comments and correspondence are in Appendix I of the CEUS SSC Report)
- CEUS SSC Project Plan dated June 2008
- Information from Workshops 1–3, including meeting agendas, lists of participants, summaries, presentations, and a photo album of participants

Note that the project GIS database is provided in a format that will allow other investigators to use the CEUS SSC database in subsequent CEUS seismic hazard assessments.

9.3.4 Use of SSC Model with Site-Specific Refinements

The seismic source characterization developed under this project is a regional characterization of seismic sources, useful as a starting point for site-specific calculations. Any site-specific application will need to be conducted according to the applicable regulatory guidance for the nuclear facility of interest (e.g., NRC Regulatory Guide 1.208, ANSI/ANS-2.27-2008). These guidance documents typically require the development of a site-specific database that might include local geologic, tectonic, geophysical, seismicity, and paleoseismic data indicative of local seismic sources that could affect the site.

9.4 Hazard Significance

A PSHA integrates a range of SSC and GMC input models and parameters, which, collectively, represent current knowledge and uncertainties. After a PSHA is completed, it is expected that new data, models, and methods will subsequently emerge within the technical community. Some of those data, models, and methods may have implications to the existing PSHA model and some will not. This section presents an approach to assessing the significance of new findings that result in new inputs to the PSHA. The approach looks at the quantitative precision in seismic hazard implied by prior studies, and derives *minimum* estimates of hazard uncertainty to use as a guide in assessing the significance of future changes to seismic hazard estimates.

9.4.1 Data Available to Evaluate the Precision of Seismic Hazard Estimates

The purpose of this section is to investigate what level of precision should be associated with seismic hazard estimates in the CEUS. In other words, how might the seismic hazard estimates change if the analysis were to be repeated with independent experts who have access to the same basic information (geology, tectonics, seismicity, ground motion equations, site characterization)? In effect, we are asking, how precise are the estimates of seismic hazard? If a data set or interpretation were to change, and that change were to cause a change in the assessed seismic hazard, how would we judge whether that change in hazard were significant or insignificant? So the question of significance is closely linked to the level of precision with which we can assess seismic hazard.

Three fundamental sets of information contribute to the precision of seismic hazard estimates:

1. Seismic sources and parameters, which may be derived by individuals or teams of experts.
2. Ground motion equations, which are generally derived by a single expert or team using available equations but are sometimes derived by multiple experts.
3. Site response estimates, which are generally derived by a single expert but are sometimes derived by multiple experts.

A realistic assumption can be made that, for seismic hazard analysis at a site, these information inputs are separate and independent. It is understood that ground motion equations are developed for a wide range of magnitudes and distances, and that site response estimates are developed for a wide range of input motions. Additionally, it is assumed that we are interested in the precision of the *mean* seismic hazard curves, rather than any particular fractile. The mean seismic hazard curve is used to make decisions regarding design levels for nuclear facilities.

Estimates of the precision in mean hazard associated with each of these inputs can be made by examining existing seismic hazard results from published studies. Table 9.4-1 indicates available studies that can be used for this purpose.

The underlying concept is that we can estimate the uncertainty in mean hazard from available studies by examining the variability in hazard caused by team-to-team variations or expert-to-expert variations in hazard. For example, if six teams are used to derive seismic sources for a hazard estimate, there will be a distribution of total hazard (i.e., annual frequency of exceedance) for a given ground-motion amplitude. This distribution will have a standard deviation σ_{TH} caused by team-to-team variability, and this standard deviation can be calculated using the conditional total hazard curves for each team. The uncertainty in *overall mean* hazard σ_{MH} caused by the different seismic source interpretations is $\sigma_{MH} = \sigma_{TH}/\sqrt{6}$, assuming the teams' hazard estimates are uncorrelated. We put aside questions of team-to-team correlation that result from common data sets, availability of published papers, and similar items, because this correlation is a condition under which we are evaluating the precision of hazard. Similar "independent" teams would have access to the same data sets and published papers.

As additional background, note that the term *mean hazard* has several meanings. The total hazard curve calculated for one team, or one ground-motion equation, or some other assumption, is a *conditional mean* hazard curve. This curve, along with others, is used to calculate σ_{TH}. The family of *conditional mean* hazard curves is used, with weights, to calculate an *overall mean* hazard curve. We are interested in the uncertainty σ_{MH} in this overall mean.

9.4.2 Observed Imprecision in Seismic Hazard Estimates

The imprecision inherent in seismic hazard calculations from past studies provides a guide as to what levels of precision we should associate with current or future studies. To this end, we use the coefficient of variation (COV) of the mean annual frequency of exceedance (the mean hazard) as the fundamental estimate of how precise or imprecise the estimates of mean hazard are. The COV is the calculated standard deviation (σ) of mean hazard divided by the mean hazard, and is a good measure of how precisely we can characterize the mean hazard. When used in this sense, the coefficient of variation is designated COV_{MH}.

9.4.2.1 Area Seismic Sources

Figures 9.4-1 and 9.4-2 show the calculated COV_{MH} as a function of ground motion amplitude and seismic hazard (i.e., annual frequency of exceedance), respectively, for study (1A) in Table 9.4-1. These COV_{MH} values were calculated at the seven test sites using only hazard from the six EPRI (1989) team interpretations of seismic sources, and do not include hazard from the New Madrid and Charleston RLME sources. At some sites (e.g., Manchester), RLME sources such as the Charlevoix zone are distant, and area sources dominate the hazard. At other sites (e.g., Savannah), the RLME hazard is dominant because the site lies very close to a seismic source zone (the Charleston seismic zone, in the case of Savannah) and the area sources contribute relatively less hazard. COV_{MH} tends to increase with decreasing annual frequency; between 10^{-4} and 10^{-6} (the mean hazard range of interest) it ranges from about 0.1 to 0.4.

Figure 9.4-3 shows COV_{MH} at four Swiss nuclear power plant sites (i.e., Beznau, Goesgen, Leibstadt, and Muehleberg) studied during the PEGASOS project (study 1B in Table 9.4-1). In that project, four experts developed seismic source interpretations. Based on these four interpretations, Figure 9.4-3 (top) plots COV_{MH}, calculated from the standard deviation of hazard σ_{MH} at each amplitude, as $\sigma_{MH} = \sigma_{TH}/\sqrt{4}$. Results from the PEGASOS project are available only for peak ground acceleration (PGA) and spectral acceleration at 1 Hz. For mean annual frequencies in the range of 10^{-4} to 10^{-6}, COV_{MH} ranges from about 0.13 to 0.3, with one set of results (PGA for Goesgen) falling as low as 0.05 (see the solid blue curve on Figure 9.4-3 top and bottom).

Regarding imprecision in seismic hazard estimates for area seismic sources, the conclusion from Figures 9.4-1 through 9.4-3 is that typical COV_{MH} values will range from perhaps 0.15 to 0.3 at a mean annual frequency of 10^{-4} to perhaps 0.2 to 0.4 at a mean annual frequency of 10^{-6}, with a wide variation in that range. A typical minimum COV_{MH} is 0.1, with one result (i.e., Goesgen PGA on Figure 9.4-3b) falling below that minimum.

9.4.2.2 RLME Seismic Sources

For seismic hazard calculations in the CEUS, two sources of RLME are the Charleston seismic zone and the New Madrid seismic zone. Nuclear plant seismic hazard studies have relied on two interpretations for these RLME sources: the WLA model (Southern Nuclear, 2008) for the Charleston seismic zone and the Geomatrix model (Exelon, 2003) for the New Madrid seismic zone. A general representation of the logic tree representing uncertainties in the Charleston seismic zone model is given in Table 9.4-2. For many sites in the southeastern United States, seismic hazard will be dominated by this source, rather than by area sources represented by multiple interpretations. COV_{MH} values for area sources were described in the previous section, but for sites dominated by RLMEs, it is reasonable that there is some uncertainty in the mean hazard coming from the RLME, even though only one interpretation is currently used (e.g., Table 9.4-2).

It is notable that weights on alternatives are generally given to one-decimal-place precision, and that while these weights indicate quantitative preferences on alternatives, an independent evaluation by another investigator might assign somewhat different weights (both because the weights themselves are imprecise and because a different investigator might assign substantially different weights). Because alternative weights would change the mean hazard at a site, there is imprecision in the current estimates of mean hazard from the base-case model.

To determine the potential effect of alternative weights, an adaptation of the statistical bootstrap technique (e.g., Efron, 1982) was used. This application has the underlying assumption that the weights given to alternative interpretations (e.g., in Table 9.4-2) are variables with distributions. It is reasonable that, to estimate a *minimum* variation on the weights given in Table 9.4-2, we should pick a COV_{WT} for the weights that correspond to a change of 0.1 in the highest weight among the alternatives for each interpretation, because this is the precision with which weights were assigned. Designating this coefficient of variation COV_{WT}, we calculate the following values:

Source geometry	COV_{WT} = 0.1/0.7 = 0.143
Maximum magnitudes	COV_{WT} = 0.1/0.3 = 0.333
Paleoseismic record length	COV_{WT} = 0.1/0.8 = 0.125
Activity rate given record	COV_{WT} = 0.1/0.4 = 0.25

The statistical bootstrap method consisted of generating random weights for the alternative interpretations given in Table 9.4-2, using the listed values as mean values and using the COV_{WT} given above to calculate standard deviations for the weights. A normal distribution for weights was assumed, truncated at 0 and 1. For each interpretation, the random weight for the alternative with the highest mean weight was generated first, and weights for the other alternatives followed. The values of these other weights are not independent, but instead depend on previously generated weights. In particular, they must sum to unity.

The paleoseismic record length is an easy example to explain because it has only two alternatives. The weight for the preferred alternative, W_1, is generated from a normal distribution with a mean of 0.8 and a standard deviation of 0.1. The weight for the other alternative, W_2, is simply 1-W_1. For 100 samples these assumptions result in the following statistics:

	W_1	W_2
Mean	~0.8	~0.2
Standard deviation	~0.1	~0.1
COV_{WT}	~0.125	~0.5

Since mean seismic hazard is linearly proportional to the weights given to alternative interpretations, the effect on COV_{MH} for W_1 and W_2 will depend on the relative contributions of the alternative interpretations to mean hazard. (As one example of a trivial case, if the mean hazard for each alternative paleoseismic record length is the same, then uncertainty in W_1 and W_2 will result in zero uncertainty in mean hazard.)

For the interpretations in Table 9.4-2 with four or five alternatives, the bootstrap application generates a random weight for the preferred alternative first, followed by the next -preferred alternative, and so on. Any symmetry in the weights (e.g., in the maximum magnitude distribution) is maintained, so that the overall mean is maintained. The mean weight of the second -preferred alternative is adjusted downward if the random weight of the preferred alternative exceeds its mean, by the ratio (1-W_1)/(1-mean[W_1]). This has the effect of maintaining a near-normal (truncated) distribution shape for the less-preferred alternatives. The last weight is set equal to one minus the sum of previous weights, so that the weights sum to unity.

The total mean hazard (annual frequency of exceedance) is the sum of weighted hazards from the available alternatives. For example, for the alternative geometries with four alternatives,

$$\text{mean (H)} = W_1 H_1 + W_2 H_2 + W_3 H_3 + W_4 H_4 \tag{9-1}$$

where the H_i's are the mean hazard conditional on geometry i. In the current context, the H_i's are constant and the W_i's are random variables, so that

$$\text{mean (H)} = \Sigma_i \, E[W_i]H_i \tag{9-2}$$

(where *E[.]* indicates expectation) and

$$\sigma_k^2 \text{ (H)} = \Sigma \, \sigma_i^2 \, H_i^2 + 2 \, \Sigma_i \, \Sigma_{j>i} \, H_i \, H_j \, cov(W_i, W_j) \tag{9-3}$$

where σ is standard deviation, *cov* is covariance, *k* indicates a specific interpretation from Table 9.4-2, and the σ_i's, H_i's, and W_i's are with respect to alternatives for that interpretation. The W_i's are correlated because, for example, a higher-than-mean value of W_1 will generally be associated with lower-than-mean values of the other W_i's, since they must sum to unity. The covariance of the W_i's can be estimated from samples generated using the bootstrap technique.

To calculate the total variance of the mean hazard (designated here as σ_{MH}^2), we assume that the contributions from the four alternatives in Table 9.4-2 are independent. This is an explicit assumption in the logic tree summarized in Table 9.4-2 (e.g., the maximum magnitude alternatives and weights apply to all geometries). We also assume that effects of uncertainties in parameters are multiplicative on hazard. For example, if a variation of weights on alternative rates reduces the hazard by 20%, and a variation of weights on alternative geometrics increases the hazard by 10%, the total effect on hazard would be $0.8 \times 1.1 = 0.88$.

Because hazard values of interest vary over several orders of magnitude, it is convenient to present uncertainties as COV_{MH}, which for total hazard H_T is defined as follows:

$$COV_{MH} = \sigma_{MH} / E[H_T] \tag{9-4}$$

Under the independence assumption, COV_{MH} can be estimated as follows:

$$COV_{MH}^2 \simeq COV_{GEOM}^2 + COV_{Mmax}^2 + COV_{SEIS}^2 + COV_{RATE}^2 \tag{9-5}$$

where Equation 9-5 neglects cross-product terms involving the COVs that are small.

Figures 9.4-4 through 9.4-6 present COV_K (where K represents GEOM, Mmax, etc.) and COV_{MH} for PGA, 10 Hz, and 1 Hz spectral accelerations, respectively, for the Charleston model developed by WLA (Southern Nuclear, 2008). These plots were calculated using hazard results at a generic site located in Columbia, South Carolina, from only the Charleston source. From these figures it is evident that the alternative Mmax distribution dominates the uncertainty in mean hazard, except at low amplitudes (i.e., at high annual frequencies of exceedance).

From Figures 9.4-4 through 9.4-6, the COV_{MH} for annual frequencies in the range of 10^{-4} to 10^{-6} is 0.25 to 0.45, with a minimum of 0.25.

Figure 9.4-7 shows a similar comparison of hazard sensitivity at the Jackson site to New Madrid alternatives, which include Mmax, seismicity rate, and alternative geometries for the three faults in the New Madrid region (designated "RFgeom" for the Reelfoot fault, "NNgeom" for the New Madrid North fault, and "NSgeom" for for the New Madrid South fault). A cluster model (Exelon, 2003) is used to calculate hazard.

Unlike the results for Charleston, the results for the New Madrid model indicate that uncertainty in the rate of seismicity is the dominant contributor to uncertainty in hazard. The sensitivity to Mmax is low because, when one fault produces a high characteristic magnitude, other faults may produce a low characteristic magnitude during the cluster of earthquakes. COV_{MH} is about 0.25 for all amplitudes, and this result will be consistent across spectral frequencies because seismicity rate affects hazard equally across spectral frequencies.

9.4.2.3 Ground Motion Equations

As indicated in Table 9.4-1, direct estimates of the uncertainty in seismic hazard caused by different interpretations of ground motion equations are available using three studies (labeled 2A, 2B, and 2C in Table 9.4-1): EPRI (2004), PEGASOS (NAGRA, 2004), and USGS (Petersen et al., 2008). These studies are described below.

<u>EPRI Equations</u>. Hazards calculated with the the EPRI (2004) ground motion equations were analyzed in a fashion similar to the Charleston seismic source, i.e., using an application of the statistical bootstrap technique. Weights given in EPRI (2004) for the various ground-motion equations depend on whether ground motions from a general source or an RLME source are being modeled, as shown in Table 9.4-3.

The ground motion models for general sources and RLME sources are used in hazard calculations in specific combinations; they are not independent.

We applied the statistical bootstrap procedure to generate random weights using the following principles:

1. The mean weights are the weights given in Table 9.4-3.
2. Weights are assigned a normal distribution.
3. Uncertainties in the randomly generated weights were controlled using standard deviations that are 0.3, 0.5, and 0.7 times the mean weight (these choices are designated "COV_{WT}" below).
4. Equations with equal weights (e.g., C1 and C3) kept this characteristic.
5. Weights for the last pair of equally weighted equations (e.g., for C7 and C9 of the general source equations) were chosen so that the sum of all weights was unity.

Under principle 3 above, the COV_{WT} values were chosen using the following reasoning. A typical weight on the higher-weighted equations in Table 9.4-3 is 0.2, and it seems reasonable that an alternative study of ground motions would assign weights for these preferred equations in the range of 0.1 to 0.3, about two-thirds of the time. Stated another way, given today's knowledge, if several equations had weights of 0.2, and those equations were re-weighted by another study, it is unlikely that the revised weights would be less than 0.1 or greater than 0.3; these cases might occur for one-third of the equations, but the other two-thirds would have results within $\pm$0.1 of the original weight of 0.2. This supports the COV_{WT} of 0.5; the alternative values of 0.3 and 0.7 are calculated to show sensitivity to this choice.

Results are presented separately for sites dominated by general sources and RLME sources, to better understand any differences caused by these two cases. The variance of mean hazard σ_{MH}^2 that results from these random weights is calculated using Equation 9-3 above, and COV_{MH} is calculated (at each ground-motion amplitude) by dividing σ_{MH} by the mean hazard at that amplitude.

<u>General Sources</u>. As an example of hazard results affected by general sources, Figure 9.4-8 shows PGA seismic hazard curves for the Manchester test site, for each of the nine general-source ground-motion equations. Curves are also shown for the mean hazard, for "sigma," which is the standard deviation of total hazard σ_{TH}, and for "classical mean sigma," the classical standard deviation of the mean, an estimate of the standard deviation of mean hazard as if the hazards from each ground-motion equation were independent. While this assumption does not hold, it is a useful comparative curve. It is calculated as $\sigma_{MH} \times \sqrt{\Sigma\, W_i^2}$, where W_i are the weights given in Table 9.4-3. (This is equivalent to calculating the standard deviation of the mean of a group of equally weighted observations using $\sigma/\sqrt{n}$.) This estimate is designated as σ_{CL} here.

Figure 9.4-9 shows the COV_{MH} from ground motion equations plotted vs. PGA level for the Manchester site, for the two methods of calculating COV_{MH} (the classical mean sigma divided by the mean, designated as COV_{CL}, and the bootstrap procedure, designated by the values of COV_{WT}). At PGA amplitudes above 0.2 g, all measures of COV_{MH} increase. This is consistent with the hazard plot on Figure 9.4-8, which shows that the relative range of hazard increases for those amplitudes, and the sigma estimates increase relative to the mean hazard.

Figure 9.4-10 plots COV_{MH} of PGA hazard vs. mean hazard for the Manchester site. Typically, the range of hazards from 10^{-4} to 10^{-6} are of most interest in seismic hazard studies for nuclear plants, and in this range, even the lowest assumption on COV_{WT} ($COV_{WT} = 0.3$) indicates that COV_{MH} is between 0.1 and 0.4. The assumption of $COV_{WT} = 0.5$ indicates results similar to COV_{CL}, but this is not a universal result, as will be demonstrated below.

Figures 9.4-11 and 9.4-12 show plots of COV_{MH} at Manchester for 10 Hz and 1 Hz, respectively. The 10 Hz COV_{MH} is similar to that for PGA, but the 1 Hz COV_{MH} (Figure 9.4-12) shows markedly higher COV_{MH} values. The reason is that the 1 Hz hazard curves (Figure 9.2-13) show a larger range and both a larger σ_{MH} and a larger σ_{CL} than do the PGA hazard curves (for PGA on Figure 9.4-8, the "sigma" curve generally lies below the mean hazard, but for 1 Hz on Figure 9.4-13, the "sigma" curve generally lies above the mean hazard). Figure 9.4-13 also shows that the "cl. mean sigma" curve peaks, relative to the mean hazard curve, at an amplitude of about 0.1 g. At higher ground motions (lower annual frequencies), the "cl. mean sigma" decreases relative to the mean hazard. This leads to decreasing COV_{CL} and COV_{WT} curves on Figure 9.4-12 for hazards in the range of 10^{-5} to 10^{-7}.

As another example of the effect of ground motion equations for general sources, Figures 9.4-14 through 9.4-16 show plots of COV_{MH} from ground motion equations for the Chattanooga test site. This site is dominated by local sources, with small contributions to hazard coming from the distant Charleston and New Madrid sources. The COV_{MH} plots are similar to those for Manchester, with PGA and 10 Hz showing COV_{MH} in the range of 0.15 to 0.25 for hazards in the range of 10^{-4} to 10^{-6}, and 1 Hz showing higher COV_{MH} (for the same reason discussed for the Manchester site).

<u>RLME Sources</u>. In the EPRI (2004) study there were 12 equations recommended for sources that can generate large-magnitude earthquakes, as indicated in Table 9.4-3. As an example, Figure 9.4-17 shows seismic PGA hazard curves for these 12 equations for the Savannah test site, along

with mean, σ_{MH}, and σ_{CL} curves. This site is located quite close to the Charleston seismic zone, and hazard at the site is dominated by that source.

Figures 9.4-18 through 9.4-20 show the COV_{MH} resulting from ground motion equations for PGA, 10 Hz, and 1 Hz respectively. At the close distance from the Savannah site to the Charleston seismic zone, the hazard curves span a small range (for hazard curves), e.g., for PGA amplitudes corresponding to mean hazards of 10^{-4} and 10^{-5}, the range of hazard among the 12 ground motion equations on Figure 9.4-17 is about a factor of 20 to 30 in annual frequency. As a result, Figure 9.4-18 shows COV_{MH} around 0.1 for COV_{WT} = 0.3, and higher COV_{MH} for higher values of COV_{WT}.

For the central case of COV_{WT} = 0.5, for 10 Hz spectral accelerations, COV_{MH} is around 0.1 for mean hazards in the range of 10^{-4} to 10^{-6}, and for 1 Hz spectral acceleration, COV_{MH} ranges from about 0.12 to 0.15.

The relative agreement among PGA hazard curves at the Savannah site results from the proximity of this site to the Charleston seismic zone. To illustrate this, seismic hazard was calculated at Columbia, South Carolina, from the Charleston seismic zone. Columbia lies roughly 150 km (93 mi.) from the center of the Charleston seismic zone. Figure 9.4-21 plots the PGA hazard curves for Columbia for the 12 ground motion equations, and plots the mean hazard, σ_{TH}, and σ_{CL}. For PGA corresponding to mean hazards of 10^{-4} and 10^{-5}, the range in hazards from the 12 ground motion equations spans two to three orders of magnitude, which is much greater than the range illustrated on Figure 9.4-17 for Savannah. As a result, the COV_{HAZ} at Columbia is larger, as illustrated on Figures 9.4-22 through 9.4-24 for PGA, 10 Hz, and 1 Hz, respectively, particularly for mean hazard values that are less than 10^{-4}.

To provide further perspective, Figures 9.4-25 through 9.4-27 plot COV_{MH} vs. mean hazard at the Chattanooga site, but only for the hazard caused by earthquakes in the New Madrid seismic zone (NMSZ). Chattanooga is about 400 km (250 mi.) from the NMSZ, and ground motion equations show a wider range of hazard at these long distances, as reflected on Figures 9.4-25 through 9.4-27, wherein the COV_{WT} = 0.5 curves indicate that COV_{MH} is between 0.2 and 0.4 for mean hazards between 10^{-4} and 10^{-6}. This confirms the trend seen with the Savannah and Columbia results that COV_{MH} increases with increasing distance from an RLME source.

Another trend that appears in the COV_{MH} plots for Savannah, Columbia, and Chattanooga is that COV_{CL} is much higher than COV_{MH} estimated by bootstrap techniques. The reason is related to the dominance of one RLME ground-motion equation, F9 in Table 9.4-3, in the mean hazard calculations (see Figures 9.4-17 and 9.4-21). The classical mean estimate of hazard uncertainty assumes that all estimates are independent, whereas the bootstrap technique maintains the symmetry in weights between RLME ground-motion equations F7 and F9 (the former gives estimates lower than equation F8, the latter gives estimates greater than F8, by a consistent multiplicative factor). This symmetry results in a lower estimate of COV_{MH} from the bootstrap technique and is important in the case of RLME sources when equation F9 results in a hazard curve that greatly exceeds the curves from other equations.

PEGASOS Study. In the PEGASOS project (NAGRA, 2004), five ground-motion experts provided recommendations on sets of ground motion equations with weights, and hazard results are available at four Swiss nuclear power plant sites for PGA and 1 Hz SA conditional on each ground-motion expert. The standard deviation of hazard σ_{MH} can be calculated for this set of conditional hazards, and COV_{MH} is taken as $\sigma_{MH}/\sqrt{5}$ divided by the overall mean hazard. Figures 9.4-28 and 9.4-29 show COV_{MH} at the four sites, plotted vs. ground motion amplitude and vs. annual frequency of exceedance, respectively. For PGA the COV_{MH} exceeds 0.2, and for 1 Hz SA the COV_{MH} exceeds 0.3, for mean hazards in the range of 10^{-4} to 10^{-6}.

USGS Study. The USGS (Petersen et al., 2008) calculation of seismic hazard for the national seismic hazard maps uses multiple weighted ground-motion equations. These allow an estimate of the COV_{MH} to be derived. Equations and weights used in the USGS study for the CEUS are shown in Table 9.4-4.

Different weights are used for background sources and for RLME sources in the USGS application. The way hazards from alternative ground-motion-prediction equations (GMPEs) are combined when the total hazard is calculated from background and RLME sources does not affect the mean hazard and is not specified in the USGS study. But the combination of hazards does affect the uncertainty in total hazard. In order to avoid the arbitrariness of adopting any specific combination rule, and with the goal of calculating the *minimum* estimate of hazard uncertainty, we assume that the GMPEs in Table 9.4-3 combine independently, and adopt the *classical standard deviation* designated σ_{CL} above. Accounting for correlations of estimates (e.g., that equation *i* for background seismicity would be associated with equation *i* for RLMEs) would increase the estimates of the uncertainty in mean hazard from the classical estimate.

Figures 9.4-30 and 9.4-31 show COV_{MH} for Chattanooga and Central Illinois, respectively, for the USGS 2008 hazards at seven spectral frequencies. Total hazard at the Chattanooga site is dominated by background seismicity, and at the Central Ilinois site is a combination of hazard from background and RLMEs, and this combination depends on spectral frequency. For both sites, COV_{MH} ranges from 0.15 to 0.25 for total mean hazard between 10^{-4} and 10^{-6}, with a minimum COV_{MH} of about 0.15.

Note that additional epistemic uncertainties are not used in the USGS GMPEs, as they are in the EPRI (2004) GMPEs. Rather, the USGS GMPEs adopts the best estimate of what each author believes are appropriate ground-motion amplitudes in the CEUS, along with aleatory uncertainties. Some of the authors, in their original publications, discuss how to extend their models to estimate epistemic uncertainties, but these extensions have not been used in the USGS model. This, along with the assumption of independence between area source and RLME estimates discussed above, contributes to the USGS COV_{MH} estimates in some cases appearing to be low relative to other estimates.

Overall, uncertainties in hazard caused by uncertainty in ground motion equations shown for the PEGASOS project (Figures 9.4-28 and 9.4-29) and from the USGS (Figures 9.4-30 and 9.4-31) are consistent with the results shown for the results in the CEUS (Figures 9.4-8 through 9.4-27). That is, hazard uncertainties are lower for high frequencies than for 1 Hz spectral amplitudes, and hazard uncertainties increase with ground motion amplitude. Focusing on COV_{MH} estimated using $COV_{WT} = 0.5$, a typical range of COV is from 0.1 to 0.45 across all spectral frequencies and amplitudes of interest, with some specific results falling outside of this range.

9.4.2.4 Site Response

Most sites in the CEUS are not classified as hard rock sites, and at these sites, uncertainty in site response plays a role in the uncertainty in site hazard calculations. Results from the PEGASOS project allow a direct estimate of the hazard uncertainty caused by uncertainty in site response calculations, because four site response experts provided recommendations on site response models, and hazard results are available at the four Swiss plant sites conditional on these four experts. The standard deviation of mean hazard σ_{MH} can be calculated for this set of conditional hazards, and COV_{MH} is taken as $\sigma_{MH}/\sqrt{4}$ divided by the overall mean hazard. Figure 9.4-32 shows COV_{MH} at the four sites for PGA and 1 Hz spectral acceleration (which are the only results available in this format), plotted vs. ground motion amplitude. COV_{MH} is relatively small for PGA, generally below 0.1. For 1 Hz spectral acceleration, COV_{MH} is small at low amplitudes and increases with amplitude. Figure 9.4-33 shows COV_{MH} plotted vs. mean hazard, where for the hazard range of 10^{-4} to 10^{-6}, and depending on spectral frequency, COV_{MH} values range from 0.03 to 0.4. Results differ among the four sites, which should be expected.

In the CEUS, an estimate is available of the uncertainty in hazard caused by alternative soil amplification models. This comes from the results of two EPRI-funded projects (EPRI, 2005a, 2005b, 2008) that calculated seismic hazard (including site response) at a group of nuclear power plants in the CEUS. Multiple models of site profiles and site characteristics were developed using available public information on the sites, and these multiple models were weighted to obtain the total site hazard. For the purposes of the current study, at each site the individual mean hazard curves for each soil model were obtained, and standard deviation of mean hazard σ_{MH} was calculated using these individual curves and weights. The classical standard deviation of the mean was then calculated as $\sigma_{CL} = \sigma_{TH} \times \sqrt{\Sigma\, W_i^2}$, where W_i are the weights for the various soil models. This calculation assumes that the estimates of hazard are independent.

Figure 9.4-34 shows COV_{MH} resulting from the alternative site response models, vs. mean hazard, for four sites with alternative site response models. COV_{MH} varies over a wide range, as might be expected for different sites, but results generally show that COV_{MH} exceeds 0.05, with one site (Site 4 for 10 Hz) showing lower COVs.

9.4.3 Conclusions on the Precision in Seismic Hazard Estimates

Results presented above are summarized in Table 9.4-5, which represents minimum COV_{MH} values observed in these sensitivity results. For reasons given above, COV_{MH} from the Savannah site and from the USGS ground-motion results are not used. Also, the COV_{MH} values from the PEGASOS study are downweighted, because only mean hazard curves conditional on each ground-motion expert are available, and these do not include within-expert variability. COV_{MH} values are summarized by spectral frequency and annual frequency of exceedance, and results are given separately for area sources and RLME sources. The last two columns represent the total COV_{MH}, calculated as the square root of the sum of squares of the individual COVs for sites affected primarily by area sources and by RLME sources. Table 9.4-5 presents COV_{MH} results for annual frequencies of exceedance of 10^{-4}, 10^{-5}, and 10^{-6}. This is a common hazard range for the seismic design of critical facilities, but note that investigations of seismic hazard for such facilities often require a wider range (e.g., 10^{-3} to 10^{-7}).

Table 9.4-5 shows that in general, minimum hazard uncertainties resulting from area source characteristics are smaller than minimum hazard uncertainties resulting from RLME source characteristics. But the reverse is true of uncertainties resulting from ground motion models, where minimum hazard uncertainties from area-source ground-motion models are larger than from RLME ground-motion models. These two effects compensate somewhat, so that total minimum uncertainties in hazard are comparable for the two types of sources. Uncertainty in site response contributes relatively little, at least for the example sites presented here from two major studies. As an overall conclusion, the minimum COV representing uncertainty in mean hazard over all spectral frequencies, and for annual mean hazards in the range of 10^{-4} to 10^{-6}, can be taken to be about 0.25 for 10^{-4}, 0.3 for 10^{-5}, and 0.35 for 10^{-6}. Because the contribution of site response uncertainty is a small part of this total, this conclusion applies to both rock and soil sites.

For decisions regarding the significance of changes in seismic hazard, the above results should be interpreted as follows. If an alternative assumption or parameter is used in a seismic hazard study, and it potentially changes the calculated mean hazard (mean annual frequency of exceedance) by less than $\pm$25% for ground motions corresponding to 10^{-4} annual frequency of exceedance, and it potentially changes the calculated hazard by less than $\pm$35% for ground motions corresponding to 10^{-6} annual frequency of exceedance, then that potential change is less than the best (highest) level of precision with which we can calculate mean seismic hazard. Under these circumstances, the potential change could be deemed not significant. For many sites we cannot be this precise, and the uncertainty in mean hazard will be higher than this, but the above interpretation gives a reasonable lower-bound guideline with which to evaluate the significance of potential changes in mean hazard. Note that regulators addressing the impacts of potential changes in seismic hazard on seismic design motions or on seismic risk-related decisions may (appropriately) require action even if potential changes are less than the guidelines given above.

Table 9.4-1
Available Information for Determining the Precision of Mean Hazard

Input	Subset of Application	Available Studies
(1) Seismic sources and parameters	Area sources	(1A) EPRI (1989) project (6 teams at 7 sites) (1B) PEGASOS project (NAGRA, 2004)
	RLME sources (Charleston, New Madrid)	(1C) Charleston (Southern Nuclear, 2008) (1D) New Madrid (Exelon, 2003)
(2) Ground motion equations	All	(2A) EPRI (2004) equations applied to 7 sites (2B) USGS equations (Petersen et al., 2008) applied to 7 sites (2C) PEGASOS study (NAGRA 2004) (5 experts applied to 4 sites)
(3) Site response	All (non-rock) sites	(3A) EPRI study (2005a, b, 2008) (1 expert applied to 45 sites) (3B) PEGASOS study (NAGRA, 2004) (4 experts applied to 4 sites)

Table 9.4-2
Summary of an Example Logic Tree Representing Uncertainties for the Charleston Seismic Zone

Interpretation	Alternatives	Weights on Alternatives	Designation[1]
Geometry of source	4 geometries	0.7, 0.1, 0.1, 0.1	GEOM
Maximum magnitude	5 values	0.1, 0.25, 0.3, 0.25, 0.1	Mmax
Paleoseismic record length	2 periods	0.8, 0.2	SEIS
Activity rate given record	5 rates	0.1, 0.2, 0.4, 0.2, 0.1	RATE

[1] Designation of curves in Figures 9.4-4 through 9.4-6

Table 9.4-3
Basic Weights Given in EPRI (2004) for Ground Motion Equations

General Source			RLME Source		
Equation	**Weight**	**Comment**	**Equation**	**Weight**	**Comment**
C1	0.065	—	F1	0.0509	—
C2	0.221	—	F2	0.173	—
C3	0.065	wt. equal to C1	F3	0.0509	wt. equal to F1
C4	0.0737	—	F4	0.0577	—
C5	0.251	—	F5	0.197	—
C6	0.0737	wt. equal to C4	F6	0.0577	wt. equal to F4
C7	0.0463	—	F7	0.0363	—
C8	0.158	—	F8	0.124	—
C9	0.0463	wt. equal to C7	F9	0.0363	wt. equal to F7
—	(not used)	—	F0	0.0401	—
—	(not used)	—	FA	0.137	—
—	(not used)	—	FB	0.0401	wt. equal to F0

Table 9.4-4
Ground Motion Equations and Weights Used in USGS 2008 National Hazard Map for CEUS

Reference	Weight for Background Seismicity	Weight for RLME Sources
Atkinson and Boore (2006; 140 bars)	0.125	0.1
Atkinson and Boore (2006; 200 bars)	0.125	0.1
Campbell (2003)	0.125	0.1
Frankel et al. (1996)	0.125	0.1
Tavakoli and Pezeshk (2005)	0.125	0.1
Silva et al. (2002)	0.125	0.1
Toro et al. (1997)	0.25	0.2
Somerville et al. (2001)	—	0.2

Table 9.4-5
Minimum COV_{MH} Values Observed in Seismic Hazard

Case	Area Sources	RLME Sources	Ground Motion (Area Sources[1])	Ground Motion (RLME Sources[1,2])	Site Response	Total COV_{MH}, General Site	Total COV_{MH}, RLME Site
PGA, 1E-4	0.15	0.27	0.20	0.15	0.05	~0.25	~0.31
PGA, 1E-5	0.18	0.31	0.25	0.22	0.05	~0.31	~0.38
PGA, 1E-6	0.20	0.40	0.30	0.28	0.05	~0.36	~0.49
10 Hz, 1E-4	0.15	0.27	0.17	0.10	0.05	~0.23	~0.29
10 Hz, 1E-5	0.18	0.31	0.25	0.13	0.05	~0.31	~0.34
10 Hz, 1E-6	0.21	0.4	0.37	0.16	0.05	~0.43	~0.43
1 Hz, 1E-4	0.10	0.25	0.30	0.12	0.05	~0.32	~0.28
1 Hz, 1E-5	0.10	0.30	0.40	0.18	0.05	~0.42	~0.35
1 Hz, 1E-6	0.10	0.35	0.50	0.23	0.05	~0.51	~0.42

[1] Excluding Savannah site
[2] Excluding USGS results

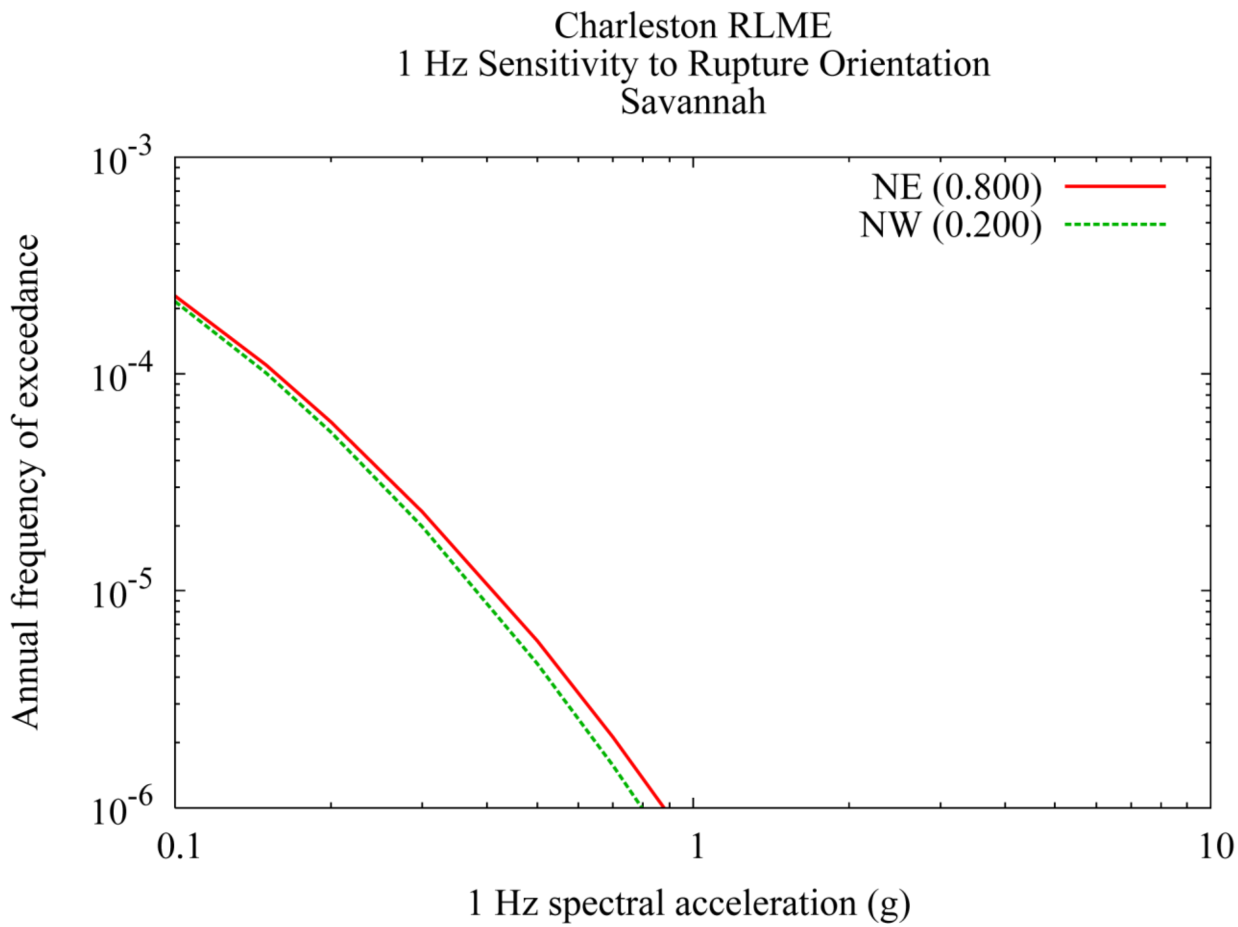

Figure 9.3-1
1 Hz sensitivity to rupture orientation at Savannah for the Charleston regional source

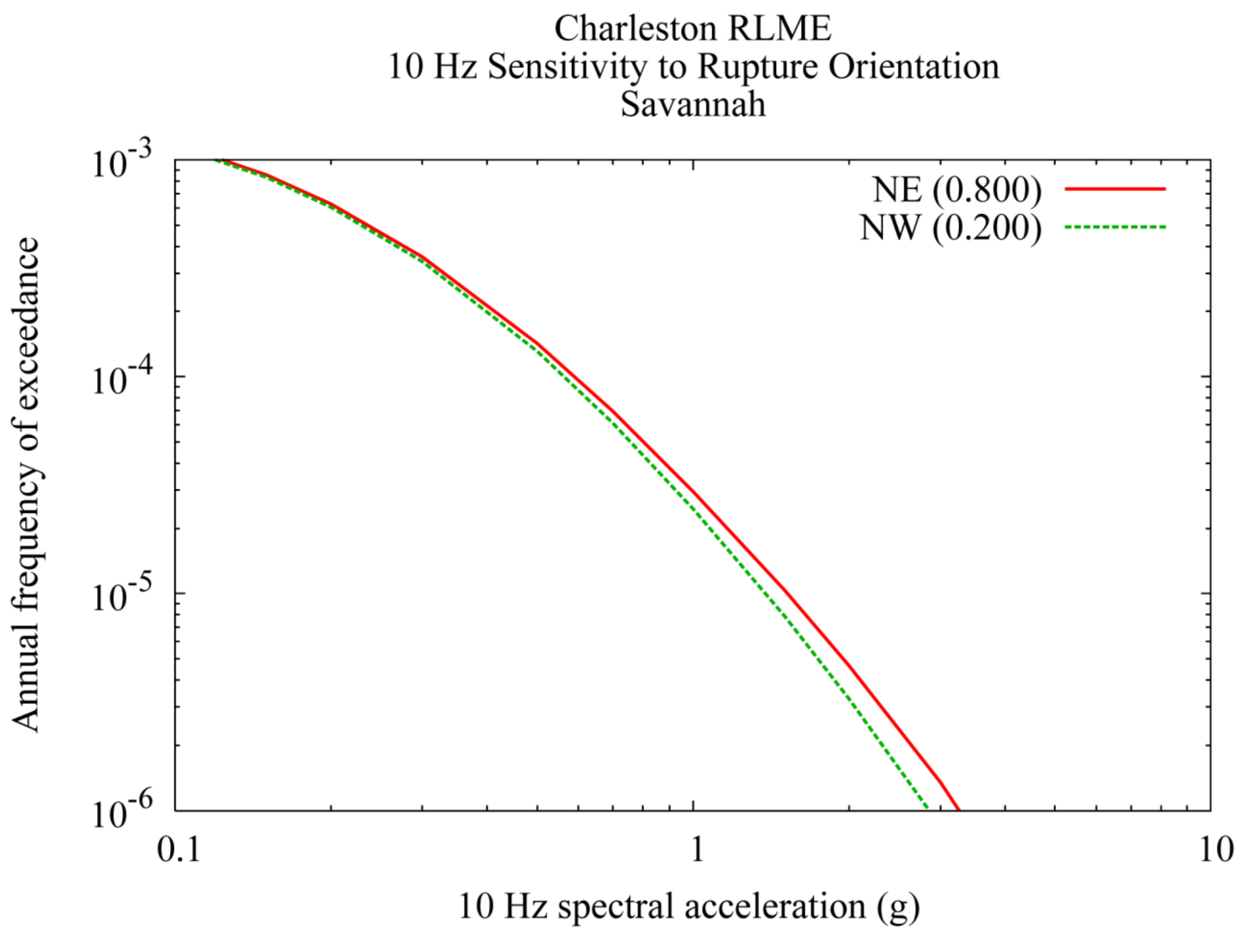

Figure 9.3-2
10 Hz sensitivity to rupture orientation at Savannah for the Charleston regional source

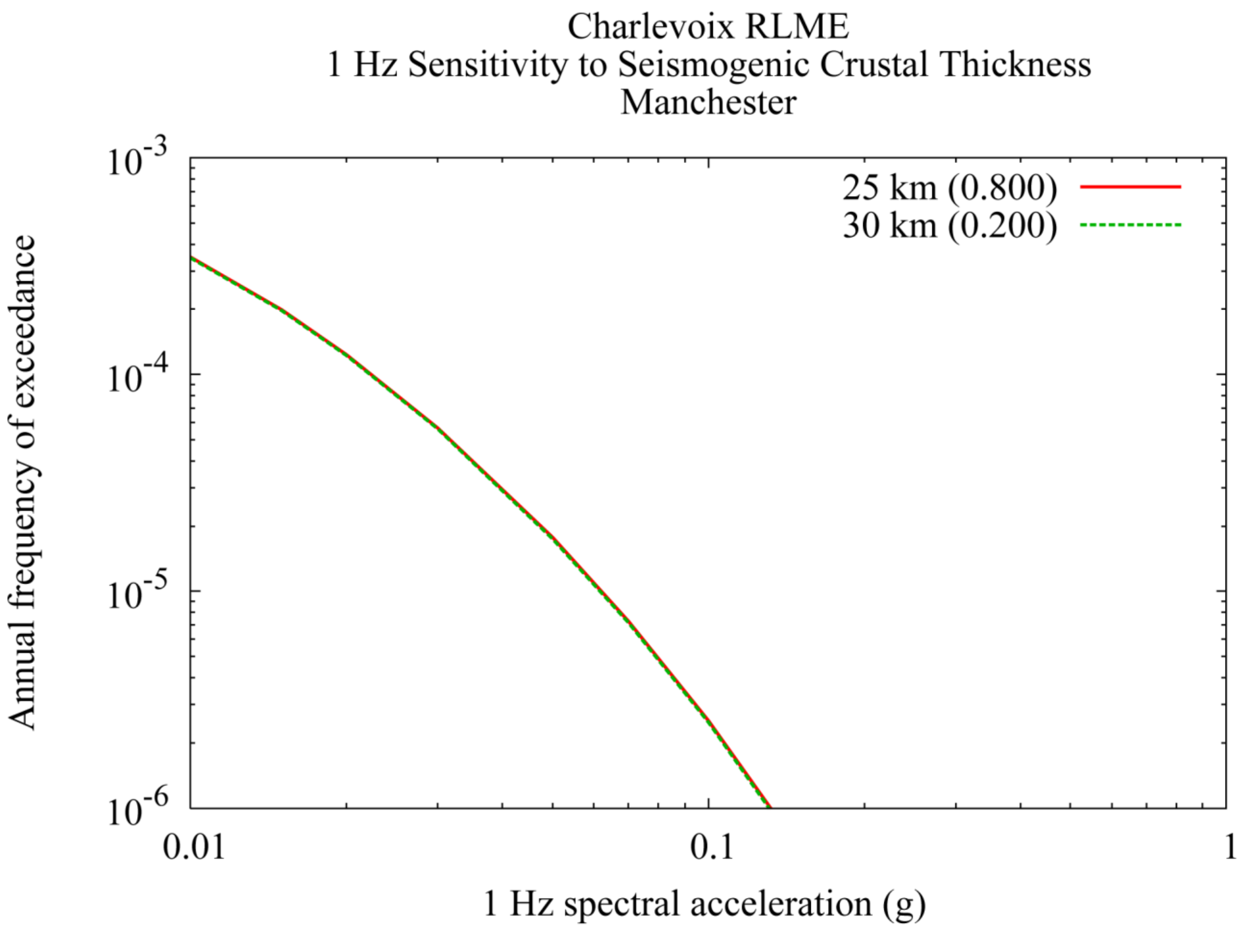

Figure 9.3-3
1 Hz sensitivity to seismogenic thickness at Manchester for the Charlevoix area source

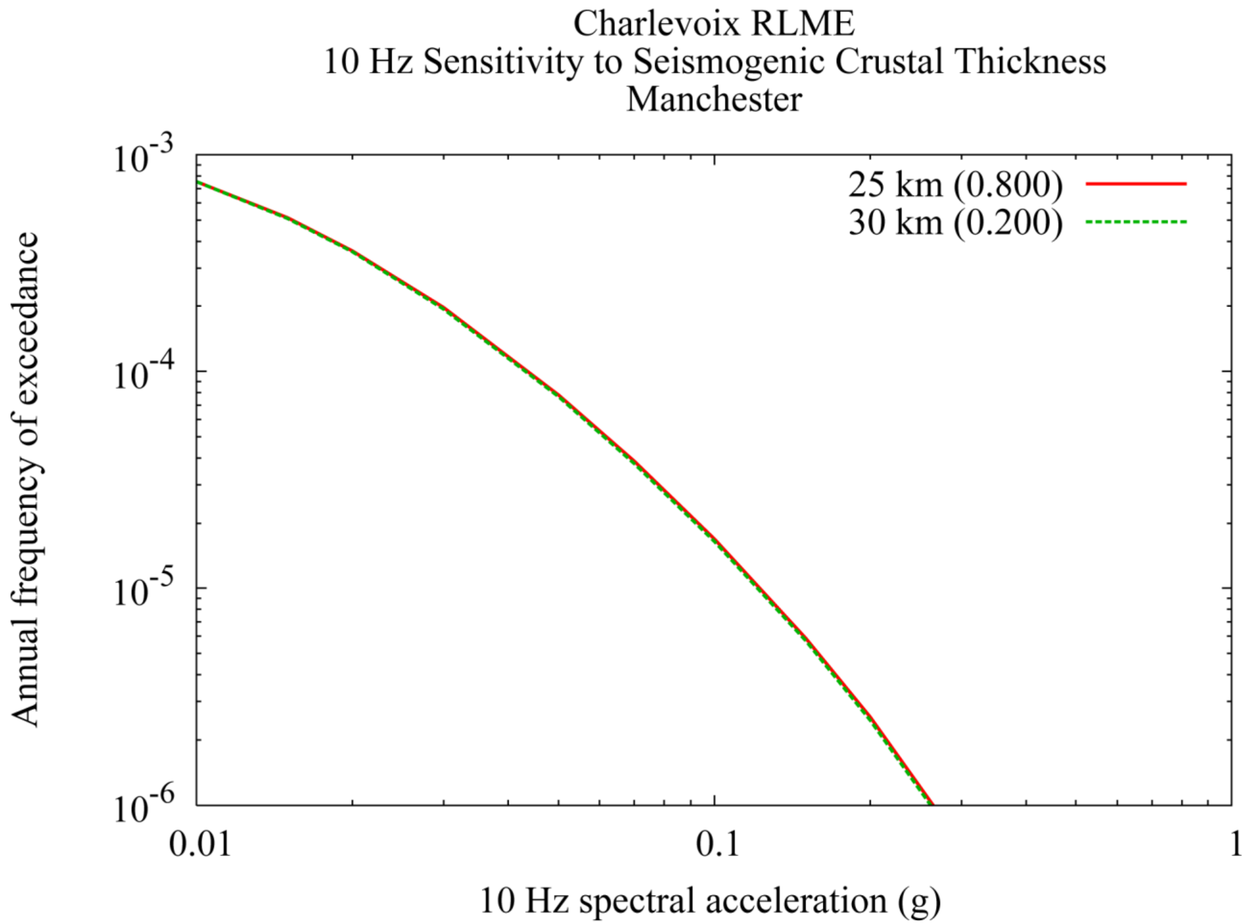

Figure 9.3-4
10 Hz sensitivity to seismogenic thickness at Manchester for the Charlevoix area source

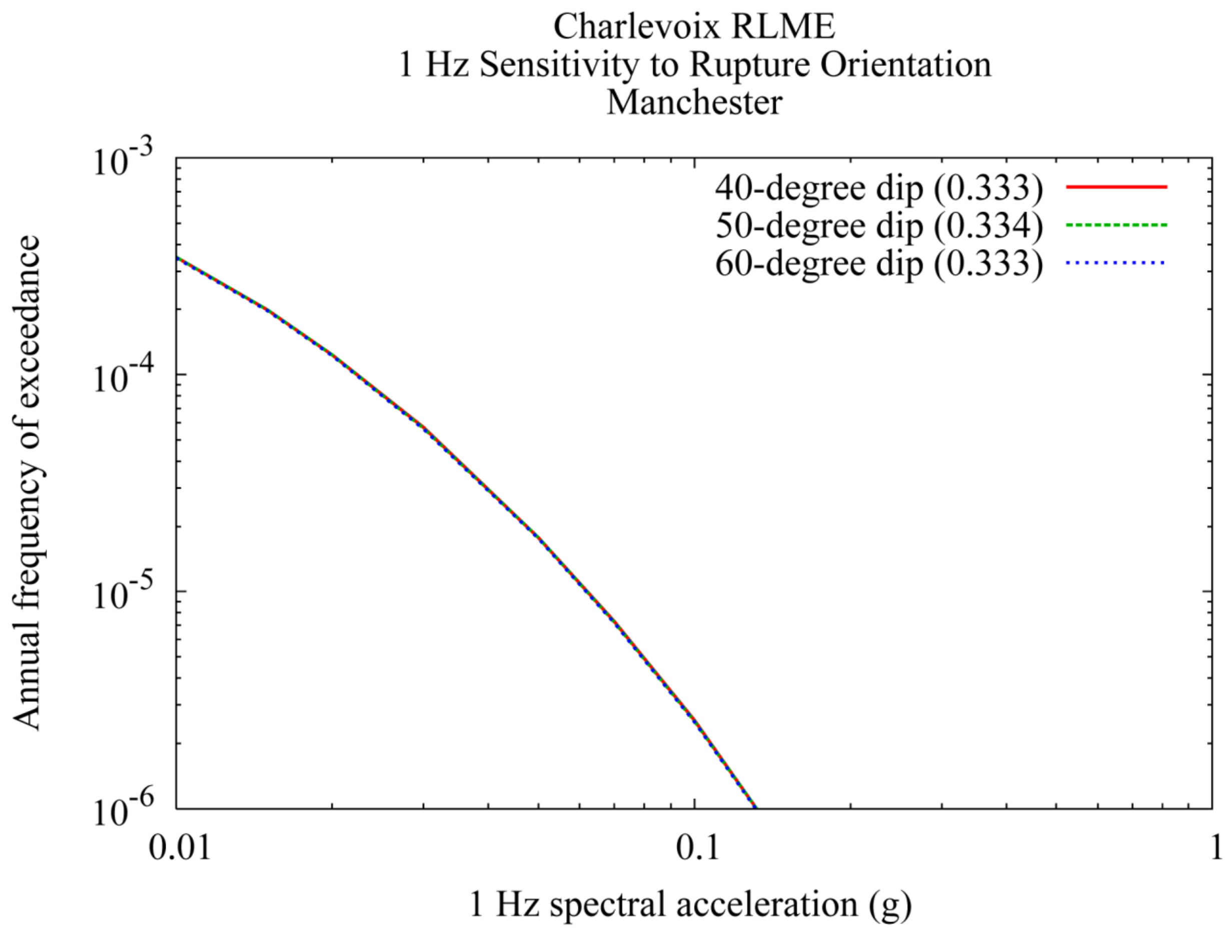

Figure 9.3-5
1 Hz sensitivity to rupture orientation (dip) at Manchester for the Charlevoix area source

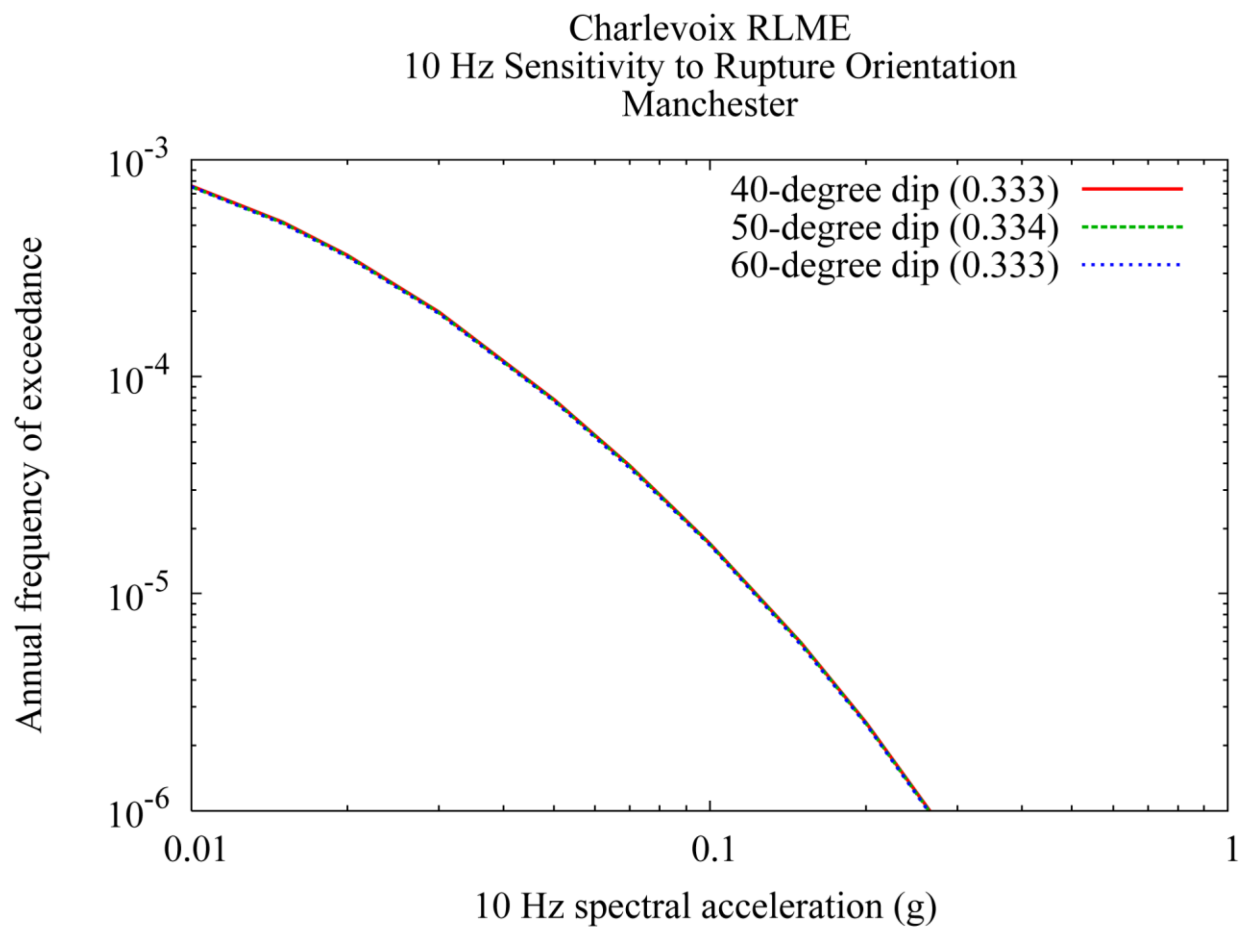

Figure 9.3-6
10 Hz sensitivity to rupture orientation (dip) at Manchester for the Charlevoix area source

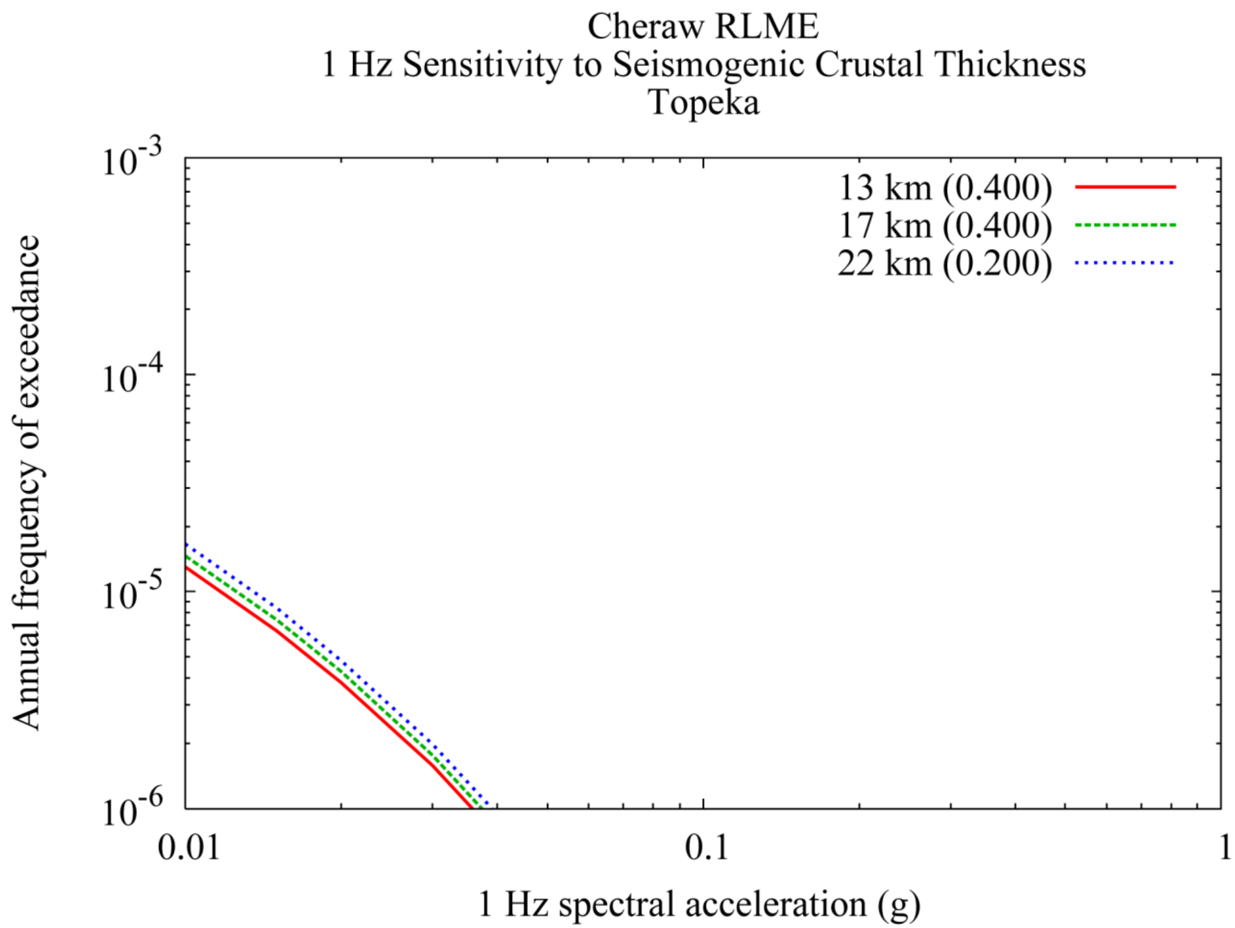

Figure 9.3-7
1 Hz sensitivity to seismogenic thickness at Topeka for the Cheraw fault source

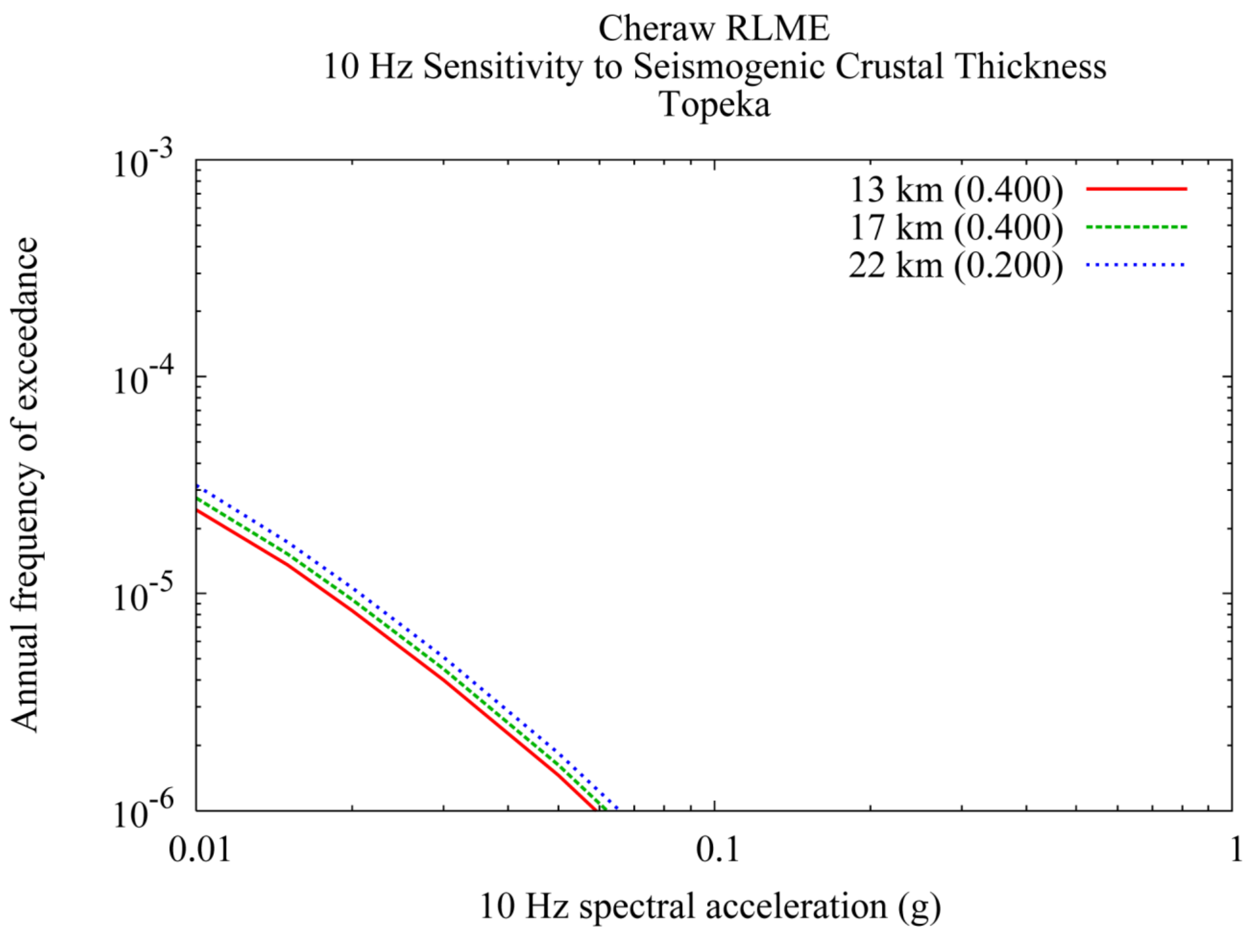

Figure 9.3-8
10 Hz sensitivity to seismogenic thickness at Topeka for the Cheraw fault source

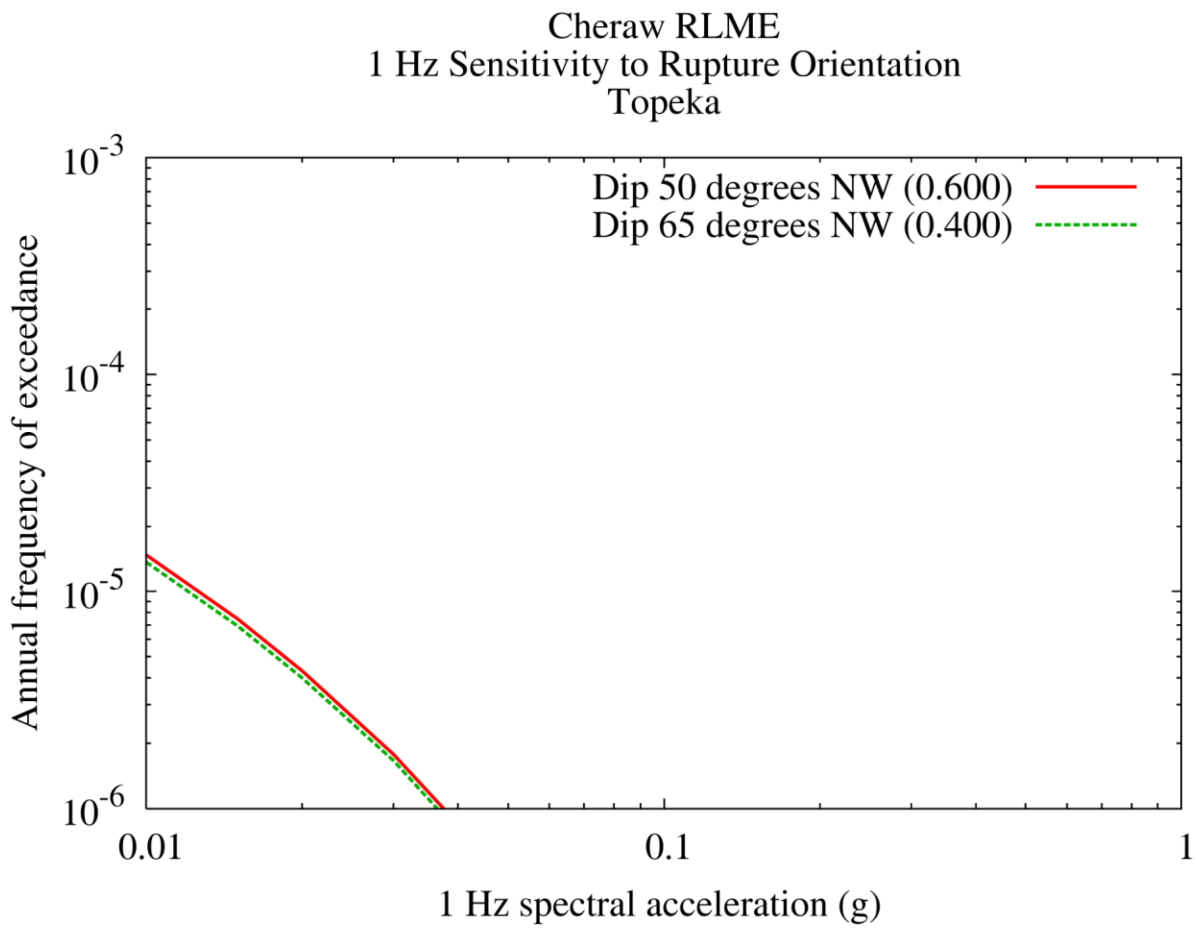

Figure 9.3-9
1 Hz sensitivity to rupture orientation (dip) at Topeka for the Cheraw fault source

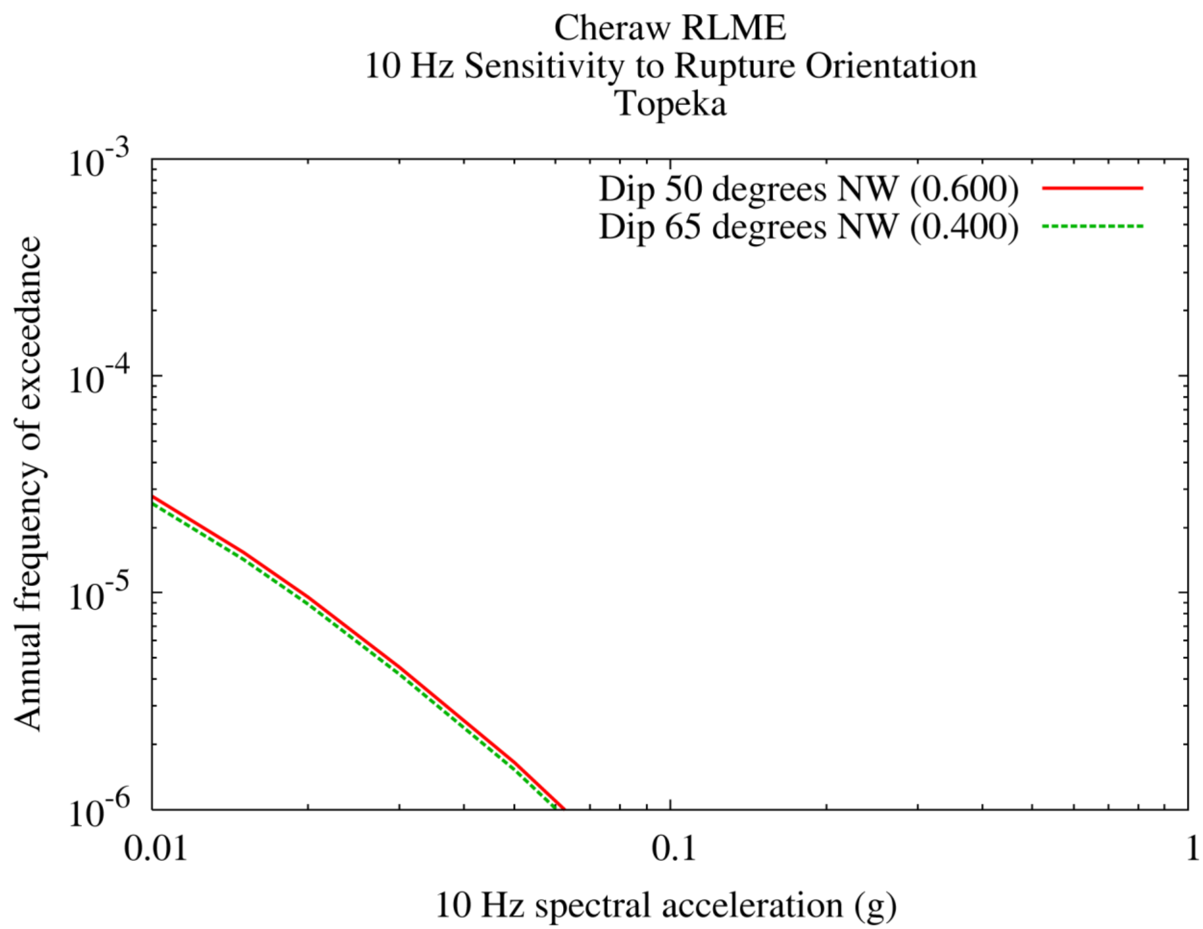

Figure 9.3-10
10 Hz sensitivity to rupture orientation at Topeka for the Cheraw fault source

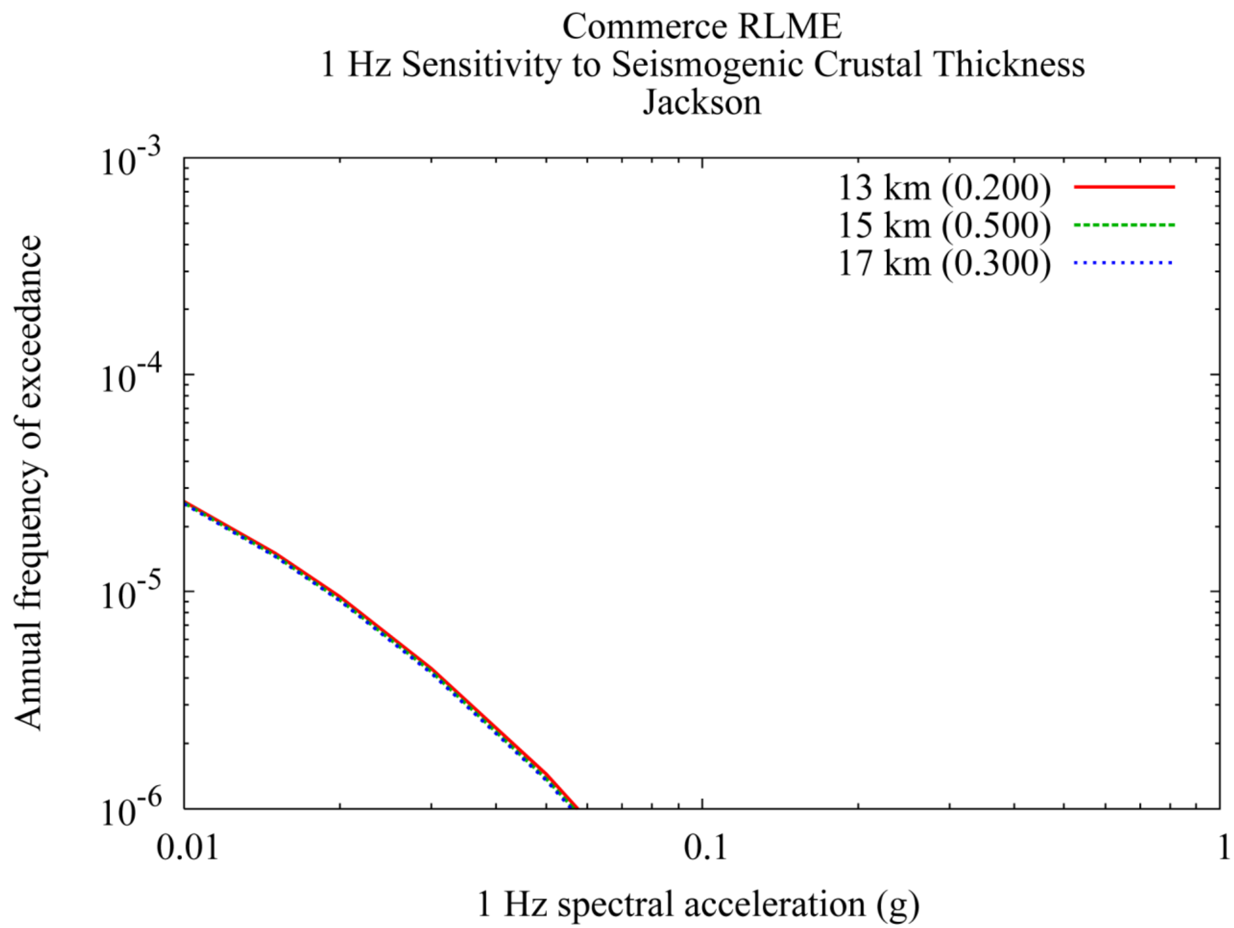

Figure 9.3-11
1 Hz sensitivity to seismogenic thickness at Jackson for the Commerce area source

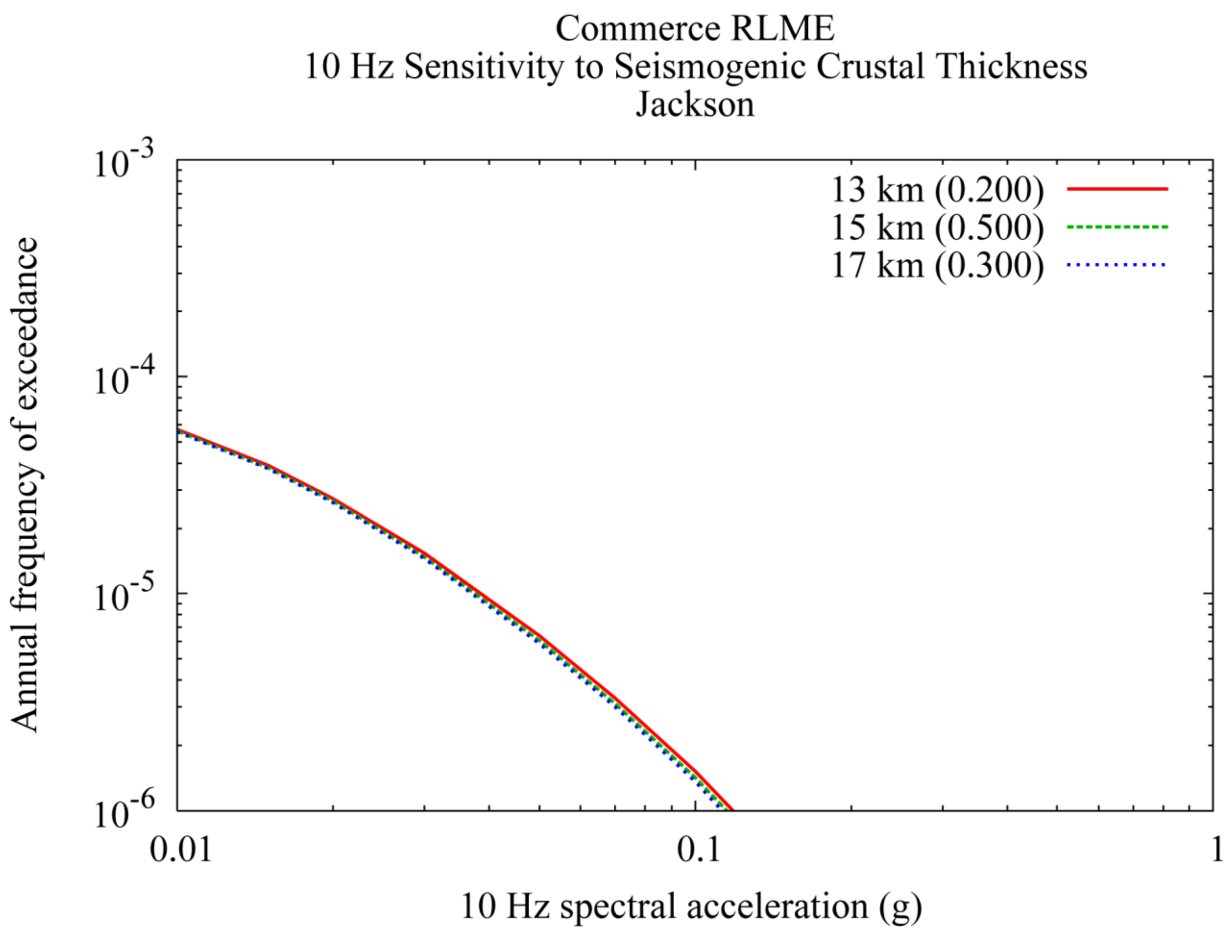

Figure 9.3-12
10 Hz sensitivity to seismogenic thickness at Jackson for the Commerce area source

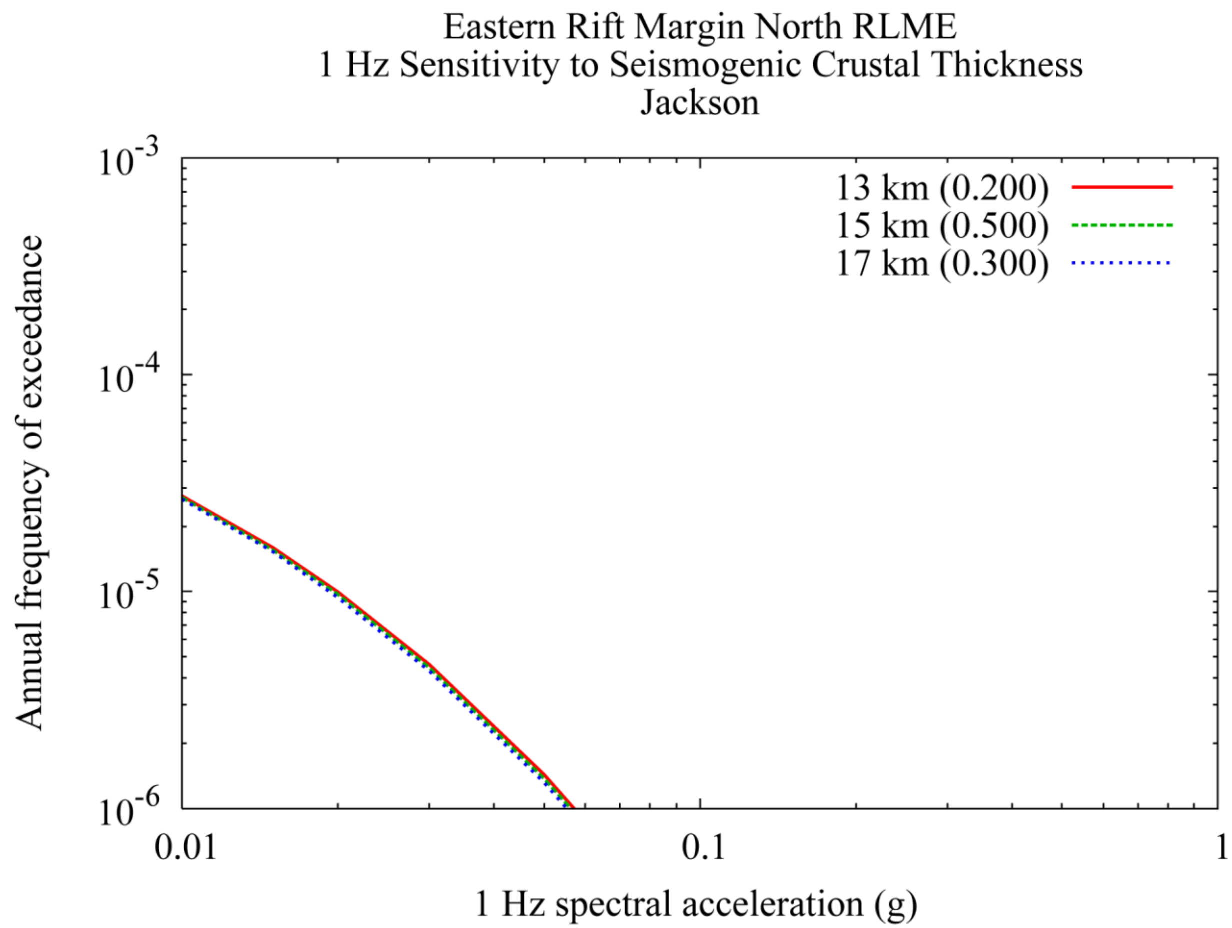

Figure 9.3-13
1 Hz sensitivity to seismogenic thickness at Jackson for the ERM-N area source

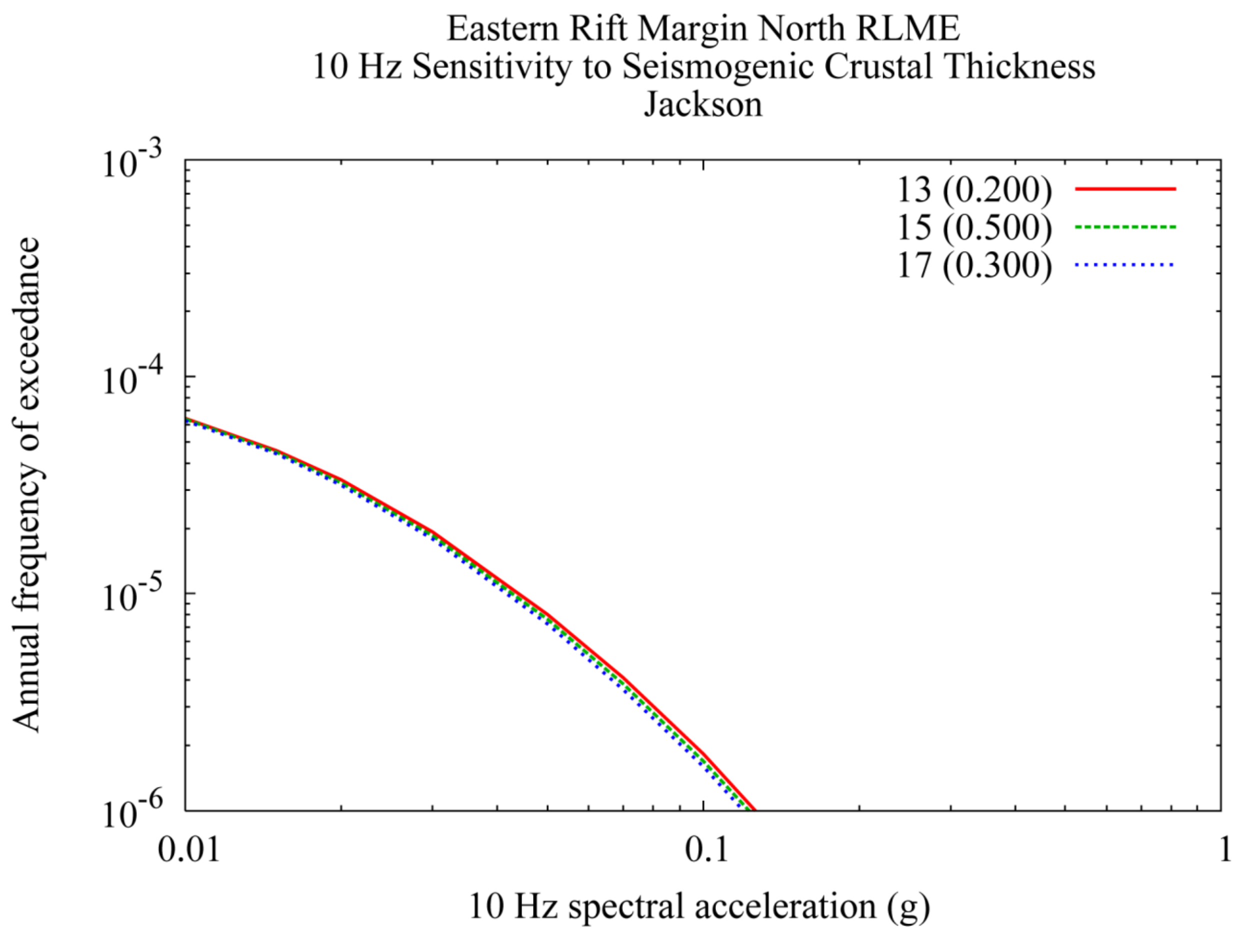

Figure 9.3-14
10 Hz sensitivity to seismogenic thickness at Jackson for the ERM-N area source

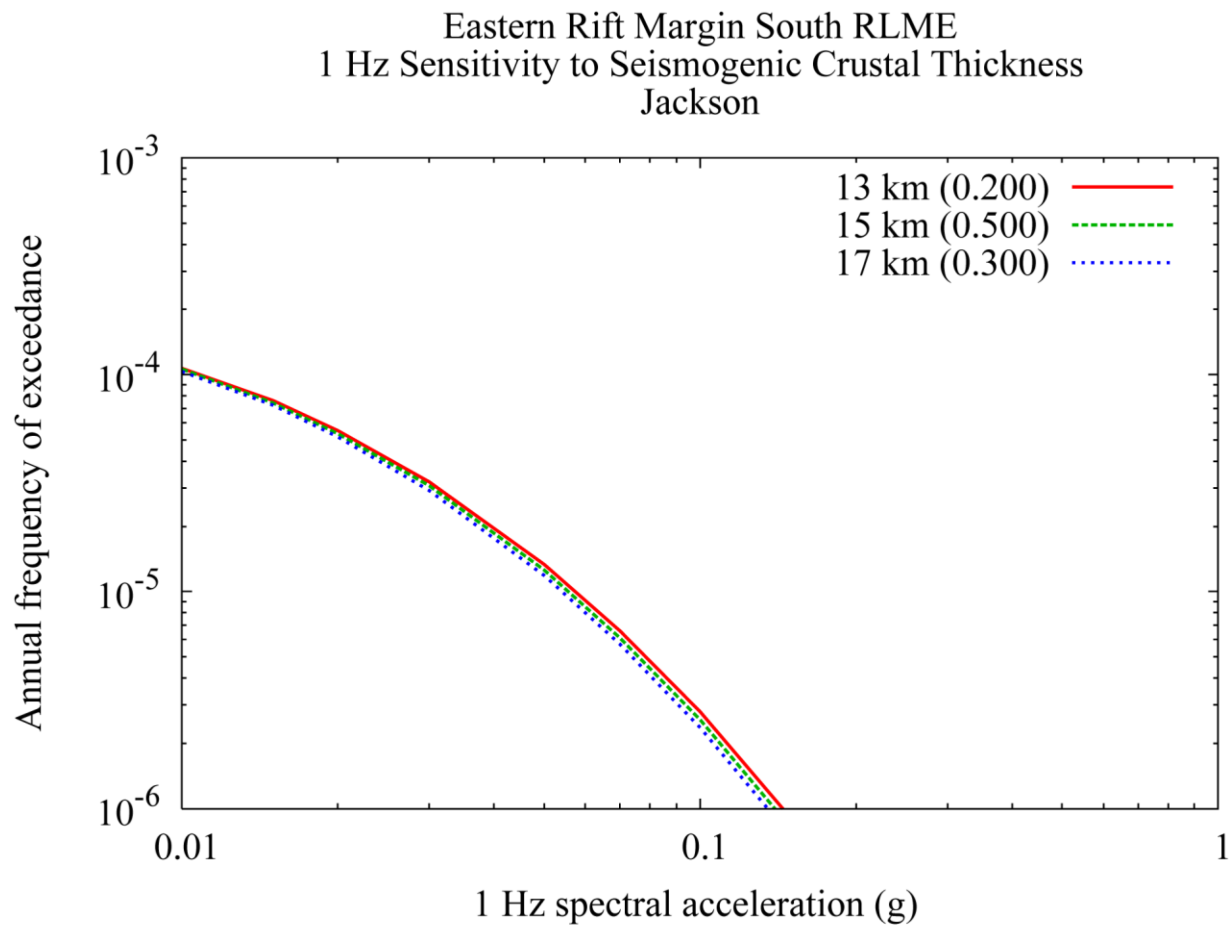

Figure 9.3-15
1 Hz sensitivity to seismogenic thickness at Jackson for the ERM-S area source

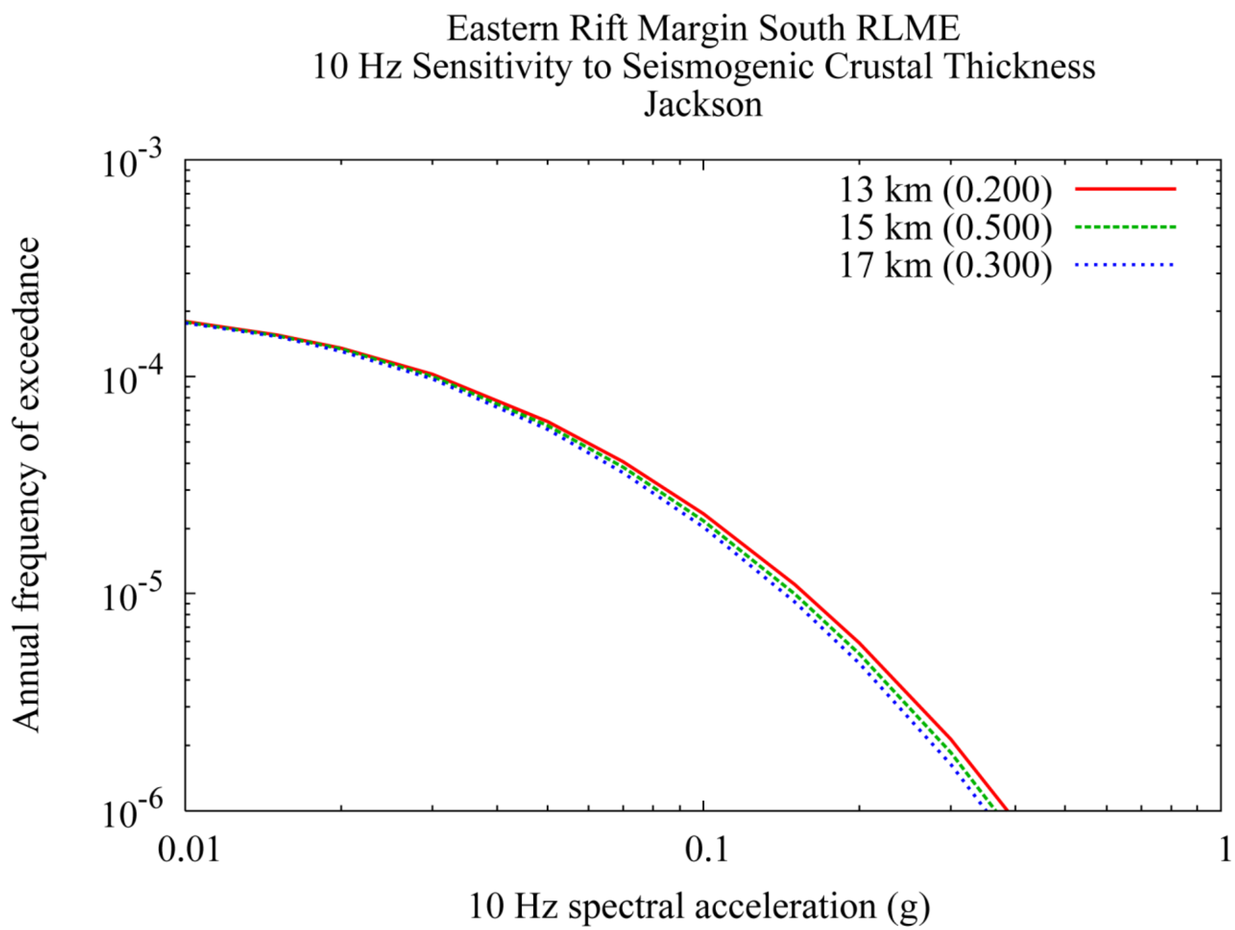

Figure 9.3-16
10 Hz sensitivity to seismogenic thickness at Jackson for the ERM-S area source

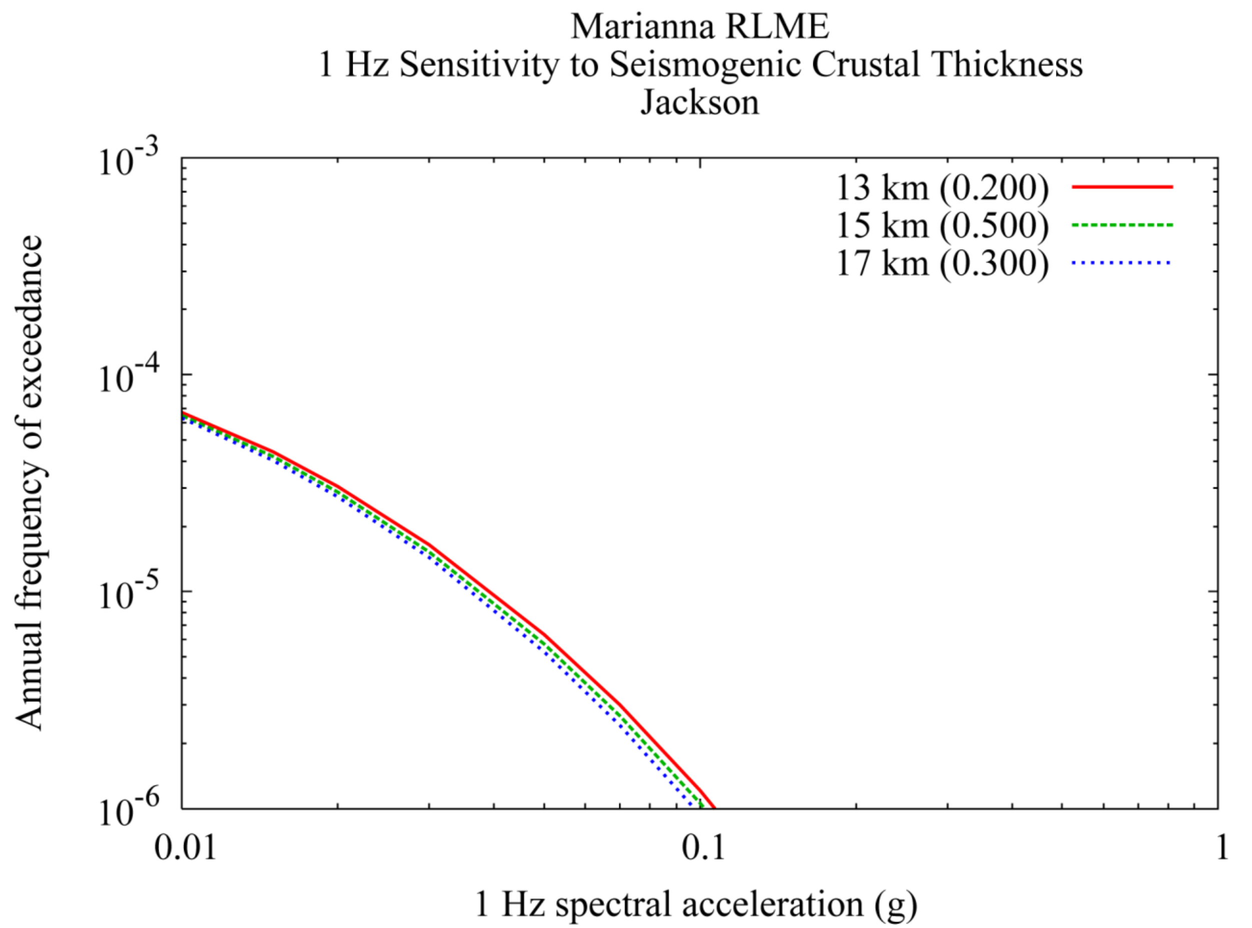

Figure 9.3-17
1 Hz sensitivity to seismogenic thickness at Jackson for the Marianna area source

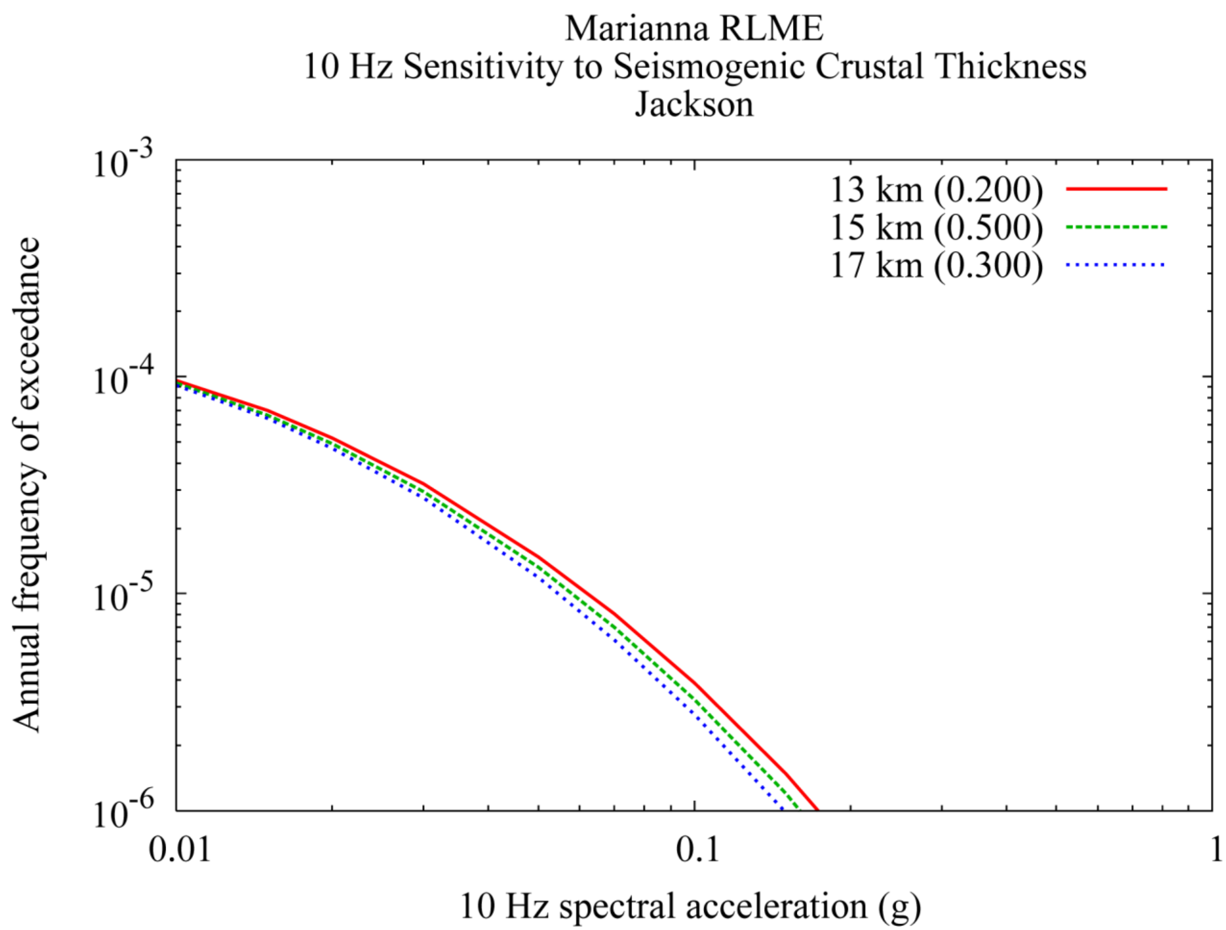

Figure 9.3-18
10 Hz sensitivity to seismogenic thickness at Jackson for the Marianna area source

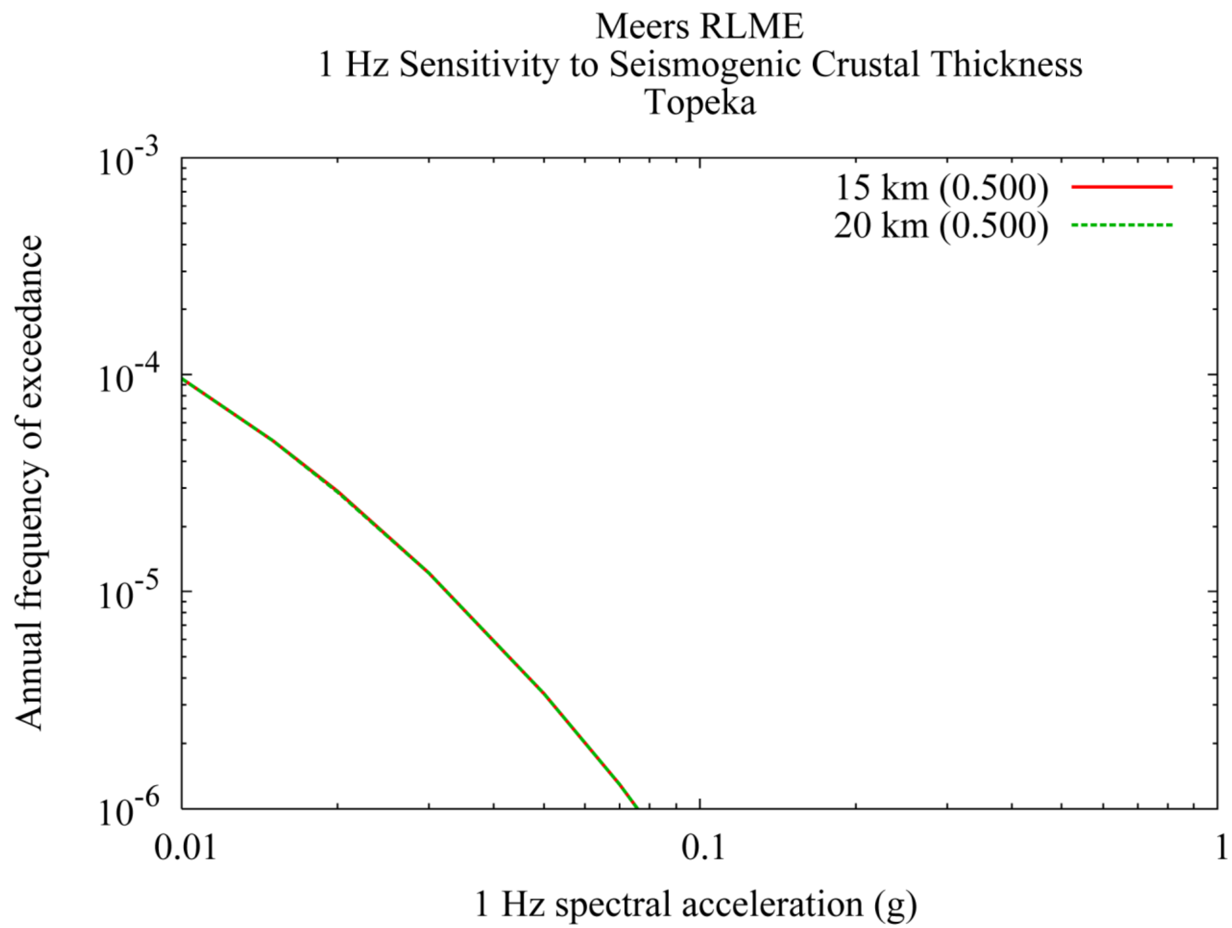

Figure 9.3-19
1 Hz sensitivity to seismogenic thickness at Topeka for the Meers fault and OKA area sources

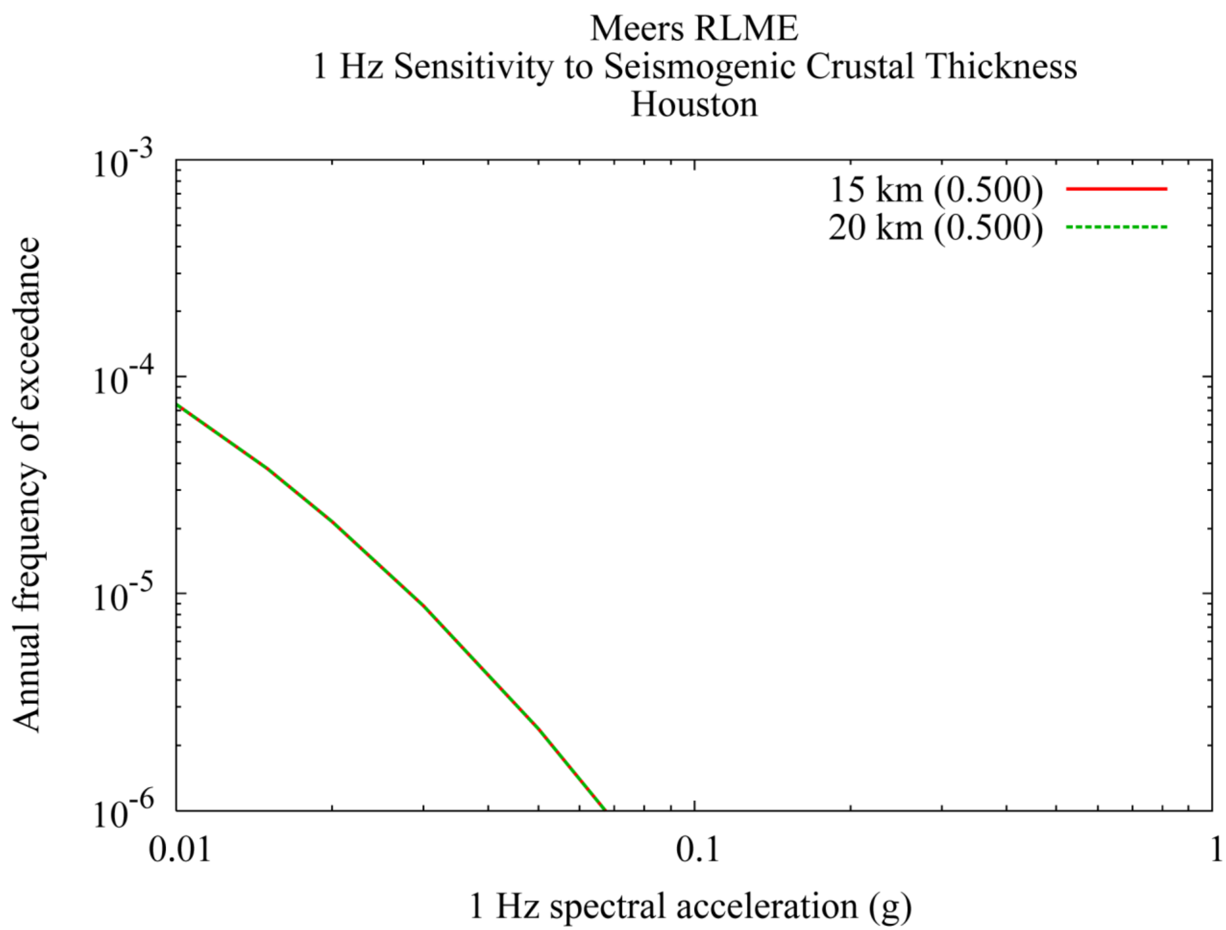

Figure 9.3-20
1 Hz sensitivity to seismogenic thickness at Houston for the Meers fault and OKA area sources

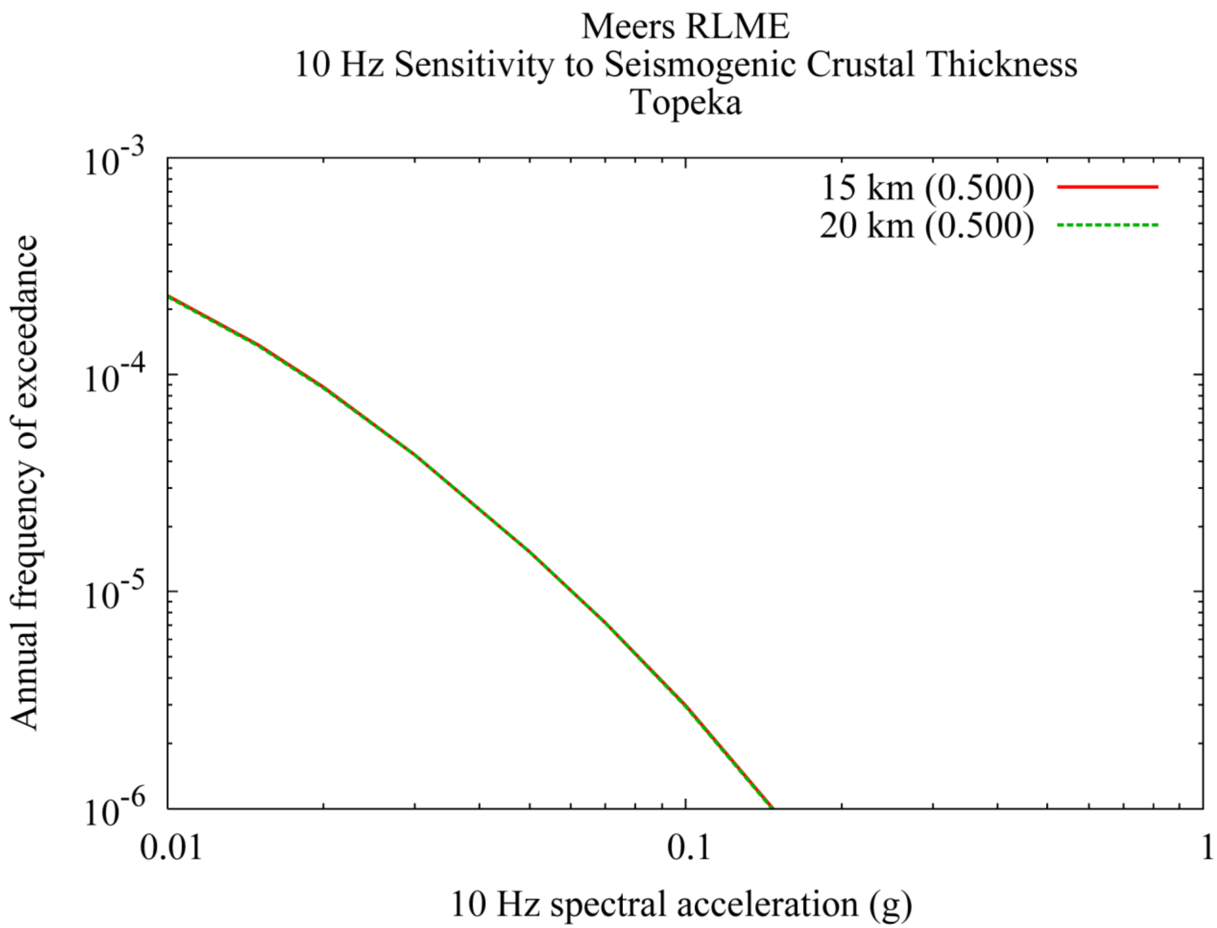

Figure 9.3-21
10 Hz sensitivity to seismogenic thickness at Topeka for the Meers fault and OKA area sources

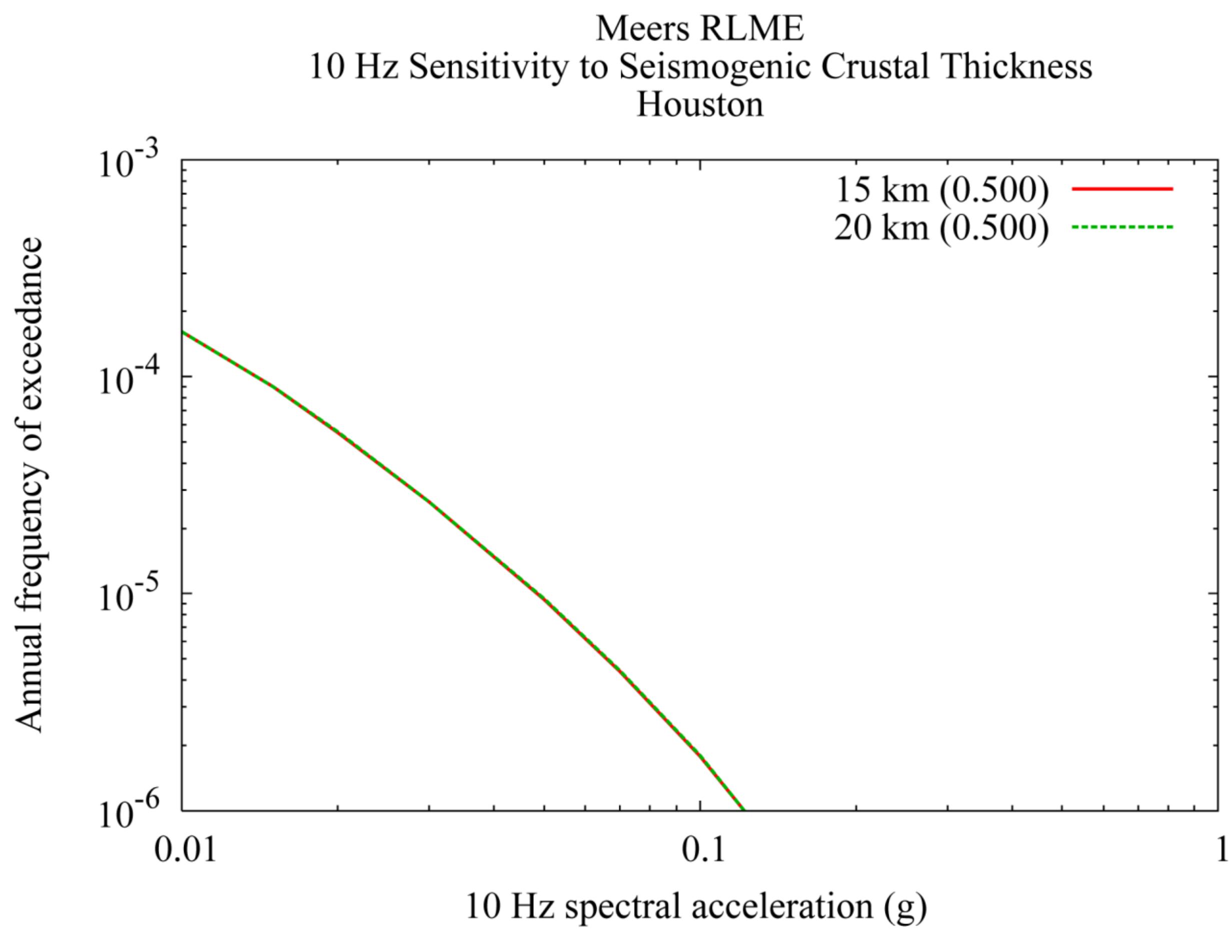

Figure 9.3-22
10 Hz sensitivity to seismogenic thickness at Houston for the Meers fault and OKA area sources

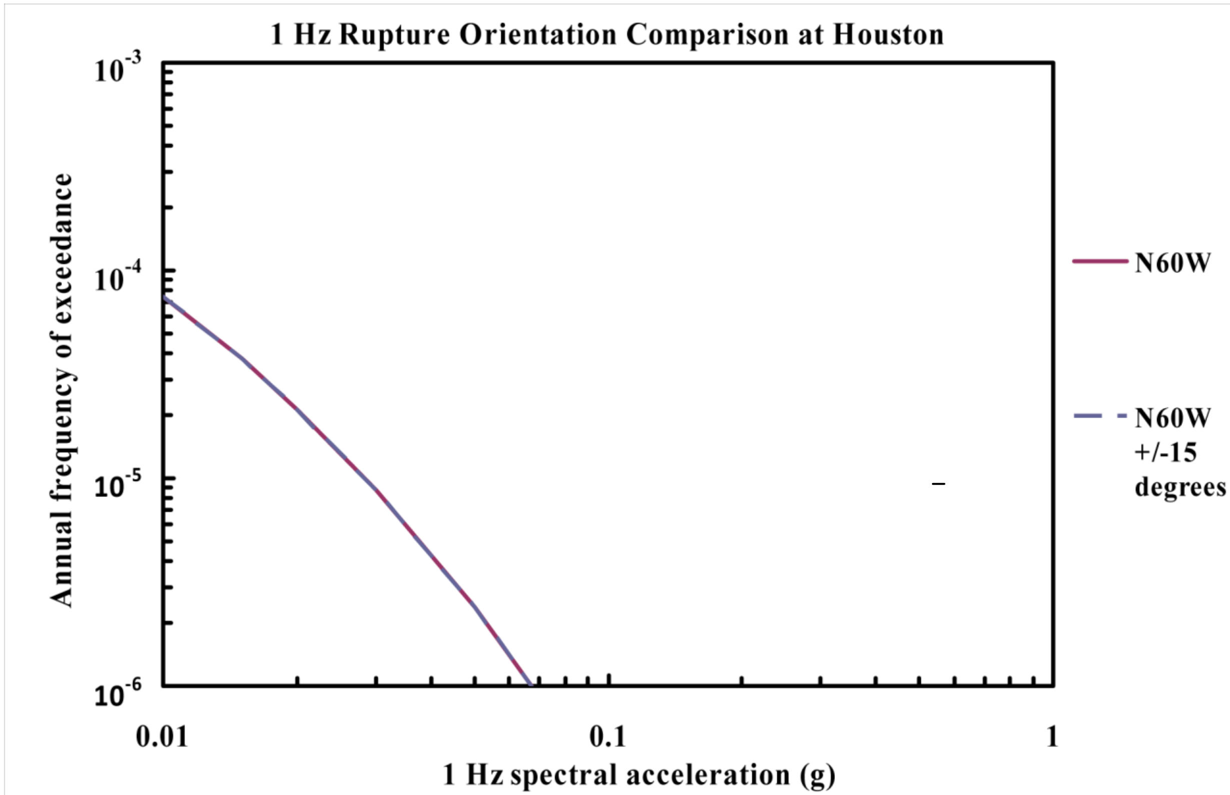

Figure 9.3-23
1 Hz sensitivity to rupture orientation at Houston for the OKA area source

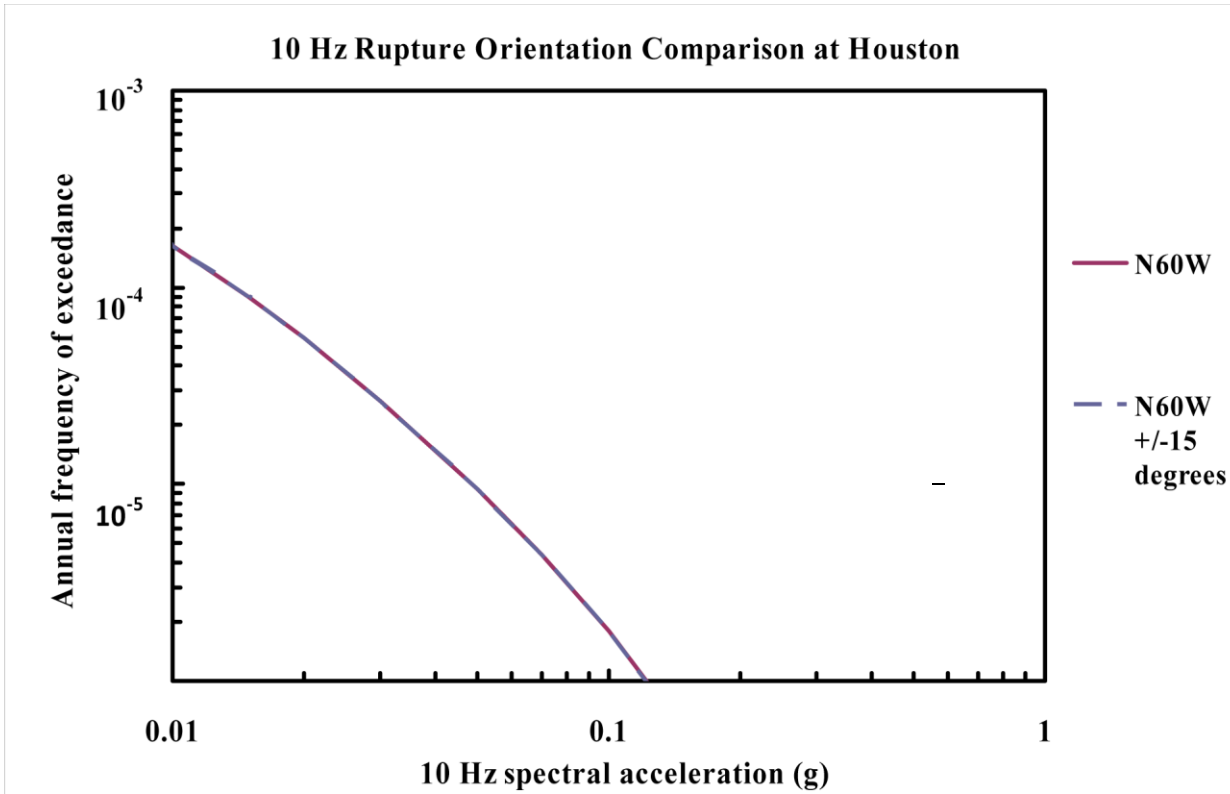

Figure 9.3-24
10 Hz sensitivity to rupture orientation at Houston for the OKA area source

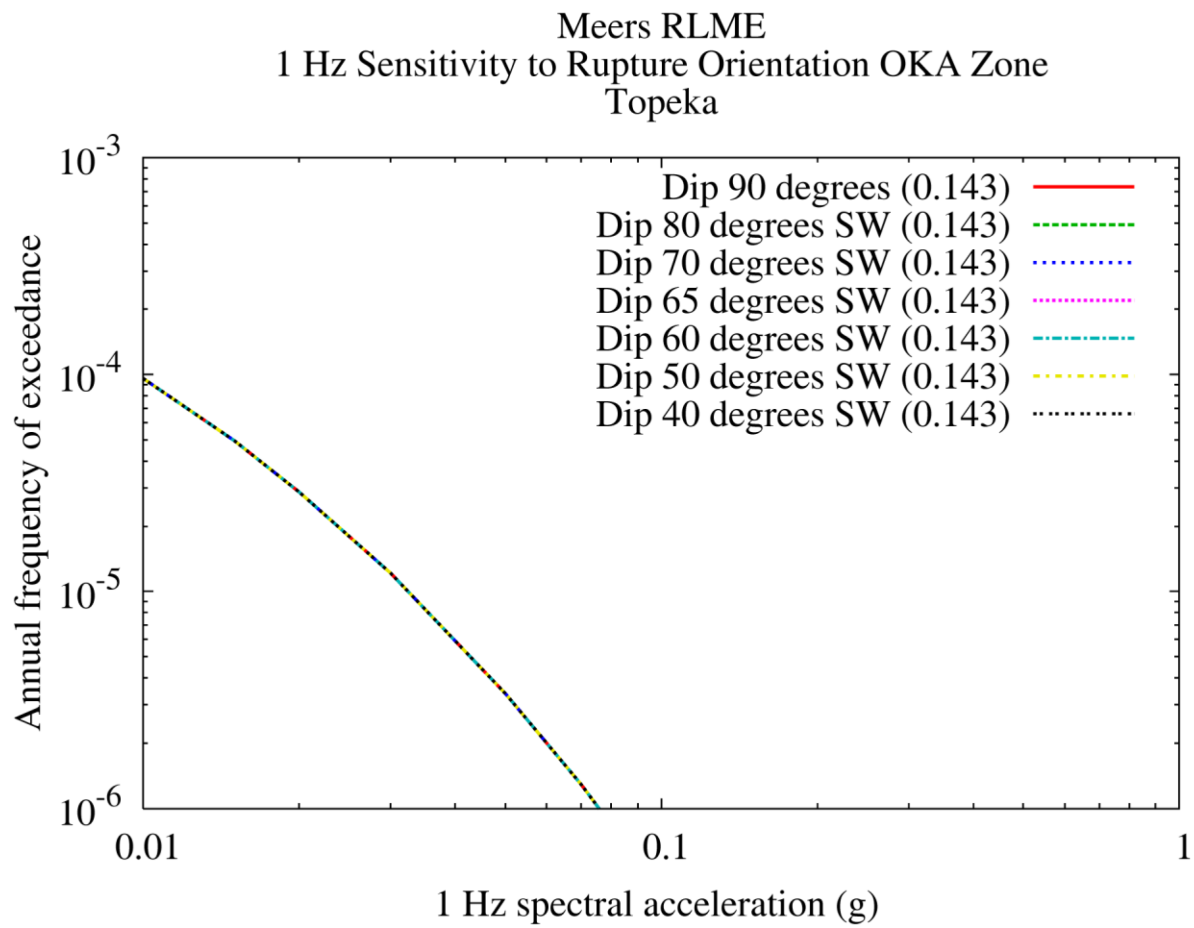

Figure 9.3-25
1 Hz sensitivity to rupture orientation (dip) at Topeka for the OKA area source

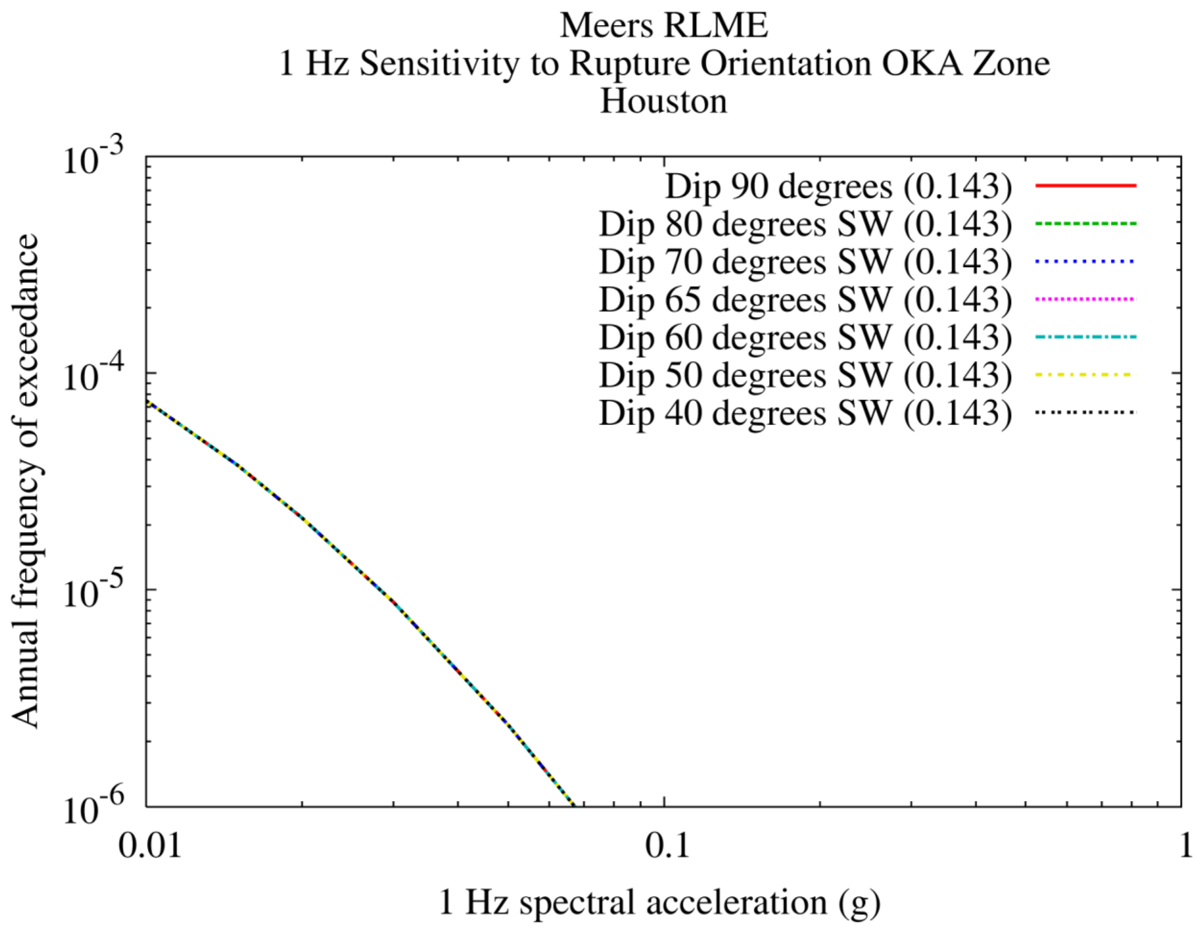

Figure 9.3-26
1 Hz sensitivity to rupture orientation (dip) at Houston for the OKA area source

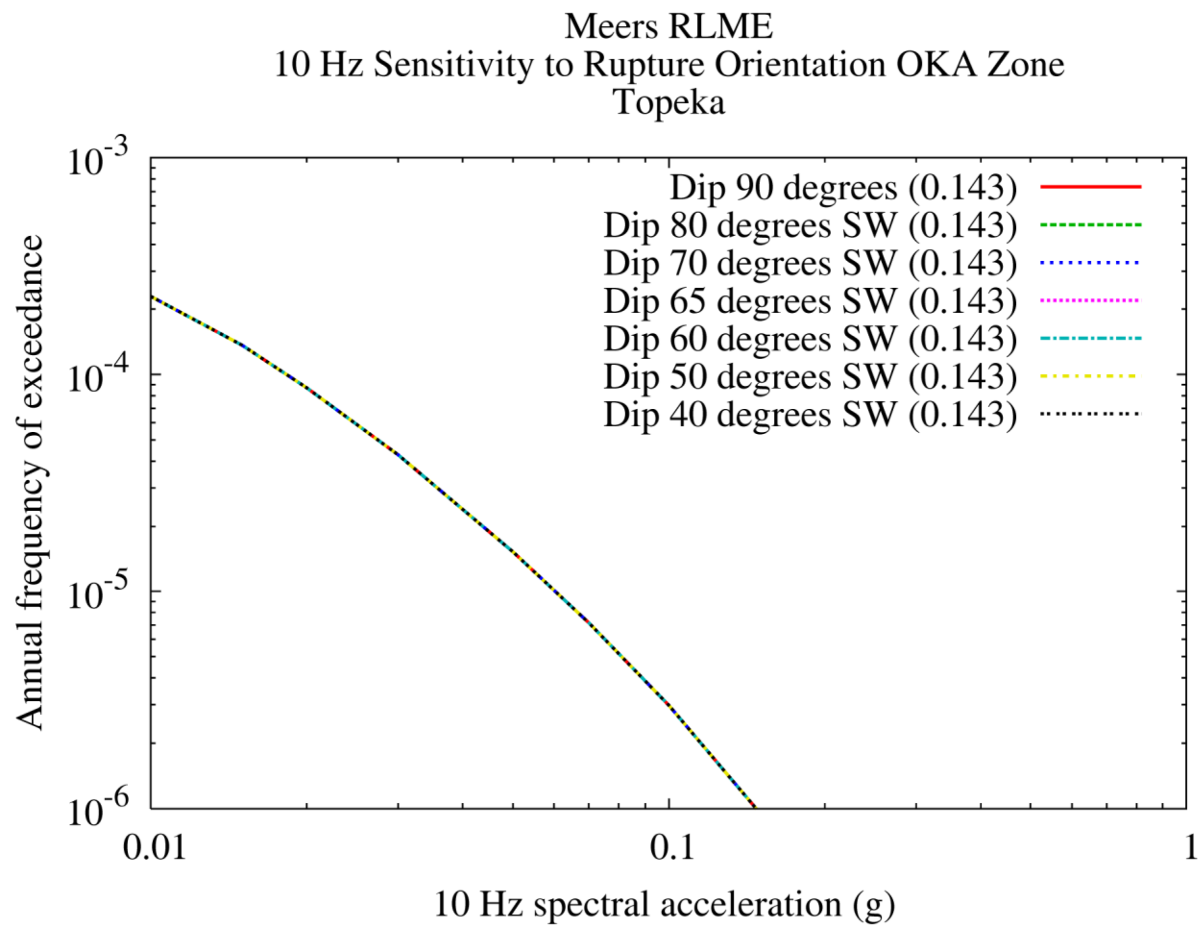

Figure 9.3-27
10 Hz sensitivity to rupture orientation (dip) at Topeka for the OKA area source

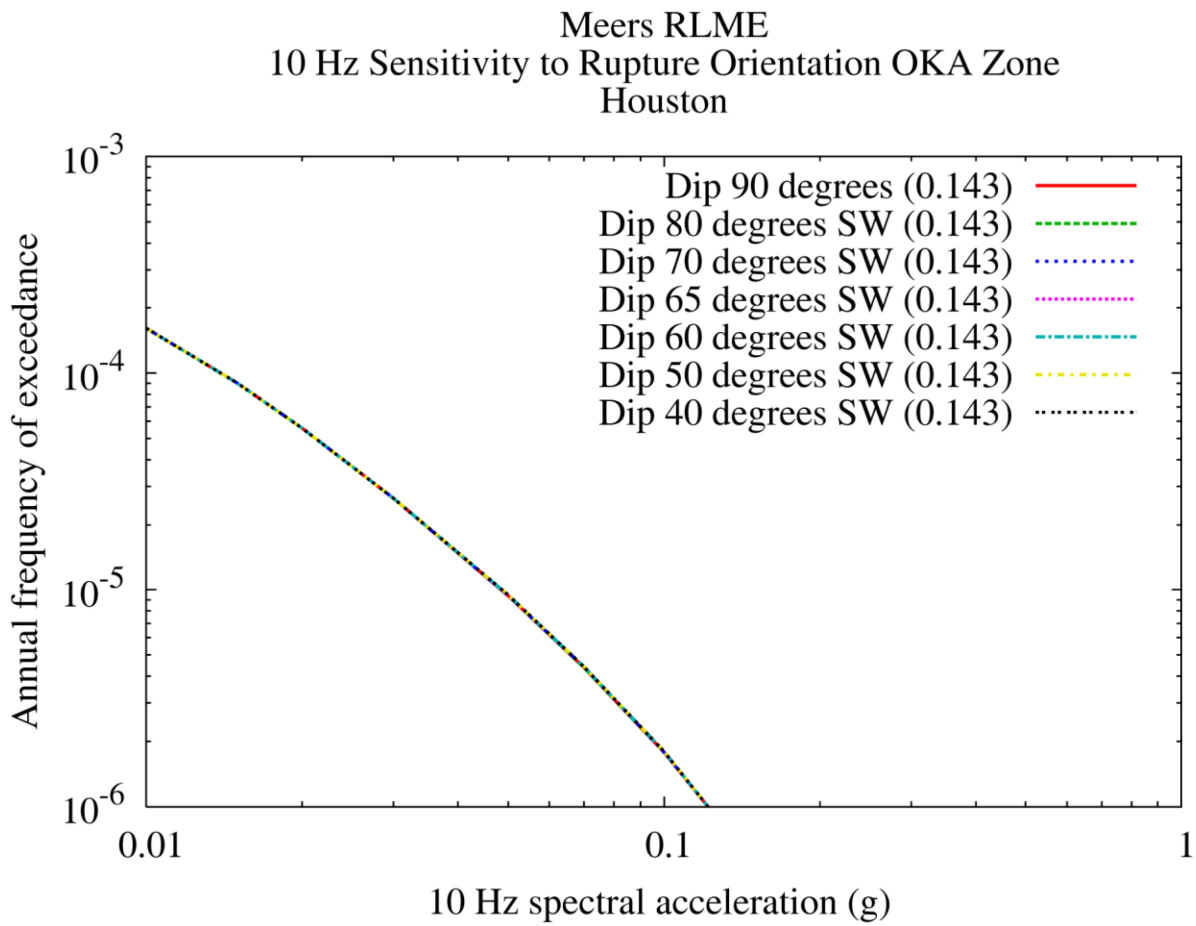

Figure 9.3-28
10 Hz sensitivity to rupture orientation (dip) at Houston for the OKA area source

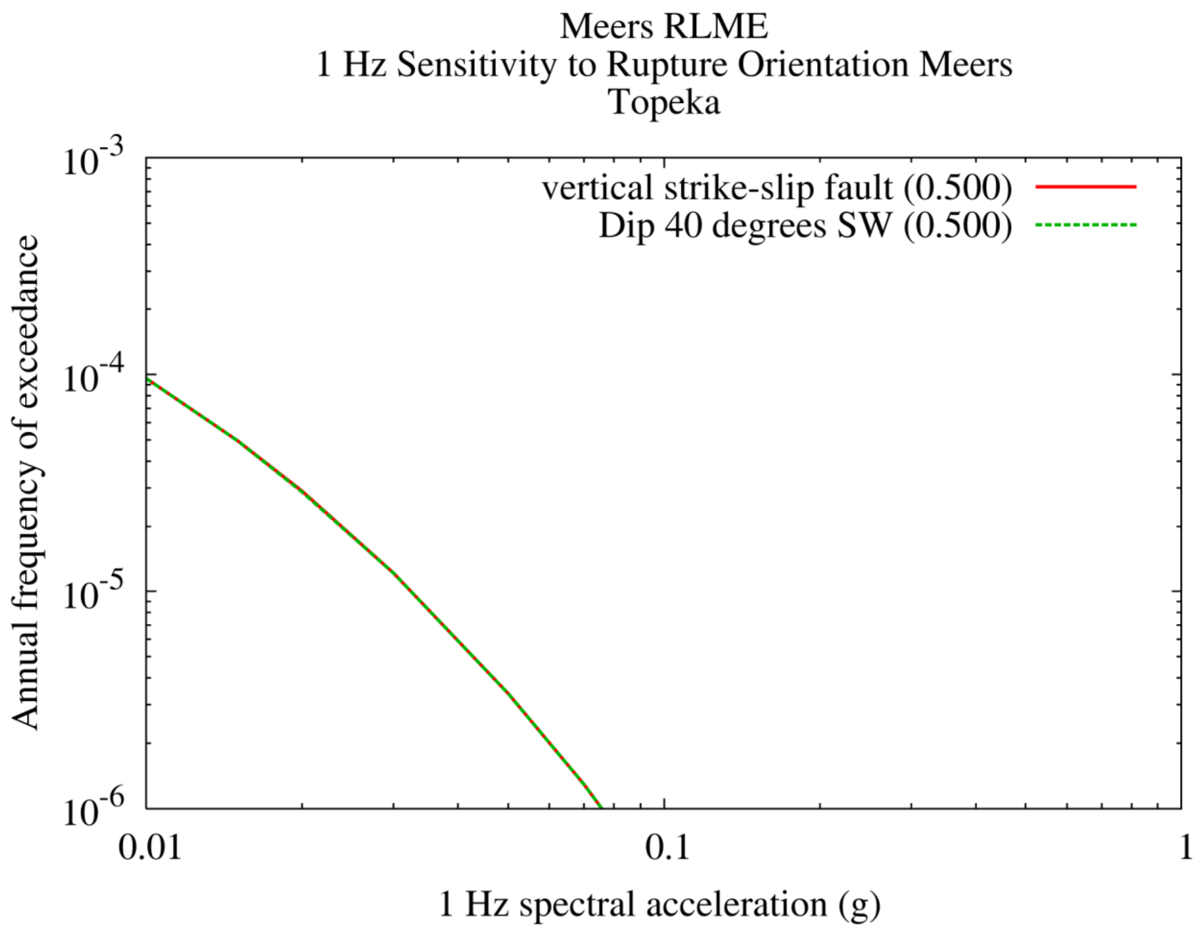

Figure 9.3-29
1 Hz sensitivity to rupture orientation (dip) at Topeka for the Meers fault source

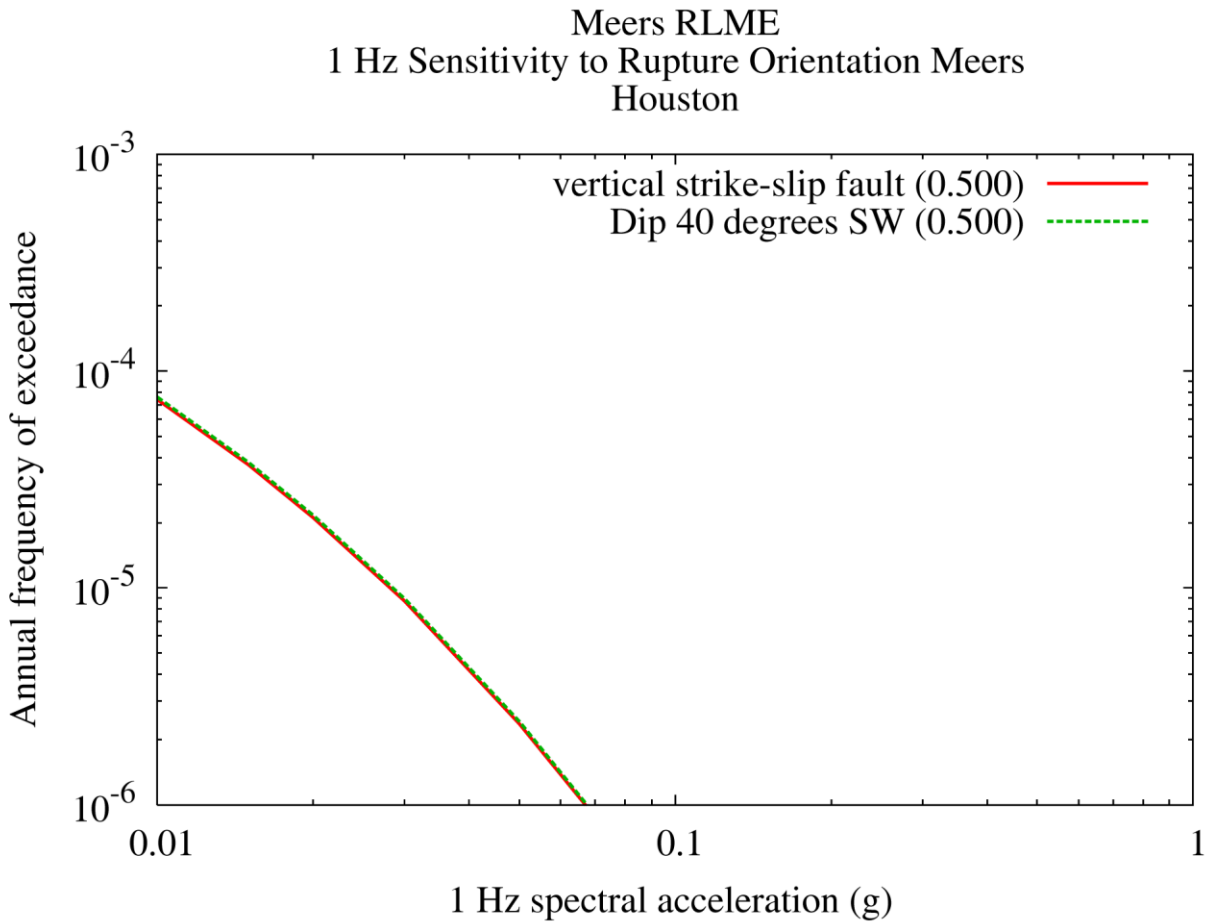

Figure 9.3-30
1 Hz sensitivity to rupture orientation (dip) at Houston for the Meers fault source

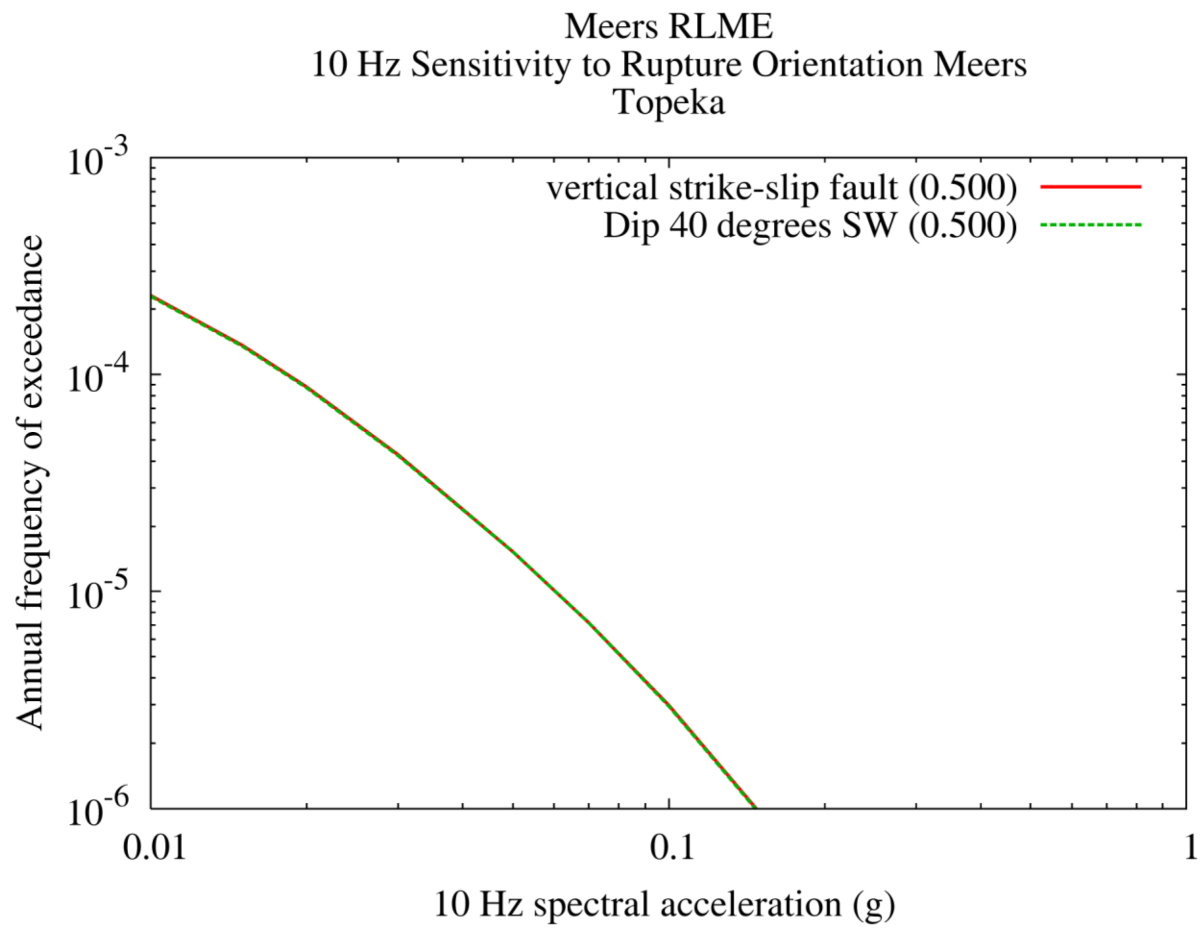

Figure 9.3-31
10 Hz sensitivity to rupture orientation (dip) at Topeka for the Meers fault source

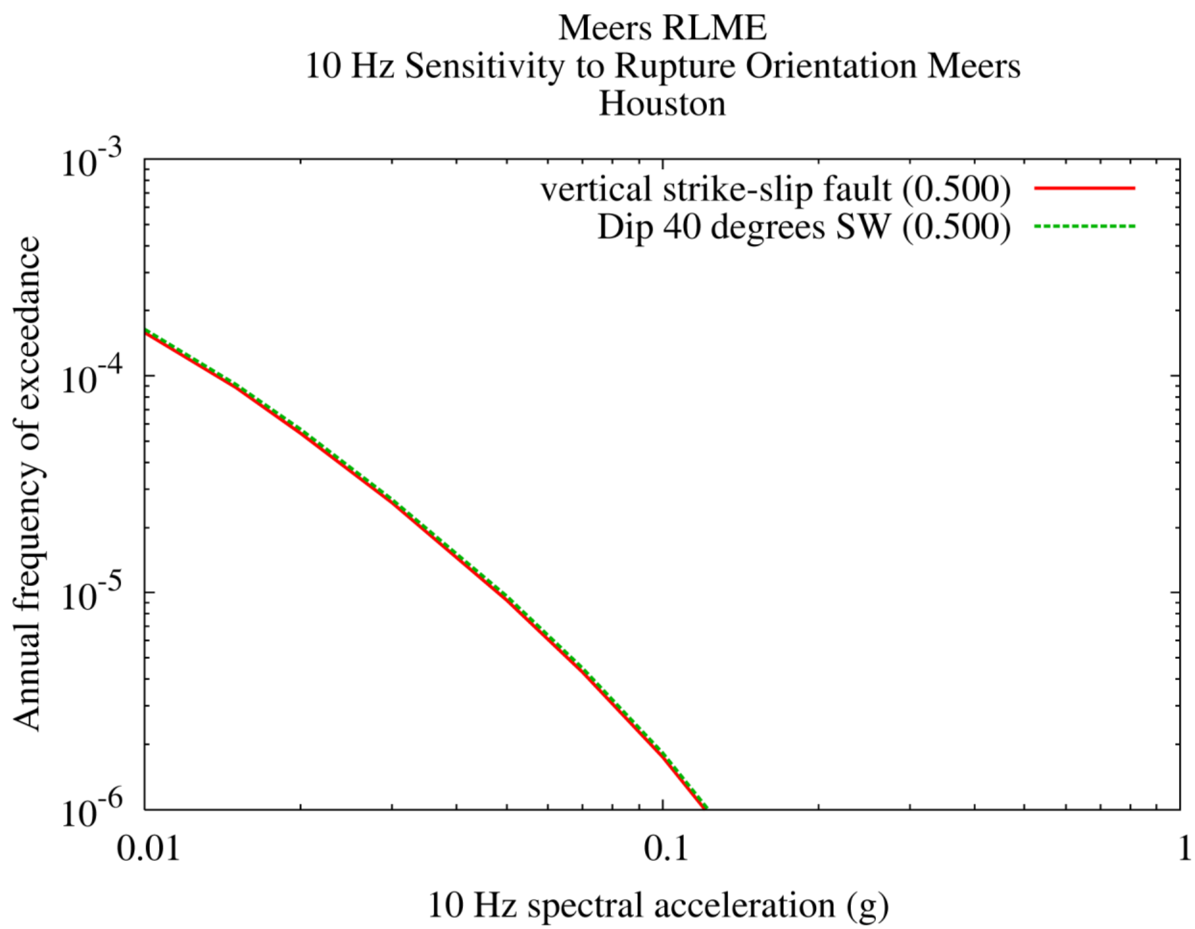

Figure 9.3-32
10 Hz sensitivity to rupture orientation (dip) at Houston for the Meers fault source

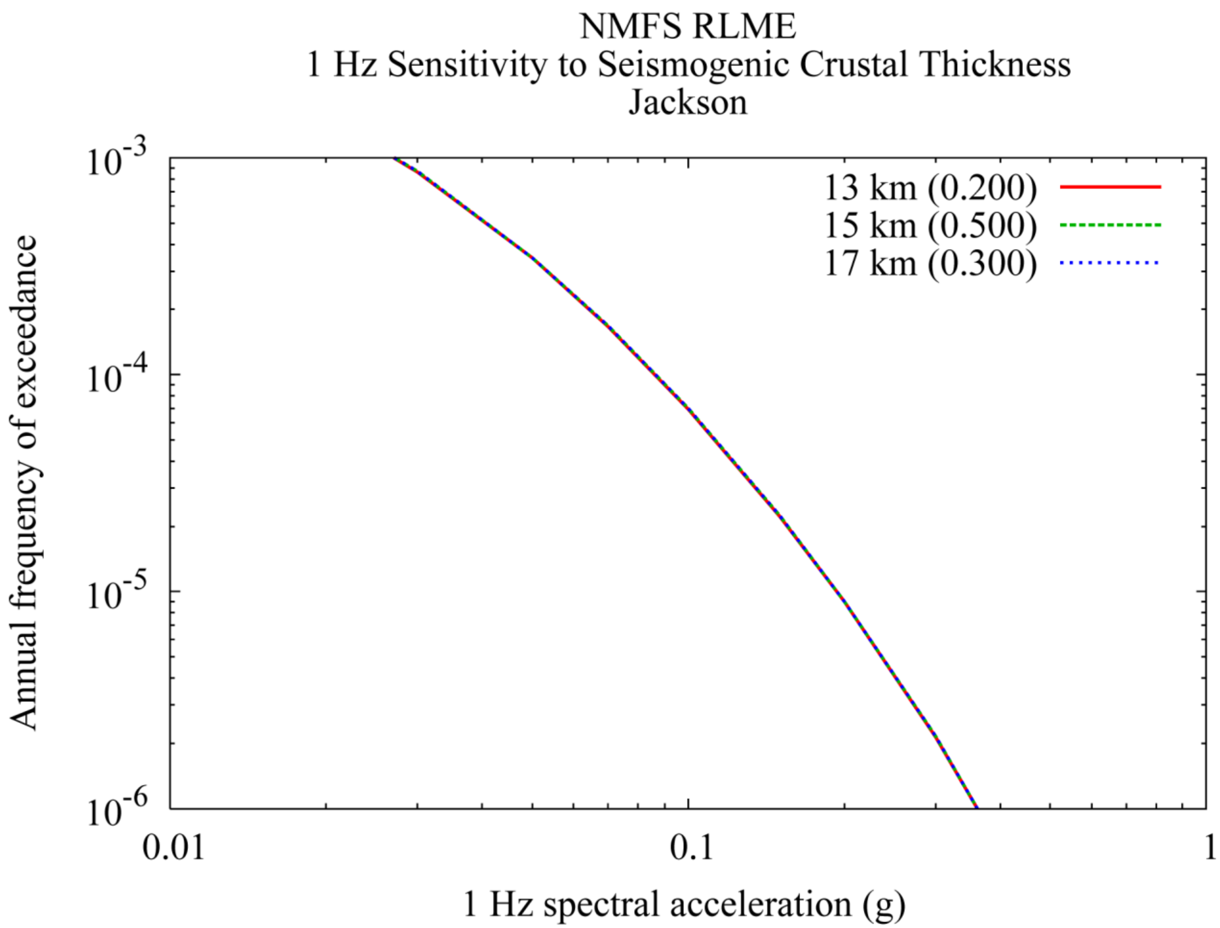

Figure 9.3-33
1 Hz sensitivity to seismogenic thickness at Jackson for the NMFS fault sources

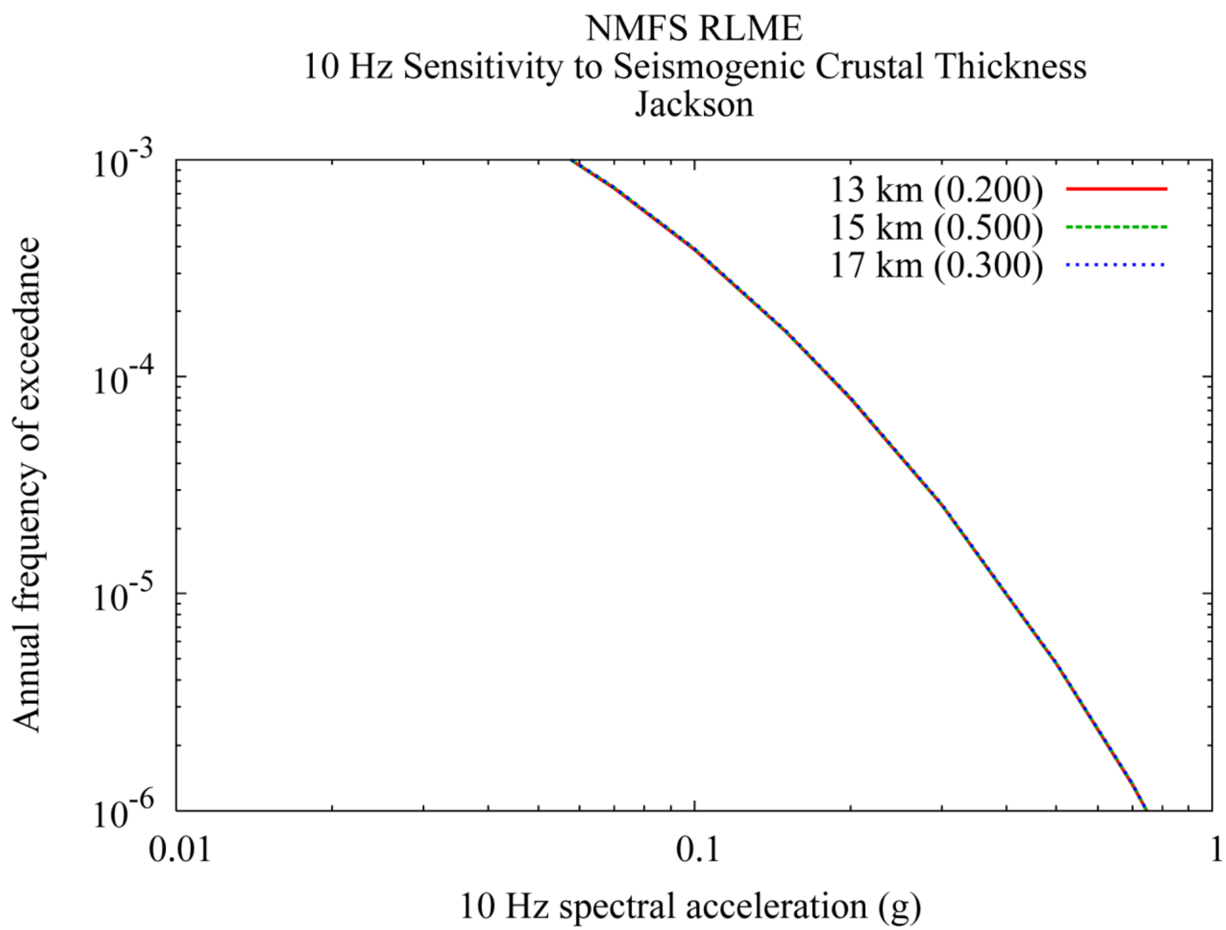

Figure 9.3-34
10 Hz sensitivity to seismogenic thickness at Jackson for the NMFS fault sources

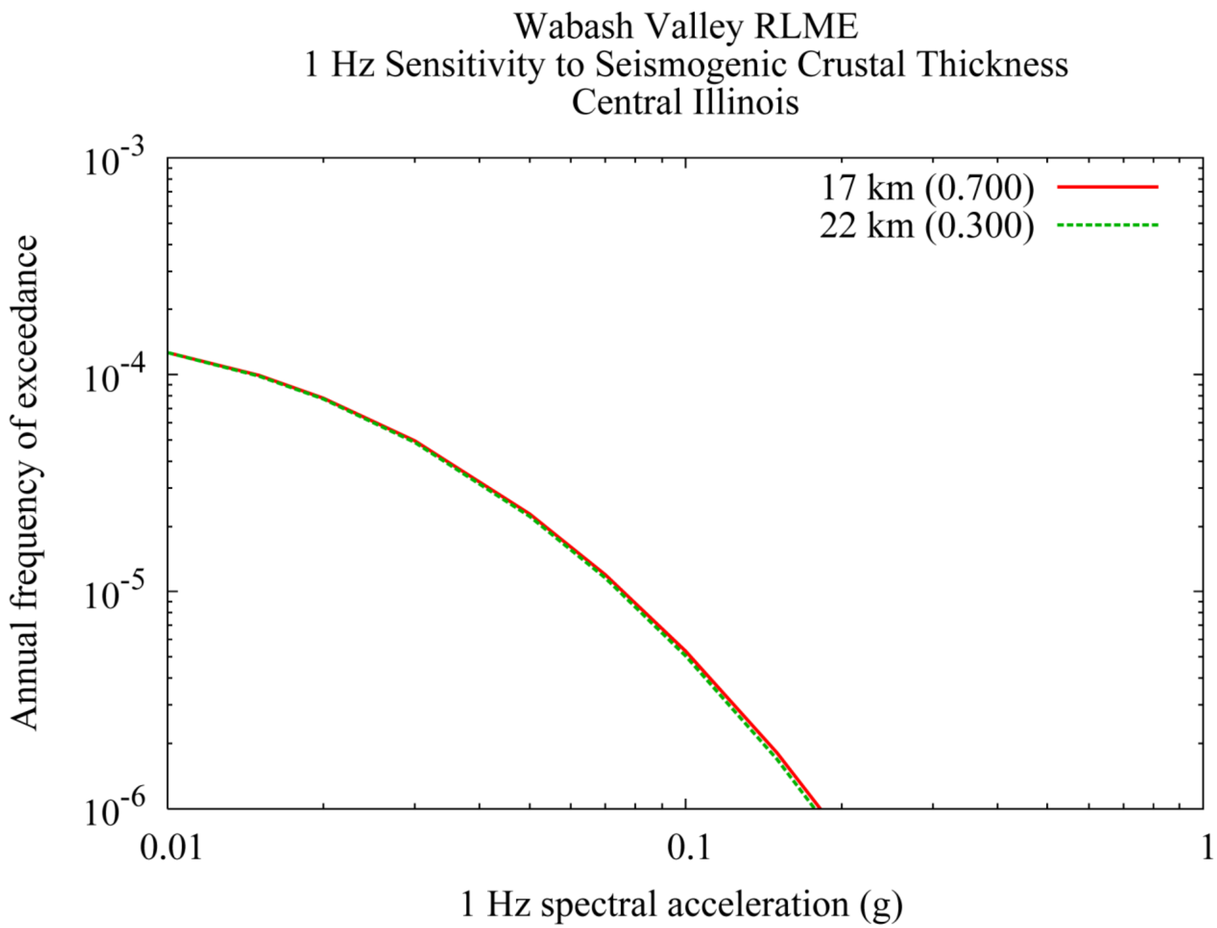

Figure 9.3-35
1 Hz sensitivity to seismogenic thickness at Central Illinois for the Wabash Valley area source

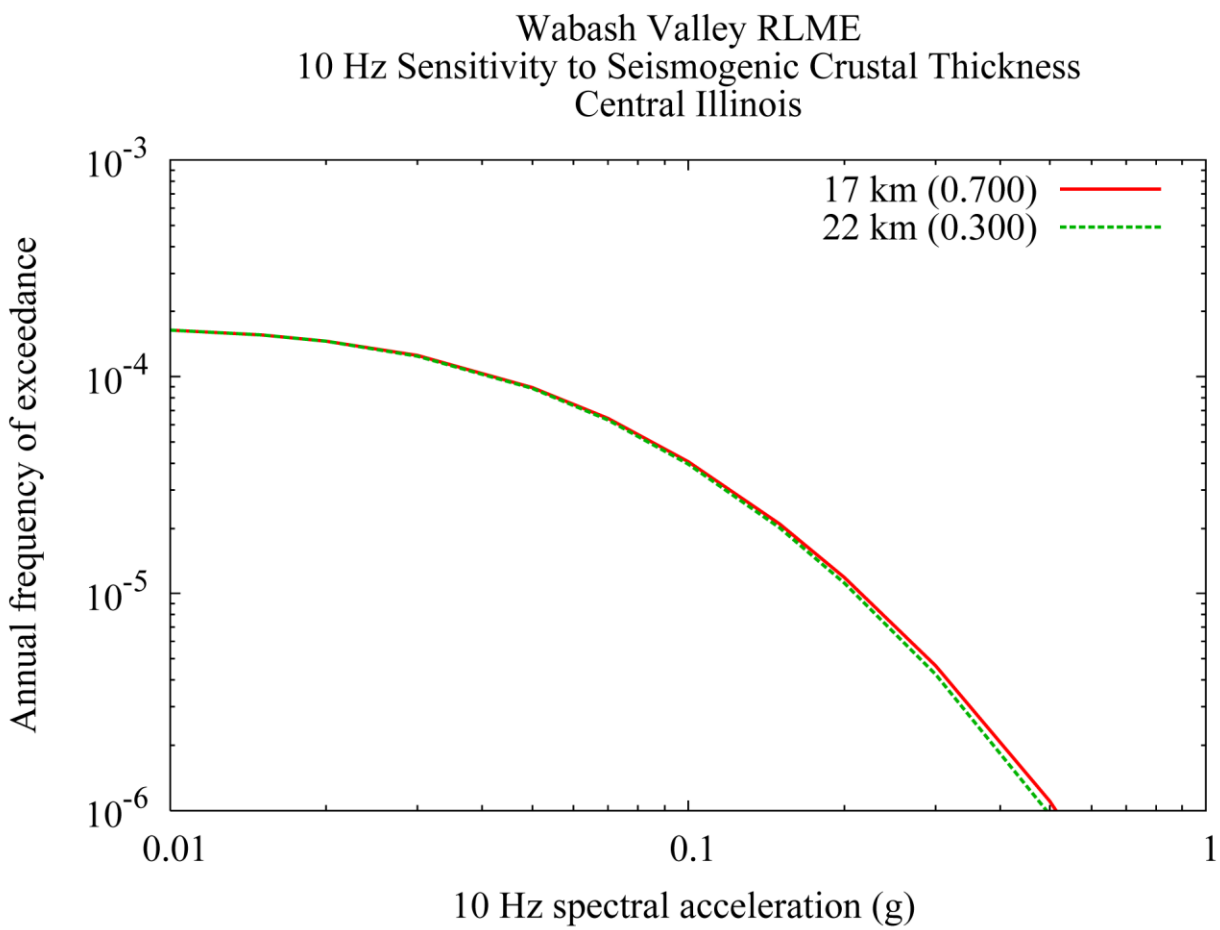

Figure 9.3-36
10 Hz sensitivity to seismogenic thickness at Central Illinois for the Wabash Valley area source

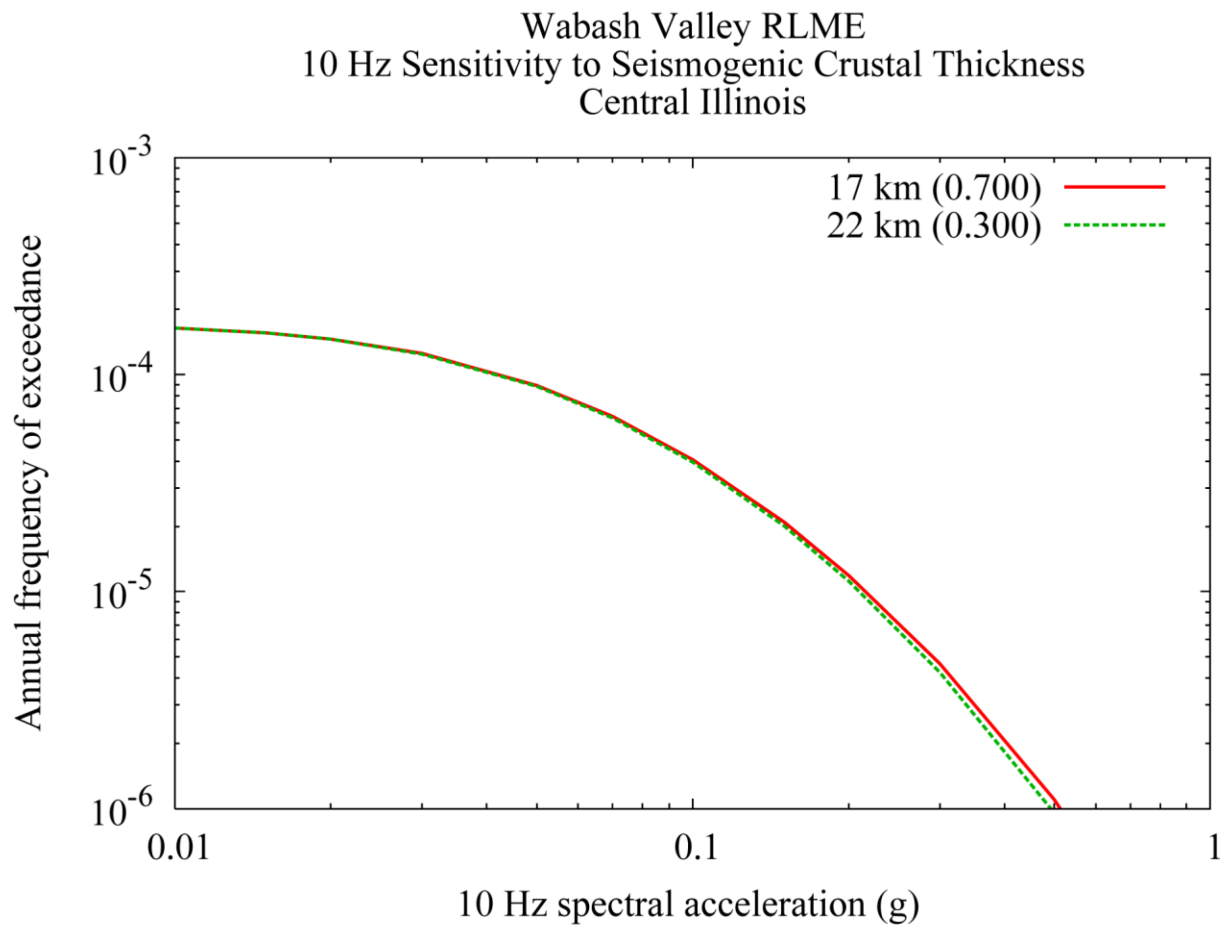

Figure 9.3-37
1 Hz sensitivity to rupture orientation (dip) at Central Illinois for the Wabash Valley area source

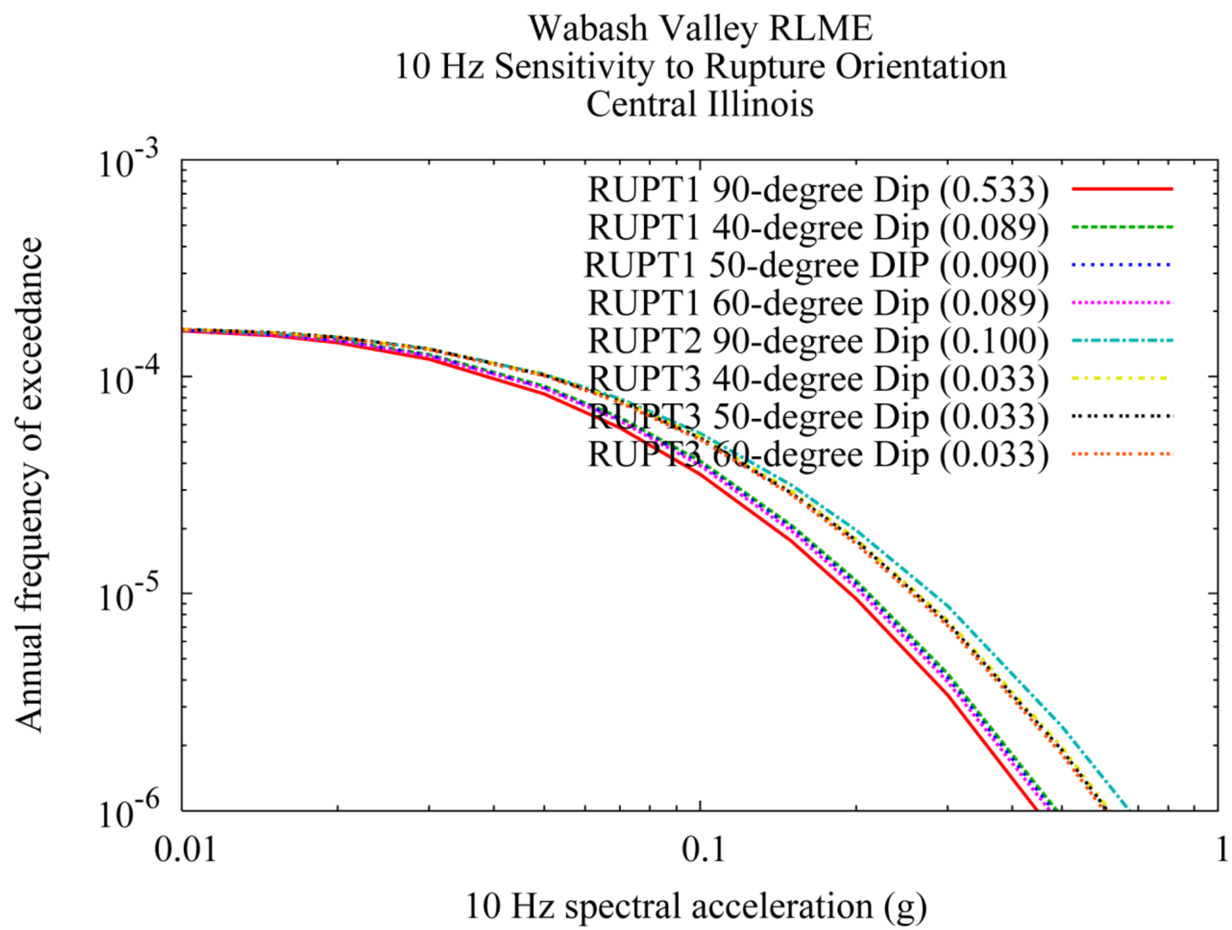

Figure 9.3-38
10 Hz sensitivity to rupture orientation (dip) at Central Illinois for the Wabash Valley area source

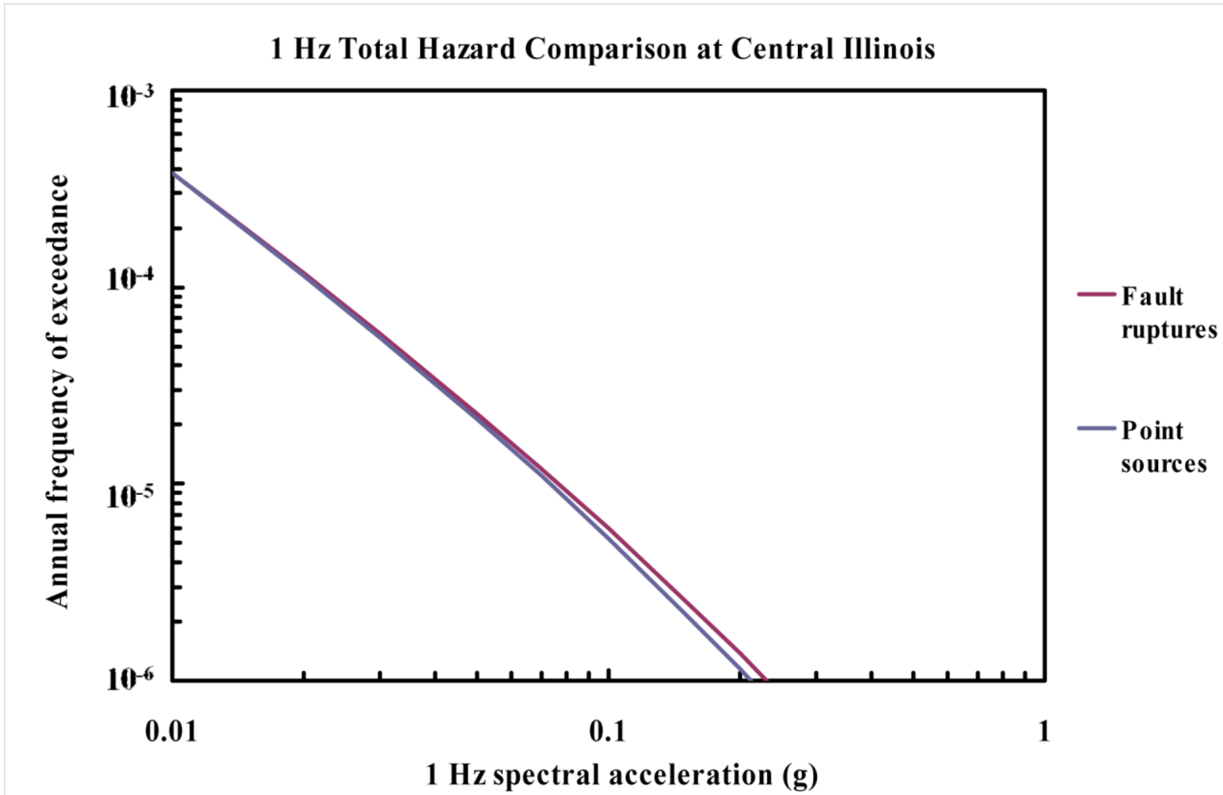

Figure 9.3-39
1 Hz sensitivity to fault ruptures vs. point source for the Central Illinois site from the Mid-C–A background source

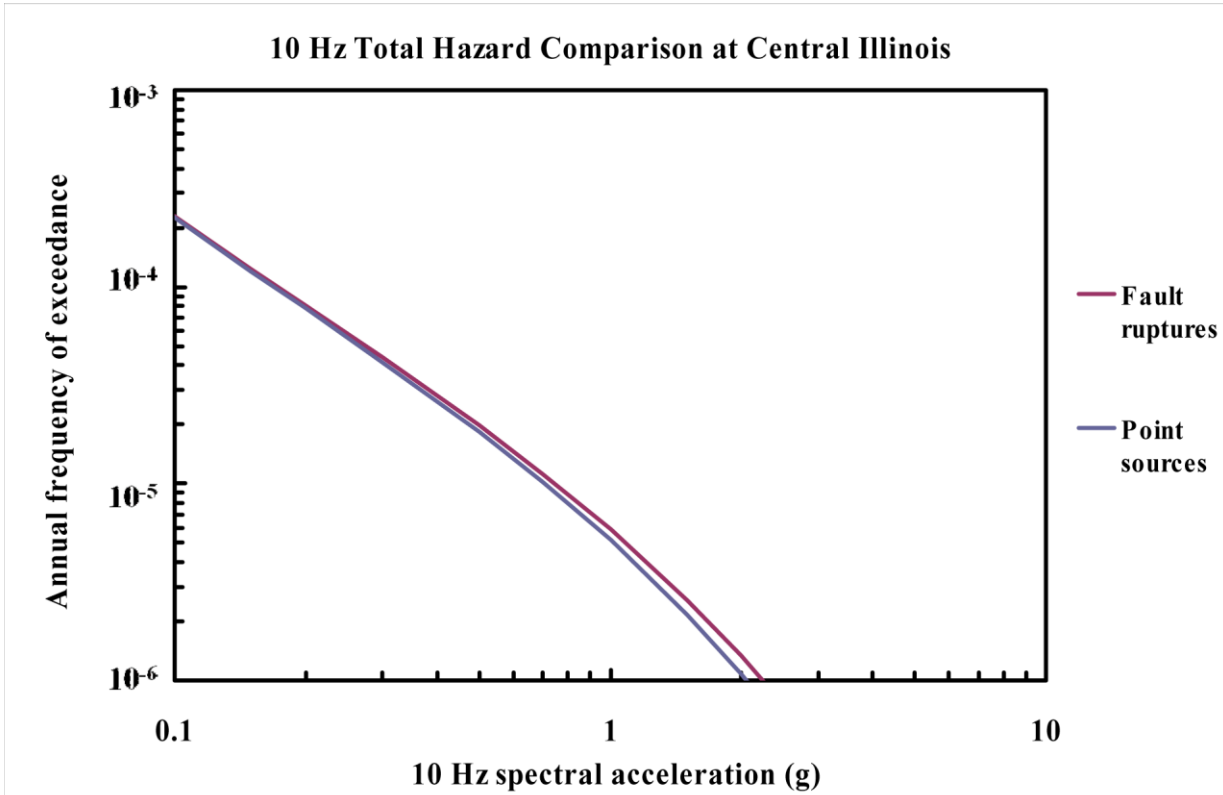

Figure 9.3-40
10 Hz sensitivity to fault ruptures vs. point source for the Central Illinois site from the Mid-C–A background source

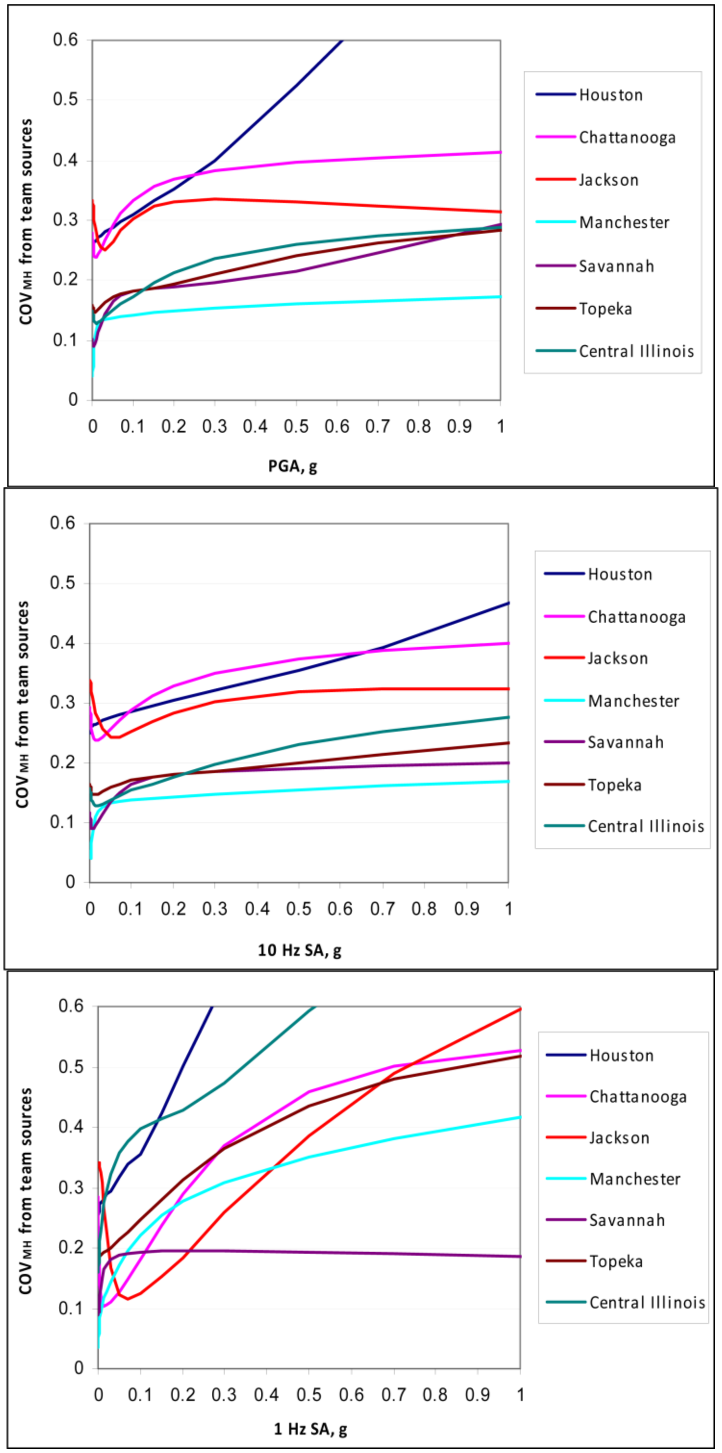

Figure 9.4-1
COV$_{MH}$ from EPRI (1989) team sources vs. ground motion amplitude for seven test sites: PGA (top), 10 Hz SA (middle), and 1 Hz SA (bottom)

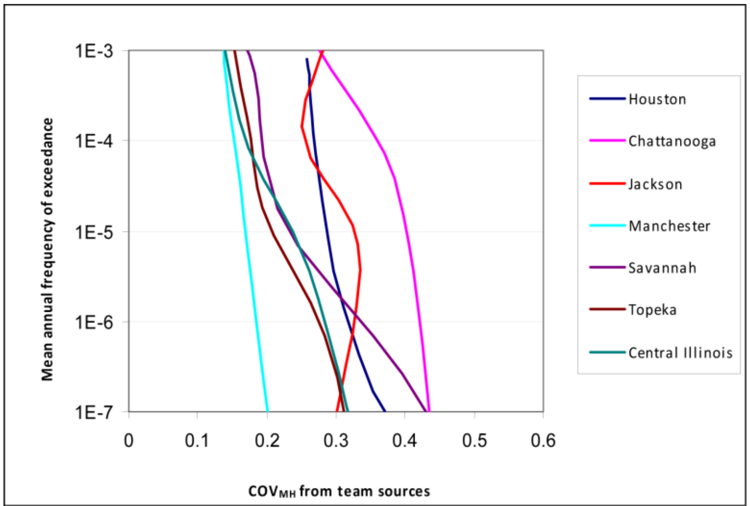

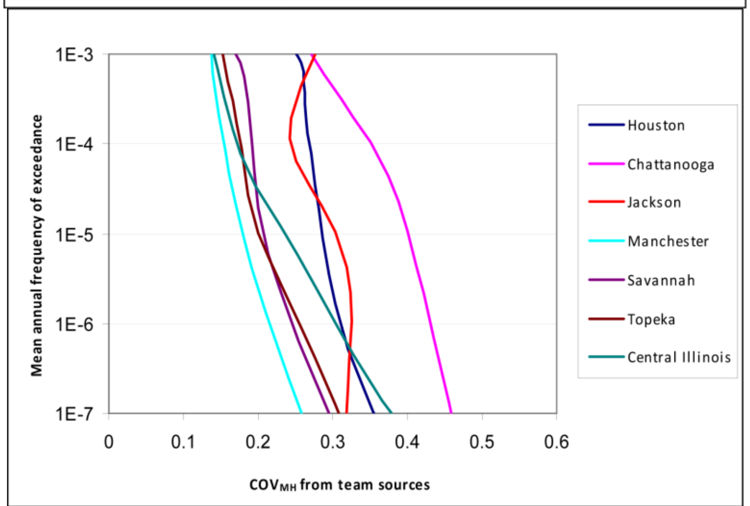

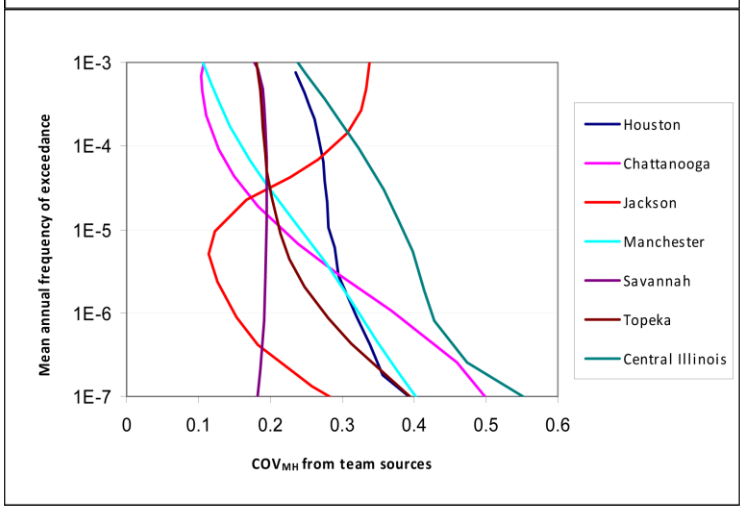

Figure 9.4-2
COV_{MH} from EPRI (1989) team sources vs. seismic hazard (i.e., annual frequency of exceedance) for seven test sites: PGA (top), 10 Hz SA (middle), and 1 Hz SA (bottom)

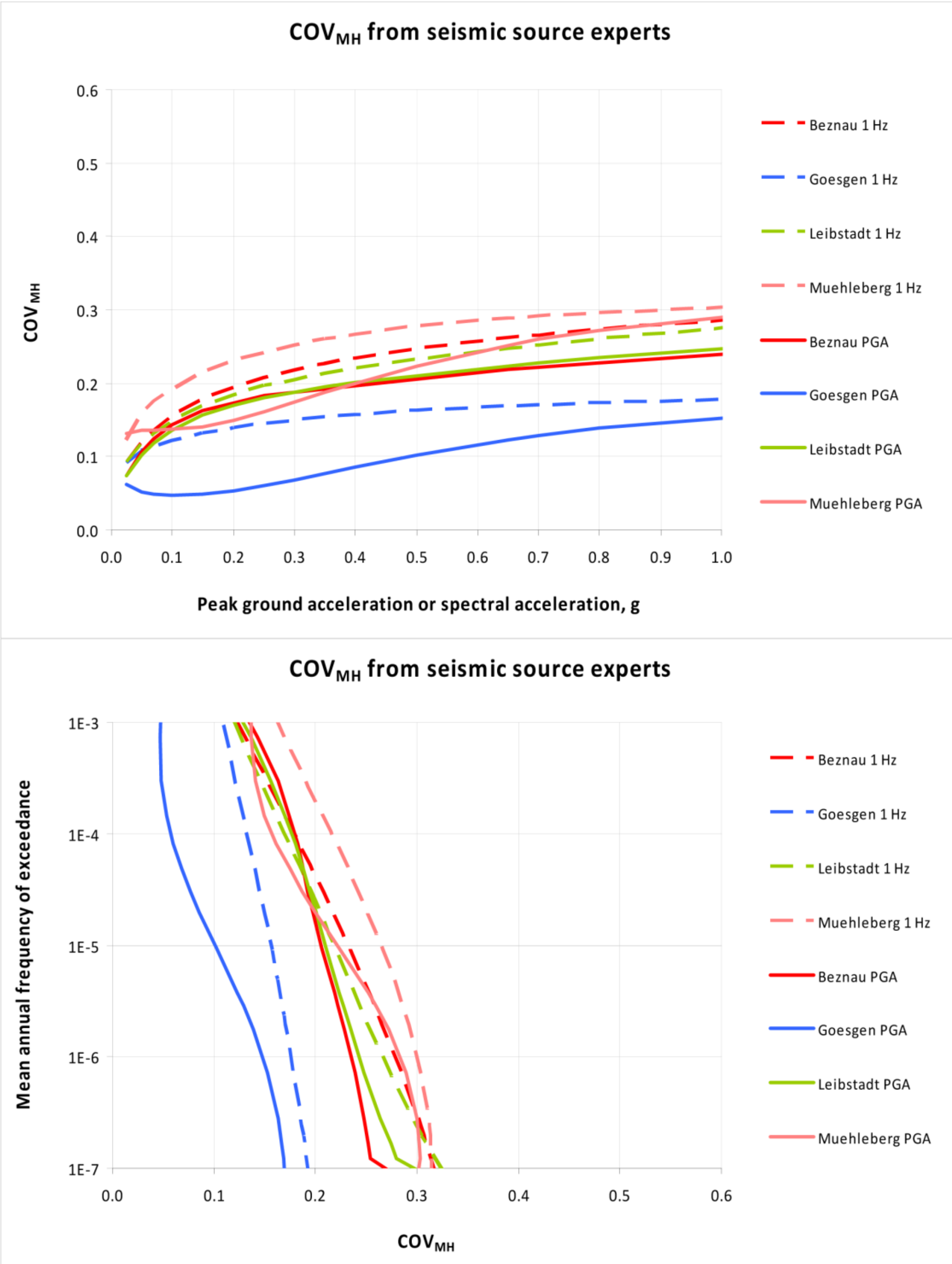

Figure 9.4-3
COV$_{MH}$ from seismic source experts (PEGASOS project) vs. amplitude (top) and annual frequency (bottom)

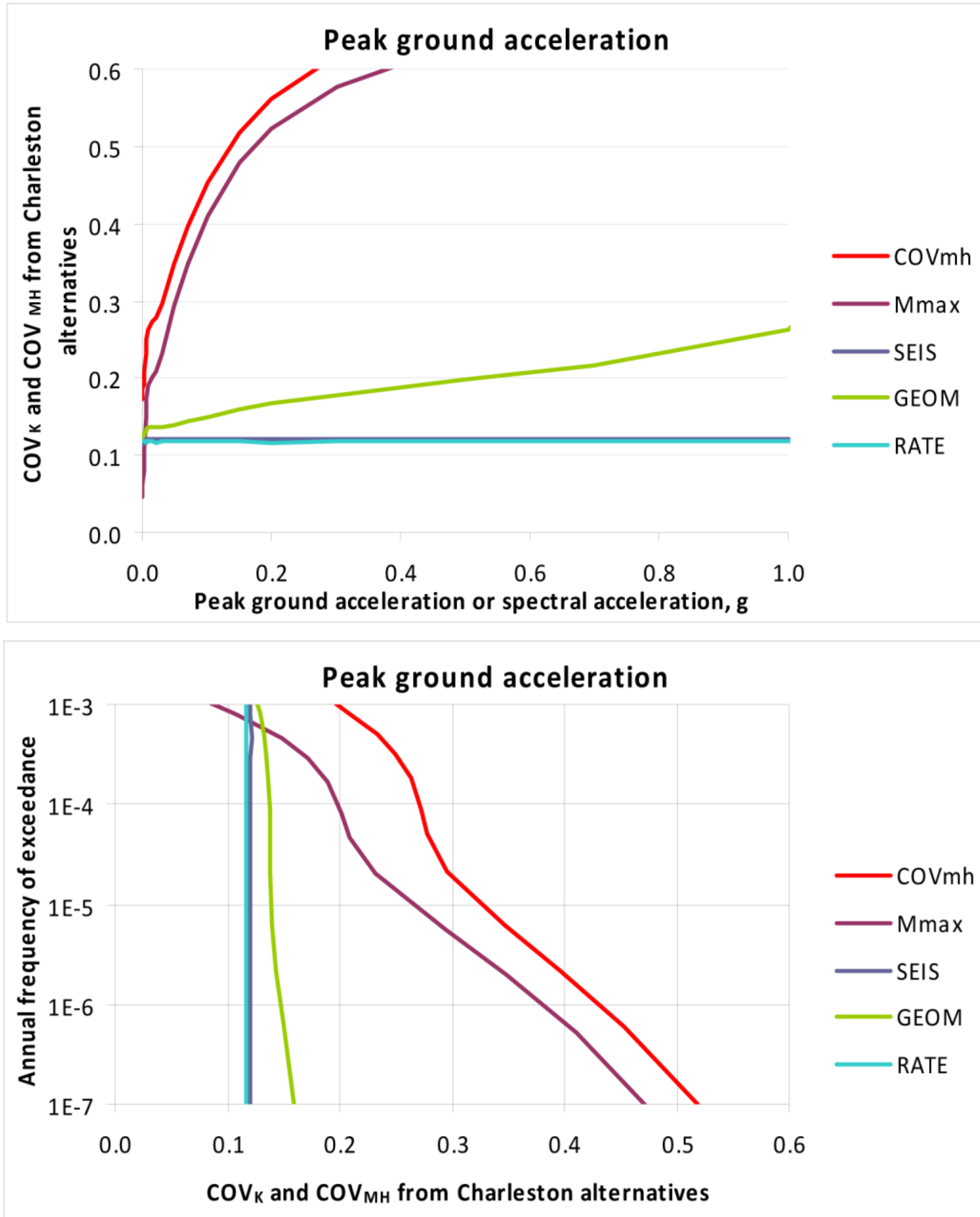

Figure 9.4-4
COV$_K$ and COV$_{MH}$ from Charleston alternatives for PGA, plotted vs. PGA amplitude (top) and hazard (bottom). COV$_{MH}$ is the total COV of mean hazard; see Table 9.4-2 for other labels for curves.

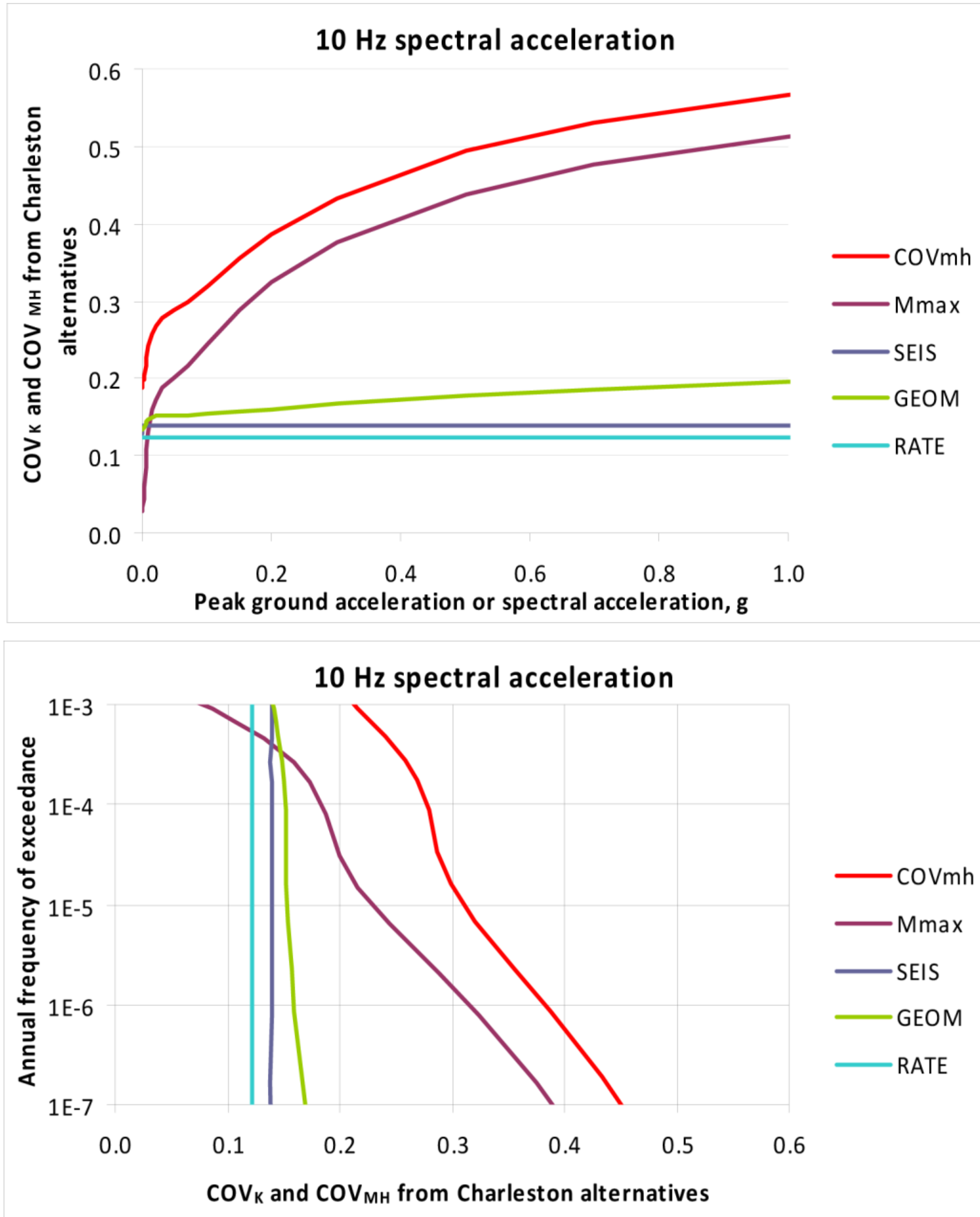

Figure 9.4-5
COV_K and COV_{MH} from Charleston alternatives for 10 Hz, plotted vs. 10 Hz amplitude (top) and hazard (bottom). COV_{MH} is the total COV of mean hazard; see Table 9.4-2 for other labels for curves.

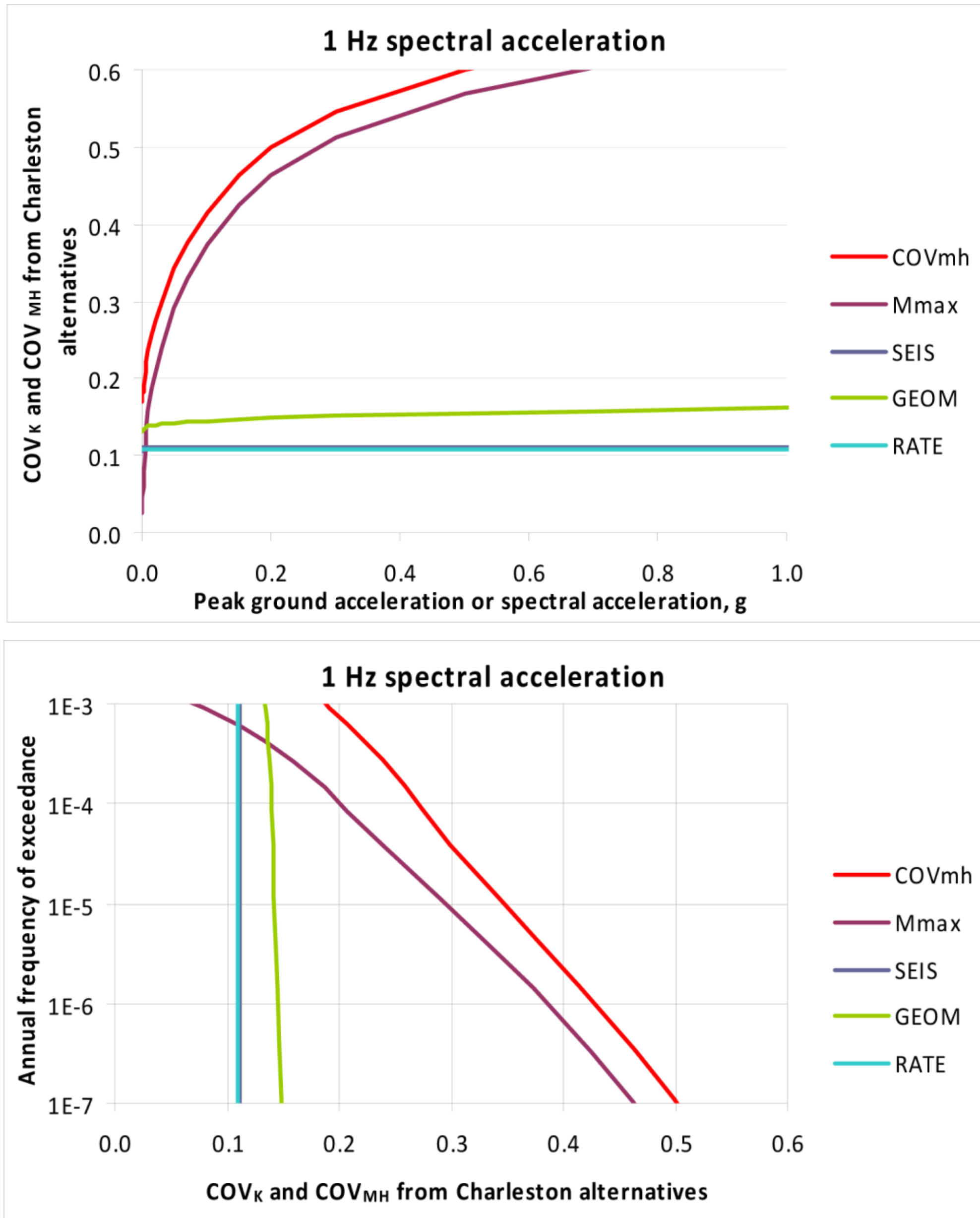

Figure 9.4-6
COV_K and COV_{MH} from Charleston alternatives for 1 Hz, plotted vs. 1 Hz amplitude (top) and hazard (bottom). COV_{MH} is the total COV of mean hazard; see Table 9.4-2 for other labels for curves..

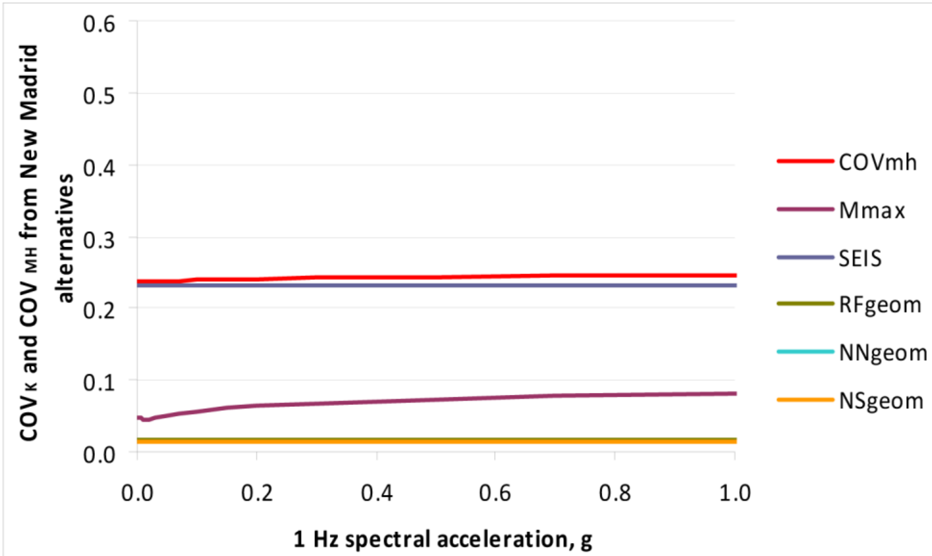

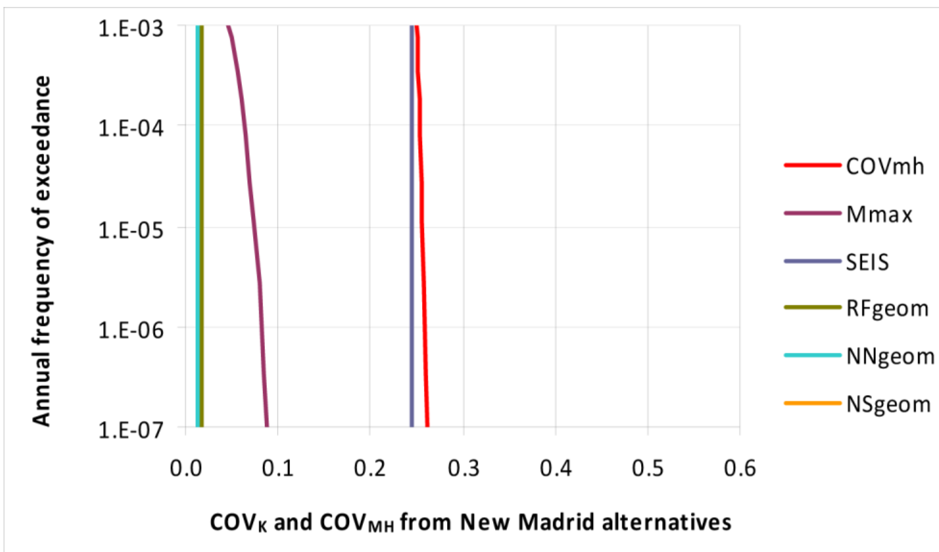

Figure 9.4-7
COV_K and COV_{MH} of total hazard from New Madrid for 1 Hz, plotted vs. 1 Hz amplitude (top) and hazard (bottom). COV_{MH} is the total COV; see the text for other labels for curves.

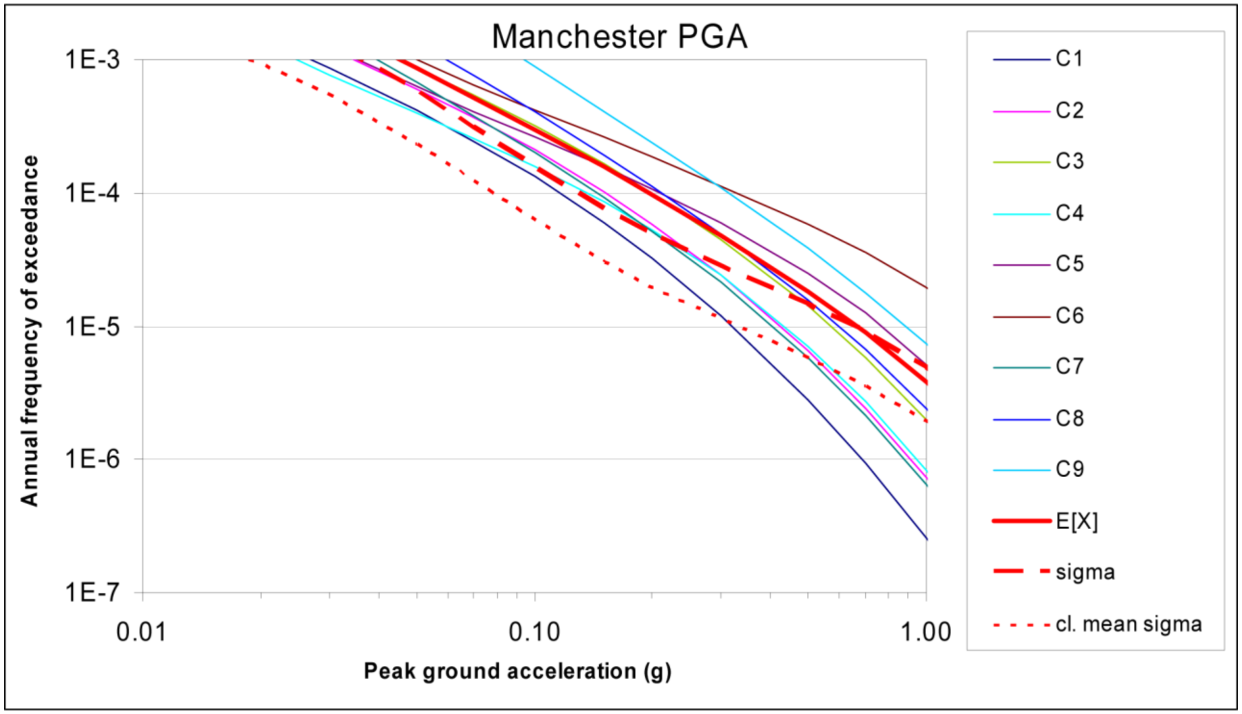

Figure 9.4-8
PGA hazard curves for Manchester test site

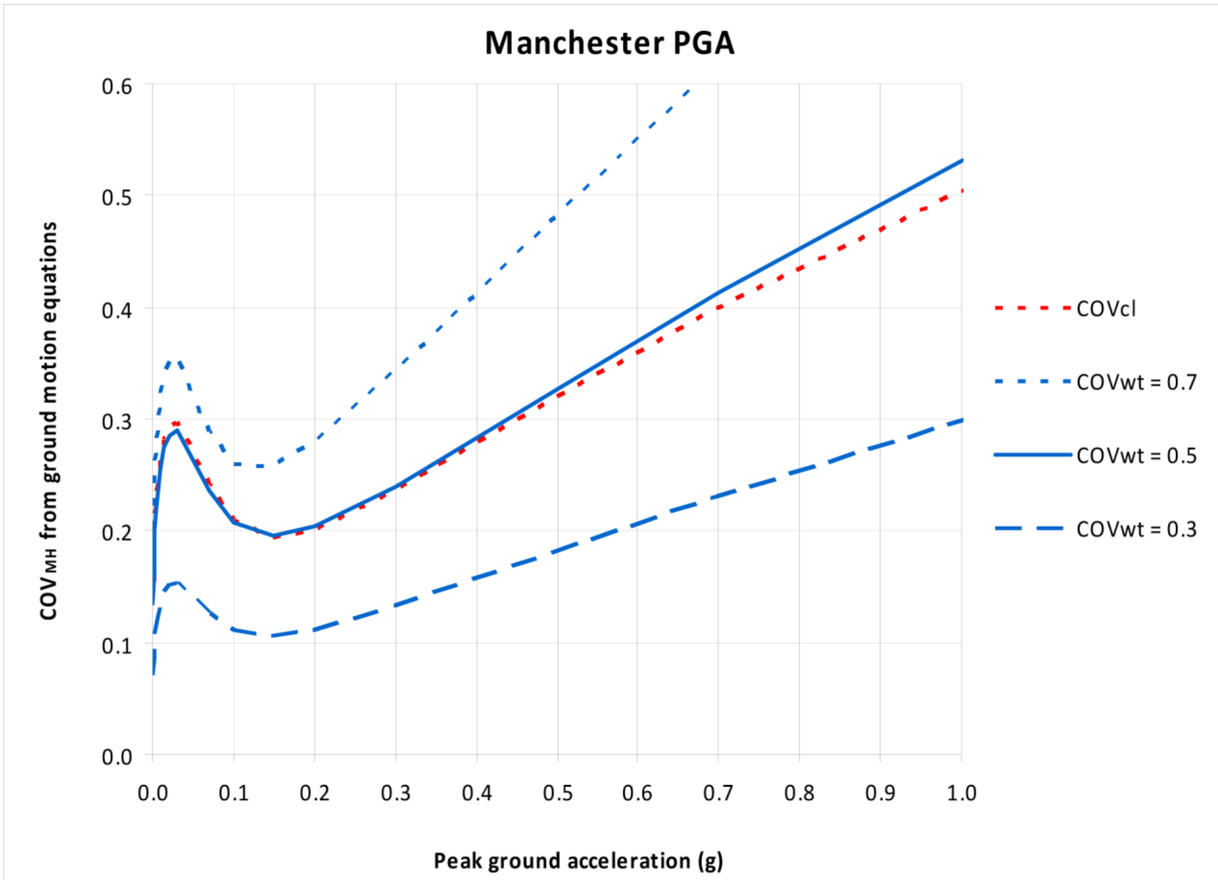

Figure 9.4-9
COV_{MH} of PGA hazard at Manchester site from ground motion equation vs. PGA

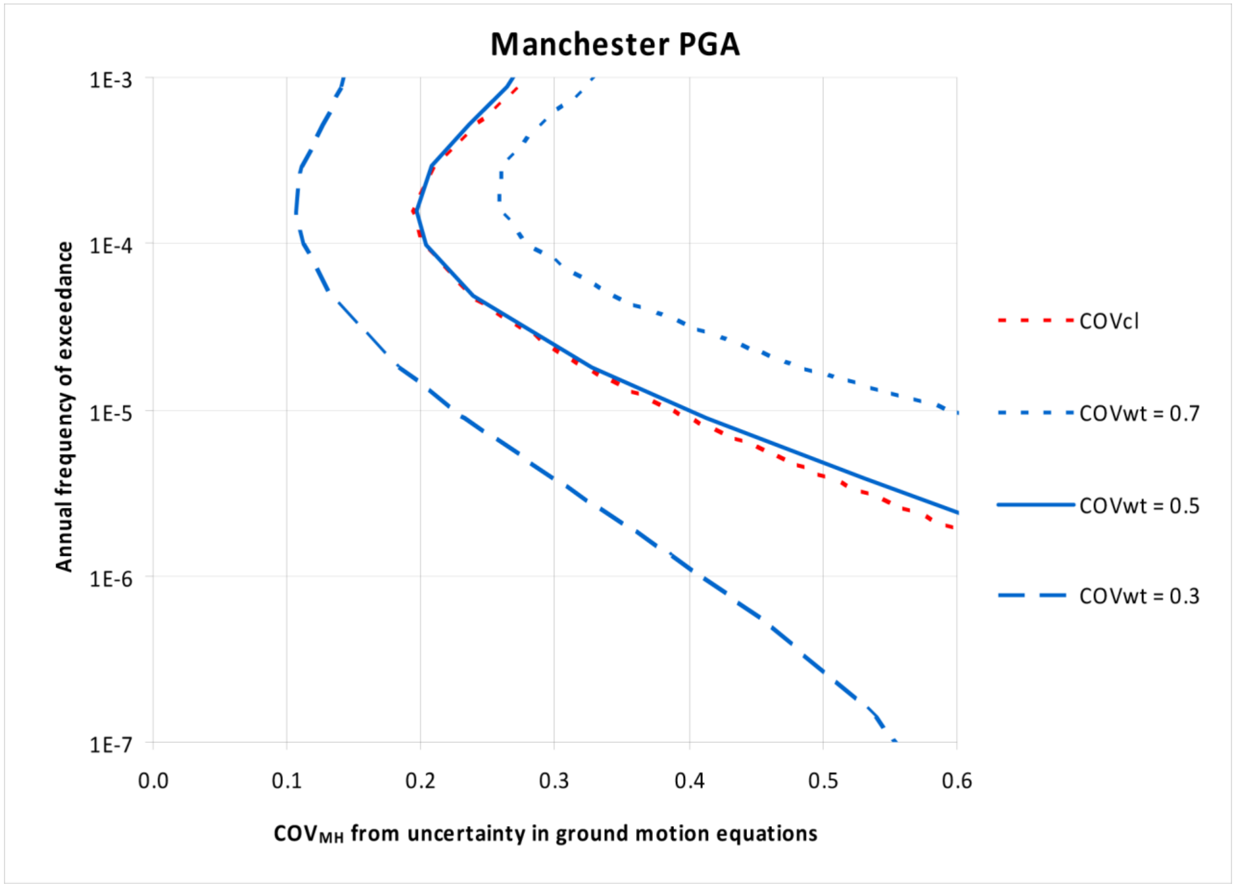

Figure 9.4-10
COV of PGA hazard at Manchester site from ground motion equation vs. hazard

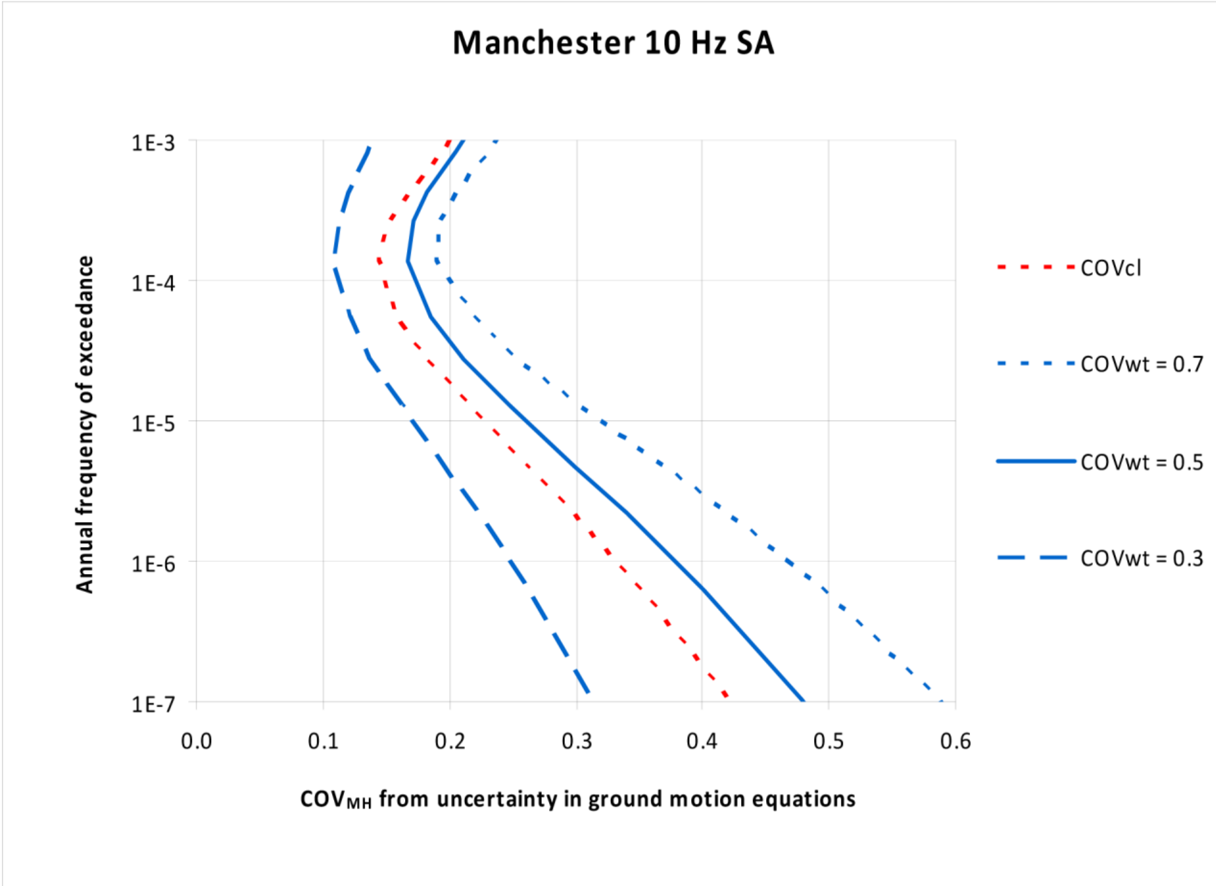

Figure 9.4-11
COV of 10 Hz hazard at Manchester site from ground motion equations vs. hazard

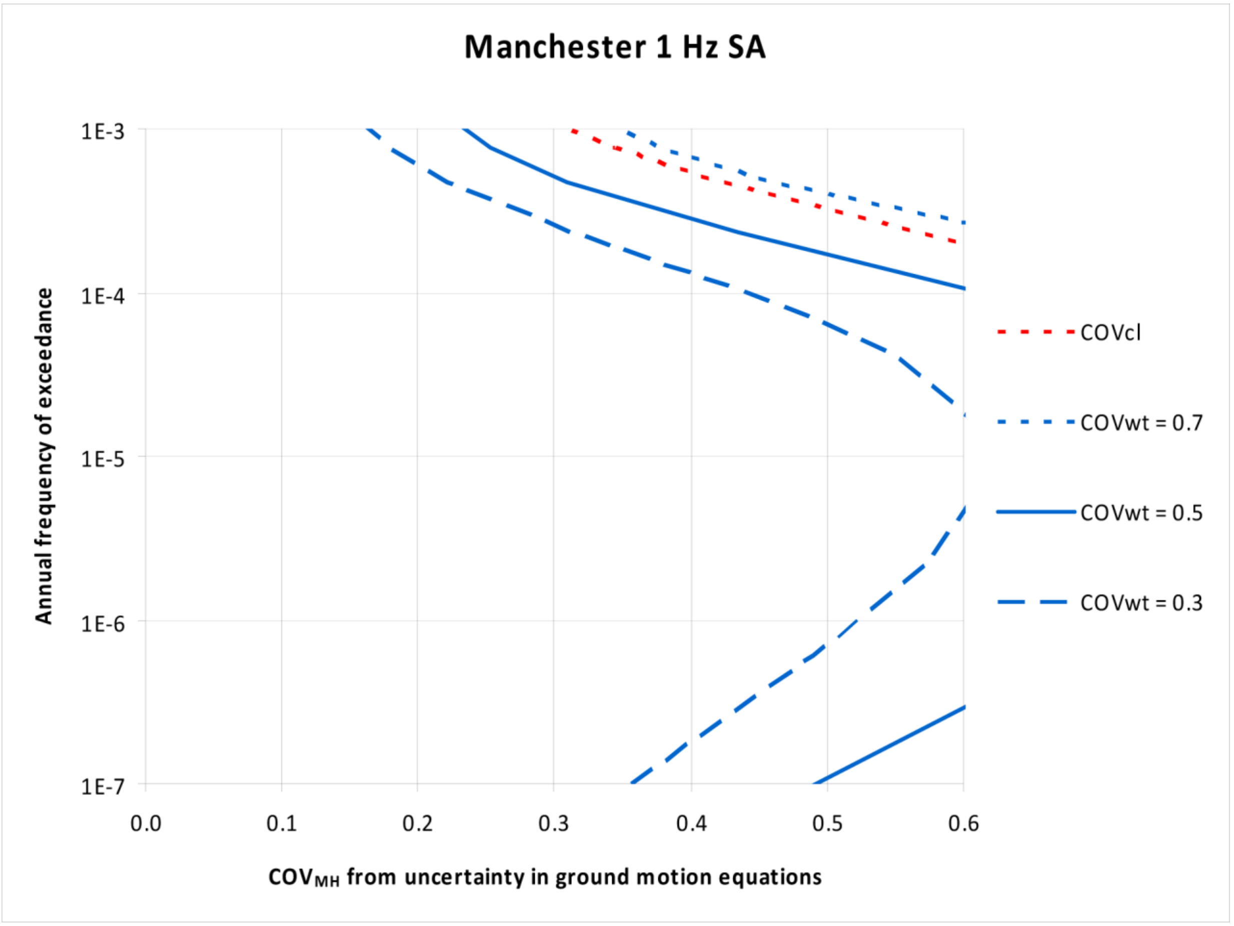

Figure 9.4-12
COV of 1 Hz hazard at Manchester site from ground motion equations vs. hazard

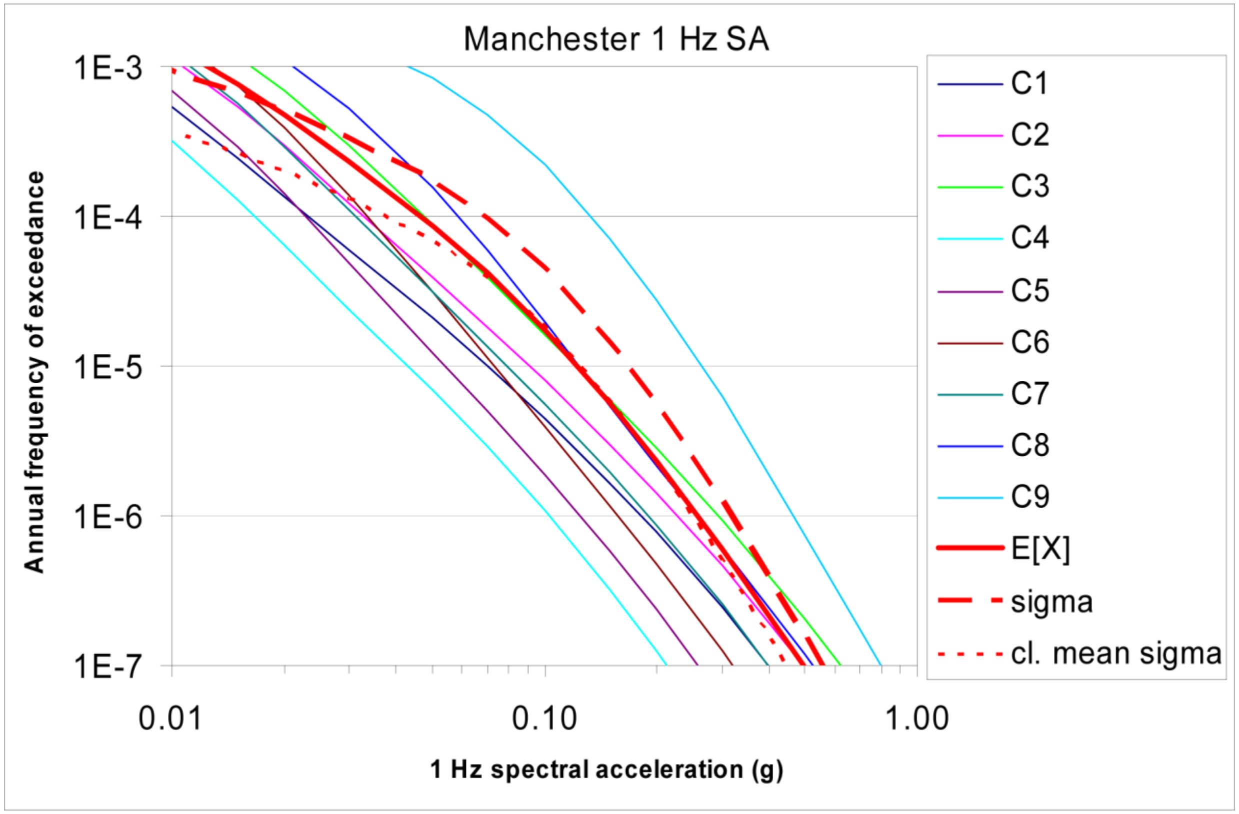

Figure 9.4-13
1 Hz spectral acceleration hazard curves for Manchester test site

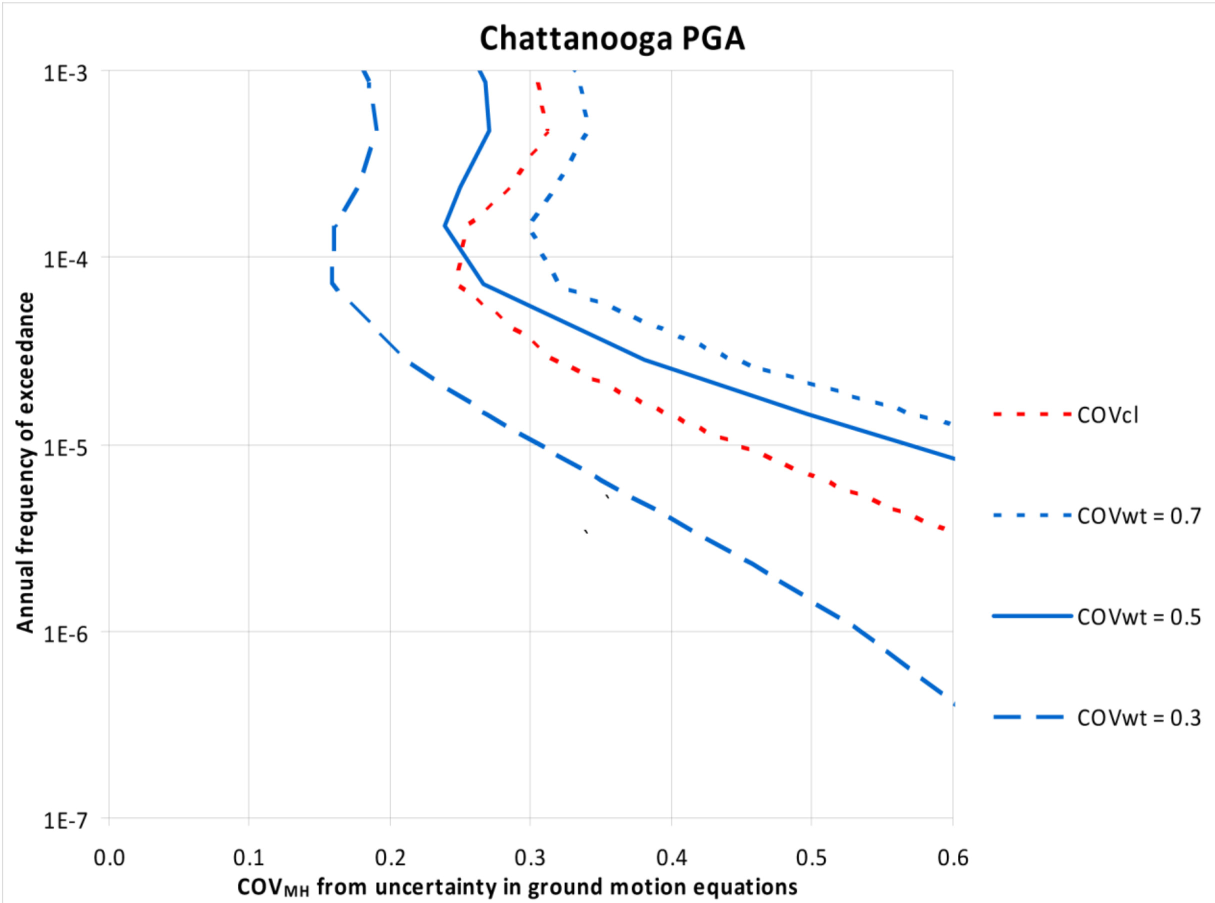

Figure 9.4-14
COV_{MH} of PGA hazard at Chattanooga from ground motion equation vs. hazard

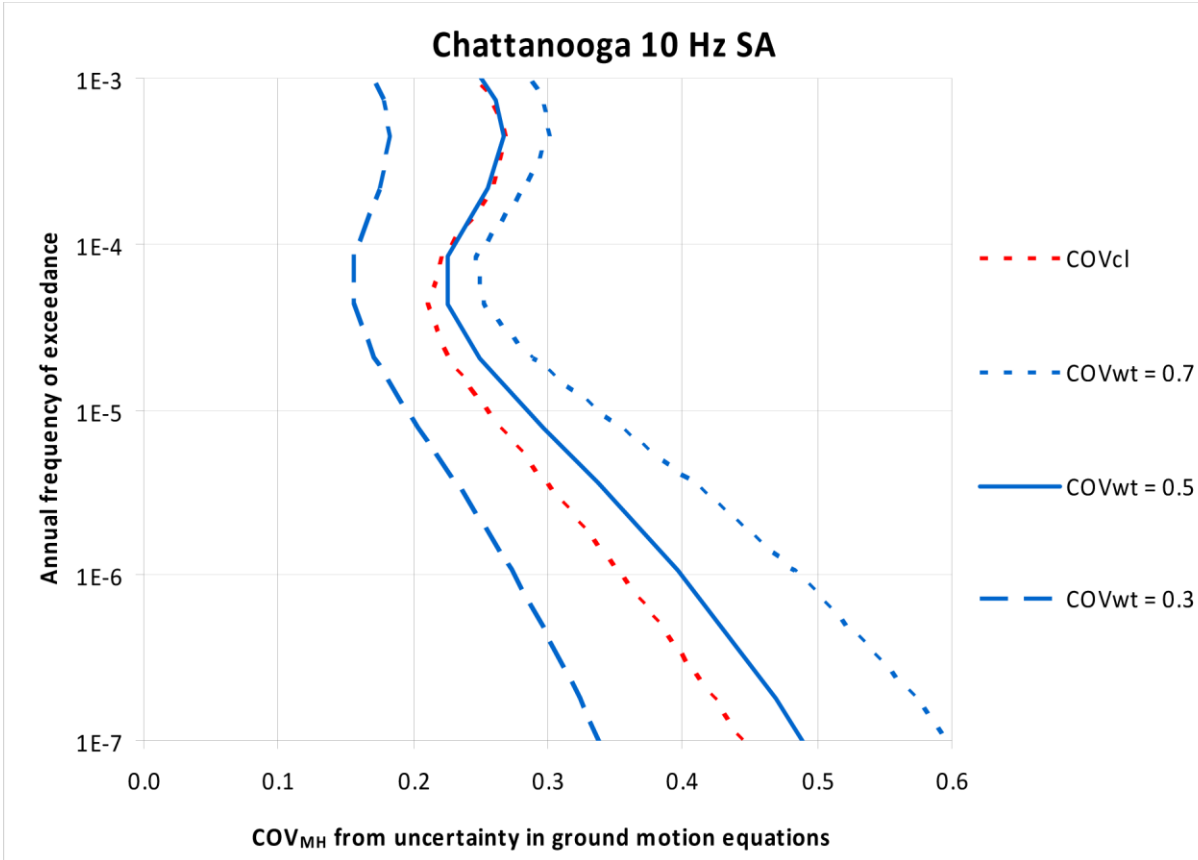

Figure9.4-15
COV_{MH} of 10 Hz hazard at Chattanooga from ground motion equation vs. hazard

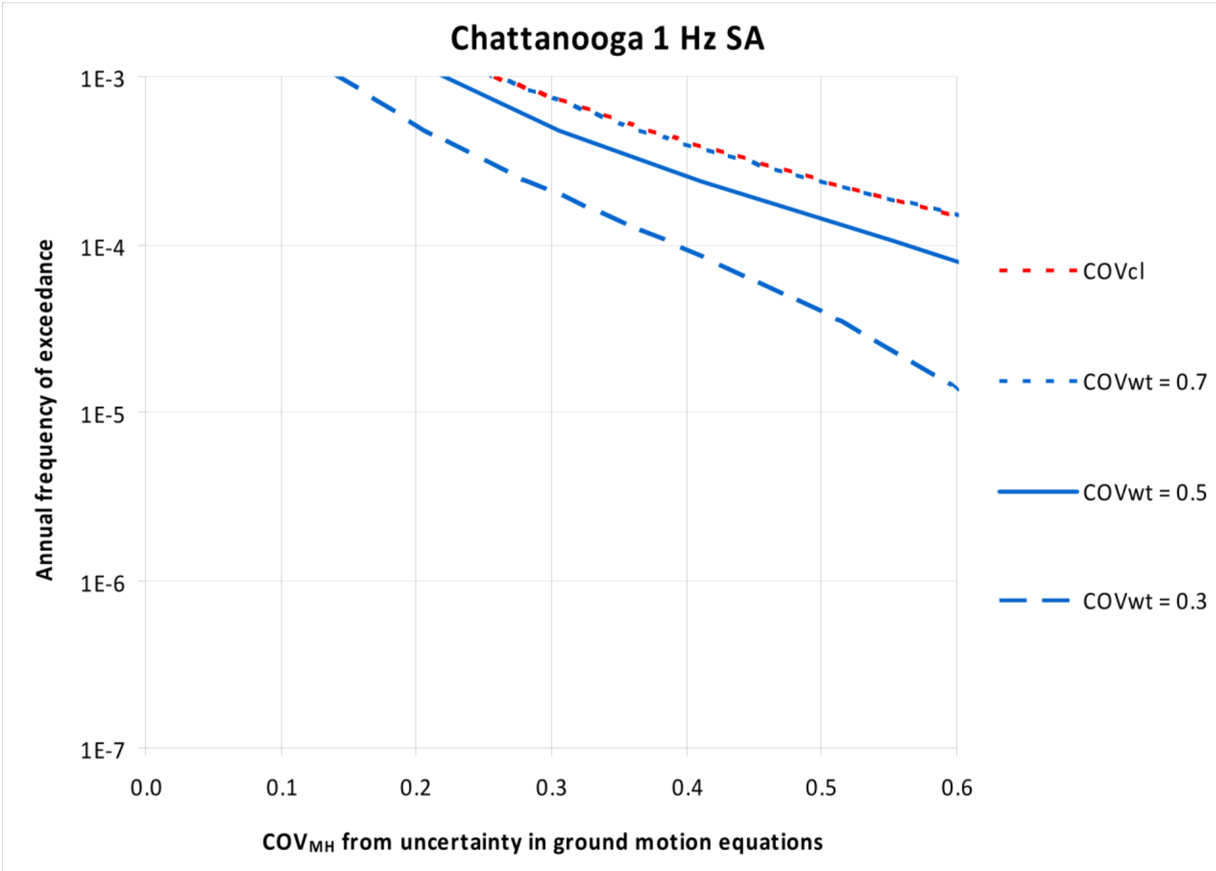

Figure 9.4-16
COV_{MH} of 1 Hz hazard at Chattanooga site from ground motion equation vs. hazard

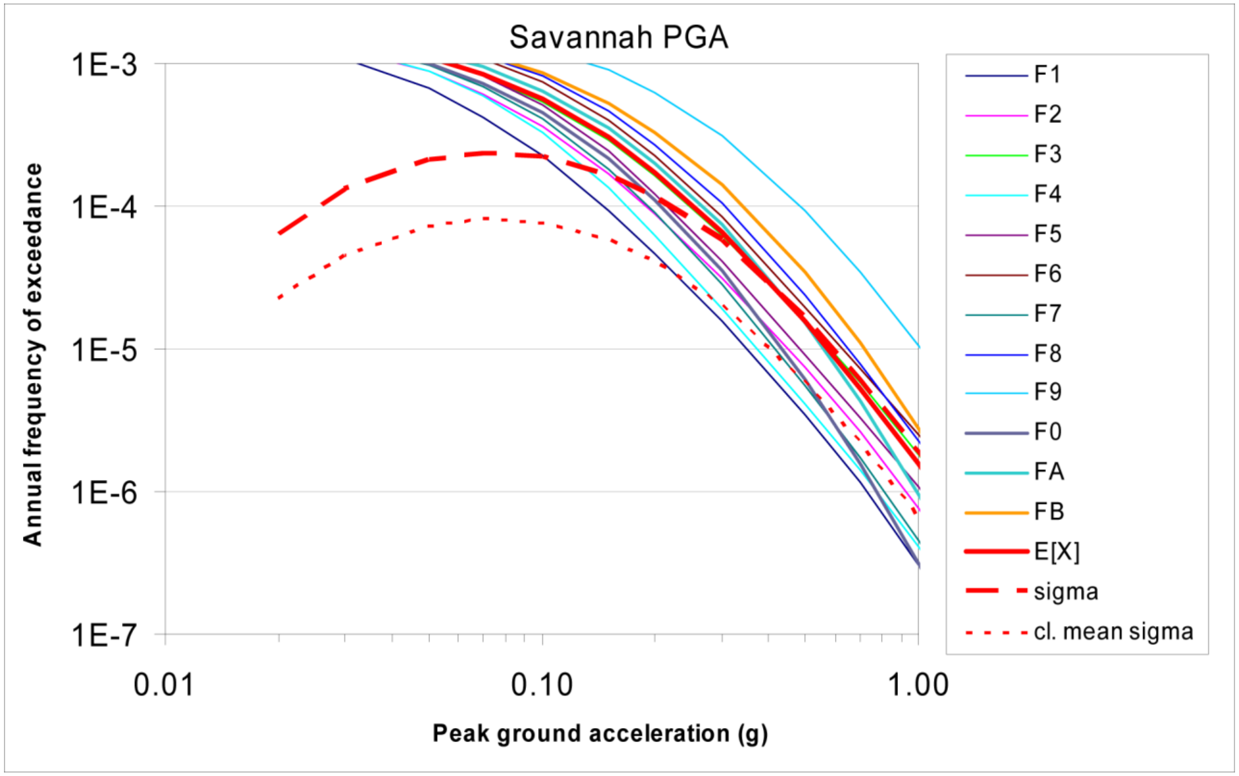

Figure 9.4-17
PGA hazard curves for Savannah test site

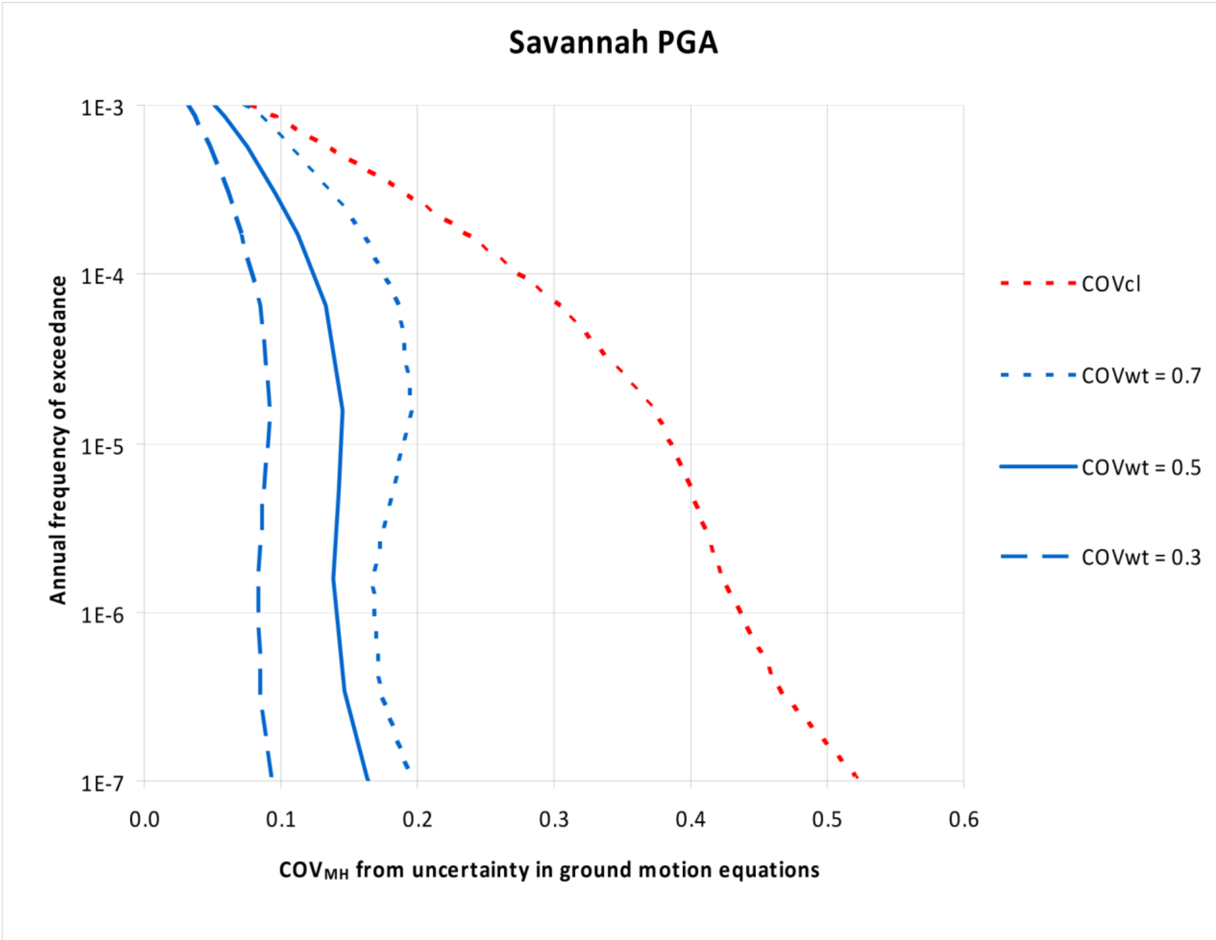

Figure 9.4-18
COV_{MH} of PGA hazard at Savannah site from ground motion equations vs. hazard

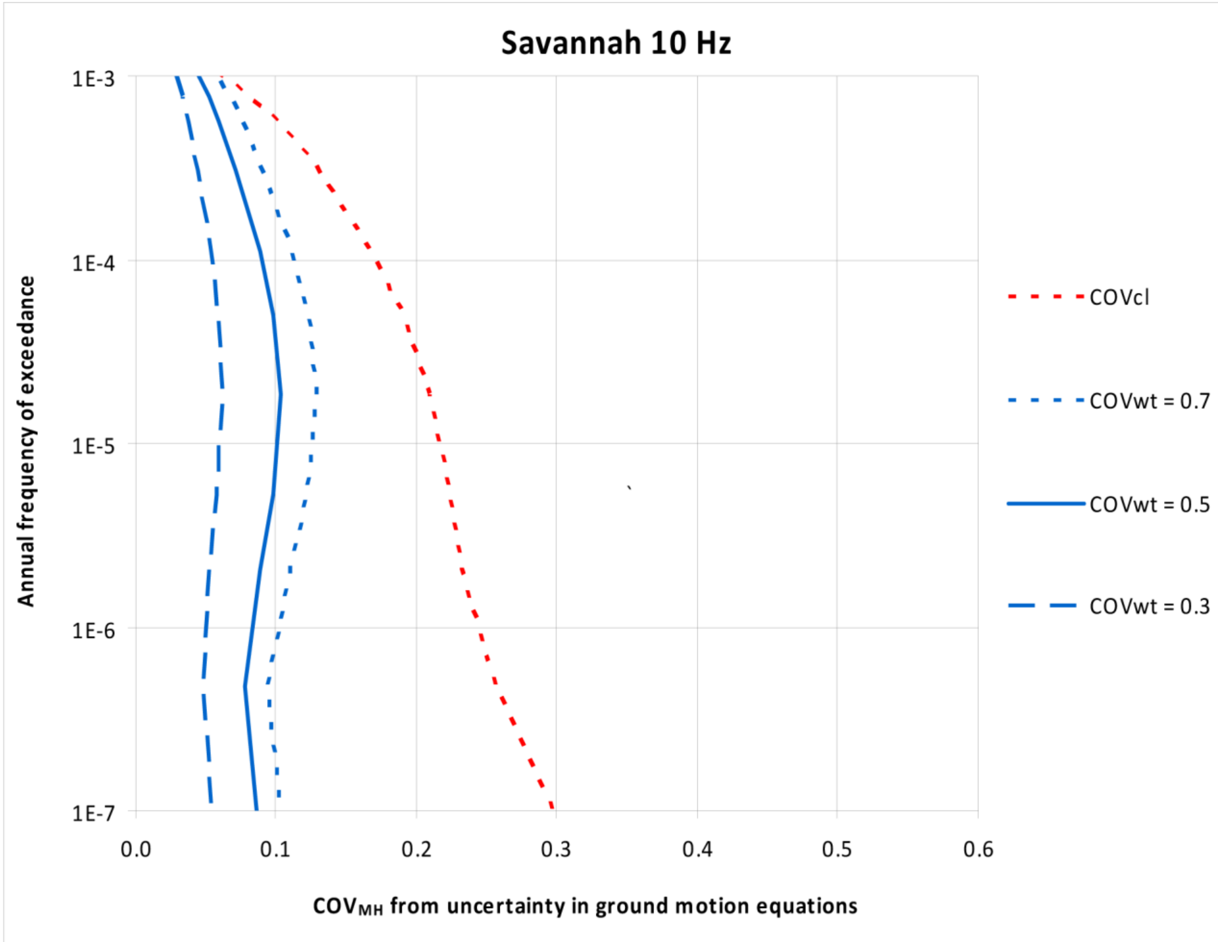

Figure 9.4-19
COV_{MH} of 10 Hz hazard at Savannah site from ground motion equations vs. hazard

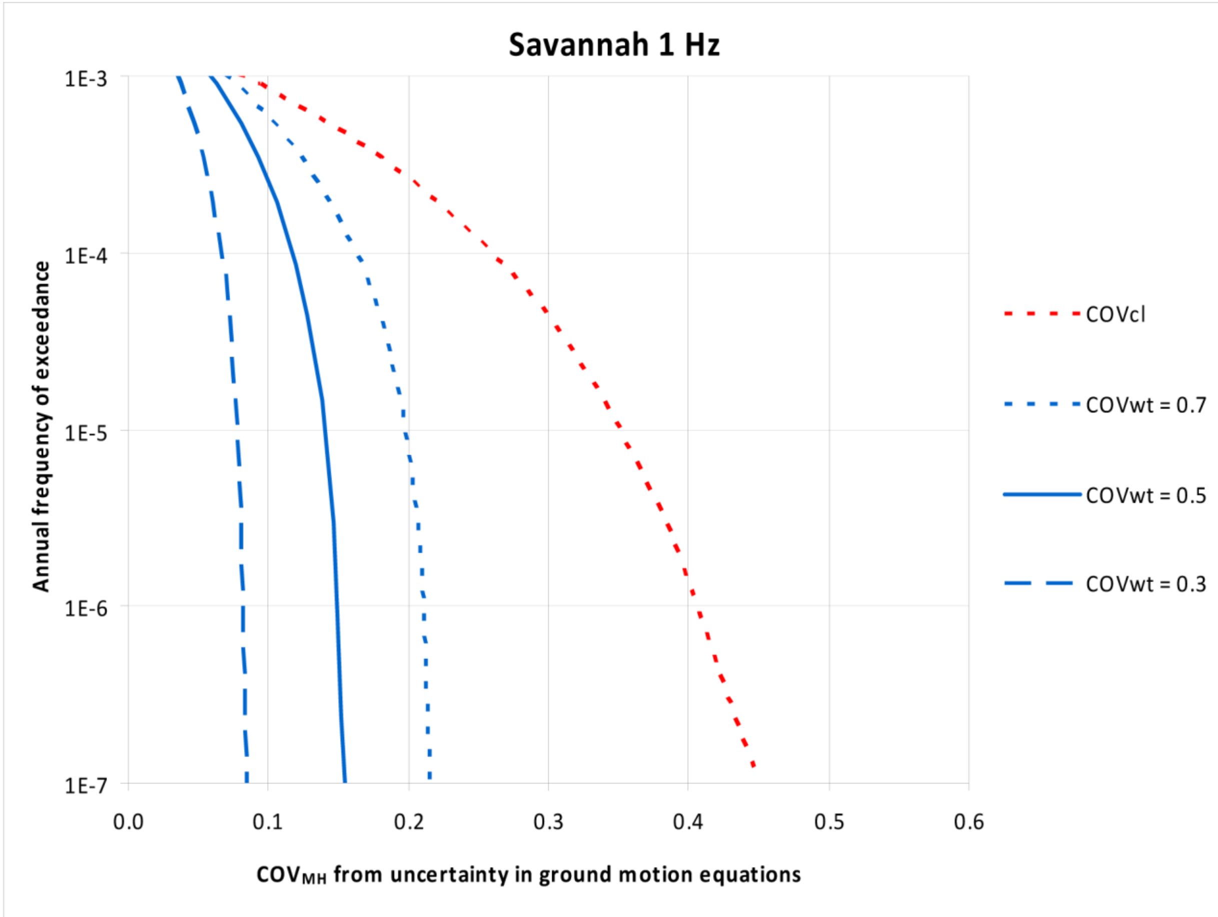

Figure 9.4-20
COV$_{MH}$ of 1 Hz hazard at Savannah site from ground motion equations vs. hazard

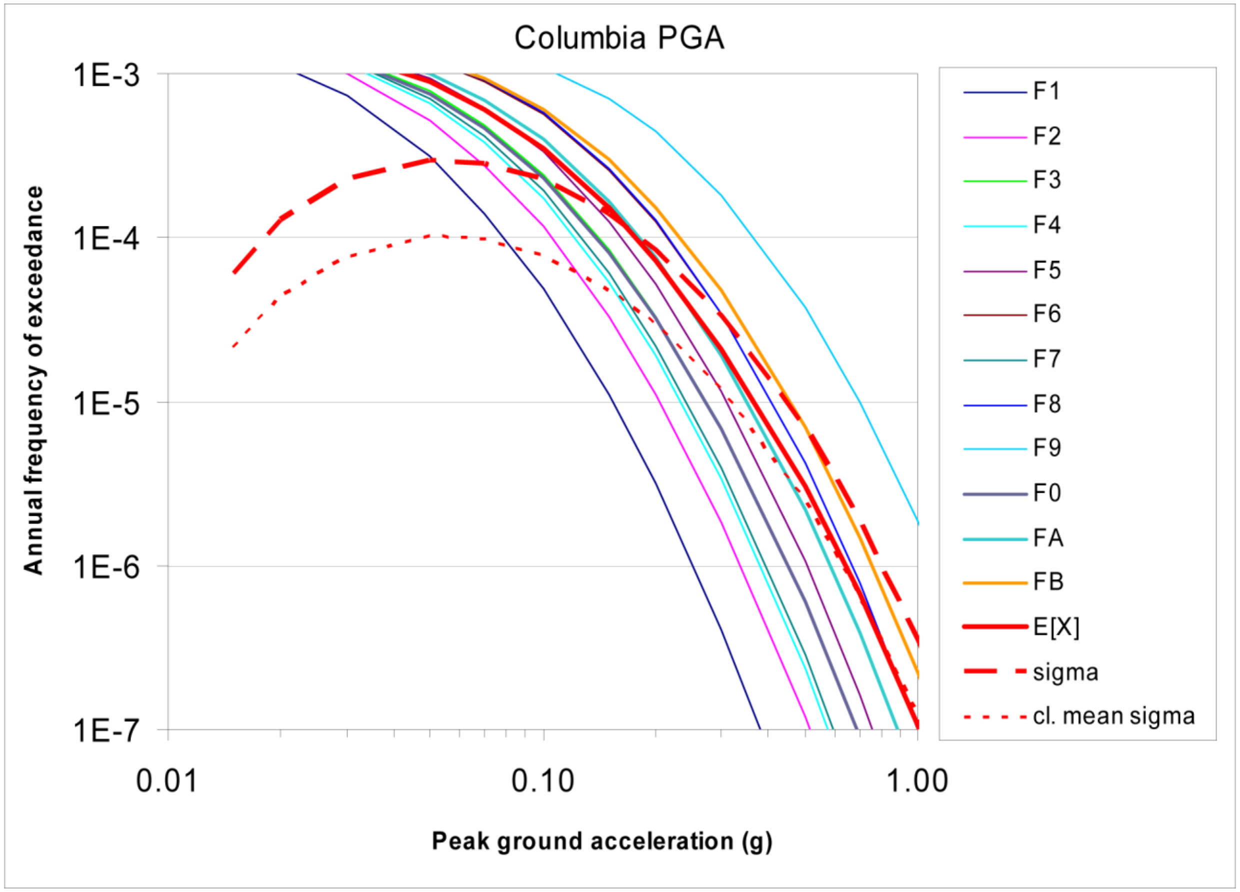

Figure 9.4-21
PGA hazard curves for Columbia site

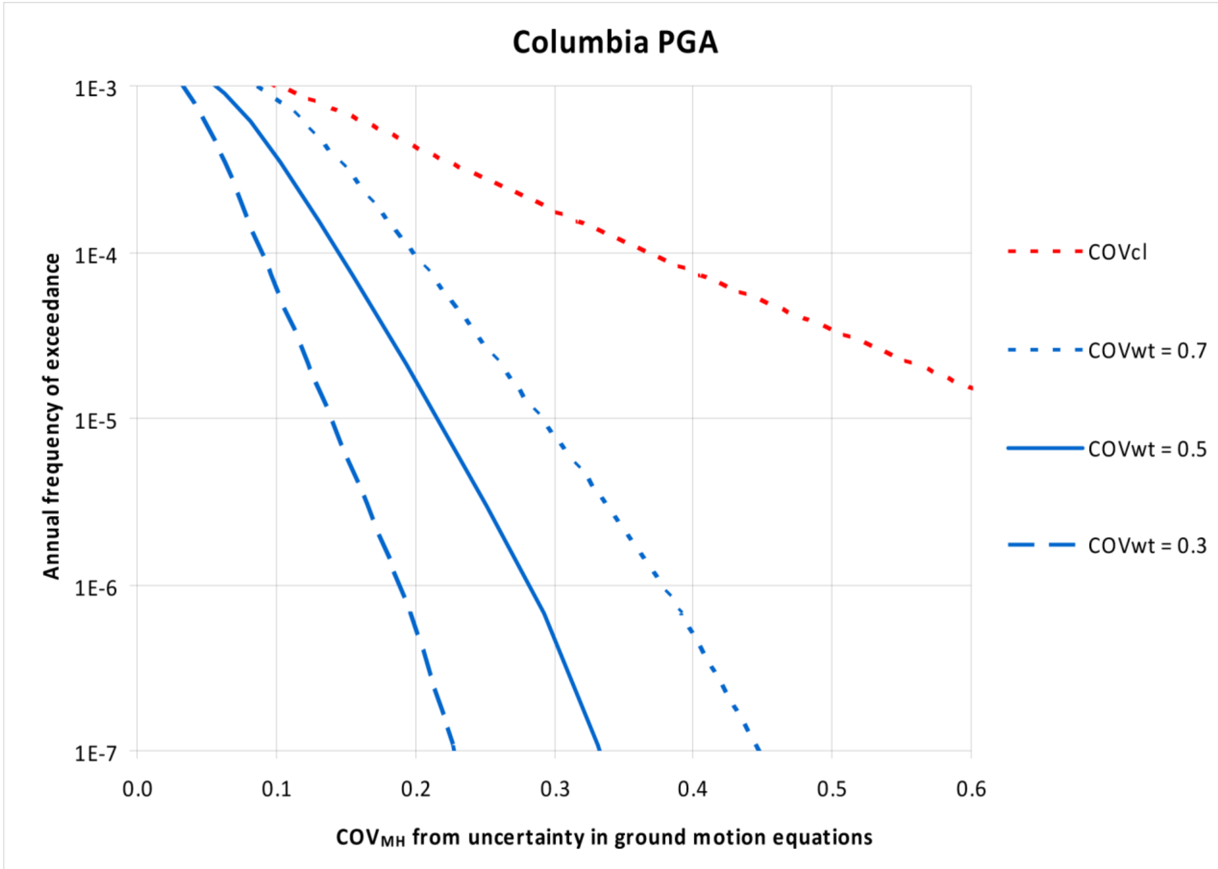

Figure 9.4-22
COV_{MH} of PGA hazard at Columbia from ground motion equations vs. hazard

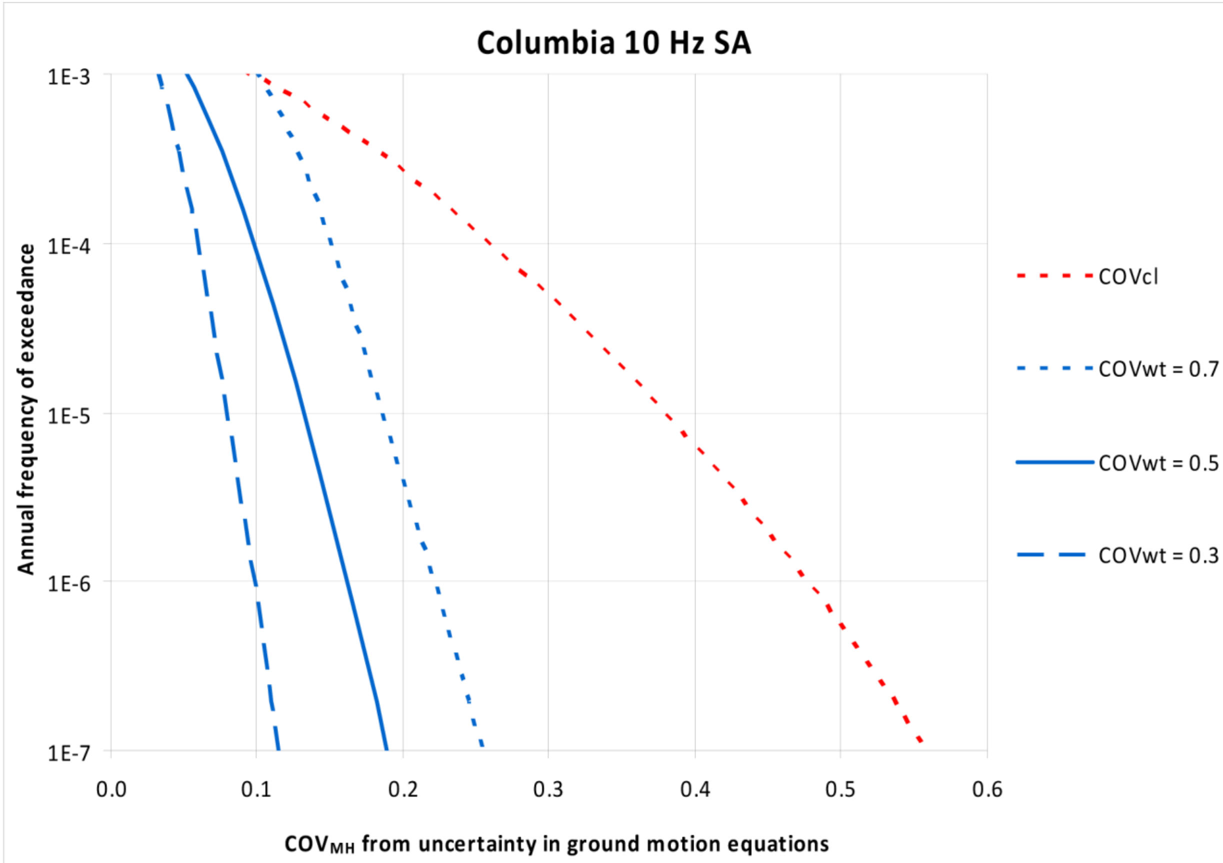

Figure 9.4-23
COV_{MH} of 10 Hz hazard at Columbia from ground motion equations vs. hazard

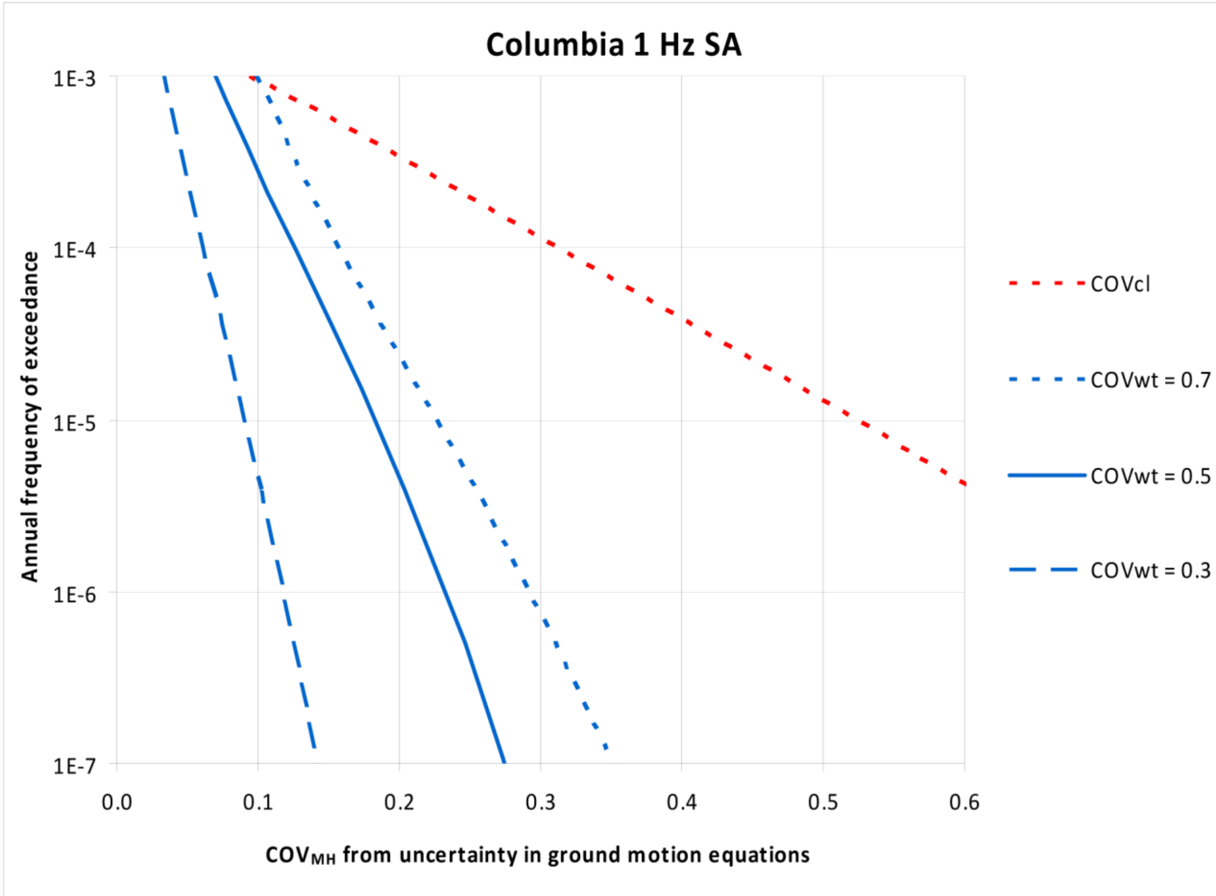

Figure 9.4-24
COV_{MH} of 1 Hz hazard at Columbia from ground motion equations vs. hazard

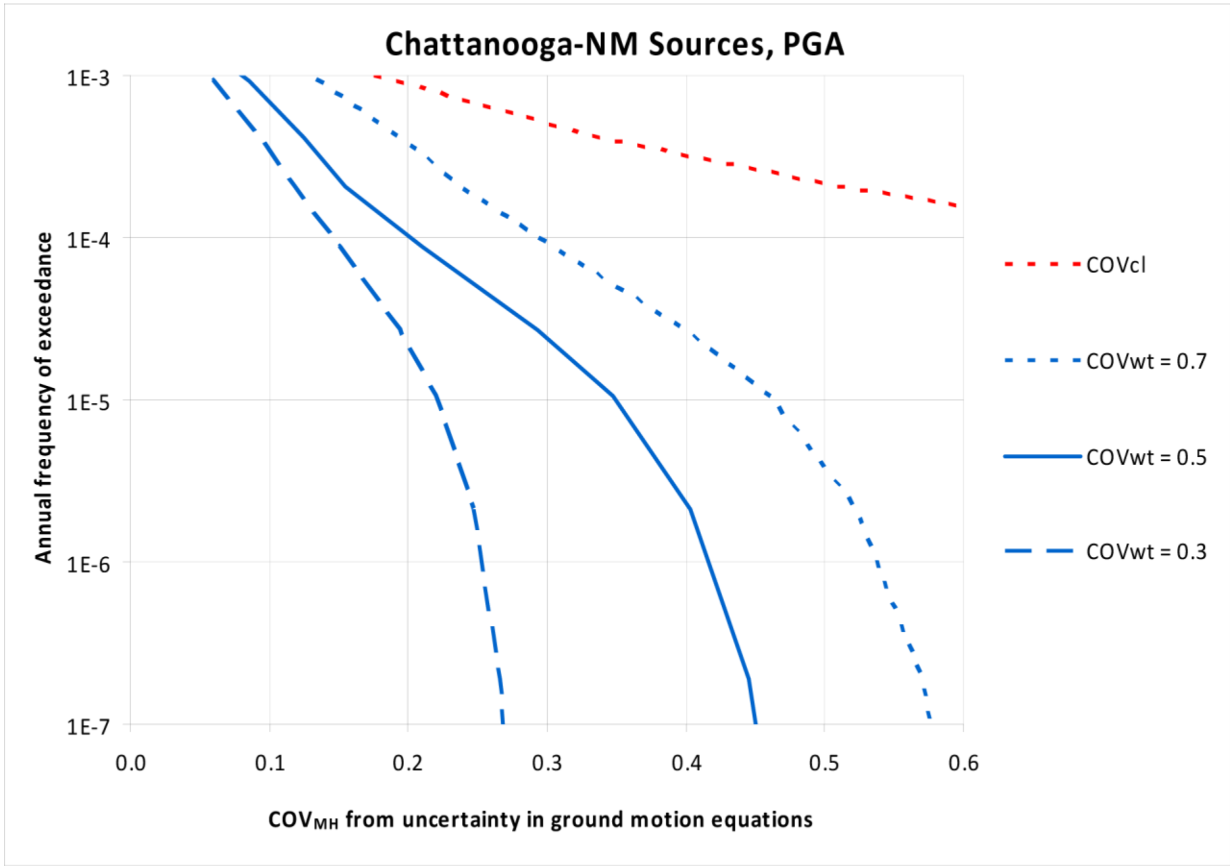

Figure 9.4-25
COV_{MH} of PGA hazard at Chattanooga (New Madrid only) vs. hazard

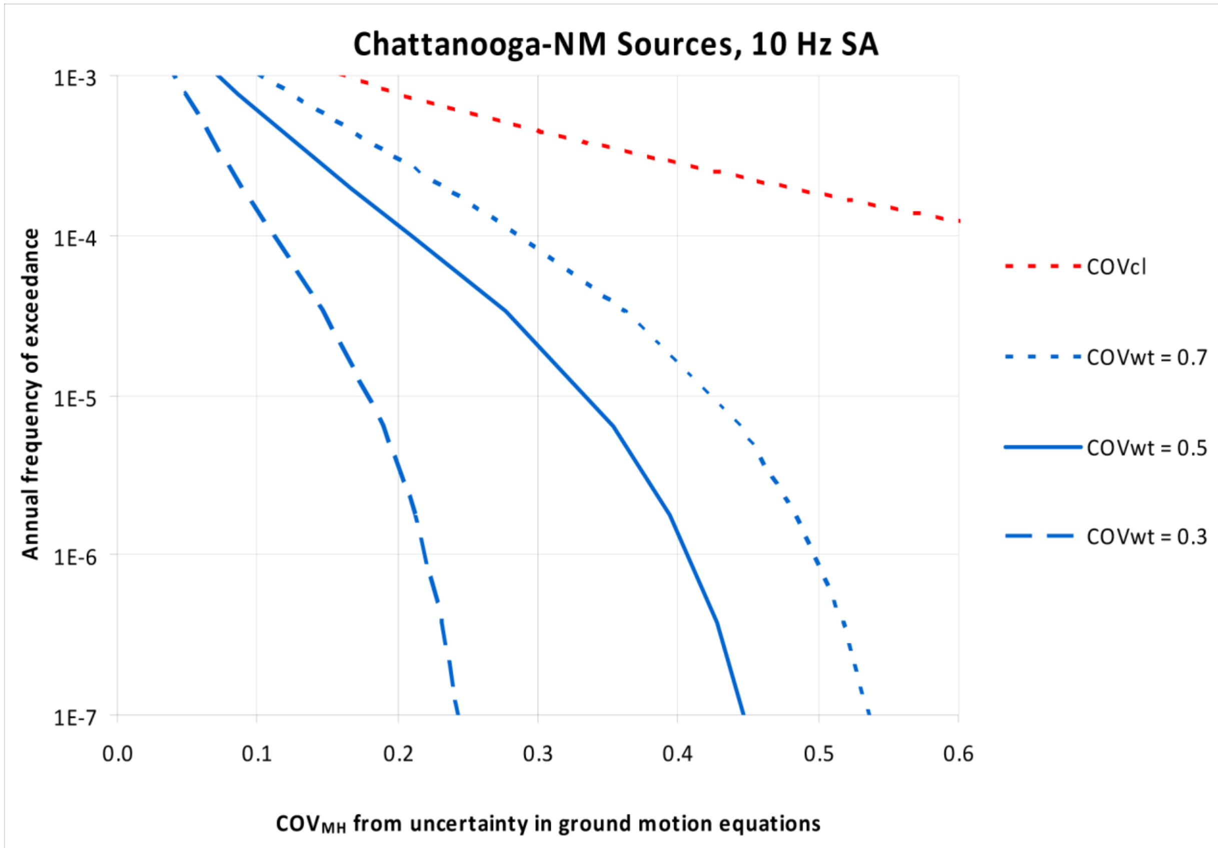

Figure 9.4-26
COV_{MH} of 10 Hz hazard at Chattanooga (New Madrid only) vs. hazard

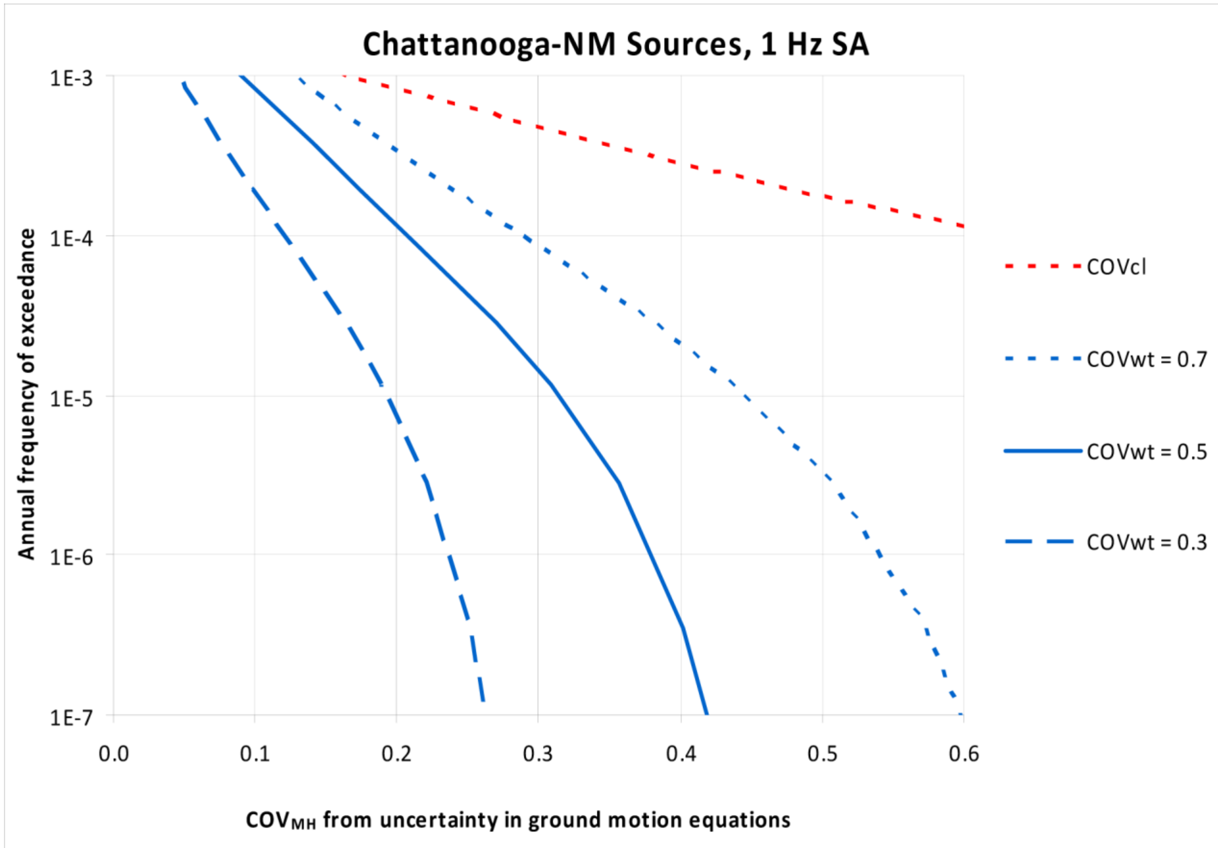

Figure 9.4-27
COV_{MH} of 1 Hz hazard at Chattanooga (New Madrid only) vs. hazard

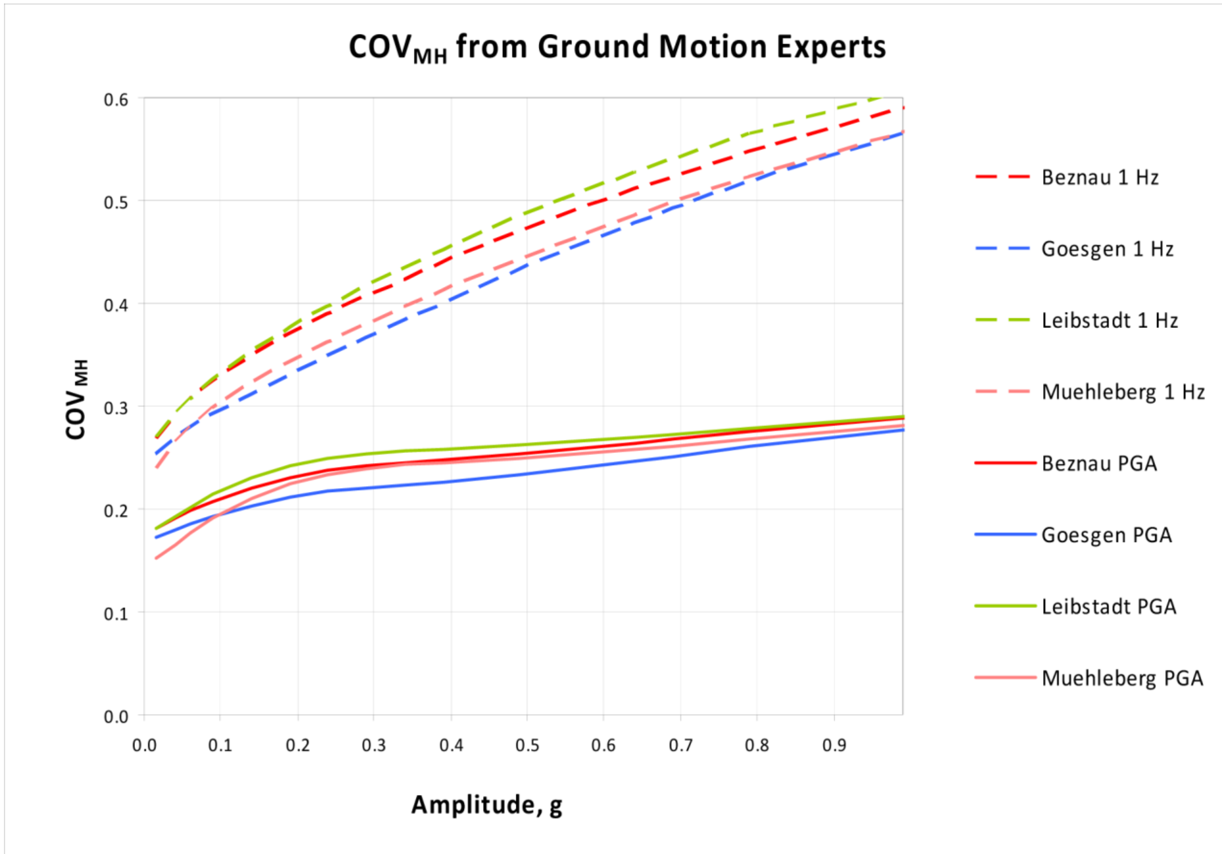

Figure 9.4-28
COV$_{MH}$ for PGA and 1 Hz SA vs. ground motion amplitude resulting from alternative ground motion experts, PEGASOS project

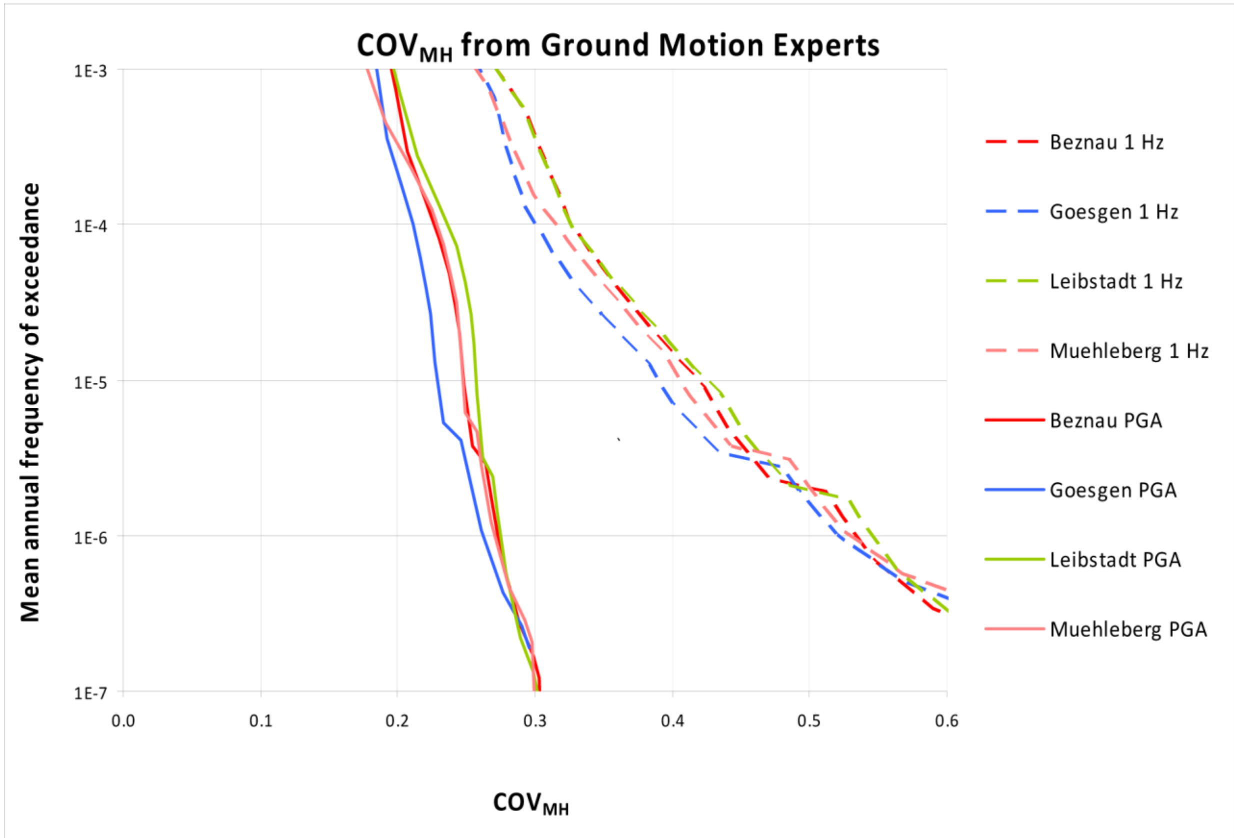

Figure 9.4-29
COV$_{MH}$ for PGA and 1 Hz SA vs. mean hazard from alternative ground motion experts, PEGASOS project

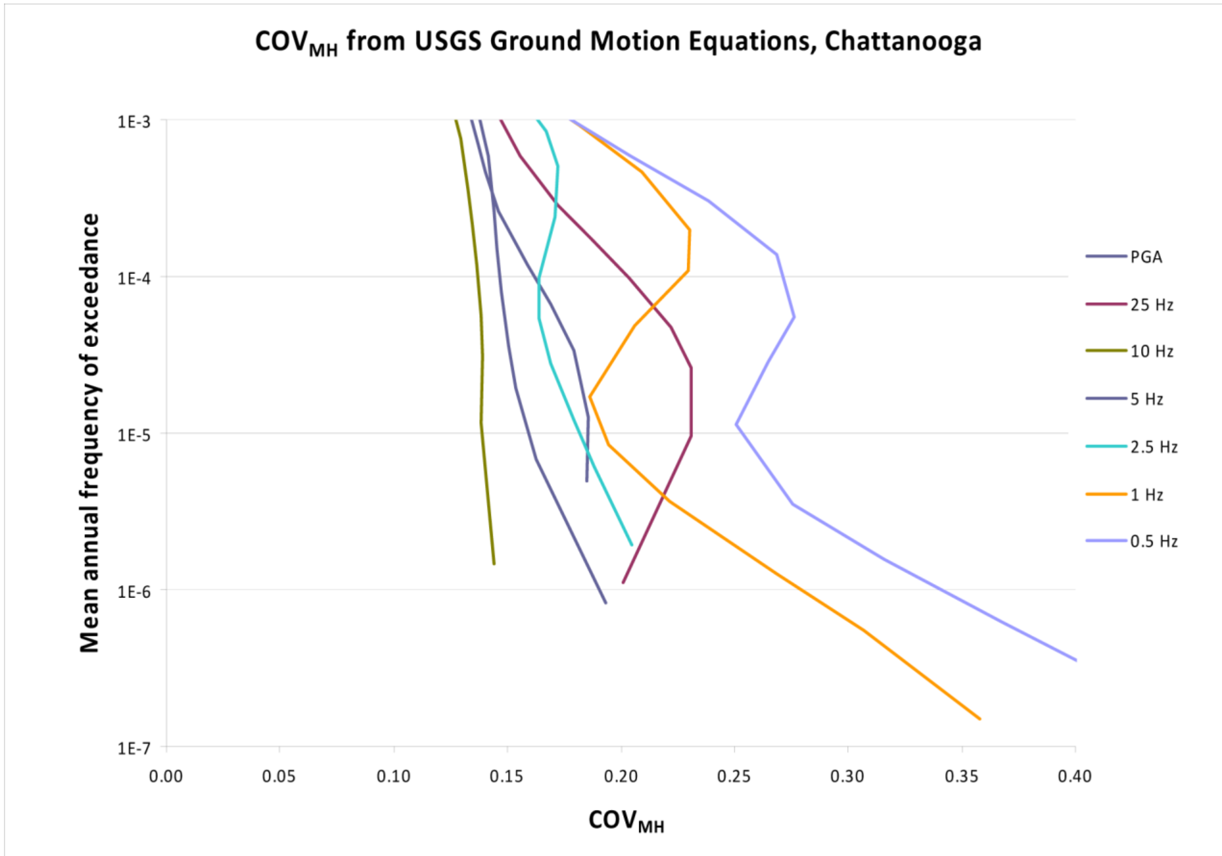

Figure 9.4-30
COV$_{HAZ}$ from ground motion equations vs. mean hazard for Chattanooga

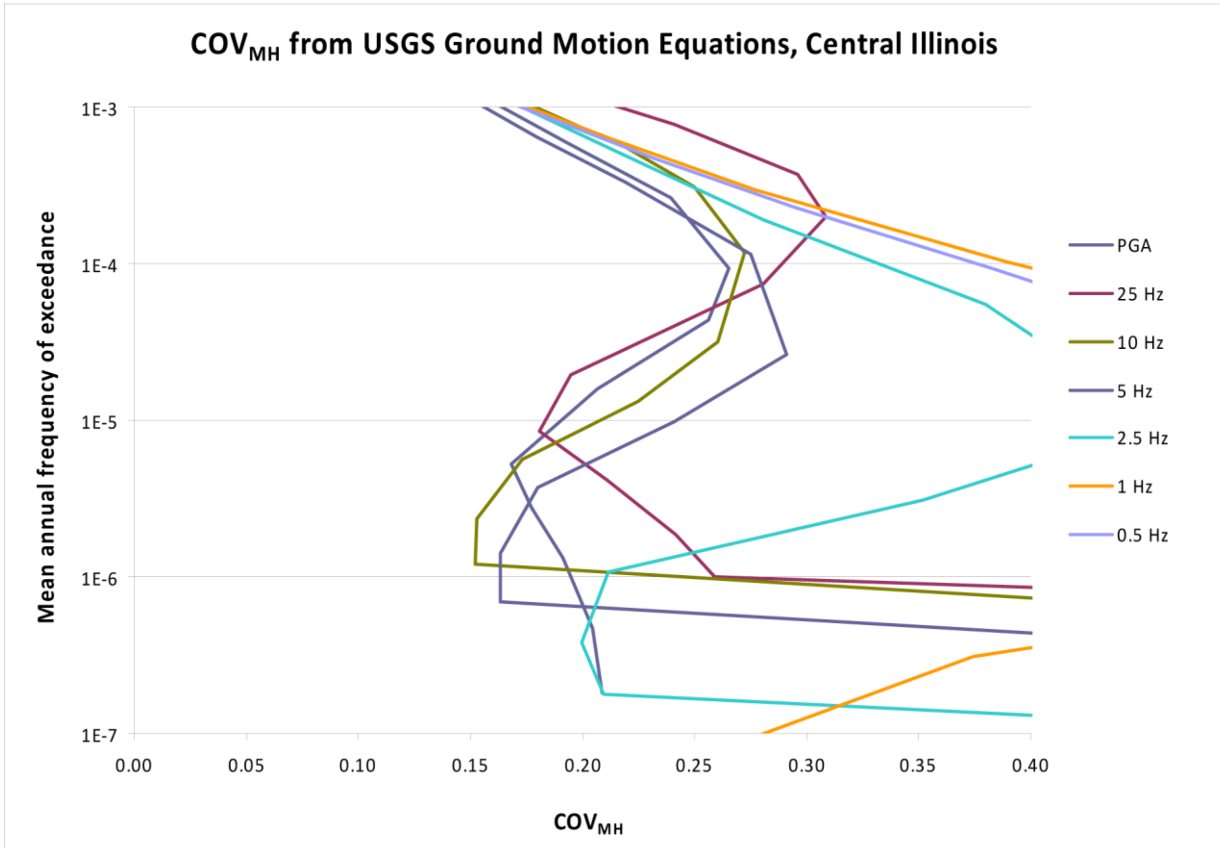

Figure 9.4-31
COV$_{MH}$ from ground motion equations vs. mean hazard for Central Illinois

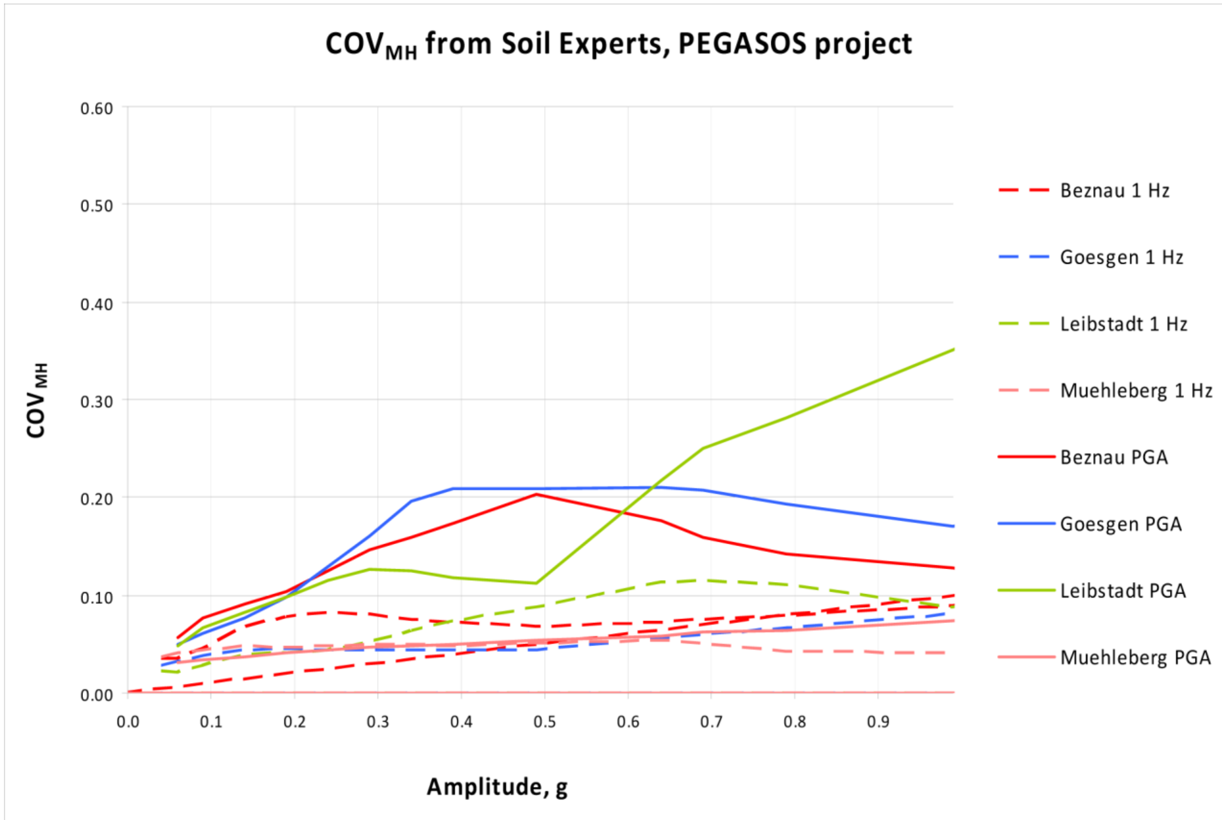

Figure 9.4-32
COV$_{MH}$ from soil experts vs. PGA and 1 Hz SA, PEGASOS project

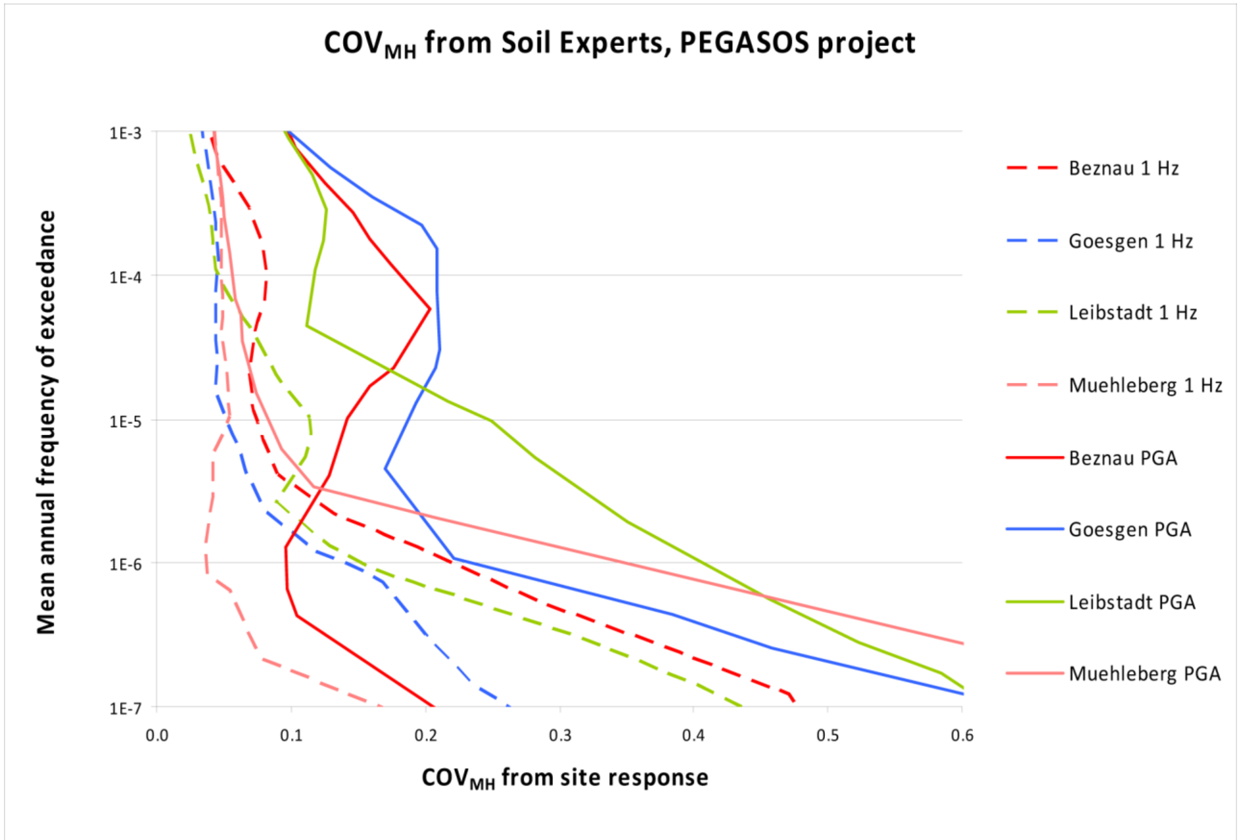

Figure 9.4-33
COV$_{MH}$ from soil experts vs. mean hazard for PGA and 1 Hz SA, PEGASOS project

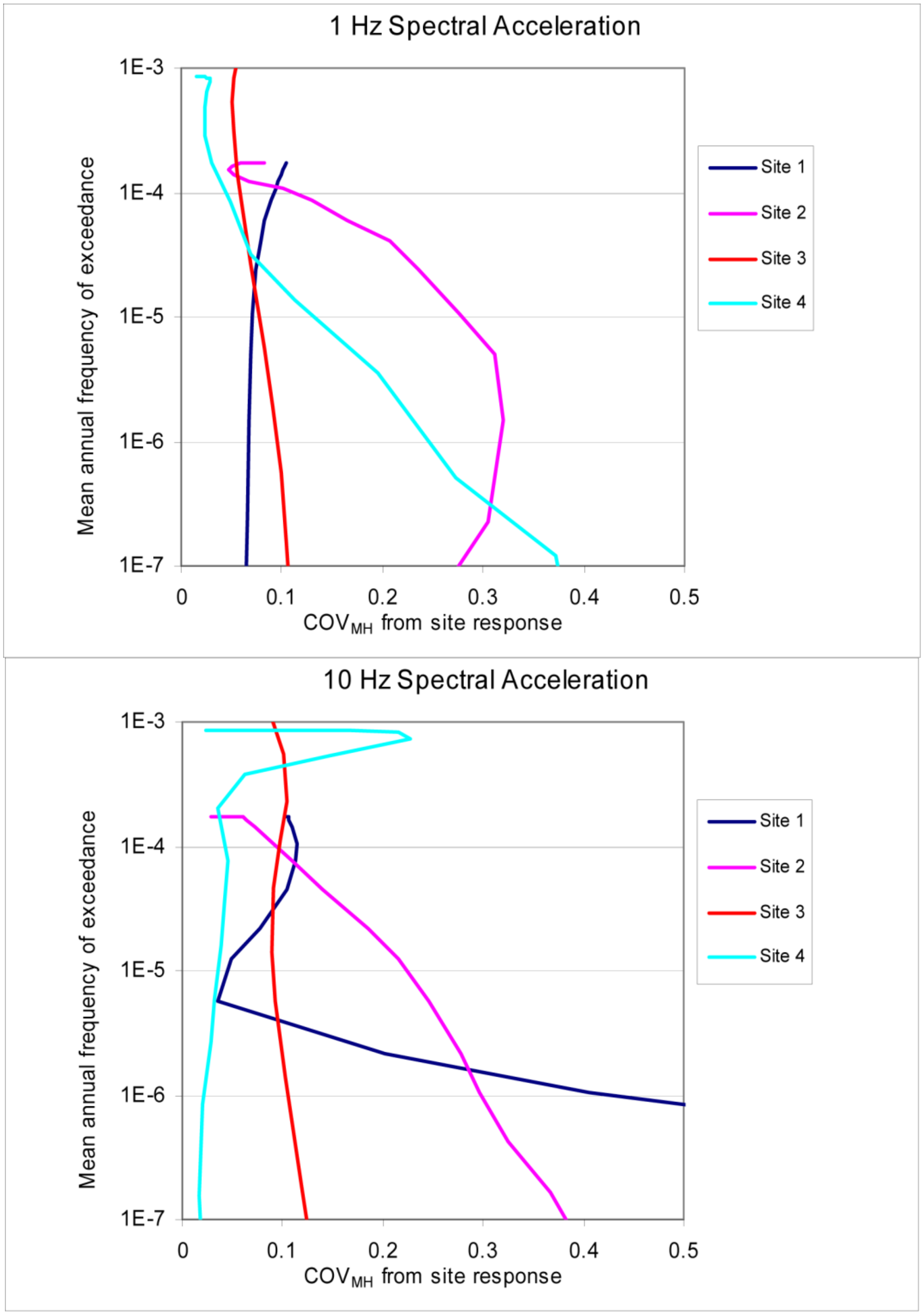

Figure 9.4-34
COV$_{MH}$ resulting from site response models vs. mean hazard for four sites, 1 Hz (top) and 10 Hz (bottom)

10

CHAPTER 10 REFERENCES

Abdel-Rahman, A.-F.M., and Kumarapeli, P.S., 1998, Geochemistry of mantle-related intermediate rocks from the Tibbit Hill volcanic suite, Quebec Appalachians: *Mineralogical Magazine*, v. 62, no. 4, pp. 487-500.

Abdel-Rahman, A.-F.M., and Kumarapeli, P.S., 1999, Geochemistry and petrogenesis of the Tibbit Hill metavolcanic suite of the Appalachian fold belt, Quebec-Vermont: A plume-related and fractionated assemblage: *American Journal of Science*, v. 299, pp. 210-237.

Adams, J., and Basham, P., 1989, The seismicity and seismotectonics of Canada east of the Cordillera: *Geoscience Canada*, v. 16, pp. 3-16.

Adams, J., and Basham, P., 1991, The seismicity and seismotectonics of eastern Canada: in Slemmons, D.B., Engdahl, E.R., Zoback, M.D., and Blackwell, D.D. (editors), *Neotectonics of North America*, Geological Society of America, Decade Map, Volume 1.

Adams, J., Basham, P.W., and Halchuk, S., 1995, Northeastern North American earthquake potential—New challenges for seismic hazard mapping: *Current Research 1995-D*, Geological Survey of Canada, pp. 91-99.

Adams, J., and Halchuk, S., 2003, *Fourth Generation Seismic Hazard Maps of Canada: Values for over 650 Canadian Localities Intended for the 2005 National Building Code of Canada*: Geological Survey of Canada, Open File 4459, 155 pp.

Adams, J., and Simmons, D.G., 1991, *Relocation of Earthquakes in the Labrador Sea and Southern Labrador*: Geological Survey of Canada Open File 2326, 103 pp.

Adams, J., Vonk, A., Pittman, D., and Vatcher, H., 1989, *New Focal Mechanisms for Southeastern Canadian Earthquakes—Volume II*: Geological Survey of Canada Open File Report 1995, 97 pp.

Adams, J., Weichert, D.H., Halchuk, S., and Basham, P.W, 1996, *Trial Seismic Hazard Maps of Canada—1995: Final Values for Selected Canadian Cities*: Geological Survey of Canada, Open File 3283, 97 pp.

Advanced National Seismic System (ANSS), Composite Earthquake Catalog, website, http://quake.geo.berkeley.edu/cnss/, last modified August 17, 2011.

Aitken, M.J., 1990, *Science-Based Dating in Archaeology*: Longman Group, London and New York, 274 pp.

Aitken, M.J., 1998, *An Introduction to Optical Dating: The Dating of Quaternary Sediments by the Use of Photon-Stimulated Luminescence*: Oxford University Press, 280 pp.

Akaike, H., 1974, A new look at the statistical model identification: *IEEE Transactions on Automatic Control*, v. 19, no. 6, pp. 716-723.

Aki, K., 1965, Maximum likelihood estimate of *b* in the formula log $N = a - bM$ and its confidence limits: *Bulletin of the Earthquake Research Institute* [University of Tokyo], v. 43, pp. 237-239.

Aleinikoff, J.N., Zartman, R.E., Walter, M., Rankin, D.W., Lyttle, P.T., and Burton, W.C., 1995, U-Pb ages of metarhyolites of the Catoctin and Mount Rogers Formations, central and southern Appalachians: Evidence for two pulses of Iapetan rifting: *American Journal of Science*, v. 295, pp. 428-454.

Allen, J.R.L., 1982, *Sedimentary Structures: Their Character and Physical Basis*: Elsevier, Amsterdam.

Ambraseys, N.N., 1988, Engineering seismology: *Earthquake Engineering and Structural Dynamics*, v. 17, pp. 1-105.

American Association of Petroleum Geologists (AAPG), 1995a, Geological Highway Map of the Northeastern Region, AAPG Highway Map number 10: American Association of Petroleum Geologists, Tulsa, Okla.

American Association of Petroleum Geologists (AAPG), 1995b, Geological Highway Map of the Southeastern Region, AAPG Highway Map number 9: Tulsa, OK: American Association of Petroleum Geologists, Tulsa, Okla.

American Nuclear Society, 2008a, *Criteria for Investigations of Nuclear Facility Sites for Seismic Hazard Assessments*: National Standard ANSI/ANS-2.27-2008.

American Nuclear Society, 2008b, *Probabilistic Seismic Hazard Analysis*: National Standard ANSI/ANS-2.29-2008.

American Petroleum Institute, 2000, Recommended Practice for Planning, Designing, and Constructing Fixed Offshore Platforms—Working Stress Design: American Petroleum Institute Standard RP 2A-WSD, 21st Edition, 242 pp.

Amick, D., and Gelinas, R., 1991, The search for evidence of large prehistoric earthquakes along the Atlantic seaboard: *Science*, v. 251, pp. 655-658.

Amick, D., Gelinas, R., Maurath, G., Cannon, R., Moore, D., Billington, E., and Kemppinen, H., 1990, *Paleoliquefaction Features along the Atlantic Seaboard*: U.S. Nuclear Regulatory Commission, NUREG/CR-5613 RA, 146 pp.

Amick, D., Maurath, G., and Gelinas, R., 1990, Characteristics of seismically induced liquefaction sites and features located in the vicinity of the 1886 Charleston, South Carolina earthquake: *Seismological Research Letters*, v. 61, no. 2, pp. 117-130.

Amick, D.C., 1990, Paleoliquefaction Investigations Along the Atlantic Seaboard with Emphasis on the Prehistoric Earthquake Chronology of Coastal South Carolina: unpublished Ph.D. dissertation, University of South Carolina.

Ammon, C.J., Herrmann, R.B., Langston, C.A., and Benz, H., 1998, Faulting parameters of the January 16, 1994 Wyomissing Hills, Pennsylvania earthquakes: *Seismological Research Letters*, v. 69, no. 3, pp. 261-269.

Anderson, K., and Spotila, J., 2001, The relationship of geologic structure to the Giles County seismic zone in Southwest Virginia, based on fracture mapping in allochthonous Paleozoic strata [abstract]: Geological Society of America *Abstracts with Programs*, v. 33, no. 2, p. 1.

Anderson, N.L., 1997, Subsurface Structure of the Commerce English Hill and Related Faults in the Benton Hills of Southeastern Missouri: Collaborative research, University of Missouri-Rolla, Department of Geology and Geophysics, and Missouri Department of Natural Resources Division of Geology and Land Survey, U.S. Geological Survey Award No. 1434-HQ-97-GR-03038, Project Summary, 4 pp.

Anderson, T.H., and Schmidt, V.A., 1983, The evolution of middle America and the Gulf of Mexico–Caribbean Sea region during Mesozoic time: *Geological Society of America Bulletin*, v. 94, pp. 941-966.

Anderson, T.W., and Lewis, C.F.M., 1975, Acoustic profiling and coring in Lake Ontario, Lake Erie and Georgian Bay: in Geological Survey of Canada Paper 75-1, Part A, pp. 373-376.

Andrus, R., and Heidari, T., 2009, Mapping liquefaction potential of soil deposits near Charleston, SC: abstract and talk presented at the meeting of the Central and Eastern U.S. (CEUS) Earthquake Hazards Program.

Angell, M., and Hitchcock, C., 2007, A geohazard perspective of recent seismic activity in the northern Gulf of Mexico: *2007 Offshore Technology Conference Proceedings*, May, Paper No. 19035, 8 pp.

Armbruster, J.G., 2002, Updates to the NCEER91 Catalog, files obtained from http://www.ldeo.columbia.edu/~armb/HIST/.

Armbruster, J.G., Seeber, L., Barstow, N., Kim, W.Y., and Horton, S., 1994, The Jan. 1994 Wyomissing Hills earthquakes (m_{bLg} = 4.0 & 4.6) in southeastern Pennsylvania: A 2-km-long northwest-striking fault illuminated by aftershocks [abstract]: *Eos, Transactions of the American Geophysical Union*, v. 75, no. 16, p. 237.

Atekwana, E.A., 1996, Precambrian basement beneath the central Midcontinent United States as interpreted from potential field data: in van der Pluijm, B.A., and Catacosinos, P.A. (editors), *Basement and Basins of Eastern North America*, Geological Society of America Special Paper 308, pp. 33-44.

Atkinson, G., 2008, Ground-motion prediction equations for eastern North America from a referenced empirical approach: Implications for epistemic uncertainty: *Bulletin of the Seismological Society of America*, v. 98, no. 3, pp. 1304-1318.

Atkinson, G.M., 1993, Earthquake source spectra in Eastern North America: *Bulletin of the Seismological Society of America*, v. 83, no. 6, pp. 1778-1798.

Atkinson, G.M., 2004a, Empirical attenuation of ground-motion spectral amplitudes in southeastern Canada and the northeastern United States: *Bulletin of the Seismological Society of America*, v. 94, no. 3, pp. 1079-1095.

Atkinson, G.M., 2004b, Erratum to "Empirical attenuation of ground-motion spectral amplitudes in southeastern Canada and the northeastern United States": *Bulletin of the Seismological Society of America*, v. 94, no. 6, pp. 2419-2423.

Atkinson, G.M., and Boore D.M., 1987, On the m_N, M relation for eastern North American earthquakes: *Seismological Research Letters*, v. 58, no. 4, pp. 119-124.

Atkinson, G.M., and Boore, D.M., 1995, Ground-motion relations for eastern North America: *Bulletin of the Seismological Society of America*, v. 85, no. 1, pp. 17-30.

Atkinson, G.M., and Boore, D.M., 2006, Earthquake ground-motion prediction equations for eastern North America: *Bulletin of the Seismological Society of America*, v. 96, pp. 2181-2205.

Atkinson, G.M., and Hanks, T.C., 1995, A high-frequency magnitude scale: *Bulletin of the Seismological Society of America*, v. 85, pp. 825-833.

Atkinson, G.M., Kaka, S.I., Eaton, D., Bent, A., Peci, V., and Halchuk, S., 2008, A very close look at a moderate earthquake near Sudbury, Ontario: *Seismological Research Letters*, v. 78, no. 1, pp. 119-131.

Atkinson, G.M., and Wald, D., 2007, Did You Feel It? Intensity data: A surprisingly good measure of earthquake ground motion: *Seismological Research Letters*, v. 78, no. 3, pp. 362-368.

Atwater, B.F., Tuttle, M.P., Schweig, E.S., Rubin, C.M., Yamaguchi, D.K., and Hemphill-Haley, E., 2004, Earthquake recurrence inferred from paleoseismology: in Gillespie, A.R., Porter, S.C., and Atwater, B.F. (editors), *The Quaternary Period in the United States*: Developments in Quaternary Science 1, Elsevier, Amsterdam and New York, pp. 331-350.

Audemard, F., and de Santis, F., 1991, Survey of liquefaction structures induced by recent moderate earthquakes: *Bulletin of the International Association of Engineering Geology*, v. 44, pp. 5-16.

Austin, J.A., Stoffa, P.L., Phillips, J.D., Oh, J., Sawyer, D.S., Purdy, G.M., Reiter, E., and Makris, J., 1990, Crustal structure of the Southeast Georgia embayment-Carolina Trough: Preliminary results of a composite seismic image of a continental suture (?) and a volcanic passive margin: *Geology*, v. 18, pp. 1023-1027.

Autin, W.J., Burns, S.F., Miller, B.J., Saucier, R.T., and Snead, J.I., 1991, Quaternary geology of the lower Mississippi Valley: in Morrison, R.B. (editor), *Quaternary Nonglacial Geology; Conterminous United States*, Geological Society of America, The Geology of North America, v. K-2, pp. 547-582.

Axtman, T.C., 1983, Structural mechanisms and oil accumulation along the Mountain View–Wayne fault, south-central Oklahoma, Part I: *Shale Shaker*, v. 34, pp. 1-11.

Aylsworth, J.M., and Lawrence, D.E., 2003, Earthquake-induced landsliding east of Ottawa: A contribution to the Ottawa Valley Landslide Project: *Geohazards 2003, Proceedings of the 3rd Canadian Conference on Geotechnique and Natural Hazards, June 9 and 10, Edmonton, Alberta, Canada*, pp. 57-64.

Aylsworth, J.M., Lawrence, D.E., and Guertin, J., 2000, Did two massive earthquakes in the Holocene induce widespread landsliding and near-surface deformation in part of the Ottawa Valley, Canada? *Geology*, v. 28, pp. 903-906.

Baird, A.F., McKinnon, S.D., and Godin, L., 2009, Stress channelling and partitioning of seismicity in the Charlevoix seismic zone, Québec, Canada: *Geophysical Journal International*, v. 179, pp. 559-568.

Baksi, A.K., 1997, The timing of Late Cretaceous alkalic igneous activity in the northern Gulf of Mexico basin, Southeastern USA: *Geology*, v. 105, pp. 629-643.

Bakun, W.H., and Hopper, M.G., 2004a, *Catalog of Significant Historical Earthquakes in the Central United States*: U.S. Geological Survey Open-File Report 2004-1086, 142 pp.

Bakun, W.H., and Hopper, M.G., 2004b, Magnitudes and locations of the 1811-1812 New Madrid, Missouri, and the 1886 Charleston, South Carolina, earthquakes: *Bulletin of the Seismological Society of America*, v. 94, no. 1. pp. 64-75.

Bakun, W.H., Johnston, A.C., and Hopper, M.G., 2003, Estimating locations and magnitudes of earthquakes in eastern North America from modified Mercalli intensities: *Bulletin of the Seismological Society of America*, v. 93, pp. 190-202.

Bakun, W.H., and McGarr, A., 2002, Differences in attenuation among the stable continental regions: *Geophysical Research Letters*, v. 29, no. 23, pp. 2121.

Bakun, W.H., and Wentworth, C.M., 1997, Estimating earthquake location and magnitude from seismic intensity data: *Bulletin of the Seismological Society of America*, v. 87, pp. 1502-1521.

Baldwin, J.N., Barron, A.D., and Kelson, K.I., Harris, J.B., and Cashman, S.M., 2002, Preliminary paleoseismic and geophysical investigation of the North Farrenburg Lineament, Farrenburg, Missouri: Deformation associated with the New Madrid North fault? *Seismological Research Letters*, v. 73, no. 3, pp. 395-413.

Baldwin, J.N., Givler, R., Brossy, C.C., Elliot, E.T., and Harris, J.B., 2008, *Geophysical and Paleoseismic Evaluation of the Penitentiary Fault and Its Association with the Commerce Geophysical Lineament, Tamms, Southern Illinois*: U.S. Geological Survey National Earthquake Hazards Reduction Program, Final Technical Report, Award 06-HQ-GR-0138, 34 pp, plus 10 figures and one plate.

Baldwin, J.N., Harris, J.B., Van Arsdale, R.B., Givler, R., Kelson, K.I., Sexton, J.L., and Lake, M., 2005, Constraints on the location of the late Quaternary Reelfoot and New Madrid North faults in the New Madrid seismic zone, Central United States: *Seismological Research Letters*, v. 76, no. 6, pp. 772-789.

Baldwin, J.N., Witter, R.C., Vaughn, J.D., Harris, J.B., Sexton, J., Lake, M., and Forman, S.L., 2006, Geological characterization of the Idalia Hill fault zone and its structural association with the Commerce geophysical lineament, Idalia, Missouri: *Bulletin of the Seismological Society of America*, v. 96, no. 6, pp. 2281-2303.

Baranoski, M.T., 2002, Structure Contour Map on the Precambrian Unconformity Surface in Ohio and Related Basement Features: A Description to Accompany Division of Geological Survey Map PG-23: Ohio Geological Survey, 19 pp.

Baranoski, M.T., Dean, S.L., Wicks, J.L., and Brown, V.M., 2009, Unconformity-bounded seismic reflection sequences define Grenville-age rift system and foreland basins beneath the Phanerozoic in Ohio: *Geosphere*, v. 5, pp. 140-151.

Barnes, A. A., 2000, An Interdisciplinary Study of Earthquake-Induced Liquefaction Features in the New Madrid Seismic Zone, Central United States: M.S. thesis, Auburn University, Alabama, 266 pp.

Barstow, N.L., Brill, K.G., Jr., Nuttli, O.W., and Pomeroy, P.W. (editors), 1981, *Approach to Seismic Zonation for Siting Nuclear Electric Power Generating Facilities in the Eastern United States*: U.S. Nuclear Regulatory Commission Report NUREG/CR-1577, pp. 98-143.

Bartholomew, M.J., and Rich, F.J., 2007, The walls of colonial Fort Dorchester: A record of structures caused by the August 31, 1886 Charleston, South Carolina, earthquake and its subsequent earthquake history: *Southeastern Geology*, v. 44, no. 4, pp. 147-169.

Basham, P.W., Weichert, D.H., and Berry, M.J., 1979, Regional assessment of seismic risk in Eastern Canada: *Bulletin of the Seismological Society of America*, v. 69, no. 5, pp. 1567-1602.

Bauer, L.M., 2006, Studies of Historic and Prehistoric Earthquake-Induced Liquefaction Features in the Meizoseismal Area of the 1811-1812 New Madrid Earthquakes, Central United States: M.S. thesis, University of Memphis, Memphis, Tennessee, 135 pp.

BC Hydro, 2008, Seismic Source Characterization for the Probabilistic Seismic Hazard Analysis for the BC Hydro Service Area: draft report, BC Hydro and Power Authority.

Bear, G.W., Rupp, J.A., and Rudman, A.J., 1997, Seismic interpretation of the deep structure of the Wabash Valley fault system: *Seismological Research Letters*, v. 68, pp. 624-640.

Bédard, J.H., and Stevenson, R., 1999, The Caldwell Group lavas of southern Quebec: MORB-like tholeiites associated with the opening of Iapetus Ocean: *Canadian Journal of Earth Sciences*, v. 36, pp. 999-1019.

Behrendt, J.C., Hamilton, R.M., Ackermann, H.D., and Henry, V.J., 1981, Cenozoic faulting in the vicinity of the Charleston, South Carolina, 1886 earthquake: *Geology*, v. 9, no. 3, pp. 117-122.

Behrendt, J.C., Hamilton, R.M., Ackermann, H.D., Henry, V.J., and Bayer, K.C., 1983, Marine multichannel seismic-reflection evidence for Cenozoic faulting and deep crustal structure near Charleston, South Carolina: in Gohn, G.S. (editor), *Studies Related to the Charleston, South Carolina Earthquake of 1886—Tectonics and Seismicity*, U.S. Geological Survey Professional Paper 1313-J, pp. J1-J29.

Behrendt, J.C., and Yuan, A., 1987, The Helena Banks strike-slip (?) fault zone in the Charleston, South Carolina, earthquake area: results from a marine, high-resolution, multichannel, seismic-reflection survey: *Geological Society of America Bulletin*, v. 98, no. 5, pp. 591-601.

Benjamin, J.R., and Cornell, C.A., 1970, *Probability, Statistics, and Decisions for Civil Engineers*: McGraw-Hill, New York, 684 pp.

Bennison, A.P., 1978, Geological Highway Map of the Great Lakes Region, AAPG Highway Map number 11, Tulsa, OK: American Association of Petroleum Geologists.

Bennison, A.P., 1990, Geological Highway Map of the Southern Rocky Mountain Region, AAPG Highway Map number 2, Tulsa, OK: American Association of Petroleum Geologists.

Bennison, A.P., and Chenoweth, P.A., 1984, Geological Highway Map of the Northern Great Plains Region, AAPG Highway Map number 12, Tulsa, OK: American Association of Petroleum Geologists.

Bennison, A.P., and Webb, J.M., 1986, Geological Highway Map of the Midcontinent Region, AAPG Highway Map number 1, Tulsa, OK: American Association of Petroleum Geologists.

Bennison, A.P., and Webb, J.M., 1989, Geological Highway Map of the Mid-Atlantic Region, AAPG Highway Map number 4, Tulsa, OK: American Association of Petroleum Geologists.

Benson, R.N., 1992, Map of exposed and buried early Mesozoic rift basins/synrift rocks of the U.S. middle Atlantic continental margin: *Delaware Geological Society*, Miscellaneous map series no. 5, 1:1,000,000 scale.

Bent, A.L., 1992, A re-examination of the 1925 Charlevoix, Quebec earthquake: *Bulletin of the Seismological Society of America*, v. 82, pp. 2097-2113.

Bent, A.L., 1995, A complex double-couple source mechanism for the M_S 7.2 1929 Grand Banks earthquake: *Bulletin of the Seismological Society of America*, v. 85, no. 4, pp. 1003-1020.

Bent, A.L., 1996a, An improved source mechanism for the 1935 Timiskaming, Quebec, earthquake from regional waveforms: *Pure and Applied Geophysics*, v. 146, no. 1, pp. 5-20.

Bent, A.L., 1996b, Source parameters of the damaging Cornwall-Massena earthquake of 1944 from regional waveforms: *Bulletin of the Seismological Society of America*, v. 86, no. 2, pp. 489-497.

Bent, A.L., 2009, *A Moment Magnitude Catalog for the 150 Largest Eastern Canadian Earthquakes*: Geological Survey of Canada, Open-File 6080, 23 pp.

Bent, A.L., 2010, Toward a moment magnitude catalog for earthquakes hazard assessment in eastern Canada [abstract]: *Seismological Research Letters*, v. 81, p. 354.

Bent, A.L., and Cassidy, J.F., 1993, The January 1992 Franklin Lake, Northwest Territories, earthquake sequence: *Bulletin of the Seismological Society of America*, v. 83, no. 2, pp. 398-415.

Bent, A.L., Drysdale, J., and Perry, H.K.C., 2003, Focal mechanisms for Eastern Canadian earthquakes, 1994-2000: *Seismological Research Letters*, v. 74, no. 4, pp. 452-468.

Bent, A.L., and Hasegawa, H.S., 1992, Earthquakes along the northwestern boundary of the Labrador Sea: *Seismological Research Letters*, v. 63, pp. 587-602.

Bent, A.L., Lamontagne, M., Adams, J., Woodgold, C.R.D., Halchuk, S., Drysdale, J., Wetmiller, R.J., and Ma, S., 2002, The Kipawa, Quebec, "Millennium" earthquake: *Seismological Research Letters*, v. 73, no. 2, pp. 285-297.

Bent, A.L., and Perry, H.K.C., 2002, Depths of Eastern Canadian earthquakes from regional data: *Seismological Research Letters*, v. 73, no. 2, pp. 273-284.

Bergantino, R.N., and Wilde, E.M., 1998a, Geologic map of the Culbertson 30' × 60' quadrangle (bedrock emphasis), northeastern Montana: Montana Bureau of Mines and Geology Open-File Report 359, scale 1:100,000.

Bergantino, R.N., and Wilde, E.M., 1998b, Geologic map of the Wolf Point 30' × 60' quadrangle (bedrock emphasis), northeastern Montana: Montana Bureau of Mines and Geology Open-File Report 358, scale 1:100,000.

Bernreuter, D.L., Savy, J.B., Mensing, R.W., Chen, J.C., and Davis, B.C., 1989, *Seismic Hazard Characterization of 69 Nuclear Plant Sites East of the Rocky Mountains*: U.S. Nuclear Regulatory Commission, NUREG/CR-5250, Volumes 1–8, Washington, D.C., January.

Bickford, M.E., Van Schmus, W.R., and Zietz, I., 1986, Proterozoic history of the Midcontinent region of North America: *Geology*, v. 14, pp. 492-496.

Biewick, L.R.H., Hardie, J.K., Williamson, C., and Amdt, H.H., 1990, *Evaluation of Coal Resources in the Eastern Part of the Fort Peck Indian Reservation, Montana*: U.S. Geological Survey Bulletin 1869, 136 pp.

Bird, D., 2001, Shear margins: Continent-ocean transform and fracture zone boundaries: *The Leading Edge* [Association of Exploration Geophysicists], February, pp. 150-159.

Bird, D.E., Burke, K., Hall, S.A., and Casey, J.F., 2005, Gulf of Mexico tectonic history: Hotspot tracks, crustal boundaries, and early salt distribution: *AAPG Bulletin*, v. 89, no. 3, pp. 311-328.

Birkeland, P.W., 1999, *Soils and Geomorphology*, 3rd Edition: Oxford University Press, New York and Oxford, 448 pp.

Boatwright, J., 1994, Regional propagation characteristics and source parameters of earthquakes in northeastern North America: *Bulletin of the Seismological Society of America*, v. 84, no. 1, pp. 1-15.

Bollinger, G.A., 1973, Seismicity and crustal uplift in the southeastern United States: *American Journal of Science*, v. 273-A, pp. 396-408.

Bollinger, G.A., 1975, A catalog of Southern United States earthquakes—1754 through 1974: *Research Division Bulletin* 101, Virginia Polytechnic Institute and State University, 68 pp.

Bollinger, G.A., 1977, Reinterpretation of the intensity data for the 1886 Charleston, South Carolina, earthquake: in Rankin, D.W. (editor), *Studies Related to the Charleston, South Carolina, Earthquake of 1886—A Preliminary Report*, U.S. Geological Survey Professional Paper 1028, pp. 17-32.

Bollinger, G.A., 1979, Attenuation of the Lg phase and the determination of m_b in the southeastern United States: *Bulletin of the Seismological Society of America*, v. 69, no. 1, pp. 45-63.

Bollinger, G.A., 1983, Speculations on the nature of seismicity at Charleston, South Carolina: in Gohn, G.S. (editor), *Studies Related to the Charleston, South Carolina, Earthquake of 1886—Tectonics and Seismicity*, U.S. Geological Survey Professional Paper 1313-T, pp. T1-T11.

Bollinger, G.A., 1992, *Specification of Source Zones, Recurrence Rates, Focal Depths, and Maximum Magnitudes for Earthquakes Affecting the Savannah River Site in South Carolina*: U.S. Geological Survey Bulletin 2017, 57 pp.

Bollinger, G.A., and Hopper, M.G., 1971, Virginia's two largest earthquakes—December 22, 1875, and May 31, 1897: *Bulletin of the Seismological Society of America*, v. 61, pp. 1033-1039.

Bollinger, G.A., Johnston, A.C., Talwani, P., Long, L.T., Shedlock, K.M., Sibol, M.S., and Chapman, M.C., 1991, Seismicity of the southeastern United States; 1698 to 1986: in Slemmons, D.B., Engdahl, E.R., Zoback, M.D., and Blackwell, D. (editors), *Neotectonics of North America*: Geological Society of America, Decade Map Volume 1, pp. 291-308.

Bollinger, G.A., Law, R.D., Pope, M.C., Wirgart, R.H., and Whitmarsh, R.S., 1992, Geologically recent near-surface faulting in the Valley and Ridge Province: New exposures of extensional faults in alluvial deposits, Giles County, SW Virginia [abstract]: Geological Society of America *Abstracts with Programs*, v. 24, no. 7, p. 152.

Bollinger, G.A., and Sibol, M.S., 1985, Seismicity, seismic reflection studies, gravity and geology of the central Virginia seismic zone: Part 1. Seismicity: *Geological Society of America Bulletin*, v. 96, no. 1, pp. 49-57.

Bollinger, G.A., and Wheeler, R.L., 1983, The Giles County seismic zone: *Science*, v. 219, pp. 1063-1065.

Bollinger, G.A., and Wheeler, R.L., 1988, *The Giles County, Virginia, Seismogenic Zone—Seismological Results and Geological Interpretations*: U.S. Geological Survey Professional Paper 1355, 85 pp.

Bommer, J.J., and Scherbaum, F., 2008, The use and misuse of logic trees in probabilistic seismic hazard analysis: *Earthquake Spectra*, v. 24, pp. 997-1009.

Boore, D.M., and Atkinson, G.M., 1987, Stochastic prediction of ground motion and spectral response parameters at hard-rock sites in eastern North America: *Bulletin of the Seismological Society of America*, v. 77, no. 2, pp. 440-467.

Boore, D.M., and Atkinson, G.M., 1992, Source spectra for the 1988 Saguenay, Quebec, earthquakes: *Bulletin of the Seismological Society of America*, v. 82, no. 2, pp. 683-719.

Boore, D.M., Campbell, K.W., and Atkinson, G.M., 2010, Determination of stress parameters for eight well-recorded earthquakes in eastern North America: *Bulletin of the Seismological Society of America*, v. 100, no. 4, pp. 1632-1645.

Bostwick, T.K., 1984, A Re-examination of the 1949 Queen Charlotte Earthquake: M.Sc. thesis, University of British Columbia, Vancouver, Canada.

Bradshaw, B., and Watkins, J., 1994, Growth-fault evolution in offshore Texas: *Transactions of the Gulf Coast Association of Geological Societies*, v. 44, pp. 103-109.

Braile, L.W., Keller, G.R., Hinze, W.J., and Lidiak, E.G., 1982, An ancient rift complex and its relation to contemporary seismicity in the New Madrid seismic zone: *Tectonics*, v. 1, pp. 225-237.

Braile, L., Hinze, W., Sexton, J., Keller, G.R., and Lidiak, E., 1984, Tectonic development of the New Madrid Seismic Zone: in Hays, W.W., and Gori, P.L. (editors), *Proceedings of the Symposium on the New Madrid Seismic Zone*, U.S. Geological Survey Open-File Report 84-770, pp. 204-233.

Braile, L.W., Hinze, W.J., Keller, G.R., Lidiak, E.G., and Sexton, J.L., 1986, Tectonic development of the New Madrid Rift Complex, Mississippi Embayment, North America: *Tectonophysics*, v. 131, pp. 1-21.

Braile, L.W., Hinze, W.J., and Keller, G.R., 1997, New Madrid seismicity, gravity anomalies, and interpreted ancient rift structures: *Seismological Research Letters*, v. 68, no. 4, pp. 599-610.

Bramlette, K.W., Secor, D.T., and Prowell, D.C., 1982, The Belair fault: A Cenozoic reactivation structure in the eastern Piedmont: *Geological Society of America Bulletin*, v. 93, pp. 1109-1117.

Brewer, J.A., 1982, Study of southern Oklahoma aulacogen, using COCORP deep seismic-reflection profiles: in Gilbert, M.C., and Donovan, R.N. (editors), *Geology of the Eastern Wichita Mountains, Southwestern Oklahoma*, Oklahoma Geological Survey Guidebook 21, pp. 31-39.

Brewer, J.A., Brown, L.D., Steiner, D., Oliver, J.E., Kaufman, S., and Denison, R.E., 1981, Proterozoic basin in the southern Midcontinent of the United States revealed by COCORP deep seismic reflection profiling: *Geology*, v. 9, pp. 569-575.

Brewer, J.A., Good, R., Oliver, J.E., Brown, L.D., and Kaufman, S., 1983, COCORP profiling across the Southern Oklahoma aulacogen: Overthrusting of the Wichita Mountains and compression within the Anadarko Basin: *Geology*, v. 11, pp. 109-114.

Bristol, H.M., and Treworgy, J.D., 1979, *The Wabash Valley Fault System in Southeastern Illinois*: Illinois State Geological Survey, Circular 509, 19 pp.

Bronk Ramsey, C., 1995, Radiocarbon calibration and analysis of stratigraphy: The OxCal program: *Radiocarbon*, v. 37, no. 2, pp. 425-430.

Bronk Ramsey, C., 2001, Development of the radiocarbon calibration program OxCal: *Radiocarbon*, v. 43, no. 2A, pp. 355-363.

Bronk Ramsey, C., 2009, Bayesian analysis of radiocarbon dates: *Radiocarbon*, v. 51, no. 1, pp. 337-360.

Broughton, A.T., Van Arsdale, R.B., and Broughton, J.H., 2001, Liquefaction susceptibility mapping in the city of Memphis and Shelby County, Tennessee (in earthquake hazard evaluation in the central United States): *Engineering Geology*, v. 62, no. 1-3, pp. 207-222.

Brown, E.J., and Ebel, J.E., 1985, An investigation of the January 1982, Gaza, New Hampshire, aftershock sequence: *Earthquake Notes*, v. 56, no. 4, pp. 125-133.

Brown, W.J., 1900, *History of the Town of Hampton Falls, New Hampshire: From the Time of the First Settlement Within Its Borders, 1640-1900*: John B. Clark Co., Manchester, N.H., v. 1, 637 pp.

Browning, S.E., 2003, Paleoseismic Studies in the New Madrid Seismic Zone, Central United States: M.S. thesis, Auburn University, Auburn, Ala., 134 pp.

Buchner, C.A., Cox, R., Skinner, C.T., Kaplan, C., and Albertson, E.S., 2010, *Data Recovery Excavations at the Laplant I Site (23NM51), New Madrid County, Missouri*: Report to U.S. Army Corps of Engineers, Memphis District.

Budnitz, R.J., Apostolakis, G., Boore, D.M., Cluff, L.S., Coppersmith, K.J., Cornell, C.A., and Morris, P.A., 1997, *Recommendations for Probabilistic Seismic Hazard Analysis: Guidance on Uncertainty and Use of Experts*: Report NUREG/CR-6372, Lawrence Livermore National Laboratory, sponsored by the U.S. Nuclear Regulatory Commission, U.S. Department of Energy, and Electric Power Research Institute.

Buffler, R.T., Watkins, J.S., Shaub, F.J., and Worzel, J.L., 1980, Structure and early geologic history of the deep central Gulf of Mexico Basin: in Pilger, R.H. (editor), *The Origin of the Gulf of Mexico and the Early Opening of the Central North Atlantic Ocean*, Louisiana Geologic Society, Baton Rouge, La.

Buffler, R.T., and Sawyer, D.S., 1985, Distribution of crust and early history, Gulf of Mexico basin: *Transactions of the Gulf Coast Association of Geological Societies*, v. 35, pp. 333-344.

Buffler, R.T., and Thomas, W.A., 1994, Crustal structure and evolution of the southwestern margin of North America and the Gulf of Mexico basin: in Speed, R.C. (editor), *Phanerozoic Evolution of North American Continent-Ocean Transitions*: Geological Society of America, DNAG Continent-Ocean Transect Volume CRV-001, pp. 219-264.

Bunker, B.J., Ludvigson, G.A., and Witzke, B.J., 1985, *The Plum River Fault Zone and the Structural and Stratigraphic Framework of Eastern Iowa*: Iowa Geological Survey, Technical Information Series Report 13, 126 pp.

Bunker, B.J., and Witzke, B.J., 1988, Central mid-continent region sedimentary cover of the craton: in Sloss, L.L. (editor), *Sedimentary Cover—North American Craton: U.S.*, Geological Society of America, The Geology of North America, v. D-2, Plate 4.

Burke, K.B.S., 2004, Historical seismicity in the Central Highlands, Passamaquoddy Bay, and Moncton regions of New Brunswick, Canada, 1817-1961: *Seismological Research Letters*, v. 75, pp. 419-431.

Burke, K.B.S., 2009, *Historical Earthquakes Felt in New Brunswick (1764, 1811-1960)*: Sadler Geophysical and Administrative Services, Fredericton, New Brunswick, 755 pp. plus 34 pp. of appendices.

Burrell, R.D., 1997, Evaluation of Faulting Characteristics and Ground Acceleration Associated with Recent Movement along the Meers Fault, Southwestern Oklahoma: M.S. thesis, Texas A&M, College Station, Tex.

Buschbach, T.C., and Kolata, D.R., 1991, Regional setting of the Illinois Basin: in Leighton, M.W., Kolata, D.R., Oltz, D.F., and Eidel, J.J. (editors), *Interior Cratonic Basins*, AAPG Memoir 51, pp. 29-55.

Byerly, G.R., 1991, Igneous activity: in Salvador, A. (editor), *The Gulf of Mexico Basin*, Geological Society of America, The Geology of North America, v. J, ch. 6, pp. 91-108.

Calais, E., Freed, A., Van Arsdale, R., and Stein, S., 2009, Time-Variable Deformation in the New Madrid Seismic Zone: presentation given at meeting of CEUS Earthquake Hazards Program, U.S. Geological Survey, October 28-29, Memphis, Tenn.

Calais, E., Han, J.Y., DeMets, C., and Nocquet, J.M., 2006, Deformation of the North American plate interior from a decade of continuous GPS measurements: *Journal of Geophysical Research*, v. 111, B06402, doi:10.1029/2005JB004253.

Calais, E., Mattioli, G., DeMets, C., Nocquet, J.M., Stein, S., Newman, A., and Rydelek, P., 2005, Tectonic strain in the interior of the North American Plate? *Nature*, v. 438, doi:10.1038/nature04428.

Calais, E., and Stein, S., 2009, Time-variable deformation in the New Madrid seismic zone: *Science*, v. 323, pp. 1442, doi:0.1126/science.1168122.

Campbell, K.W., 2003, Prediction of strong ground motion using the hybrid empirical method and its use in the development of ground-motion (attenuation) relations in eastern North America: *Bulletin of the Seismological Society of America*, v. 93, pp. 1012-1033.

Cannon, W.F., 1994, Closing of the Midcontinent rift—A far-field effect of Grenvillian compression: *Geology*, v. 22, pp. 155-158.

Cannon, W.F., Green, A.G., Hutchinson, D.R., and nine others, 1989, The North American Midcontinent Rift beneath Lake Superior from GLIMPCE seismic reflection profiling: *Tectonics*, v. 8, no. 2, pp. 305-332.

Cannon, W.F., Lee, M.W., Hinze, W.J., Schulz, K.J., and Green, A.G., 1991, Deep crustal structure of the Precambrian basement beneath northern Lake Michigan, midcontinent North America: *Geology,* v. 19, pp. 207-210.

Castilla, R.A., and Audemard, F.A., 2007, Sand blows as a potential tool for magnitude estimation of pre-instrumental earthquakes: *Journal of Seismology*, v. 11, pp. 473-487, doi:10.1007/s10950-007-9065-z.

Cavallini, F., and Rebez, A., 1996, Representing earthquake intensity-magnitude relationship with a nonlinear function: *Bulletin of the Seismological Society of America*, v. 86, no. 1A, pp. 73-78.

Cawood, P.A., McCausland, P.J.A., and Dunning, G.R., 2001, Opening Iapetus: Constraints from the Laurentian margin in Newfoundland: *Geological Society of America Bulletin*, v. 113, pp. 443-453.

Center for Earthquake Research and Information (CERI), New Madrid Earthquake Catalog, website, http://folkworm.ceri.memphis.edu/catalogs/html/cat_nm.html.

Cetin, H., 2003, Comment on "Known and suggested Quaternary faulting in the midcontinent United States by Russell L. Wheeler and Anthony Crone": *Engineering Geology,* v. 69, pp. 193-210.

Cetin, K.O., Seed, R.B., Kiureghian, A.D., Tokimatsu, K., Harder, Jr., L.F., Kayen, R.E., and Moss, R.E.S., 2004, Standard penetration test-based probabilistic and deterministic assessment of seismic soil liquefaction potential: *Journal of Geotechnical and Geoenvironmental Engineering*, v. 130, no. 12, pp. 1314-1340.

Champion, J., Mueller, K., Tate, A., and Guccione, M., 2001, Geometry, numerical models and revised slip rate for the Reelfoot fault and trishear fault-propagation fold, New Madrid seismic zone: *Engineering Geology*, v. 62, pp. 31-49.

Chapman, M.C., 1996, Focal mechanisms and the geometry of basement faults in the eastern Tennessee seismic zone: *Seismological Research Letters*, v. 67, no. 2, p. 35.

Chapman, M.C., and Beale, J.N., 2008, Mesozoic and Cenozoic faulting imaged at the epicenter of the 1886 Charleston, South Carolina earthquake: *Bulletin of the Seismological Society of America*, v. 98, pp. 2533-2542.

Chapman, M.C., and Beale, J.N., 2009, Results of reprocessing seismic reflection data near Summerville, SC: abstract and talk presented at the meeting of the Central and Eastern U.S. (CEUS) Earthquake Hazards Program.

Chapman, M.C., and Beale, J.N., 2010, On the geologic structure at the epicenter of the 1886 Charleston, South Carolina, earthquake: *Bulletin of the Seismological Society of America*, v. 100, no. 3, pp. 1010-1030.

Chapman, M.C., Beale, J.N., and Hole, J.A., 2007, *Attenuation in the Atlantic Coastal Plain of Virginia and Cenozoic Faulting Imaged in the Epicentral Area of the 1886 Charleston, South Carolina Earthquake, Using Data from Seismic Reflection Profiles*: Final report, U.S. Geological Survey Award Nos. 07-HQ-GR-0042 and 06-HQ-GR-0109, 34 pp.

Chapman, M.C., and Bollinger, G.A., 1984, Reliability of focal depth estimates from a small network: *Earthquake Notes*, v. 55, no. 4, pp. 16-25.

Chapman, M.C., and Krimgold, F., 1994, Seismic Hazard Assessment for Virginia: report prepared for the Virginia Department of Emergency Services and the Federal Emergency Management Agency, Virginia Tech Seismological Observatory, Blacksburg, Va., 62 pp.

Chapman, M.C., Munsey, J.W., Powell, C.A., Whisner, S.C., and Whisner, J., 2002, The eastern Tennessee seismic zone: Summary after 20 years of network monitoring: *Seismological Research Letters*, v. 73, no. 2, p. 245.

Chapman, M.C., Powell, C.A., Vlahovic, G., and Sibol, M.S., 1997, A statistical analysis of earthquake focal mechanisms and epicenter locations in the eastern Tennessee seismic zone: *Bulletin of the Seismological Society of America*, v. 87, no. 6, pp. 1522-1536.

Chapman, M.C., and Talwani, P., 2002, Seismic Hazard Mapping for Bridge and Highway Design in South Carolina: South Carolina Department of Transportation report.

Chester, J.S., and Tuttle, M.P., 2000, *Paleoseismology Study in the Cache River Valley, Southern Illinois*: Annual Project Summary submitted to the U.S. Geological Survey National Earthquake Hazards Reduction Program, Contract No. 1434-HQ-98-GR-00013 and GR-00015, 6 pp.

Chiu, J.M., Chen, K.C., Yang, Y.T. and Johnston, A., 1990, A high resolution PANDA experiment in the central New Madrid seismic zone [abstract]: Geological Society of America *Abstracts with Programs*, v. 7, no. 17.

Chiu, J.M., Johnston, A.C., and Yang, Y.T., 1992, Imaging the active faults of the central New Madrid seismic zone using PANDA array data: *Seismological Research Letters*, v. 63, no. 3, pp. 375-393.

Chiu, S.-C.C., Chiu, J.-M., and Johnston, A.C., 1997, Seismicity of the southeastern margin of Reelfoot rift, central United States: *Seismological Research Letters*, v. 68, no. 5, pp. 785-796.

Choi, J., Jin, K., Enkhbayar, D., Bayasgalan, A., and Kim, Y., 2009, Fault segmentation and slip distribution along the 1957 Gobi-Altay earthquake rupture, Mongolia [abstract]: American Geophysical Union, Fall Meeting, Abstract T33B-1910.

Christenson, G., 1990, The Florida lineament: in Kinsland, G., and Cagle, A. (editors): *Transactions of the Gulf Coast Association of Geological Societies*, v. 40, pp. 99-115.

Clendenin, C.W., Lowell, G.R., and Niewendorp, C.A., 1993, Sequencing Reelfoot extension based on relations from southeast Missouri and interpretations of the interplay between offset preexisting zones of weakness: *Tectonics*, v. 12., pp. 703-712.

Clendenin, C.W., Niewendorp, C.A., and Lowell, G.R., 1989, Reinterpretation of faulting in southeast Missouri: *Geology*, v. 17, pp. 217-220.

Coffin, J., 1845, A Sketch of the History of Newbury, Newburyport, and West Newbury, 1635–1845: S.G. Drake, Boston, Mass., 416 pp.

Coffman, J.D., Gilbert, M.C., and McConnell, D.A., 1986, An interpretation of the crustal structure of the southern Oklahoma aulacogen satisfying gravity data: in Gilbert, M.C. (editor), *Petrology of the Cambrian Wichita Mountains Igneous Suite*: Oklahoma Geological Survey, Guidebook 23, Norman, Okla.

Collier, J.W., 1998, Geophysical investigations of liquefaction features in the New Madrid seismic zone: Northeastern Arkansas and southeastern Missouri: M.S. thesis, Auburn University, Auburn, Ala., 163 pp.

Collins, E., 2004, Summary of the Balcones fault zone, central Texas: A prominent zone of Tertiary normal faults marking the western margin of the Texas coastal plain, Field Trip Guidebook, Volume 24: Austin, TX, Austin Geological Society, pp. 81-89.

Colquhoun, D.J., Woollen, I.D., Van Nieuwenhuise, D.S., Padgett, G.G., Oldham, R.W., Boylan, D.C., Bishop, J.W., and Howell, P.D., 1983, Surface and subsurface Stratigraphy, Structure and aquifers of the South Carolina coastal plain: SCDHEC Report ISBN 0-9613154-0-7, 78 pp.

Colton, R.B., 1963a, Geologic Map of the Brockton Quadrangle, Roosevelt and Richland Counties, Montana: U.S. Geological Survey Miscellaneous Geologic Investigations Map I-362, 1 sheet, scale 1:62,5000.

Colton, R.B., 1963b, Geologic Map of the Poplar Quadrangle, Roosevelt, Richland, and McCone Counties, Montana: U.S. Geological Survey Miscellaneous Geologic Investigations Map I-367, 1 sheet, scale 1:62,5000.

Cook, F.A., 1984, Geophysical anomalies along strike of the southern Appalachian Piedmont: *Tectonics*, v. 3, no. 1, pp. 45-61.

Cook, F.A., Albaugh, D.S., Brown, L.D., Kaufman, S., Oliver, J.E., and Hatcher R.D., Jr., 1979, Thin-skinned tectonics in the crystalline southern Appalachians: COCORP seismic reflection profiling of the Blue Ridge and Piedmont: *Geology*, v. 7, pp. 563-567.

Cook, F.A., Albaugh, D.S., Brown, L.D., Kaufman, S., Oliver, J.E., and Hatcher, R.D., Jr., 1980, The Brevard fault: A subsidiary thrust fault to the southern Appalachian sole thrust: in Wones, D.R. (editor), *Proceedings of the Caledonide Orogen Project, The Caledonides in the U.S.A.*, Department of Geological Sciences, Virginia Polytechnic Institute and State University, pp. 205-213.

Cook, F.A., Brown, L.D., Kaufman, S., Oliver, J.E., and Petersen, T.A., 1981, COCORP seismic profiling of the Appalachian orogen beneath the Coastal Plain of Georgia: *Geological Society of America Bulletin*, v. 92, no. 10, pp. 738-748.

Cook, F.A., and Oliver, J.E., 1981, The late Precambrian—Early Paleozoic continental edge in the Appalachian orogen: *American Journal of Science*, v. 281, pp. 993-1008.

Cook, F.A., and Vasudevan, K., 2003, Are there relict crustal fragments beneath the Moho? *Tectonics*, v. 22, no. 3, 1026, doi:10.1029/2001TC001341.

Cook, F.A., and Vasudevan, K., 2006, Reprocessing and enhanced interpretation of the initial COCORP Southern Appalachians traverse: *Tectonophysics*, v. 420, pp. 161-174.

Coppersmith, K.J., Bommer, J.J., Kammerer, A.M., and Ake, J., 2010, Implementation guidance for SSHAC Level 3 and 4 processes: *10th International Probabilistic Safety and Management Conference, Seattle, Wash., June 7-11*.

Cornell, C.A., and Van Marke, E.H., 1969, The major influences on seismic risk: *Proceedings of the Third World Conference on Earthquake Engineering, Santiago, Chile*, v. A-1, pp. 69-93.

Coruh, C., Bollinger, G.A., and Costain, J.K., 1988, Seismogenic structures in the Central Virginia seismic zone: *Geology*, v. 16, no. 8, pp. 748-751.

Counts, R., Van Arsdale, R., and Woolery, E., 2009b, Paleoseismic Features Within the Wabash Valley Seismic Zone in Western Kentucky: presentation given at meeting of CEUS Earthquake Hazards Program, U.S. Geological Survey, October 28-29, Memphis, Tenn.

Counts, R.C., Durbin, J.M., and Obermeier, S.F., 2008, Seismic ground-failure features in the vicinity of the Lower Wabash and Ohio River valleys: in Counts, M.H., and Counts, R.C. (editors), *From the Cincinnati Arch to the Illinois Basin: Geological Field Excursions Along the Ohio River Valley*: Geological Society of America Field Guide 12, pp. 57-79.

Counts, R.C., Van Arsdale, R.B., and Woolery, E.W., 2009a, Investigation of Quaternary displacement on the Uniontown fault, western Kentucky [abstract]: Geological Society of America *Abstracts with Programs*, v. 41, no. 1, p. 20.

Cox, R.T., 1988, Evidence of Quaternary ground tilting associated with the Reelfoot rift zone, northeast Arkansas: *Southeastern Geology*, v. 28, no. 4, pp. 211-224.

Cox, R.T., 1994, Analysis of drainage-basin symmetry as a rapid technique to identify areas of possible Quaternary tilt-block tectonics: An example from the Mississippi Embayment: *Geological Society of America Bulletin*, v. 106, pp. 571-581.

Cox, R.T., 2002, Investigation of Seismically-Induced Liquefaction in the Southern Mississippi Embayment: U.S. Geological Survey National Earthquake Hazards Reduction Program, Final Technical Report, Award No. 01-HQGR-0052, 15 pp.

Cox, R.T., 2009, Investigations of Seismically-Induced Liquefaction in Northeast Louisiana: U.S. Geological Survey National Earthquake Hazards Reduction Program, Final Technical Report, Award No. 08-HQGR-0008.

Cox, R.T., and Van Arsdale, R.B., 1997, Hotspot origin of the Mississippi Embayment and its possible impact on contemporary seismicity: *Engineering Geology*, v. 46, pp. 201-216.

Cox, R.T., Van Arsdale, R.B., Harris, J.B., Forman, S.L., Beard, W., and Galluzzi, J., 2000, Quaternary faulting in the southern Mississippi Embayment and implications for tectonics and seismicity in an intraplate setting: *Geological Society of America Bulletin*, v. 112, no. 11, pp. 1724-1735.

Cox, R.T., Van Arsdale, R.B., and Harris, J.B., 2001, Identification of possible Quaternary deformation in the northeastern Mississippi Embayment using quantitative geomorphic analysis of drainage-basin asymmetry: *Geological Society of America Bulletin*, v. 113, pp. 615-624.

Cox, R.T., Van Arsdale, R.B., Harris, J.B., and Larsen, D., 2001, Neotectonics of the southeastern Reelfoot rift zone margin, central United States, and implications for regional strain accommodation: *Geology*, v. 29, no. 5, pp. 419-422.

Cox, R.T., Forman, S.L., Woods, J., Galluzzi, J., Hall, L., Semko, A., and McHugh, J., 2002, New data of Holocene tectonism in the southern Mississippi Embayment [abstract]: *Seismological Research Letters*, v. 73, pp. 246-247.

Cox, R.T., and Van Arsdale, R.B., 2002, The Mississippi Embayment, North America: A first order continental structure generated by the Cretaceous superplume mantle event: *Journal of Geodynamics*, v. 34, pp. 163-176, doi:10.1016/S0604-3707(02)00019-4.

Cox, R.T., Van Arsdale, R.B., and Larsen, D., 2002, Paleoseismology of the Southeastern Margin of the Reelfoot Rift in the Vicinity of Memphis, Tennessee: Final technical report, U.S. Geological Survey Award No. 02-HQ-GR-0025, 15 pp.

Cox, R.T., Harris, J.B., Hill, A.A., Forman, S.L., Gardner, C., and Csontos, R., 2004, More evidence for young tectonism along the Saline River fault zone, southern Mississippi Embayment: AGU Fall Meeting Supplement, Abstract T41F-1289, *Eos, Transactions of the American Geophysical Union*, v. 85, no. 47, p. 311.

Cox, R.T., and Larsen, D., 2004, Investigation of Seismically-Induced Liquefaction in the Southern Mississippi Embayment: National Earthquake Hazards Reduction Program, Final Technical Report No. 03HQGR0011, 19 pp.

Cox, R.T., Larsen, D., Forman, S.L., Woods, J., Morat, J., and Galluzzi, J., 2004, Preliminary assessment of sand blows in the southern Mississippi Embayment: *Bulletin of the Seismological Society of America*, v. 94, pp. 1125-1142.

Cox, R.T., Larsen, D., and Hill, A.A., 2004, More paleoliquefaction data from southeastern Arkansas: Implications for seismic hazards: Geological Society of America Joint Northeastern and Southeastern Section Meeting, Washington, D.C.

Cox, R.T., Cherryhomes, J., Harris, J.B., Larsen, D., Van Arsdale, R.B., and Forman, S.L., 2006, Paleoseismology of the southeastern Reelfoot rift in western Tennessee and implications for intraplate fault zone evolution: *Tectonics*, v. 25, TC3019, doi:10.1029/2005TC001829, 17 pp.

Cox, R.T., Hill, A.A., Larsen, D., Holzer, T., Forman, S.L., Noce, T., Gardner, C., and Morat, J., 2007, Seismotectonic implications of sand blows in the southern Mississippi embayment: *Engineering Geology*, v. 89, pp. 278-299.

Cox, R.T., and Gordon, J., 2008, Sand blows on Late Quaternary surfaces in northeast Louisiana [abstract]: Geological Society of America *Abstracts with Programs*, v. 40, no. 6, p. 151.

Cramer, C.H., Schweig, E.S., and Tuttle, M.P., 2006, The possibility of northeastward unilateral rupture for the January 23, 1812 New Madrid earthquake [abstract]: *Seismological Research Letters*, v. 77, no. 1, p. 107.

Cramer, C.H., 2001, A seismic hazard uncertainty analysis for the New Madrid seismic zone: *Engineering Geology*, v. 62, pp. 251-266.

Craven, J.A., 1995a, Paleoseismological Study in the New Madrid Seismic Zone Using Geological and Archeological Features to Constrain Ages of Liquefaction Deposits: M.S. thesis, University of Memphis, 51 pp.

Craven, J.A., 1995b, Evidence of paleoseismicity within the New Madrid seismic zone at a late Mississipian Indian occupation site in the Missouri Bootheel [abstract]: Geological Society of America *Abstracts with Programs*, 1995 Annual Meeting, p. A-394.

Crone, A.J., 1992, Structural relations and earthquake hazards of the Crittenden County fault zone, Northeastern Arkansas: *Seismological Research Letters*, v. 63, no. 3, pp. 249-262.

Crone, A.J. (compiler), 1994, Fault number 1031b, Meers fault, in Quaternary fault and fold database of the United States: U.S. Geological Survey website, http://earthqakes.usgs.gov/regional/qfaults.

Crone, A.J. (compiler), 1997, Fault number 2330, Cheraw fault, in Quaternary fault and fold database of the United States: U.S. Geological Survey website, http://earthquakes.usgs.gov/regional/qfaults, accessed July 3, 2009.

Crone, A.J., 1998a, Defining the southwestern end of the Blytheville arch, northeastern Arkansas: Delimiting a seismic source zone in the New Madrid region: *Seismological Research Letters*, v. 69, no. 4, pp. 350-358.

Crone, A.J. (compiler), 1998b, Fault number 1032, Crooked Creek fault, in Quaternary fault and fold database of the United States: U.S. Geological Survey website, http://earthquakes.usgs.gov/regional/qfaults.

Crone, A.J., De Martini, P.M., Machette, M.N., Okumura, K., and Prescott, J.R., 2003, Paleoseismicity of two historically quiescent faults in Australia: Implications for fault behavior in stable continental regions: *Bulletin of the Seismological Society of America*, v. 93, no. 5, pp. 1913-1934.

Crone, A.J., and Luza, K.V., 1990, Style and timing of Holocene surface faulting on the Meers fault, southwestern Oklahoma: *Geological Society of America Bulletin*, v. 102, pp. 1-17.

Crone, A.J., and Machette, M.N., 1995, Holocene movement on the Cheraw fault, SE Colorado—Another hazardous late Quaternary fault in the stable continental interior [abstract]: *Eos, Transactions of the American Geophysical Union*, 1995 Fall Meeting Program, v. 76, no. 46, November 7, 1995 supplement, p. F362.

Crone, A.J., Machette, M.N., and Bowman, J.R., 1997, Episodic nature of earthquake activity in stable continental regions revealed by palaeoseismicity studies of Australian and North American Quaternary faults: *Australian Journal of Earth Sciences*, v. 44, pp. 203-214.

Crone, A.J., Machette, M.N., Bradley, L., and Mahan, S.A., 1997, Late Quaternary Surface Faulting on the Cheraw Fault, Southeastern Colorado: U.S. Geological Survey Geologic Investigations Map I-2591, includes 7 pp. pamphlet.

Crone, A.J., and Schweig, E.S. (compilers), 1994, Fault number 1023, Reelfoot scarp and New Madrid seismic zone: Quaternary fault and fold database of the United States, U.S. Geological Survey website, http://earthquakes.usgs.gov/regional/qfaults, accessed August 7, 2009.

Crone, A.J., and Wheeler, R.L., 2000, *Data for Quaternary Faults, Liquefaction Features, and Possible Tectonic Features in the Central and Eastern United States, East of the Rocky Mountain Front*: U.S. Geological Survey Open-File Report 00-0260, 342 pp.

Crough, S.T., 1981, Mesozoic hotspot epeirogeny in eastern North America: *Geology*, v. 9, pp. 2-6.

Csontos, R., and Van Arsdale, R., 2008, New Madrid seismic zone fault geometry: *Geosphere*, v. 4, no. 5, pp. 802-813.

Csontos, R., Van Arsdale, R., Cox, R., and Waldron, B., 2008, Reelfoot rift and its impact on Quaternary deformation in the central Mississippi River valley: *Geosphere*, v. 4, no. 1, pp. 145-158.

Csontos, R.M., 2007, Three-Dimensional Modeling of the Reelfoot Rift and New Madrid Seismic Zone: Ph.D. dissertation, University of Memphis, Memphis, Tenn., 92 pp.

Culotta, R.C., Pratt, T., and Oliver, J., 1990, A tale of two sutures: COCORP’s deep seismic surveys of the Grenville province in the eastern U.S. midcontinent: *Geology*, v. 18, pp. 646-649.

Cumbest, R.J., Price, V., and Anderson, E.E., 1992, Gravity and magnetic modeling of the Dunbarton Basin, South Carolina: *Southeastern Geology*, v. 33, no. 1, pp. 37-51.

Curtis, B.F., 1988, Sedimentary rocks in the Denver basin: in Sloss, L.L. (editor), *Sedimentary Cover—North American Craton*, U.S. Geological Society of America, The Geology of North America, v. D-2, ch. 7, pp. 109-221.

Cushing, E.M., Boswell, E.H., and Hosman, R.L., 1964, *General Geology of the Mississippi Embayment*: USGS Professional Paper 448-B, 28 pp.

Daniels, D.L., Zietz, I., and Popenoe, P., 1983, Distribution of subsurface lower Mesozoic rocks in the southeastern United States, as interpreted from regional aeromagnetic and gravity maps: in Gohn, G.S. (editor), *Studies Related to the Charleston, South Carolina, Earthquake of 1886—Tectonics and Seismicity*, U.S. Geological Survey Professional Paper 1313-K, pp. K1-K24.

Dart, R.L., and Swolfs, H.S., 1998, Contour mapping of relic structures in the Precambrian basement of the Reelfoot rift, North American midcontinent: *Tectonics*, v. 17, no. 2, pp. 235-249.

Darton, N.H., 1950, *Configuration of the Bedrock Surface of the District of Columbia and Vicinity*: U.S. Geological Survey Professional Paper 217, 41 pp.

Davis, S.D., Pennington, W.D., and Carlson, S.M., 1989, *A Compendium of Earthquake Activity in Texas*: Geological Circular 89-3, Bureau of Economic Geology, The University of Texas at Austin, 27 pp.

Dawers, N.H., and Seeber, L., 1991, Intraplate faults revealed in crystalline bedrock in the 1983 Goodnow and 1985 Ardsley epicentral areas, New York: *Tectonophysics*, v. 186, pp. 115-131.

Dellinger, J., and Nettles, M., 2006, The 10 February 2006, magnitude 5.2 Gulf of Mexico earthquake: Insights and implications: *Society of Exploration Geophysicists*, 1 p.

Dellinger, J.A., Dewey, J.W., Blum, J., and Nettles, M., 2007, Relocating and characterizing the 10 Feb 2006 "Green Canyon" Gulf of Mexico earthquake using oil-industry data: *Eos Transactions of the American Geophysical Union*, v. 88, p. 52, Fall Meeting Supplement, Abstract S13F-01.

Dellinger, J., Ehlers, J., and Clarke, R., 2007, The Green Canyon event as recorded by the Atlantis OBS Node Survey: *Offshore Technology Conference Proceedings*, Paper 18588.

Dennis, A.J., Shervais, J.W., Mauldin, J., Maher, H.D., Jr., and Wright, J.E., 2004, Petrology and geochemistry of Neoproterozoic volcanic arc terranes beneath the Atlantic Coastal Plain, Savannah River site, South Carolina: *Geological Society of America Bulletin*, v. 116, pp. 572-593.

Dewey, J.W., and Dellinger, J.A., 2008, *Location of the Green Canyon (Offshore Southern Louisiana) Seismic Event of February 10, 2006*: U.S. Geological Survey Open-File Report 2008-1184, 30 pp.

Dewey, J.W., and Gordon, D.W., 1984, Map Showing Recomputed Hypocenters of Earthquakes in the Eastern and Central United States and Adjacent Canada, 1925–1980: U.S. Geological Survey Miscellaneous Field Studies Map MF-1699, 1 sheet, scale 1:250,000, 39 pp. pamphlet.

DeWispelare, A.R., Herren, L.T., Miklas, M.P., and Clemen, R.T., 1993, *Expert Elicitation of Future Climate in the Yucca Mountain Vicinity*: Report NRC-02-88-005, Center for Nuclear Waste Regulatory Analyses, San Antonio, Tex.

de Witt, W., and Bayer, K.C., 1986, Seismicity, seismic reflection, gravity, and geology of the Central Virginia Seismic Zone: Part 3. Gravity: Discussion and reply: *Geological Society of America Bulletin*, v. 97, Discussion, pp. 1285-1286.

Dickerson, P.W., and Muehlberger, W.R., 1994, Basins of the Big Bend segment of the Rio Grande rift, Trans-Pecos Texas: in Keller, G.R., and Cather, S.M. (editors), *Basins of the Rio Grande Rift: Structure, Stratigraphy, and Tectonic Setting*: Geologic Society of America Special Paper 291, pp. 283-297.

Dineva, S., Eaton, D., and Mereu, R., 2004, Seismicity of the southern Great Lakes: Revised earthquake hypocenters and possible tectonic controls: *Bulletin of the Seismological Society of America*, v. 94, no. 5, pp. 1902-1918.

Dionne, J.-C., 2001, Relative sea-level changes in the St. Lawrence estuary from deglaciation to present day: in Weddle, T.K., and Retelle, M.J. (editors), *Deglacial History and Relative Sea-Level Changes, Northern New England and Adjacent Canada*, Geological Society of America Special Paper 351, pp. 271-284.

Doar, W.R. III, and Willoughby, R.H., 2006, Revision of the Pleistocene Dorchester and Summerville scarps, the inland limits of the Penholoway Terrace, central South Carolina: abstract and poster presented at the 2006 annual meeting of the Southeastern Section of the Geological Society of America, available at http://www.dnr.sc.gov/geology/segsa.htm, accessed May 25, 2009.

Doig, R., 1990, 2300 yr history of seismicity from silting events in Lake Tadoussac, Charlevoix, Quebec: *Geology*, v. 18, pp. 820-823.

Doig, R., 1991, Effects of strong seismic shaking in lake sediments, and earthquake recurrence interval, Témiscaming, Quebec: *Canadian Journal of Earth Sciences*, v. 28, pp. 1349-1352.

Doig, R., 1998, 3000-year paleoseismological record from the region of the 1988 Saguenay, Quebec, earthquake: *Bulletin of the Seismological Society of America*, v. 88, pp. 1198-1203.

Dokka, R.K., Sella, G.F., and Dixon, T.H., 2006, Tectonic control of subsidence and southward displacement of southeast Louisiana with respect to stable North America: *Geophysical Research Letters*, v. 33, Paper no. 23308, 5 pp.

Dominion Nuclear North Anna, LLC, North Anna Early Site Permit Application Response to Request for Additional Information No. 3, 2004, 114 pp.

Drahovzal, J.A., 1992, The origin and evolution of the East Continent Rift Basin [abstract]: Geological Society of America *Abstracts with Programs*, v. 24, p. A-330.

Drahovzal, J.A., 1994, Basin-floor fan complexes: A new exploration strategy for the Rough Creek Graben: in Ridgley, J.L., Drahovzal, J.A., Keith, B.D., and Kolata, D.R. (editors), *Proceedings of the Illinois Basin Energy and Mineral Resources Workshop, September 12-13, 1994, Evansville, Indiana*: Kentucky Geological Survey, Open-File Report 94-12 (Illinois State Geological Survey, Open-File Report 94-4; Indiana Geological Survey, Open-File Report 94-12; U.S. Geological Survey Open-File Report 94-298), pp. 7-8.

Drahovzal, J.A., 1997, Proterozoic sequences and their implications for Precambrian and Cambrian geologic evolution of western Kentucky: Evidence from seismic-reflection data: *Seismological Research Letters*, v. 68, no. 4, pp. 553-566.

Drahovzal, J.A., 2009, Rifts in the Midcontinent: East Continent Rift Basin, Rough Creek Graben and the Rome Trough: presentation given at CEUS SSC Project Workshop #2, February 18-20, Palo Alto, Calif.

Drahovzal, J.A., Harris, D.C., Wickstrom, L.H., Walker, D., Baranoski, M.T., Keith, B., and Furer, L.C., 1992, *The East Continent Rift Basin: A New Discovery*, Ohio Geological Survey Information Circular 57, Columbus, Ohio, pp. 1-25.

Drysdale, J.A., and Cajka, M.G., 1989, Intensity distribution of the 1988 M6 Saguenay earthquake: paper presented at Seismological Society of America Eastern Section meeting, Lexington, Ky., October.

Du, W.-X., Kim, W.-Y., and Sykes, L.R., 2003, Earthquake source parameters and state of stress for the northeastern United States and southeastern Canada from analysis of regional seismograms: *Bulletin of the Seismological Society of America*, v. 93, no. 4, pp. 1633-1648.

DuBar, J.R., Ewing, T.E., Lundelius, E.L., Otvos, E.G., and Winker, C.D., 1991, Quaternary geology of the Gulf of Mexico coastal plain: in Morrison, R.B. (editor), *Quaternary Nonglacial Geology: Conterminous U.S.*, The Geological Society of America, The Geology of North America, v. K-2, pp. 583-610.

Du Berger, R., Roy, D.W., Lamontagne, M., Woussen, G., North, R.G., and Wetmiller, R.J., 1991, The Saguenay (Quebec) earthquake of November 25, 1988: Seismologic data and geologic setting: in Mareschal, J.-C. (editor), Intraplate Deformation, Neotectonics, Seismicity, and the State of Stress in Eastern North America, *Tectonophysics* (special issue), v. 186, pp. 59-74.

Dunbar, J.A., and Sawyer, D.S., 1987, Implications of continental crust extension for plate reconstruction: an example from the Gulf of Mexico: *Tectonics*, v. 6, pp. 739-755.

Duncan, R.A., 1984, Age progressive volcanism in the New England seamounts and the opening of the central Atlantic Ocean: *Journal of Geophysical Research*, v. 89, pp. 9980-9990.

Dunn, M.M., and Chapman, M.C., 2006, Fault orientation in the eastern Tennessee seismic zone: A study using the double-difference earthquake location algorithm: *Seismological Research Letters*, v. 77, no. 4, pp. 494-504.

Dunn, M., Horton, S., DeShon H., and Powell, C., 2010, High-resolution earthquake relocation in the New Madrid seismic zone: *Seismological Research Letters*, v. 81, no. 2, pp. 406-413.

Dura-Gomez, I., and Talwani, P., 2008, A revised seismotectonic framework for the Charleston, South Carolina earthquakes [abstract]: *Abstracts with Programs*, *American Geophysical Union Annual Fall Meeting*, S42A-06.

Dura-Gomez, I., and Talwani, P., 2009, Finding faults in the Charleston area, South Carolina: 1. Seismological data: *Seismological Research Letters*, v. 80, no. 5, pp. 883-900.

Dutton, C.E., 1889, *The Charleston Earthquake of August 31, 1886*: U.S. Geological Survey Ninth Annual Report, 1887-88, pp. 203-528.

Easton, R.M., and Carter, T.R., 1995, Geology of the Precambrian basement beneath the Paleozoic of Southwestern Ontario: in Ojakangas, R.W., Dickas, A.B., and Green, J.C. (editors), *Basement Tectonics*, v. 10, pp. 221-264.

Eaton, D.W., Dineva, S., and Mereu, R., 2006, Crustal thickness and V_P/V_S variations in the Grenville orogen (Ontario, Canada) from analysis of teleseismic receiver functions: *Tectonophysics*, v. 420, pp. 223-238.

Ebel, J.E., 1994, The m_{LG}(F) magnitude scale: A proposal for its use for northeastern North America: *Seismological Research Letters*, v. 65, no. 2, pp. 157-166.

Ebel, J.E., 1996, The seventeenth century seismicity of northeastern North America: *Seismological Research Letters*, v. 67, no. 3, pp. 51-68.

Ebel, J.E., 2000, A reanalysis of the 1727 earthquake at Newbury, Massachusetts: *Seismological Research Letters*, v. 71, no. 3, pp. 364-374.

Ebel, J.E., 2001, A new look at the 1755 Cape Ann, Massachusetts earthquake [abstract]: *Eos, Transactions of the American Geophysical Union*, v. 82, p. S271.

Ebel, J.E., 2006a, The Cape Ann, Massachusetts earthquake of 1755: A 250th anniversary perspective: *Seismological Research Letters*, v. 77, no. 1, pp. 74-86.

Ebel, J.E., 2006b, Thoughts Concerning Earthquake Sources in the Northeastern U.S.: presentation given at CEUS Workshop on National Seismic Hazard Maps, May 9, Boston.

Ebel, J.E., 2009, On the magnitude of the 1663 Charlevoix, Quebec earthquake [abstract]: *Seismological Research Letters*, v. 80, no. 2, p. 343.

Ebel, J.E., Bonjer, K.-P., and Oncescu, M.C., 2000, Paleoseismicity: Seismicity evidence for past large earthquakes: *Seismological Research Letters*, v. 71, no. 2, pp. 283-294.

Ebel, J.E., and Bouck, B.R., 1988, New focal mechanisms for the New England region: Constraints on the regional stress regime: *Seismological Research Letters*, v. 59, no. 4, pp. 183-187.

Ebel, J.E., and Hart, K., 2001, Observational evidence for amplification of earthquake ground motions in Boston and vicinity: *Civil Engineering Practice*, v. 16, no. 2, pp. 5-16.

Ebel, J.E., Somerville, P.G., and McIver, J.D., 1986, A study of the source parameters of some large earthquakes of northeastern North America: *Journal of Geophysical Research*, v. 91, no. B8, pp. 8231-8247.

Eberhart-Phillips, D., Richardson, R.M., Sbar, M.L., and Herrmann, R.B., 1981, Analysis of the 4 February 1976 Chino Valley, Arizona, earthquake: *Bulletin of the Seismological Society of America*, v. 71, no. 3, pp. 787-801.

Efron, B., 1982, *The Jackknife, the Bootstrap, and Other Resampling Plans*: Society for Industrial and Applied Mathematics, Philadelphia, Penn., 92 pp.

Electric Power Research Institute (EPRI), 1988, *Seismic Hazard Methodology for the Central and Eastern United States*: 10 volumes, EPRI-NP-4726.

Electric Power Research Institute (EPRI), 1989, *Probabilistic Seismic Hazard Evaluations at Nuclear Plant Sites in the Central and Eastern United States: Resolution of the Charleston Earthquake Issue*: EPRI Technical Report EPRI NP-6395-D.

Electric Power Research Institute (EPRI), 1993, *Guidelines for Determining Design Basis Ground Motions*: EPRI TR-102293, 5 volumes.

Electric Power Research Institute (EPRI), 2004, *CEUS Ground Motion Project Final Report*: EPRI Report 1009684, December.

Electric Power Research Institute (EPRI), 2005a, *Program on Technology Innovation: Assessment of a Performance-Based Approach for Determining Seismic Ground Motions for New Plant Sites, Volume 1: Performance-Based Design Spectra*, EPRI TR-1012044, August.

Electric Power Research Institute (EPRI), 2005b. *Program on Technology Innovation: Assessment of a Performance-Based Approach for Determining Seismic Ground Motions for New Plant Sites, Volume 2: Seismic Hazard Results at 28 Sites*: EPRI TR-1012045, August.

Electric Power Research Institute (EPRI), 2006, *Program on Technology Innovation: Truncation of the Lognormal Distribution and Value of the Standard Deviation for Ground Motion Models in the Central and Eastern United States*: EPRI TR-1014381, August.

Electric Power Research Institute (EPRI), 2008a, *Assessment of Seismic Hazard at 34 U.S. Nuclear Plant Sites*: EPRI TR-1016736, August.

Electric Power Research Institute (EPRI), 2008b, *Project Plan: Central and Eastern United States Seismic Source Characterization for Nuclear Facilities*: Technical Update 1016756, June.

Ellsworth, W.L., 2003, Magnitude and Area Data for Strike Slip Earthquakes (Appendix D): in Working Group on California Earthquake Probabilities (editor), *Earthquake Probabilities in the San Francisco Bay Region: 2002-2031*, U.S. Geological Survey, Open-File Report 03-214.

Ellsworth, W.L., Matthews, M.V., Nadeau, R.M., Nishenko, S.P., Reasenberg, P.A., and Simpson, R.W., 1999, A physically-based earthquake recurrence model for estimation of long-term earthquake probabilities, *Proceedings of the Workshop on Earthquake Recurrence: State of the Art and Directions for the Future, Istituto Nazionale de Geofisica. Rome, Italy, February 22-25*.

Engdahl, E.R., and Villaseñor, A., 2002, Global seismicity—1900–1999: in Lee, W.H.K., Kanamori, H., Jennings, P.C., and Kisslinger, C. (editors), *International Handbook of Earthquake and Engineering Seismology*, International Association of Seismology and Physics of the Earth's Interior (IASPEI), pp. 665-690.

Ervin, G.P., and McGinnis, L.D., 1975, Reelfoot rift; reactivated precursor to the Mississippi embayment: *Geological Society of America Bulletin*, v. 86, pp. 1287-1295.

Ewing, T.E., 1991, Structural framework: in Salvador, A. (editor), *The Gulf of Mexico Basin*, Geological Society of America, The Geology of North America, v. J, ch. 3, pp. 31-52.

Ewing, T.E., and Lopez, R.F., 1991, Principal structural features Gulf of Mexico basin: in Salvador, A. (editor), *The Gulf of Mexico Basin*, Geological Society of America, The Geology of North America, v. J, Plate 2.

Exelon Generation Company, LLC, 2003, Early site permit (ESP) application for property co-located with existing Clinton Power Station (CPS) facility in Illinois: U.S. Nuclear Regulatory Commission document accession no. ML032721596, filed September 25.

Exelon Generation Company, LLC, 2004, Early Site Permit (ESP) Application for the Clinton ESP Site: letter to the U.S. Nuclear Regulatory Commission with responses to requests for additional information, October 11.

Faill, R.T., 1997a, A geologic history of the north-central Appalachians. Part 1. Orogenesis from the Mesoproterozoic through the Taconic orogeny: *American Journal of Science*, v. 297, pp. 551-619.

Faill, R.T., 1997b, A geologic history of the north-central Appalachians. Part 2. The Appalachian basin from the Silurian through the Carboniferous: *American Journal of Science*, v. 297, pp. 729-761.

Faill, R.T., 1998, A geologic history of the north-central Appalachians. Part 3. The Alleghany orogeny: *American Journal of Science*, v. 298, pp. 131-179.

Faill, R.T. (compiler), 2004, *Earthquake Catalog and Epicenter Map of Pennsylvania*: Pennsylvania Department of Conservation and Natural Resources.

Fakundiny, R.H., and Pomeroy, P.W., 2002, Seismic-reflection profiles of the central part of the Clarendon-Linden fault system of western New York in relation to regional seismicity: *Tectonophysics*, v. 353, pp. 173-213.

Faure, S., Tremblay, A., and Angelier, J., 1996a, Alleghenian paleostress reconstruction in the northern Appalachians: Intraplate deformation between Laurentia and Gondwana: *Geological Society of America Bulletin*, v. 108, pp. 1467-1480.

Faure, S., Tremblay, A., and Angelier, J., 1996b, State of intraplate stress and tectonism of northeastern America since Cretaceous times, with particular emphasis on the New England–Quebec igneous province: *Tectonophysics*, v. 255, pp. 111-134.

Faure, S., Tremblay, A., and Malo, M., 2004, Reconstruction of Taconian and Acadian paleostress regimes in the Quebec and northern New Brunswick Appalachians: *Canadian Journal of Earth Sciences*, v. 41, pp. 619-634.

Faure, S., Tremblay, A., Malo, M., and Angelier, J., 2006, Paleostress analysis of Atlantic crustal extension in the Quebec Appalachians: *The Journal of Geology*, v. 114, pp. 435-448.

Faust, T.H., Fujita, K., Mackey, K.G., Ruff, L.J., and Ensign, R.C., 1997, The September 2, 1994 Central Michigan earthquake: *Seismological Research Letters*, v. 68, no. 3, pp. 460-464.

Faye, R.E., and Prowell, D.C., 1982, *Effects of Late Cretaceous and Cenozoic Faulting on the Geology and Hydrology of the Coastal Plain near the Savannah River, Georgia and South Carolina*: U.S. Geological Survey Open-File Report 82-156.

Felzer, K.R., 2008, Calculating California seismicity rates: in Field, E.H., Dawson, T.E., Felzer, K.R., Frankel, A.D., Gupta, V., Jordan, T.H., Parsons, T., Petersen, M.D., Stein, R.S., Weldon II, R.J., and Wills, C.J. (editors), *The Uniform California Earthquake Rupture Forecast, Version 2 (UCERF 2)*, USGS Open File Report 2007-1437.

Fenneman, N.M., and Johnson, D.W., 1946, Physiographic Divisions of the Conterminous United States: U.S. Geological Survey Water Resources Maps and GIS Data, http://water.usgs.gov/GIS/dsdl/physio.gz.

Filion, L., Quinty, F., and Bégin, C., 1991, A chronology of landslide activity in the valley of Rivierre du Gouffre, Charlevoix, Quebec: *Canadian Journal of Earth Sciences*, v. 28, pp. 103-118.

Fischer-Boyd, K., and Schumm, S.A., 1995, Geomorphic evidence of deformation in the northern part of the New Madrid seismic zone: in Shedlock, K.M., and Johnston, A.C. (editors), *Investigations of the New Madrid Seismic Zone*, U.S. Geological Survey Professional Paper 1538-R, 35 pp.

Fisk, H.N., 1944, *Geological Investigation of the Alluvial Valley of the Lower Mississippi River*: Corps of Engineers, U.S. Army, conducted for the Mississippi River Commission, Vicksburg, Miss., 170 pp.

Fletcher, J.B., and Sykes, L.R., 1977, Earthquakes related to hydraulic mining and natural seismicity in western New York State: *Journal of Geophysical Research*, v. 82, pp. 3767-3780.

Foland, K.A., Gilbert, L.A., Sebring, C.A., and Jiang-Fen, C., 1986, 40Ar/39Ar ages for plutons of the Monteregian Hills: Evidence for a single episode of Cretaceous magmatism: *Geological Society of America Bulletin*, v. 97, pp. 966-974.

Forman, S.L., Pierson, J., and Lepper, K., 2000, Luminescence geochronology: in Noller, J.S., Sowers, J.M., and Lettis, W.R. (editors), *Quaternary Geochronology: Methods and Applications*, American Geophysical Union, AGU Reference Shelf 4, pp. 157-175.

Forsyth, D.A., 1981, Characteristics of the Western Quebec seismic zone: *Canadian Journal of Earth Sciences*, v. 18, pp. 103-118.

Forsyth, D.A., Milkereit, B., Davidson, A., Hanmer, S., Hutchinson, D.R., Hinze, W.J., and Mereu, R.F., 1994, Seismic images of a tectonic subdivision of the Grenville orogen beneath Lakes Ontario and Erie: *Canadian Journal of Earth Sciences*, v. 31, pp. 229-242.

Forsyth, D.A., Milkereit, B., Zelt, C.A., White, D.J., Easton, R.M., and Hutchinson, D.R., 1994, Deep structure beneath Lake Ontario: Crustal-scale Grenville subdivisions: *Canadian Journal of Earth Sciences*, v. 31, pp. 255-270.

Forte, A.M., Mitrovica, J.X., Moucha, R., Simmons, N.A., and Grand, S.P., 2007, Descent of the ancient Farallon slab drives localized mantle flow below the New Madrid seismic zone: *Geophysical Research Letters*, v. 34, L04308, doi:10.1029/2006GL027895.

Fox, J., 2002, *An R and S-Plus Companion to Applied Regression*: Sage Publications, 328 pp.

Frankel, A., 1994, Implications of felt area-magnitude relations for earthquake scaling and the average frequency of perceptible ground motion: *Bulletin of the Seismological Society of America*, v. 84, no. 2, pp. 462-465.

Frankel, A., 1995, Mapping seismic hazard in the central and eastern United States: *Seismological Research Letters*, v. 66, no. 4, pp. 8-21.

Frankel, A., Mueller, C., Harnhard, T., Perkins, D., Leyendecker, E.V., Dickman, N., Hanson, S., and Hopper, M., 1996, *National Seismic-Hazard Maps: Documentation June 1996*: U.S. Geological Survey Open-File Report 96-532.

Frankel, A.D., Petersen, M.D., Mueller, C.S., Haller, K.M., Wheeler, R.L., Leyendecker, E.V., Wesson, R.L., Harmsen, S.C., Cramer, C.H., Perkins, D.M., and Rukstales, K.S., 2002, *Documentation for the 2002 Update of the National Seismic Hazard Maps*: U.S. Geological Survey Open-File Report 02-420, 33 pp.

Fraser, G.S., Thompson, T.A., Olyphant, G.A., Furer, L., and Bennett, S.W., 1997, Geomorphic response to tectonically-induced ground deformation in the Wabash Valley: *Seismological Research Letters*, v. 68, no. 4, pp. 662-674.

Frohlich, C., and Davis, S.D., 2002, *Texas Earthquakes*: University of Texas Press, 275 pp.

Fujita, K., and Sleep, N.H., 1991, A re-examination of the seismicity of Michigan: *Tectonophysics*, v. 186, nos. 1-2, pp. 75-106.

Fukuda, J., and Johnson, K.M., 2008, A fully Bayesian inversion for spatial distribution of fault slip with objective smoothing: *Bulletin of the Seismological Society of America*, v. 98, no.3, pp. 1128-1146.

Funck, T., Jackson, H.R., Louden, K.E., Kehler, S.A., and Wu, Y., 2004, Crustal structure of the northern Nova Scotia rifted continental margin (eastern Canada): *Journal of Geophysical Research*, v. 109, B09102, doi:10.1029/2004JB003008.

Gagliano, S.M., 2005, Effects of earthquakes, fault movements, and subsidence on the south Louisiana landscape: *Journal of the Louisiana Section of the American Society of Civil Engineers*, v. 13, no. 2, pp. 5-7, 19-22.

Gangopadhyay, A., and Sen, M., 2008, A possible mechanism for the spatial distribution of seismicity in northern Gulf of Mexico: *Geophysical Journal International*, v. 175, pp. 1141-1153.

Gangopadhyay, A., and Talwani, P., 2005, Fault intersections and intraplate seismicity in Charleston, South Carolina: Insights from a 2-D numerical model: *Current Science*, v. 88, pp. 1,609-1,616.

Gardner, J.K., and Knopoff, L., 1974, Is the sequence of earthquakes in Southern California, with aftershocks removed, Poissonian? *Bulletin of the Seismological Society of America*, v. 64, no. 5, pp. 1363-1367.

Garrity, C.P., and Soller, D.R., 2009, Database of the Geologic Map of North America—Adapted from the Map by J.C. Reed, Jr. and others (2005): U.S. Geological Survey Data Series 424, http://pubs.usgs.gov/ds/424/.

Garrote, J., Cox, R.T., Swann, C., and Ellis, M., 2006, Tectonic geomorphology of the southeastern Mississippi Embayment in northern Mississippi, USA: *Geological Society of America Bulletin*, v. 118, pp. 1160-1170.

Gassman, S., Talwani, P., and Hasek, M., 2009, Magnitudes of Charleston, South Carolina Earthquakes from In Situ Geotechnical Data: presentation given at meeting of CEUS Earthquake Hazards Program, U.S. Geological Survey, October 28-29, Memphis, Tenn.

Gates, A.E., and Costa, R.E., 1998, Multiple reactivations of rigid basement block margins: Examples in the northern Reading Prong, USA: in Gilbert, M.C., Hogan, J.P. (editors), *Basement Tectonics 12: Central North America and Other Regions*, Kluwer Academic Publishers, Dordrecht, The Netherlands, pp. 123-153.

Gay, S.P., Jr., 2003a, The Nemaha trend—A system of compressional thrust-fold, strike-slip structural features in Kansas and Oklahoma, Part 1: *Shale Shaker*, Oklahoma City Geological Society, July/August, pp. 9-17.

Gay, S.P., Jr., 2003b, The Nemaha trend—A system of compressional thrust-fold, strike-slip structural features in Kansas and Oklahoma (Part 2, Conclusion): *Shale Shaker*, Oklahoma City Geological Society, July/August, pp. 39-49.

Gelinas, R., Cato, K., Amick, D., and Kemppinen, H., 1998, *Paleoseismic Studies in the Southeastern United States and New England*: U.S. Nuclear Regulatory Commission Report, NUREG/CR-6274.

General Bathymetric Chart of the Oceans (GEBCO), International Hydrographic Organization (IHO), Intergovernmental Oceanographic Commission (IOC), 2009, GEBCO_08 Grid, version 20091120, http://www.gebco.net.

Geomatrix Consultants, Inc., 1997, *Seismic Hazard in Southern Ontario, Final Report, Part 1: Seismic Source Models, Recurrence Models and Ground Motion Attenuation Models*: prepared for the Atomic Energy Control Board of Canada, March.

Gesch, D.B., 2007, The National Elevation Dataset: in Maune, D. (editor), Digital Elevation Model Technologies and Applications: *The DEM Users Manual*, 2nd Edition: American Society for Photogrammetry and Remote Sensing, Bethesda, Md., pp. 99-118.

Gilbert, M.C., 1982, Geologic setting of the eastern Wichita Mountains with a brief discussion of unresolved problems: in Gilbert, M.C.G., and Donovan, R.N. (editors), *Geology of the Eastern Wichita Mountains, Southwestern Oklahoma*, Oklahoma Geological Survey Guidebook 21, Norman, Okla., pp. 1-30.

Gilbert, M.C., 1983a, The Meers fault of southwestern Oklahoma: Evidence for possible strong quaternary seismicity in the midcontinent: *EOS, Transactions of the American Geophysical Union*, v. 64, abstract T21B-13, p. 313.

Gilbert, M.C., 1983b, Timing and chemistry of igneous events associated with the Southern Oklahoma Aulacogen: *Tectonophysics*, v. 94, pp. 439-455.

Givler, R., and Baldwin, J., 2009, Commerce Geophysical Lineament and Northwestern Margin of the New Madrid Seismic Zone: Summary of Recent Research in Southeastern Missouri and Southern Illinois: presentation given at CEUS SSC Project Workshop #2, February 18-20, Palo Alto, Calif.

Globensky, Y., 1987, *Geologie des Basses-Terres du Saint-Laurent*: Ministère des Richesses Naturelles, Quebec, MM 85-02, 63 pp. and map (1:250000) no. 1999.

Glover L., III, Costain, J.K., and Çoruh, C., 1995, Tectonics of the central Appalachian orogen in the vicinity of corridor E-3: With implications for the tectonics of the southern Appalachians: in E-3 Southwestern Pennsylvania to Baltimore Canyon Trough: Geological Society of America, Geology of North America, North American Continent/Ocean Transect Program, Explanatory Pamphlet for Transect 19, pp. 1-49.

Gomberg, J. and Ellis, M., 1994, Topography and tectonics of the central New Madrid seismic zone: Results of numerical experiments using a three-dimensional boundary element program: *Journal of Geophysical Research*, v. 99, no. B10, pp. 20,299–20,310.

Gomberg, J., and Wolf, L., 1999, Possible cause for an improbable earthquake—The 1997 M_w 4.9 southern Alabama earthquake and hydrocarbon recovery: *Geology*, v. 27, no. 4, pp. 367-370.

Good, R., Brown, L.D., Oliver, J.E., and Kaufman, S., 1983, COCORP deep seismic reflection traverse across the southern Oklahoma aulacogen: in Bally, A.W. (editor), *Seismic Expression of Structural Styles: A Picture and Work Atlas, Volume 3*, AAPG Studies in Geology, v. 15, pp. 3.2.2-33–3.2.2-37.

Gordon, J., and Cox, R.T., 2008, Recurrent Mesozoic and Cenozoic faulting along the southern margin of the North American craton [abstract]: Geological Society of America *Abstracts with Programs*, v. 40, no. 6, p. 151.

Gordon, M.B., Mann, P., Caceres, D., and Flores, R., 1997, Cenozoic tectonic history of the North America–Caribbean plate boundary zone in western Cuba: *Journal of Geophysical Research*, v. 102, pp. 10,055-10,082.

Gouin, P., 2001, *Historical Earthquakes Felt in Quebec: From 1534 to March 1925, as Revealed by the Local Contemporary Literature*: Guérin, Montréal, 1491 pp.

Grana, J.P., and Richardson, R.M., 1996, Tectonic stress within the New Madrid seismic zone: *Journal of Geophysical Research*, v. 101, pp. 5445-5458.

Granger, D.E., Kirchner, J.W., and Finkel, R.C., 1997, Quaternary downcutting rate of the New River, Virginia, measured from differential decay of cosmogenic ^{26}Al and ^{10}Be in cave-deposited alluvium: *Geology*, v. 25, pp. 107-110.

Grant, L.B., and Sieh, K., 1994, Paleoseismic evidence of clustered earthquakes on the San Andreas Fault in the Carrizo Plain, California: *Journal of Geophysical Research*, v. 99, no. B4, pp. 6819-6841.

Gray, G.G., Pottorf, R.J., Yurewic, D.A., Mahon, K.I., Pevear, D.R., and Chuchla, R.J., 2001, Thermal and chronological record of syn- to post-Laramide burial and exhumation, Sierra Madre Oriental, Mexico: in Bartolini, C., Buffler, R.T., and Cantu-Chapa, A. (editors), *The Western Gulf of Mexico Basin: Tectonics, Sedimentary Basins, and Petroleum Systems*: AAPG Memoir 75, pp. 159-181.

Green, R.A., 2001. Ph Energy-Based Evaluation and Remediation of Liquefiable Soils: Ph.D. dissertation, Virginia Polytechnic Institute and State University, 394 pp.

Green, R.A., Obermeier, S.F., and Olson, S.M., 2004a, The role of paleoliquefaction studies in performance-based earthquake engineering in the central-eastern United States: *Proceedings of the 13th World Conference on Earthquake Engineering, Vancouver, B.C., Canada, August 1–6, 2004*, Paper 1643.

Green, R.A., Obermeier, S.F., and Olson, S.M., 2004b, *Geotechnical Analysis of Paleoseismic Shaking Using Liquefaction Features: Part II. Field Examples*: Report UMCEE 04-08, Department of Civil and Environmental Engineering, University of Michigan, Ann Arbor, Mich., 85 pp.

Green, R.A., Obermeier, S.F., and Olson, S.M., 2005, Engineering geologic and geotechnical analysis of paleoseismic shaking using liquefaction effects: Field examples: *Engineering Geology*, v. 76, pp. 263-293.

Gresko, M.J., 1985, Analysis and Interpretation of Compressional (P Wave) and Shear (SH Wave) Reflection Seismic and Geologic Data over the Bane Dome, Giles County, Virginia: unpublished Ph.D. thesis, Virginia Polytechnic Institute and State University, Blacksburg, VA, 74 pp.

Grier, M.E., 1995, *Brittle Faulting Along the St. Lawrence Valley from Kingston to Cornwall*: prepared for the Atomic Energy Control Board, Report INFO-0578, 23 pp.

Grollimund, B.R., and Zoback, M.D., 2001, Did deglaciation trigger intraplate seismicity in the New Madrid seismic zone? *Geology*, v. 29, no. 2, pp. 175-178.

Grubbs, F.E., 1950, Sample criteria for testing outlying observations: *Annals of Mathematical Statistics*, v. 21, no. 1, pp. 27-58.

Grünthal, G., 1985, The up-dated earthquake catalogue for the German Democratic Republic and adjacent areas—Statistical data characteristics and conclusions for hazard assessment: *Proceedings of the 3rd International Symposium on the Analysis of Seismicity and Seismic Risk*, Liblice Castle, Czechoslovakia, June 17–22, pp. 19-25.]

Guccione, M.J., 2005, Late Pleistocene and Holocene paleoseismology of an intraplate seismic zone in a large alluvial valley, the New Madrid seismic zone, Central USA: *Tectonophysics*, v. 408, pp. 237-264.

Guccione, M.J., Marple, R., and Autin, W.J., 2005, Evidence for Holocene displacements on the Bootheel fault (lineament) in southeastern Missouri: Seismotectonic implications for the New Madrid region: *Geological Society of America Bulletin*, v. 117, pp. 319-333, doi:10.1130/B25435.1.

Guccione, M.J., Mueller, K., Champion, J., Shepherd, S., and Odhiambo, B., 2002, Stream response to repeated co-seismic folding, Tiptonville Dome, western Tennessee: *Geomorphology*, v. 43, pp. 313-349.

Guccione, M.J., and VanArsdale, R.B., 1995, *Origin and Age of the St. Francis Sunklands Using Drainage Patterns and Sedimentology*: Final Report submitted to the U.S. Geological Survey, Award Number 1434-93-G-2354.

Guccione, M.J., Van Arsdale, R.B., and Hehr, L.H., 2000, Origin and age of the Manila high and associated Big Lake "Sunklands," New Madrid seismic zone, northeastern Arkansas: *Geological Society of America Bulletin*, v. 112, pp. 579-590.

Gutenberg, B., and Richter, C.F., 1956, Earthquake magnitude, intensity, energy and acceleration: *Bulletin of the Seismological Society of America*, v. 46, pp. 105-145.

Hajic, E.R., and Wiant, M.D., 1997, Dating of Prehistoric Earthquake Liquefaction in Southeastern and Central Illinois: Final technical report submitted to the U.S. Geological Survey National Earthquake Hazards Reduction Program, Contract No. 1434-95-G-2599, 63 pp.

Hajic, E.R., Wiant, M.D., and Oliver, J.J., 1995, Distribution and Dating of Prehistoric Earthquake Liquefaction in Southeastern Illinois, Central U.S.: Final technical report submitted to the U.S. Geological Survey National Earthquake Hazards Reduction Program, Contract No. 1434-93-G-2359, 33 pp.

Halchuk, S., 2009, *Seismic Hazard Earthquake Epicentre File (SHEEF) Used in the Fourth Generation Seismic Hazard Maps of Canada*: Geological Survey of Canada, Open File 6208, 1 CD-ROM.

Hall, D.J., Cavanaugh, T.D., Watkins, J.S., and McMillen, 1982, The rotational origin of the Gulf of Mexico based on regional gravity data: in Watkins, J.S., and Drake, C.L. (editors), *Studies in Continental Margin Geology*, AAPG Memoir No. 34, pp. 115-126.

Hall, S.A., and Najmuddin, I.J., 1994, Constraints on the tectonic development of the Gulf of Mexico provided by magnetic anomaly data: *Journal of Geophysical Research*, v. 99, pp. 7161-7175.

Ham, W.E., Denison, R.E., and Merritt, C.A., 1964, *Basement Rocks and Structural Evolution of Southern Oklahoma*: Normal, Okla., Oklahoma Geological Survey Bulletin 95, 302 pp.

Hamburger, M.W., Rybakov, V., Lowry, A., Shen-Tu, B., and Rupp, J.A., 2002, Preliminary results from a GPS geodetic network in the southern Illinois basin: *Seismological Research Letters*, v. 73, no. 5, pp. 762-775.

Hamburger, M., Galgana, G., and Johnson, K., 2008, Geodetic observations from the region surrounding the M 5.2 Mt. Carmel, Illinois earthquake: *Eos, Transactions of the American Geophysical Union*, v. 89, no. 53, Fall Meeting Supplement, Abstract G21A-0664.

Hamburger, M., Galgana, G., and Johnson, K., 2009, Is There a Connection Between Seismicity and Deformation in the New Madrid and Wabash Valley Seismic Zones? presentation given at meeting of CEUS Earthquake Hazards Program, U.S. Geological Survey, October 28-29, Memphis, Tenn.

Hamilton, R.M., and Zoback, M.D., 1982, Tectonic features of the New Madrid seismic zone from seismic reflection profiles: in McKeown, F.A., and Pakiser, L.C. (editors), *Investigations of the New Madrid, Missouri, Earthquake Region*, U.S. Geological Survey Professional Paper 1236, pp. 55-82.

Hamilton, R.M., Behrendt, J.C., and Ackermann, H.D., 1983, Land multichannel seismic-reflection evidence for tectonic features near Charleston, South Carolina: in Gohn, G.S. (editor), *Studies Related to the Charleston, South Carolina Earthquake of 1886—Tectonics and Seismicity*, U.S. Geologic Survey Professional Paper 1313-I, pp. I1-I18.

Hanks, T.C., Abrahamson, N.A., Boore, D.M., Coppersmith, K.J, and Knepprath, N.E., 2009, *Implementation of the SSHAC Guidelines for Level 3 and 4 PSHAs—Experience Gained from Actual Applications*: U.S. Geological Survey Open-File Report 2009-1093, 66 pp.

Hanks, T.C., and Bakun, W.H., 2002, A bilinear source-scaling model for M-log A observations of continental earthquakes: *Bulletin of the Seismological Society of America*, v. 92, pp. 1841-1846.

Hanks, T.C., and Kanamori, H., 1979, A moment magnitude scale: *Journal of Geophysical Research*, v. 84, no. B5, pp. 2348-2350.

Hansen, M.C., 1987, July 1986 Auglaize County earthquake: *Ohio Geology*, The Ohio Seismic Network, Ohio Geological Survey, Fall.

Hansen, M.C., 1993, Earthquakes and seismic risk in Ohio: *Ohio Geology*, The Ohio Seismic Network, Ohio Geological Survey, Summer.

Hansen, M.C., Larsen, G.E., Swinford, E.M., and Ruff, L.J., 2001, Seismic Spotlight Shines on Ashtabula: *Ohio Geology*, The Ohio Seismic Network, Ohio Geological Survey, No. 3.

Hanson, K.L., Swan, F.H., Wesling, J.R., and Kelson, K.I., 1997, Quaternary deformation along the Criner fault, Oklahoma: A case study for evaluating tectonic versus landslide faulting [abstract]: American Geophysical Union Spring Meeting, Baltimore, Md.

Harden, J.W., 1982, A quantitative index of soil development from field descriptions: Examples from a chronosequence in central California: *Geoderma*, v. 28, pp. 1-28.

Harden, J.W., and Taylor, E.M., 1983, A quantitative comparison of soil development in four climatic regions: *Quaternary Research*, v. 20, pp. 342-359.

Hardie, J.K., and Arndt, H.H., 1988, Geology, Structure, and Coal Beds of the Fort Union Formation in the Eastern Part of the Fort Peck Indian Reservation, Daniels, Roosevelt, and Sheridan Counties, Montana: U.S. Geological Survey Coal Investigations Map C-122-A, 1 sheet, scale 1:100,000.

Harris, J.B., and Street, R.L., 1997, Seismic investigation of near-surface geological structure in the Paduach, Kentucky, area: Application to earthquake hazards evaluation: *Engineering Geology*, v. 46, pp. 369-383.

Harrison, R., and Schultz, A., 2008, A tectonic model for the midcontinent U.S. lithosphere based on structural analyses of Mesoproterozoic through Cenozoic deformation: *Eos, Transactions of the American Geophysical Union*, v. 89, no. 53, Fall Meeting Supplement, Abstract S42A-03.

Harrison, R.W., 1997, Bedrock geologic map of the St. Louis 30 × 60 quadrangle, Missouri and Illinois, U.S. Geological Survey Miscellaneous Investigations Series Map I-2533, scale 1:100,000.

Harrison, R.W., Hoffman, D., Palmer, J.R., Vaughn, J.D., and Schultz, A., 1995, Late Quaternary deformation on the English Hill fault, southeast Missouri [abstract]: Geological Society of America *Abstracts with Programs*, v. 26, no. 6, p. A-389.

Harrison, R.W., Hoffman, D., Vaughn, J.D., Palmer, J.R., Wiscombe, C.L., McGeehin, J.P., Stephenson, W.J., Odum, J.K., Williams, R.A., and Forman, S.L., 1999, An example of neotectonism in a continental interior: Thebes Gap, Midcontinent, United States: *Tectonophysics*, v. 305, pp. 399-417.

Harrison, R.W., Palmer, J.R., Hoffman, D., Vaughn, J.D., Repetski, J.E., Frederiksen, N.O., and Forman, S.L., 2002, Geologic Map of the Scott City 7.5-Minute Quadrangle, Scott and Cape Girardeau Counties, Missouri: U.S. Geological Survey Geologic Investigation Series Map I-2744, with accompanying article.

Harrison, R.W., and Schultz, A., 1994, Strike-slip faulting at Thebes Gap, Missouri and Illinois: Implications for New Madrid tectonism: *Tectonics*, v. 13, no. 2, pp. 246-257.

Harrison, R.W., and Schultz, A., 2002, Tectonic framework of the southwestern margin of the Illinois basin and its influence on neotectonism and seismicity: *Seismological Research Letters*, v. 73, no. 5, pp. 698-731.

Harry, D.L., and Londono, J., 2004, Structure and evolution of the central Gulf of Mexico continental margin and coastal plain, southeast United States: *Geological Society of America Bulletin*, v. 116, pp. 188-199.

Hartline, C.S., 1995, Deep Structural Analysis Related to the Akron Magnetic Boundary Using Geophysical Well Logs and Potential Field Data, East Central Ohio: M.S. thesis, University of Akron, Akron, Ohio.

Harvard University Seismology, Centroid Moment Tensor Project catalog, now (since 2006) at Lamont-Doherty Earth Observatory and known as the Global CMT Project catalog.

Hatcher, R.D., Jr., Osberg, P.H., Drake, A.A., Jr., Robinson, P. and Thomas, W.A., 1990, Tectonic map of the U.S. Appalachians, Plate 1: in Hatcher, R.D. Jr., Thomas, W.A. and Viele, G.W. (editors), *The Appalachian-Ouachita Orogen in the United States*, The Geological Society of America, The Geology of North America, v. F-2.

Hatcher, R.D., Jr., Bream, B.R., and Merschat, A.J., 2007, Tectonic map of the southern and central Appalachians: A tale of three orogens and a complete Wilson Cycle: in R.D. Hatcher, Jr., M.P. Carlson, Martinez Catalan, J.R. (editors), *4-D Framework of Continental Crust, Geological Society of America Memoir*, v. 200, pp. 595-632.

Hatcher, R.D., Jr., Colquhoun, D.J., Secor, D.T., Cook, F.S., Dillon, W.P., Klitgord, K., Popenoe, P., Merschat, C.E., Wiener, L.S., Milici, R.C., Nelson, A.E., Sheridan, R.E., and Snoke, A.W., 1994, *Centennial Continent/Ocean Transect #18, E-5—Cumberland Plateau to Blake Plateau*: The Geological Society of America, two maps and text, 56 pp.

Hatcher, R.D., Jr., and Zietz, I., 1980, Tectonic implications of regional aeromagnetic and gravity data from the southern Appalachians: in Wones, D.R. (editor), *Proceedings, The Caledonides in the U.S.A.*, IGCP Project 27, Virginia Polytechnic Institute and State University Memoir 2, pp. 235-244.

Hauser, E.C., 1993, Grenville foreland thrust belt hidden beneath the eastern U.S. midcontinent: *Geology*, v. 21, pp. 61-64.

Heaman, L.M., and Kjarsgaard, B.A., 2000, Timing of eastern North American kimberlite magmatism: Continental extension of the Great Meteor hotspot track? *Earth and Planetary Science Letters*, v. 178, pp. 253-268.

Heidbach, O., Tingay, M., Barth, A., Reinecker, J., Kurfess, D., and Müller, B., 2008, The World Stress Map database release 2008, http://dc-app3-14.gfz-potsdam.de.

Heigold, P.C., 1972, *Notes on the Earthquake of September 15, 1972, in Northern Illinois*: Illinois State Geological Survey, Environmental Geology Note 59, 15 pp.

Heigold, P.C., and Kolata, D.R., 1993, Proterozoic crustal boundary in the southern part of the Illinois Basin: *Tectonophysics*, v. 217, pp. 307-319.

Heigold, P.C., and Larson, T.H., 1994, *Geophysical Investigations of Possible Recent Ground Deformation and Neotectonism in White County, Illinois*: Illinois State Geological Survey, Open File Series 1994-5, 22 pp.

Hendricks, J.D., 1988, *Bouguer Gravity of Arkansas*: U.S. Geological Survey Professional Paper 1474, 31 pp.

Herrmann, R.B., 1978, A seismological study of two Attica, New York earthquakes: *Bulletin of the Seismological Society of America*, v. 68, pp. 641-651.

Herrmann, R.B., 1979, Surface wave focal mechanisms for eastern North American earthquakes with tectonic implications: *Journal of Geophysical Research*, v. 84, no. B7, pp. 3547-3552.

Herrmann, R.B., and Ammon, C.J., 1997, Faulting parameters of earthquakes in the New Madrid, Missouri, region: *Engineering Geology*, v. 46, pp. 299-311.

Herrmann, R.B., and Canas, J.A., 1978, Focal mechanism studies in the New Madrid seismic zone: *Bulletin of the Seismological Society of America*, v. 68, pp. 1095-1102.

Herrmann, R.B., and Kijko, A., 1983, Short-period *Lg* magnitudes: Instrument, attenuation, and source effects: *Bulletin of the Seismological Society of America*, v. 73, no. 6A, pp. 1835-1850.

Herrmann, R.B., and Nuttli, O.T., 1982, Magnitude: The relation of M_L to m_{bLg}: *Bulletin of the Seismological Society of America*, v. 72, no. 2, pp. 389-397.

Herrmann, R.B., Park, S.-K., and Wang, C-Y., 1981, The Denver earthquakes of 1967-1968: *Bulletin of the Seismological Society of Amer*ica, v. 71, no. 3, pp. 731-745.

Hersi, O.S., Lavoie, D., and Nowlan, G.S., 2003, Reappraisal of the Beekmantown Group sedimentology and stratigraphy, Montréal area, southwestern Quebec: Implications for understanding the depositional evolution of the Lower-Middle Ordovician Laurentian passive margin of eastern Canada: *Canadian Journal of Earth Sciences*, v. 40, pp. 149-176.

Heyl, A.V., 1972, The 38th parallel lineament and its relation to ore deposits: *Economic Geology*, v. 67, pp. 879-894.

Hibbard, J., 2004, The Appalachian orogen: in van der Pluijm, B., and Marshak, S. (editors), *Earth Structure: An Introduction to Structural Geology and Tectonics*, W.W. Norton & Co., New York, pp. 582-592.

Hibbard, J.P., van Staal, C.R., and Rankin, D.W., 2007, A comparative analysis of pre-Silurian crustal building blocks of the northern and the southern Appalachian orogen: *American Journal of Science*, v. 307, pp. 1-22.

Hibbard, J.P., van Staal, C.R., Rankin, D.W., and Williams, H., 2006, *Lithotectonic Map of the Appalachian Orogen, Canada–United States of America*: Geological Society of Canada, map 2096A, 1:1,500,000 scale.

Higgins, M.D., and van Breemen, O., 1998, The age of the Sept Iles layered mafic intrusion, Canada: Implications for the late Neoproterozoic/Cambrian history of southeastern Canada: *The Journal of Geology*, v. 106, pp. 421-431.

Hildenbrand, T.G., 1982, Model of the southeastern margin of the Mississippi Valley graben near Memphis, Tennessee, from interpretation of truck-magnetometer data: *Geology*, v. 10, pp. 476-480.

Hildenbrand, T.G., 1985, Rift structure of the northern Mississippi Embayment from the analysis of gravity and magnetic data: *Journal of Geophysical Research*, v. 90, pp. 12,607-12,622.

Hildenbrand, T.G., and Hendricks, J.D., 1995, Geophysical setting of the Reelfoot rift and relations between rift structures and the New Madrid seismic zone: in Shedlock, K.M., and Johnston, A.C. (editors), *Investigations of the New Madrid Seismic Zone*, U.S. Geological Survey Professional Paper 1538-E, 30 pp.

Hildenbrand, T.G., and Kucks, R.P., 1992, Filtered Magnetic Anomaly Maps of Missouri, U.S. Geological Survey Geophysical Investigations Series Map GP-1000, 2 sheets, scale 1:1,000,000.

Hildenbrand, T.G., Kucks, R.P., and Sweeney, R.E., 1983, Digital Magnetic-Anomaly Map of central United States: Description of Major Features: U.S. Geological Survey Geophysical Investigations Map GP-955, scale 1:2,500,000.

Hildenbrand, T.G., McBride, J.H., and Ravat, D., 2002, The Commerce geophysical lineament and its possible relation to Mesoproterozoic igneous complexes and large earthquakes in the central Illinois basin: *Seismological Research Letters*, v. 73, no. 5, pp. 640-659.

Hildenbrand, T.G., and Ravat, D., 1997, Geophysical setting of the Wabash Valley fault system: *Seismological Research Letters,* v. 68, no. 4, pp. 567-585.

Hildenbrand, T.G., Stuart, W.D., and Talwani, P., 2001, Geologic structures related to New Madrid earthquakes near Memphis, Tennessee, based on gravity and magnetic interpretations: *Engineering Geology,* v. 62, pp. 105-121.

Himes, L., Strauder, W., and Herrmann, R.B., 1988, Indications of active faults in the New Madrid seismic zone from precise locations of hypocenters: *Seismological Research Letters*, v. 59, pp. 123-131.

Hinze, W.J., 1996, The crust of the northern U.S. craton: A search for beginnings: in van der Pluijm, B.A., and Catacosinos, P.A. (editors), *Basement and Basins of Eastern North America*, Geological Society of America Special Paper 308, pp. 187-201.

Hinze, W.J., Allen, D.J., Braile, L.W., and Mariano, J., 1997, The Midcontinent Rift System: A major Proterozoic continental rift: in Ojakangas, R.W., Dickas, A.B., and Green, J.C. (editors), *Middle Proterozoic to Cambrian Rifting, Central North America*, Geological Society of America Special Paper 312, pp. 7-35.

Hinze, W.J., and Hildenbrand, T.G., 1988, The utility of geopotential field data in seismotectonic studies in the Eastern United States: *Seismological Research Letters*, v. 59, no. 4, pp. 289-297.

Hinze, W.J., Kellogg, R.L., and O’Hara, N.W., 1975, Geophysical studies of the basement geology of southern peninsula of Michigan: *AAPG Bulletin*, v. 59, no. 9, pp. 1562-1584.

Hodych, J.P., and Cox, R.A., 2007, Ediacaran U-Pb zircon dates for the Lac Matapédia and Mt. St.-Anselme basalts of the Quebec Appalachians: Support for a long-lived mantle plume during the rifting phase of Iapetus opening: *Canadian Journal of Earth Sciences,* v. 44, pp. 565-581.

Hoehn, M.H., 1991, An Integrated Geophysical Study of the Grenville Province in the Greater Lake Erie Region: M.S. thesis, Purdue University, West Lafayette, Ind.

Holbrook, J., Autin, W.J., Rittenour, T.M., Marshak, S., and Goble, R.J., 2006, Stratigraphic evidence for millennial-scale temporal clustering of earthquakes on a continental-interior fault: Holocene Mississippi River floodplain deposits, New Madrid seismic zone, USA: *Tectonophysics*, v. 420, pp. 431-454.

Holbrook, W.S., Purdy, G.M., Sheridan, R.E., Glover III, L., Talwani, M., Ewing, J., and Hutchinson, D., 1994, Seismic structure of the U.S. Mid-Atlantic continental margin: *Journal of Geophysical Research*, v. 99, no. B9, pp. 17871-17891.

Holbrook, W.S., Reiter, E.C., Purdy, G.M., Sawyer, D., Stoffa, P.L., Austin, J.A., Oh, J., and Makris, J., 1994, Deep structure of the U.S. Atlantic continental margin, offshore South Carolina, from coincident ocean bottom and multichannel seismic data: *Journal of Geophysical Research*, v. 99, no. B5, pp. 9155-9178.

Horton, J.W., Jr., and Dicken, C.L., 2001, *Preliminary Digital Geologic Map of the Appalachian Piedmont and Blue Ridge, South Carolina Segment*: U.S. Geological Survey Open-File Report 01-298, 1:500,000 scale.

Horton, S.P., Kim, W.Y., and Withers, M., 2005, The 6 June 2003 Bardwell, Kentucky, earthquake sequence: Evidence for a locally perturbed stress field in the Mississippi embayment: *Bulletin of the Seismological Society of America*, v. 95, pp. 431-445.

Hosman, R.L., 1996, *Regional Stratigraphy and Subsurface Geology of Cenozoic Deposits, Gulf Coastal Plain, South-Central United States*: U.S. Geological Survey Professional Paper 1416-G, 35 pp.

Hough, S., Armbruster, J.G., Seeber, L., and Hough, J.F., 2000, On the modified Mercalli intensities and magnitudes of the 1811-1812 New Madrid earthquakes: *Journal of Geophysical Research*, v. 105, no. B10, pp. 23,839-23,864.

Hough, S.E., 2009, The 1811-1812 New Madrid Sequence: Mainshocks, Aftershocks, and Beyond: presentation given at meeting of CEUS Earthquake Hazards Program, U.S. Geological Survey, October 28-29, Memphis, Tenn.

Hough, S.E., Bilham, R., Mueller, K., Stephenson, W., Williams, R., and Odum, J., 2005, Wagon loads of sand blows in White County, Illinois: *Seismological Research Letters*, v. 76, no. 3, pp. 373-386.

Hough, S.E., and Martin, S., 2002, Magnitude estimates of two large aftershocks of the 16 December 1811 New Madrid earthquake: *Bulletin of the Seismological Society of America*, v. 92, no. 8, pp. 3259-3268.

Hough, S.E., and Page, M., 2011, Toward a consistent model for strain accrual and release for the New Madrid, central United States: *Journal of Geophysical Research*, v. 116, B03311, doi:10.1029/2010JB007783.

Hough, S.E., and Seeber, L., 1991, Seismological constraints on source properties on the mb = 4.0, 1985 Ardsley, New York, earthquake: A characteristic rupture? *Journal of Geophysical Research*, v. 96, no. B11, pp. 18,183-18,195.

Howe, J.R., 1985, Tectonics, Sedimentation, and Hydrocarbon Potential of the Reelfoot Aulacogen: M.S. thesis, University of Oklahoma, Norman, Okla., 109 pp.

Howell, P.D., and van der Pluijm, B.A., 1999, Structural sequences and styles of subsidence in the Michigan basin: *Geological Society of America Bulletin*, v. 111, no. 7, pp. 974-991.

Hu, K., Gassman, S.L., and Talwani, P., 2002a, In-situ properties of soils at paleoliquefaction sites in the South Carolina Coastal Plain: *Seismological Research Letters*, v. 73, pp. 964-978.

Hu, K., Gassman, S.L., and Talwani, P., 2002b, Magnitudes of prehistoric earthquakes in the South Carolina Coastal Plain from geotechnical data: *Seismological Research Letters*, v. 73, pp. 979-991.

Hughes, S., and Luetgert, J.H., 1991, Crustal structure of the western New England Appalachians and the Adirondack Mountains: *Journal of Geophysical Research*, v. 96, pp. 16471-16,494.

Hurd, O., 2010, Stress measurement update for the Central Eastern United States, conducted as part of CEUS SSC Project, 5 pp.

Hutchinson, D.R., Grow, J.A., and Klitgord, K.D., 1983, Crustal structure beneath the southern Appalachians; nonuniqueness of gravity modeling: *Geology*, v. 11, pp. 611-615.

Hutchinson, D.R., Klitgord, K.D., and Detrick, R.S., 1986, Rift basins of the Long Island platform: *Geological Society of America Bulletin*, v. 97, pp. 688-702.

Hutchinson, D.R., Pomeroy, P.W., Wold, R.J., and Halls, H.C., 1979, A geophysical investigation concerning the continuation of the Clarendon-Linden fault across Lake Ontario: *Geology*, v. 7, pp. 206-210.

Illinois State Geological Survey (ISGS), 1995, Structural Features in Illinois - 1995 - Line Features (Axial or Flexure) of Anticlines, Synclines and Monoclines. http://www.isgs.illinois.edu/nsdihome/outmeta/IL_Struct_Feat_Clines_1995_Ln.html

Iman, R.L., and Conover, W.J., 1980, Small sample sensitivity analysis techniques for computer models, with an application to risk assessment: Communications in Statistics—Theory and Methods, v. 9, pp. 1749-1842.

International Seismological Centre (ISC), website, http://www.isc.ac.uk/.

Jackson, M.P.A., 1982, *Fault Tectonics of the East Texas Basin*: Geological Circular 82-4, Bureau of Economic Geology, University of Texas, Austin, 31 pp.

Jacobeen, F.H., 1972, *Seismic Evidence for High Angle Reverse Faulting in the Coastal Plain of Prince Georges and Charles County, Maryland*: Maryland Geological Survey Information Circular 13, 21 pp.

Jacobi, R.D., 2002, Basement faults and seismicity in the Appalachian Basin of New York State: *Tectonophysics*, v. 353, pp. 75-113.

Jacobi, R., and Fountain, J., 1993, The southern extension and reactivations of the Clarendon-Linden fault system: *Geographie physique et Quaternaire*, v. 47, no. 3, pp. 285-302.

Jacobi, R., and Fountain, J., 1996, *Determination of the Seismogenic Potential of the Clarendon-Linden Fault System in Allegany County*: Final report to New York State Energy Research and Development Agency, 2,106 pp., 31 oversize maps.

Jacobi, R.D., and Fountain, J., 2002, The character and reactivation history of the southern extension of the seismically active Clarendon-Linden Fault System, western New York State: *Tectonophysics*, v. 353, pp. 215-262.

Jacques, J.M., Price, A.D., and Bain, J.F., 2004, Digital integration of potential fields and geologic datasets for plate tectonic and basin dynamic modeling—The first step towards identifying new play concepts in the Gulf of Mexico basin: *The Leading Edge*, Association of Exploration Geophysicists, April.

James, D.E., Smith, T.J., and Steinhart, J.S., 1968, Crustal structure of the middle Atlantic states: *Journal of Geophysical Research*, v. 73, pp. 1983-2007.

Jenny, H., 1941, *Factors of Soil Formation*: McGraw-Hill, New York, 281 pp.

Jenny, H., 1961, Derivation of state factor equations of soils and ecosystems: *Soil Science Society of America Journal*, v. 25, pp. 385-388.

Joeckel, R.M., Carlson, M.P., Summerside, S.C., and Leach, J.P., 2003, Earthquake history, seismicity, and related tectonics in Nebraska: *Geological Society of America*, Paper No. 17-6, http://gsa.confex.com/gsa/2003NC/finalprogram/abstract_50624.htm, accessed August 10, 2009.

Johnston, A.C., 1994, Seismotectonic interpretations and conclusions from the stable continental region seismicity database: in Schneider, J.F. (editor), *The Earthquakes of Stable Continental Regions—Volume 1: Assessment of Large Earthquake Potential*, Electric Power Research Institute, Report TR-102261, v. 1, sect. 4, pp. 1-103.

Johnston, A.C., 1996a, Seismic moment assessment of earthquakes in stable continental regions—I. Instrumental seismicity: *Geophysical Journal International*, v. 124, pp. 381-414.

Johnston, A.C., 1996b, Seismic moment assessment of earthquakes in stable continental regions—II. Historical seismicity: *Geophysical Journal International*, v. 125, pp. 639-678.

Johnston, A.C., 1996c, Seismic moment assessment of earthquakes in stable continental regions—III. New Madrid 1811-1812, Charleston 1886, and Lisbon 1755: *Geophysical Journal International*, v. 126, pp. 314-344.

Johnston, A.C., Coppersmith, K.J., Kanter, L.R., and Cornell, C.A., 1994, *The Earthquakes of Stable Continental Regions: Final Report Submitted to Electric Power Research Institute (EPRI)*: TR-102261, 5-volume proprietary report prepared for Electric Power Research Institute, Palo Alto, California.

Johnston, A.C., and Kanter, L.R., 1990, Earthquakes in stable continental crust: *Scientific American*, v. 262, pp. 68-75.

Johnston, A.C., and Nava, S.J., 1990, Seismic-hazard assessment in the central United States: in Krinitzsky, E.L., and Slemmons, D.B., *Neotectonics in Earthquake Evaluation, Geological Society of America Reviews in Engineering Geology*, v. 8, pp. 47-58.

Johnston, A.C., Reinbold, D.J., and Brewer, S.I., 1985, Seismotectonics of the southern Appalachians: *Bulletin of the Seismological Society of America*, v. 75, pp. 291-312.

Johnston, A.C., and Schweig, E.S., 1996, The enigma of the New Madrid earthquakes of 1811-1812: *Annual Review of Earth and Planetary Sciences*, v. 24, pp. 339-384.

Jones, F.B., Long, L.T., and McKee, J.H., 1977, Study of the attenuation and azimuthal dependence of seismic-wave propagation in the southeastern United States: *Bulletin of the Seismological Society of America*, v. 67, no. 6, pp. 1503-1513.

Jones-Cecil, M., 1995, Structural controls of Holocene reactivation of the Meers fault, southwestern Oklahoma, from magnetic studies: *Geological Society of America Bulletin*, v. 107, pp. 98-112.

Kafka, A., Schlesinger-Miller, E.A., and Barstow, N.L., 1985, Earthquake activity in the greater New York City area: Magnitudes, seismicity, and geologic structures: *Bulletin of the Seismological Society of America*, v. 75, pp. 1285-1300.

Kafka, A.L., 2007, Does seismicity delineate zones where future large earthquakes are likely to occur in intraplate environments? in Stein, S., and Mazzotti, S. (editors), *Continental Intraplate Earthquakes: Science, Hazard, and Policy Issues*, Geological Society of America Special Paper 425, pp. 35-48, doi:10.1130/2007.2425(03).

Kafka, A.L., 2009, Use of Seismicity to Define Seismic Sources: Application to Eastern North America: presentation given at CEUS SSC Project Workshop #2, February 18-20, Palo Alto, Calif.

Kamo, S.L., Gower, C.F., and Krogh, T.E., 1989, Birthdate for the Iapetus Ocean? A precise U-Pb and baddeleyite age for the Long Range dykes, southeast Labrador: *Geology*, v. 17, no. 7, pp. 602-605.

Kamo, S.L., Krogh, T.E., and Kumarapeli, P.S., 1995, Age of the Grenville dyke swarm, Ontario-Quebec: Implications for the timing of Iapetan rifting: *Canadian Journal of Earth Sciences*, v. 32, pp. 273-280.

Kanamori, H., 1977, The energy release in great earthquakes, *Journal of Geophysical Research*, v. 82, pp. 2,981-2,987.

Kanter, L.R., 1994, Tectonic interpretation of stable continental crust: in Johnston, A.C., Coppersmith, K.J., Kanter, L.R., and Cornell, C.A., 1994, *The Earthquakes of Stable Continental Regions, Volume 1: Assessment of Large Earthquake Potential*, Final Report TR-102261-V1, a five-volume proprietary report prepared for Electric Power Research Institute (EPRI), Palo Alto, Calif., chapter 2, pp. 2-1–2-98.

Karlo, J.F., and Shoup, R.C., 2000, Classifications of syndepositional systems and tectonic provinces of the northern Gulf of Mexico: AAPG Search and Discovery article #30004.

Karlstrom, K.E., and Keller, G.R. (editors), 2005, *The Rocky Mountain Region—An Evolving Lithosphere: Tectonics, Geochemistry, and Geophysics*: American Geophysical Union Geophysical Monograph 154, 441 pp.

Karner, G.D., and Watts, A.B., 1983, Gravity anomalies and flexure of the lithosphere at mountain ranges: *Journal of Geophysical Research*, v. 88, pp. 10,449-10,477.

Kaufmann, R.D., and Long, L.T., 1996, Velocity structure and seismicity of southeastern Tennessee: *Journal of Geophysical Research*, v. 101, no. B4, pp. 8531-8542.

Kean, A.E., and Long, L.T., 1981, A seismic refraction line along the axis of the southern Piedmont and crustal thicknesses in the southeastern United States: *Earthquake Notes*, v. 51, no. 4, pp. 3-13.

Keen, C.E., and Potter, D.P., 1995a, The transition from a volcanic to a nonvolcanic rifted margin off eastern Canada: *Tectonics*, v. 14, no. 2, pp. 359-371.

Keen, C.E., and Potter, D.P., 1995b, Formation and evolution of the Nova Scotia rifted margin: Evidence from deep seismic reflection data: *Tectonics*, v. 14, no. 4, pp. 918-932.

Keller, G.R., 2010, An Integrated Geophysical Analysis of the MidContinent Rift System: Internal report submitted as part of the CEUS SSC Project.

Keller, G.R., Bland, A.E., and Greenberg, J.K., 1982, Evidence for a major Late Precambrian tectonic event (rifting?) in the eastern Midcontinent region, United States: *Tectonics*, v. 1, no. 2, pp. 213-223.

Keller, G.R., and Hatcher Jr., R.D., 1999, Some comparisons of the structure and evolution of the southern Appalachian-Ouachita orogen and portions of the Trans-European Suture Zone region: *Tectonophysics*, v. 314, pp. 43-68.

Keller, G.R., and Stephenson, R.A., 2007, The southern Oklahoma and Dniepr-Donets aulacogens: A comparative analysis: in Hatcher, R.D., Jr., Carlson, M.P., McBride, J.H., and Martínez Catalán, J.R. (editors), *4-D Framework of Continental Crust*: Geological Society of America Memoir 200, pp. 127-143.

Keller, M.R., Robinson, E.S., and Glover III, L., 1985, Seismicity, seismic reflection, gravity, and geology of the central Virginia seismic zone: Part 3. Gravity: *Geological Society of America Bulletin*, v. 96, pp. 1,580-1,584.

Kelson, K.I., Van Arsdale, R.B., Simpson, G.D., and Lettis, W.R., 1992, Assessment of the style and timing of surficial deformation along the Central Reelfoot scarp, Lake County, Tennessee: *Seismological Research Letters*, v. 63, no. 3, pp. 349-356.

Kelson, K.I., and Swan, F.H., 1990, Paleoseismic history of the Meers fault, southwestern Oklahoma, and its implications for evaluations of earthquake hazards in the central and eastern United States: in Weiss, A.J. (editor), *Proceedings of the Seventeenth Water Reactor Safety Information Meeting*, Nuclear Regulatory Commission, NUREG/CP-0105, pp. 341-365.

Kelson, K.I., Simpson, G.D., Van Arsdale, R.B., Harris, J.B., Haraden, C.C., and Lettis, W.R., 1996, Multiple late Holocene earthquakes along the Reelfoot fault, central New Madrid seismic zone: *Journal of Geophysical Research*, v. 101, no. B-3, pp. 6151-6170.

Kenner, S.J., 2003, Effects of driving stress and rheology on the temporal and spatial distribution of faulting within intraplate seismic zones: *Eos, Transactions of the American Geophysical Union*, v. 84, no. 46, Fall Meeting Supplemental, Abstract T21B-04.

Kenner, S.J., and Segall, P., 2000, A mechanical model for intraplate earthquakes: Application to the New Madrid seismic zone: *Science*, v. 289, pp. 2329-2332, doi:10.1126/science.289.5488.2329.

Kijko, A., 2004, Estimation of the maximum earthquake magnitude, m_{max}: *Pure and Applied Geophysics*, v. 161, pp. 1-27.

Kijko, A., and Graham, G., 1998, ‘‘Parametric-historic’’ procedure for probabilistic seismic hazard analysis: Part I: Assessment of maximum regional magnitude m_{max}: *Pure and Applied Geophysics*. v. 152, pp. 413-442.

Kijko, A., Graham, G., Singh, M., Roblin, D., and Brandt, M.B.C., 2009, Probabilistic PGA and spectral acceleration seismic hazard maps for South Africa [abstract]: Invited lecture, Workshop R1 “Earthquake Hazard,” the IASPEI General Assembly in Cape Town, January 11-16.

Kim, W.-Y., 1998, The M_{L} scale in eastern North America: *Bulletin of the Seismological Society of America*, v. 99, no. 4, pp. 935-951.

Kim, W.-Y., 2003, The 18 June 2002 Caborn, Indiana, earthquake: Reactivation of ancient rift in the Wabash Valley seismic zone? *Bulletin of the Seismological Society of America*, v. 93, no. 5, pp. 2201-2211.

Kim, W.-Y., and Chapman, M., 2005, The 9 December 2003 central Virginia earthquake sequence: A compound earthquake in the Central Virginia seismic zone: *Bulletin of the Seismological Society of America*, v. 95, no. 6, pp. 2428-2445.

Kim, W.-Y, Dineva, S., Ma, S., and Eaton, D., 2006, The 4 August 2004, Lake Ontario, earthquake: *Seismological Research Letters*, v. 77, no. 1, pp. 65-73.

King, P.B., and Beikman, H.M. (compilers), 1974, Geologic Map of the United States: U.S. Geological Survey, 3 sheets, scale 1:2,500,000.

King, E.R., and Zietz, I., 1978, The New York–Alabama lineament: Geophysical evidence for a major crustal break in the basement beneath the Appalachian basin: *Geology*, v. 6, pp. 312-318.

Kirkham, R.M., and Rogers, W.P., 1981, Earthquake potential in Colorado—A preliminary evaluation: *Colorado Geological Survey Bulletin 43*, 171 pp., 3 plates.

Klasner, J.S., Cannon, W.F., and Van Schmus, W.R., 1982, The pre-Keweenawan history of the southern Canadian Shield and its influence on formation of the Midcontinent Rift: in Wold, R.J., and Hinze, W.J. (editors), *Geology and Tectonics of the Lake Superior Basin*: Geological Society of America Memoir 156, pp. 27-46.

Klitgord, K.D., Hutchinson, D.R., and Schouten, H., 1988, U.S. Atlantic continental margin; Structural and tectonic framework: in Sheridan, R.E., and Grow, J.A. (editors), *The Atlantic Continental Margin, U.S.*, Geological Society of America, The Geology of North America, v. I-2, ch. 3, pp. 19-55.

Klitgord, K.D., Popenoe, P., and Schouten, H., 1984, Florida: A Jurassic transform plate boundary: *Journal of Geophysical Research*, v. 89, pp. 7753-7772.

Klose, C.D., and Seeber, L., 2007, Shallow seismicity in stable continental regions: *Seismological Research Letters*, v. 78, no. 5, pp. 554-562.

Koff, L.R., 1978, Tectonics of the Oklahoma City Uplift, Central Oklahoma: unpublished M.S. thesis, University of Oklahoma, 64 pp.

Kolata, D.R., and Hildenbrand, T.G., 1997, Structural underpinnings and neotectonics of the southern Illinois basin: An overview: *Seismological Research Letters*, v. 68, no. 4, p. 499.

Kolata, D.R., and Nelson, W.J., 1991 Tectonic history of the Illinois Basin: in Leighton, M.W., Kolata, D.R., Oltz, D.F., and Eidel, J.J. (editors), *Interior Cratonic Basins*, AAPG Memoir 51, Chapter 18, pp. 263-285.

Kolata, D.R., Buschbach, T.C., and Treworgy, J.D., 1978, *The Sandwich Fault Zone of Northern Illinois*: Illinois State Geological Survey Circular 505, 26 pp.

Krinitzsky, E.L., 1950, Geological Investigation of Faulting in the Lower Mississippi Valley: U.S. Army Corps of Engineers Waterways Experiment Station, Technical Memorandum 3-311, 50 pp.

Kuenen, P.H., 1958, Experiments in geology: *Transactions of the Geological Society of Glasgow*, v. 23, pp. 1-28.

Kulkarni, R.B., Youngs, R.R., and Coppersmith, K.J., 1984, Assessment of confidence intervals for results of seismic hazard analysis: in *Proceedings, Eighth World Conference on Earthquake Engineering, San Francisco*, v. 1, pp. 263-270.

Kumarapeli, P.S., 1985, Vestiges of Iapetan rifting in the craton west of the northern Appalachians: *Geoscience Canada*, v. 12, no. 2, pp. 54-59.

Kumarapeli, P.S., 1993, A plume-generated segment of the rifted margin of Laurentia, Southern Canadian Appalachians, seen through a completed Wilson Cycle: *Tectonophysics*, v. 29, pp. 47-55.

Kumarapeli, P.S., and Saull, V.A., 1966, The St. Lawrence valley system: A North American equivalent of the East African rift system: *Canadian Journal of Earth Sciences*, v. 3, pp. 639-658.

Kumarapeli, S., St. Seymour, K., Pintson, H., and Hasselgren, E., 1988, Volcanism on the passive margin of Laurentia: An early Paleozoic analogue of Cretaceous volcanism on the northeastern American margin: *Canadian Journal of Earth Sciences*, v. 25, pp. 1824-1833.

Kuribayashi, E., and Tatsuoka, F., 1975, Brief review of liquefaction during earthquakes in Japan: *Soils and Foundations*, v. 15, pp. 81-92.

Lamontagne, M., 1987, Seismic activity and structural features in the Charlevoix region, Québec: *Canadian Journal of Earth Sciences*, v. 24, pp. 2118-2129.

Lamontagne, M., 1999, Rheological and Geological Constraints on the Earthquake Distribution in the Charlevoix Seismic Zone: Ph.D. thesis, Carleton University, published as Geological Survey of Canada Open-File Report, D-3778, 353 pp.

Lamontagne, M., 2009, Description and analysis of the earthquake damage in the Quebec City region between 1608 and 2008: *Seismological Research Letters*, v. 80, no. 3, pp. 514-424.

Lamontagne, M., Bent, A.L., Woodgold, C.R.D., Ma, S., and Peci, V., 2004, The 16 March 1999 m_N 5.1 Côte-Nord earthquake: The largest earthquake ever recorded in the lower St. Lawrence seismic zone, Canada: *Seismological Research Letters*, v. 75, no. 2, pp. 299-316.

Lamontagne, M., Halchuk, S., Cassidy, J. F., and Rogers, G. C., 2007, *Significant Canadian Earthquakes, 1600-2006*: Geological Survey of Canada, Open-File 5539, 32 pp.

Lamontagne, M., Halchuck, S., Cassidy, J.F., and Rogers, G.C., 2008, Significant Canadian earthquakes of the period 1600-2006: *Seismological Research Letters*, v. 79, pp. 211-223.

Lamontagne, M., Hasegawa, H., Forsyth, D., Buchbinder, G., and Cajka, M., 1994, The Mont-Laurier, Quebec, earthquake of 19 October 1990 and its seismotectonic environment: *Bulletin of the Seismological Society of America*, v. 84, pp. 1506-1522.

Lamontagne, M., Keating, P., and Perreault, S., 2003, Seismotectonic characteristics of the lower St. Lawrence seismic zone, Quebec: Insights from geology, magnetics, gravity, and seismics: *Canadian Journal of Earth Sciences*, v. 40, pp. 317-336.

Lamontagne, M., Keating, P., and Toutin, T., 2000, Complex faulting confounds earthquake research in the Charlevoix seismic zone, Québec: *Eos, Transactions of the American Geophysical Union*, v. 81, pp. 26, 289, 292, 293.

Lamontagne, M., and Ranalli, G., 1996, Thermal and rheological constraints on the earthquake depth distribution in the Charlevoix, Canada, intraplate seismic zone: *Tectonophysics*, v. 257, pp. 55-69.

Lamontagne, M., and Ranalli, G., 1997, Faults and spatial clustering of earthquakes near La Malbaie, Charlevoix seismic zone, Canada: *Seismological Research Letters*, v. 68, no. 2, pp. 337-352.

Lamont-Doherty Cooperative Seismographic Network, LCSN Earthquake Catalog: http://almaty.ldgo.columbia.edu:8080/data.search.html, last updated July 22, 2011.

Langenheim, V.E., and Hildenbrand, T.G., 1997, Commerce geophysical lineament—Its source, geometry, and relation to the Reelfoot rift and New Madrid seismic zone: *Geological Society of America Bulletin*, v. 109, no. 5, pp. 580-595.

Larson, E.E., Patterson, P.E., Curtis, G., Drake, K., and Mutschler, F.E., 1985, Petrologic, paleomagnetic, and structural evidence of a Paleozoic rift system in Oklahoma, New Mexico, Colorado, and Utah: *Geological Society of America Bulletin.*, v. 96, pp. 1364-1372.

Larson, T.H., 2001, *The Earthquake of September 2, 1999, in Northern Illinois: Big Lessons from a Small Earthquake*: Illinois State Geological Survey, Environmental Geology Notes 153, 22 pp.

Larson, T.H., 2002, The earthquake of 2 September 1999 in northern Illinois: Intensities and possible neotectonism: *Seismological Research Letters*, v. 73, no. 5. pp. 732-738.

Larson, T.H., Bauer, R.A., Su, W.-J., Devera, J.A., Seid, M., Hester, N.C., Elrick, S.D., and Korose, C.P., 2009, Analysis of effects from the April 18, 2008 Illinois earthquake [abstract]: *Seismological Research Letters,* v. 80, no. 2, pp. 301-302.

LASE Study Group, 1986, Deep structure of the U.S. East Coast passive margin from large aperture seismic experiments (LASE): *Marine and Petroleum Geology*, v. 3, pp. 234-242.

Lavoie, D., Burden, E., and Lebel, D., 2003, Stratigraphic framework for the Cambrian-Ordovician rift and passive margin successions from southern Quebec to western Newfoundland: *Canadian Journal of Earth Sciences*, v. 40, pp. 177-205.

Law, K.T., 1990, Analysis of soil liquefaction during the 1988 Saguenay earthquake: *Proceedings of the 43rd Canadian Geotechnical Conference, Quebec*, v. 1, pp. 189-196.

Law, R.D., Pope, M.C., Wirgart, R.H., Bollinger, G.A., and Whitmarsh, R.S., 1992, Geologically recent near-surface folding and faulting in the Valley and Ridge province—New exposures of extensional faults in alluvial sediments, Giles County, SW Virginia [abstract]: *Seismological Research Letters*, v. 63, pp. 609-610.

Law, R.D., Pope, M.C., Wirgart, R.H., Eriksson, K.A., Carpenter, D., Robinson, E.S., and Bollinger, G.A., 1993, Geologically recent near-surface folding and faulting in the Valley and Ridge Province: New exposures of extensional faults in alluvial sediments, Giles County, SW Virginia [abstract]: *Eos, Transactions of the American Geophysical Union*, v. 74, no. 16, p. 282.

Law, R.D., Pope, M.C., Wirgart, R.H., Eriksson, K.A., Robinson, E.S., Sayer, S., Phinney, E.J., and Bollinger, G.A., 1994, Geologically recent near-surface faulting and folding in Giles County, southwest Virginia: New exposures of extensional and apparent reverse faults in alluvial sediments between Pembroke and Pearisburg: *Proceedings of the U.S. Nuclear Regulatory Commission for 1994, Twenty-First Water Reactor Safety Information Meeting, October 25-27, 1993, Bethesda, Maryland*, NUREG/CP-0133, v. 3, pp. 415-432.

Law, R.D., Robinson, E.S., Cyrnak, J.S., Sayer, S., Williams, R.T., Callis, J., and Pope, M., 1997, Geologically-recent faulting and folding of alluvial sediments near Pearisburg, Giles County, Virginia—Tectonic faulting or karst subsidence in origin? [abstract]: *Eos, Transactions of the American Geophysical Union*, v. 78, no. 17 (supplement), p. S316.

Law, R.D., Robinson, E.S., Pope, M., and Williams, R.T., 2000, Folding and faulting of Plio-Pleistocene sediments in Giles County, SW Virginia: 1) Surface data and interpretation [abstract]: Geological Society of America *Abstracts with Programs*, v. 32, no. 2, p. A-57.

Law, R.D., Robinson, E.S., Sayer, S., Cyrnak, J.S., Williams, R.T., Callis, J., and Pope, M., 1998, Geologically-recent faulting and folding of alluvial sediments near Pearisburg, Giles County, Virginia—Tectonic faulting or karst subsidence in origin? in Dennison, J.M., and Stewart, K.G. (editors), *Geologic Field Guide to Extensional Structures along the Allegheny Front in Virginia and West Virginia near the Giles County Seismic Zone: Southeastern Section*, Geological Society of America, Charleston, West Virginia, March 28-29, 1998, Guidebook, pp. 95-101.

LDRL (Luminescence Dating Research Laboratory, University of Illinois at Chicago), 2010, Luminescence Tutorial—Optically Stimulated Luminescence (OSL), website accessed June 10, 2010, http://www.uic.edu/labs/ldrl/osl.html.

Leblanc, G., 1981, A closer look at the September 16, 1732, Montreal earthquake: *Canadian Journal of Earth Sciences*, v. 18, pp. 539-550.

Leblanc, G., and Burke, K.B.S., 1985, Re-evaluation of the 1817, 1855, 1869, and 1904 Maine–New Brunswick area earthquakes: *Earthquake Notes*, v. 56, pp. 107-123.

Lehmann, E.L., 1959, *Testing Statistical Hypotheses*: John Wiley and Sons, New York, 150 pp.

Lemieux, Y., Tremblay, A., and Lavoie, D., 2003, Structural analysis of supracrustal faults in the Charlevoix area, Quebec: Relation to impact cratering and the St-Laurent fault system: *Canadian Journal of Earth Sciences*, v. 40, pp. 221-235.

Lennon, G., 1986, *Identification of a Northwest Trending Seismogenic Graben near Charleston, South Carolina*: U.S. Nuclear Regulatory Commission Report, NUREG/CR-4075, 43 pp.

Leon, E., 2003, Effect of Aging of Sediments on Paleoliquefaction Evaluation in the South Carolina Coastal Plain*:* unpublished Ph.D. dissertation, University of South Carolina, 181 pp.

Leon, E., Gassman, S.L., and Talwani, P., 2005, Effect of soil aging on assessing magnitudes and accelerations of prehistoric earthquakes: *Earthquake Spectra*, v. 21, pp. 737-759.

Leonard, M., 2010, Earthquake fault scaling: Self-consistent relating of rupture length, width, average displacement, and moment release: *Bulletin of the Seismological Society of America*, v. 100, no. 5A, pp. 1971-1988.

Lepper, K., 2007, Optically stimulated luminescence dating—An introduction: *New Mexico Geology*, v. 29, no. 4, p. 111.

Levesque, C., Locat, J., and Leroueil, S., 2006, Dating submarine mass movements triggered by earthquakes in the Upper Saguenay Fjord, Quebec, Canada: *Norwegian Journal of Geology*, v. 86, pp. 231-242.

Li, A., Forsyth, D.W., and Fischer, K.M., 2003, Shear velocity structure and azimuthal anisotropy beneath eastern North America from Rayleigh wave inversion: *Journal of Geophysical Research*, v. 108, doi:10.1029/2002JB002259.

Li, Q., Liu, M., and Stein, S., 2009, Spatiotemporal complexity of continental intraplate seismicity: Insights from geodynamic modeling and implications for seismic hazard estimation: *Bulletin of the Seismological Society of America*, v. 99, no. 1, pp. 52-60.

Li, Q., Liu, M., Zhang, Q., and Sandvol, E., 2007, Stress evolution and seismicity in the central-eastern United States: Insights from geodynamic modeling: in Stein, S., and Mazzotti, S. (editors), *Continental Intraplate Earthquakes: Science, Hazard, and Policy Issues*, Geological Society of America Special Paper 425, pp. 149-166.

Li, Y., Doll, C., and Toksoz, M.N., 1995, Source characterization and fault plane determinations for M_{bLg} = 1.2 to 4.4 earthquakes in the Charlevoix seismic zone, Quebec, Canada: *Bulletin of the Seismological Society of America*, v. 85, pp. 1604-1621.

Li, Y., Schweig, E. S., Tuttle, M. P., and Ellis, M. A., 1998, Evidence for large prehistoric earthquakes in the northern New Madrid seismic zone, central United States: *Seismological Research Letters,* v. 69, no. 3, pp. 270-276.

Liang, C., and Langston, C.A., 2009, Three-dimensional crustal structure of eastern North America extracted from ambient noise: *Journal of Geophysical Research*, v. 114, p. B03310.

Liao, T., Mayne, P.W., Tuttle, M.P., Schweig, E.S., Van Arsdale, R.B., 2002, CPT site characterization for seismic hazards in the New Madrid seismic zone: *Soil Dynamics and Earthquake Engineering*, v. 22, pp. 943-950.

Lidiak, E.G., and Hinze, W.J., 1993, Grenville province in the subsurface of eastern United States: in Rankin, D.W., Chiarenzelli, J.R., Drake, A.A., Jr., Goldsmith, R., Hall, L.M., Hinze, W.J., Isachsen, Y.W., Lidiak, E.G., McLelland, J., Mosher, S., Ratcliffe, N.M., Secor, D.T., Jr., and Whitney, P.R. (editors), Chapter 5—Proterozoic rocks east and southeast of the Grenville front: in Reed, J.C., Jr., Bickford, M.E., Houston, R.S., Link, P.K., Rankin, D.W., Sims, P.K., and Van Schmus, W.R. (editors), *Precambrian: Conterminous U.S.*, Geological Society of America, The Geology of North America, v. C-2, pp. 353-365.

Liu, L., and Zoback, M.D., 1997, Lithospheric strength and intraplate seismicity in the New Madrid seismic zone: *Tectonic*s, v. 16, no. 4, pp. 585-595.

Locat, J., 2008, Localisation et magnitude du séisme du 5 février 1663 (Québec) revues à l'aide des mouvements de terrain: in Locat, J., Perret, D., Turmel, D., Demers, D., and Leroueil, S. (editors), *Proceedings of the 4th Canadian Conference on Geohazards: From Causes to Management*, Presse de l'Université Laval, Quebec, pp. 429-444.

Lombardi, A.M., 2003, The maximum likelihood estimator of *b*-value for mainshocks: *Bulletin of the Seismological Society of America*, v. 93, no. 5, pp. 2082-2088.

Long, L.T., and Kaufmann, R.D., 1994, The velocity structure and seismotectonics of southeastern Tennessee: *Seismological Research Letters*, v. 65, no. 3/4, p. 223.

Longuépée, H., and Cousineau, P.A., 2005, Reappraisal of the Cambrian glauconite-bearing Anse Maranda Formation, Quebec Appalachians: From deep-sea turbidites to clastic shelf deposits: *Canadian Journal of Earth Sciences*, v. 42, pp. 259-272.

Lowe, D.R., 1975, Water escape structures in coarse-grained sediment: *Sedimentology*, v. 22, pp. 157-204.

Lowe, D.R., and LoPiccolo, R.D., 1974, The characteristics and origins of dish and pillar structures: *Journal of Sedimentary Petrology*, v. 44, pp. 484-501.

Luza, K.V., and Lawson, J.E., 1993, *Oklahoma Seismic Network*: U.S. Nuclear Regulatory Commission, NUREG/CR-6034, 33 pp.

Luza, K.V., Madole, R.F., and Crone, A.J., 1987a, *Investigation of the Meers Fault in Southwestern Oklahoma*: U.S. Nuclear Regulatory Commission, NUREG/CR-4937, 55 pp.

Luza, K.V., Madole, R.F., and Crone, A.J., 1987b, *Investigation of the Meers Fault, Southwestern Oklahoma*: Oklahoma Geological Society, Norman, OK, Special Publication 87-1, 75 pp.

Luzietti, E.A., Kanter, L.R., Schweig, E.S., Shedlock, K.M., and Van Arsdale, R.B., 1992, Shallow deformation along Crittenden County fault zone near the southeastern boundary of the Reelfoot rift, northeast Arkansas: *Seismological Research Letters*, v. 63, no. 3, pp. 263-275.

Lyakhovsky, V., Ben-Zion, Y., and Agnon, A., 2001, Earthquake cycle, fault zones, and seismicity patterns in a rheologically layered lithosphere: *Journal of Geophysical Research*, v. 106, no. B3, pp. 4103-4120.

Ma, S., and Atkinson, G.M., 2006, Focal depths for small to moderate earthquakes ($m_N \geq 2.8$) in western Quebec, southern Ontario, and northern New York: *Bulletin of the Seismological Society of America*, v. 96, pp. 609-623.

Ma, S., and Eaton, D.W., 2007, Western Quebec seismic zone (Canada): Clustered, midcrustal seismicity along a Mesozoic hot spot track: *Journal of Geophysical Research*, v. 112, B06305, doi:10.1029/2006JB004827.

Ma, S., Eaton, D.W., and Adams, J., 2008, Intraplate seismicity of a recently deglaciated shield terrane: A case study from northern Ontario, Canada: *Bulletin of the Seismological Society of America*, v. 98, no. 6, pp. 2828-2848.

Maceira, M., Ammon, C.J., and Herrmann, R.B., 2000, Faulting parameters of the September 25, 1998 Pymatuning, Pennsylvania earthquake: *Seismological Research Letters*, v. 71, no. 6, pp. 742-752.

Madabhushi, S., and Talwani, P., 1990, Composite fault plane solutions of recent Charleston, South Carolina, earthquakes: *Seismological Research Letters*, v. 61, no. 3-4, p. 156.

Madabhushi, S., and Talwani, P., 1993, Fault plane solutions and relocations of recent earthquakes in Middleton Place-Summerville seismic zone near Charleston, South Carolina: *Bulletin of the Seismological Society of America*, v. 83, no. 5, pp. 1442-1466.

Madole, R.F., 1986, The Meers fault: Quaternary stratigraphy and evidence for late Holocene movement: in Donovan, R.N. (editor), *The Slick Hills of Southwestern Oklahoma—Fragments of an Aulacogen*: Oklahoma Geological Society, Norman, Okla., Guidebook 24, pp. 55-67.

Madole, R.F., 1988, Stratigraphic evidence of Holocene faulting in the mid-continent: The Meers fault, southwestern Oklahoma: *Geological Society of America Bulletin*, v. 100, pp. 392-401.

Magnani, B., and McIntosh, K., 2009, Towards an Understanding of the Long-Term Deformation of the Mississippi Embayment: U.S. Geological Survey, Final Technical Report (08HQGR0089), 19 pp.

Magnani, M.B., Mitchell, L., and Waldron, B., 2009, Long-Term Deformation History in the Mississippi Embayment: The Mississippi Seismic Survey: presentation given at meeting of CEUS Earthquake Hazards Program, U.S. Geological Survey, October 28-29, Memphis, Tenn.

Mahan, S., Counts, R., Tuttle, M., and Obermeier, S., 2009, Can OSL Be Used to Date Paleoliquefaction Events? presentation given at meeting of CEUS Earthquake Hazards Program, U.S. Geological Survey, October 28-29, Memphis, Tenn.

Mahan, S.A. and Crone, A.J., 2006, Luminescence dating of paleoliquefaction features in the Wabash River Valley of Indiana: in Wise, R.A. (editor), *Proceedings of the 4th New World Luminescence Dating and Dosimetry Workshop, Denver, Colorado*: U.S. Geological Survey Open-File Report 2006-1351, 22 pp.

Mai, P.M., Spudich, P., and Boatwright, J., 2005, Hypocenter locations in finite-source rupture models: *Bulletin of the Seismological Society of America*, v. 95, no. 3, pp. 965-980.

Manspeizer, W., DeBoer, J., Costain, J.K., Froelich, A.J., Coruh, C., Olsen, P.E., McHone, G.J., Puffer, J.H., and Prowell, D.C., 1989, Post-Paleozoic activity: in Hatcher Jr., R.D., Thomas, W.A., and Viele, D.W. (editors), *The Appalachian-Ouachita Orogen in the United States*, Geological Society of America, The Geology of North America, v. F2, pp. 319-374.

Marple, R., and Miller, R., 2006, Association of the 1886 Charleston, South Carolina, earthquake and seismicity near Summerville with a 12º bend in the East Coast fault system and Triple-Fault Junctions: *Southeastern Geology*, v. 44, no. 3, pp. 101-127.

Marple, R., and Talwani, P., 1993, Evidence of possible tectonic upwarping along the South Carolina Coastal Plain from an examination of river morphology and elevation data: *Geology*, v. 21, pp. 651-654.

Marple, R., and Talwani, P., 2000, Evidence for a buried fault system in the Coastal Plain of the Carolinas and Virgina—Implications for neotectonics in the southeastern United States: *Geological Society of America Bulletin*, v. 112, pp. 200-220.

Marple, R.T., and Talwani, P., 2004, Proposed Shenandoah Fault and East Coast–Stafford Fault system and their implications for eastern U.S. tectonics: *Southeastern Geology*, v. 43, no. 2, pp. 57-80.

Marshak, S., and Paulsen, T., 1996, Midcontinent U.S. fault and fold zones: A legacy of Proterozoic intracratonic extensional tectonism? *Geology*, v. 24, no. 2, pp. 151-154.

Marshak, S., and Paulsen, T., 1997, Structural style, regional distribution, and seismic implications of midcontinent fault-and-fold zones, United States: *Seismological Research Letters*, v. 68, no. 4. pp. 511-520.

Martin, J.R., and Clough, G.W., 1994, Seismic parameters from liquefaction evidence: *Journal of Geotechnical Engineering*, v. 120, no. 8, pp. 1345-1361.

Marton, G., and Buffler, R.T., 1994, Jurassic reconstruction of the Gulf of Mexico basin: *International Geology Review*, v. 36, pp. 545-586.

Mateker, E.J., Phelan, M.J., and Scharon, L., 1966, Geophysical evidence for a northeast crustal lineament near St. Louis: *Eos, Transactions of the American Geophysical Union*, v. 47, p. 192.

Mateker, E.J., and Segar, R.L., 1965, Gravity investigation along the eastern flank of the Ozark uplift: *Eos, Transactions of the American Geophysical Union*, v. 46, p. 160.

Matthews, M.V., Ellsworth, W.L., and Reasenberg, P.A., 2002, A Brownian model for recurrent earthquakes: *Bulletin of the Seismological Society of America*, v. 92, pp. 2233-2250.

Matton, G., and Jebrak, M., 2009, The Cretaceous Peri-Atlantic Alkaline Pulse (PAAP): Deep mantle plume origin or shallow lithospheric break-up? *Tectonophysics*, v. 469, pp. 1-12.

Mayer, L., and Wentworth, C.M., 1983, Geomorphic differences east and west of the Stafford fault system, northeastern Virginia [abstract]: Geological Society of America *Abstracts with Programs*, v. 15, p. 56.

Mayne, P.W., 2001, Cone Penetration Testing for Seismic Hazards Evaluation in Memphis and Shelby County, Tennessee: U.S. Geological Survey, Earthquake Hazards Program, Final Report (00-HQ-GR-0025), 21 pp.

Mazzotti, S., 2009, Strain (and Stress) Constraints on Seismicity in the St. Lawrence Valley: presentation given at CEUS SSC Project Workshop #2, February 18-20, Palo Alto, Calif.

Mazzotti, S., and Adams, J., 2005, Rates and uncertainties on seismic moment and deformation rates in Eastern Canada: *Journal of Geophysical Research*, v. 110, B09301, doi:10.1029/2004JB003510.

McBride, J.H., Hatcher, R.D., Jr., Stephenson, W.J., and Hooper, R.J., 2005, Integrating seismic reflection and geological data and interpretations across and internal basement massif: The southern Appalachian Pine Mountain window, USA: *Geological Society of America Bulletin*, v. 117, no. 5/6, pp. 669-686.

McBride, J.H., Hildenbrand, T.G., Stephenson, W.J., and Potter, C.J., 2002, Interpreting the earthquake source of the Wabash Valley seismic zone (Illinois, Indiana, and Kentucky) from seismic reflection, gravity, and magnetic intensity: *Seismological Research Letters*, v. 73, no. 5, pp. 660-686.

McBride, J.H., and Kolata, D.R., 1999, Upper crust beneath the central Illinois basin, United States: *Geological Society of America Bulletin*, v. 111, no. 3, pp. 375-394.

McBride, J.H., Kolata, D.R., and Hildenbrand, T.G., 2001, Refining the target for EarthScope in the central Midcontinent [abstract]: EarthScope Workshop: Making and Breaking a Continent, Snowbird, Colo., October 10-12.

McBride, J.H., Kolata, D.R., and Hildenbrand, T.G., 2003, Geophysical constraints on understanding the origin of the Illinois basin and its underlying crust: *Tectonophysics*, v. 363, pp. 45-78.

McBride, J.H., Leetaru, H.E., Bauer, R.A., Tingey, B.E., and Schmidt, S.E.A., 2007, Deep faulting and structural reactivation beneath the southern Illinois basin: *Precambrian Research*, v. 157, pp. 289-313, doi:10.1016/j.precamres.2007.02.020.

McBride, J.H., and Nelson, K.D., 1988, Integration of COCORP deep reflection and magnetic anomaly analysis in the southeastern United States: Implications for origin of the Brunswick and East Coast magnetic anomalies: *Geological Society of America Bulletin*, v. 100, pp. 436-445.

McBride, J.H., and Nelson, W.J., 1999, Style and origin of mid-Carboniferous deformation in the Illinois Basin, USA—Ancestral Rockies deformation? *Tectonophysics*, v. 305, pp. 249-273.

McBride, J.H., Nelson, W.J., and Stephenson, W.J., 2002, Integrated geological and geophysical study of Neogene and Quaternary-age deformation in the northern Mississippi embayment: *Seismological Research Letters*, v. 73, no. 5, pp. 597-627.

McBride, J.H., Pugin, A.J.M., Nelson, W.J., Larson, T.H., Sargent, S.L., Devera, J.A., Denny, F.B., and Woolery, E.W., 2003, Variable post-Paleozoic deformation detected by seismic reflection profiling across the northwestern “prong” of New Madrid seismic zone: *Tectonophysics*, v. 368, pp. 171-191.

McBride, J.H., Sargent, M.L., and Potter, C.J., 1997, Investigating possible earthquake-related structure beneath the southern Illinois basin from seismic reflection: *Seismological Research Letters*, v. 68 no. 4, pp. 641-649.

McCartan, L., Lemon, E.M., Jr., and Weems, R.E., 1984, *Geologic Map of the Area Between Charleston and Orangeburg, South Carolina*: U.S. Geological Series Miscellaneous Investigations Series Map I-1472, 1: 250,000-scale.

McCausland, P.J.A., and Hodych, J.P., 1998, Paleomagnetism of the 550 Ma Skinner Cove volcanics of western Newfoundland and the opening of the Iapetus Ocean: *Earth and Planetary Science Letters*, v. 163, pp. 15-29.

McCausland, P.J.A., Hodych, J.P., and Dunning, G.R., 1997, Evidence from western Newfoundland for the final breakup of Rodinia? U-Pb age and paleolatitude of the Skinner Cove volcanic: *Abstract Volume, Geological Association of Canada 1997 Annual Meeting,* p. A-99.

McConnell, D.A., 1989, Determination of offset across the northern margin of the Wichita uplift, southwest Oklahoma: *Geological Society of America Bulletin*, v. 101, pp. 1317-1332.

McConnell, D.A., and Gilbert, M.C., 1990, Cambrian extensional tectonics and magmatism within the southern Oklahoma aulacogen: *Tectonophysics*, v. 174, pp. 147-157.

McFall, G.H., 1993, Structural elements and neotectonics of Prince Edward County, Southern Ontario: *Geographie physique et Quaternaire*, v. 47, no. 3, pp. 303-312.

McHone, J.G., 1996, Constraints on the mantle plume model for Mesozoic Alkaline intrusions in northeastern North America: *The Canadian Mineralogist*, v. 34, pp. 325-334.

McHone, J.G., 2000, Non-plume rifting during the opening of the central Atlantic Ocean: *Tectonophysics*, v. 316, pp. 287-296.

McHuron, E.J., and Rice, R.H., 1974, Tectonic evolution of the Gulf Coast: Relation to nuclear power plant site selection and design criteria [abstract]: Geological Society of America *Abstracts with Programs*, v. 6, no. 7, pp. 863-864.

McKeever, S.W.S., 2001, Optically stimulated luminescence dosimetry: *Nuclear Instruments and Methods in Physics Research Section B: Beam Interactions with Materials and Atoms*, v. 184, no. 1-2, pp. 29-54.

McKenna, J., Stein, S., and Stein, C.A., 2007, Is the New Madrid seismic zone hotter and weaker than its surroundings? in Stein, S., and Mazzotti, S. (editors), *Continental Intraplate Earthquakes: Science, Hazard, and Policy Issues*, Geological Society of America Special Paper 425, pp. 167-175, doi:10.1130/2007.2425(12).

McKeown, F.A., Hamilton, R.M., Diehl, S.F., and Glick, E.E., 1990, Diapiric origin of the Blytheville and Pascola arches in the Reelfoot rift, east-central United States: Relation to New Madrid seismicity: *Geology*, v. 18, pp. 1158-1162.

McLaughlin, K.L., Barker, T.G., and Bennet, T.J., 1997, Evaluation of National Seismograph Network Detection Capabilities, Final Report, NUREG/CR-6448, Volume 2, MFD-TR-97-15804: Prepared for the Division of Engineering Technology Office of Nuclear Regulatory Research, U.S. Nuclear Regulatory Commission, October.

McNulty, W.E., and Obermeier, S.F., 1997, *Liquefaction Evidence for Two Holocene Paleo-earthquakes in Central and Southwestern Illinois*: U.S. Geological Survey Open-File Report 97-435, 14 pp.

McNulty, W.E., and Obermeier, S.F., 1999, Liquefaction evidence for at least two strong Holocene paleoearthquakes in central and southwestern Illinois, USA: *Environmental and Engineering Geoscience*, v. 5, no. 2, pp. 133-146.

McPhee, J.P., 1983, Regional Gravity Analysis of the Anna, Ohio, Seismogenic Region: M.S. thesis, Purdue University, West Lafayette, Ind., 100 pp.

Mereu, R.F., Wang, D., Kuhn, O., Forsyth, D.A., Green, A.G., Morel, P., Buchbinder, G.G.R., Crossley, D., Schwarz, E., duBerger, R., Brooks, C., and Clowes, R., 1986, The 1982 COCRUST seismic experiment across the Ottawa-Bonnechere graben and Grenville Front in Ontario and Quebec: *Geophysical Journal International*, v. 84, pp. 491-514.

Metropolis, N., Rosenbluth, A.W., Rosenbluth, M.N., Teller, A.H., and Teller, E., 1953, Equation of state calculations by fast computing machines: *Journal of Chemical Physics*, v. 21, pp. 1087-1092.

Metzger, A.G., Armbruster, J.G., and Seeber, L., 2000, Documentation, Location and Size-Estimation of "New" Historical Earthquakes in the Central United States: Continuation: U.S. Geological Survey Contract No. 1434-HQ-97-GR-03064, Final Technical Report, 12 pp., 2 appendices.

Miao, Q., and Langston, C.A., 2008, Spatial distribution of earthquake energy release in the central United States from a global point of view: *Seismological Research Letters*, v. 79, pp. 33-40.

Mickus, K.L., and Keller, G.R., 1992, Lithospheric structure of the south-central United States: *Geology*, v. 20, pp. 335-338.

Mihills, R.K., and Van Arsdale, R.B., 1999, Late Wisconsin to Holocene deformation in the New Madrid seismic zone: *Bulletin of the Seismological Society of America*, v. 89, pp. 1019-1024.

Milkereit, B., Forsyth, D.A., Green, A.G., Davidson, A., Hanmer, S., Hutchinson, D.R., Hinze, W.J., and Mereu, R.F., 1992, Seismic images of a Grenvillian terrane boundary: *Geology*, v. 20, pp. 1027-1030.

Miller, A.C., and Rice, T.R., 1983, Discrete approximations of probability distributions: *Management Science*, v. 29, pp. 352-362.

Miller, R.D., Steeples, D.W., and Myers, P.B., 1990, Shallow seismic reflection survey across the Meers fault, Oklahoma: *Geological Society of America Bulletin*, v. 102, pp. 18-25.

Mills, H.H., 1985, *Descriptions of Backhoe Trenches Dug on New River Terraces Between Radford and Pearisburg, Virginia, June 1981*: U.S. Geological Survey Open File Report 85-474.

Mills, H.H., 1986, Possible differential uplift of New River terraces in southwestern Virginia: *Neotectonics*, v. 1, pp. 75-86.

Mitchell, B.J., Nuttli, O.W., Herrmann, R.B., Stauder, W., 1991, Seismotectonics of the central United States: in Slemmons, D.B., Engdahl, E.R., Zoback, M.D., and Blackwell, D.D. (editors), *Neotectonics of North America*: Geological Society of America, Decade Map Volume 1, pp. 245-260.

Mixon, R.B., and Newell, W., 1978, *The Faulted Coastal Plain Margin at Fredericksburg, Virginia*: Tenth Annual Virginia Geological Field Conference.

Moench, R.H., and Aleinikoff, J.N., 2003, Stratigraphy, geochronology, and accretionary terrane settings of two Bronson Hill arc sequences, northern New England: *Physics and Chemistry of the Earth*, v. 28, pp. 113-160; originally published in 2002 (v. 27, pp. 47-95); republished because of editorial errors.

Mooney, W.D., Andrews, M.C., Ginzburg, A., Peters, D.A., and Hamilton, R.M., 1983, Crustal structure of the northern Mississippi Embayment and a comparison with other continental rift zones: in Morgan, P., and Baker, B.H. (editors), Processes of Continental Rifting, *Tectonophysics*, v. 94, pp. 327-348.

Mooney, W.D., and Ritsema, J., 2009, Mmax and lithospheric structure in Central and Eastern North America [abstract]: *Proceedings, Meeting of Central and Eastern U.S. (CEUS) Earthquake Hazards Program, October 28-29, 2009, Memphis, TN*, U.S. Geological Survey Memphis, TN, office, p. 25.

Morgan, W.J., 1983, Hotspot tracks and the early rifting of the Atlantic: *Tectonophysics*, v. 94, pp. 123-139.

Morton, R.A., Purcell, N.A., and Patterson, R.L., 2001, *Shallow Stratigraphic Evidence of Subsidence and Faulting Induced by Hydrocarbon Production in Coastal Southeast Texas*: U.S. Geological Survey Open-File Report 01-274, 40 pp.

Moulis, A., 2002, The Development of a Moment-Magnitude Based Earthquake Catalog for the Northeastern United States: M.S. thesis, Boston College.

Mueller, C., Hopper, M., and Frankel, A., 1997, *Preparation of Earthquake Catalogs for the National Seismic Hazard Maps—Contiguous 48 States*: U.S. Geological Survey Open-File Report 97-464, 36 pp.

Mueller, K., Champion, J., Guccione, M., and Kelson, K., 1999, Fault slip rates in the modern New Madrid seismic zone: *Science*, v. 286, pp. 1135-1138.

Mueller, K., Hough, S.E., and Bilham, R., 2004, Analysing the 1811-1812 New Madrid earthquakes with recent instrumentally recorded aftershocks: *Nature*, v. 429, pp. 284-288.

Mueller, K., and Pujol, J., 2001, Three-dimensional geometry of the Reelfoot blind thrust: Implications for moment release and earthquake magnitude in the New Madrid seismic zone: *Bulletin of the Seismological Society of America*, v. 91, pp. 1563-1573.

Munsey, J.W., 2006, Identification of “New” Historic Earthquakes in the Central and Eastern United States through Online Keyword Searches: Unpublished Report of River Operations, Tennessee Valley Authority, February.

Munsey, J.W., and Bollinger, G.A., 1985, Focal mechanism analyses for Virginia earthquakes (1978-1984): *Bulletin of the Seismological Society of America*, v. 75, pp. 1,613-1,636.

Munson, P.J., and Munson, C.A., 1996, *Paleoliquefaction Evidence for Recurrent Strong Earthquakes since 20,000 yr BP in the Wabash Valley of Indiana: Final Report*: submitted to the U.S. Geological Survey, March, 137 pp.

Munson, P.J., Munson, C.A., and Pond, E.C., 1995, paleoliquefaction evidence for a strong Holocene earthquake in south-central Indiana: *Geology*, v. 23, pp. 325-328.

Munson, P.J., Obermeier, S.M., Munson, C.A., and Hajic, E.R., 1997, Liquefaction evidence for Holocene and latest Pleistocene in the southern halves of Indiana and Illinois—A preliminary overview: *Seismological Research Letters*, v. 68, no. 4, pp. 523-536.

Murphy, J.B., and Keppie, J.D., 2005, The Acadian orogeny in the northern Appalachians: *International Geology Review*, v. 47, pp. 663-687.

Murray, A.S., and Olley, J.M., 2002, Precision and accuracy in the optically stimulated luminescence dating of sedimentary quartz—An overview: *Geochronometria*, v. 21, pp. 1-16.

Murray, G.E., 1961, *Geology of the Atlantic and Gulf Coastal Province of North America*: Harper & Brothers, New York, 692 pp.

Nábělek, J., and Suárez, G., 1989, The 1983 Goodnow earthquake in the central Adirondacks, New York: Rupture of a simple, circular crack: *Bulletin of the Seismological Society of America*, v. 79, no. 6, pp. 1762-1777.

Nagihara, S., and Jones, K.O., 2005, Geothermal heat flow in the northeast margin of the Gulf of Mexico: *AAPG Bulletin*, v. 89, pp. 821-831.

NAGRA (Nationale Genossenschaft für die Lagerung radioaktiver Abfälle), 2004, *Probabilistic Seismic Hazard Analysis for Swiss Nuclear Power Plant Sites* (PEGASOS Project), Volume 1, Final Report, Wettingen, Switzerland, July 31.

National Agriculture Imagery Program (NAIP), 2006, NAIP aerial imagery: U.S. Department of Agriculture (USDA), Farm Service Agency, Aerial Photography Field Office.

National Earthquake Database (NEDB), website, http://earthquakescanada.nrcan.gc.ca/stndon/NEDB-BNDS, last modified March 17, 2011.

National Earthquake Information Center (NEIC) Preliminary Determination of Epicenters (PDE), website, http://earthquake.usgs.gov/earthquakes/eqarchives/epic/, last modified May 5, 2011.

National Earthquake Prediction Evaluation Council (NEPEC), 2011, Letter and report from the Independent Expert Panel on New Madrid Seismic Zone Earthquake Hazards to Marcia McNutt, Director of the U.S. Geological Survey: Letter dated April 18, 2011, http://earthquake.usgs.gov/aboutus/nepec/reports/NEPEC_LettertoMcNutt4-18-11.pdf, and report dated April 16, 2011, 26 pp., http://earthquake.usgs.gov/aboutus/nepec/reports/NEPEC_NMSZ_expert_panel_report.pdf.

Nelson, K.D., Arnow, J.A., McBride, J.H., Willemin, J.H., Huang, J., Zheng, L., Oliver, J.E., Brown, L.D., and Kaufman, S., 1985, New COCORP profiling in the southeastern United States—Part I: Late Paleozoic suture and Mesozoic rift basin: *Geology*, v. 13, pp. 714-718.

Nelson, K.D., McBride, J.H., Arnow, J.A., Wille, D.M., Brown, L.D., Oliver, J.E., and Kaufman, S., 1987, Results of recent COCORP profiling in the Southeastern United States: *Geophysical Journal of the Royal Astronomical Society*, v. 89, pp. 141-146.

Nelson, K.D., and Zhang, J., 1991, A COCORP deep reflection profile across the buried Reelfoot rift, south-central United States: *Tectonophysics*, v. 197, pp. 271-293.

Nelson, W.J., 1995, *Structural Features in Illinois*: Illinois State Geological Survey Bulletin 100, 144 pp.

Nelson, W.J., Denny, F.B., Devera, J.A., Follmer, L.R., and Masters, J.M., 1997, Tertiary and Quaternary tectonic faulting in southernmost Illinois: *Engineering Geology*, v. 46, pp. 235-258.

Nelson, W.J., Denny, F.B., Follmer, L.R., and Masters, J.M., 1999, Quaternary grabens in southernmost Illinois: Deformation near an active intraplate seismic zone: *Tectonophysics*, v. 305, pp. 381-397.

Nelson, W.J., and Lumm, D.K., 1987, *Structural Geology of Southeastern Illinois and Vicinity*: Illinois State Geological Survey, Department of Energy and Natural Resources, Circular 538, 70 pp.

Nettles, M., 2006, Two unusual seismic events in the Gulf of Mexico: IRIS Annual Workshop, June 8-10, 2006, Westward Look Resort, Tucson, Arizona.

Nettles, M., 2007, Analysis of the February10, 2006, Gulf of Mexico earthquake from global and regional seismic data: *2007 Offshore Technology Conference Proceedings*, paper no. 19099.

Newell, W.L., 1985, Architecture of the Rappahannock estuary—Neotectonics in Virginia: in Morisawa, M., and Hack, J.T. (editors), *Tectonic Geomorphology*, Allen and Unwin, Winchester, Mass., pp. 322-342.

Newman, A., Stein, S., Weber, J., Engeln, J., Mao, A., and Dixon, T., 1999, Slow deformation and lower seismic hazard at the New Madrid seismic zone: *Science*, v. 284, no. 5414, pp. 619-621.

Nguyen, B.V., and Herrmann, R.B., 1992, Determination of source parameters for central and eastern North American earthquakes (1982-1986): *Seismological Research Letters*, v. 63, no. 4, pp. 567-586.

NICE (Northern Interior Continental Evolution) Working Group: Holm, D.K., Anderson, R., Boerboom, T.J., Cannon, W.F., Chandler, V., Jirsa, M., Miller, J., Schneider, D.A., Schulz, K.J., and Van Schmus, W.R., 2007, Reinterpretation of Paleoproterozoic accretionary boundaries of the north-central United States based on a new aeromagnetic-geologic compilation: *Precambrian Research,* v. 157, pp. 71-79.

Nicholson, C., and Wesson, R.L., 1990, *Earthquake Hazard Associated with Deep Well Injection—A Report to the U.S. Environmental Protection Agency*: U.S. Geological Survey Bulletin 1951.

Nicholson, C., Roeloffs, E., and Wesson, R.L., 1988, The northeastern Ohio earthquake of 31 January 1986: Was it induced? *Bulletin of the Seismological Society of America*, v. 78, no. 1, pp. 188-217.

Nielsen, R.J., 1982, *Stanford Data Base for Earthquakes in the United States*: The John A. Blume Earthquake Engineering Center Report No. 58, Stanford University, 117 pp.

Niemi, T.M., Ferris, A.N., and Abers, G.A., 2004, Investigation of microearthquakes, macroseismic data, and liquefaction associated with the 1867 Wamego earthquake in eastern Kansas: *Bulletin of the Seismological Society of America*, v. 94, no. 6, pp. 2317-2329.

Noger, M.C. (compiler), 1988, *Geologic Map of Kentucky*, Sesquicentennial edition of the Kentucky Geological Survey: Kentucky Geological Survey, Series 11, 1 sheet, 1:500,000.

Noller, J.S., and Forman, S.L., 1998, Luminescence geochronology of liquefaction features near Georgetown, South Carolina: in Sowers, J.M., Noller, J.S., and Lettis, W.R. (editors), *Dating and Earthquakes: Review of Quaternary Geochronology and Its Application to Paleoseismology*: U.S. Nuclear Regulatory Commission Report, NUREG/CR-5562, pp. 4.49-4.57.

Ntzoufras, I., 2009, *Bayesian Modeling Using WinBUGS*: John Wiley and Sons.

Nunn, J.A., 1985, State of stress in the northern Gulf Coast: *Geology*, v. 13, pp. 429-432.

Nuttli, O.W., 1973, Seismic wave attenuation and magnitude relations for eastern North America: *Journal of Geophysical Research*, v. 78, pp. 876-885.

Nuttli, O.W., 1974, Magnitude-recurrence relation for central Mississippi Valley earthquakes: *Bulletin of the Seismological Society of America*, v. 64, pp. 1189-1207.

Nuttli, O.W., 1983, Catalog of Central United States earthquakes Since 1800 of mb>3.0: Saint Louis University, St, Louis, Mo.

Nuttli, O.W., Bollinger, G.A., and Griffiths, D.W., 1979, On the relation between modified Mercalli intensity and body-wave magnitude: *Bulletin of the Seismological Society of America*, v. 69, pp. 893-909.

Nuttli, O., and Brill, K., 1981, Earthquake source zones in the central United States determined from historical seismicity: in Barstow, N.L., Brill, K.G., Nuttli, O.W., and Pomeroy, P.W. (editors), Approach to seismic zonation for siting nuclear electric power generating facilities in the eastern United States, U.S. Nuclear Regulatory Commission Report NUREG/CR-1577, pp. 98-143.

Nyquist, J.E., and Wang, H.F., 1988, Flexural modeling of the Midcontinent rift: *Journal of Geophysical Research*, v. 93, no. B8, pp. 8852-8868.

Nystrom, P.G., Jr., 1996, *Earthquake Hazards Map of the South Carolina Coastal Plain*: South Carolina Geological Survey Generalized Geologic Map Series GGMS-2, scale 1:400,000.

Obermeier, S., 1996, Summary of 1995 paleoliquefaction field search in the vicinity of Perry, Ohio: Letter submitted to Dr. Andrew Murphy, U.S. Nuclear Regulatory Commission, May 23, 10 pp.

Obermeier, S., and Pond, E., 1999, Issues in using liquefaction features for paleoseismic analysis: *Seismological Research Letters*, v. 70, pp. 34-56.

Obermeier, S.F., 1989, The New Madrid Earthquakes: An Engineering-Geologic Interpretation of Relict Liquefaction Features: U.S. Geological Survey Professional Paper 1336-B, 114 pp.

Obermeier, S.F., 1995, Paleoseismic liquefaction studies—Central U.S. and Pacific Northwestern U.S.: in Jacobsen, M.L. (compiler), *National Earthquake Hazards Reduction Program Annual Project Summaries: XXXVI, Volume II*, U.S. Geological Survey Open-File Report 95-210, pp. 606-609.

Obermeier, S., 1996a, Summary of 1995 Paleoliquefaction Field Search in the Vicinity of Perry, Ohio: Letter submitted to Dr. Andrew Murphy, U.S. Nuclear Regulatory Commission, May 23, 10 pp.

Obermeier, S.F., 1996b, Using liquefaction-induced features for paleoseismic analysis: in McCalpin, J.P. (editor), *Paleoseismology*, Academic Press, ch. 7, pp. 331-396.

Obermeier, S.F., 1998, Liquefaction evidence for strong earthquakes of Holocene and latest Pleistocene ages in the states of Indiana and Illinois, USA: *Engineering Geology*, Elsevier Science, v. 50, pp. 227-254.

Obermeier, S.F., 2009, Using liquefaction-induced and other soft-sediment features for paleoseismic analysis: *International Geophysics*, v. 95, pp. 499-566.

Obermeier, S.F., and McNulty, W.E., 1998, Paleoliquefaction evidence for seismic quiescence in central Virginia during late and middle Holocene time [abstract]: *Eos, Transactions of the American Geophysical Union*, v. 79, no. 17, p. S342.

Obermeier, S.F., Bleurer, N.K., Munson, C.A., Munson, P.J., Marin, W.S., McWilliams, K.M., Tabaczynski, D.A., Odum J.K., Rubin, M., and Eggert, D.L., 1991, Evidence of strong earthquake shaking in the lower Wabash Valley from prehistoric liquefaction features: *Science*, v. 251, pp. 1061-1063.

Obermeier, S.F., Jacobson, R.B., Smoot, J.P., Weems, R.E., Gohn, G.S., Monroe, J.E., and Powars, D.S., 1990, *Earthquake-Induced Liquefaction Features in the Coastal Setting of South Carolina and in the Fluvial Setting of the New Madrid Zone*: U.S. Geological Survey Professional Paper 1504.

Obermeier, S.F., Martin, J.R., Frankel, A.D., Youd, T.L., Munson, P.J., Munson, C.A., and Pond, E.C., 1993, *Liquefaction Evidence for One or More Strong Holocene Earthquakes in the Wabash Valley of Southern Indiana and Illinois, with a Preliminary Estimate of Magnitude*: U.S. Geological Survey Professional Paper 1536, 27 pp.

Obermeier, S.F., Pond, E.C., and Olson, S.M., with contributions by Green, R.A., Stark, T.D., and Mitchell, J.K., 2001, *Paleoliquefaction Studies in Continental Settings: Geologic and Geotechnical Factors in Interpretations and Back-Analysis*: U.S. Geological Survey Open-File Report 01-29, 75 pp., http://pubs.usgs.gov/of/2001/of01-029/revision.html.

Obermeier, S.F., Weems, R.E., Jacobson, R.B., and Gohn, G.S., 1989, Liquefaction evidence for repeated Holocene earthquakes in the Coastal Region of South Carolina: *Annals of the New York Academy of Sciences*, v. 558, pp. 183-195.

O'Brien, M.J., and Lyman, R.L., 1999, *Seriation, Stratigraphy, and Index Fossils: The Backbone of Archaeological Dating*, Plenum Press, New York, 261 pp.

O'Dowd, C.R., Eaton, D., Forsyth, D., and Asmis, H.W., 2004, Structural fabric of the Central Metasedimentary Belt of southern Ontario, Canada, from deep seismic profiling: *Tectonophysics*, v. 388, pp. 145-159.

Odum, J.K., Luzietti, E.A., Stephenson, W.J., Shedlock, K.M., and Michael, J.A., 1995, High-resolution, shallow, seismic reflection surveys of the northwest Reelfoot rift boundary near Marston, Missouri: in Shedlock, K.M., and Johnston, A.C. (editors), *Investigations of the New Madrid Seismic Zone*, U.S. Geological Survey Professional Paper 1538-P, 24 pp.

Odum, J.K., Stephenson, W.J., Shedlock, K.M., and Pratt, T.L., 1998, Near-surface structural model for deformation associated with the February 7, 1812, New Madrid, Missouri, earthquake: *Geological Society of America Bulletin*, v. 110, no. 2, pp. 149-162.

Odum, J.K., Stephenson, W.J., and Williams, R.A., 2003, Variable near-surface deformation along the Commerce segment of the Commerce geophysical lineament, southeast Missouri to southern Illinois, USA: in McBride, J.H., and Stephenson, W.J. (editors), Contributions to Neotectonics and Seismic Hazard from Shallow Geophysical Imaging, *Tectonophysics* (special issue), v. 368, nos. 1-4, pp. 155-170.

Odum, J.K., Stephenson, W.J., and Williams, R.A., 2010, Multi-source, high-resolution seismic-reflection imaging of Meeman-Shelby fault and a possible tectonic model for a Joiner Ridge–Manila high stepover structure in the Upper Mississippi embayment region: *Seismological Research Letters*, v. 81, no. 4, pp. 647-663.

Odum, J.K., Stephenson, W.J., Williams, R.A., Devera, J.A., and Staub, J.R., 2002, Near-surface faulting and deformation overlying the Commerce geophysical lineament in southern Illinois: *Seismological Research Letters*, v. 73, no. 5, pp. 687-697.

Odum, J.K., Stephenson, W.J., Williams, R.A., Worley, D.M., Guccione, M.J., and Van Arsdale, R.B., 2001, High-resolution seismic-reflection imaging of shallow deformation beneath the northeast margin of the Manila high at Big Lake, Arkansas: *Engineering Geology*, v. 62, pp. 91-103.

Oh, J., Austin, J.A., Phillips, J.D., Coffin, M.F., and Stoffa, P.L., 1995, Seaward-dipping reflectors offshore the southeastern United States: Seismic evidence for extensive volcanism accompanying sequential formation of the Carolina Trough and Blake Plateau basin: *Geology*, v. 21, no. 1, pp. 9-12.

Ohio Geological Survey, Ohio Seismic Network Catalog and Maps of Ohio Earthquakes, website, http://www.dnr.state.oh.us/geosurvey/html/eqcatlog/tabid/8302/Default.aspx, last updated December 22, 2010.

Oklahoma Geological Survey, Earthquake Catalog, website, http://www.okgeosurvey1.gov/level2/okeqcat.index.html, last updated March 13, 2011.

Olsen, P.E., Froelich, A.J., Daniels, D.L., Smoot, J.P., and Gore, P.J.W., 1991, Rift basins of early Mesozoic age: in Horton, J.W., Jr., and Zullo, V.A. (editors), *The Geology of the Carolinas*, University of Tennessee Press, Knoxville, pp.142-170.

Olson, S.M., 2009, Quantifying Uncertainties in Paleoliquefaction Studies: presentation given at CEUS SSC Project Workshop #2, February 18-20, Palo Alto, Calif.

Olson, S.M., Green, R.A., and Obermeier, S.F., 2005a, Geotechnical analysis of paleoseismic shaking using liquefaction effects: A major updating: *Engineering Geology*, v. 76, pp. 235-261.

Olson, S.M., Green, R.A., and Obermeier, S.F., 2005b, Revised magnitude bound relation for the Wabash Valley seismic zone of the central United States: *Seismological Research Letters*, v. 76, no. 6, pp. 756-771.

Olson, S.M., Obermeier, S.F., and Stark, T.D., 2001, Interpretation of Penetration Resistance for Back-Analysis at Sites of Previous Liquefaction: *Seismological Research Letters*, v. 72, no. 1, pp. 46-59.

Olson, S.M., Wen, Y.K., Song, J., Johnson, C.I., and Muhammad, K., 2007, *Quantifying Uncertainties in Paleoliquefaction Studies*: Final report, USGS NEHRP Award No. 06-HQ-GR-0013, December.

Ouassaa, K., and Forsyth, D.A., 2002, Interpretation of seismic and potential field data from western New York State and Lake Ontario: *Tectonophysics*, v. 353, pp. 115-149.

Owen, H. G., 1987, Deformation processes in unconsolidated sands: *Geological Society of London Special Publications 1987*, v. 29, pp. 11-24.

Pacific Earthquake Engineering Research Center (PEER), 2010, Next Generation Attenuation Relationships for Central & Eastern US (NGA-East): http://peer.berkeley.edu/ngaeast /index.html.

Palmer, J.R., Hoffman, D., Stephenson, W.J., Odum, J.K., and Williams, R.A., 1997a, Shallow seismic reflection profiles and geological structure in the Benton Hills, southeast Missouri: *Engineering Geology*, v. 46, pp. 217-233.

Palmer, J.R., Shoemaker, M., Hoffman, D., Anderson, N.L., Vaughn, J.D., and Harrison, R.W., 1997b, Seismic evidence of Quaternary faulting in the Benton Hills area, southeast Missouri: *Seismological Research Letters*, v. 68, pp. 650-661.

Parzen, E., 1962, *Stochastic Processes*: Holden-Day, San Francisco.

Parrish, S., and Van Arsdale, R., 2004, Faulting along the southeastern margin of the Reelfoot rift in northwestern Tennessee revealed in deep seismic reflection profiles: *Seismological Research Letters*, v. 75, pp. 782-791.

Pavich, M.J., Leo, G.W., Obermeier, S.F., and Estabrook, J.R., 1989, *Investigations of the Characteristics, Origin, and Residence Time of the Upland Residual Mantle of the Piedmont of Fairfax County, VA*: U.S. Geological Survey Professional Paper 1352, 114 pp.

Pavlides, L., 1994, Continental margin deposits and the Mountain Run fault zone of Virginia: Stratigraphy and tectonics: in Drake, A.A., Jr., and Pavlides, L. (editors), *Stratigraphic Notes, 1993*: U.S. Geological Survey Bulletin 2076-B, 9 pp.

Pavlides, L., Babyarchick, A.B., Newell, W.L., and Pavich, J.J., 1983, Late Cenozoic faulting along the Mountain Run fault zone, central Virginia Piedmont [abstract]: Geological Society of America *Abstracts with Programs*, v. 15, no. 2, p. 55.

Pazzaglia, F.J., 1999, Active tectonics in a passive margin setting: in Hanson, K.L., Kelson, K.I., Angell, M.A., and Lettis, W.R., (editors), *Techniques for Identifying Faults and Determining Their Origins*, NUREG/CR-5503, pp. A-143-A-183.

Peel, F.J., 2007, The setting and possible mechanism of the 2006 Green Canyon seismic event: Offshore Technology Conference, Houston, Texas, 30 April–3 May, 2007.

Peel, F.J., Travis, C.J., and Hossack, J.R., 1995, Genetic structural provinces and salt tectonics of the Cenozoic offshore U.S. Gulf of Mexico: A preliminary analysis: in Jackson, M.P.A., Roberts, D.G., and Snelson, S. (editors), *Salt Tectonics: A Global Perspective*, American Association of Petroleum Geologists Memoir 65, pp. 153-175.

Pe-Piper, G., and Piper, D.J.W., 2004, The effects of strike-slip motion along the Cobequid-Chedabucto-southwest Grand Banks fault system on the Cretaceous-Tertiary evolution of Atlantic Canada: *Canadian Journal of Earth Sciences*, v. 41, pp. 799-808.

Perry, W.J., Jr., 1989, *Tectonic Evolution of the Anadarko Basin Region, Oklahoma*: U.S. Geological Survey Bulletin 1866-A, pp. A1-A19.

Petersen, M.D., Frankel, A.D., Harmsen, S.C., Mueller, C.S., Haller, K.M., Wheeler, R.L., Wesson, R.L., Oliver, Y.Z, Boyd, S., Perkins, D.M., Luco, N., Field, E.H., Wills, C.J., and Rukstales, K.S., 2008, *Documentation for the 2008 Update of the United States National Seismic Hazard Maps*: USGS Open-File Report 2008-1128, 128 pp.

Pierce, K.L., 1986, Dating methods: in Geophysics Study Committee, Geophysics Research Forum, National Research Council (authors), *Active Tectonics: Impact on Society*, The National Academies Press, Washington, D.C., ch. 13, pp. 195-214.

Pierre, J.-R., and Lamontagne, M., 2004, The 20 April 2002, M_w 5.0 Au Sable Forks, New York, earthquake: A supplementary source of knowledge on earthquake damage to lifelines and buildings in eastern North America: *Seismological Research Letters*, v. 75, no. 5, pp. 626-636.

Pindell, J., 1985, Alleghenian reconstruction and subsequent evolution of the Gulf of Mexico, Bahamas, and proto-Caribbean: *Tectonics*, v. 4, pp. 1-39.

Pindell, J., 1993, Regional synopsis of Gulf of Mexico and Caribbean evolution: in Pindell, J., and Perkins, B. (editors), *Mesozoic and Early Cenozoic Development of the Gulf of Mexico and Caribbean Region, A Context for Hydrocarbon Exploration*, Gulf Coast Section Society of Economic Paleontologists and Mineralogists Foundation 13th Annual Research Conference, pp. 251-271.

Pindell, J., and Dewey, J.F., 1982, Permo-Triassic reconstruction of western Pangea and the evolution of the Gulf of Mexico/Caribbean region: *Tectonics*, v. 1, pp. 179-211.

Pindell, J., and Kennan, L., 2001, Kinematic evolution of the Gulf of Mexico and Caribbean: *Petroleum Systems of Deep-Water Basins: Global and Gulf of Mexico Experience*, Proceedings of the GCSSEPM Foundation 21st Annual Research Conference, 2-5 December 2001, pp. 193-220.

Pindell, J., Kennan, L., and Barrett, S., 2000, Putting it all together again: *American Association of Petroleum Geologists Explorer*, v. 21, pp. 34-37.

Pindell, J., Kennan, L., Stanek, K.P., Maresch, W.V., and Draper, G., 2006, Foundations of Gulf of Mexico and Caribbean evolution: Eight controversies resolved: *Geologica Acta*, v. 4, pp. 303-341.

Pomeroy, P.W., Simpson, D.W., and Sbar, M.L., 1976, Earthquakes triggered by surface quarrying—The Wappingers Falls, New York sequence of June, 1974: *Bulletin of the Seismological Society of America*, v. 66, no. 3, pp. 685-700.

Pond, E.C., 1996, Seismic Parameters from the Central United States Based on Paleoliquefaction Evidence in the Wabash Valley: Ph.D. dissertation, Virginia Polytechnic Institute, Blacksburg, Virginia, 583 pp.

Pond, E.C., and Martin, J.R., II, 1996, Seismic Parameters from the Central United States Based on Paleoliquefaction Evidence in the Wabash Valley: Final Report submitted to U.S. Geological Survey.

Pond, E.C., and Martin, J.R., 1997, Estimated magnitudes and accelerations associated with prehistoric earthquakes in the Wabash Valley region of the central United States: in Kolata, D.R., and Hildenbrand, T.G. (editors), Investigations of the Illinois Basin Earthquake Region, *Seismological Research Letters*, v. 68, pp. 611-623.

Poole, W.H., Sanford, B.V., Williams, H., and Kelley, D.G., 1970, Geology of southeastern Canada: in Douglas, R.J.W. (editor), *Geology and Economic Minerals of Canada*, Geological Survey of Canada Economic Geology Report 1, pp. 228-304.

Potter, C.J., and Drahovzal, J.A., 1994, The regional configuration of the Cambrian Reelfoot–Rough Creek–Rome rift system: in Ridgley, J.L., Drahovzal, J.A., Keith, B.D., and Kolata, D.R. (editors), *Proceedings of the Illinois Basin Energy and Mineral Resource Workshop*, U.S. Geological Survey Open-File Report 94-298, pp. 34-35 (also Kentucky Geological Survey, Open-File Report 94-12; Illinois State Geological Survey, Open-File Report 94-4; and Indiana Geological Survey, Open-File Report 94-12).

Potter, C.J., Drahovzal, J.A., Sargent, M.L., and McBride, J.H., 1997, Proterozoic structure, Cambrian rifting, and younger faulting as revealed by a regional seismic reflection network in the southern Illinois Basin: *Seismological Research Letters*, v. 68, no. 4, pp. 537-552.

Potter, C.J., Goldhaber, M.B., Heigold, P.C., and Drahovzal, J.A., 1995, Structure of the Reelfoot–Rough Creek Rift System, Fluorspar Area Fault Complex, and Hicks Dome, southern Illinois and western Kentucky—New constraints from regional seismic reflection data: in Shedlock, K.M., and Johnston, A.C. (editors), *Investigations of the New Madrid Seismic Zone*, U.S. Geological Survey Professional Paper 1538-Q, 19 pp.

Powell, C.A., 2002, Three-dimensional velocity structure in the New Madrid and other SCR seismic zones: *Eos, Transactions of the American Geophysical Union*, v. 83, no. 47, Fall Meeting Supplement, Abstract S22D-04.

Powell, C.A., Bollinger, G.A., Chapman, M.C., Sibol, M.S., Johnston, A.C., and Wheeler, R.L., 1994, A seismotectonic model for the 300-kilometer-long Eastern Tennessee seismic zone: *Science*, v. 264, pp. 686-688.

Pratt, T., 2009, Insights into the Structure and Long-Term Deformation in the New Madrid Region from Seismic Reflection Profiles: presentation given at meeting of CEUS Earthquake Hazards Program, U.S. Geological Survey, October 28-29, Memphis, Tenn.

Pratt, T., Culotta, R., Hauser, E., Nelson, D., Brown, L., Kaufman, S., Oliver, J., and Hinze, W., 1989, Major Proterozoic basement features of the eastern Midcontinent of North America revealed by recent COCORP profiling: *Geology*, v. 17, no. 6, pp. 505-509.

Pratt, T.L., Coruh, C., and Costain, J.K., 1988, A geophysical study of the Earth's crust in central Virginia: implications for Appalachian crustal structure: *Journal of Geophysical Research*, v. 93, no. B6, pp. 6,649-6,667.

Pratt, T.L., Hauser, E.C., and Nelson, K.D., 1992, Widespread buried Precambrian layered sequences in the U.S. Mid-continent: Evidence for large Proterozoic depositional basins: *AAPG Bulletin*, v. 76, no. 9, pp. 1384-1401.

Preisendorfer, R.W., 1988, *Principal Component Analysis in Meteorology and Oceanography*: Elsevier Science Ltd.

Prentice, C.S., Rizza, M., and Ritz, J.R., 2010, The Bogd and Bulnay faults of Mongolia: Slip rate and earthquake recurrence along two intracontinental strike-slip faults [abstract]: American Geophysical Union, Fall Meeting, Abstract T42A-08.

Progress Energy Carolinas, Inc., 2008, Shearon Harris Nuclear Power Plants Units 2 and 3, Docket Nos. 52-022 and 52-023, Supplement 1 to response to requests for additional information letter 030 related to basic geologic and seismic information, December 30, 2008, 66 pp.

Prowell, D.C., 1983, *Index of Faults of Cretaceous and Cenozoic Age in the Eastern United States*: U.S. Geological Survey Miscellaneous Field Studies Map MF-1269, 2 sheets, scale 1:2,500,000.

Prowell, D.C., 1988, Cretaceous and Cenozoic tectonism on the Atlantic coastal margin: in Sheridan, R.E., and Grow, J.A. (editors), *The Atlantic Continental Margin*, Geological Society of America, The Geology of North America, v. 1-2, pp. 557-564.

Prowell, D.C., and O'Connor, B.J., 1978, Belair fault zone; evidence of Tertiary fault displacement in eastern Georgia: *Geology*, v. 6, pp. 681-684.

Puffer, J.H., 2002, A late neoproterozoic eastern Laurentian superplume: Location, size, chemical composition, and environmental impact: *American Journal of Science*, v. 302, pp. 1-27.

Pujol, J., Johnston, A., Chiu, J.-M., and Yang, Y.-T., 1997, Refinement of thrust faulting models for the central New Madrid seismic zone: *Engineering Geology*, v. 46, pp. 281-298.

Pulli, J.J., and Guenette, M.J., 1981, The Chelmsford-Lowell, Massachusetts, earthquake of 23 November 1980: Depth control and fault plane solution: *Bulletin of the Seismological Society of America*, v. 71, no. 4, pp. 1369-1372.

Purser, J.L., and Van Arsdale, R.B., 1998, Structure of the Lake County uplift: New Madrid seismic zone: *Bulletin of the Seismological Society of America*, v. 88, no. 5, pp. 1204-1211.

Al-Qadhi, O., 2010, Geophysical Investigation of Paleoseismological Features in Eastern Arkansas, USA: Ph.D. dissertation, University of Arkansas at Little Rock, 277 pp.

Ramelli, A.R., and Slemmons, D.B., 1986, Neotectonic activity of the Meers fault: in Donovan, R.N. (editor), *The Slick Hills of Southwestern Oklahoma—Fragments of an Aulacogen*, Guidebook 24, Oklahoma Geological Society, Norman, Okla., pp. 45-54.

Ramelli, A.R., and Slemmons, D.B., 1990, Implications of the Meers Fault on seismic potential in the central United States: in Krinitzsky, E.L., and Slemmons, D.B. (editors), *Neotectonics in Earthquake Evaluation: Reviews in Engineering Geology*, Volume 8, Geological Society of America, pp. 59-75.

Ramelli, A.R., Slemmons, D.B., and Brocoum, S.J., 1987, *The Meers Fault: Tectonic Activity in Southwestern Oklahoma*: Washington, D.C., U.S. Nuclear Regulatory Commission, NUREG/CR-4852, 25 pp.

Ratcliffe, N.M., 1987, Basaltic rocks in the Rensselaer Plateau and Chatham slices of the Taconic allochthon: Chemistry and tectonic setting: *Geological Society of America Bulletin*, v. 99, pp. 511-528.

Ravat, D., Finn, C., Hill, P., Kucks, R., Phillips, J., Blakely, R., Bouligand, C., Sabaka, T., Elshayat, A., Aref, A., and Elawadi, E., 2009, *A Preliminary, Full Spectrum, Magnetic Anomaly Grid of the United States with Improved Long Wavelengths for Studying Continental Dynamics: A Website for Distribution of Data*: U.S. Geological Survey, Open-File Report 2009-1258, 2 pp.

Reagor, B.G., Stover, C.W., and Algermissen, S.T., 1980, Seismicity Map of the State of South Carolina: U.S. Geological Survey Miscellaneous Field Studies Map MF-1225.

Reasenberg, P., 1985, Second-order moment of central California seismicity, 1969–1982: *Journal of Geophysical Research*, v. 90, no. B7, pp. 5479-5495.

Reed, J.C., Jr., 1993, Map of the Precambrian rocks of the conterminous United States and some adjacent parts of Canada: in Reed, J.C., Jr., Bickford, M.E., Houston, R.S., Link, P.K., Rankin, D.W., Sims, P.K., and Van Schmus, W.R., (editors), *Precambrian: Conterminous U.S.*, Geological Society of America, The Geology of North America, v. C-2, Plate 1, scale 1:5,000,000.

Reimer, P.J., Baillie, M.G.L., Bard, E., Bayliss, A., Beck, J.W., Blackwell, P.G., Bronk Ramsey, C., Buck, C.E., Burr, G., Edwards, R.L., Friedrich, M., Grootes, P.M., Guilderson, T.P., Hajdas, I., Heaton, T.J., Hogg, A.G., Hughen, K.A., Kaiser, K.F., Kromer, B., McCormac, F.G., Manning, S.W., Reimer, R.W., Richards, D.A., Southon, J., Turney, C.S. M., van der Plicht, J., and Weyhenmeyer, C., 2009, IntCal09 and Marine09 radiocarbon age calibration curves, 0–50,000 years cal BP: *Radiocarbon*, v. 51, no. 4, pp. 1111-1150.

Reinbold, D.J., and Johnston, A.C., 1987, *Historical Seismicity in the Southern Appalachian Seismic Zone*: U.S. Geological Survey Open-File Report 87-433, 40 pp.

Reiter, L., 1990, *Earthquake Hazard Analysis: Issues and Insights*: Columbia University Press, New York.

René, R.M., and Stanonis, F.L., 1995, Reflection seismic profiling of the Wabash Valley fault system in the Illinois basin: in Shedlock, K.M., and Johnston, A.C. (editors), *Investigations of the New Madrid Seismic Zone*, U.S. Geological Survey Professional Paper 1538-O.

Renfro, H.B., and Feray, D.E., 1979, Geological Highway Map of Texas, H.B. Renfro Memorial Edition, Tulsa, OK: American Association of Petroleum Geologists.

Renfro, H.B., and Feray, D.E., 1997, Geological Highway Map Northern Rocky Mountain Region, AAPG Highway Map number 5, Tulsa, OK: American Association of Petroleum Geologists.

Rhea, S., 1987, Wave conversions from earthquakes and a new velocity model for the South Carolina coastal plain: *Bulletin of the Seismological Society of America*, v. 77, no. 6, pp. 2143-2151.

Rhea, S., 1995, *Seismotectonic Maps in the Vicinity of New Madrid, Missouri Database*: U.S. Geological Survey Open-File Report 95-0574, 10 pp.

Richter, C.F., 1935, An instrumental earthquake magnitude scale: *Bulletin of the Seismological Society of America*, v. 25, no. 1, pp. 1-32.

Riihimaki, C.A., Anderson, R.S., Safran, E.B., Dethier, D.P., Finkel, R.C., and Bierman, P.R., 2006, Longevity and progressive abandonment of the Rocky Flats surface, Front Range, Colorado: *Geomorphology*, v. 78, pp. 265-278.

Rimando, R.E., and Benn, K., 2005, Evolution of faulting and paleo-stress field within the Ottawa graben, Canada: *Journal of Geodynamics*, v. 39, pp. 337-360.

Robinson, E.S., Law, R.D., and Williams, R.T., 2000, Folding and faulting of Plio-Pleistocene sediments in Giles County, SW Virginia—(3) Seismic refraction, potential fields, and borehole data [abstract]: Geological Society of America *Abstracts with Programs*, v. 32, no. 2, p. 70.

Robinson, E.S., Sayer, S., and Law, R.D., 1993, A seismic refraction and electrical resistivity survey of faulted alluvial deposits in Giles County, VA [abstract]: *Eos, Transactions of the American Geophysical Union*, v. 74, no. 16, p. 282.

Rocher, M., Tremblay, A., Lavoie, D., and Campeau, A., 2003, Brittle fault evolution of the Montréal area (St Lawrence Lowlands, Canada): Rift-related structural inheritance and tectonism approached by palaeostress analysis: *Geological Magazine*, v. 140, pp. 157-172.

Rockwell, T.K., Lindvall, S., Herzberg, M., Murbach, D., Dawson, T., and Berger, G., 2000, Paleoseismology of the Johnson Valley, Kickapoo, and Homestead Valley faults: Clustering of earthquakes in the eastern California shear zone: *Bulletin of the Seismological Society of America*, v. 90, no. 5, pp. 1200-1236.

Roden-Tice, M.K., Brandt, J.A., and Tremblay, A., 2009, Apatite fission-track evidence for Late Paleozoic to Early Mesozoic unroofing and potential fault reactivation along the Saguenay River graben, Quebec [abstract]: Geological Society of America *Abstracts with Programs*, v. 41, no. 3, p. 32.

Roden-Tice, M.K., and Tice, S.J., 2005, Regional-scale mid-Jurassic to late Cretaceous unroofing from the Adirondack Mountains through central New England based on apatite fission-track and (U-Th)/He thermochronology: *The Journal of Geology*, v. 113, pp. 535-552.

Roden-Tice, M.K., Tice, S.J., and Schofield, I.S., 2000, Evidence for differential unroofing in the Adirondack Mountains, New York State, determined by apatite fission-track thermochronology: *The Journal of Geology,* v. 108, pp. 155-169.

Roden-Tice, M.K., West, D.P., Jr., Potter, J.K., Raymond, S.M., and Winch, J.L., 2009, Presence of a long-term lithospheric thermal anomaly: Evidence from apatite fission-track analysis in northern New England: *Journal of Geology*, v. 117, pp. 627-641.

Roden-Tice, M.K., and Wintsch, R.P., 2002, Early Cretaceous normal faulting in southern New England: Evidence from apatite and zircon fission-track ages: *The Journal of Geology,* v. 110, pp. 159-178.

Rogers, G.C., 1986, Seismic gaps along the Queen Charlotte fault: *Earthquake Prediction Research*, v. 4, pp. 1-11.

Rohs, C.R., and Van Schmus, V.R., 2007, Isotopic connections between basement rocks exposed in the St. Francois Mountains and the Arbuckle Mountains, southern mid-continent, North America: *International Journal of Earth Sciences*, v. 96, pp. 599-611.

Rondenay, S., Bostock, M.G., Hearn, T.M., White, D.J., Wu, H., Senechal, G., Ji, S., and Mareschal, M., 2000, Teleseismic studies of the lithosphere below the Abitibi-Grenville Lithoprobe transect: *Canadian Journal of Earth Sciences*, v. 37, pp. 415-426.

Rondot, J., 1979, *Reconnaissances Géologiques dans Charlevoix-Saguenay*: Ministère des Richesses Naturelles du Québec, Rapport DPV-682, 44 pp.

Rowan, M.G., Jackson, M.P.A., and Trudgill, B.D., 1999, Salt-related fault families and fault welds in the northern Gulf of Mexico: *AAPG Bulletin*, v. 83, no. 9, pp. 1454-1484.

Ruff, L., LaForge, R., Thorson, R., Wagner, T., and Goudaen, F., 1994, *Geophysical Investigations of the Western Ohio–Indiana Region: Final Report 1986–September 1992*: U.S. Nuclear Regulatory Commission, NUREG/CR-3145, prepared for the Division of Engineering, Office of Nuclear Regulatory Research.

Ruffman, A., and Peterson, J., 1988, *Pre-Confederation Historical Seismicity of Nova Scotia with an Examination of Selected Later Events*: Geological Survey of Canada Open File 1917, three volumes.

Russ, D.P., 1979, Late Holocene faulting and earthquake recurrence in the Reelfoot Lake area, northwestern Tennessee: *Geological Society of America Bulletin*, v. 90, no. 11, pp. 1013-1018.

Russ, D.P., 1982, *Style and Significance of Surface Deformation in the Vicinity of New Madrid, Missouri: Investigations of the New Madrid, Missouri, Earthquake Region*: U.S. Geological Survey Professional Paper 1236-H.

Russo, R.M., 2006, Earthquakes in the Gulf of Mexico: University of Florida, Department of Geological Sciences, http://www.clas.ufl.edu/users/russo/florida_eq.html.

Saint Louis University Earthquake Center, website, http://www.eas.slu.edu/Earthquake_Center/, last modified 2011.

Salvador, A., 1991a, Origin and development of the Gulf of Mexico Basin: in Salvador, A. (editor), *The Gulf of Mexico Basin*, Geological Society of America, The Geology of North America, v. J, ch. 14, pp. 389-444.

Salvador, A., 1991b, Triassic-Jurassic: in Salvador, A. (editor), *The Gulf of Mexico Basin*, Volume J, Geological Society of America, pp. 131-180.

Sandia National Laboratories (SNL), 2008, Probabilistic Volcanic Hazard Analysis Update (PVHA-U) for Yucca Mountain, Nevada: TDR-MGR-PO-000001 REV 01, Las Vegas, Nev.

Sanford, A.R., Lin, K.-W., Tsai, I.-C., and Jaksha, L.H., 2002, *Earthquake Catalogs for New Mexico and Bordering Areas: 1869–1998*: The New Mexico Bureau of Geology and Mineral Resources, Circular 210, 15 pp.

Sarwar, G., 2002, Northern Gulf of Mexico: A passive or passive active margin? AAPG Search and Discovery article #90007, AAPG Annual Meeting, 6 pp.

Saucier, R., 1991, Geoarchaeological evidence of strong prehistoric earthquakes in the New Madrid (Missouri) seismic zone: *Geology*, v. 19, pp. 296-298.

Saucier, R.T., 1977, *Effects of the New Madrid Earthquake Series in the Mississippi Alluvial Valley*: U.S. Army Corps of Engineers Waterways Experiment Station Miscellaneous Paper S-77-5.

Saucier, R.T., 1989, Evidence for episodic sand-blow activity during the 1811-12 New Madrid (Missouri) earthquake series: *Geology*, v. 17, pp. 103-106.

Saucier, R.T., 1994, *Geomorphology and Quaternary Geologic History of the Lower Mississippi*: U.S. Army Corps of Engineers Waterways Experiment Station, vols. 1 and 2, 364 pp. and 28 plates.

Saucier, R.T., and Smith, L.M., 1986, *Geomorphic Mapping and Landscape Classification of the Ouachita and Saline River Valleys, Arkansas*: Archeological Assessments, Inc., Report No. 51, Nashville, Ark.

Sawyer, D.S., Buffler, R.T., and Pilger, R.H., Jr., 1991, The crust under the Gulf of Mexico basin: in Salvador, A. (editor), *The Gulf of Mexico Basin*, Geological Society of America, The Geology of North America, v. J, ch. 4, pp. 53-72.

Scharnberger, C.K., 1990, A history of Pennsylvania earthquakes: *Scholars*, v. 1, no. 2, pp. 4-9.

Scharnberger, C.K., 1991a, The great Pennsylvania earthquake that never was: *Pennsylvania Geology*, v. 23, no. 2, pp. 3-8.

Scharnberger, C.K., 1991b, The pseudoearthquakes of 21 and 23 February, 1954, in Wilkes-Barre, Pennsylvania: *Seismological Research Letters*, v. 62, pp. 135-138.

Schlische, R.W., 1993, Anatomy and evolution of the Triassic-Jurassic continental rift system, eastern North America: *Tectonics*, v. 12, no. 4, pp. 1,026-1,042.

Schlische, R.W., 2003, Progress in Understanding the Structural Geology, Basin Evolution, and tectonic History of the Eastern North America Rift System: in LeTourneau, P.M., and Olsen, P.E. (editors), *The Great Rift Valleys of Pangea in Eastern North America—Volume 1. Tectonics, Structure, and Volcanism*: Columbia University Press, New York, pp. 21-64.

Schlische, R.W. and Olsen, P.E., 1990, Quantitative filling model for continental extensional basins with application to the early Mesozoic rifts of eastern North America: *Journal of Geology*, v. 98, pp. 135-155.

Schlische, R.W., Young, S.S., Ackerman, R.V., and Gupta, A., 1996, Geometry and scaling relations of a population of very small rift-related normal faults: *Geology*, v. 24, no. 8, pp. 683-686.

Schlupp, A., and Cisternas, A., 2007, Source history of the 1905 great Mongolian earthquake (Tsetserleg, Bulnay): *Geophysical Journal International*, v. 169, no. 3, pp. 1115-1131.

Schneider, J.A., and Mayne, P.W., 2000, *Liquefaction Response of Soils in Mid-America Evaluated by Seismic Cones Test*: Mid-America Earthquake Center Report MAE-GT-3A, 292 pp.

Schneider, J.A., Mayne, P.W., and Rix, G.J., 2001, geotechnical site characterization in the greater Memphis area using CPT, *Engineering Geology*, v. 62, no. 1-3, pp. 169-184.

Scholz, C.H., 1998, Earthquakes and friction laws: *Nature*, v. 391, pp. 37-42.

Schulte, S.M., and Mooney, W.D., 2005, An updated global earthquake catalogue for stable continental regions: Reassessing the correlation with ancient rifts: *Geophysical Journal International*, v. 161, pp. 707-721.

Schumm, S.A., and Spitz, W.J., 1996, Geological influences on the lower Mississippi River and its alluvial valley: *Engineering Geology*, v. 45, pp. 245-261.

Schwartz, D., Hecker, S., Ponti, D., Bayasgalan, A., Lund, W., and Stenner, H., 2009, 1998 USGS Expedition to Mongolia, Scientific Background and Field Plan, USGS Earthquake Hazards Program website, http://earthquake.usgs.gov/research/geology/mongolia98/.

Schwartz, D.P., and Coppersmith, K.J., 1984, Fault behavior and characteristic earthquakes: examples from the Wasatch and San Andreas fault zones: *Journal of Geophysical Research*, v. 89, no. B7, pp. 5681-5698.

Schwartz, S.Y., and Christensen, D.H., 1988, The 12 July 1986 St. Mary's Ohio earthquake and recent seismicity in the Anna, Ohio seismogenic zone: *Seismological Research Letters*, v. 59, pp. 57-62.

Schweig, E.S., and Ellis, M.A., 1992, Distributed faulting along the Bootheel lineament—Smoothing over the rough spots in the New Madrid seismic zone [abstract]: *Seismological Research Letters*, v. 63, no. 1, pp. 50.

Schweig, E.S., and Ellis, M.A., 1994, Reconciling short recurrence intervals with minor deformation in the New Madrid seismic zone: *Science*, v. 264, pp. 1308-1311.

Schweig, E.S., III, and Marple, R.T., 1991, Bootheel lineament: A possible coseismic fault of the great New Madrid earthquakes: *Geology*, v. 19, p. 1025-1028.

Schweig, E.S., and Van Arsdale, R.B., 1996, Neotectonics of the upper Mississippi embayment: *Engineering Geology*, v. 45, nos. 1-4, pp. 185-203.

Schweig, E.S., III, Shen, F., Kanter, L.R., VanArsdale, R.B., Luzietti, E.A., Shedlock, K.M., and King K.W., 1992, Shallow seismic reflection survey of the Bootheel lineament area, southeastern Missouri: *Seismological Research Letters*, v. 63, pp. 285-296.

Science Applications International Corporation(SAIC), 2002, Seismic investigation report for siting of a potential on-site CERCLA waste disposal facility at the Paducah Gaseous Diffusion Plant, Paducah, Kentucky: Report prepared by SAIC Engineering, Inc., Oak Ridge, Tennessee, for Bechtel Jacobs Company and the U.S. Department of Energy Office of Environmental Management, DOE/OR/07-2038&D1, August.

Science Applications International Corporation (SAIC), 2004, Seismic Investigation Report for Siting of a Potential On-Site CERCLA Waste Disposal Facility at the Paducah Gaseous Diffusion Plant, Paducah, Kentucky: unpublished consultant report dated March 2004, by SAIC for U.S. Department of Energy.

Scott, G.R., 1970, *Quaternary Faulting and Potential Earthquakes in East-Central Colorado:* U.S. Geological Survey Professional Paper 700-C, pp. C11-C18.

Scott, G.R., Taylor, R.B., Epis, R.C., and Wobus, R.A., 1978, Geologic map of the Pueblo 1° × 2° quadrangle, south-central Colorado: U.S. Geological Survey Miscellaneous Geologic Investigations I-1022.

Seborowski, K.D., Williams, G., Kelleher, J.A., and Statton, C.T., 1982, Tectonic implications of recent earthquakes near Annsville, New York: *Bulletin of the Seismological Society of America*, v. 72, no. 5, pp. 1601-1609.

Seeber, L., and Armbruster, J., 1995, Seismogenesis and structure in the Lake Erie–Lake Ontario region of the U.S. from a global perspective: *Program, List of Participants and Abstracts from the Atomic Energy Control Board Workshop on Seismic Hazard Assessment in Southern Ontario, Ottawa, Ontario, June 19-21*, INFO-0604-1, pp. D5-D20.

Seeber, L., and Armbruster, J.G., 1981, The 1886 Charleston, South Carolina earthquake and the Appalachian detachment: *Journal of Geophysical Research*, v. 86, no. B9, pp. 7874-7894.

Seeber, L., and Armbruster, J.G., 1988, Seismicity along the Atlantic Seaboard of the U.S.; Intraplate neotectonics and earthquake hazard: in Sheridan, R.E., and Grow, J.A. (editors), *The Atlantic Continental Margin: U.S.,* Geological Society of America, The Geology of North America, v. I-2, ch. 30, pp. 565-582.

Seeber, L., and Armbruster, J.G., 1989, Low-displacement seismogenic faults and nonstationary seismicity in the eastern United States: *Annals of the New York Academy of Sciences*, v. 558, pp. 21-39.

Seeber, L., and Armbruster, J.G., 1991, *The NCEER-91 Earthquake Catalog: Improved Intensity-Based Magnitudes and Recurrence Relations for U.S. Earthquakes East of New Madrid*: Technical Report NCEER-91-0021, National Center for Earthquake Engineering Research, State University of New York at Buffalo.

Seeber, L., and Armbruster, J.G., 1993, Natural and induced seismicity in the Lake Erie–Lake Ontario region: Reactivation of ancient faults with little neotectonic displacement: *Géographie physique et Quaternaire,* v. 47, no. 3, pp. 363-378.

Seeber, L., Armbruster, J.G., and Kim, W.-Y., 2004, A fluid-injection-triggered earthquake sequence in Ashtabula, Ohio: Implications for seismogenesis in stable continental regions: *Bulletin of the Seismological Society of America,* v. 94, no. 1, pp. 76-87.

Seeber, L., Armbruster, J.G., Kim, W.-Y., and Barstow, N., 1998, The 1994 Cacoosing Valley earthquakes near Reading, Pennsylvania: A shallow rupture triggered by quarry unloading, *Journal of Geophysical Research*, v. 103, no. B10, pp. 24,505-24,521.

Seeber, L., and Dawers, N., 1989, Characterization of an intraplate seismogenic fault in the Manhattan Prong, Westchester, Co., N.Y.: *Seismological Research Letters*, v. 60, no. 2, pp. 71-78.

Seeber, L., Kim, W.-Y., Armbruster, J.G., Du, W.-X., Lerner-Lam, A.L., and Friberg, P., 2002, The April 20 2002 Mw = 5.0 earthquake near Au Sable Forks, Adirondacks, New York: A first glance at a new sequence: *Seismological Research Letters*, v. 73, pp. 480-489.

Seed, H.B., and Idriss, I.M., 1982, *Ground Motions and Soil Liquefaction During Earthquakes*: Earthquake Engineering Research Institute monograph, Berkeley, Calif., 134 pp.

Serpa, L.D., Setzer, T., Farmer, H., Brown, L.D., Oliver, J.E., Kaufman, S., Sharp, J., and Steeples, D.W., 1984, Structure of the southern Keeweenawan rift from COCORP surveys across the midcontinent geophysical anomaly in northeastern Kansas: *Tectonics*, v. 3, no. 3, pp. 367-384.

Sexton, J.L., and Jones, P.B., 1986, Evidence for recurrent faulting in the New Madrid seismic zone from Mimi-Sosie high-resolution reflection data: *Geophysics*, v. 51, no. 9, pp. 1760-1788.

Sexton, J.L., Braile, L.W., Hinze, W.J., and Campbell, M.J., 1986, Seismic reflection profiling studies of a buried Precambrian rift beneath the Wabash Valley fault zone: *Geophysics*, v. 51, no. 3, pp. 640-660.

Sharps, J.A., 1976, Geologic Map of the Lamar Quadrangle, Colorado and Kansas: U.S. Geological Survey Miscellaneous Geologic Investigations I-944, scale 1:250,000.

Shedlock, K.M., 1987, *Earthquakes Recorded by the South Carolina Seismic Network (1974–1986)*: U.S. Geological Survey Open-File Report No. 87-437.

Sheridan, R.E., Musser, D.L., Glover, L., Talwani, P., Ewing, J.I., Holbrook, W.S., Purdy, G.M., Hawman, R., and Smithson, S., 1993, Deep seismic reflection data of EDGE U.S. Mid-Atlantic continental-margin experiment: Implications for Appalachian sutures and Mesozoic rifting and magmatic underplating: *Geology*, v. 21, pp. 563-567.

Shoemaker. K., Hamburger, M.W., Pavlis, G.L., Horton, S.P., and Withers, M.M., 2009, Hypocentral relocations of the 2008 Mt. Carmel, Illinois aftershock sequence [abstract]: American Geophysical Union, Fall Meeting, Abstract S51B-1421.

Al-Shukri, H., Lemmer, R.E., Mahdi, H., and Connelly, J.B., 2005, Spatial and temporal characteristics of paleoseismic features in the southern terminus of the New Madrid seismic zone in eastern Arkansas: *Seismological Research Letters*, v. 76, pp. 502-511.

Al-Shukri, H., Mahdi, H., Al Kadi, O., and Tuttle, M., 2009, Spatial and Temporal Characteristic of Paleoseismic Features in the Southern Terminus of the New Madrid Seismic Zone in Eastern Arkansas: Final Technical Report Submitted to the U.S. Geological Survey under USGS External Grant No. 07HQGR0069.

Al-Shukri, H., Mahdi, H., and Tuttle, M., 2006, Three-dimensional imaging of earthquake-induced liquefaction features with ground penetrating radar near Marianna, Arkansas: *Seismological Research Letters*, v. 77, pp. 505-513.

Shumway, A.M., 2008, Focal mechanisms in the northeast New Madrid seismic zone: *Seismological Research Letters*, v. 79, no. 3, pp. 469-477.

Sibol, M.S., Bollinger, G.A., and Birch, J.B., 1987, Estimation of magnitudes in central and eastern North America using intensity and felt area: *Bulletin of the Seismological Society of America*, v. 77, no. 5, pp. 1635-1654.

Sibson, R.H., 1982, Fault zone models, heat flow, and the depth distribution of earthquakes in the continental crust of the United States: *Bulletin of the Seismological Society of America*, v. 72, no. 1, pp. 151-163.

Sibson, R.H., 1984, Roughness at the base of the seismogenic zone: Contributing factors: *Journal of Geophysical Research*, v. 89, pp. 5791-5799.

Sibson, R.H., 2007, Au-quartz mineralization near the base of the continental seismogenic zone: *Geological Society, London, Special Publications*, v. 272, no. 1, pp. 519-532.

Sibson, R.H., and Xie, G., 1998, Dip range for intracontinental reverse fault ruptures: Truth not stranger than friction? *Bulletin of the Seismological Society of America*, v. 88, no. 4, pp. 1014-1022.

Silva, W., Gregor, N., and Darragh, R., 2002, Development of regional hard rock attenuation relations for central and eastern North America: internal report from Pacific Engineering, November 1, http://www.pacificengineering.org/CEUS/Development%20of%20Regional%20Hard_ABC.pdf.

Silva, W., Wong, I., Siegel, T., Gregor, N., Darragh, R., and Lee, R., 2003, Ground motion and liquefaction simulation of the 1886 Charleston, South Carolina, earthquake: *Bulletin of the Seismological Society of America*, v. 93, no. 6, pp. 2717-2736.

Silverman, B.W., 1986, *Density Estimation for Statistics and Data Analysis*: Chapman and Hall, London, Monographs on Statistics and Applied Probability series, No. 26.

Sims, J.D., 1973, Earthquake-induced structures in sediments of Van Norman Lake, San Fernando California: *Science*, v. 182, pp. 161-163.

Sims, J.D., 1975, Determining earthquake recurrence intervals from deformational structures in young lacustrine sediments: *Tectonophysics*, v. 29, pp. 141-153.

Sims, J.D., and Garvin, C.D., 1995, Recurrent liquefaction at Soda Lake, California, induced by the 1989 Loma Prieta earthquake, and 1990 and 1991 aftershocks: Implications for paleoseismicity studies: *Bulletin of the Seismological Society of America*, v. 85, pp. 51-65.

Sims, P.K., 1990, Precambrian Basement Map of the Northern Midcontinent, U.S.A.: U.S. Geological Survey Miscellaneous Investigations Series Map I-1853A, scale 1:1,000,000, 1 sheet.

Sims, P.K., and Peterman, Z.E., 1986, Early Proterozoic Central Plains orogen: A major buried structure in the north-central United States: *Geology*, v. 14, pp. 488-491.

Sims, P.K., Card, K.D., Morey, G.B., and Peterman, Z.E., 1980, The Great Lakes tectonic zone—A major crustal structure in central North America: *Geological Society of America Bulletin*, v. 91; no. 12, pp. 690-698, doi:10.1130/0016-7606(1980)91<690:TGLTZA>2.0.CO;2.

Sims, P.K., Kisvarsanyi, E.B., and Morey, G.B., 1987, *Geology and Metallogeny of Archean and Proterozoic Basement Terranes in the Northern Midcontinent, U.S.A.—An Overview*: U.S. Geological Survey Bulletin 1815, 51 pp.

Sims, P.K., Saltus, R.W., and Anderson, E.D., 2005, *Preliminary Precambrian Basement Structure Map of the Continental United States—An Interpretation of Geologic and Aeromagnetic Data*: U.S. Geological Survey Open-File Report 2005-1029.

Sleep, N.H., 1990, Monteregian hotspot track: A long-lived mantel plume: *Journal of Geophysical Research*, v. 95, no. B13, pp. 21,983-21,990.

Smalley, R., Jr., Ellis, M.A., Paul, J., and VanArsdale, R.B., 2005, Space geodetic evidence for rapid strain rates in the New Madrid seismic zone of the central USA: *Nature*, v. 435, pp. 1088-1090, doi:10.1038/nature03642.

Smith, W.A. and Talwani, P., 1985, Preliminary interpretation of a detailed gravity survey in the Bowman and Charleston, S.C. seismogenic zones [abstract]: Geological Society of America *Abstracts with Programs*, v. 17, no. 2, p. 137.

Smith, W.E.T., 1962, Earthquakes of eastern Canada and adjacent areas: 1534–1927: *Publications of the Dominion Observatory*, v. XXVI, no. 5, pp. 271-302.

Smith, W.E.T., 1966, Earthquakes of eastern Canada and adjacent areas: 1928–1959: *Publications of the Dominion Observatory*, v. XXXII, no. 3, pp. 87-121.

Smoot, J.P., 1985, The closed-basin hypothesis and its use in facies analysis of the Newark Supergroup: in Robinson, G.R., Jr., and Froelich, A.J. (editors), *Proceedings of the Second US Geological Survey Workshop on the Early Mesozoic Basins of the Eastern U.S.*, United States Geological Survey Circular, v. 946, pp. 4-10.

Soderberg, R.K., and Keller, G.R., 1981, Geophysical evidence for a deep basin in western Kentucky: *AAPG Bulletin*, v. 65, pp. 226-234.

Soller, D.R., and Reheis, M.C. (compilers), 2004, Surficial Materials in the Conterminous United States: U.S. Geological Survey Open-File Report 03-275, scale 1:5,000,000.

Soller, D.R., Reheis, M.C., Garrity, C.P., and Van Sistine, D.R., 2009, Map Database for Surficial Materials in the Conterminous United States: U.S. Geological Survey Data Series 425, scale 1:5,000,000, http://pubs.usgs.gov/ds/425/.

Somerville, P., Collins, N., Abrahamson, N., Graves, R., and Saikia, C., 2001, *Ground Motion Attenuation Relations for the Central and Eastern United States, Final Report, June 30, 2001*: external research project funded by U.S. Geological Survey Award No. 99HQGR0098, 38 pp.

Somerville, P., Collins, N., and Graves, R., 2005, *Magnitude-Rupture Area Scaling of Large Strike-Slip Earthquakes*: USGS NEHRP Final Report, Award No. 05-HQ-GR-0004.

Somerville, P., and Saikia, C., 2000, Ground motion attenuation relations for the Central and Eastern United States: progress report to the USGS, January 28, 2000, URS Greiner Woodward Clyde, Pasadena, 10 pp.

Somerville, P.G., McLaren, J.P., Saikia, C.K., and Helmberger, D.V., 1990, The 25 November 1988 Saguenay, Quebec, earthquake: Source parameters and the attenuation of strong ground motion: *Bulletin of the Seismological Society of America*, v. 80, no. 5, pp. 1118-1143.

Sonley, E., and Atkinson, G.M., 2005, Empirical relationship between moment magnitude and Nuttli magnitude for small-magnitude earthquakes in southern Canada: *Seismological Research Letters*, v. 76, no. 6, pp. 752-755.

South Carolina Seismic Network, 2005, List of Earthquakes in Charleston Between 1974 and 2002, webpage, http://scsn.seis.sc.edu/projects/SCSN/history/html/1974_2002Eqweb.htm.

South Carolina Seismic Network, South Carolina Earthquake Catalog, website, http://www.seis.sc.edu/projects/SCSN/.

Southern Nuclear Co., 2008, Vogtle Early Site Permit Application, Revision 4, Part 2—Site Safety Analysis Report, Chapter 2, “Site Characteristics”: see Updated Charleston Seismic Source (UCSS) model in Section 2.5.2.2.2.4, U.S. Nuclear Regulatory Commission document accession no. ML081020220, March 28.

Sparlin, M.A., and Lewis, R.D., 1994, Interpretation of the magnetic anomaly over the Omaha Oil Field, Gallatin County, Illinois: *Geophysics*, v. 59, no. 7, pp. 1092-1099.

Spencer, C., Green, A., Morel-a-l’Huissier, P., and Milkereit, B, 1989, The extension of Grenville basement beneath the northern Appalachians: Results from the Quebec-Maine seismic reflection and refraction surveys: *Tectonics*, v. 8, no. 4, pp. 677-696.

Spitz, W.J., and Schumm, S.A., 1997, Tectonic geomorphology of the Mississippi Valley between Osceola, Arkansas, and Friars Point, Mississippi: *Engineering Geology*, v. 46, pp. 259-280.

Stahle, D.W., Cook, E.R., and White, J.W.C., 1985, Tree-ring dating of bald cypress and the potential for millennia-long chronologies in the Southeast: *American Antiquity*, v. 50, pp. 796-802.

Stahle, D.W., Fye, F.K., and Therrell, M.D., 2004, Interannual to decadal climate and streamflow variability estimates from tree rings: in Gillespie, A.R., Porter, S.C., and Atwater, B.F. (editors), *The Quaternary Period in the United States*, Developments in Quaternary Science Volume 1, Elsevier, Amsterdam and New York, pp. 491-504.

Stark, T.D., 2002, Interpretation of Ground Shaking from Paleoliquefaction Features, U.S. Geological Survey, Annual Technical Report.

Stark, T.J., 1997, The East Continent Rift Complex: Evidence and conclusions: in Ojakangas, R.W., Dickas, A.B., and Green, J.C. (editors), *Middle Proterozoic to Cambrian Rifting, Central North America*, Geological Society of America Special Paper 312, pp. 253-266.

Stauder, W., 1982, Present-day seismicity and identification of active faults in the New Madrid seismic zone: in Pakiser, L., and McKeown, F.A. (editors), Investigations of the New Madrid Missouri Earthquake Region: U.S. Geological Survey Professional Paper 1236-C, pp. 21-30.

Stein, S., and Newman, A., 2004, Characteristic and uncharacteristic earthquakes as possible artifacts: Applications to the New Madrid and Wabash seismic zones: *Seismological Research Letters*, v. 75, pp. 170-184.

Steltenpohl, M.G., Zietz, I., Horton, J.W., Jr., and Daniels, D.L., 2010, New York–Alabama lineament: A buried right-slip fault bordering the Appalachians and mid-continent North America: *Geology*, v. 38, no. 6, pp. 571-574.

Stephenson, W.J., Odum, J.K., Williams, R.A., Pratt, T.L., Harrison, R.W., and Hoffman, D., 1999, Deformation and Quaternary faulting in southeast Missouri across the Commerce geophysical lineament: *Bulletin of the Seismological Society of America*, v. 89, no. 1, pp. 140-155.

Stephenson, W.J., Shedlock, K.M., and Odum, J.K., 1995, Characterization of the Cottonwood Grove and Ridgely faults near Reelfoot Lake, Tennessee, from high-resolution seismic reflection data: in Shedlock, K.M., and Johnston, A.C. (editors), *Investigations of the New Madrid Seismic Zone*, U.S. Geological Survey Professional Paper 1538-I, 10 pp.

Stepp, J.C., 1972, Analysis of completeness of the earthquake sample in the Puget Sound area and its effect on statistical estimates of earthquake hazard: *Proceedings of the International Conference on Microzonation*, v. 2, pp. 897-910.

Stepp, R., and Revetta, F.A., 2008, The Au Sable Forks, NY earthquake of April 20, 2002: Geological Society of America *Abstracts with Programs*, v. 40, no. 2, p. 67.

Stevenson, D.A., and McCulloh, R.P., 2001, *Earthquakes in Louisiana*: Louisiana Geological Survey, Public Information Series No. 7, 8 pp.

Stewart, D.B., Wright, B.E., Unger, J.D., Phillips, J.D., and Hutchinson, D.R. (principal compilers), 1993, Global Geoscience Transect 8: Quebec–Maine–Gulf of Maine Transect, Southeastern Canada, Northeastern United States of America: U.S. Geological Survey Miscellaneous Investigations Series Map I-2329.

St. Julien, P., and Hubert, C., 1975, Evolution of the Taconian orogen in the Quebec Appalachians: *American Journal of Science*, v. 275-A, pp. 337-362.

Stock, C., and Smith, E., 2002, Adaptive kernel estimation and continuous probability representation of historical earthquake catalogs: *Bulletin of the Seismological Society of America*, v. 92, no. 3, pp. 904-912.

St-Onge, G., Mulder, T., Piper, D.J.W., Hillaire-Marcel, C., and Stoner, J.S., 2004, Earthquake and flood-induced turbidites in the Saguenay Fjord (Québec): A Holocene paleoseismicity record: *Quaternary Science Reviews*, v. 23, pp. 283-294.

Stover, C.W., and Coffman, J.L., 1993, *Seismicity of the United States, 1568-1989 (Revised)*: U.S. Geological Survey Professional Paper 1527, 418 pp.

Stover, C.W., Reagor, G., and Algermissen, S.T., 1984, *United States Earthquake Data File*: U.S. Geological Survey Open-File Report 84-225, 123 pp.

Street, R., 1984, Some recent *Lg* phase displacement densities and their implication with respect to the prediction of ground motion in Eastern North America: *Bulletin of the Seismological Society of America*, v. 74, no. 2, pp. 757-762.

Street, R., Bollinger, G.A., and Woolery, E., 2002, Blasting and other mining-related activities in Kentucky: A source of earthquake misidentification: *Seismological Research Letters*, v. 73, no. 5, pp. 739-750.

Street, R., and Lacroix, A., 1979, An empirical study of New England seismicity: 1727-1977, *Bulletin of the Seismological Society of America*, v. 69, no. 1, pp. 159-175.

Street, R.L., Herrmann, R.B., and Nuttli, O.W., 1975, Spectral characteristics of the Lg wave generated by Central United States earthquakes: *Geophysical Journal of the Royal Astronomical Society*, v. 41, pp. 51-63.

Street, R.L., and Turcotte, F.T., 1977, A study of northeastern North American spectral moments, magnitudes, and intensities: *Bulletin of the Seismological Society of America*, v. 67, no. 3, pp. 599-614.

St. Seymour, K., and Kumarapeli, P.S., 1995, Geochemistry of the Grenville dyke swarm: Role of plume-source mantle in magma genesis: *Contributions to Mineralogy and Petrology*, v. 120, pp. 29-41.

Stuart, W.D., Hildenbrand, T.G., and Simpson, R.W., 1997, Stressing of the New Madrid seismic zone by a lower crust detachment fault: *Journal of Geophysical Research*, v. 102, no. B12, pp. 27,623-27,633.

Stuiver, M., Long A., Kra, R.S., and Devine, J.M. (editors), 1993, Calibration 1993 issue: *Radiocarbon*, v. 35, no. 1, 244 pp.

Stuiver, M., and Pearson, G.W., 1993, High-precision bidecadal calibration of the radiocarbon time scale, AD 1950-500 BC and 2500-6000 BC: *Radiocarbon*, v. 35, no. 1, pp. 1-25.

Stuiver, M., and Reimer, P.J., 1993, Extended ^{14}C data base and revised CALIB 3.0 ^{14}C age calibration program: *Radiocarbon*, v. 35, pp. 215-230.

Stuiver, M., Reimer, P.J., and Braziunas, T.F., 1998, High-precision radiocarbon age calibration for terrestrial and marine samples: *Radiocarbon*, v. 40, no. 3, pp. 1127-1151.

Stuiver, M., Reimer, P.J., and Reimer, R.W., 2005, CALIB Radiocarbon Calibration, Version 6.0 program and documentation, http://calib.qub.ac.uk/calib/.

Su, W.J., and McBride, J.H., 1999, Final Technical Report—Study of a Potential Seismic Source Zone in South-Central Illinois: Technical Report Submitted to the U.S. Geological Survey under USGS External Grant No. 99-HQ-GR-0075.

Swan, F.H., Wesling, J.R., Hanson, K.A., Kelson, K.I., and Perman, R.C., 1993, *Draft Report: Investigation of the Quaternary Structural and Tectonic Character of the Meers Fault (Southwestern Oklahoma)*: Geomatrix Consultants, Inc., San Francisco, CA, 104 pp. plus appendices.

Swanson, M.T., 1986, Preexisting fault control for Mesozoic basin formation in eastern North America: *Geology*, v. 14, pp. 419-422.

Sykes, L.R., Armbruster, J.G., Kim, W.-K., and Seeber, L., 2008, Observations and tectonic setting of historic and instrumentally located earthquakes in the greater New York City–Philadelphia area: *Bulletin of the Seismological Society of America*, v. 98, no. 4, pp. 1696-1719.

Syvitski, J.P.M., and Schafer, C.T., 1996, Evidence for an earthquake-triggered basin collapse in Saguenay Fjord, Canada: *Sedimentary Geology*, v. 104, pp. 127-153.

Talma, A.S., and Vogel, J.C., 1993, A simplified approach to calibrating C14 dates: *Radiocarbon*, v. 35, pp. 317-322.

Talwani, M., and Abreau, V., 2000, Inferences regarding initiation of oceanic crust formation from the U.S. East Coast margin and conjugate South Atlantic margins: in Mohriak, W., and Talwani, M. (editors), *Atlantic Rifts and Continental Margins, Geophysical Monograph*, v. 115, pp. 211-233.

Talwani, M., Ewing, J., Sheridan, R.E., Holbrook, W.S., and Glover III, L., 1995, The EDGE experiment and the U.S. Coast magnetic anomaly: in Banda, E., Talwani, M., and Torne, M. (editors), *Rifted Ocean-Continent Boundaries, NATO/ARW Series Book*, v. 3, pp. 155-181.

Talwani, M., Ewing, J., Sheridan, R.E., Musser, D.L., Glover III, L., Holbrook, S., and Purdy, M., 1992, EDGE lines of the U.S. Mid-Atlantic margin and the East Coast magnetic anomaly: *Eos, Transactions of the American Geophysical Union*, v. 73, no. 14, Fall meeting supplement, pp. 490-491.

Talwani, P., 1982, An internally consistent pattern of seismicity near Charleston, South Carolina: *Geology*, v. 10, pp. 655-658.

Talwani, P., 1999, Fault geometry and earthquakes in continental interiors: *Tectonophysics*, v. 305, pp. 371-379.

Talwani, P., 2000, The Charleston earthquake cycle: *Seismological Research Letters*, v. 71, no. 1, 121 pp.

Talwani, P., 2009, The Source and Magnitude of the Charleston Earthquakes: presentation given at CEUS SSC Project Workshop #2, February 18-20, Palo Alto, Calif.

Talwani, P., Amick, D.C., and Schaeffer, W.T., 1999, *Paleoliquefaction Studies in the South Carolina Coastal Plain*: U.S. Nuclear Regulatory Commission Report NUREG/CR 6619, 109 pp.

Talwani, P., and Cox, J., 1985, Paleoseismic evidence for recurrence of earthquakes near Charleston, South Carolina: *Science*, v. 228, pp. 379-381.

Talwani, P., and Dura-Gomez, I., 2009, Finding faults in the Charleston Area, South Carolina: 2. Complementary data, *Seismological Research Letters*, v. 80, no. 5, pp. 901-919.

Talwani, P., Dura-Gomez, I., Gassman, S., Hasek, M., and Chapman, A., 2008, Studies related to the discovery of a prehistoric sandblow in the epicentral area of the 1886 Charleston SC earthquake: Trenching and geotechnical investigations: *Program and Abstracts, Eastern Section of the Seismological Society of America*, p. 50.

Talwani, P., and Katuna, M., 2004, *Macroseismic Effects of the 1886 Charleston Earthquake*: Carolina Geological Society Field Trip Guidebook, 18 pp.

Talwani, P., Rajendran, C.P., Rajendran, K., and Madabhushi, S., 1993, *Assessment of Seismic Hazard Associated with Earthquake Source in the Bluffton-Hilton Head Area*: Technical Report SCUREF Task Order 41, University of South Carolina at Columbia, 85 pp.

Talwani, P., and Schaeffer, W., 2001, Recurrence rates of large earthquakes in the South Carolina Coastal Plain based on paleoliquefaction data: *Journal of Geophysical Research*, v. 106, pp. 6621-6642.

Tanaka, A., 2004, Geothermal gradient and heat flow data in and around Japan (II): Crustal thermal structure and its relationship to seismogenic layer: *Earth, Planets Space*, v. 56, pp. 1195-1199.

Tanaka, A., and Ishikawa, Y., 2002, Temperature distribution and focal depth in the crust of the northeastern Japan: *Earth, Planets Space*, v. 54, pp. 1109-1113.

Tanaka, A., and Ito, H., 2002, Temperature at the base of the seismogenic zone and its relationship to the focal depth of the western Nagano Prefecture area: *Journal of the Seismological Society of Japan*, v. 55, pp. 1-10. (in Japanese with English abstract)

Tanaka, A., Yamano, M., Yano, Y., and Sasada, M., 2004, Geothermal gradient and heat flow data in and around Japan (I): Appraisal of heat flow from geothermal gradient data: *Earth, Planets Space*, v. 56, pp. 1191-1194.

Tarr, A.C., and Rhea, S., 1983, Seismicity near Charleston, South Carolina, March 1973 to December 1979: in Gohn, G.S. (editor), *Studies Related to the Charleston, South Carolina Earthquake of 1886—Tectonics and Seismicity*, U.S. Geological Survey Professional Paper 1313-R, pp. R1-R17.

Tarr, A.C., Talwani, P., Rhea, S., Carver, D., and Amick, D., 1981, Results of recent South Carolina seismological studies: *Bulletin of the Seismological Society of America*, v. 71, no. 6, pp. 1883-1902.

Tavakoli, B., and Pezeshk, S., 2005, Empirical-stochastic ground-motion prediction for eastern North America: *Bulletin of the Seismological Society of America*, v. 95, pp. 2283-2296.

Tavernier, S.A., and Williams, R.T., 2002, Basement faults in the East Tennessee seismic zone: Observations from the Swan Creek gas field [abstract]: Geological Society of America Joint Annual Meeting, North-Central Section and Southeastern Section, Paper no. 21-0.

Taylor, K.B., Herrmann, R.B., Hamburger, M.W., Pavlis, G.L., Johnston, A., Langer, C., and Lam, C., 1989, The southeastern Illinois earthquake of 10 June 1987: *Seismological Research Letters*, v. 60, pp. 101-110.

Taylor, S.R., and Toksöz, M.N., 1982, Measurements of interstation phase and group velocities and *Q* using Wiener filtering: *Bulletin of the Seismological Society of America*, v. 72, pp. 73-91.

Teague, A.G., Bollinger, G.A., and Johnston, A.C., 1986, Focal mechanism analyses for eastern Tennessee earthquakes (1981-1983): *Bulletin of the Seismological Society of America*, v. 76, pp. 95-109.

Texas BEG, 1997, Tectonic Map of Texas: Bureau of Economic Geology (BEG), University of Texas, Austin.

Thomas, W.A., 1976, Evolution of Ouachita-Appalachian continental margin: *Journal of Geology*, v. 84, pp. 323-342.

Thomas, W.A., 1985, The Appalachian-Ouachita connection: Paleozoic orogenic belt at the southern margin of North America: *Annual Review of Earth and Planetary Sciences*, v. 13, pp. 175-199.

Thomas, W.A., 1988, Early Mesozoic faults of the northern Gulf Coastal Plain in the context of opening of the Atlantic Ocean: in Manspeizer, W. (editor), *Triassic-Jurassic Rifting: Continental Breakup and the Origin of the Atlantic Ocean and Passive Margins*, Developments in Geotectonics series, vol. 22, Elsevier, pp. 463-476.

Thomas, W.A., 1990, Cross sections of Appalachian-Ouachita orogen beneath Gulf Coastal Plain: in Hatcher, R.D. Jr., Thomas, W.A. and Viele, G.W. (editors), *The Appalachian-Ouachita Orogen in the United States*, The Geological Society of America, The Geology of North America, v. F-2, Plates 9 and 11.

Thomas, W.A., 1991, The Appalachian-Ouachita rifted margin of southeastern North America: *Geological Society of America Bulletin*, v. 103, pp. 415-431.

Thomas, W.A., 2006, Tectonic inheritance at a continental margin [2005 GSA presidential address]: *GSA Today*, v. 16, no. 2, pp. 4-11.

Thomas, W.A., 2009, Ouachita Sub-Detachment Structures: presentation given at CEUS SSC Project Workshop #2, February 18-20, Palo Alto, Calif.

Tinti, S., and Mulargia, F., 1985, Effects of magnitude uncertainties on estimating the parameters in the Gutenberg-Richter frequency-magnitude law: *Bulletin of the Seismological Society of America*, v. 75, pp. 1681-1697.

Todd, E., and Ammon, C.J., 2007, Characteristics of recent seismic activity in the Gulf of Mexico: *Eos, Transactions of the American Geophysical Union*, 2007 Annual Fall Meeting Supplement, v. 88, no. 52, Abstract S52B-03.

Toro, G.R., Abrahamson, N.A., and Schneider, J.F., 1997, A model of strong ground motions from earthquakes in central and eastern North America—Best estimates and uncertainties: *Seismological Research Letters*, v. 68, pp. 41-57.

Toro, G.R., and McGuire, R.E., 1987, An investigation into earthquake ground motion characteristics in eastern North America: *Bulletin of the Seismological Society of America*, v. 77, pp. 468-489.

Toro, G.R., and Silva, W.J., 2001, Scenario Earthquakes for Saint Louis, MO, and Memphis, TN, and Seismic Hazard Maps for the Central United States Region Including the Effect of Site Conditions: Final Technical Report, prepared for Risk Engineering, Inc., Boulder, Colo., under USGS External Grant No. 1434-HQ-97-GR-02981.

Tréhu, A., Morel-à-l'Huissier, P., Meyer, R., and 13 others, 1991, Imaging the Midcontinent Rift beneath Lake Superior using large aperture seismic data: *Geophysical Research Letters*, v. 16, no. 4, pp. 625-628.

Trehu, A.M., Ballard, A., Dorman, L.M., Gettrust, J.F., Klitgord, K.D., and Schreiner, A., 1989, Structure of the lower crust beneath the Carolina Trough, U.S. Atlantic Margin: *Journal of Geophysical Research*, v. 94, pp. 10,585-10,600.

Tremblay, A., and Castonguay, S., 2002, Structural evolution of the Laurentian margin revisited (southern Quebec Appalachians): Implications for the Salinian orogeny and successor basins: *Geology*, v. 30, pp. 79-82.

Tremblay, A., and Lemieux, Y., 2001, *Supracrustal Faults of the St. Lawrence Rift System Between Cap-Tourmente and Baie-Saint-Paul, Quebec*: Geological Survey of Canada, Current Research 2001-D15, 21 pp.

Tremblay, A., and Pinet, N., 2005, Diachronous supracrustal extension in an intraplate setting and the origin of the Connecticut Valley—Gaspé and Merrimack troughs, northern Appalachians: *Geological Magazine*, v. 142, pp. 7-22.

Tremblay, A., Long, B., and Massé, M., 2003, Supracrustal faults of the St. Lawrence rift system, Québec: Kinematics and geometry as revealed by field mapping and marine seismic reflection data: *Tectonophysics*, v. 369, pp. 231-252.

Tremblay, A., Ruffet, G., and Castonguay, S., 2000, Acadian metamorphism in the Dunnage zone of southern Québec, Northern Appalachians: 40Ar/39Ar evidence for collision diachronism: *Geological Society of America Bulletin*, v. 112, pp. 136-46.

Trenkamp, R., and Talwani, P., n.d., GPS Derived Strain and Strain Zonation near Charleston, South Carolina: unpublished report ca. 2005.

Treworgy, J.D., 1981, *Structural Features in Illinois—A Compendium*: Illinois State Geological Survey Circular 519, 22 pp.

Trumbore, S.E., 1989, AMS ^{14}C measurements of fractionated soil organic matter: an approach to deciphering the soil carbon cycle: *Radiocarbon*, v. 31, no. 3, pp. 644-654.

Tuttle, M., 2006, Paleoseismic investigation of long-term rates of large earthquakes in the Charlevoix and proposed Rabaska site areas: Preliminary report prepared for Rabaska, Inc., October 9.

Tuttle, M., and Barstow, N., 1996, Liquefaction-related ground failure: A case study in the New Madrid seismic zone, Central United States: *Bulletin of the Seismological Society of America*, v. 86, pp. 636-645.

Tuttle, M., and Chester, J.S., 2005, Paleoseismology Study in the Cache River Valley, Southern Illinois: U.S. Geological Survey, Earthquake Hazards Program, Final Technical Report (Award No. HQ98GR00015), 14 pp.

Tuttle, M., Chester, J., Lafferty, R., Dyer-Williams, K., and Cande, B., 1999, *Paleoseismology Study Northwest of the New Madrid Seismic Zone*: U.S. Nuclear Regulatory Commission, NUREG/CR-5730, 98 pp.

Tuttle, M., Chester, J.S., Lafferty, R., Dyer-Williams, K., Haynes, M., Cande, R., and Sierzchula, M., 1998, Liquefaction features in southwestern Illinois and southeastern Missouri and their implications for paleoseismicity [abstract]: *Eos, Transactions of the American Geophysical Union*, v. 79, p. S342.

Tuttle, M., Law, T., Seeber, L., and Jacob, K., 1990, Liquefaction and ground failure in Ferland, Quebec, triggered by the 1988 Saguenay earthquake: *Canadian Geotechnical Journal*, v. 27, pp. 580-589.

Tuttle, M., and Seeber, L., 1991, Historic and prehistoric earthquake-induced liquefaction in Newbury, Massachusetts: *Geology*, v. 19, no. 6, pp. 594-597.

Tuttle, M.P., 1994, *The Liquefaction Method for Assessing Paleoseismicity*: U.S. Nuclear Regulatory Commission, NUREG/CR-6258, 38 pp.

Tuttle, M.P., 1999, Late Holocene Earthquakes and Their Implications for Earthquake Potential of the New Madrid Seismic Zone, Central United States: Ph.D. dissertation, University of Maryland, 250 pp.

Tuttle, M.P., 2000, Paleoseismological Study in the St. Louis Region: U.S. Geological Survey, Earthquake Hazards Program, Final Technical Report (99-HQ-GR-0032), 29 pp.

Tuttle, M.P., 2001, The use of liquefaction features in paleoseismology: Lessons learned in the New Madrid seismic zone, central United States: *Journal of Seismology*, v. 5, pp. 361-380.

Tuttle, M.P., 2005a, Improving the Earthquake Chronology for the St. Louis Region: U.S. Geological Survey, Earthquake Hazards Program, Annual Project Summary (05HQGR0045), 6 pp.

Tuttle, M.P., 2005b, Paleoseismological Study in the St. Louis Region: Collaborative Research: Final Technical Report, U.S. Geological Survey External Research Award No. 1434-HQ99GR0032, 29 pp.

Tuttle, M.P., 2007, Re-evaluation of Earthquake Potential and Source in the Vicinity of Newburyport, Massachusetts, U.S. Geological Survey, Earthquake Hazards Program, Final Technical Report (01HQGR0163).

Tuttle, M.P., 2008, Paleoseismological investigations at the East Site, The Gilmore/Tyronza Mitigation Project: in *Data Recovery at the Tyronza Sites, Poinsett County, Arkansas, The East Site (3P0610)*, technical report to Arkansas State Highway and Transportation Department, v. 4, pp. 259-277.

Tuttle, M.P., 2009, Re-evaluation of Earthquake Potential and Source in the Vicinity of Newburyport, Massachusetts: *U.S. Geological Survey, Earthquake Hazards Program*, Final Technical Report (03HQGR0031).

Tuttle, M.P., 2010, Search for and Study of Sand Blows at Distant Sites Resulting from Prehistoric and Historic New Madrid Earthquakes: Collaborative Research, M. Tuttle & Associates and Central Region Hazards Team, U.S. Geological Survey, Final Technical Report (02HQGR0097), 48 pp.

Tuttle, M.P., and Atkinson, G.M., 2010, Localization of large earthquakes in the Charlevoix seismic zone, Quebec, Canada, during the past 10,000 years: *Seismological Research Letters*, v. 81, pp. 140-147.

Tuttle, M.P., Collier, J., Wolf, L.W., and Lafferty, R.H., 1999, New evidence for a large earthquake in the New Madrid seismic zone between A.D. 1400 and 1670: *Geology*, v. 27, no. 9, pp. 771-774.

Tuttle, M.P., Cowie, P., and Wolf, L., 1992, Liquefaction induced by modern earthquakes as a key to paleoseismicity: A case study of the 1988 Saguenay earthquake: in Weiss, A. (editor), *Proceedings of the Nineteenth International Water Reactor Safety Information Meeting*, NUREG/CP-0119, v. 3, pp. 437-462.

Tuttle, M.P., Dyer-Williams, K., and Barstow, N.L., 2002, Paleoliquefaction study of the Clarendon-Linden fault system, western New York State: *Tectonophysics*, v. 353, pp. 263-286.

Tuttle, M.P., Hengesh, J., Tucker, K.B., Lettis, W., Deaton, S.L., and Frost, J.D., 2002, Observations and comparisons of liquefaction features and related effects induced by the Bhuj earthquake: *Earthquake Spectra*, v. 18, Supplement A, pp. 79-100.

Tuttle, M.P., Lafferty, R.H., Chester, J.S., and Haynes, M., 1996, Evidence of earthquake-induced liquefaction north of the New Madrid seismic zone, central United States: *Seismological Research Letters*, v. 67, no. 2, p. 58.

Tuttle, M.P., Lafferty, R.H., Guccione, M.J., Schweig, E.S., Lopinot, N., Cande, R.F., Dyer-Williams, K., and Haynes, M., 1996, Use of archaeology to date liquefaction features and seismic events in the New Madrid seismic zone, central United States: *Geoarchaeology: An International Journal*, v. 11, no. 6, pp. 451-480.

Tuttle, M.P., Lafferty, R.H., III, and Schweig, E.S., III, 1998, *Dating of Liquefaction Features in the New Madrid Seismic Zone and Implications for Earthquake Hazard*: U.S. Nuclear Regulatory Commission, NUREG/GR-0017, 77 pp.

Tuttle, M.P., and Schweig, E., 2004, *Search for and Study of Sand Blows at Distant Sites Resulting from Prehistoric and Historic New Madrid earthquakes:* U.S. Geological Survey, Annual Technical Report.

Tuttle, M.P., Schweig, E., III, Campbell, J., Thomas, P.M., Sims, J.D., and Lafferty, R.H., III, 2005, Evidence for New Madrid earthquakes in A.D. 300 and 2350 B.C.: *Seismological Research Letters*, v. 76, no. 4, pp. 489-501.

Tuttle, M.P., and Schweig, E.S., 1995, Archeological and pedological evidence for large earthquakes in the New Madrid seismic zone, central United States: *Geology*, v. 23, no. 3, pp. 253-256.

Tuttle, M.P., and Schweig, E.S., 1996, Recognizing and dating prehistoric liquefaction features: Lessons learned in the New Madrid seismic zone, central United States: *Journal of Geophysical Research*, v. 101, no. B3, pp. 6171-6178.

Tuttle, M.P., and Schweig, E.S., 2000, *Towards a Paleoearthquake Chronology for the New Madrid Seismic Zone*: U.S Geological Survey, Earthquake Hazards Program, Annual Project Summary (99HQGR0022), 9 pp.

Tuttle, M.P., and Schweig, E.S., 2001, *Towards a Paleoearthquake Chronology of the New Madrid Seismic Zone*: U.S. Geological Survey, Earthquake Hazards Program, Progress Report (99HQGR0022), 28 pp.

Tuttle, M.P., Schweig, E.S., and Dyer-Williams, K., 2004, Paleoseismology Study in the St. Louis region, USGS Final Technical Report.

Tuttle, M.P., Schweig, E.S., Sims, J.D., Lafferty, R.H., Wolf, L.W., and Haynes, M.I., 2002, The earthquake potential of the New Madrid seismic zone: *Bulletin of the Seismological Society of America*, v. 92, no. 6, pp. 2080-2089.

Tuttle, M.P., Seeber, L., and Bradley, L., 1987, Liquefaction of glaciomarine sediments during the 1727 earthquake in Newburyport, Massachusetts: in Jacob, K.H. (editor), *Proceedings from the Symposium on Seismic Hazards, Ground Motions, Soil-Liquefaction and Engineering Practice in Eastern North America*, NCEER Technical Report NCEER-87-0025, pp. 467-479.

Tuttle, M.P., Al-Shukri, H., and Mahdi, H., 2006, Very large earthquakes centered southwest of the New Madrid seismic zone 5,000-7,000 years ago: *Seismological Research Letters*, v. 77, pp. 755-770.

Tuttle, M.P., Sims, J.D., Dyer-Williams, K., Lafferty III, R.H., and Schweig III, E.S., 2000, Dating of Liquefaction Features in the New Madrid Seismic Zone: U.S. Nuclear Regulatory Commission, NUREG/GR-0018, 42 pp.

Tuttle, M.P., Such, R., and Seeber, L., 1989, Ground failure associated with the November 25th, 1988 Saguenay earthquake in Quebec Province, Canada: in Jacob, K. (editor), *The 1988 Saguenay Earthquake of November 25, 1988, Quebec, Canada: Strong Motion Data, Ground Failure Observations, and Preliminary Interpretations*, Buffalo, N.Y., National Center for Earthquake Engineering Research, pp. 1-23.

Tuttle, M.P., and Wolf, L.W., 2003, Towards a Paleoearthquake Chronology of the New Madrid Seismic Zone: U.S. Geological Survey, Earthquake Hazards Program, Progress Report (01-HQ-GR-0164), 38 pp.

Urgeles, R., Locat, J., Lee, H.J., and Martin, F., 2002, The Saguenay Fjord, Quebec, Canada: Integrating marine geotechnical and geophysical data for spatial seismic slope stability and hazard assessment: *Marine Geology*, v. 185, pp. 319-340.

U.S. Geological Survey (USGS), 2003, Poster of the Fort Payne, Alabama Earthquake of 29 April 2003—Magnitude 4.6: earthquake summary, http://earthquake.usgs.gov/earthquakes/eqarchives/poster/2003/20030429.php.

U.S. Geological Survey (USGS), 2005, Shuttle Radar Topography Mission (SRTM) 3 Arc Second (~90 meter) data: Earth Resources Observation and Science (EROS) Center, http://eros.usgs.gov/#Find_Data/Products_and_Data_Available/SRTM.

U.S. Geological Survey (USGS), Crustal Database, 2008, Seismic Properties of North America and the Surrounding Ocean Basins, website, http://earthquake.usgs.gov/research/structure /crust/nam.php.

U.S. Geological Survey (USGS), Did You Feel It? website, http://earthquake.usgs.gov /earthquakes/dyfi/, last modified August 3, 2011.

U.S. Geological Survey (USGS), 2010, Earthquake Database (see Section 5.2.1.1.4)

U.S. Geological Survey (USGS), [multiple dates], Quaternary Fault and Fold Database for the United States: continuously updated, http://earthquakes.usgs.gov/regional/qfaults.

U.S. Geological Survey (USGS), Routine United States Mining Seismicity catalog, website, http://earthquake.usgs.gov/earthquakes/eqarchives/mineblast/, last modified August 17, 2011.

U.S. Nuclear Regulatory Commission (NRC), 2007, *Regulatory Guide 1.208: A Performance-Based Approach to Define the Site-Specific Earthquake Ground Motion*: Office of Nuclear Regulatory Research, March.

U.S. Nuclear Regulatory Commission (NRC), 2012, Practical Implementation Guidelines for SSHAC Level 3 and 4 Hazard Studies: NUREG-2117, Office of Nuclear Regulatory Research, 138 pp.

Utsu, T., 1966, A statistical significance test of the difference in b-value between two earthquake groups: *Journal of Physics of the Earth*, v. 14, pp. 37-40.

Valentino, D.W., and Gates, A.E., 1995, Iapetan rift-related turbidite-fan deposits from the central Appalachian Piedmont: *American Journal of Science*, v. 295, pp. 78-97.

Van Arsdale, R., Bresnahan, R., McCallister, N., and Waldron, B., 2007, Upland Complex of the central Mississippi River valley: Its origin, denudation, and possible role in reactivation of the New Madrid seismic zone: in Stein, S., and Mazzotti, S. (editors), *Continental Intraplate Earthquakes: Science, Hazard, and Policy Issues*, Geological Society of America Special Paper 425, pp. 177-192, doi:10.1130/2007.2425(13).

Van Arsdale, R., Counts, R., and Woolery, E., 2009, Quaternary Displacement Along the Hovey Lake Fault of Southern Indiana and Western Kentucky: NEHRP Final report submitted to the U.S. Geological Survey, External Grant Number 07-HQ-GR-0052, 11 pp.

Van Arsdale, R., Purser, J., Stephenson, W., and Odum, J., 1998, Faulting along the southern margin of Reelfoot Lake, Tennessee: *Bulletin of the Seismological Society of America*, v. 88, no. 1, pp. 131-139.

Van Arsdale, R., Ward, C., and Cox, R., 1989, *Post-Pennsylvanian reactivation along the Washita Valley fault, Southern Oklahoma*: U.S. Nuclear Regulatory Commission report, NUREG/CR 5375, 48 pp.

Van Arsdale, R.B., 1986, Quaternary displacement on faults within the Kentucky River fault system of east-central Kentucky: *Geological Society of America Bulletin*, v. 97, no. 11, pp. 1382-1392.

Van Arsdale, R.B., 1998, *Seismic Hazards of the Upper Mississippi Embayment*: U.S. Army Corps of Engineers Waterways Experiment Station Contract Report GL-98-1, 126 pp.

Van Arsdale, R.B., 2000, Displacement history and slip rate on the Reelfoot fault of the New Madrid seismic zone: *Engineering Geology*, v. 55, no. 4, pp. 219-226.

Van Arsdale, R.B., 2009, *Adventures Through Deep Time: The Central Mississippi River Valley and Its Earthquakes*: Geological Society of America Special Paper 455, 107 pp.

Van Arsdale, R.B., Cox, R., and Harris, J., 2002, Investigation of Faulting Beneath the City of Memphis and Shelby County, Tennessee: NEHRP Final report submitted to the U.S. Geological Survey, External Grant Number 02GQGR0053, 33 pp.

Van Arsdale, R.B., Cox, R.T., Johnston, A.C., Stephenson, W.J., and Odum, J.K., 1999, Southeastern extension of the Reelfoot fault: *Seismological Research Letters*, v. 70, no. 3, pp. 348-359.

Van Arsdale, R.B., Schweig, E.S., Kanter, L.R., Williams, R.A., Shedlock, K.M., and King, K.W., 1992, Preliminary shallow seismic reflection survey of Crowley's Ridge, northeast Kansas: *Seismological Research Letters*, v. 63, no. 3, pp. 309-320.

Van Arsdale, R.B., and Sergeant, R.E., 1992, *Post-Pliocene Displacement on Faults Within the Kentucky River Fault System of East-Central Kentucky*: Kentucky Geological Survey, Series 11, Reprint 34, reprinted from U.S. Nuclear Regulatory Commission Report NUREG/CR-4685 (1987), 36 pp.

Van Arsdale, R.B., and TenBrink, R.K., 2000, Late Cretaceous and Cenozoic Geology of the New Madrid Seismic Zone: *Bulletin of the Seismological Society of America*, v. 90, no. 2, pp. 345-356, doi:10.1785/0119990088.

Van Arsdale, R.B., Williams, R.A., Schweig, E.S., Shedlock, K.M., Odum, J.K., and King, K.W., 1995, The origin of Crowley's Ridge, northeastern Arkansas: Erosional remnant or tectonic uplift? *Bulletin of the Seismological Society of America*, v. 85, no. 4, pp. 963-985.

Van Avendonk, H.J.A, Lavier, L.L., Shillington, D.J., and Manatschal, G., 2009, Extension of continental crust at the margin of the eastern Grand Banks Newfoundland: *Tectonophysics*, v. 468, no. 1-4, pp. 131-148.

Van Dyck, J., 1986, Statistical Analysis of Earthquake Catalogs: Ph.D. thesis, Massachusetts Institute of Technology, 430 pp.

van Lanen, X., and Mooney, W.D., 2007, Integrated geologic and geophysical studies of North American continental intraplate seismicity: in Stein, S., and Mazzotti, S. (editors), *Continental Intraplate Earthquakes: Science, Hazard, and Policy Issues*, Geological Society of America Special Paper 425, pp. 101-112.

Van Schmus, W.R., 1992, Tectonic setting of the Midcontinent Rift System: *Tectonophysics*, v. 213, pp. 1-15.

Van Schmus, W.R., Bickford, M.E., and Turek, A., 1996, Proterozoic geology of the east-central Midcontinent basement: in van der Pluijm, B.A., and Catacosinos, P.A. (editors), *Basement and Basins of Eastern North America*, Geological Society of America Special Paper 308, pp. 7-32.

Van Schmus, W.R., Schneider, D.A., Holm, D.K., Dodson, S., and Nelson, B.K., 2007, New insights into the southern margin of the Archean-Proterozoic boundary in the north-central United States based on U-Pb, Sm-Nd, and Ar-Ar geochronology: *Precambrian Research*, v. 157, pp. 80-105.

Vaughn, J.D., 1991, Evidence for multiple generations of seismically induced liquefaction features in the Western Lowlands, southeast Missouri [abstract]: *Seismological Research Letters*, v. 62, p. 189.

Vaughn, J.D., 1992, Active tectonics in the Western Lowlands of southeast Missouri: An initial assessment: *Missouri Department Natural Resources Special Publication No. 8*, pp. 54-59.

Vaughn, J.D., 1994, *Paleoseismological Studies in the Western Lowlands of Southeast Missouri*: Report to NEHRP Annual External Program, Contract No. 14-08-0001-G1931, 27 pp.

Vaughn, J.D., Obermeier, S.F., Hatcher, R.D., Howard, C.W., Mills, H.H., and Whisner, S.C., 2010, Evidence for one or more major late-Quaternary earthquakes and surface faulting in the East Tennessee seismic zone [abstract]: *Seismological Research Letters*, v. 81, no. 2, p. 323.

Velasco, M., Van Arsdale, R., Waldron, B., Harris, J., and Cox, R., 2005, Quaternary faulting beneath Memphis, Tennessee: *Seismological Research Letters*, v. 76, no. 5, pp. 598-614.

Veneziano, D., and Van Dyck, J., 1985, Statistical discrimination of aftershocks and their contribution to seismic hazard: in *Seismic Hazard Methodology for Nuclear Facilities in the Eastern U.S.*, Volume 2, Appendix A-4, EPRI/SOG Draft 85-1.

Viele, G.W., and Thomas, W.A., 1989, Tectonic synthesis of the Ouachita orogenic belt: in Hatcher, R.D., Jr., Thomas, W.A., and Viele, G.W. (editors), *The Appalachian-Ouachita Orogen in the United States*, Geological Society of America, The Geology of North America, v. F-2, pp. 695-728.

Virginia Tech Seismological Observatory, Southeastern United States Seismic Network (SEUSSN) bulletins and southeastern U.S. earthquake catalog, website, http://www.geol.vt.edu/outreach/vtso/anonftp/catalog/.

Vlahovic, G., Powell, C.A., Chapman, M.C., and Sibol, M.S., 1996, P and S wave velocity structure and hypocenter locations in the eastern Tennessee seismic zone: *Seismological Research Letters*, v. 67, no. 2, p. 59.

Vlahovic, G., Powell, C., Chapman, M., and Sibol, M., 1998, Joint hypocenter-velocity inversion for the Eastern Tennessee seismic zone: *Journal of Geophysical Research*, v. 103, no. B3, pp. 4879-4896.

Vogel, J.C., Fuls, A., Visser, E., and Becker, B., 1993, Pretoria calibration curve for short lived samples: *Radiocarbon*, v. 33, pp. 73-86.

Wald, D., Quitoriano, V., Dengler, L., and Dewey, J., 1999. Utilization of the Internet for rapid community intensity maps: *Seismological Research Letters*, v. 70, pp. 680-697.

Walker, M., 2005, *Quaternary Dating Methods*: John Wiley and Sons, Ltd, West Sussex, England, 286 pp.

Walker, W.M., 2006, Structural Analysis of the Criner Hills, South-Central Oklahoma: M.S. thesis, Baylor University, Waco, Tex.

Walker, J.D., and Geissman, J.W., compilers, 2009, Geologic Time Scale: Geological Society of America, doi: 10.1130/2009.CTS004R2C.

Walsh, G.J., and Aleinikoff, J.N., 1999, U-Pb zircon age of metafelsite from the Pinney Hollow Formation: Implications for the development of the Vermont Appalachians: *American Journal of Science*, v. 299, pp. 157-170.

Watkins, J.S., Bradshaw, B.E., Huh, S., Li, R., and Zhang, J., 1996, Structure and distribution of growth faults in the northern Gulf of Mexico OCS: in Jones, J., and Freed, R.L. (editors), *Structural Framework of the Gulf of Mexico*, Special Publication of the Association of Geological Societies, 45th Annual Research Conference of the Gulf Coast Section SEPM, San Antonio, Texas, October 2-4, 1996, pp. 63-77.

Watkins, J.S., and Buffler, R.T., 1996, Gulf of Mexico deepwater frontier exploration potential: in Jones, J., and Freed, R.L. (editors), *Structural Framework of the Gulf of Mexico*, Special Publication of the Association of Geological Societies, 45th Annual Research Conference of the Gulf Coast Section SEPM, San Antonio, Texas, October 2-4, 1996, pp. 79-92.

Watkins, J.S., MacRae, G., and Simmons, G., 1996, Bipolar simple-shear rifting responsible for distribution of mega-salt basins in Gulf of Mexico? in Jones, J., and Freed, R.L. (editors), *Structural Framework of the Gulf of Mexico*, Special Publication of the Association of Geological Societies, 45th Annual Research Conference of the Gulf Coast Section SEPM, San Antonio, Texas, October 2-4, 1996, pp. 297-305.

Weems, R.E., and Edwards, L.E., 2007, Post-middle Miocene origin of modern landforms in the eastern Piedmont of Virginia: *Stratigraphy*, v. 4, no. 1, pp. 35-48.

Weems, R.E., and Lewis, W.C., 2002, Structural and tectonic setting of the Charleston, South Carolina, region: Evidence from the Tertiary stratigraphic record: *Geological Society of America Bulletin*, v. 114, no. 1, pp. 24-42.

Weems, R.E., and Obermeier, S.F., 1990, The 1886 Charleston earthquake—An overview of geological studies: in *Proceedings of the U.S. Nuclear Regulatory Commission Seventeenth Water Reactor Safety Information Meeting*, NUREG/CP-0105, v. 2, pp. 289-313.

Weems, R.E., Obermeier, S.F., Pavich, M.J., Gohn, G.S., and Rubin, M., 1986, Evidence for Three Moderate to Large Prehistoric Holocene Earthquakes Near Charleston, South Carolina: in *Proceedings of the 3rd U.S. National Conference on Earthquake Engineering, Charleston, South Carolina*, v. 1, pp. 3-13.

Weichert, D.H., 1980, Estimation of the earthquake recurrence parameters for unequal observation periods for different magnitudes: *Bulletin of the Seismological Society of America*, v. 70, no. 4, pp. 1337-1346.

Wells, D.L., and Coppersmith, K.J., 1994, New empirical relationships among magnitude, rupture length, rupture width, rupture area, and surface displacement: *Bulletin of the Seismological Society of America*, v. 84, pp. 974-1,002.

Wentworth, C.M., and Mergner-Keefer, M., 1983, Regenerate faults of of small Cenozoic offset—Probable earthquake sources in the southeastern United States: in Gohn, G.S. (editor), *Studies Related to the Charleston, South Carolina, Earthquake of 1886—Tectonics and Seismicity*, U.S. Geological Survey Professional Paper 1313-S, pp. S1-S20.

Wesnousky, S.G., 2008, Displacement and geometrical characteristics of earthquake surface ruptures: Issues and implications for seismic-hazard analysis and the process of earthquake rupture: *Bulletin of the Seismological Society of America*, v. 98, no. 4, pp. 1609-1632.

Wesnousky, S.G., and Johnson, D.L., 1996, Stratigraphic, paleosol, and C-14 evidence for a large pre-1811 magnitude earthquake in the New Madrid seismic zone: *Seismological Research Letters*, v. 67, no. 2, p. 60.

Wesson, R.L., and Nicholson, C. (editors), 1986, *Studies of the January 31, 1986, Northeastern Ohio Earthquake—A Report to the U.S. Nuclear Regulatory Commission*: U.S. Geological Survey Open-File Report 86-331.

West, D.P., Jr., and Roden-Tice, M.K., 2003, Late Cretaceous reactivation of the Norumbega fault zone, Maine: Evidence from apatite fission-track ages: *Geology*, v. 31, pp. 649-652.

Weston Observatory Northeast Earthquake Catalogs, website, http://www.bc.edu/research/westonobservatory/northeast/eqcatalogs.html, last updated May 16, 2011.

Wetmiller, R.J., and Adams, J., 1990, An earthquake doublet in the Charlevoix seismic zone, Quebec: *Current Research, Part B, Geological Survey of Canada*, Paper 90-1, pp. 105-113.

Wetmiller, R.J., Adams, J., Anglin, F.M., Hasegawa, H.S., and Stevens, A.E., 1984, Aftershock sequences of the 1982 Miramichi, New Brunswick, earthquakes: *Bulletin of the Seismological Society of America*, v. 74, pp. 621-653.

Wheeler, R.L., 1995, Earthquakes and the cratonward limit of Iapetan faulting in eastern North America: *Geology*, v. 23, no. 2, pp. 105-108.

Wheeler, R.L., 1996, Relative seismic hazards of six Iapetan rifts and grabens in southeastern North America [abstract]: *Seismological Research Letters*, v. 67, no. 2, p. 60.

Wheeler, R.L., 1997, Boundary separating the seismically active Reelfoot rift from the sparsely seismic Rough Creek graben, Kentucky, and Illinois: *Seismological Research Letters*, v. 68, no. 4, pp. 586-598.

Wheeler, R.L. (compiler), 1999a, Fault number 707, Brockton-Froid fault zone, in Quaternary fault and fold database of the United States: U.S. Geological Survey website, http://earthquakes.usgs.gov/regional/qfaults.

Wheeler, R.L. (compiler), 1999b, Fault number 924, Gulf-margin normal faults, Texas, in Quaternary fault and fold database of the United States: U.S. Geological Survey website, http://earthquakes.usgs.gov/regional/qfaults.

Wheeler, R.L., 2002, Distinguishing seismic from non-seismic soft-sediment structures: Criteria from seismic hazard analysis: in Ettensohn, F.R., Rast, N., and Brett, C.E., eds., *Ancient Seismites*, Geological Society of America Special Paper 359, pp. 1-11.

Wheeler, R.L., 2005, *Known or Suggested Quaternary Tectonic Faulting, Central and Eastern United States—New and Updated Assessments for 2005*: U.S. Geological Survey Open-File Report 2005-1336, 40 pp.

Wheeler, R.L., 2009, *Methods of Mmax Estimation East of the Rocky Mountains*: U.S. Geological Survey Open-File Report 2009-1018, 44 pp.

Wheeler, R.L., and Cramer, C.H., 2002, Updated seismic hazard in the southern Illinois basin: Geological and geophysical foundations for use in the 2002 USGS national seismic-hazard maps: *Seismological Research Letters*, v. 73, no. 5, pp. 776-791.

Wheeler, R.L., and Crone, A.J., 2001, Known and suggested Quaternary faulting in the midcontinent United States: *Engineering Geology*, v. 62, pp. 51-78.

Wheeler, R.L., and Crone, A.J., 2003, Reply to "Comment on evaluation of Meers fault, Oklahoma in 'Known and suggested Quaternary faulting in the midcontinent United States' by Russell L. Wheeler and Anthony J. Crone": *Engineering Geology*, v. 69, pp. 211-215.

Wheeler, R.L., and Frankel, A.D., 2000, Geology in the 1996 USGS seismic-hazard maps, central and eastern United States: *Seismological Research Letters*, v. 71, pp. 273-282.

Wheeler, R.L., and Johnston, A.C., 1992, Geologic implications of earthquake source parameters in central and eastern North America: *Seismological Research Letters*, v. 63, no. 4, pp. 491-505.

Wheeler, R.L., Rhea, S., and Dart, R.L., 1994, Map Showing Structure of the Mississippi Valley Graben in the Vicinity of New Madrid, Missouri: U.S. Geological Survey Miscellaneous Field Studies Map MF-2264-D.

Wheeler, R.L., Rhea, S., Diehl, S.F., Drahovzal, J.A., Bear, G.W., and Sargent, M.L., 1997, Seismotectonic Map Showing Faults, Igneous Rocks, and Geophysical and Neotectonic Features in the Vicinity of the Lower Wabash Valley, Illinois, Indiana, and Kentucky: U.S. Geological Survey Geologic Investigations Series I-2583-D, scale 1:250,000.

Whisner, S.C., Hatcher, R.D., Jr., and Munsey, J.W., 2003, Disturbed sediments in the East Tennessee seismic zone: Evidence of large prehistoric earthquakes in East Tennessee? *Southeastern Geology*, v. 42, no. 2, pp. 1-16.

White, D.J., Easton, R.M., Culshaw, N.G., Milkereit, B., Forsyth, D.A., Carr, S., Green, A.G., and Davidson, A., 1994, Seismic images of the Grenville orogen in Ontario: *Canadian Journal of Earth Sciences*, v. 31, pp. 293-307.

White, D.J., Forsyth, D.A., Asudeh, I., Carr, S.D., Wu, H., Easton, R.M., and Mereu, R.F., 2000, A seismic-based cross-section of the Grenville orogen in southern Ontario and western Quebec: *Canadian Journal of Earth Sciences*, v. 37, pp. 183-192.

White, G., 1980, Permian-Triassic continental reconstruction of the Gulf of Mexico−Caribbean area: *Nature*, v. 283, pp. 823-826.

Whitmeyer, S.J., and Karlstrom, K.E., 2007, Tectonic model for the Proterozoic growth of North America: *Geosphere*, v. 3, no. 4, pp. 220-259.

Widmann, B.L. (compiler), 1997a, Fault number 2327, Ute Pass fault zone, in Quaternary fault and fold database of the United States: U.S. Geological Survey website, http://earthquakes.usgs.gov/regional/qfaults, accessed April 28, 2009.

Widmann, B.L. (compiler), 1997b, Fault number 2328, Rampart Range fault, in Quaternary fault and fold database of the United States: U.S. Geological Survey website, http://earthquakes.usgs.gov/regional/qfaults, accessed May 5, 2009.

Widmann, B.L. (compiler), 1997c, Fault number 2329, Goodpasture fault, in Quaternary fault and fold database of the United States: U.S. Geological Survey website, http://earthquakes.usgs.gov/regional/qfaults, accessed May 6, 2009.

Wildermuth, E., and Talwani, P., 2001, A detailed gravity survey of a pull-apart basin in northeast South Carolina [abstract]: Geological Society of America *Abstracts with Programs*, v. 33, no. 6, p. 240.

William Lettis & Associates, Inc. (WLA), 2006, Investigation of Holocene Faulting at Proposed C-746 Landfill Expansion: prepared for Kentucky Research Consortium for Energy and Environment, UK/KRCEE Doc # P17.6 2006, University of Kentucky.

Williams, D.A., 1991, *Paleozoic Geology of the Ottawa–St. Lawrence Lowland, Southern Ontario*: Ontario Geological Survey, Open File Report 5770, 292 pp.

Williams, H., 1978, Tectonic Lithofacies Map of the Appalachian Orogen, Map 1a: Memorial University of Newfoundland, St. Johns.

Williams, H., and Hatcher, R.D., Jr., 1983, Appalachian suspect terranes: in Hatcher, R.D., Jr., Williams, H., and Zietz, I. (editors), *The Tectonics and Geophysics of Mountain Chains*, Geological Society of America Memoir 158, pp. 33-53.

Williams, R.A., Luzietti, E.A., and Carver, D.L., 1995, High-resolution seismic imaging of Quaternary faulting on the Crittenden County fault zone, New Madrid seismic zone, northeastern Arkansas: *Seismological Research Letters*, v. 66, no. 3, pp. 42-57.

Williams, R.A., Stephenson, W.J., and Odum, J.K., 2009, Post-Eocene Deformation Observed in Seismic Profiles Across the Southwestern Blytheville Arch, Crowley's Ridge, and Western Reelfoot Rift Margin, Arkansas: presentation given at meeting of CEUS Earthquake Hazards Program, U.S. Geological Survey, October 28-29, Memphis, Tenn.

Williams, R.A., Stephenson, W.J., Odum, J.K., and Worley, D.M., 2001, Seismic-reflection imaging of Tertiary faulting and related post-Eocene deformation 20 km north of Memphis, Tennessee: *Engineering Geology*, v. 62, pp. 79-90.

Williams, R.T., Robinson, E.S., and Law, R.D., 2000, Folding and faulting of Plio-Pleistocene sediments in Giles County, SW Virginia—(2) Ground-penetrating radar and seismic reflection data [abstract]: Geological Society of America *Abstracts with Programs*, v. 32 no. 2, p. 83.

Williamson, S.C., 1996, Observations on the Capability of the Criner Fault, Southern Oklahoma: M.S. thesis, Texas A&M, College Station, Tex.

Willoughby, R.H., and Nystrom, P.G., Jr., 2005, Generalized Geologic Map of South Carolina: South Carolina Geological Survey Generalized Geologic Map Series GGMS, scale 1:1,000,000.

Wintle, A.G. and Murray, A.S., 1997, The Relationship Between Quartz Thermoluminescence, Photo-Transferred Luminescence, and Optically Stimulated Luminescence: Radiation Measurements, v. 27, no. 4, pp. 611-624.

Wise, D.U., and Faill, R.T., 1998, Lancaster County seismic zone (Penna.): Reactivation of a Taconic structural feature [abstract]? Geological Society of America *Abstracts with Programs*, v. 30, no. 7, pp. A-320.

Withers, M.M., Herrmann, R.B., and Benz, H.M., 2009, Introduction and background for the April 18, 2008 Illinois earthquake [abstract]: *Seismological Research Letters*, v. 80, no. 2, p. 301.

Withjack, M.O., Schlische, R.W., and Olsen, P.E., 1998, Diachronous rifting, drifting, and inversion on the passive margin of central eastern North America: An analog for other passive margins: *AAPG Bulletin*, v. 82, no. 5A, pp. 817-835.

Withjack, M.O., Schlische, R.W., and Olsen, P.E., 2002, Rift-basin structure and its influence on sedimentary systems: in Renault, R.W., and Ashley, G.M. (editors), *Sedimentation in Continental Rifts*, SEPM (Society for Sedimentary Geology) Special Publication, no. 73, pp. 57-81.

Wolf, L.W., 2004, *Geophysical Investigations of Earthquake-Induced Liquefaction Features in the New Madrid Seismic Zone*: Earthquake Hazards Program, Final Technical Report (01HQGR0003), 36 pp.

Wolf, L.W., Collier, J., Tuttle, M., and Bodin, P., 1998, Geophysical reconnaissance of earthquake-induced liquefaction features in the New Madrid seismic zone: *Journal of Applied Geophysics*, v. 39, pp. 121-129.

Wolf, L.W., Tuttle, M.P., Browning, S., and Park, S., 2006, Geophysical surveys of earthquake-induced liquefaction deposits in the New Madrid seismic zone: *Geophysics*, v. 71, no. 6, pp. B223-230.

Wong, I., Olig, S., Dober, M., Wright, D., Nemser, E., Lageson, D., Silva, W., Stickney, M.S., Lemieux, M., and Anderson, L., 2005, *Probabilistic Earthquake Hazard Maps for the State of Montana*: Montana Bureau of Mines and Geology, Special Publication 117, 72 pp.

Woolery, E.W., 2005, Geophysical and geological evidence of neotectonic deformation along the Hovey Lake fault, lower Wabash Valley fault system, central United States: *Bulletin of the Seismological Society of America*, v. 95, no. 3, pp. 1193-1201.

Woolery, E.W., and Street, R., 2002, Quaternary fault reactivation in the Fluorspar Area fault complex of western Kentucky: Evidence from shallow SH-wave reflection profiles: *Seismological Research Letters*, v. 73, no. 5, pp. 628-639.

Woolery, E.W., Baldwin, J., Kelson, K., Hampson, S., and Givler, R., 2009, Site-Specific Fault Rupture Hazard Assessment—Fluorspar Area Fault Complex, Western Kentucky: presentation given at meeting of CEUS Earthquake Hazards Program, U.S. Geological Survey, October 28-29, Memphis, Tenn.

Working Group on California Earthquake Probabilities (Working Group), 2003, *Earthquake Probabilities in the San Francisco Bay Region: 2002-2031*: U.S. Geological Survey Open-File Report 03-214.

Wu, S., Bally, A.W., and Cramez, C., 1990, Allochthonous salt, structure and stratigraphy of the north-eastern Gulf of Mexico. Part II: Structure: *Marine and Petroleum Geology*, v. 7, no. 4, pp. 334-370.

Yang, H., Zhu, L., and Chu, R., 2009, Determination of the fault plane for the April 18, 2008 Illinois earthquake by detecting and relocating aftershocks [abstract]: *Seismological Research Letters*, v. 80, no. 2, pp. 302-303.

Youd, T.L., 1984, Geologic effects—Liquefaction and associated ground failure: U.S. Geological Survey Open-File Report 84-760, pp. 210-232.

Youd, T.L., Idriss, I.M., Andrus, R.D., Arango, I., Castro, G., Christian, J.T., Dobry, R., Finn, W.D.L., Harder, L.F., Hynes, M.E., Ishihara, K., Koester, J.P., Liao, S.S.C., Marcuson, W.F., Martin, G.R., Mitchell, J.K., Moriwaki, Y., Power, M.S., Robertson, P.K., Seed, R.B., and Stokoe, K.H., 2001, Liquefaction resistance of soils: Summary report from the 1996 NCEER and 1998 NCEER/NSF workshops on evaluation of liquefaction resistance of soils: *Journal of Geotechnical and Geoenvironmental Engineering*, v. 127, no. 4, pp. 297-313.

Youngs, R.R., and Coppersmith, K.J., 1985, Implications of fault slip rates and earthquake recurrence models to probabilistic hazard estimates: *Bulletin of the Seismological Society of America*, v. 75, pp. 939-964.

Zartman, R.E., 1977, Geochronology of some alkalic rock provinces in eastern and central United States: *Annual Review of Earth and Planetary Sciences*, v. 5, pp. 257-286.

Zelt, C.A., Forsyth, D.A., Milkereit, B., White, D.J., and Asudeh, I., 1994, Seismic structure of the Central Metasedimentary Belt, southern Grenville Province: *Canadian Journal of Earth Sciences*, v. 31, pp. 243-254.

Zhang, Q., Sandvol, E., and Liu, M., 2009a, Lithospheric velocity structure of the New Madrid Seismic Zone: A joint teleseismic and local P tomographic study: *Geophysical Research Letters*, v. 36, doi:10.1029/2009GL037687.

Zhang, Q., Sandvol, E., and Liu, M., 2009b, Tomographic *Pn* velocity and anisotropy structure in the central and eastern United States: *Bulletin of the Seismological Society of America*, v. 99, pp. 422-427.

Zoback, M.D., 2010, Update to stress map of the CEUS, conducted as part of CEUS SSC Project.

Zoback, M.D., Hamilton, R.M., Crone, A.J., Russ, D.P., McKeown, F.A., and Brockman, S.R., 1980, Recurrent intraplate tectonism in the New Madrid seismic zone: *Science*, v. 209, pp. 971-976.

Zoback, M.D., and Zoback, M.L., 1991, Tectonic stress field of North America and relative plate motions: in Slemmons, D.B., Engdahl, E.R., Zoback, M.D., and Blackwell, D.D. (editors), *Neotectonics of North America*, Geological Society of America, Decade Map Volume 1.

Zoback, M.L., 1992, Stress field constraints on intraplate seismicity in eastern North America: *Journal of Geophysical Research*, v. 97, no. B8, pp. 11,761-11,782.

Zoback, M.L., and Zoback, M.D., 1989, Tectonic stress field of the continental U.S.: in Pakiser, L.C., and Mooney, W.D. (editors), *Geophysical Framework of the Continental United States*, GSA Memoir, v. 172, pp. 523-539.

11

CHAPTER 11
GLOSSARY OF KEY TERMS

Definitions provided in this Glossary were compiled from multiple reference sources, including the SSHAC guidance in NUREG/CR-6372 (Budnitz et al., 1997), NUREG-2117 (NRC, 2012), and McGuire (2004). The Glossary definitions are consistent with the use of the terms in the CEUS SSC Project report and may not correspond exactly to definitions appearing in regulatory documents of NRC or DOE. For additional geological terms, the reader is referred to a standard glossary of geology (e.g., Neuendorf, K.K.E., Mehl, J.P., Jr., and Jackson, J.A., 2005, *Glossary of Geology*, 5th Edition, American Geological Institute, Alexandria, Va., 779 pp.). Throughout this report, designations for formal (capitalized) divisions of time periods followed a Geological Society of America geologic time scale (Walker and Geissman, 2009), provided in Figure 11-1.

Active Fault: A fault that has slipped in geologically recent time, has a clear association with earthquakes, and is likely to slip again in the future. Quaternary faults (i.e., those whose most recent slip was in the past 1.6–1.7 Myr) are generally considered to be active.

Active Source: A seismic source that is capable of generating moderate- to large-magnitude ($M \geq 5$) earthquakes.

Aleatory Uncertainty: The uncertainty that is inherent in a random phenomenon and cannot be reduced by acquiring additional data or information. Examples include future earthquake locations and magnitudes.

Area Source: A region of the earth's crust that is assumed for PSHA to have relatively uniform seismic source characteristics.

Background Source: A regional-scale area source.

Bayesian Approach: An approach to determine a maximum magnitude distribution defined by Johnston et al. (1994) that uses a prior distribution for Mmax developed from the worldwide Stable Continental Region (SCR) database. It assumes that crust with the same characteristics (extension history, age, stress state, angle of structure relative to stress) has the same *prior* distribution of Mmax. The approach updates the prior distribution with a likelihood function that includes local information on the maximum observed magnitude and numbers of observed earthquakes of various magnitude. The result is a *posterior* distribution of Mmax for an individual seismic source.

***b*-value:** A parameter describing the decrease in the relative frequency of occurrence of earthquakes of increasing sizes. It is the slope of a straight line relating absolute or relative frequency (plotted logarithmically in base 10) to earthquake magnitude. It is referred to as β when using natural logarithms.

Coefficient of Variation (COV): A statistical term that measures the relative variation of a quantity. It is calculated as the standard deviation of the quantity divided by the mean of the quantity.

Conceptual SSC Framework: The seismotectonic and seismic hazard-informed context within which data are evaluated and seismic sources are defined and characterized.

Data Evaluation Table: A table developed for a particular seismic source identified in the CEUS SSC Project that provides a summary of the data used for seismic source characterization, including the quality of the data and the reliance placed on it for SSC.

Data Summary Table: A table developed for a particular seismic source identified in the CEUS SSC Project that records the data considered and summarizes the potential relevance that the data may have to seismic source characterization.

Declustering: A statistical approach that removes foreshocks and aftershocks to produce a catalog of independent main shocks consistent with the requirements of a PSHA model. Comparison with a variety of declustering approaches used by the USGS and others showed that the results are essentially the same.

Distance, Epicentral: The distance from the epicenter to a specific location (site).

Distance, Fault: The shortest distance from the fault to a specific location (site).

Distance, Hypocentral: The distance from the hypocenter to a specific location (site).

Earthquake: A sudden motion or trembling of the earth caused by the abrupt release of accumulated strain.

Epistemic Uncertainty: The uncertainty that arises from lack of knowledge about a model or a parameter, which can be reduced by the accumulation of additional information. Epistemic uncertainty is reflected in the different outcomes of viable alternative models, interpretations, and/or assumptions operating on the same data. Examples include geometry of seismotectonic zones and assessed source parameters such as maximum magnitude.

Evaluator Expert: An expert who is capable of evaluating the relative credibility of multiple alternative hypotheses to explain a set of observations. Requires considering the available data, listening to proponent and other evaluator experts, questioning the technical basis for their conclusions, and challenging the proponent’s position.

Expert Elicitation: A formal expert assessment technique of conventional decision analysis in which experts are led through a series of assessment steps to address narrowly defined questions about specific uncertain quantities within their area of expertise.

Expert Assessment: The use of expert judgment to address technical questions and their uncertainties.

Fault: A fracture surface or zone in the earth across which there has been relative displacement.

Fault, Dip-Slip: A fault in which the relative displacement is along the direction of the dip of the fault plane; either downdip (normal fault) or updip (reverse fault).

Fault, Normal: A dip-slip fault in which the block above the fault has moved downward relative to the block below, representing crustal extension.

Fault, Reverse: A dip-slip fault in which the block above the fault has moved upward relative to the block below, and the fault dip is >45°.

Fault Slip Rate: The amount of displacement on a fault divided by the time period over which the displacement took place.

Fault, Strike-Slip: A fault in which the relative displacement is along the strike of the fault plane, either right- or left-lateral.

Fault, Thrust: A dip-slip fault in which the block above the fault has moved upward relative to the block below, and the fault dip is <45°, representing crustal compression.

Fault Zone: The zone of deformation comprising a fault, which may be hundreds of meters wide.

Focal Mechanism: A geometrical representation of earthquake faulting expressed in terms of the strike and dip of the fault plane and the rake angle of the slip vector with respect to the fault plane.

Future Earthquake Characteristics: The expected characteristics of future earthquakes that occur within a particular seismic source. The characteristics identified (e.g., style of faulting, orientation of rupture) are those that are potentially important to ground motion prediction equations.

Geon: A 100-million-year interval of geologic time starting with the present and continuing backward through time. Geons are named according to the number representing geologic age divided by 100 million. Geologic ages less than 100 million years would be in geon 0. For example, an age of 1,650 million years would belong to geon 16.

Hazard Calculation: The calculation of annual frequencies with which seismic ground-motion amplitudes will be exceeded as a result of possible earthquakes in the region. The results of this calculation may be represented as mean annual frequencies ("mean hazard curves") or fractile annual frequencies ("fractile hazard curves").

Hazard-Informed Approach: An assessment methodology for characterizing seismic sources that places greatest emphasis and focus on those seismic source elements that are most important to the hazard analysis results.

Hazard Input Document (HID): A report that provides the documentation necessary for users to implement the input model (e.g., the SSC or GMC model) in PSHA calculations for future applications. The HID includes the logic tree structure (with all branches and weights) for each seismic source, but it does not include the technical basis or justification for the elements of the model.

Hypocenter: The point in the earth at which an earthquake is initiated. Also referred to as the *focus*.

Informed Technical (Scientific) Community: A hypothetical construct of the SSHAC guidelines that embodies the community distribution of uncertainty sought by the SSHAC process at any study level. The goal of a SSHAC process is to "represent the center, body, and range of the views of the informed technical community." "Informed" means that the technical community is familiar with the project-specific databases and that the individuals have gone through the interactive SSHAC process. Recent SSHAC implementation guidance (NRC, 2011) has replaced the terminology to avoid confusion. In that guidance, the goal of the SSHAC process is said to be twofold: (1) to consider the data, models, and methods of the larger technical community; and (2) to represent the center, body, and range of technically defensible interpretations.

Intensity: A measure of the effects (e.g., damage) of an earthquake at a particular place. Commonly used scales are Rossi-Forel, Mercalli, and modified Mercalli.

Liquefaction/Paleoliquefaction: The temporary conversion of water-saturated, unconsolidated soils (sediments) into a medium that behaves like a fluid. It can occur as a secondary hazard related to strong shaking from an earthquake. The age, location, and extent of liquefaction can be used to estimate the size and location of prehistoric earthquakes.

Logic Tree: A series of nodes and branches to sequence the assessments in an analysis by describing alternative models or parameter values or both. At each node, there is a set of branches that represent the range of alternative credible models or parameter values; the branch weights must sum to unity at each node. The weights on the branches of logic trees reflect scientific judgments in the relative confidence in the alternative models.

Longevity, Hazard Studies: The length of time a hazard study is considered adequate for continued use.

Magnitude (general): A measure of earthquake size, classically determined by taking the common logarithm (base 10) of the largest ground motion recorded during the arrival of a seismic wave type and applying a standard correction for distance to the epicenter.

Magnitude, Adjusted (M*): Moment magnitude adjusted to correct for a bias that results from the propagation of uncertainty in magnitude estimates through the magnitude conversion process.

Magnitude, Body-Wave (m_b): Magnitude derived from the largest displacement amplitude of body waves.

Magnitude, Coda-Wave (M_C): Magnitude derived from the amplitude and duration of the seismic coda (latter part of a seismic wave train).

Magnitude, Duration (M_D): Magnitude derived from the total duration of the measured seismic wave train.

Magnitude, Lg (m_{bLg}): Magnitude derived from the displacement amplitude of Lg waves; often used in Eastern North America because it can be accurately measured from typical low-gain seismographs at long distances from the source.

Magnitude, Moment (M, M_w): Magnitude derived from the scalar seismic moment, M_o. Approximately equal to local magnitude for moderate earthquakes, and to surface-wave magnitude for large earthquakes. As discussed in Hanks and Kanamori (1979), M_w is derived from Kanamori's (1977) magnitude scale based on strain energy drop and is given by the relationship log(M_o in dyne-cm) = $1.5M_w + 16.1$. Hanks and Kanamori (1979) defined the moment magnitude scale **M** using the relationship **M** = ⅔log(M_o in dyne-cm)-10.7. The result is a 0.03-magnitude unit difference between M_w and **M** for the same value of M_o.

Magnitude, Richter or Local (M_L): Common logarithm of the trace amplitude (in microns) of a standard Wood-Anderson seismograph located on firm ground 100 km from the epicenter. Correction tables are used to account for other distances and ground conditions.

Magnitude, Surface-Wave (M_S): Earthquake magnitude determined from the maximum amplitude of 20-second period surface waves.

Maximum Magnitude (M_{max}): The largest earthquake that a seismic source is assessed to be capable of generating. The maximum magnitude is the upper bound to recurrence curves.

Modeling Uncertainty: The epistemic uncertainty that results from the use of various models to explain observed data and predict future phenomena. In principle, it can be reduced or eliminated by further testing, data accumulation, or more detailed modeling. It is one source of epistemic uncertainty.

Paleoseismic/Paleoseismicity: Term referring to the science of evaluating prehistoric earthquakes through the geological analyses of the surficial strata and landforms that have been created, deformed, and/or offset by earthquakes.

Participatory Peer Review: As defined in SSHAC guidance, an ongoing review throughout an entire project that allows reviewers to observe and comment on the process followed and the technical assessments developed. Reviewers must be recognized experts on the subject matter under review ("peers" in the true sense).

Probability of Activity: The likelihood that a particular tectonic feature is seismogenic and will localize moderate-to-large ($M \geq 5$) earthquakes.

Probabilistic Seismic Hazard Analysis: An analytical methodology that estimates the likelihood that various levels of earthquake-caused ground motions will be exceeded at a given location in a given future time period.

Project Manager: As defined in SSHAC guidance, a dedicated full-time professional who is the point of contact between the project and the project sponsor(s), and who is responsible for ensuring adherence to scope, schedule, budgets, and contractual requirements. The PM organizes workshops and keeps the sponsor(s) apprised of progress.

Proponent Expert: An expert who advocates a particular hypothesis or technical position.

Rate of Seismicity: Rate of occurrence of earthquakes above some specified magnitude for a specific region.

Recurrence, Recurrence Rate, Recurrence Curve: The frequency of earthquake occurrence of various magnitudes often expressed by the Gutenberg-Richter relation.

Recurrence Interval: The mean time period between earthquakes of a given magnitude on a fault or in a region.

Recurrence Model: A model to express the relative number or frequency of earthquakes having different magnitudes. A common recurrence model is the exponential magnitude distribution.

Recurrence Model (Poisson, Renewal): A model to express the relative number of earthquakes of different magnitudes that occur within or associated with a particular seismic source. Two models that are commonly used to represent the temporal elements of a recurrence model are Poisson and Renewal. In the Poisson model, the time between consecutive earthquakes follows an exponential distribution and there is no dependence of the timing of the next earthquake with the timing or size of earlier earthquakes. In the Renewal model, the time between consecutive events is assumed to be related to the release and accumulation of strain such that there is a relation between the timing of the most recent event and time to the next event.

Resource Expert: A technical expert who has either site-specific knowledge or expertise with a particular methodology or procedure useful to the evaluator experts in developing the community distribution.

RLME Source: A seismic source identified in the CEUS SSC Project as the location of repeated (more than one) large-magnitude (**M** ≥ 6.5) earthquakes; paleoseismic evidence is used to define the source's recurrence rate.

Seismicity: The occurrence, intensity, and distribution of earthquakes in a region; also refers to the the frequency and depths of these earthquakes.

Seismic Moment: Scalar measurement of the size of an earthquake. It is the product of the area of rupture, the average slip on the fault, and the shear modulus of the crustal rocks. It is typically expressed in units of dyne-cm.

Seismic Source: Traditionally, in a probabilistic seismic hazard analysis, a region or volume of the earth's crust that has uniform earthquake potential or uniform earthquake-generating characteristics. In this project, unique seismic sources (faults, regions) are spatially defined to account for distinct differences in earthquake recurrence rate, maximum earthquake magnitude, expected future earthquake characteristics, and probability of generating earthquakes of magnitude 5 or larger.

Seismic Source Characteristics: The parameters that characterize a seismic source for PSHA, including source geometry, maximum magnitude, earthquake recurrence, and future earthquake characteristics.

Seismic Source Zones: See "Area Source." Volumes within the earth where future earthquakes are expected to occur. The geometry of seismic sources in the CEUS SSC Project is defined by differences in earthquake recurrence rate, maximum earthquake magnitudes, future earthquake characteristics, and the probability of activity of tectonic features.

Seismic Zone: A region showing relatively elevated levels of observed seismicity.

Seismogenic: Capable of generating tectonically significant earthquakes (M ≥ 5).

Seismotectonic Province: A region of the earth's crust having similar seismicity and tectonic characteristics.

Sensitivity Analysis: The calculation of the effect that a particular input parameter or model has on the ouput of a seismic hazard analysis. This may be represented as multiple hazard curves for these alternative input assumptions.

Smoothing: The spatial variation in the rate of activity (*a*-value of the earthquake recurrence relationship) and the *b*-value (slope of the recurrence curve).

Source Zone: See **Area Source**.

Spatial Clustering: Observed or inferred proximity of earthquake occurrences.

Spatial Stationarity: A model in which the locations of future earthquakes are assessed to follow the spatial distribution of past earthquakes.

SSC Model: A seismic source characterization model to represent the parameters that characterize a seismic source for PSHA, including source geometry, probability of activity, maximum magnitude, and earthquake recurrence.

SSHAC (Senior Seismic Hazard Analysis Committee): A committee sponsored by the NRC, DOE, and EPRI to review the state-of-the-art in PSHA and to develop methodologies for using expert judgment and treating uncertainties in seismic hazard analyses. The report of the SSHAC is given in Budnitz et al. (1997), which is also called the SSHAC guidelines.

SSHAC Methodology: The recommended methodology for conducting a PSHA given in Budnitz et al. (1997).

SSHAC Assessment Level: See **SSHAC Study Level**

SSHAC Study Level: One of four "Study Levels" (also called SSHAC Levels) identified in the SSHAC guidelines, ranging from Level 1 projects, which involve very few participants, to Level 4 projects, which involve multiple participants and workshops.

Stability: Characteristic of a hazard input model such as the SSC model that properly quantifies current knowledge and uncertainties such that the identification of new data, models, and methods will not lead to the need to significantly revise the model.

Stable Continental Region: A region of the earth's crust that is defined by Johnston et al. (1994) as having particular characteristics relative to the age and style of most recent tectonism.

Technical Integrator (TI): A SSHAC term for an individual or team responsible for considering the data, models, and methods of the larger technical (scientific) community and for assessing and representing the center, body, and range of technically defensible interpretations in a seismic hazard model. In this project, this was done using a SSHAC Level 3 assessment process.

Tectonic Province: See **Seismotectonic Province**.

Temporal Clustering: Occurrences of multiple closely timed earthquakes separated by longer periods of quiescence. Events that tend to cluster represent a deviation from a stationary Poisson process.

Upper-Bound Magnitude: See **Maximum Magnitude**.

Uncertainty: A general term. See **Epistemic Uncertainty** and **Aleatory Uncertainty**.

Variance: The expected value, taken with respect to its probability distribution, of the squared deviation of an aleatory variable from its expected value.

Weight: A numerical value ($\leq$1.0 or 100%) assigned to alternative credible models or parameter values. Weights reflect scientific judgments that any particular model or parameter value is the correct model or parameter.

Zonation: The process of developing seismic source maps (or a set of seismic zones).

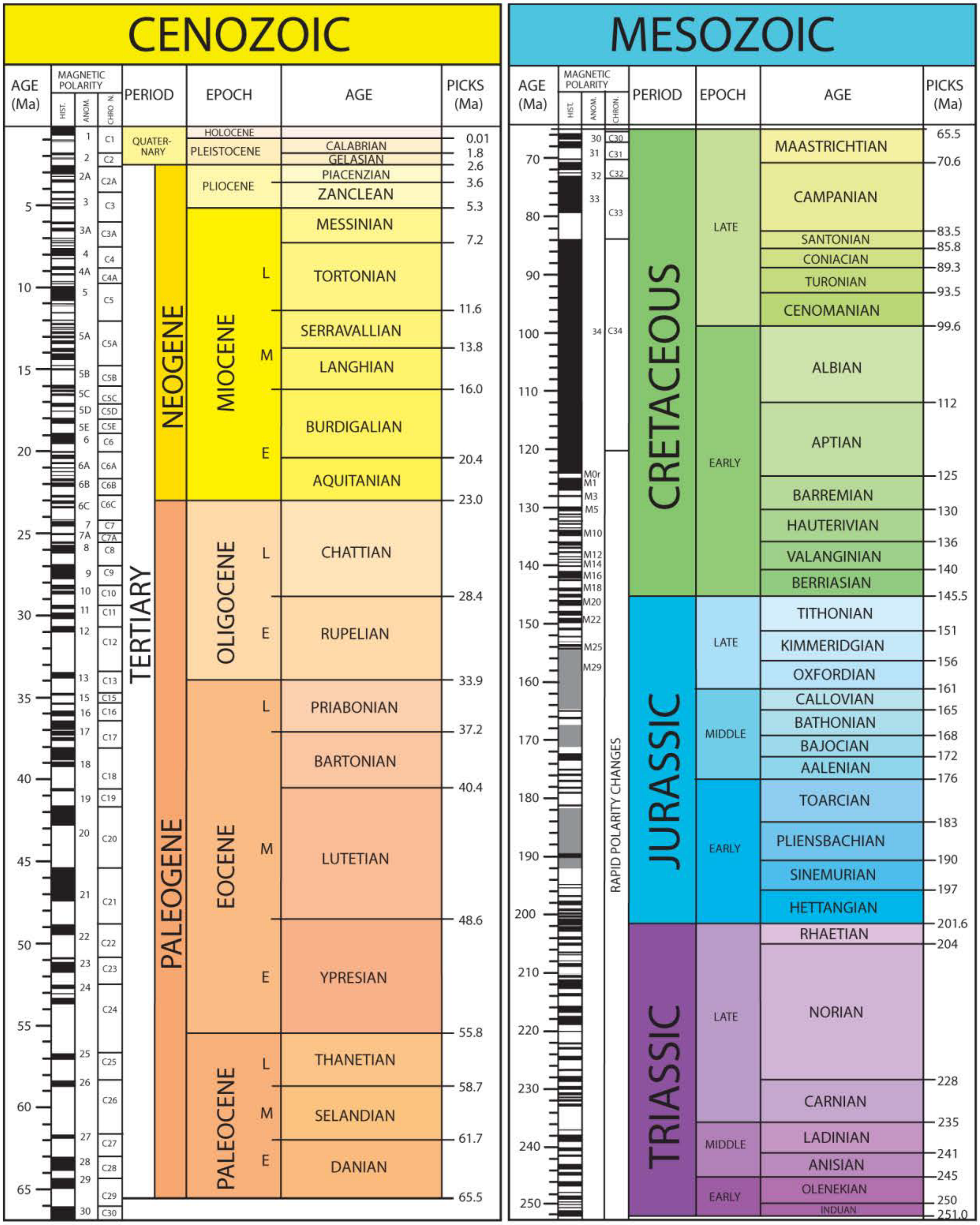

Figure 11-1
Geologic time scale (Walker and Geissman, 2009)

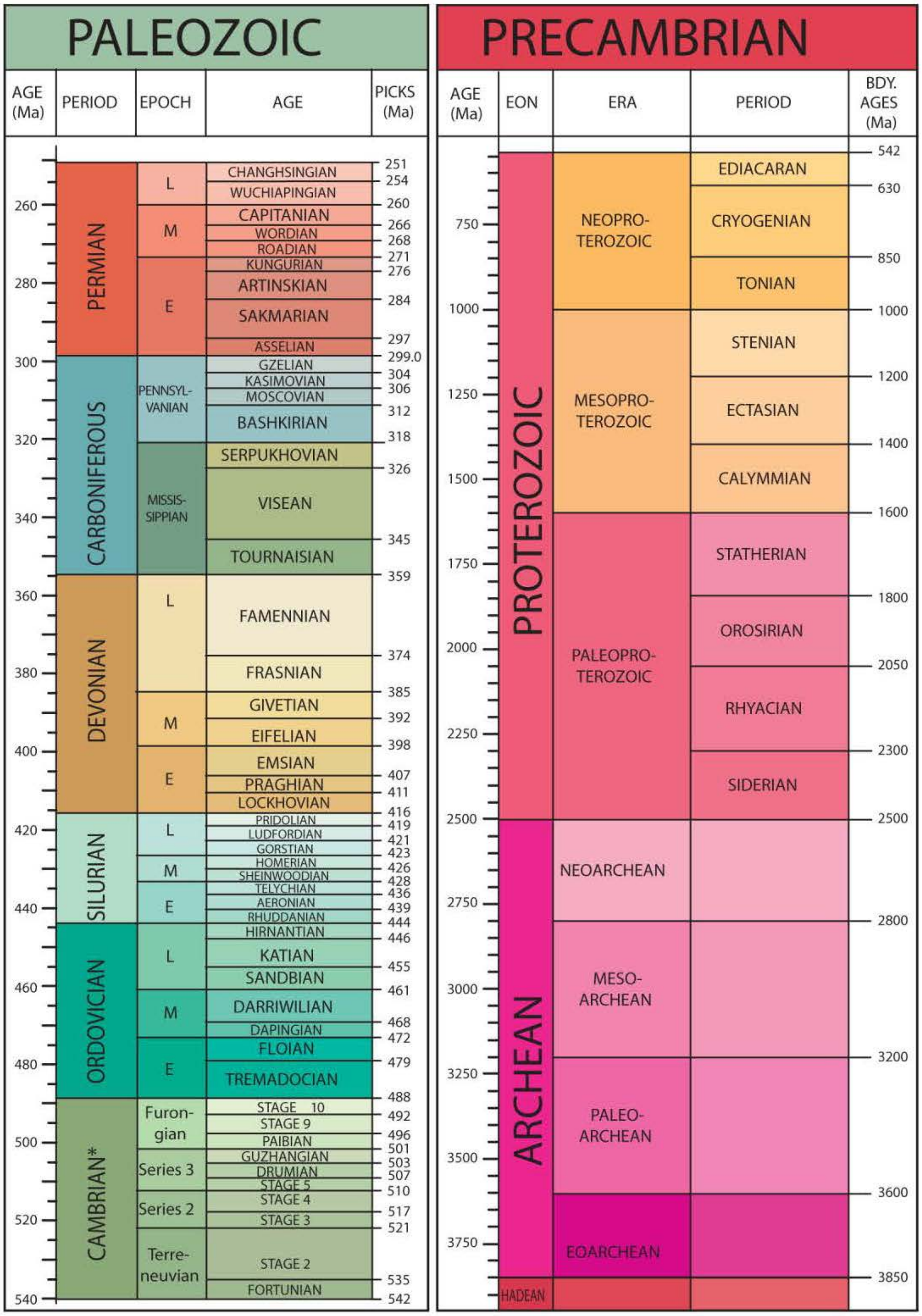

Figure 11-1
Geologic time scale (continued)

NRC FORM 335 (12-2010) NRCMD 3.7

U.S. NUCLEAR REGULATORY COMMISSION

BIBLIOGRAPHIC DATA SHEET

(See instructions on the reverse)

1. REPORT NUMBER **(Assigned by NRC, Add Vol., Supp., Rev., and Addendum Numbers, if any.)**

NUREG-2115
Vol. 3

2. TITLE AND SUBTITLE

Central and Eastern United States Seismic Source Characterization for Nuclear Facilities

Volume 3: Chapters 8 to 11

3. DATE REPORT PUBLISHED

MONTH	YEAR
January	2012

4. FIN OR GRANT NUMBER

K6877

5. AUTHOR(S)

G. Stirewalt (NRC), L. Salomone (Savannah River Nuclear Solutions, LLC), S. McDuffie (DOE), K. Coppersmith (Coppersmith Consulting, Inc), Fugro William Lettis & Associates, Inc.: C. Fuller, R. Hartleb, W. Lettis, S. Lindvall, R. McGuire, G. Toro, D. Slayter, R. Cumbest, A. Shumway, F. Syms, AMEC Geomatrix, Inc: L. Glaser, K. Hanson, R. Youngs, S. Bozkurt, V. Montaldo Falero, R. Perman, R. McGuire (Risk Engineering), M. Tuttle (M. Tuttle & Associates)

6. TYPE OF REPORT

Technical

7. PERIOD COVERED *(Inclusive Dates)*

8. PERFORMING ORGANIZATION - NAME AND ADDRESS *(If NRC, provide Division, Office or Region, U.S. Nuclear Regulatory Commission, and mailing address; if contractor, provide name and mailing address.)*

U.S. Nuclear Regulatory Commission, Office of Nuclear Regulatory Research, Washington DC 20555
U.S. Department of Energy, 1000 Independence Avenue SW, Washington DC 20585
Electric Power Research Institute, 3420 Hillview Avenue, Palo Alto, CA 94304

9. SPONSORING ORGANIZATION - NAME AND ADDRESS *(If NRC, type "Same as above"; if contractor, provide NRC Division, Office or Region, U.S. Nuclear Regulatory Commission, and mailing address.)*

U.S. Nuclear Regulatory Commission, Office of Nuclear Regulatory Research, Washington DC 20555
U.S. Department of Energy, 1000 Independence Avenue SW, Washington DC 20585
Electric Power Research Institute, 3420 Hillview Avenue, Palo Alto, CA 94304

10. SUPPLEMENTARY NOTES

11. ABSTRACT *(200 words or less)*

This report describes a new seismic source characterization (SSC) model for the Central and Eastern United States (CEUS). It will replace the Seismic Hazard Methodology for the Central and Eastern United States, EPRI Report NP-4726 (July 1986) and the Seismic Hazard Characterization of 69 Nuclear Plant Sites East of the Rocky Mountains, Lawrence Livermore National Laboratory Model, (Bernreuter et al., 1989). The objective of the CEUS SSC Project is to develop a new seismic source model for the CEUS using a Senior Seismic Hazard Analysis Committee (SSHAC) Level 3 assessment process. The goal of the SSHAC process is to represent the center, body, and range of technically defensible interpretations of the available data, models, and methods. Input to a probabilistic seismic hazard analysis (PSHA) consists of both seismic source characterization and ground motion characterization. These two components are used to calculate probabilistic hazard results (or seismic hazard curves) at a particular site. This report provides a new seismic source model.

12. KEY WORDS/DESCRIPTORS *(List words or phrases that will assist researchers in locating the report.)*

Probabilistic seismic hazard analysis (PSHA)
Seismic source characterization (SSC)
Seismic source characterization model
Central and Eastern United States (CEUS)

13. AVAILABILITY STATEMENT

unlimited

14. SECURITY CLASSIFICATION

(This Page)
unclassified

(This Report)
unclassified

15. NUMBER OF PAGES

16. PRICE